



QA: QA

TDR-DSD-MD-000001 REV 00

March 2004

DOE SNF Phase I and II Summary Report

By
Horia Radulescu
Dennis Moscalu
Mehmet Saglam

Prepared for:
U.S. Department of Energy
Office of Civilian Radioactive Waste Management
Office of Repository Development
1551 Hillshire Drive
Las Vegas, Nevada 89134-6321

Prepared by:
Bechtel SAIC Company, LLC
1180 Town Center Drive
Las Vegas, Nevada 89144

Under Contract Number
DE-AC28-01RW12101

DISCLAIMER

This report was prepared as an account of work sponsored by an agency of the United States Government. Neither the United States Government nor any agency thereof, nor any of their employees, nor any of their contractors, subcontractors or their employees, makes any warranty, express or implied, or assumes any legal liability or responsibility for the accuracy, completeness, or any third party's use or the results of such use of any information, apparatus, product, or process disclosed, or represents that its use would not infringe privately owned rights. Reference herein to any specific commercial product, process, or service by trade name, trademark, manufacturer, or otherwise, does not necessarily constitute or imply its endorsement, recommendation, or favoring by the United States Government or any agency thereof or its contractors or subcontractors. The views and opinions of authors expressed herein do not necessarily state or reflect those of the United States Government or any agency thereof.

Bechtel SAIC Company, LLC

DOE SNF Phase I and II Summary Report

TDR-DSD-MD-000001 REV 00

March 2004

Originator:

Horia R. Radulescu
Horia R. Radulescu (All sections except 6.5 and 10)

03/02/04
Date

Dennis R. Moscalu
Dennis R. Moscalu (Sections 6.5 and 10 only)

03/02/04
Date

M. Saglam
Mehmet Saglam (Sections 6.5 and 10 only)

03/02/04
Date

Checker:

Abdelhalim
Abdelhalim Alsaed

03/02/04
Date

Quality Engineering Representative:

Darrell Svalstad
Darrell Svalstad

03/02/04
Date

Responsible Manager:

Daniel A. Thomas
Daniel A. Thomas
Risk and Criticality Department

03/02/2004
Date

INTENTIONALLY LEFT BLANK

CHANGE HISTORY

<u>Revision Number</u>	<u>Interim Change No.</u>	<u>Date</u>	<u>Description of Change</u>
00	0	03/02/2004	Initial Issue.

INTENTIONALLY LEFT BLANK

EXECUTIVE SUMMARY

There are more than 250 forms of U.S. Department of Energy (DOE)-owned spent nuclear fuel. Due to the variety of the spent nuclear fuel, the National Spent Nuclear Fuel Program (NSNFP) has designated nine representative fuel groups for disposal criticality analyses based on fuel matrix, primary fissile isotope, and enrichment. For each fuel group, a fuel type that represents the characteristics of all fuels in that group has been selected for detailed analysis. The DOE-owned spent nuclear fuel will be loaded into the DOE standardized canisters (or multicanister overpacks for N-Reactor fuel), which will be codisposed with five (two for N-Reactor fuel) defense high-level waste glass canisters in a waste package. The results of the analyses performed will be used to develop waste acceptance criteria. The items that are important to criticality control are identified based on the analysis needs and result sensitivities. The eight DOE fuel groups covered in this report, the representative fuel type for each group, and the neutron absorbers used for criticality control are listed in Table ES-1.

Table ES-1. The DOE Spent Nuclear Fuel Groups and Their Representative Fuel Types

DOE Fuel Group	Representative Fuel Type	Neutron Absorber
Mixed Oxide (MOX)	Fast Flux Test Facility (FFTF) Driver Assembly	Gd Alloy
Uranium-Zirconium Hydride (UZrH)	Training, Research, Isotope General Atomic (TRIGA) – Fuel Life Improvement Program (FLIP) Rod	Gd Alloy
U-Mo and U-Zr Alloys	Enrico Fermi Fuel Pin	Gd Shot
Highly Enriched Uranium (HEU) Oxide	Shippingport - Pressurized Water Reactor (PWR) Assembly	None
²³³ U/Th Oxide	Shippingport - Light Water Breeder Reactor (LWBR) Seed Assembly	Gd Shot
U Metal	N-Reactor Assembly	None
HEU-AI	Melt and Dilute (MD) Form	Gd
U/Th Carbide	Fort Saint Vrain Reactor (FSVR) Assembly	None

The analyses have been performed by following the methodology documented in *Disposal Criticality Analysis Methodology Topical Report (YMP 2003)* and submitted to the U.S. Nuclear Regulatory Commission for approval. The methodology includes analyzing the geochemical and environmental processes that can breach the waste package and degrade the waste forms and other internal components, as well as the structural, thermal, shielding, and intact and degraded component criticality analyses.

The structural, thermal, shielding, and intact and degraded component criticality analyses performed for each fuel type waste package configuration met the design criteria as defined in *DOE and Commercial Waste Package System Description Document (BSC 2003a)*.

CONTENTS

Page

CONTENTS

Page

1	INTRODUCTION.....	1-1
1.1	PURPOSE.....	1-1
1.2	SCOPE.....	1-1
2	DESIGN INFORMATION.....	2-1
2.1	WASTE PACKAGE.....	2-1
2.2	DHLW GLASS POUR CANISTERS.....	2-6
2.3	DOE STANDARDIZED SNF CANISTER.....	2-7
2.3.1	Internals of FFTF DOE SNF Canister.....	2-9
2.3.2	Internals of TRIGA DOE SNF Canister.....	2-10
2.3.3	Internals of Shippingport PWR DOE SNF Canister.....	2-11
2.3.4	Internals of Enrico Fermi DOE SNF Canister.....	2-13
2.3.5	Internals of Shippingport LWBR DOE SNF Canister.....	2-16
2.3.6	Internals of Melt and Dilute DOE SNF Canister.....	2-18
2.3.7	Internals of FSVR DOE SNF Canister.....	2-18
2.4	N-REACTOR MULTICANISTER OVERPACK.....	2-18
2.4.1	MCO Basket for Mark IV.....	2-22
2.4.2	MCO Basket for Mark IA Fuels.....	2-24
3	SUMMARY OF FUEL CHARACTERISTICS.....	3-1
3.1	DOE SNF GROUPING AND RATIONALE.....	3-1
3.1.1	Background on DOE SNF Grouping.....	3-1
3.1.2	Criticality Grouping Selection.....	3-2
3.1.3	Fuel Groups.....	3-4
3.2	DESCRIPTION OF REPRESENTATIVE FUEL TYPES.....	3-6
3.2.1	FFTF.....	3-6
3.2.2	TRIGA.....	3-9
3.2.3	Shippingport PWR.....	3-18
3.2.4	Enrico Fermi.....	3-22
3.2.5	Shippingport LWBR.....	3-24
3.2.6	N-Reactor.....	3-31
3.2.7	Melt and Dilute.....	3-34
3.2.8	Fort Saint Vrain.....	3-35
3.3	STRUCTURAL.....	3-42
3.4	THERMAL.....	3-42
3.4.1	DHLW Glass.....	3-42
3.4.2	FFTF.....	3-45
3.4.3	TRIGA.....	3-45
3.4.4	Shippingport PWR.....	3-46
3.4.5	Enrico Fermi.....	3-47
3.4.6	Shippingport LWBR.....	3-49

CONTENTS (Continued)

	Page
3.4.7 N-Reactor	3-50
3.4.8 Melt and Dilute.....	3-53
3.4.9 FSVR.....	3-53
3.5 SHIELDING SOURCE TERM	3-55
3.5.1 DHLW Glass	3-55
3.5.2 FFTF	3-58
3.5.3 TRIGA.....	3-58
3.5.4 Shippingport PWR	3-60
3.5.5 Enrico Fermi.....	3-60
3.5.6 Shippingport LWBR.....	3-61
3.5.7 N-Reactor	3-62
3.5.8 Melt and Dilute.....	3-63
3.5.9 FSVR.....	3-64
3.6 MATERIAL COMPOSITIONS	3-65
4 FUNCTIONS AND DESIGN CRITERIA.....	4-1
4.1.1 Structural Criteria.....	4-1
4.1.2 Thermal Criteria	4-3
4.1.3 Shielding Criteria	4-3
4.1.4 Degradation and Geochemistry Criteria.....	4-3
4.1.5 Intact and Degraded Criticality Criteria	4-4
5 ASSUMPTIONS	5-1
5.1 STRUCTURAL	5-1
5.1.1 The Viability Assessment Design Waste Package Containment Barriers Have Solid Connections at the Adjacent Surfaces	5-1
5.1.2 Target Surface Elastic Characteristics.....	5-1
5.1.3 MCO Internals Mass Distribution Simplification	5-1
5.1.4 The Total Mass of DOE SNF Canister Loaded with MD Ingots is Distributed Uniformly Within the Volume of the Canister.....	5-2
5.1.5 Mass of FSVR Fuel Element is Distributed Uniformly Within its Volume	5-2
5.1.6 Mass of DHLW Glass Canister is Distributed Uniformly Within its Volume	5-2
5.2 THERMAL	5-3
5.2.1 The Axial Power Peaking Factor (PPF) for the FFTF SNF Assemblies, TRIGA, and Enrico Fermi SNF Pins is 1.25.....	5-3
5.2.2 The Volumetric Heat Generation of DHLW Glass Canisters and Shippingport PWR C2 S2 SNF Assemblies is Uniform	5-3
5.2.3 The Axial PPF for Shippingport LWBR SNF is 2.0	5-3
5.2.4 The First Arrival and Emplacement of Shippingport LWBR SNF Will Occur in 2010	5-4
5.2.5 Heat Output of the Shippingport LWBR Seed SNF is Held Constant after 2030.....	5-4
5.2.6 The MCO Contains Intact Mark IV Fuel Elements Only	5-4

CONTENTS (Continued)

	Page	
5.2.7	Basis for the Heat Output History of Hanford DHLW Glass Canisters.....	5-4
5.2.8	The Thermal Conductivity of the DHLW Glass is Equal to that of Borosilicate Glass, and its Density and Specific Heat to that of Pyrex Glass	5-5
5.2.9	The Heat Output of the MCO Filled with Mark IV Fuels is Constant over the Entire Period of Emplacement	5-5
5.2.10	The Zircaloy-2 Cladding of the Mark IV Fuel Pins is Completely Oxidized	5-5
5.2.11	Basis for 2-MCO/2-DHLW Waste Package Surface Temperature History	5-6
5.2.12	The Fill Gas Within the N-Reactor Waste Package is Same as the Gas Filling the MCO	5-6
5.2.13	The DHLW Glass Filling the Hanford 4.5-m- (15-ft-) long Canister Has an Age of Zero.....	5-6
5.2.14	A Two-Dimensional Finite Element Representation of a Cross-Section of the Waste Package is Representative of the Hottest Portion of the Waste Package.....	5-6
5.2.15	The Thermal Conductivity of Helium at Atmospheric Pressure is Representative of the Waste Package Conditions	5-7
5.2.16	Modeling only Conduction and Radiation Heat Transfer Provides Conservative Results	5-7
5.2.17	The Equations for Unirradiated Graphite are Used to Calculate the Thermal Conductivity of the Graphite Block.....	5-8
5.2.18	The Glass Volume in the Hanford 4.5-m- (15-ft-) long Canister is 1.08 m ³	5-8
5.2.19	The Fill Gas Used in the DOE SNF Canister is Air	5-8
5.3	SHIELDING	5-8
5.3.1	For FFTF, TRIGA, and Fermi SNF the Contents of the DOE SNF Canister are Homogenized Inside the Cavity of Canister	5-8
5.3.2	An Axial PPF of 1.25 is used for the FFTF, TRIGA, Fermi, and Shippingport PWR SNF Source	5-9
5.3.3	The dose rate due to secondary gamma rays is negligible	5-9
5.3.4	The inner, the outer brackets, and the divider plates supporting the DHLW glass canisters in the waste package are neglected.....	5-9
5.3.5	The active fuel region of the Shippingport LWBR seed fuel assembly, Shippingport PWR C2 S1 fuel assembly and FSVR fuel element is homogenized inside its transverse dimensions.....	5-10
5.3.6	The Shippingport LWBR fuel source terms has an axial PPF factor of 2.0	5-10
5.3.7	The density of the SRS DHLW glass is 2.56 g/cm ³	5-10
5.3.8	The head and neck of the DHLW glass canisters are neglected.....	5-10
5.3.9	The source distribution of the N-Reactor SNF has axial PPF of 2.0.....	5-11
5.3.10	For elements' composition with weight percent range, the midpoint value is assumed.....	5-11

CONTENTS (Continued)

	Page
5.3.11	The MD ingots do not contain a liner, and the ingot stack occupies the entire cavity volume of the 18-in-outer diameter DOE SNF canister 5-11
5.3.12	The MD ingots composition consists of 13.2 ± 5 wt% uranium with aluminum being the balance element 5-12
5.4	INTACT AND DEGRADED COMPONENT CRITICALITY 5-12
5.4.1	Preirradiation nuclear fuel compositions were used..... 5-12
5.4.2	Ident-69 pin containers are assumed to contain a most reactive configuration of FFTF fuel pins for the intact fuel cases 5-12
5.4.3	The DHLW canister is represented as a right circular cylinder completely filled with DHLW glass and the flanged head and neck are neglected..... 5-12
5.4.4	The radial FFTF pellet spacing in degraded cladding configurations never becomes greater than the original pitch of the DFA..... 5-13
5.4.5	The erbium burnable neutron absorber for fresh TRIGA nuclear fuel was neglected. 5-13
5.4.6	The neutron absorber for the TRIGA waste package is made of Alloy 22 with 8 at% of gadolinium 5-13
5.4.7	For Fermi SNF, the impurities in the undegraded fuel matrix (B, C, Cr, Fe, Ni, N, O, Zr, Cu, and others) are replaced with molybdenum (Mo).... 5-14
5.4.8	If aluminum is present in the DOE SNF canister its degradation (oxidizing) produces AlOOH (diaspore)..... 5-14
5.4.9	For the degraded configurations with intact fuel pins, the pins are assumed to be stacked at the bottom of the waste package in a regular array..... 5-14
5.4.10	Boron in two end plates of the Shippingport PWR SNF subassembly were represented as water..... 5-14
5.4.11	The iron in the iron shot and Stainless Steel degrades to goethite rather than hematite 5-15
5.4.12	The length of the FSVR fuel in the fuel elements is same as the length of the fuel elements 5-15
5.4.13	A most reactive fissile concentration is used for the FSVR fuel that is shown to bound fuel compositions for actual fuel elements 5-15
5.5	GENERAL 5-16
5.5.1	The limits for each fuel group, which are established by the technical information related to that specific SNF, are bounding 5-16
5.5.2	SRS Design-Basis DHLW glass fills the 4.5-m-long glass pour canisters 5-16
6	ANALYSIS METHODOLOGY 6-1
6.1	STRUCTURAL 6-1
6.2	THERMAL 6-2
6.3	SHIELDING 6-2
6.4	GEOCHEMISTRY 6-2
6.4.1	Design Analysis..... 6-3

CONTENTS (Continued)

	Page
6.4.2 Basic Design Approach for Geochemistry Analysis.....	6-8
6.5 CRITICALITY METHODOLOGY	6-9
7 STRUCTURAL ANALYSIS	7-1
7.1 FFTF	7-1
7.1.1 Description of the Finite-Element Representation	7-1
7.1.2 Results with No Credit for the Structural Components of the DOE SNF Canister.....	7-2
7.1.3 Results with Structural Credit for the DOE SNF Canister Components.....	7-2
7.1.4 Summary	7-3
7.2 TRIGA	7-4
7.2.1 Description of the Finite-Element Representation	7-4
7.2.2 Results with No Credit for the TRIGA SNF Rod Inside of the DOE SNF Canister	7-5
7.2.3 Summary	7-7
7.3 SHIPPINGPORT PWR.....	7-7
7.3.1 Description of the Finite-Element Representation	7-7
7.3.2 Results of Structural Calculations	7-9
7.3.3 Summary	7-10
7.4 ENRICO FERMI	7-10
7.4.1 Description of the Finite-Element Representation	7-10
7.4.2 Results	7-12
7.4.3 Summary	7-12
7.5 SHIPPINGPORT LWBR.....	7-13
7.5.1 Description of the Finite-Element Representation	7-13
7.5.2 Results	7-14
7.5.3 Summary	7-16
7.6 N-REACTOR.....	7-16
7.6.1 Description of the Finite Element Representation	7-16
7.6.2 Results of Structural Calculations	7-18
7.6.3 Summary	7-18
7.7 ALUMINUM-BASED FUELS (MELT AND DILUTE).....	7-19
7.7.1 Description of the Finite Element Representation	7-19
7.7.2 Results of Structural Calculations	7-20
7.8 FORT SAINT VRAIN.....	7-21
7.8.1 Description of the Finite Element Representation	7-21
7.8.2 Results	7-22
7.8.3 Summary	7-23
8 THERMAL ANALYSIS	8-1
8.1 FFTF	8-1
8.1.1 Thermal Design Analysis	8-1
8.1.2 Calculations and Results	8-3
8.1.3 Summary	8-4
8.2 TRIGA	8-4

CONTENTS (Continued)

	Page
8.2.1 Design Analysis.....	8-4
8.2.2 Calculations and Results	8-5
8.2.3 Summary	8-8
8.3 SHIPPINGPORT PWR.....	8-8
8.3.1 Thermal Design Analysis	8-8
8.3.2 Calculations and Results	8-8
8.3.3 Summary	8-10
8.4 ENRICO FERMI	8-11
8.4.1 Thermal Design Analysis	8-11
8.4.2 Calculations and Results	8-13
8.4.3 Summary	8-15
8.5 SHIPPINGPORT LWBR.....	8-15
8.5.1 Thermal Design Analysis	8-15
8.5.2 Calculations and Results	8-16
8.5.3 Summary	8-20
8.6 N-REACTOR.....	8-20
8.6.1 Thermal Design Analysis	8-20
8.6.2 Calculations and Results	8-22
8.6.3 Summary	8-24
8.7 MELT AND DILUTE.....	8-24
8.8 FORT SAINT VRAIN.....	8-24
8.8.1 Calculations and Results	8-24
8.8.2 Summary	8-26
8.9 CONCLUSIONS.....	8-26
9 SHIELDING ANALYSIS.....	9-1
9.1 FFTF	9-1
9.1.1 Waste Package Containing Hanford DHLW and FFTF Fuel.....	9-4
9.1.2 Waste Package Containing Only Hanford DHLW Canisters.....	9-5
9.1.3 Summary	9-5
9.2 TRIGA	9-6
9.3 SHIPPINGPORT PWR.....	9-9
9.4 ENRICO FERMI	9-11
9.5 SHIPPINGPORT LWBR.....	9-14
9.6 N-REACTOR.....	9-17
9.7 ALUMINUM-BASED FUELS (MELT AND DILUTE).....	9-20
9.8 FORT SAINT VRAIN.....	9-24
10 CRITICALITY ANALYSIS.....	10-1
10.1 FFTF SNF WASTE PACKAGE	10-2
10.1.1 Degradation Scenarios and Configurations.....	10-3
10.1.2 Criticality Calculations and Results	10-5
10.1.3 ROP for Configurations of Waste Package Containing FFTF SNF.....	10-12
10.1.4 Selection of the Criticality Benchmark Experiments Used in the Validation of the Criticality Model	10-13

CONTENTS (Continued)

	Page
10.1.5	Comparison between ROA of Benchmark Experiments and ROP 10-14
10.1.6	Calculation of the Lower Bound Tolerance Limit 10-15
10.1.7	Summary of Criticality Model Results and Validation for the Waste Package Containing FFTF SNF 10-15
10.2	TRIGA SNF 10-18
10.2.1	Degradation Scenarios and Configurations 10-19
10.2.2	Criticality Calculations and Results 10-21
10.2.3	ROP for Configurations of Waste Package Containing TRIGA DOE SNF 10-27
10.2.4	Selection of the Criticality Benchmark Experiments 10-28
10.2.5	Comparison between ROA of Benchmark Experiments and ROP 10-31
10.2.6	Calculation of the Lower Bound Tolerance Limit 10-32
10.2.7	Summary of the Criticality Model Results and Validation for the Waste Package 10-33
10.3	SHIPPINGPORT PWR SNF 10-36
10.3.1	Degradation Scenarios and Configurations 10-36
10.3.2	Criticality Calculations and Results 10-39
10.3.3	Range of Parameters for Configurations of Waste Package Containing Shippingport PWR DOE SNF 10-43
10.3.4	Selection of the Criticality Benchmark Experiments 10-44
10.3.5	Comparison Between ROA of Benchmark Experiments and ROP 10-45
10.3.6	Calculation of the Lower Bound Tolerance Limit 10-46
10.3.7	Summary of Criticality Model Results and Validation for the Waste Package Containing Shippingport PWR SNF 10-46
10.4	ENRICO FERMI 10-49
10.4.1	Degradation Scenarios and Configurations 10-49
10.4.2	Criticality Calculations and Results 10-52
10.4.3	Range of Parameters for Configurations of Waste Package Containing Enrico Fermi DOE SNF 10-61
10.4.4	Selection of the Criticality Benchmark Experiments Used in the Validation of the Criticality Model 10-63
10.4.5	Comparison Between ROA of Benchmark Experiments and ROP 10-63
10.4.6	Summary of Criticality Model Results and Validation for the Waste Package Containing Enrico Fermi DOE SNF 10-67
10.5	SHIPPINGPORT LWBR SNF 10-70
10.5.1	Degradation Scenarios and Configurations 10-71
10.5.2	Criticality Calculations and Results 10-73
10.5.3	Range of Parameters for Configurations of Waste Package Containing Shippingport LWBR DOE SNF 10-81
10.5.4	Selection of the Criticality Benchmark Experiments Used in the Validation of the Criticality Model 10-82
10.5.5	Comparison Between ROA of Benchmark Experiments and ROP 10-84
10.5.6	Calculation of the Lower Bound Tolerance Limit 10-85

CONTENTS (Continued)

	Page
10.5.7 Summary of Criticality Model Results and Validation for the Waste Package Containing Shippingport LWBR SNF	10-86
10.6 N-REACTOR.....	10-89
10.6.1 Degradation Scenarios and Configurations.....	10-89
10.6.2 Criticality Calculations and Results	10-92
10.6.3 Selection of the Criticality Benchmark Experiments Used in the Validation of the Criticality Model	10-100
10.7 MELT AND DILUTE SNF	10-106
10.7.1 Degradation Scenarios and Configurations.....	10-107
10.7.2 Range of Parameters for Configurations of Waste Package Containing Melt and Dilute DOE SNF	10-114
10.7.3 Selection of the Criticality Benchmark Experiments Used in the Validation of the Criticality Model	10-115
10.7.4 Comparison Between ROA of Benchmark Experiments and ROP	10-116
10.7.5 Calculation of the Lower Bound Tolerance Limit	10-117
10.7.6 Summary of the Criticality Model Results and Validation for the Waste Package Containing Melt and Dilute SNF	10-117
10.8 FSVR SNF	10-120
10.8.1 Degradation Scenarios and Configurations.....	10-121
10.8.2 Criticality Calculations and Results	10-122
10.8.3 Range of Parameters for Configurations of Waste Package Containing FSVR DOE SNF	10-130
10.8.4 Selection of the Criticality Benchmark Experiments Used in the Validation of the Criticality Model	10-131
10.8.5 Comparisons between ROA of Benchmark Experiments and ROP.....	10-132
10.8.6 Summary of Criticality Model Results and Validation for FSVR SNF ..	10-134
11 CONCLUSIONS.....	11-137
11.1 STRUCTURAL	11-137
11.2 THERMAL	11-137
11.3 SHIELDING	11-137
11.4 CRITICALITY	11-138
12 REFERENCES.....	12-1
12.1 DOCUMENTS CITED.....	12-1
12.2 CODES, STANDARDS, REGULATIONS, AND PROCEDURES.....	12-9
12.3 DATA, LISTED BY DATA TRACKING NUMBER.....	12-10
12.4 SOFTWARE CODES.....	12-10

FIGURES

		Page
2-1.	Cross-Section of the 5-DHLW/DOE Spent Nuclear Fuel Waste Package (Viability Assessment Design).....	2-2
2-2.	Cross-Sectional Representation of the 5-DHLW/DOE Waste Package in an As-Loaded Condition.....	2-4
2-3.	Cross-Section View of the 2-MCO/2-DHLW Waste Package in an As-Loaded Condition.....	2-5
2-4.	DHLW Glass Pour Canister.....	2-7
2-5.	Plan View of the 18-in-Outer Diameter DOE Standardized Spent Nuclear Fuel Canister.....	2-8
2-6.	Cross-Sectional Representation of the FFTF DOE Spent Nuclear Fuel Canister in an As-Loaded Condition.....	2-9
2-7.	Cross-Sectional Representation of an Arrangment of TRIGA-SS Rods in a DOE Spent Nuclear Fuel Canister.....	2-10
2-8.	Isometric View of the TRIGA DOE Spent Nuclear Fuel Canister.....	2-11
2-9.	Emplacement of the Advanced Neutron Absorber Matrix Tubes in the TRIGA DOE Spent Nuclear Fuel Canister Basket.....	2-11
2-10.	Cross-Sectional Representation of the Shippingport PWR DOE Spent Nuclear Fuel Canister in an As-Loaded Condition.....	2-12
2-11.	Isometric View of the Shippingport PWR DOE Spent Nuclear Fuel Canister.....	2-12
2-12.	Schematic of -01 and -02 Shipping Canisters.....	2-13
2-13.	Schematic of -04 Canister.....	2-14
2-14.	Cross-Sectional Representation of the Enrico Fermi DOE Spent Nuclear Fuel Canister in an As-Loaded Condition.....	2-15
2-15.	Enrico Fermi Fuel Pins in a 4-in-Diameter Pipe.....	2-15
2-16.	Cross-Sectional Representation of the Shippingport LWBR DOE Spent Nuclear Fuel Canister in an As-Loaded Condition.....	2-17
2-17.	Isometric View of the Shippingport LWBR DOE Spent Nuclear Fuel Canister.....	2-17
2-18.	Multicanister Overpack With Four Intact and One Scrap Mark IV Baskets.....	2-19
2-19.	Example of Loading Arrangements in Multicanister Overpacks.....	2-21
2-20.	Mark IV Spent Nuclear Fuel Intact Elements Storage.....	2-23
2-21.	Mark IV Spent Nuclear Fuel Scrap Elements Storage Basket.....	2-24
2-22.	Mark IA Spent Nuclear Fuel Intact Elements Storage Basket.....	2-25
2-23.	Mark IA Spent Nuclear Fuel Scrap Material Storage Basket.....	2-26
2-24.	Isometric Representation of One Half of Mark IA Spent Nuclear Fuel Scrap Material Storage Basket.....	2-27
3-1.	FFTF Test Fuel Assembly.....	3-7
3-2.	FFTF DFA Cross-Section.....	3-7
3-3.	Standard DFA Fuel Pin.....	3-8
3-4.	Cross-Section View of Partially Loaded Ident-69 Fuel Pin Container.....	3-8
3-5.	Sketch of Aluminum-Clad TRIGA Rods (TRIGA-AI).....	3-11
3-6.	Sketch of TRIGA-SS Rods.....	3-12
3-7.	Cross-Section Sketch of TRIGA-SS Rod.....	3-13
3-8.	Sketch of Standard Fuel-Follower Control Rod.....	3-15

FIGURES (Continued)

	Page
3-9. Sketch of ACPR Fuel-Follower Control Rod Element	3-16
3-10. Shippingport C2 S2 Spent Nuclear Fuel Assembly	3-19
3-11. Shippingport C2 S2 Spent Nuclear Fuel Subassembly Cross-Section.....	3-20
3-12. Shippingport C2 S2 Spent Nuclear Fuel Fuel Plate	3-22
3-13. Enrico Fermi Fuel Pin Details (all dimensions are in inches).....	3-23
3-14. Schematic Representation of Seed Fuel Assembly and Rods	3-25
3-15. Layout of Fuel Rods in a Seed Assembly	3-30
3-16. Characteristic N-Reactor Fuel Types	3-33
3-17. Standard FSVR Fuel Element	3-37
3-18. Cross-Section View of Fertile and Fissile Fuel Particles Used in FSVR.....	3-38
6-1. Internal Criticality Master Scenarios, Part 1	6-5
6-2. Internal Criticality Master Scenarios, Part 2	6-6
7-1. Stresses in 5-DHLW/DOE SNF-Long Waste Package Loaded with FFTF Fuel.....	7-3
7-2. Stresses in the 5-DHLW/DOE SNF-Short Waste Package Loaded with TRIGA Fuel.....	7-6
7-3. Stresses Inside of the DOE Spent Nuclear Fuel Canister Loaded with TRIGA Fuel.....	7-6
7-4. Stresses in 5-DHLW/DOE SNF-Long Waste Package Loaded with Shippingport PWR Fuel	7-8
7-5. Stresses in the DOE Spent Nuclear Fuel Canister Loaded with Shippingport PWR Fuel	7-10
7-6. Stresses in the 5-DHLW/DOE SNF-Short Waste Package Loaded with Enrico Fermi Fuel	7-12
7-7. Stresses in the 5-DHLW/DOE SNF-Long Waste Package	7-14
7-8. Stresses in the DOE Spent Nuclear Fuel Canister.....	7-15
7-9. Cross-Section View of Tipover (Case 1 Orientation)	7-17
7-10. Cross-Section View of Tipover (Case 2 Orientation)	7-17
8-1. Node Locations and Numbers on Part 1 of the Finite-element Representation (Waste Package Basket and Hanford 15-ft DHLW Canister).....	8-2
8-2. Node Locations and Numbers on Part 2 of the Finite-element Representation (Ident-69 Fuel Pin Container).....	8-2
8-3. Temperature History for FFTF Waste Package	8-4
8-4. The Finite Element Representation of TRIGA Waste Package	8-5
8-5. Location of DOE Spent Nuclear Fuel Canister Temperature Nodes	8-6
8-6. Temperature History for TRIGA Waste Package	8-6
8-7. Peak Temperature versus Distance from the Center of the Waste Package.....	8-7
8-8. Finite-element Representation of the 5-DHLW/DOE SNF-Long Waste Package	8-9
8-9. Finite-element Representation of the Shippingport PWR C2 S2 Spent Nuclear Fuel Assembly.....	8-9
8-10. Axial Temperature Profile of the 5-DHLW/DOE SNF-Long Waste Package	8-10

FIGURES (Continued)

		Page
8-11.	Node Locations and Numbers of the Finite-Element Representation of Waste Package with Fermi Spent Nuclear Fuel Canister and the DHLW Canisters	8-12
8-12.	Node Locations and Numbers of the Finite-Element Representation of Fermi Spent Nuclear Fuel Canister	8-13
8-13.	Temperature History for Enrico Fermi Waste Package	8-14
8-14.	Finite-Element Representation of the 5-DHLW/DOE SNF-Long Waste Package.....	8-15
8-15.	Finite-Element Representation of the Shippingport LWBR Seed Assembly Fuel (One-Sixth Section)	8-16
8-16.	DHLW Peak Temperature Versus Time	8-18
8-17.	Radial Temperature Profile of the Waste Package.....	8-19
8-18.	2-MCO/2-DHLW Waste Package Configurations.....	8-20
8-19.	Cross-Section View of the 2-MCO/2-DHLW Waste Package for the Thermal Analysis	8-21
8-20.	Cross-Section of the MCO	8-21
8-21.	Peak Temperatures – Configuration 1	8-23
8-22.	Peak Temperatures – Configuration 2	8-23
8-23.	Plot of Temperature Versus Time at Points along Waste Package Radius	8-25
8-24.	Plot of Temperature Versus Time for the FSVR Spent Nuclear Fuel Element	8-25
9-1.	Axial and Transversal Cross-Sections of MCNP Geometry Representation for FFTF Waste Package.....	9-2
9-2.	Radial Segments Used for Dose-Rate Calculations	9-3
9-3.	MCNP Estimates for Dose Rates in rem/h over Axial Surfaces and Segments.....	9-4
9-4.	Vertical and Horizontal Cross-Sections of MCNP Geometry Representation.....	9-7
9-5.	Radial-Surface Segments of the Waste Package Used in Dose Rate Calculations	9-8
9-6.	Waste Package Cross-Sections of MCNP Geometry Representation	9-9
9-7.	Radial Surfaces and Segments of the Waste Package Used in Dose Rate Calculations	9-10
9-8.	Vertical and Horizontal Cross-Sections of MCNP Geometry Representation.....	9-12
9-9.	Surfaces and Segments Used for Dose-Rate Calculations	9-13
9-10.	Vertical and Horizontal Cross-Sections of the MCNP Geometry Representation.....	9-15
9-11.	Surfaces and Segments Used for Dose-Rate Calculations	9-16
9-12.	Waste Package Cross-Section of MCNP Geometry Representation and the Angular Segments Used in Dose Rate Calculations	9-18
9-13.	Radial and Axial Surfaces and Segments of the Waste Package Used in Dose Rate Calculations.....	9-19
9-14.	Vertical and Horizontal Cross-Sections of MCNP Geometry Representation.....	9-21
9-15.	Surfaces and Segments (axial and radial) Used for Dose Rate Calculations	9-22
9-16.	Angular Segments of the Waste Package Outer Radial Surface Used in Dose Rate Calculations.....	9-23
9-17.	Vertical and Horizontal Cross-Sections of MCNP Geometry Representation.....	9-25
9-18.	Surfaces and Segments (Axial and Radial) Used for Dose Rate Calculations.....	9-26
9-19.	Angular Segments of the Waste Package Outer Radial Surface Used in Dose Rate Calculations.....	9-27

FIGURES (Continued)

	Page
10-1. Cross-Section View of the 5-HLW/DOE SNF-Long Waste Package (Viability Assessment Design) with Six DFAs	10-6
10-2. Cross-Section View of the Degraded Configuration of the Waste Package with an Intact Ident-69 Container	10-9
10-3. TRIGA Waste Package and DOE Spent Nuclear Fuel Canister Dimensions	10-22
10-4. Cross-Section of the DOE Spent Nuclear Fuel Canister (Basket Intact, Cladding Degraded)	10-23
10-5. Cross-Section of the DOE Spent Nuclear Fuel Canister (Fuel Partially Fractured) ..	10-24
10-6. Cross-Section of the DOE Spent Nuclear Fuel Canister (Stainless Steel Tubes Degraded)	10-25
10-7. Cross-Section of the DOE Spent Nuclear Fuel Canister with Advanced Neutron Absorber Matrix between the Rods	10-25
10-8. Cross-Section of the DOE Spent Nuclear Fuel Canister (Fuel Degraded).....	10-26
10-9. Cross-Section View of the 5-DHLW/DOE Spent Nuclear Fuel-Long Waste Package.....	10-39
10-10. Cross-Section View of the Configuration with Degraded Guide Plates and Intact Spent Nuclear Fuel	10-40
10-11. Partially Degraded Fuel Cluster in the Waste Package	10-41
10-12. Cross-Section View of the Waste Package Showing the Contents of the DOE Spent Nuclear Fuel Canister for the Intact-Mode Analysis	10-53
10-13. Different Arrangement of Fuel Pins Inside 4-in-diameter Pipes.....	10-54
10-14. Waste Package Showing a Partially Degraded, More Compact Arrangement of Pipes Inside the DOE Spent Nuclear Fuel Canister	10-55
10-15. Hexagonal Close-Packed Arrangement of the Pipes.....	10-56
10-16. Cross-Section View of the Degraded Waste Package Configuration with Degraded Fuel Mixture in 4-in-Diameter Pipes	10-58
10-17. Cross-Section View of the Waste Package Showing the Contents of the DOE Spent Nuclear Fuel Canister for the Intact-Mode Analysis	10-73
10-18. Intact Assembly Surrounded by Degraded Contents of the DOE Spent Nuclear Fuel Canister in an Intact Waste Package	10-75
10-19. Different Arrangements of Fuel Pins Inside DOE Spent Nuclear Fuel Canister	10-77
10-20. Cross-Section View of the Degraded Configuration with Intact Fuel Pins Dispersed within the DOE Canister Shell	10-77
10-21. Cross-Section of the MCO Loaded with 54 Mark IV Fuel Elements in the Intact Basket	10-92
10-22. Cross-Section of the MCO Loaded with 48 Mark IA Fuel Elements in the Intact Basket	10-93
10-23. Fuel Elements Collapsed at the Bottom of the MCO	10-95
10-24. Center Post Snapped at the Bottom of the MCO.....	10-96
10-25. Intact Fuel Elements in a Degraded Basket.....	10-96
10-26. MCO Combined	10-98
10-27. Cross-Section View of the 5-DHLW/DOE Waste Package in an As-Loaded (Intact) Configuration.....	10-110

FIGURES (Continued)

	Page
10-28. Cross-Section View of an Infinitely Long Mixture of Uranium and Water, Reflected with Water.....	10-111
10-29. Cross-Section View of Degraded Fuel in an Intact Waste Package.....	10-112
10-30. Cross-Section View of the 5-DHLW/DOE Waste Package Intact Configuration ...	10-123
10-31. Configuration with Fissile Material in Solution in the Lower Half of the Coolant Channels and Voids of the Fuel Element	10-125
10-32. Configuration with the Fuel Elements Broken into Six Pieces.....	10-126
10-33. Configuration with Graphite Block Broken into Rubble and Fuel Compacts Axially Aligned Forming “Fuel Rods” (level arrangement).....	10-127
10-34. Configuration with Graphite Block Broken into Rubble and Fuel Compacts Axially Aligned Forming “Fuel Rods” (mound arrangement).....	10-127

TABLES

	Page
ES-1. The DOE Spent Nuclear Fuel Groups and Their Representative Fuel Types.....	vii
1-1. The DOE Spent Nuclear Fuel Groups and Their Representative Fuel Types.....	1-2
2-1. 5-DHLW/DOE SNF-Long Waste Package Dimensions and Material Specifications (Viability Assessment Design)	2-1
2-2. 5-DHLW/DOE SNF-Long Waste Package Dimensions and Material Specifications (Licence Application Design).....	2-3
2-3. 2-MCO/2-DHLW Waste Package Dimensions and Material Specifications.....	2-6
2-4. Geometry and Material Specifications for DHLW Glass Pour Canisters	2-7
3-1. Uranium and Plutonium Content of a Fresh DFA.....	3-9
3-2. TRIGA-SS FLIP Dimensions and Fuel Loading	3-14
3-3. Beginning-of-Life Characteristics for Four TRIGA Spent Nuclear Fuel Rod Types	3-17
3-4. Nominal Compositions and Densities of TRIGA UZrH Fuels	3-17
3-5. TRIGA Spent Nuclear Fuel Type Quantities	3-17
3-6. TRIGA SNF-Element Lengths.....	3-18
3-7. Geometry and Material Specifications for the Shippingport C2 S2 Assembly.....	3-21
3-8. Isotopic Composition of the Uranium	3-24
3-10. As-Built Characteristics of Seed Fuel Rods	3-27
3-11. Further As-Built Characteristics of Fuel Rods in the Seed Region.....	3-27
3-12. Average As-Built Cladding Dimensions for all Core Regions	3-28
3-13. Plenum Spring Dimensions for All Core Regions	3-28
3-14. Estimated Masses of Unirradiated Fuel Rod Components for All Core Regions	3-28
3-15. Average As-Built Fissile Loading of Assemblies from All Core Regions	3-29
3-16. Composition of the Seed Assembly with Maximum Fissile Loading.....	3-29
3-17. N-Reactor Fresh Fuel Elements Description.....	3-32
3-18. Calculated Cladding Thickness for Mark IA and Mark IV Fuel Elements.....	3-34
3-19. Values Used for the MD Ingots Composition	3-35
3-20. Physical Characteristics of FSVR Fuel Elements	3-35
3-21. FSVR Fuel Particle Characteristics (all dimensions are in μm).....	3-40
3-22. FSVR Fuel Compact Composition Used.....	3-41
3-23. Heat Output History of a Hanford 4.5-m- (15-ft-) Long DHLW Glass Canister.....	3-43
3-24. Heat Output History of an SRS 3.0-m- (10-ft-) Long DHLW Glass Canister	3-44
3-25. FFTF Spent Nuclear Fuel Assembly Heat Output	3-45
3-26. TRIGA-AI/SS Standard Assembly Heat Output as a Function of Decay Time and Burnup (Low Burnups)	3-46
3-27. TRIGA-SS FLIP Heat Output as a Function of Decay Time and Burnup (High Burnups)	3-46
3-28. Heat Output of the Shippingport PWR Spent Nuclear Fuel and the Waste Package.....	3-47
3-29. Heat Output History of the Enrico Fermi Spent Nuclear Fuel and the Waste Package.....	3-48

TABLES (Continued)

	Page
3-30. Heat Output of the Shippingport LWBR Spent Nuclear Fuel and the Waste Package.....	3-49
3-31. Axial Peaking Factors Estimated from Peak and Average Burnups.....	3-50
3-32. Upper Bound of the 2-MCO/2-DHLW Waste Package Surface Temperature.....	3-51
3-33. 2-MCO/2-DHLW Waste Package Heat Output History.....	3-52
3-34. Maximum Heat Output History of the FSVR Waste Package.....	3-53
3-35. FSVR Waste Package Boundary Conditions.....	3-54
3-36. Gamma and Neutron Sources for a 3-m- (10-ft-) Long Canister Loaded with SRS DHLW Glass at Day One after Pouring.....	3-56
3-37. Gamma Sources for a Hanford 4.5-m- (15-ft-) Long DHLW Glass Canister at One Day Decay Time.....	3-57
3-38. Neutron Sources for a Hanford DHLW Glass Canister at One Day Decay Time.....	3-57
3-39. Gamma and Neutron Sources for a FFTF Type 4.1 (Outer) Assembly at 150 MWd/kg Burnup (decay of 5 years).....	3-58
3-40. Total Gamma Source for the Maximum Burnup TRIGA-SS FLIP Element.....	3-59
3-41. Neutron Source at 20-Year Decay Time for the TRIGA-SS FLIP SNF Element.....	3-59
3-42. Gamma and Neutron Sources of the Shippingport C2 S1 Fuel Assembly at Year 2005.....	3-60
3-43. Gamma Sources for a Typical Fermi Spent Nuclear Fuel Assembly at 9,404-Day Cooling Time.....	3-61
3-44. Gamma Source Terms of a Shippingport LWBR Spent Nuclear Fuel Seed Assembly at Year 2005.....	3-62
3-45. Maximum Gamma Source Term per MCO.....	3-63
3-46. Gamma and Neutron Source Terms per Kilogram of Melt and Dilute Ingots.....	3-64
3-47. Gamma and Neutron Sources per FSVR Fuel Element.....	3-65
3-48. Chemical Composition of ASTM B 575 (Alloy 22) (UNS N06022).....	3-65
3-49. Chemical Composition of ASTM A 516 Grade 70 Carbon Steel (UNS K02700).....	3-66
3-50. Chemical Composition of Stainless Steel Type 304.....	3-66
3-51. Chemical Composition of Stainless Steel Type 304L (UNS S30403).....	3-66
3-52. Chemical Composition of SS Type 316L (UNS S31603).....	3-67
3-53. Chemical Composition of Zircaloy-2 (UNS R60802).....	3-67
3-54. Chemical Composition of Zircaloy-4 (UNS R60804).....	3-67
3-55. Composition of the Advanced Neutron Absorber Matrix.....	3-68
3-56. Chemical Composition of SRS DHLW Glass.....	3-68
4-1. Summary of Load Combinations for Normal and Hypothetical Accident Conditions for the Waste Package at the Repository on the Surface and to the Emplaced Condition.....	4-2
4-2. Summary of Load Combinations for Normal and Hypothetical Accident Conditions for the Waste Package at the Repository in the Emplaced Postclosure Condition on Pallet.....	4-3
6-1. Containment Structure Allowable Stress-Limit Criteria.....	6-2

TABLES (Continued)

		Page
7-1.	5-DHLW/DOE SNF-Long Waste Package FEA Stress Results	7-2
7-2.	5-DHLW/DOE SNF-Short Waste Package FEA Stress Results	7-5
7-3.	True Stress of Alloy 22 and Stainless Steel Type 316NG	7-19
7-4.	Maximum Stress Intensities	7-20
7-5.	True Stress of Alloy 22 and Stainless Steel Type 316NG	7-21
7-6.	Maximum Stress Intensities Comparison	7-22
8-1.	Physical Locations of Nodes of Interest	8-3
8-2.	Peak Temperatures and Time of Occurrence for Each Case	8-4
8-3.	Peak Temperature Histories of Fuel Cladding and Glass	8-7
8-4.	Time and Location of Peak Temperature	8-7
8-5.	Physical Locations of Nodes of Interest	8-9
8-6.	Peak Temperatures and Time of Occurrence for Each DOE Spent Nuclear Fuel Canister Fill Gas	8-10
8-7.	Physical Locations of Nodes of Interest	8-14
8-8.	Enrico Fermi Peak Fuel Temperatures and Time of Occurrence	8-14
8-9.	Peak Temperature versus Time for Various Components	8-17
8-10.	Peak Temperatures and Time of Occurrence for Each DOE Spent Nuclear Fuel Canister Fill Gas: Configuration 1	8-22
8-11.	Peak Temperatures and Time of Occurrence for Each DOE Spent Nuclear Fuel Canister Fill Gas: Configuration 2	8-22
9-1.	Total Radial Dose Rates Averaged over a Height of 60 cm	9-4
9-2.	Dose Rates Averaged over Segment d	9-5
9-3.	Radial Gamma Dose Rates Averaged over a Height of 60 cm	9-5
9-4.	Dose Rates in rem/h Averaged over Segment d	9-5
9-5.	Gamma Dose Rates Averaged over Waste Package Outer Radial Surface	9-8
9-6.	Gamma Dose Rates Averaged over Waste Package Axial Surfaces	9-8
9-7.	Dose Rates on Waste Package Outer Radial Surface	9-10
9-8.	Dose Rates on Waste Package Axial Surfaces	9-11
9-9.	Radial Dose Rates Averaged over Waste Package Outer-Radial Surface	9-14
9-10.	Axial Dose Rates Averaged over a 30-cm Radius Surface	9-14
9-11.	Axial Dose Rates Averaged over the Circular Segment Outside the 30-cm Radius	9-14
9-12.	Dose Rates on the Waste Package Outer Radial Surface	9-16
9-13.	Dose Rates on the Waste Package Axial Surfaces	9-17
9-14.	Dose Rates on Waste Package Outer Radial Surface	9-20
9-15.	Dose Rates on Segments of Waste Package Axial Surfaces	9-20
9-16.	Dose Rates Averaged over Axial and Radial Segments of the Waste Package Outer-Radial and Axial Surfaces	9-23
9-17.	Dose Rates Averaged Over Angular Segments of the Waste Package Outer- Radial Surface	9-24
9-18.	Dose Rates Averaged over Axial and Radial Segments of the Waste Package Outer-Radial and Axial Surfaces	9-27

TABLES (Continued)

	Page
9-19. Dose Rates Averaged Over Angular Segments of the Waste Package Outer-Radial Surface	9-28
10-1. Critical Benchmarks Selected for Validation of the Criticality Model for the Limiting Cases of FFTF Spent Nuclear Fuel Waste Package	10-14
10-2. Summary of Geochemistry and Criticality Analyses for Internal Configurations (phase I and II) of the Waste Package Containing FFTF Spent Nuclear Fuel	10-17
10-3. Materials and Thicknesses for TRIGA Spent Nuclear Fuel Waste Package.....	10-19
10-4. Critical Benchmarks Selected for Validation of the Criticality Model for TRIGA Spent Nuclear Fuel	10-30
10-5. Lower Bound Tolerance Limits for Benchmark Subsets Representative for the Configurations of the Waste Package Containing TRIGA Spent Nuclear Fuel.....	10-33
10-6. Summary of Geochemistry and Criticality Analyses for Internal Configurations (Phase I and II) of the Waste Package Containing TRIGA Spent Nuclear Fuel.....	10-35
10-7. Materials and Thicknesses.....	10-37
10-8. Critical Benchmarks Selected for Validation of the Criticality Model for Shippingport PWR Spent Nuclear Fuel.....	10-45
10-9. Summary of Geochemistry and Criticality Analyses for Internal Configurations (Phase I and II) of the Waste Package Containing Shippingport PWR Spent Nuclear Fuel	10-48
10-10. Materials and Thicknesses.....	10-51
10-11. Critical Benchmarks Selected for Validation of the Criticality Model for Enrico Fermi Spent Nuclear Fuel.....	10-64
10-12. Lower-Bound Tolerance Limits for Benchmark Subsets Representative for the Configurations of the Waste Package Containing Enrico Fermi Spent Nuclear Fuel.....	10-67
10-13. Summary of Geochemistry and Criticality Analyses for Internal Configurations (Phase I and II) of the Waste Package Containing Enrico Fermi Spent Nuclear Fuel.....	10-69
10-14. Materials and Thicknesses.....	10-72
10-15. Critical Benchmarks Selected for Validation of the Criticality Model for Shippingport LWBR Spent Nuclear Fuel.....	10-83
10-16. Lower Bound Tolerance Limits for Benchmark Subsets Representative for the Configurations of the Waste Package Containing Shippingport LWBR Spent Nuclear Fuel	10-86
10-17. Summary of Geochemistry and Criticality Analyses for Internal Configurations (Phase I and II) of the Waste Package Containing Shippingport LWBR Spent Nuclear Fuel	10-88
10-18. Materials and Thicknesses.....	10-90
10-19. Critical Benchmarks Selected for Validation of the Criticality Model for N-Reactor Spent Nuclear Fuel.....	10-101
10-20. Lower Bound Tolerance Limits for Benchmark Subsets Representative for the Configurations of the Waste Package Containing N-Reactor Spent Nuclear Fuel ..	10-103

TABLES (Continued)

	Page
10-21. Summary of Geochemistry and Criticality Analyses for Internal Configurations (Phase I and II) of the Waste Package Containing N-Reactor Spent Nuclear Fuel .	10-105
10-22. Materials and Thicknesses.....	10-108
10-23. Critical Benchmarks Selected for Validation of the Criticality Model for Melt and Dilute Spent Nuclear Fuel	10-116
10-24. Summary of Geochemistry and Criticality Analyses for Internal Configurations (Phase I and II) of the Waste Package Containing Melt and Dilute LWBR Spent Nuclear Fuel	10-119
10-25. Materials and Thicknesses.....	10-121
10-26. Critical Benchmarks Selected for Validation of the Criticality Model for FSVR Spent Nuclear Fuel	10-132
10-27. Lower Bound Tolerance Limits for Benchmark Subsets Representative for the Configurations of the Waste Package Containing FSVR Spent Nuclear Fuel.....	10-134
10-28. Summary of Geochemistry and Criticality Analyses for Internal Configurations (Phase I and II) of the Waste Package Containing Shippingport LWBR Spent Nuclear Fuel	10-136

INTENTIONALLY LEFT BLANK

ACRONYMS AND ABBREVIATIONS

ACPR	Annular Core Pulsed Reactor
AENCF	average energy of neutron causing fission
ANSI	American National Standards Institute
ASME	American Society of Mechanical Engineers
ASTM	American Society for Testing and Materials
BOL	beginning of life
BPVC	Boiler and Pressure Vessel Code
DBE	design basis event
DFA	driver fuel assembly
DFTL	distribution free tolerance limit
DHLW	Defense High-Level Waste
DOE	Department of Energy
DWPF	Defense Waste Processing Facility
EDA	Enhanced Design Alternative
EOL	end of life
EM	Environmental Management
EPA	U.S. Environmental Protection Agency
FEA	finite element analysis
FFTF	Fast Flux Test Facility
FLIP	Fuel Life Improvement Program
FSVR	Fort St. Vrain
FSVR	Fort St. Vrain Reactor
HLW	high-level waste
HEU	highly-enriched uranium
ID	inner diameter
INEEL	Idaho Nuclear Engineering and Environmental Laboratory
IP	internal to the package
LSTC	Livermore Software Technology Corporation
LUTB	Lower Uniform Tolerance Band
LWBR	Light Water Breeder Reactor
MOX	mixed-oxide
MT	metric tons
MW	megawatt
MTHM	metric tons of heavy metal
MCO	multicanister overpacks
MD	melt and dilute
NDTL	normal distribution tolerance limit

ACRONYMS AND ABBREVIATIONS (Continued)

NRC	U.S. Nuclear Regulatory Commission
NSNFP	National Spent Nuclear Fuel Program
NSNFPDB	National Spent Nuclear Fuel Program
OCRWM	Office of Civilian Radioactive Waste Management
OD	outer diameter
OIC	other internal components
PPF	power peaking factor
PWR	pressurized water reactor
ROA	range of applicability
ROP	range of parameters
SDD	System Description Document
SNF	spent nuclear fuel
SRS	Savannah River Site
SS	stainless steel
UNS	Universal Numbering System
TMI	Three Mile Island
TRIGA	Test, Research, Isotopes, General Atomics
TSPA	total system performance assessment
TSPA-LA	Total System Performance Assessment for the License Application
TSPA-SR	Total System Performance Assessment for the Site Recommendation
TSPA-VA	Total System Performance Assessment for the Viability Assessment
YMP	Yucca Mountain Project

1 INTRODUCTION

1.1 PURPOSE

There are more than 250 forms of U.S. Department of Energy (DOE)-owned spent nuclear fuel (SNF). Due to the variety of the spent nuclear fuel, the National Spent Nuclear Fuel Program (NSNFP) has designated nine representative fuel groups for disposal criticality analyses based on fuel matrix, primary fissile isotope, and enrichment. For each fuel group, a fuel type that represents the characteristics of all fuels in that group has been selected for detailed analysis. The DOE SNF will be loaded into the DOE standardized SNF canisters (or multiccanister overpacks [MCOs] for N-Reactor SNF), which will be codisposed with five (two for N-Reactor SNF) defense high-level waste glass (DHLW) canisters in a waste package. The results of the analyses performed will be used to develop waste acceptance criteria. The items that are important to criticality control are identified based on the analysis needs and result sensitivities. The analyses have been performed according to *Disposal Criticality Analysis Methodology Topical Report* (YMP 2003). The methodology includes analyzing the geochemical and environmental processes that can breach the waste package and degrade the waste forms and other internal components, as well as the intact and degraded component criticality analyses. This report also provides the structural, thermal, and shielding analyses of the waste package to ensure that the repository waste acceptance criteria have been met.

The purpose of this report is to summarize eight Phase I and II technical reports that cover the evaluation of codisposal viability of DOE SNF. The evaluations consisted of structural, thermal, shielding, geochemistry, and intact and degraded component criticality analyses. All the analyses performed met the design criteria as defined in *DOE and Commercial Waste Package System Description Document* (BSC 2003a).

Technical Work Plan for: Department of Energy Spent Nuclear Fuel Criticality and TSPA Work Packages (BSC 2003b) concluded that the development of this report is subject to *Quality Assurance Requirements and Description* (DOE 2003) controls. There are no limitations on the use of this report.

1.2 SCOPE

This technical report summarizes the structural, thermal, shielding, geochemistry, intact and degraded component criticality analyses that were performed for the evaluation of codisposal viability for eight fuel types, which were designated as representative for eight DOE SNF groups (Table 1-1). The selection of the representative fuel type for each group is explained in Section 3.1.

Table 1-1. The DOE Spent Nuclear Fuel Groups and Their Representative Fuel Types

DOE SNF Group	Representative Fuel Type
Mixed Oxide (MOX)	Fast Flux Test Facility (FFTF) Driver Assembly
Uranium-Zirconium Hydride (UZrH)	Training, Research, Isotope General Atomic (TRIGA) – Fuel Life Improvement Program (FLIP) Rod
U-Mo and U-Zr Alloys	Enrico Fermi Fuel Pin
Highly Enriched Uranium (HEU) Oxide	Shippingport - Pressurized Water Reactor (PWR) Assembly
²³³ U/Th Oxide	Shippingport - Light Water Breeder Reactor (LWBR) Seed Assembly
U Metal	N-Reactor Assembly
HEU-Al	Melt and Dilute (MD) Form
U/Th Carbide	Fort Saint Vrain Reactor (FSVR) Assembly

2 DESIGN INFORMATION

This section describes the waste package design and internal components or identifies the basis of major parameters.

2.1 WASTE PACKAGE

The waste package for FFTF, TRIGA, Shippingport PWR, Enrico Fermi, Shippingport LWBR, Melt and Dilute (MD) and FSVR DOE SNF contains five DHLW glass canisters surrounding a DOE 18-in-outer diameter standardized canister loaded with DOE SNF. There are two versions for this type of waste package design, the Viability Assessment design; used for the codisposal evaluations of FFTF, TRIGA, Shippingport PWR, and Enrico Fermi SNF), and the License Application design (used for the codisposal evaluations of Shippingport LWBR, MD and FSVR DOE SNF).

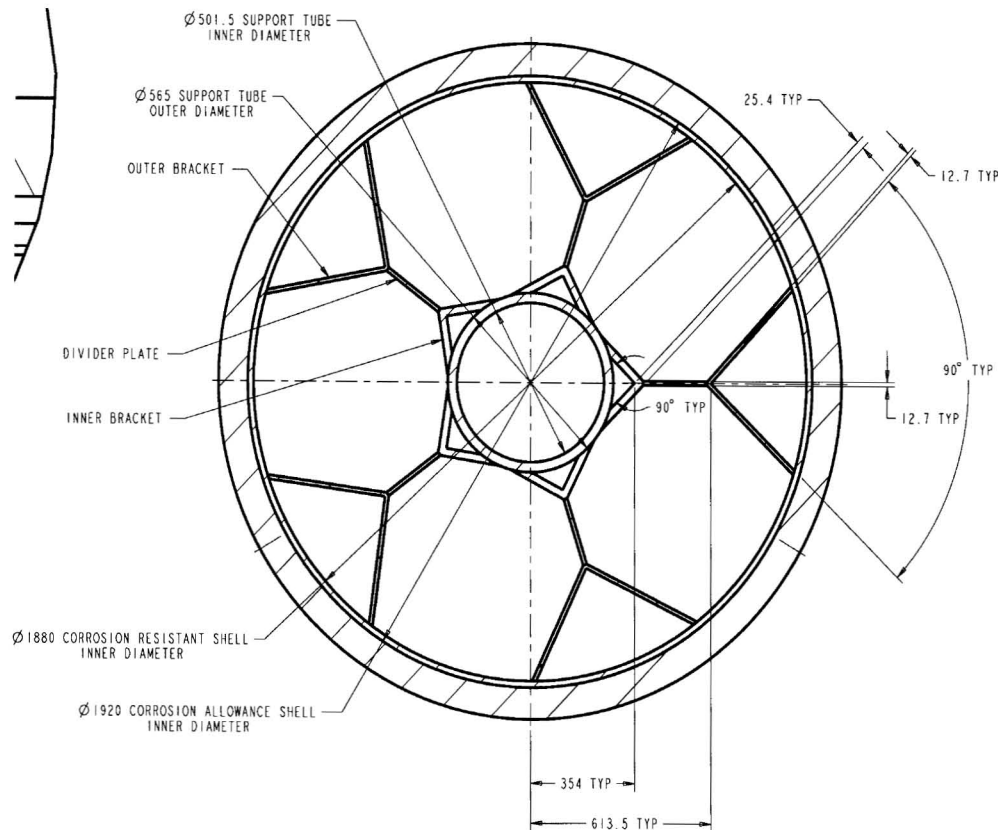
The inner barrier of the 5-DHLW/DOE SNF-long waste package Viability Assessment design (DOE 1998a) is 20.0-mm thick high-nickel alloy ASTM B 575 (Alloy 22) and serves as a corrosion-resistant material. The outer barrier is 100.0-mm thick carbon steel (ASTM A 516 Grade 70) and serves as a corrosion-allowance material (CRWMS M&O 1997a, pp. 56 and 72). The outer diameter of the waste package is 2,120.0 mm and the length of the inside cavity is 4,617.0 mm (CRWMS M&O 1998a, Attachment I), which is designed to accommodate Hanford 4.5-m- (15-ft-) long DHLW glass canisters. The lids of the inner barrier are 25.0 mm thick; those of the outer barrier, 110.0 mm thick. There is a 30.0-mm gap between the inner and outer barrier upper lids. Each end of the waste package has a 225.0-mm long skirt. Table 2-1 summarizes the dimensions and materials of the 5-DHLW/DOE SNF-long waste package.

Table 2-1. 5-DHLW/DOE SNF-Long Waste Package Dimensions and Material Specifications (Viability Assessment Design)

Component	Material	Parameter	Dimension (mm)
Outer barrier shell	Carbon Steel (ASTM A 516 Grade 70)	Thickness	100.0
		Outer diameter	2,120.0
Inner barrier shell	High-Nickel Alloy (ASTM B 575)	Thickness	20.0
		Inner length	4,617.0
Top and bottom outer barrier lids	Carbon Steel (ASTM A 516 Grade 70)	Thickness	110.0
Top and bottom inner barrier lids	High-Nickel Alloy (ASTM B 575)	Thickness	25.0
Gap between the upper inner and outer closure lids	Air	Thickness	30.0
Support tube	Carbon Steel (ASTM A 516 Grade 70)	Outer diameter	565.0
		Inner diameter (ID)	501.5
		Length	4,607.0

Source: CRWMS M&O 1998a, Attachment I

The DOE SNF canister is placed in a 31.8-mm thick carbon steel (ASTM A 516 Grade 70) support tube with a nominal outer diameter of 565.0 mm. The support tube is connected to the waste package inside wall by a web-like structure of carbon steel (ASTM A 516 Grade 70) basket plates to support five 4.5-m-long DHLW glass canisters (Figure 2-1). The support tube and the plates are 4,607.0 mm long.



Source: CRWMS M&O 1998a

Figure 2-1. Cross-Section of the 5-DHLW/DOE Spent Nuclear Fuel Waste Package (Viability Assessment Design)

The barrier materials and dimensions of the 5-DHLW/DOE SNF-short waste package Viability Assessment design (DOE 1998a) are identical to those used for the 5-DHLW/DOE SNF-long waste package, except the inside cavity, and the support tube and plates lengths, which are equal to 3,040.0 mm, and 3,030.0 mm, respectively. The 5-DHLW/DOE SNF-short waste package is designed to accommodate five Savannah River Site (SRS) 3-m-long DHLW canisters (CRWMS M&O 1998a, Attachment I).

The License Application design for 5-DHLW/DOE SNF-long waste package is described in *Repository Design Project, RDP/PA IED Typical Waste Package Components Assembly (2)* (BSC 2003c). This type of waste package will be loaded with FFTF, Shippingport PWR, Shippingport LWBR, and FSVR DOE SNF. The shell materials of the waste package are typical of those used for commercial SNF waste package. The waste package design consists of two concentric cylindrical shells. The inner shell is a 50.0-mm-thick cylinder of Stainless Steel Type 316 NG (nuclear grade, also identified as SA-240). The outer shell is composed of 25.0-mm-thick high-nickel alloy ASTM B 575 (Alloy 22) and its outer diameter is 2,030.0 mm. The length of waste package's inside cavity is 4,617.0 mm, which is designed to accommodate five 4.5-m (15-ft) Hanford DHLW glass canisters. The lid of the inner shell is 105.0-mm thick. The outer shell flat bottom lid is 25.0-mm thick and the outer shell flat closure lid is 10.0-mm thick. Table 2-2 summarizes the dimensions and materials of the waste package.

Table 2-2. 5-DHLW/DOE SNF-Long Waste Package Dimensions and Material Specifications (License Application Design)

Component	Material	Parameter	Dimension (mm)
Outer barrier shell	High-Nickel Alloy (ASTM B 575)	Thickness	25.0
		Outer diameter	2,030.0
Inner barrier shell	Stainless Steel Type 316 NG (SA-240)	Thickness	50.0
		Inner length	4,617.0
Top and bottom outer barrier lids	High-Nickel Alloy (ASTM B 575)	Thickness	25.0
Closure lid (only at the top)	High-Nickel Alloy (ASTM B 575)	Thickness	10.0
Top and bottom inner barrier lids	Stainless Steel Type 316 NG (SA-240)	Thickness	105.0
Gap between the top inner and closure lids	Air	Thickness	30.0
Gap between the top outer and closure lids	Air	Thickness	30.0
Gap between the bottom inner and outer lids	Air	Thickness	70.0
Support tube	Carbon Steel (ASTM A 516 Grade 70)	Outer diameter	565.0
		Inner diameter	501.5
		Length	4,607.0

Source: BSC 2003c

Similarly to the 5-DHLW/DOE SNF-long waste package Viability Assessment design, the DOE SNF canister is placed in a support tube connected to the inside wall of the waste package by a web-like structure of basket plates to support five 4.5-m-long DHLW glass canisters, as shown in Figure 2-2. The support tube and the plates are identical to those pertaining to the Viability Assessment design of the 5-DHLW/DOE SNF-long waste package.

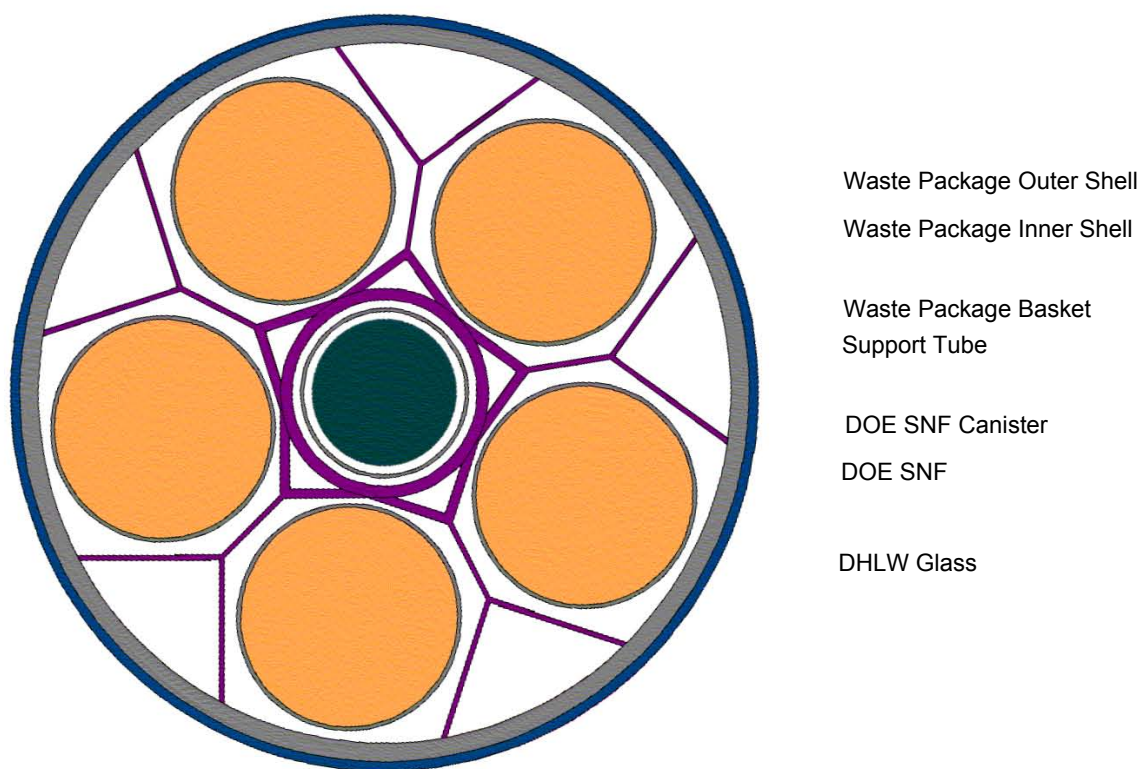


Figure 2-2. Cross-Section Representation of the 5-DHLW/DOE Waste Package in an As-Loaded Condition

The 5-DHLW/DOE SNF-short waste package License Application design is described in *Repository Design Project, RDP/PA IED Typical Waste Package Components Assembly (2)* (BSC 2003c). This type of waste package will be loaded with TRIGA, Enrico Fermi, and Melt and Dilute DOE SNF. The design is very similar to that of 5-DHLW/DOE SNF-long waste package, except the length of the inside cavity, which in this case is 3,040.0 mm, and the lid of the inner shell, which is 80.0-mm thick. Similarly to the 5-DHLW/DOE SNF-short waste package Viability Assessment design, the DOE SNF canister is placed in a support tube connected to the inside wall of the waste package by a web-like structure of basket plates to support five SRS 3-m-long DHLW glass canisters, as shown in Figure 2-2. The support tube and the plates are identical to those pertaining to the Viability Assessment design of the 5-DHLW/DOE SNF-short waste package.

The N-Reactor waste package contains two DHLW canisters and two MCOs loaded with N-Reactor DOE SNF. The main reasons for the difference with the 5-DHLW/DOE SNF waste package design are: (1) Although the MCO has the same basic shell diameter as the DHLW canisters, it also has a slightly larger diameter collar at one end, which would make for a very tight fit in the standard-diameter waste package if five canisters were used; (2) The two DOE SNF canisters are placed in opposition so that the four-canister configuration is balanced around the cylinder axis. This latter capability is important if the closure weld is implemented by rotating the waste package on a turntable. A side-by-side placement is also considered because this could occur from a misload. Such misload configurations are discussed in *Evaluation of Codisposal Viability for U-Metal (N Reactor) DOE-Owned Fuel* (CRWMS M&O 2001a, Sections 6 and 7).

The 2-MCO/2-DHLW waste package design is based on *Repository Design Project, RDP/PA IED Typical Waste Package Components Assembly (2)* (BSC 2003c). The waste package design consists of two concentric cylindrical shells that have the same thickness and material composition as the shells in 5-DHLW/DOE SNF-long waste package design. The outside diameter of the waste package is 1,734.0 mm and the length of the inside cavity is 4,617.0 mm, which is designed to accommodate two Hanford 4.5-m- (15-ft-) long DHLW glass canisters. The lid of the inner shell is 105.0 mm thick. The outer shell flat bottom lid is 25.0 mm thick and the outer shell flat closure lid is 10.0 mm thick. There are two 10.0-mm-thick carbon steel plates (made of ASTM A 516 Grade 70, and called separation plates) that divide the waste package in four quarters as shown in Figure 2-3. The two N-Reactor MCOs are placed on a 5.0-mm-thick carbon steel (ASTM A 516 Grade 70) support cylinder with a diameter of 600.0 mm topped by a 5.0-mm fuel support plate made of carbon steel. Table 2-3 summarizes the 2-MCO/2-DHLW waste package dimensions and materials.

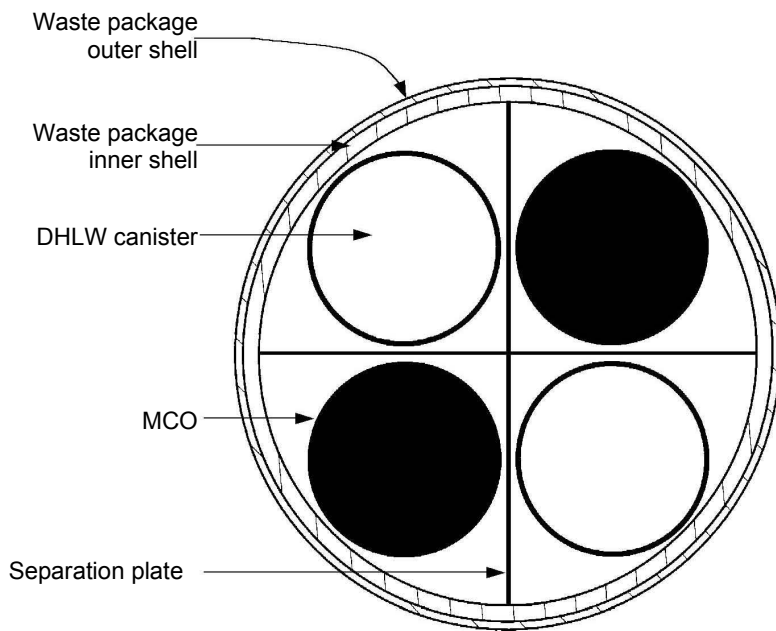


Figure 2-3. Cross-Section View of the 2-MCO/2-DHLW Waste Package in an As-Loaded Condition

Table 2-3. 2-MCO/2-DHLW Waste Package Dimensions and Material Specifications

Component	Material	Parameter	Dimension (mm)
Outer shell	High-Nickel Alloy (ASTM B 575)	Thickness	25.0
		Outer diameter	1734.0
Inner shell	Stainless Steel Type 316 NG (SA-240)	Thickness	50.0
		Inner cavity length	4617.0
Inner shell lid	Stainless Steel Type 316 NG (SA-240)	Thickness	105.0
Extended outer shell lid	High-Nickel Alloy (ASTM B 575)	Thickness	25.0
Outer shell flat closure lid	High-Nickel Alloy (ASTM B 575)	Thickness	10.0
Fuel support cylinder	Carbon Steel (ASTM A 516 Grade 70)	Outer diameter	600.0
		Inner diameter	590.0
		Length	270.0
Separation plates	Carbon Steel (ASTM A 516 Grade 70)	Thickness	10.0
Fuel support plate	Carbon Steel (ASTM A 516 Grade 70)	Thickness	5.0

Source: BSC 2003c

2.2 DHLW GLASS POUR CANISTERS

The SRS Defense Waste Processing Facility (DWPF) high-level radioactive waste canister, as shown in Figure 2-4, is a cylindrical Stainless Steel Type 304L shell. The outer diameter of the cylindrical shell is 610.0 mm, the wall thickness is 9.525 mm, and the nominal length is 3,000.0 mm (CRWMS M&O 2000a, p. 13). The flanged head and neck of the canister are 225.6-mm high. The DHLW glass occupies approximately 85 percent of the volume of the canister. The glass mass is 1,682 kg (CRWMS M&O 2000a, p. 13) and the maximum total mass of the canister is 2,500 kg (BSC 2003a, Table 2). The nominal dimensions of the canister are used for the analyses.

There is no long SRS DHLW glass canister. Therefore, the Hanford 4.5-m- (15-ft-) long DHLW glass canister (similar to that shown in Figure 2-4) is used in the 5-DHLW/DOE SNF-long waste package. Since the composition of the Hanford DHLW glass has not yet been specified, it is assumed to be the same as the SRS DHLW glass (see Assumption 5.5.2). The Hanford DHLW glass canister is a 4,570.0-mm-long cylindrical Stainless Steel Type 304L shell with an outer diameter of 610.0 mm (24.0 in) (BSC 2003a, Table 2) and a wall thickness of 10.5 mm (Taylor 1997, pp. 1 and 2). The maximum loaded canister mass is 4,200 kg and the fill volume is 87 percent (Taylor 1997, pp. 1 and 2). The nominal dimensions of the canister were used for the analyses. The geometry and material specifications for DHLW glass canisters are given in Table 2-4.

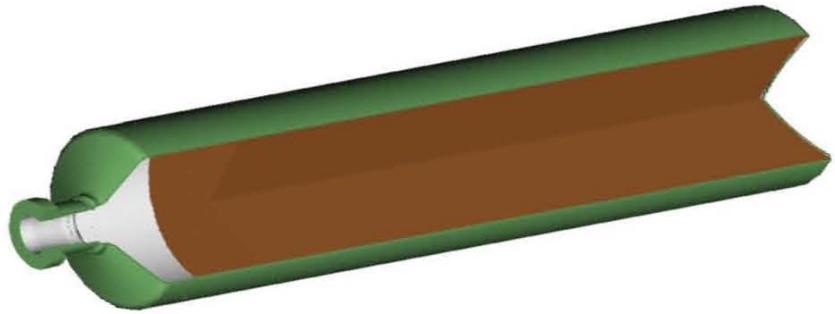


Figure 2-4. DHLW Glass Pour Canister

Table 2-4. Geometry and Material Specifications for DHLW Glass Pour Canisters

Material/Parameter	Hanford 4.5-m (15-ft) Canister	SRS 3-m (10-ft) Canister
Material	Stainless Steel Type 304L	Stainless Steel Type 304L
Outer diameter	610.0 mm ^a	610.0 mm ^c
Total mass of canister and glass	4,200 kg ^b	2,500 kg ^a
Fill volume of glass in canister	87% ^b	85% ^c
Wall thickness	10.5 mm ^b	9.525 mm ^c
Length	4,570.0 mm ^a	3,000.0 mm ^c

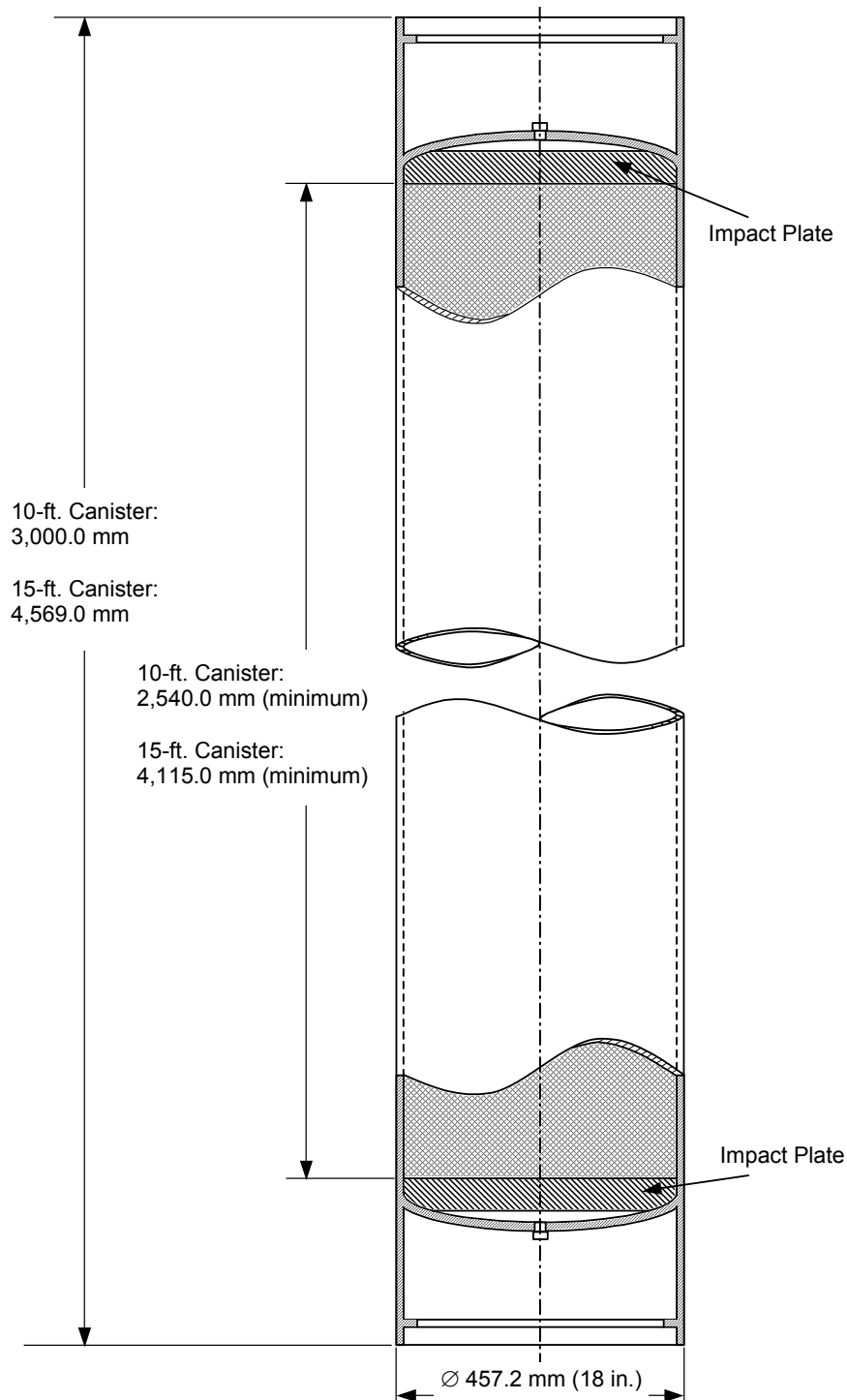
Sources: ^a BSC 2003a, Table 2

^b Taylor 1997, pp. 1 and 2

^c CRWMS M&O 2000a, p. 13

2.3 DOE STANDARDIZED SNF CANISTER

The conceptual design for the standardized DOE SNF canister is taken from *Preliminary Design Specification for Department of Energy Standardized Spent Nuclear Fuel Canisters* (DOE 1999a, pp. 5 and A-2). The canister (Figure 2-5) is a right circular cylinder of Stainless Steel Type 316L with an outer diameter of 457.2 mm (18.0 in) and a wall thickness of 9.5 mm (0.375 in). There are two types of DOE SNF canisters: long and short. The minimum internal length of the long canister is 4,115.0 mm and the nominal overall length is 4,569.0 mm (approximately 15 ft). The minimum internal length of the short canister is 2,540.0 mm and the nominal overall length is 3,000.0 mm (approximately 10 ft). There is a curved carbon steel (ASTM A 516 Grade 70) impact plate, 50.8-mm (2.0-in) thick, at the top and bottom boundaries of the canister. The maximum loaded mass is 2,721 kg for the long canister, and 2,270 kg for the short canister (DOE 1999a, Table 3.2).



Source: DOE 1999a, p. A-2

NOTE: Figure not to scale.

Figure 2-5. Plan View of the 18-in-Outer Diameter DOE Standardized Spent Nuclear Fuel Canister

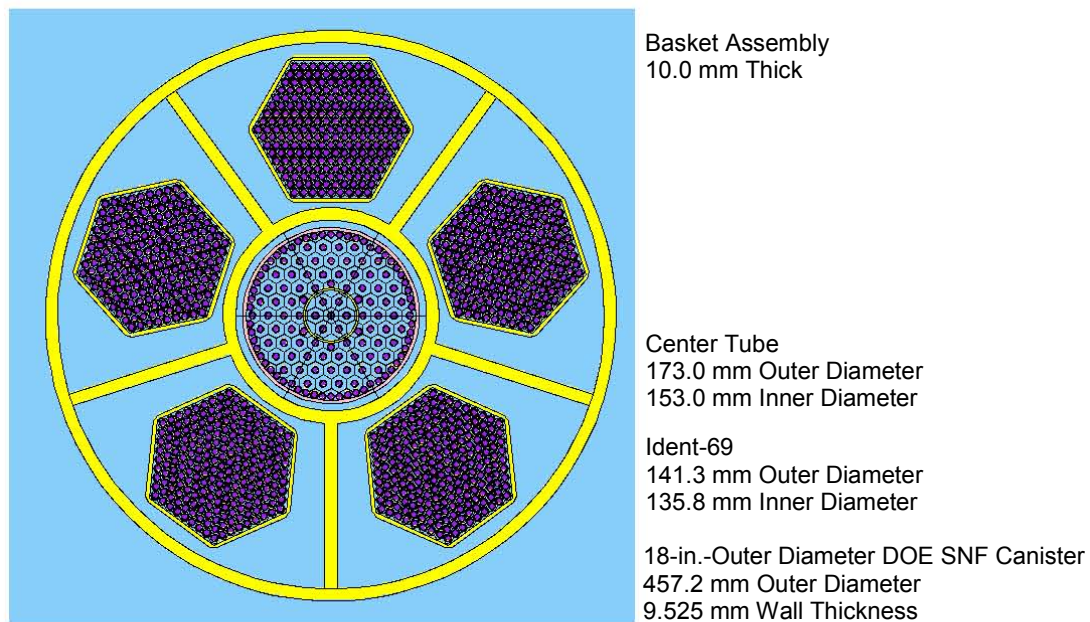
The DOE standardized SNF canisters that will be loaded with FFTF, TRIGA, Shippingport PWR, Enrico Fermi, and Shippingport LWBR fuels contain a basket, which is not a standard part of the DOE SNF canister. The basket design is modified for each specific fuel type. The basket

provides structural support, and acts as a guide for the fuel assemblies and pin containers during loading. Additionally, for the FFTF and TRIGA SNF the basket provides material for controlling criticality in the form of gadolinium added to its composition.

2.3.1 Internals of FFTF DOE SNF Canister

The source of information in this section is Section 2.1.3 of *Evaluation of Codisposal Viability for MOX (FFTF) DOE-Owned Fuel* (CRWMS M&O 1999a).

The FFTF SNF will be loaded in 15-ft-long DOE standardized SNF canisters (outer diameter of 18 in) that contain six basket locations (one center position surrounded by five outer positions). Either an Ident-69 fuel pin container or a driver fuel assembly (DFA) can be placed in the center position. All outer positions are filled with DFAs only. A cross-section view of the DOE SNF canister containing five FFTF assemblies and an Ident-69 fuel pin container is shown in Figure 2-6.



Source: CRWMS M&O 1999a, p. 9

Figure 2-6. Cross-Sectional Representation of the FFTF DOE Spent Nuclear Fuel Canister in an As-Loaded Condition

The basket consists of a cylindrical center tube and five divider plates extending radially from the center tube to the DOE SNF canister wall as shown in Figure 2-6. The center tube inner diameter is 153.0 mm and its wall thickness is 10.0 mm. The divider plates are 10.0 mm thick. The basket length is 4,095.0 mm (20.0 mm shorter than the minimum internal length), and for controlling criticality gadolinium is added to its composition.

2.3.2 Internals of TRIGA DOE SNF Canister

The source of information in this section is Section 2.1.3 of *Evaluation of Codisposal Viability for UZrH (TRIGA) DOE-Owned Fuel* (CRWMS M&O 2000b).

The TRIGA SNF will be loaded in 10-ft-long DOE standardized SNF canisters (outer diameter of 18 in). A basket for the DOE SNF canister will be constructed to hold 37 fuel rods. The basket will be welded together at the top and bottom with the bottom of the tubes welded to a steel base plate. For rods with maximum length of 774.7-mm, three such baskets will be stacked in the DOE SNF canister to provide basket locations for 111 rods per canister. For rods with maximum length of 1143.0 mm, two such baskets will be stacked in the DOE SNF canister to provide 74 rods per canister. For rods with maximum length of 1689.1 mm, one such basket will be placed in the DOE SNF canister to provide 37 rods per canister. A cross-sectional representation of an arrangement of TRIGA stainless steel (TRIGA-SS) rods in an 18-in.-outer diameter DOE standardized SNF canister is shown in Figure 2-7 and an isometric view is provided in Figure 2-8.

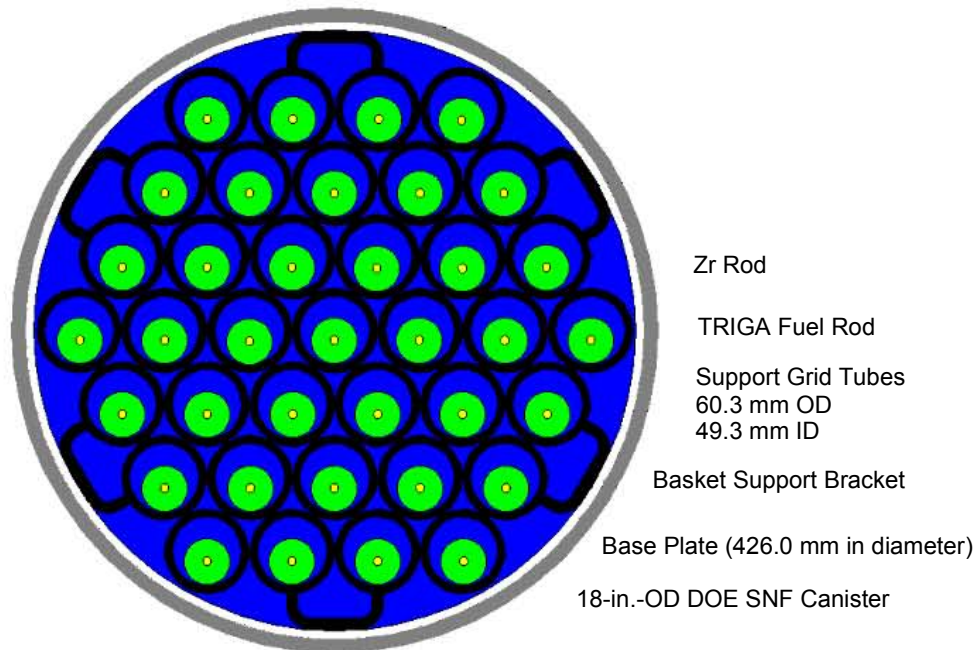


Figure 2-7. Cross-Sectional Representation of an Arrangement of TRIGA-SS Rods in a DOE Spent Nuclear Fuel Canister

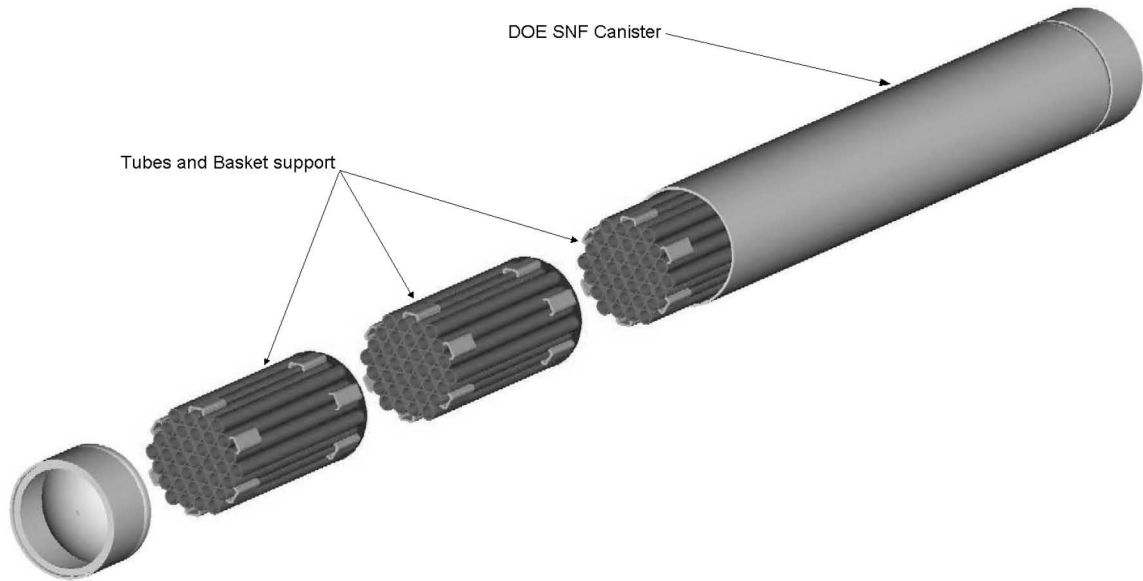


Figure 2-8. Isometric View of the TRIGA DOE Spent Nuclear Fuel Canister

A 1-mm-thick advanced neutron absorber matrix tube (Alloy-4 with 8 at % Gd) is placed inside of 12 structural tubes per basket. The options considered for the emplacement of the advanced neutron absorber matrix tubes throughout the basket are shown in Figure 2-9.

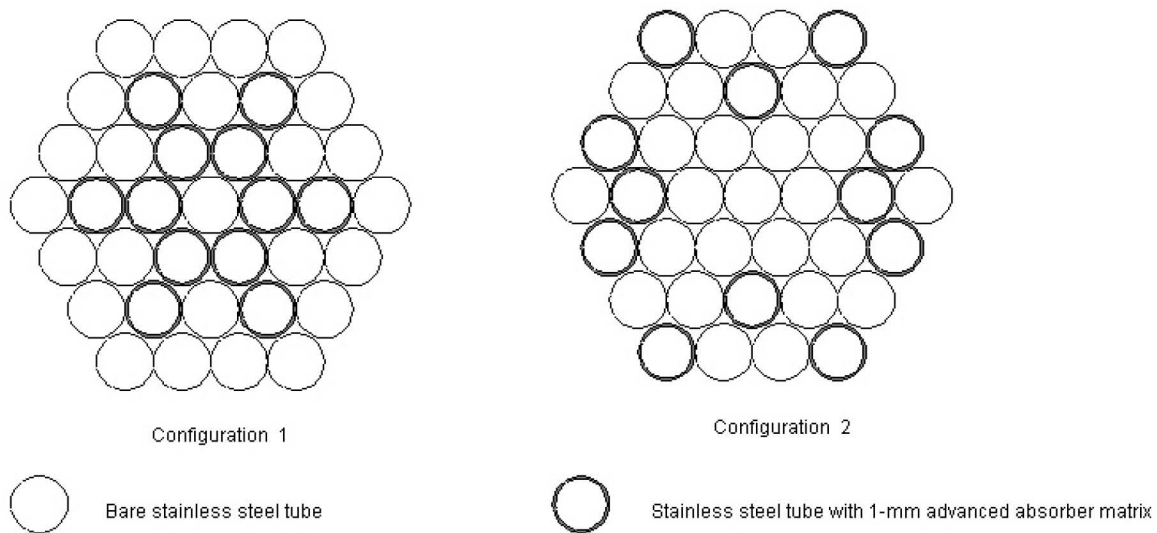


Figure 2-9. Emplacement of the Advanced Neutron Absorber Matrix Tubes in the TRIGA DOE Spent Nuclear Fuel Canister Basket

2.3.3 Internals of Shippingport PWR DOE SNF Canister

The source of information in this section is Section 2.1.3 of *Evaluation of Codisposal Viability for HEU Oxide (Shippingport PWR) DOE-Owned Fuel (CRWMS M&O 2000c)*.

The Shippingport PWR SNF will be loaded in 15-ft-long DOE standardized SNF canisters (outer diameter of 18 in). Each canister will hold a single Shippingport PWR Core 2 Seed 2 SNF assembly in a specially designed basket. Figure 2-10 is a cross-sectional representation of the DOE SNF canister containing one Shippingport PWR assembly. An isometric view of the DOE SNF canister and the Shippingport PWR basket assembly is shown in Figure 2-11. The basket consists of a 208.0-mm-square grid constructed of 9.5-mm-thick Stainless Steel Type 316L plates. The basket height is 2,681.0 mm.

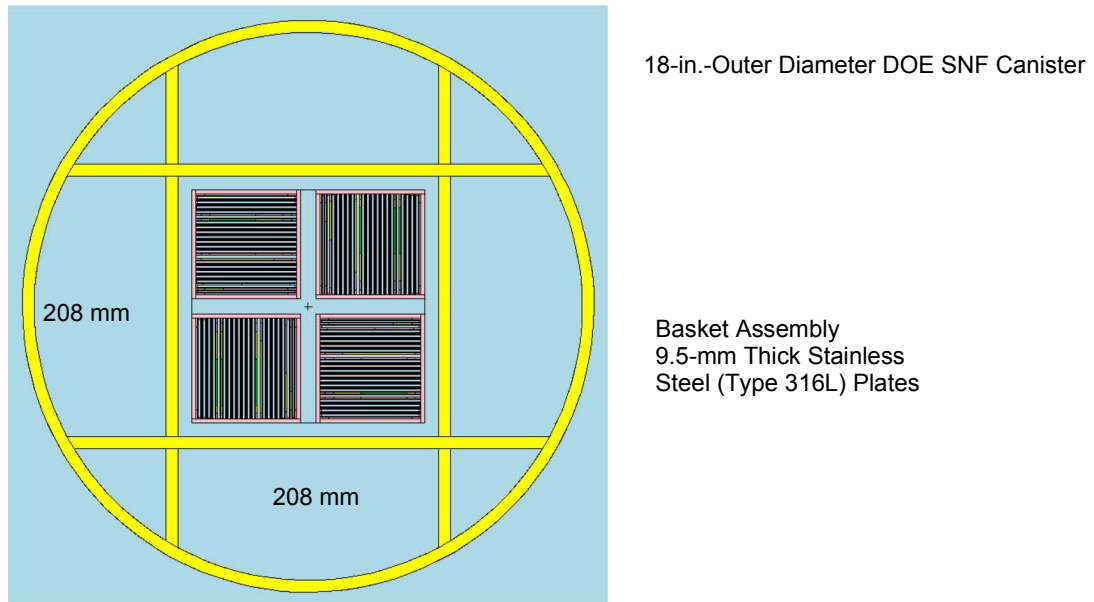


Figure 2-10. Cross-Sectional Representation of the Shippingport PWR DOE Spent Nuclear Fuel Canister in an As-Loaded Condition

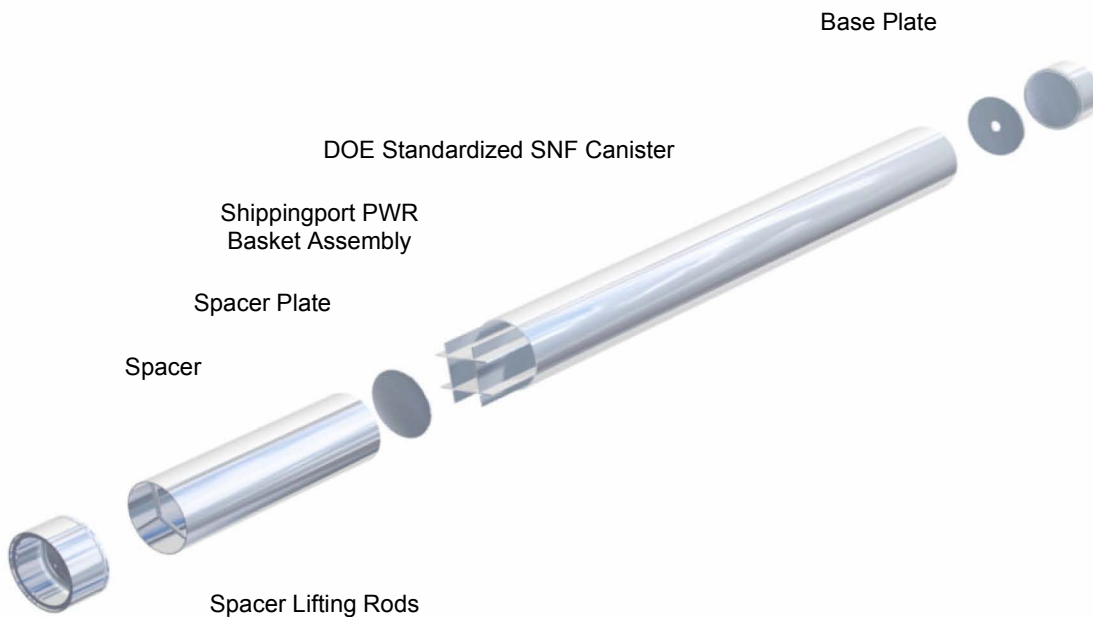
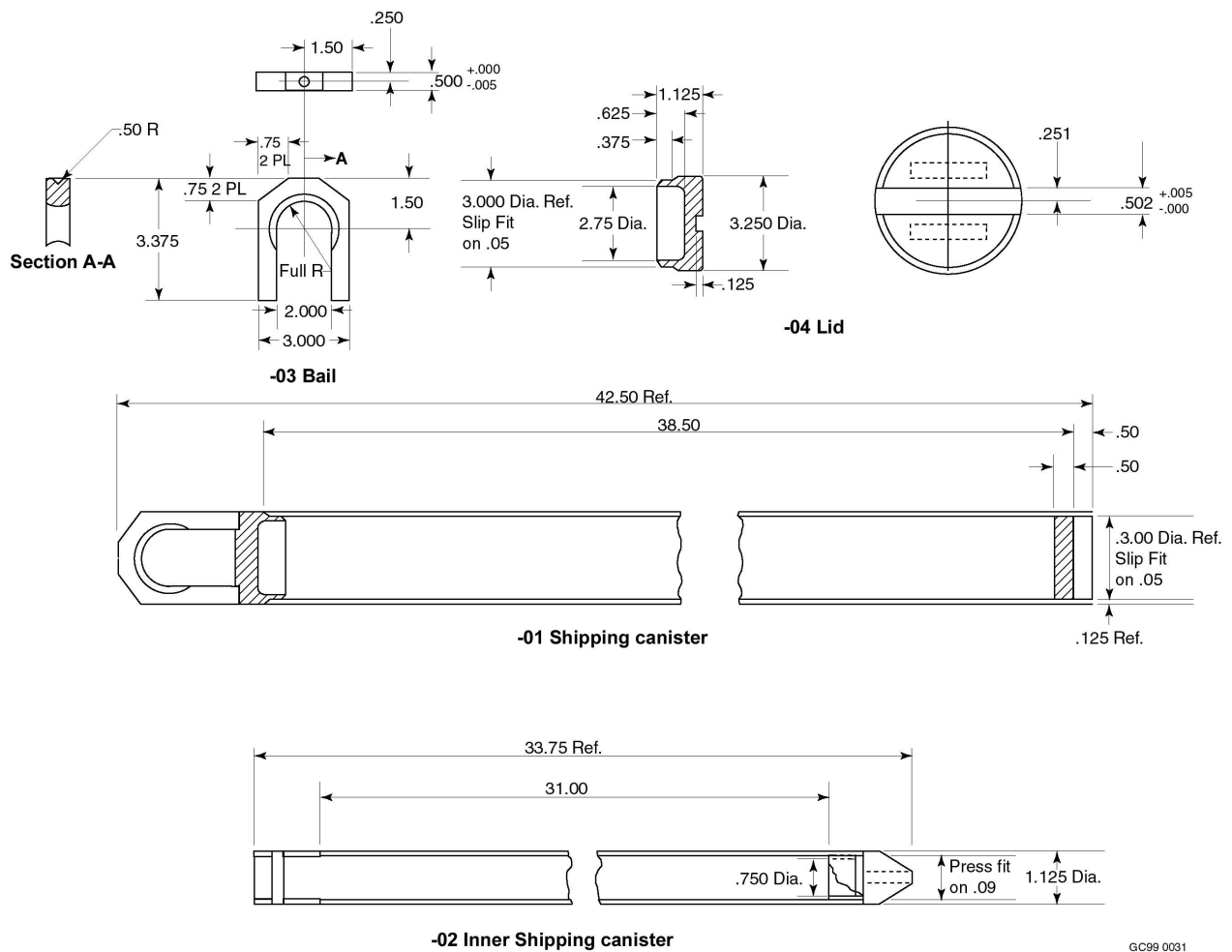


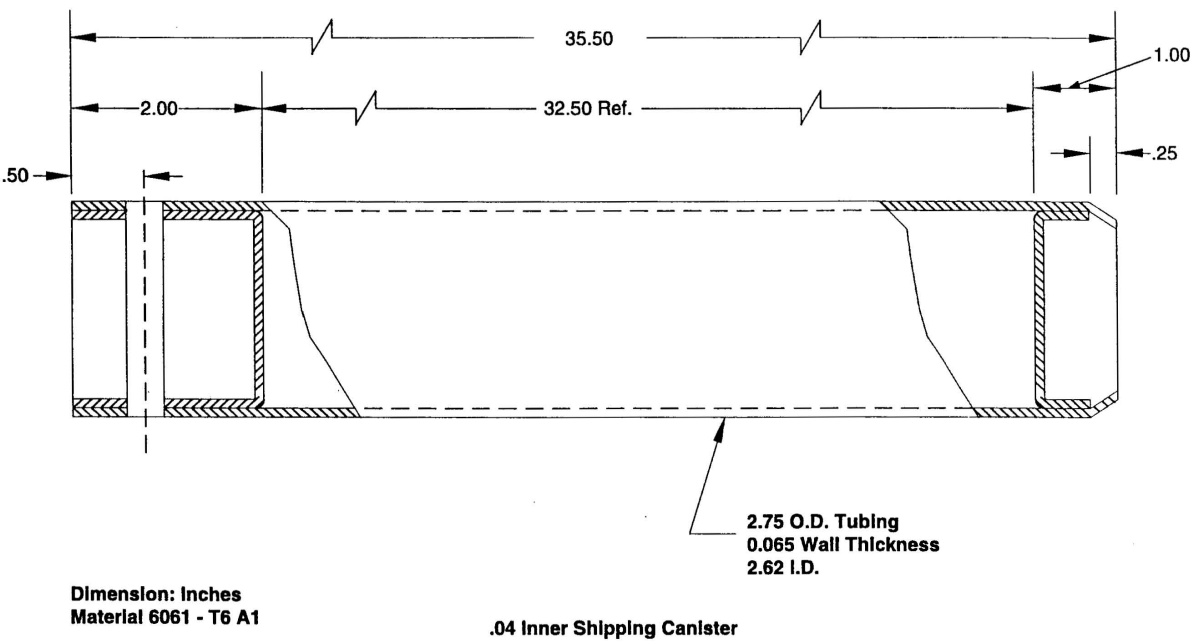
Figure 2-11. Isometric View of the Shippingport PWR DOE Spent Nuclear Fuel Canister



Source: DOE 1999b, p. 14

NOTE: Dimensions in inches.

Figure 2-12. Schematic of -01 and -02 Shipping Canisters



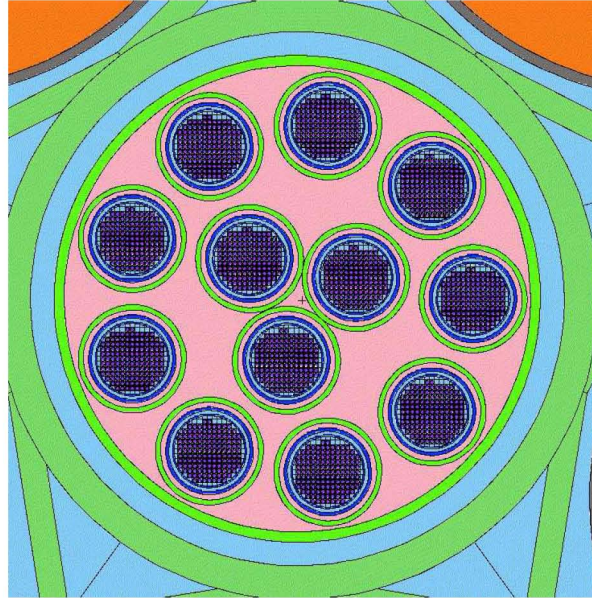
ICPP-A-14141
(6-96)

Source: DOE 1999b, p. 15
NOTE: Dimensions in inches.

Figure 2-13. Schematic of -04 Canister

18-in-outer diameter
DOE SNF Canister

4-inch-Diameter Pipe
Containing 140 Fuel
Pins



Source: CRWMS M&O 1999b

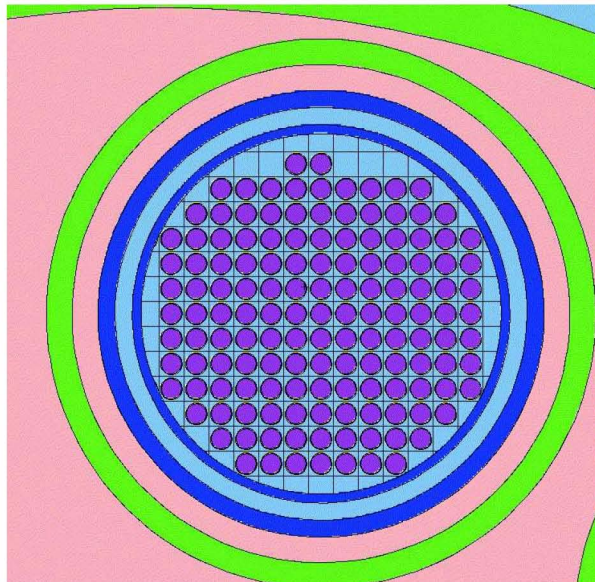
Figure 2-14. Cross-Sectional Representation of the Enrico Fermi DOE Spent Nuclear Fuel Canister in an As-Loaded Condition

A Typical 4-inch-
Diameter Pipe

-01 Canister

-04 Canister

Fuel Pins



Source: CRWMS M&O 1999b

Figure 2-15. Enrico Fermi Fuel Pins in a 4-in-Diameter Pipe

The 191 de-rodged fuel sections (26,740 clad fuel pins) were the focus of the disposal evaluation (CRWMS M&O 2000d) to support repository licensing. The design dimensions of the -01 and -04 canisters are shown in Figures 2-12 and 2-13. The bare fuel pins with the swaged, pointed ends as shown in Figure 2-15 are to be qualified for shipment. In each -04 canister, 140 pins were loose-packed without any supporting/spacing mechanism (Figure 2-14 [the grid lines in Figures 2-14 and 2-15 are part of the computer code representation used for evaluation and do

not represent any types of matrix or structured packing]). Air fill the voids inside the -04 aluminum storage canisters.

For codisposal, the Enrico Fermi SNF is to be stored inside the DOE SNF canister, as described above. Figure 2-14 is a cross-sectional representation of the initial, proposed storage configuration. As shown in this figure, the proposed arrangement is that nine 4-in-diameter steel pipes that are located near the inside wall, and three steel pipes are located in a cluster at the center of the DOE SNF canister. The 12 steel pipes are welded to a base plate to form a basket. There are also dividers welded between the pipes and a lifting rod in the basket structure. Two such baskets are stacked axially inside the DOE SNF canister. The space between all the 4-in steel pipes is filled with iron shot (CRWMS M&O 1996) to exclude water (prevent neutron moderation) and provide support for the steel pipes. The iron shot is also a mechanism for introducing the neutron absorber, such as gadolinium phosphate ($GdPO_4$), either in the iron shot or in the form of a mixture.

2.3.5 Internals of Shippingport LWBR DOE SNF Canister

The source of information in this section is Section 2.1.3 of *Evaluation of Codisposal Viability for Th/U Oxide (Shippingport LWBR) DOE-Owned Fuel* (CRWMS M&O 2000e).

The Shippingport LWBR DOE SNF will be loaded in 15-ft-long DOE standardized SNF canisters (outer diameter of 18 in). The canister holds a single Shippingport LWBR SNF seed assembly in a specially designed basket. Figure 2-16 is a cross-sectional representation of the DOE SNF canister containing one Shippingport LWBR assembly. An isometric view of the DOE SNF canister and the Shippingport LWBR basket assembly is shown in Figure 2-17. The basket consists of a 295.0 mm by 257.0 mm rectangular grid. The basket plate is Stainless Steel Type 316L with a 9.5-mm thickness. Inside the basket is placed a spacer that has the role of limiting the length of space available for the Shippingport LWBR seed assembly to 3,350 mm that is slightly greater than the maximum length of the intact assemblies, including the shipping plates (3327.4 mm). The purpose of this limitation is to avoid significant movements of the assembly within the space available, during the handling of the DOE SNF canister, with the potential of damaging the assembly and the DOE SNF canister components. The spacer consists of a 293.0 mm by 255.0 mm rectangular tube made of 9.5-mm-thick plates that has a 19.1-mm-thick plate attached at the end closer to the assembly location. The spacer plates are made of Stainless Steel Type 316L.

The void space inside the DOE SNF canister will be filled with shot consisting of a mixture of Al and $GdPO_4$. This mixture has the role of a neutron absorber intended to prevent criticality inside the waste package.

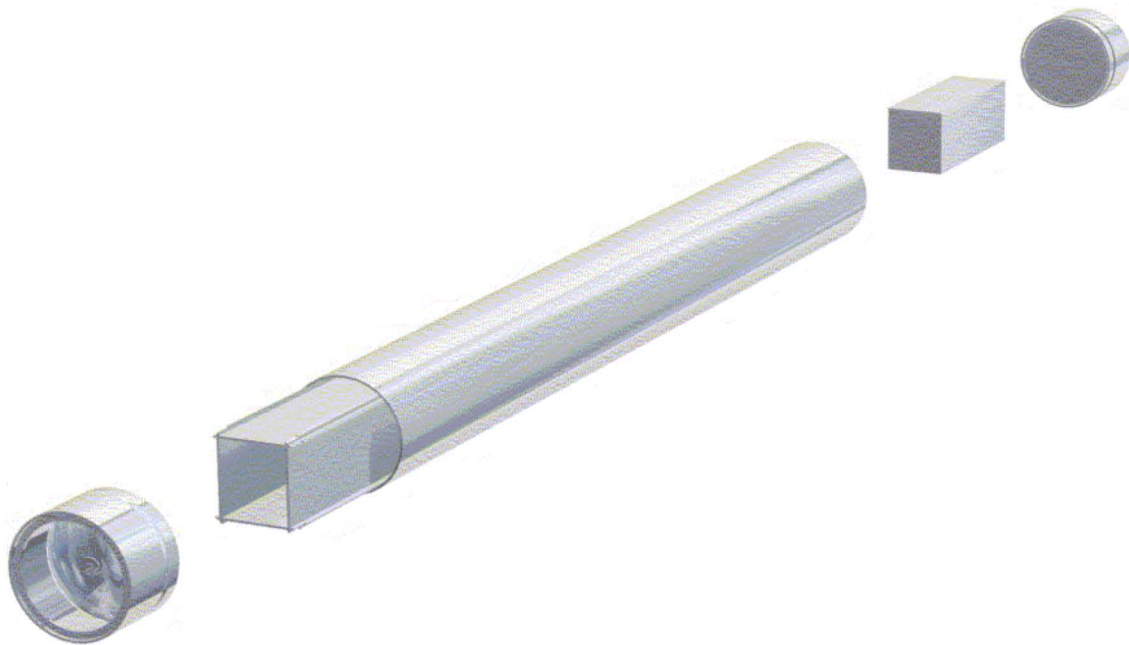
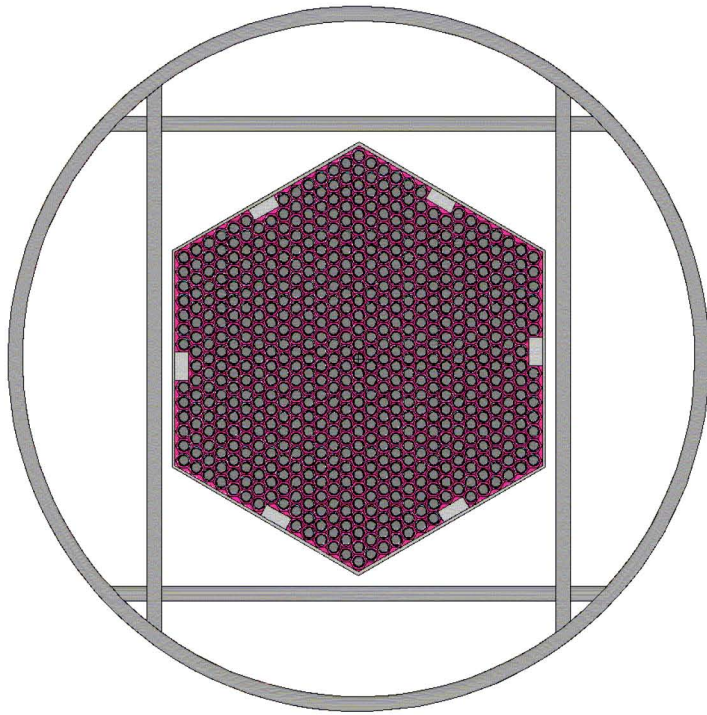


Figure 2-17. Isometric View of the Shippingport LWBR DOE Spent Nuclear Fuel Canister

2.3.6 Internals of Melt and Dilute DOE SNF Canister

Melt and Dilute (MD) ingots will be loaded in 10-ft-long DOE standardized SNF canisters (outer diameter of 18 in) (BSC 2001a). The MD ingots are homogeneous monolithic cylinders composed primarily of U-Al alloy (BSC 2001b, Section 3). These ingots will range in height from 381.0 to 762.0 mm (15 to 30 in) and will likely be contained in a plain carbon steel crucible liner. The crucible liner will have a maximum outer diameter of 393.7 to 419.1 mm (15.5-16.5 in) and a thickness of up to 12.5 mm (0.5 in) (BSC 2001b, Section 3). No internal basket structure is used inside the DOE SNF canister loaded with MD ingots (BSC 2001a). The DOE standardized SNF canister will contain three to six MD ingots, depending on the dimensions of the ingots.

2.3.7 Internals of FSVR DOE SNF Canister

The source of information in this section is Section 2.1.3 of *Evaluation of Codisposal Viability for Th/U Carbide (Fort Saint Vrain HTGR) DOE-Owned Fuel* (BSC 2001c), except where noted otherwise.

FSVR SNF will be loaded in 15-ft-long DOE standardized SNF canisters (outer diameter of 18 in). The DOE standardized SNF canister will contain up to five FSVR SNF elements, which are hexagonal graphite blocks 793.0 mm (31.22 in) high and 360.0 mm (14.172 in) across flats (Taylor 2001). No internal basket structure and no neutron absorber intended to prevent criticality will be present inside the DOE SNF canister loaded with FSVR SNF.

2.4 N-REACTOR MULTICANISTER OVERPACK

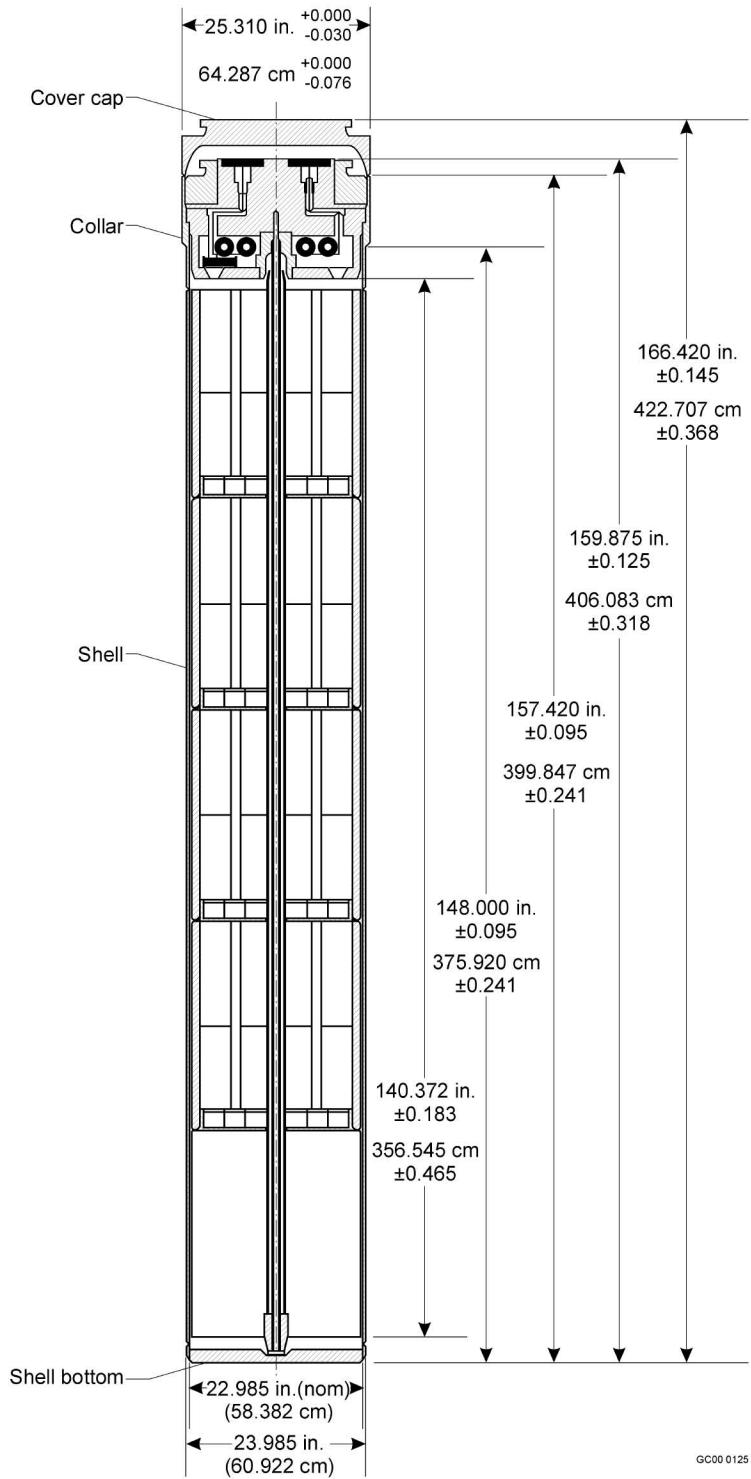
The source of information in this section is *Evaluation of Codisposal Viability for U-Metal (N Reactor) DOE-Owned Fuel* (CRWMS M&O 2001a), except where noted otherwise.

Development of the MCO grew out of the Tri-Party Agreement among the State of Washington, Department of Ecology; U.S. Environmental Protection Agency, Region 10; and the DOE. Part of the agreement mandated removal of SNF from the wet-storage environment in the K-Basins because of the potential environmental concerns posed by continued wet-storage (DOE 2000a).

The MCO was initially developed as an interim dry-storage container for the various N-Reactor fuels. With an evolutionary design, it may also end up being used as the package for transport and disposal in the repository.

Current wet storage of N-Reactor SNF required a package design that allows for both underwater loading of the fuel elements and in situ drying of the MCO and its contents after loading.

One canister design has been proposed for use in the packaging, transport, and disposal of the N-Reactor fuels. The canister design (Figure 2-18) includes a nominal length of 4198.37 mm (165.29 in) and a maximum outer diameter of 642.9 mm (25.31 in). Beyond these basic dimensions, fuel-specific internals have been designed for each canister based on the known maximum lengths of the fuels (Mark IV or IA) contained therein.



Source: DOE 2000a, p. 24

Figure 2-18. Multicanister Overpack With Four Intact and One Scrap Mark IV Baskets

The MCOs are constructed out of Stainless Steel Type 304L (ASTM A 240/A 240M-03b) having an outside diameter 60.92 cm (23.985 in) and a wall thickness of 1.27 cm (0.5 in) (Figure 2-18). The top portion of the MCO has a slightly larger diameter (64.29 cm [25.31 in]) than the overall

tube body in order to accommodate the top mechanical closure device. The overall length of the MCO is 422.71 cm (166.42 in) with an inner cavity height to the top of the stacked baskets of 356.55 cm (140.372 in). The bottom plate has a thickness of 5.11 cm (2.01 in). There is a metal structure that adds another 57.91 cm (22.80 in) to the top of the MCO above the basket that is best approximated as a solid, Stainless Steel Type 304L shield plug (DOE 2000a, p. 23).

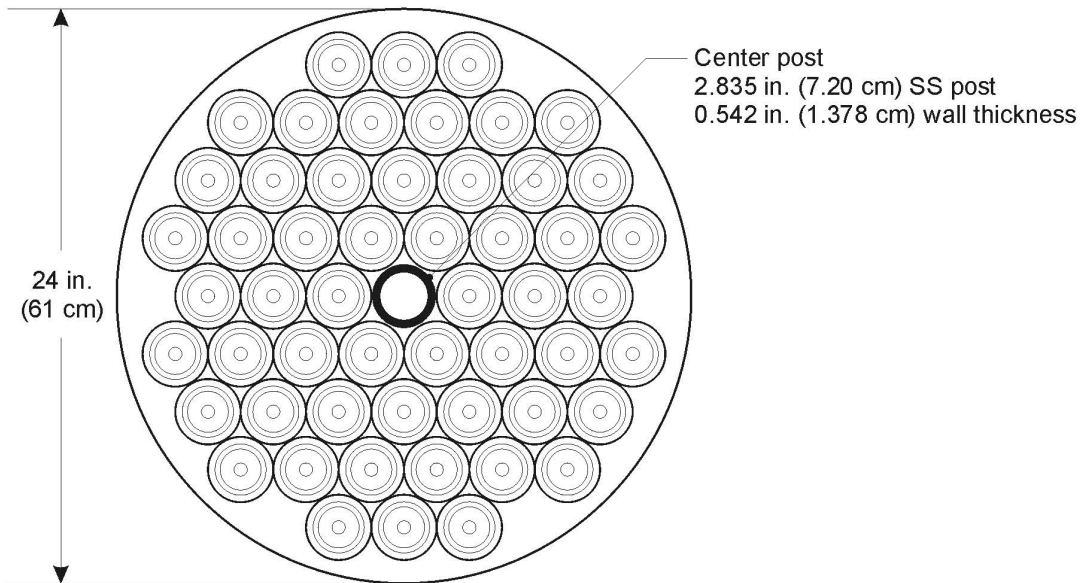
In addition, a central post constructed out of Stainless Steel Type 304L is present in the MCOs (Figure 2-19). This central post is associated with the stacked baskets, and each post is drilled to facilitate water removal from the bottom of the MCO after underwater loading. In the case of the Mark IV fuel baskets, the post outer diameter is 7.20 cm (2.835 in) with a 1.38 cm (0.54 in) thick wall. The Mark IA fuel and scrap baskets use a 16.83 cm (6.625 in) post diameter and a 4.46 cm (1.755 in [max.]) drilled hole in the center for a 6.18 cm (2.435 in) wall thickness.

In order to distinguish between what constitutes intact versus scrap material for MCO basket loading, the following generic guidelines are used for differentiating material segregation between baskets.

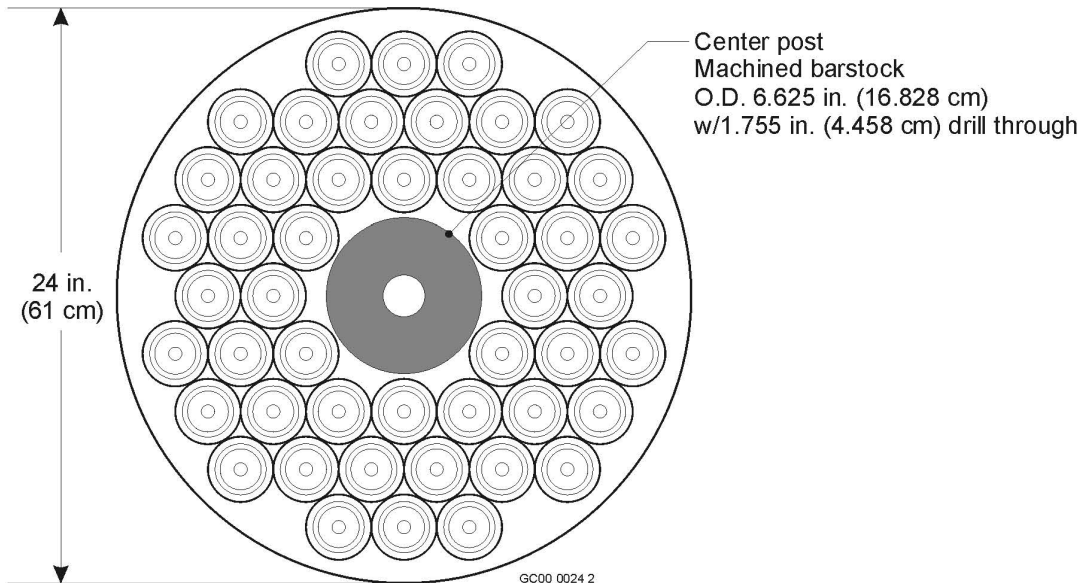
Scrap cans consist of material with a maximum dimension as small as 6.35 mm (1/4 in), but can also consist of pieces as large as entire fuel elements which do not fit in bottom plate sockets of the fuel basket (DOE 2000a, p. 23).

“Intact” fuels, suitable for loading in MCO fuel baskets, are defined as material that is loaded to form fuel element pairs, at least one end of the outer element fits within the hole machined in the plate of the fuel basket, and the inner element fits within the outer element. Both elements must seat within the fuel basket holes such that the top of either element does not exceed the basket height. Fuel element segments may be stacked (outer segments on intact inner or inner segments in intact outer) to form element pairs in a fuel basket position. The height of stacked segments can not exceed the length of intact element supporting the segment stack (DOE 2000a, p. 26).

Loading Arrangement for Mark IV Fuel in MCO Container



Loading Arrangement for Mark IA Fuel in MCO Container



Source: DOE 2000a, p. 25

Figure 2-19. Example of Loading Arrangements in Multicanister Overpacks

2.4.1 MCO Basket for Mark IV

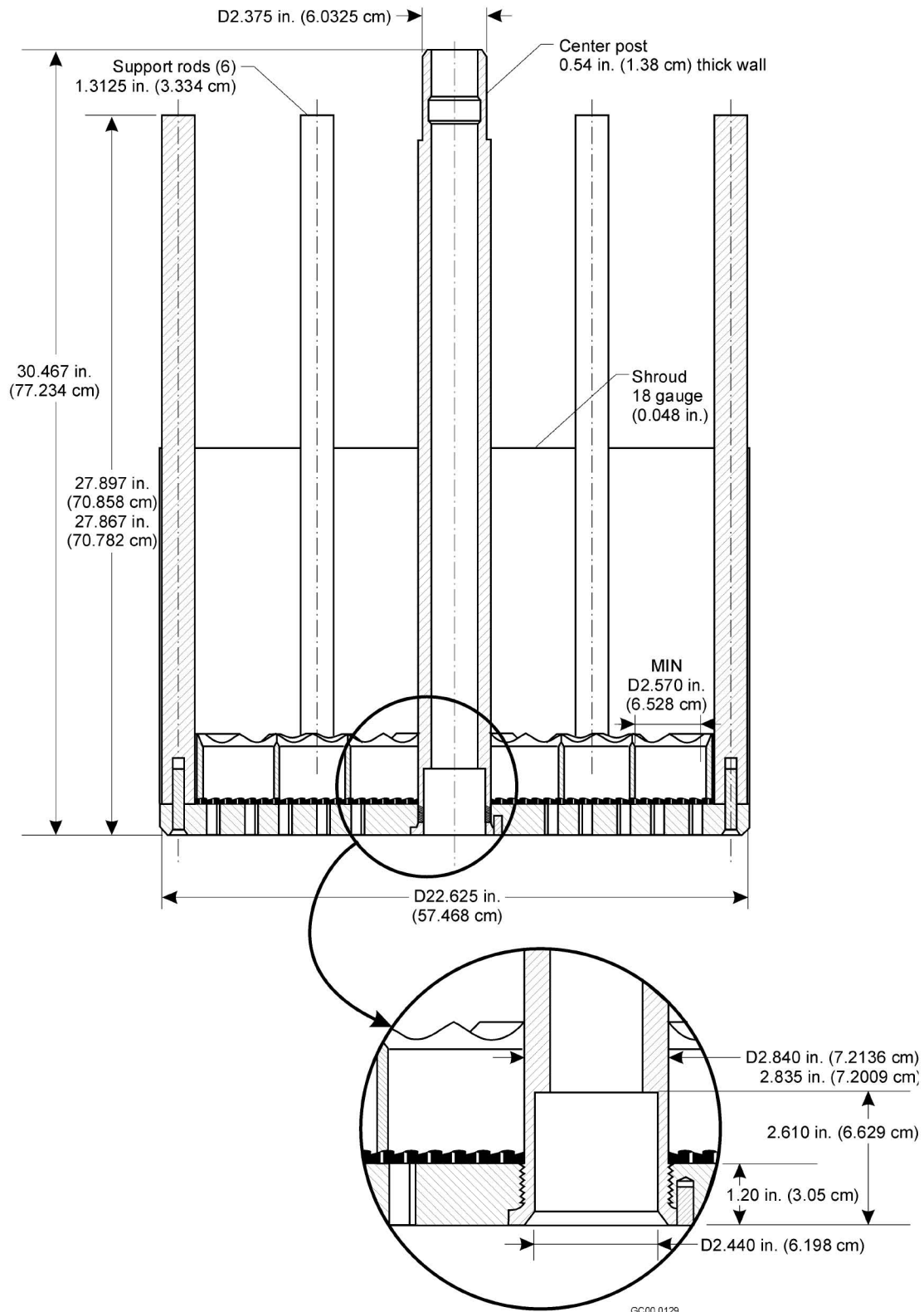
The Mark IV fuel consists of an inner element with a preirradiation enrichment of 0.947 percent and an outer element with a preirradiation enrichment of 0.947 percent. The length of the Mark IV fuel ranges from 44.2 cm (17.4-in) to 66.3 cm (26.1 in). Analyses are based on the 66 cm (26.1 in) long elements. The pertinent dimensions and weights for Mark IV elements are given in *N Reactor (U-Metal) Fuel Characteristics for Disposal Criticality Analysis* (DOE 2000a).

The proposed configuration consists of 54 Mark IV elements per basket (Figure 2-19) loaded in an upright position. Five baskets containing Mark IV spent nuclear fuel are then placed into an MCO. Previous criticality safety calculations (DOE 2000a, p. 26) allow two of the five baskets within the MCO to contain scrap or degraded Mark IV fuel. Heat transfer considerations indicate that a maximum of two scrap baskets may be loaded in an MCO and that they must be placed into the MCO as top and bottom baskets. The Mark IV scrap baskets are limited to a maximum of 980 kg and use a 0.95 percent enrichment value. Scrap basket design does not limit the mass of scrap in a basket; the scrap limits are based on spills of the baskets in the K Basins where there is sludge containing fissile material on the floor.

The Mark IV basket is an annular type basket constructed of Stainless Steel Type 304L (Figure 2-20). The 54 elements are housed in the annular section (Figure 2-19). The center post is comprised of a 7.201 cm (2.835 in) outer diameter cylinder made of stainless steel, with a wall thickness of 1.378 cm (0.54 in). There are six, Stainless Steel Type 304L, round-bar support rods of 3.33 cm (1.3125 in) diameter equally spaced around the outer periphery of the basket. These rods aid in distributing the axial load of the fuel/scrap baskets when the MCO is in the vertical position.

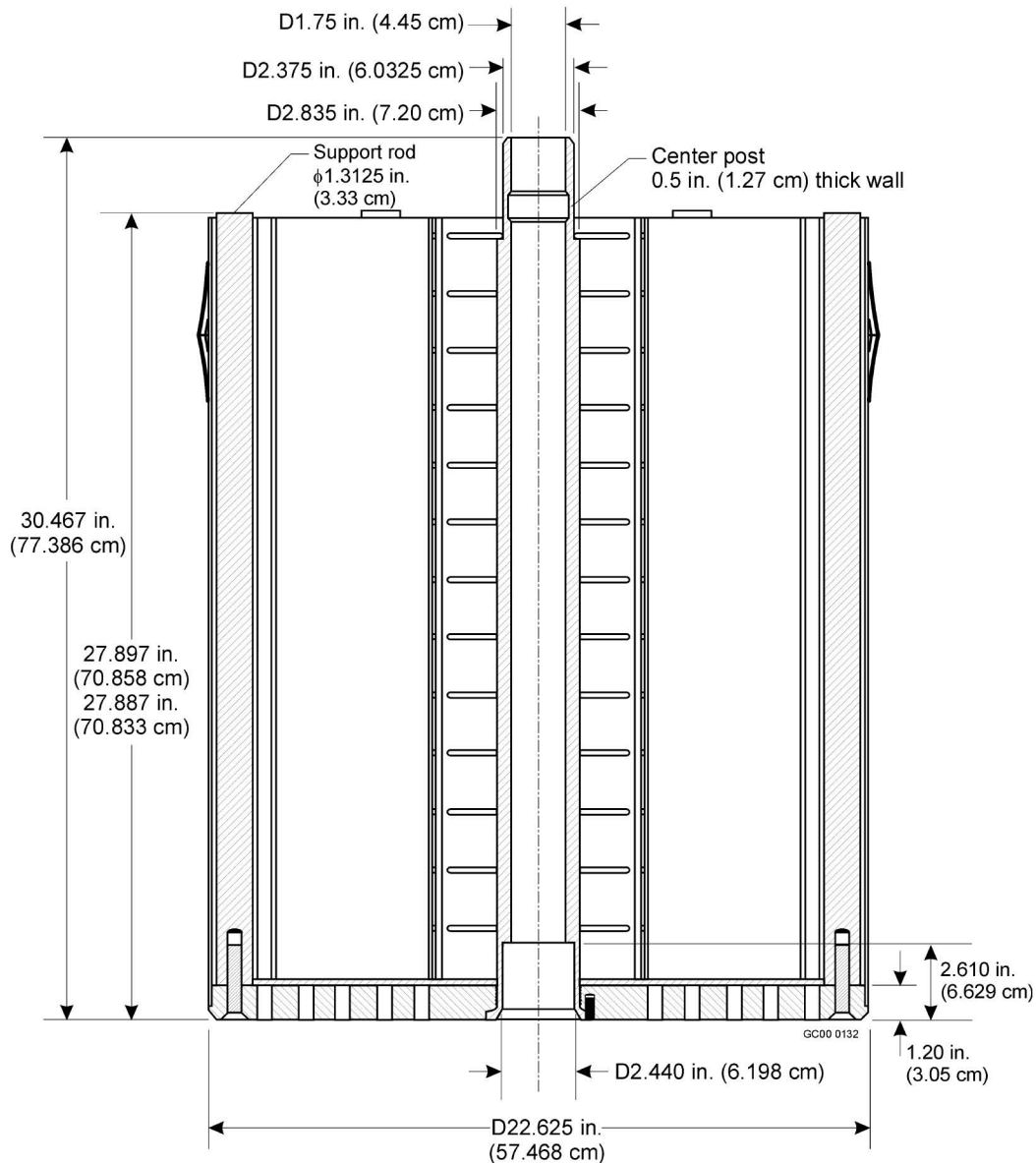
The basket used to house intact Mark IV fuel elements has an outer shell that extends approximately 35.6 cm (approximately 14 in), the height of the bucket. The outside shell is constructed of 18-gauge (0.048 in) Stainless Steel Type 304L. The outer shell outer diameter is 57.47 cm (22.625-in diameter). Each of the baskets, for intact elements, contains an aluminum spacer guide at the bottom of the basket. This spacer is approximately 6.35 cm (2.5 in) thick axially and arranges the Mark IV elements in the triangular pitch configuration at a typical center-to-center pitch of 6.99 cm (2.75 in) shown in Figure 2-19. The inside height of the basket is 67.30 cm (26.496 in) with an overall outer height of 70.86 cm (27.897 in). The perforated plate at the basket base is 3.05 cm (1.20 in) thick.

The Mark IV scrap basket is also an annular type basket constructed primarily of Stainless Steel Type 304L (Figure 2-21). The Mark IV scrap material is housed in the annular section. The center post is a 7.20 cm (2.835 in) outer diameter stainless steel pipe with a wall thickness of 1.38 cm (0.54 in) and an 18-gauge (0.048 in) stainless steel sheet metal outer shell. The outer diameter of the outer shell is 57.47 cm (22.625 in). The basket bottom plate is constructed from 3.05 cm (1.20 in) thick stainless steel with 1.27-cm (0.5-in) drain holes drilled through. The scrap baskets do not contain the aluminum element spacer guide at the bottom of the basket. The scrap baskets are divided equally into six compartments separated by six, full-height copper plates (ASM 1961, p. 1010) that are 0.318 cm (0.125 in) thick. The center of these assembled, truncated arcs forms a hexagon with a 17.78 cm (7.0 in) dimension across the flats (Figure 2-24 in Section 2.4.2 is an example of scrap basket structure). The outer height of the shroud (in cross-section) is 19.84 cm (7.81 in). The outer shroud height is 69.09 cm (27.20 in).



Source: DOE 2000a, p. 28

Figure 2-20. Mark IV Spent Nuclear Fuel Intact Elements Storage

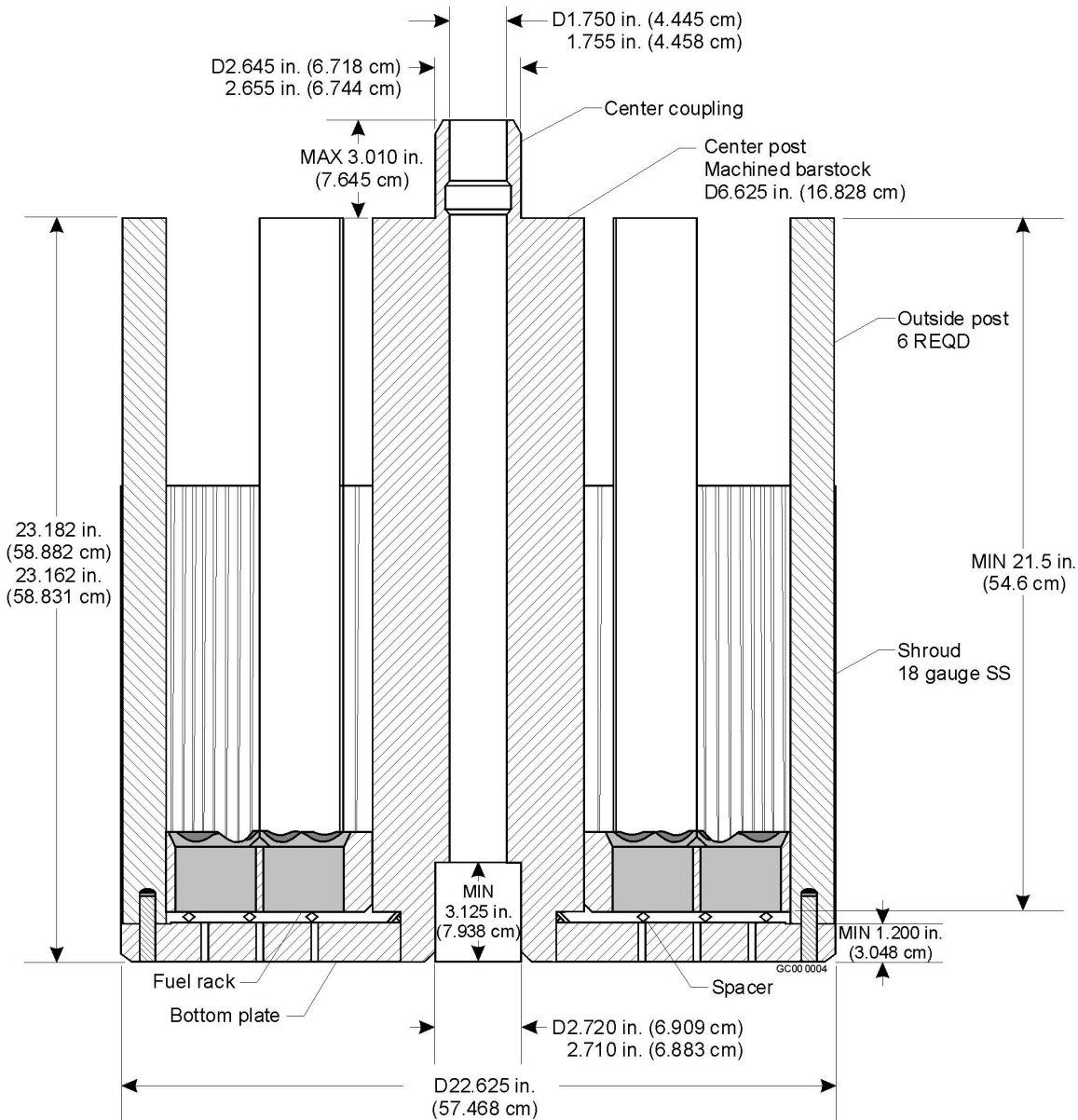


Source: DOE 2000a, p. 29

Figure 2-21. Mark IV Spent Nuclear Fuel Scrap Elements Storage Basket

2.4.2 MCO Basket for Mark IA Fuels

The basket is an annular type basket constructed of Stainless Steel Type 304L (Figure 2-22). The center post is machined stainless steel barstock (actual dimension of 16.83 cm [6.625 in]), and the wall thickness is 6.19 cm (2.4375 in). The outer wall of the basket is an 18-gauge stainless steel sheet metal with 57.47 cm (22.625 in) inner diameter outer shell. The 48 elements are housed in the annular section. The overall basket outer height is 58.88 cm (23.182 in). The basket bottom plate is constructed from 3.05 cm (1.20 in) thick stainless steel with drain holes drilled through. Each of the baskets contains an aluminum spacer guide at the bottom of the basket. This spacer is approximately 6.35 cm (2.5 in) thick and arranges the elements in the triangular pitch configuration at a typical center-to-center pitch of 6.99 cm (2.75 in) as shown in Figure 2-19.

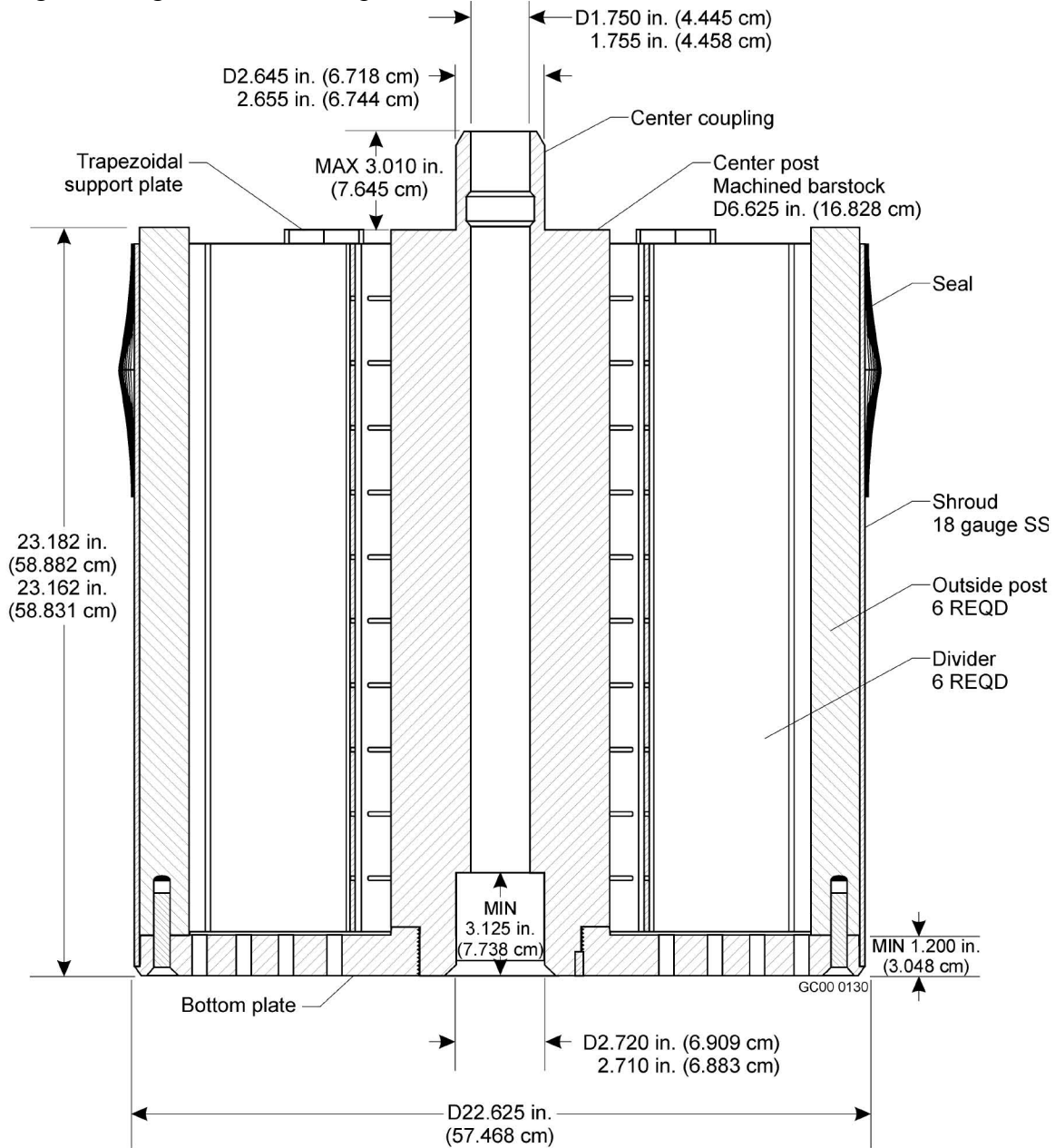


Source: DOE 2000a, p. 31

Figure 2-22. Mark IA Spent Nuclear Fuel Intact Elements Storage Basket

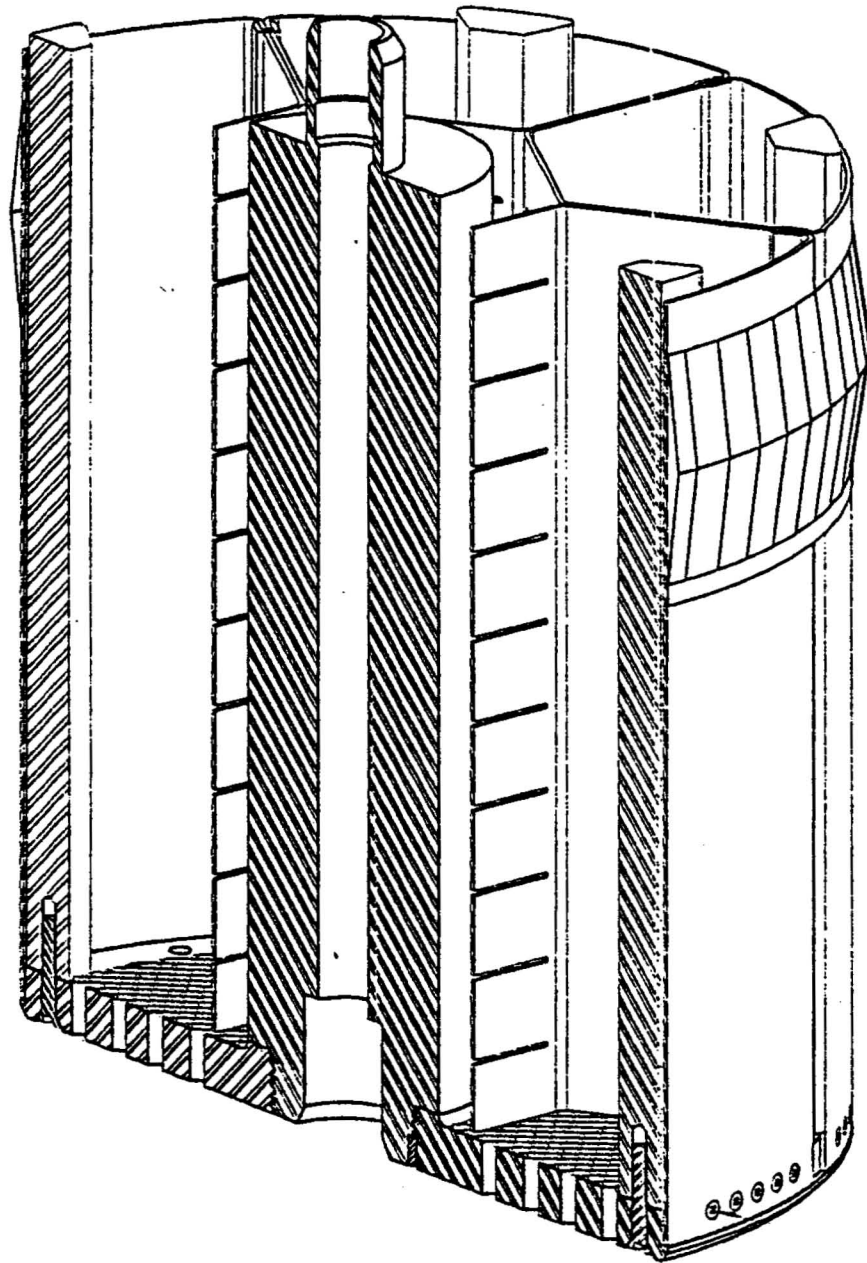
The scrap baskets do not have the aluminum spacer element guide located at the bottom (Figure 2-22). Scrap consists of various sized pieces and sections from Mark IA elements that have structurally failed. The scrap baskets (Figures 2-23 and 2-24) are divided into six individual compartments consisting of 0.318 cm (0.125 in) thick copper plate material (ASM 1961, p. 1010). Each compartment occupies a 60° arc (six segments) within the canister. Six trapezoidal posts (equally spaced radially on the outer periphery of the basket) provide structural support and a small degree of standoff (58.88 cm [23.182 in]) height from the basket shroud (56.64 cm [22.30 in]). The basket shroud element is shaped like a truncated (on the pointed end) piece of pie. The 60° arc is formed on a 28.41 cm (11.185 in) outer radius and an

overall height from the outside of the radius to the outside of the flat truncation of 17.48 cm (6.88 in). The flat-to-flat inside dimension of the hex shape formed by the joined surfaces of the scrap shrouds measures 22.54 cm (8.875 in). A trapezoid piece of Stainless Steel Type 304L bar stock is centered within each compartment on the outer radius. The following trapezoid cross-section dimensions (maximums) include a 3.73 cm (1.47 in) height, 3.18 cm (1.25 in) short base, a projected 7.96 cm (3.134 in) long base with 0.635 cm (0.25 in) radius on those corners. The thickness of the bottom plate of the basket is 3.05 cm (1.20 in). The overall outer diameter of each basket is 57.47 cm (22.625 in). The Mark IA scrap baskets are limited to a maximum loading to 575 kg and used a 1.25 percent enrichment value.



Source: DOE 2000a, p. 32

Figure 2-23. Mark IA Spent Nuclear Fuel Scrap Material Storage Basket



Source: DOE 2000a, p. 33

Figure 2-24. Isometric Representation of One Half of Mark IA Spent Nuclear Fuel Scrap Material Storage Basket

INTENTIONALLY LEFT BLANK

3 SUMMARY OF FUEL CHARACTERISTICS

3.1 DOE SNF GROUPING AND RATIONALE

The source of information in this section is *DOE Spent Nuclear Fuel Grouping in Support of Criticality, DBE, TSPA-LA* (DOE 2000b), except where noted otherwise.

3.1.1 Background on DOE SNF Grouping

The main goal of grouping the DOE SNF is to supply characterization data in a cost-effective manner to support DOE SNF management and disposal without increased risk to the public, environment, or worker safety. The DOE SNF grouping by the NSNFP has been an evolving process that is described in Section 5.1 of *DOE Spent Nuclear Fuel Information in Support of TSPA-SR* (DOE 2002).

First, the data needs required to meet the NRC and Environmental Protection Agency (EPA) regulations were evaluated. Two fuel parameters, fuel matrix and cladding, were identified to have primary influence on the behavior of DOE SNF. These behaviors are (a) release rate and (b) time-to-failure (i.e., the fuel's chemical and physical stability). Seven other parameters (burnup, initial enrichment, cladding integrity, fuel geometry, radionuclide inventory, fission gas release, and moisture content) were identified as having only secondary influences on fuel behavior.

Based on these findings, the DOE SNF was grouped into 11 groups for testing purposes. However, the 11 groups suggested are inconvenient for other analysis needs such as criticality evaluations in support of repository disposal. Subsequent discussion among the DOE SNF programs proposed that the DOE SNF inventory be first reduced to 34 DOE SNF groups based on fuel matrix, cladding, cladding condition, and enrichment. These parameters are the basis used in selecting the SNF grouping.

From these 34 DOE groups, it was determined that the groups may be further reduced to support both TSPA and criticality analyses. Specifically, the 34 groups of SNF were further reduced to 16 groups for the TSPA and 13 groups for criticality analyses purposes. The representative fuel in each condensed group was selected based generally on the quantity of the SNF within that specific group. These DOE SNF groups were used in the TSPA-VA analyses. U-metal fuel was used as the design basis DOE fuel that bounds the entire DOE SNF inventory.

In November 1998, the NSNFP decided to further refine and document the grouping process based on plan and cost estimate for the remaining work required to complete and submit a license application to the NRC. The grouping of DOE SNF was expanded to support site recommendation and licensing analyses in three major areas: criticality, design basis events, and performance assessment. The detailed rationale for grouping DOE SNF for each of these areas is covered in the report *DOE Spent Nuclear Fuel Grouping in Support of Criticality, DBE, TSPA-LA* (DOE 2000b). For disposal criticality analyses, nine DOE SNF groups and representative fuels types have been designated, out of which eight groups are addressed in this report (listed in Table 1-1).

3.1.2 Criticality Grouping Selection

While providing a relatively small contribution to the total metric tons of heavy metal (MTHM) within the repository (2,233 MTHM of the 7,000 MTHM allowed for defense-related materials, and 63,000 MTHM for commercial), the DOE SNF has many unique characteristics not found in commercial fuels that impact nuclear evaluations.

Commercial fuels are evaluated based on whether they are either PWR or boiling water reactor (BWR) type fuels. These fuels have very narrow range of enrichment (3.75 ± 0.5 percent enrichment), well defined lengths and cross-sectional dimensions, relatively uniform cladding and fuel composition, and closely controlled burnup values. Conversely, SNF within the DOE inventory exhibits a high degree of variability in terms of:

- Fuel matrix (metal, graphite, oxide, ceramic)
- Fissile material composition (metal, carbide, oxide, metal alloy)
- Cladding (aluminum, stainless steel, zirconium, other)
- Fissile species (^{235}U , ^{233}U , ^{239}Pu)
- Enrichment (0.7 percent to more than 90 percent ^{235}U)
- Burnup value (several days for test elements to several years in demonstration reactors)
- Physical condition (intact, disrupted, particulate)
- Cross-sectional dimension (from less than half centimeter to approximately half meter)
- Length (from several centimeters to several meters).

Each of the above parameters in some way affects the predicted behavior of the SNF relative to the potential releasable quantity of radionuclide material per packaging and behavior of the fissile material in what is eventually predicted to become a degraded waste package.

3.1.2.1 Fissile Species and Enrichment

The fissile species tested or used in various DOE reactors includes both ^{233}U and ^{235}U as well as ^{239}Pu . The related parameter designating the amount of fissile species compared to the rest of the actinide mix, referred to as enrichment, is a primary driver and determines whether a system can achieve criticality. The ability to assemble a critical mass of fissile material is very dependent on the overall enrichment of the fuel matrix.

3.1.2.2 Fuel Compound/Matrix

The components of the fuel compound/matrix that are important to grouping fuels are the mix of actinides and the compound. Solubility issues based on actinide species may affect fissile material movement both within a breached SNF canister and waste package, and transport once

outside a waste package on a long-term basis. Actual solubility differences between all chemical forms of uranium and plutonium in a common system are separated by at least two orders of magnitude, with uranium being the more soluble of the species. Similar differences in solubility are also noted between uranium and thorium, with the thorium species being less soluble. In a closed system such as a breached DOE SNF canister that retains water and soluble materials at equilibrium, new issues are raised with respect to fissile material transport, both within and outside/away from the waste package. For less robust fuels (e.g., U-Al_x), the fissile material may separate from the aluminum in the matrix and fuel cladding and move away from the basket structure to accumulate in the bottom of the DOE SNF canister. In other cases, the fuel basket structure inside the canister may degrade before the fuels, leading to intact fuel consolidation inside the canister. Both of these cases must be addressed in criticality analyses.

The various fuel matrix properties (e.g., carbides, oxides, metals, and ceramics) selected for the various fuels in the DOE inventory are of interest when segregating fuels by matrix. Introduction of water into the waste package through a breach must be examined. Given scenarios that allow for the formation of a chemical equilibrium (bathtub) versus a flow-through model, the various fuel matrices (in conjunction with the cladding and the internal basket structure) are expected to behave differently.

3.1.2.3 Cladding

Cladding for most of the DOE SNF can be considered either durable or nondurable with respect to eventual waste package breach for the postulated repository conditions. The nondurable cladding would generally include both aluminum and stainless steel (includes the high nickel alloys such as Inconel).

The durable cladding materials include specifically the zirconium (similar to commercial cladding) and the special case silicon carbide coating on some of the carbide fuel particles in graphite. There is a variety of zirconium alloys associated with the DOE fuels, because many were developmental tests of zirconium alloys leading to the various Zircaloy materials used in the commercial industry. Because the condition of even the durable cladding may be in question for many fuels, both extremes of intact and of degraded cladding must be considered in developing degraded configurations. For this reason, cladding is not an important parameter in grouping.

The bulk carbon associated with the graphite fuels is an inert material and is expected to retain much of its structural shape even after waste package breach. While graphite offers some neutron moderator (water) exclusion, it does not preclude water contact with the coated particles and provides some degree of moderation.

Cladding material does play a part in the analysis of fuel in a degraded SNF package. Within the DOE SNF inventory, many of the fuels have unique dimensions that will require a fuel-specific basket or structure within the DOE SNF canister. For the nondurable cladding material or that with unknown condition, early exposure of the fuel matrix to water could facilitate movement and/or redistribution of fissile material inside the DOE SNF canister prior to gross failure of the internal canister structure or the canister itself. For the more durable cladding, the canister internals might degrade prior to the cladding, thereby resulting in a different set of assumptions

relative to movement of fissile material within a breached DOE SNF canister. Both of these cases have added implications if neutron absorbers are included in the basket material for reactivity control.

3.1.2.4 Burnup

A fresh fuel assumption with no credit for burnable absorbers is made for DOE fuels, so burnup analysis becomes a relatively unimportant component for grouping. In the special cases of breeder or converter reactors, adjustments may need to be made to the beginning-of-life (BOL) fissile loading to account for the production of other fissile species because they generally affect the fuel reactivity calculations. In this case, burnup data are needed to support criticality analyses.

Burnup cannot be ignored, however, because the knowledge of that value is needed to calculate both thermal response of the package over time when loaded with the prescribed number of fuel elements and also the shielding calculations of a standard DOE SNF canister.

3.1.3 Fuel Groups

The NSNFP has designated nine representative fuel groups for disposal criticality analyses based on fuel matrix, primary fissile isotope, and enrichment. For each fuel group, a fuel type that represents the characteristics of all fuels in that group has been selected for detailed analysis.

3.1.3.1 U Metal (representative type: N-Reactor fuel)

The N-Reactor fuels constitute by far the greatest quantity (in MTHM) of SNF within the DOE inventory. Within this group of fuels, the Mark 1A and Mark IV fuels encompass over 90 percent of the fuel mass within this group. Current plans for packaging and disposal of these fuels include the use of MCOs (described in Section 2.4).

Two different enrichment values are represented with the Mark 1A (1.15 percent smeared enrichment) and Mark IV (0.947 percent enriched) fuels. For purposes of criticality analysis, the Mark 1A fuel provided the most reactive fuel for loading within the MCO and would be considered to be the bounding case fuel. The Mark 1A fuel constitutes approximately 1/3 of the total N-Reactor mass.

3.1.3.2 MOX (representative type: FFTF fuel)

MOX fuels were used exclusively as test fuels within the DOE complex. The FFTF fuels, while not necessarily the most highly enriched within the grouping, provided the basis for analyzing multiple fuel assemblies within a single canister. Within the MOX fuel grouping, the FFTF fuels contain approximately 2,332 kg of fissile material; no other type fuel within the grouping contains more than 50.0 kg. Furthermore, of the several plutonium enrichments ranging from 22.43 to 29.28 percent, the driver fuel assembly (DFA) Type 4.1 with 29 percent or greater enrichment was used as the base case for analysis. Proposed fissile masses per DOE SNF canister are as great for these fuels as for any combination of other fuel types within this group.

3.1.3.3 U-Mo and U-Zr Alloys (representative type: Enrico Fermi fuel)

The U-metal alloy fuels are dominated by the Fermi (Core 1 and 2) fuels at nearly 1,000 kg of fissile material in 214 canisters; as such, they comprise 96.48 percent of the fissile mass in this group. The Fermi fuels also represent the best documentation of any fuel type within this group.

3.1.3.4 HEU Oxide (representative type: Shippingport PWR fuel)

Shippingport PWR fuels consist of two different cores, both with highly enriched plate fuels (93.2 percent @ BOL), but with slightly different fissile loads. Data from both cores is used in the analyses; Core 1 data is used for the calculated burnup values for thermal and shielding analyses, and the Core 2 fissile mass is used in the criticality analysis.

3.1.3.5 ²³³U/Th Oxide (representative type: Shippingport LWBR fuel)

Shippingport LWBR fuels provide a uniquely distinctive fuel in many ways. All of the fuel types in this grouping originate from the same reactor. The nature of the reactor design dictated differences in fissile loadings and the size of the various assemblies. Some of the blanket assemblies contain a higher fissile mass than the seed assemblies, but an atom-density/unit volume equivalent to the seed assemblies. Their size is too large for disposal in an 18-in. canister, and disposal in a 24-in. canister is questionable, even with significant neutron poisoning. In addition, all these fuels are composed of high ²³³U enrichments (approximately 98 percent) mixed in binary fuel pellets of UO₂ (~5.2 wt percent U[max.]) with a thoria (ThO₂) matrix.

3.1.3.6 U/Th Carbide (representative type: Fort St. Vrain fuel)

Two demonstration commercial reactors generated distinctive graphite fuel types, Peach Bottom and FSVR. The fuels used a combination of UC₂ and ThC₂ fuel particles embedded in a graphite matrix. The two fuel types have many common properties; their greatest difference is the physical size of the fuel assembly and how they end up being packaged for criticality safety.

3.1.3.7 UZrH (representative type: TRIGA fuel)

The TRIGA fuel elements have been constructed in a variety of configurations (differing cladding materials, a variety of enrichments). These fuels are unique in that they incorporate a moderator in the matrix as zirconium hydride. The selection of the fuel type for criticality analysis within this group represents a departure from previous criteria applied to the other fuel groups. Within the other fuel groups, the quantity of fuel along with available characterization data was a determining feature in selection. Within the UZrH group, the TRIGA FLIP fuels with their 70 percent ²³⁵U enrichments constitute the most conservative case for codisposal evaluation because of the high reactivity of the fuels.

3.1.3.8 HEU-Al (representative type: Melt and Dilute form)

Earlier studies with aluminum fuels evolved around the Massachusetts Institute of Technology reactor fuel design. Subsequent decisions set the use of melt and dilute form (with depleted uranium) to reduce the enrichment levels below 20 percent. While there is some small effect on

the expected allowable fissile mass per SNF canister, the greater effect is the standardized shape and composition of the new waste form created with the ingots generated in the melt and dilute process.

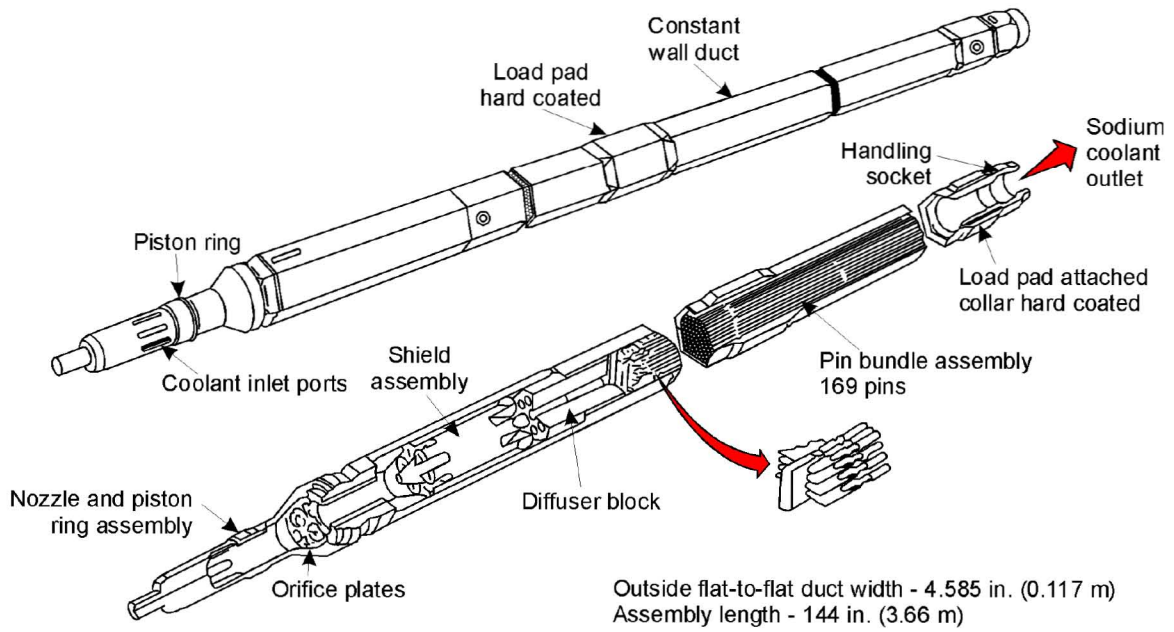
3.1.3.9 LEU Oxide (representative type: Three Mile Island debris)

Within the DOE SNF inventory are a number of fuel assemblies from commercial reactors. Among these fuels are 344 canisters containing the core debris from the Three Mile Island Unit 2 accident. This DOE SNF group is outside the scope of this report.

3.2 DESCRIPTION OF REPRESENTATIVE FUEL TYPES

3.2.1 FFTF

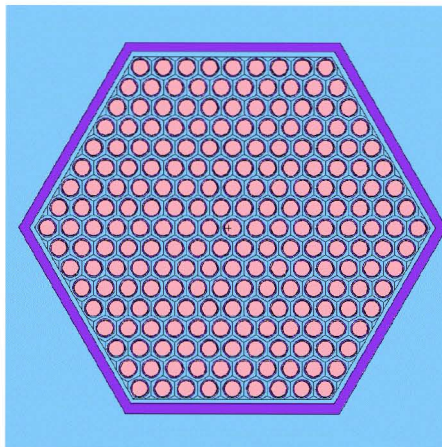
The source of FFTF fuel information is *FFTF (MOX) Fuel Characteristics for Disposal Criticality Analysis* (DOE 1998b). The FFTF standard driver fuel assembly (DFA) contains 217 cylindrical fuel pins and is hexagonally shaped. An axial view of a typical test fuel (169 fuel pins) assembly is shown in Figure 3-1 and a cross-section view of a typical DFA (217 fuel pins) appears in Figure 3-2 – the hexagonal cells seen in the figure are an artifact of the analysis modeling. The assembly is 3,657.6 mm long. The overall height of a fuel pin is 2,372.36 mm for Type 3.1 and 4.1 fuel pins, and 2,377.44 mm for Type 3.2 and 4.2 fuel pins. The Stainless Steel Type 316 cladding is 0.381 mm (0.015 in) thick. The inner and outer diameters of the cladding are 5.08 mm (0.200 in) and 5.842 mm (0.230 in), respectively. Each fuel pin has a 914.4 mm (36 in) long fuel region containing fuel pellets with an outer diameter of 4.9403 mm (0.1945 in). The fuel region is centered 1,663.7 mm (65.5 in) from the bottom of the assembly. Each fuel pin is helically wrapped with a 1.4224 mm (0.056 in) diameter Stainless Steel Type 316 wire to provide lateral spacing along its length. The wire pitch is 304.8 mm (12 in). The fuel pins are arranged with a triangular pitch within the hexagonal duct. The fuel density is reported as 90.4 percent of the theoretical density, which corresponds to a fuel pellet density of 10.02 g/cm³. The mixed oxide (MOX – UO_{1.96} and PuO_{1.96}) fuel region is followed by 20.32 mm (0.8 in) of natural UO₂ insulator pellets and 144.78 mm (5.7 in) of Inconel 600 reflector on each end. The density of natural uranium insulator pellets is 10.42 ± 0.22 g/cm³. The reflector outer diameter is 4.8133 mm (0.1895 in). Above the top reflector are a Stainless Steel Type 302 spring (125.5 mm long by 0.8052 mm in diameter) and a Stainless Steel Type 316 plenum (862.1 mm long with a 4.9022 mm outer diameter and 0.1397 mm wall thickness). The maximum spring volume is 2.7264 cm³. The fuel pin is closed with top and bottom caps having a 5.842 mm diameter. The length of the top cap is 104.6 mm. The bottom cap length for Type 3.1 and 4.1 fuels is 35.6 mm. The bottom cap length for Type 3.2 and 4.2 fuels is 40.6 mm. Each fuel pin weighs 455 g. A simplified axial view of a fuel pin is shown in Figure 3-3. The fuel enrichments and isotopic fractions for all four types of fresh FFTF fuel are given in Table 3-1. Note that Type 3.1 and 4.1 fuel pins and Type 3.2 and 4.2 fuel pins have the same dimensions.



C98 0682 1

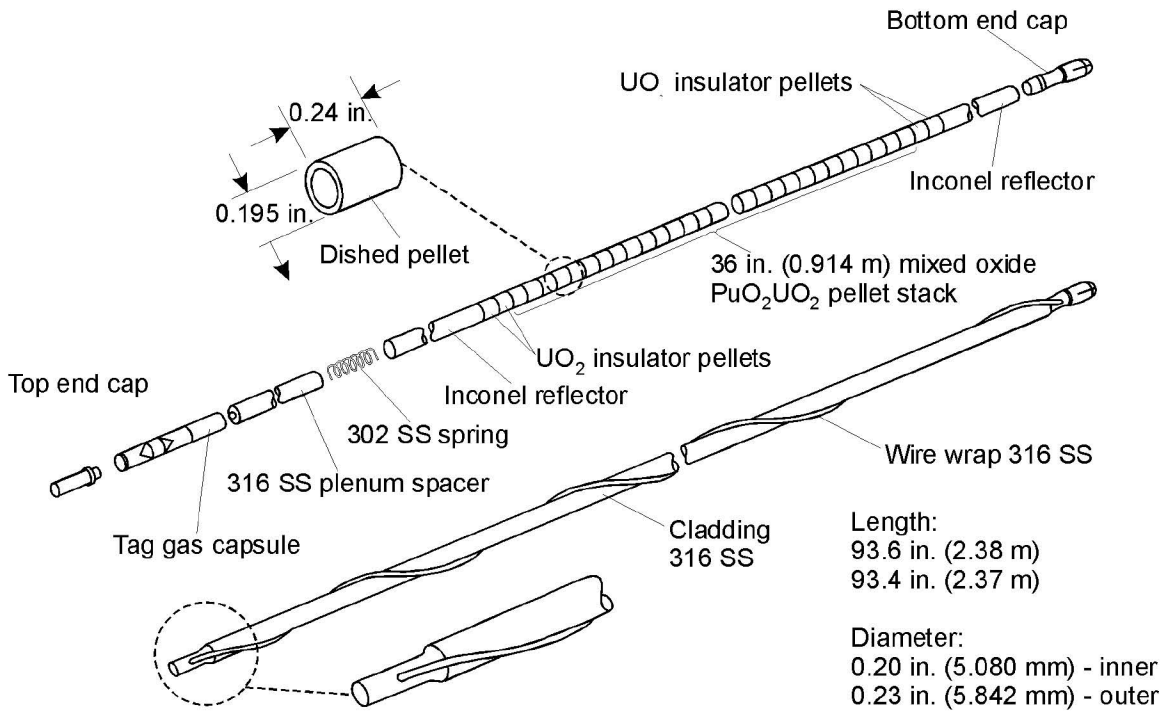
Source: DOE 1998b, Figure 3.1

Figure 3-1. FFTF Test Fuel Assembly



Source: DOE 1998b, Figure 3.2

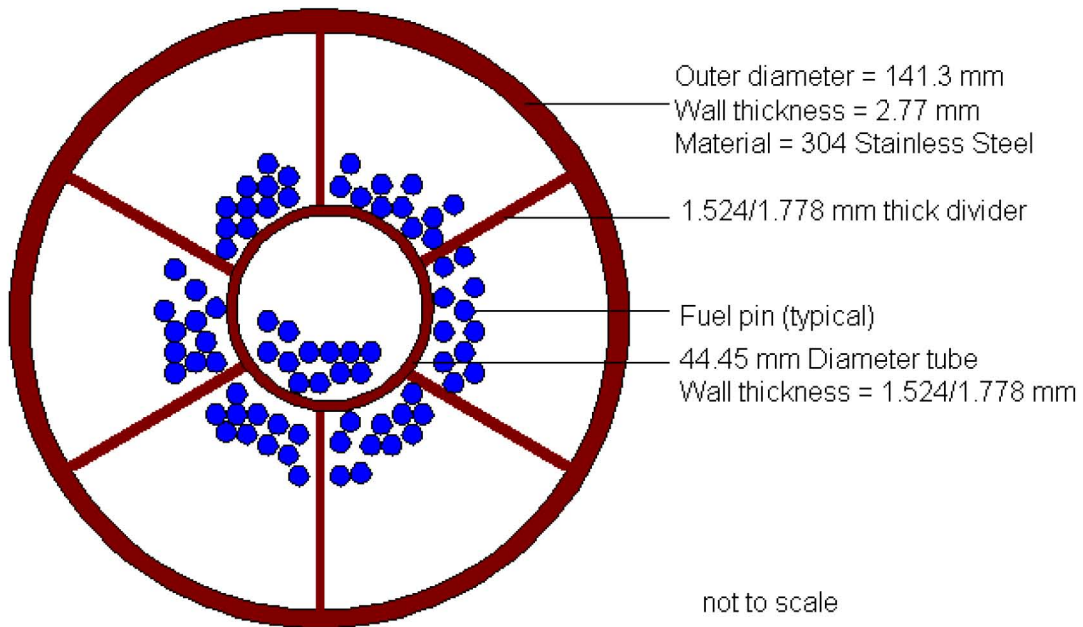
Figure 3-2. FFTF DFA Cross-Section



C98 0662 2

Source: DOE 1998b, Figure 3.3

Figure 3-3. Standard DFA Fuel Pin



Source: CRWMS M&O 1999a, Figure 2-9

Figure 3-4. Cross-Section View of Partially Loaded Ident-69 Fuel Pin Container

Table 3-1. Uranium and Plutonium Content of a Fresh DFA

		Driver Fuel Type				
		3.1	3.2	4.1	4.2	
Plutonium	Enrichment (%Pu/[Pu+U])	27.37	22.43	29.28	25.14	
	Assembly content (kg)	9.071	7.421	9.722	8.333	
	Fuel pin content (g)	41.8	34.2	44.8	38.4	
	Isotopic fraction	²³⁹ Pu	0.8696	0.8696	0.8711	0.8711
		²⁴⁰ Pu	0.1173	0.1173	0.1163	0.1163
²⁴¹ Pu		0.0104	0.0104	0.0102	0.0102	
Uranium	Enrichment (%U/[Pu+U])	72.63	77.57	70.72	74.86	
	Assembly content (kg)	24.070	25.666	23.481	24.813	
	Fuel pin content (g)	110.9	118.3	108.2	114.3	
	Isotopic fraction	²³⁵ U	0.007	0.007	0.002	0.002
		²³⁸ U	0.993	0.993	0.998	0.998

Source: DOE 1998b, Table 3.1

NOTE: Each assembly nominally holds 1.5 kg of uranium in insulator pellets.

The DFA comprises a hexagonal duct that surrounds the fuel pins, discriminator, inlet nozzle, neutron shield and flow orifice region, load pads, and handling socket. The duct is made of Stainless Steel Type 316 with a wall thickness of 3.048 mm (0.12 in). The duct-tube outer dimension is 116.205 mm (4.575 in) across the hexagonal flats and 131.064 mm (5.16 in) across the opposite hexagonal points. The fuel pin pitch is 7.2644 mm (0.286 in). The maximum assembly width is determined by the load pads, which are 138.1125 mm (5.4375 in) wide across the opposite hexagonal points. The assembly is 3657.6 mm (144 in) high. Total weight of a DFA is 172.819 kg.

Some of the assemblies have been disassembled and the fuel pins placed in fuel pin containers named Ident-69 pin containers. Although there are several types of pin containers, the most reactive pin container is the compartmented model, which can hold up to 217 fuel pins. The total container length is 3,657.6 mm (144 in). The Ident-69 containers are made with 5-in Stainless Steel Type 304L pipe (actual outer diameter is 5.563 in or 141.30 mm) with a transition to 2.5 in pipe (actual outer diameter is 2.875 in, or 73.02 mm) at 431.8 mm (17 in) from the bottom. The inside diameter of the container is 135.763 mm (5.345 in). The fuel pins are supported on a grid plate with 1.5875 mm (0.0625 in) diameter holes. The central compartment has inside and outside radii of 20.701 mm (0.815 in) and 22.225 mm (0.875 in), respectively. The empty weight of an Ident-69 container is 59.09 kg (130 lb.). A cross-section view of a partially loaded Ident-69 fuel pin container is shown in Figure 3-4.

3.2.2 TRIGA

Six hundred sixty-five TRIGA SNF rods are stored at the Idaho National Engineering and Environmental Laboratory (INEEL) and approximately 290 fuel rods are stored within several TRIGA reactor facility sites.

TRIGA reactors utilize solid fuel rods, in which the zirconium-hydride matrix is homogeneously combined with the enriched uranium and loaded into cylindrical rods 38.1 mm (1.5 in) in diameter and 762.0-mm (30.0-in) long.

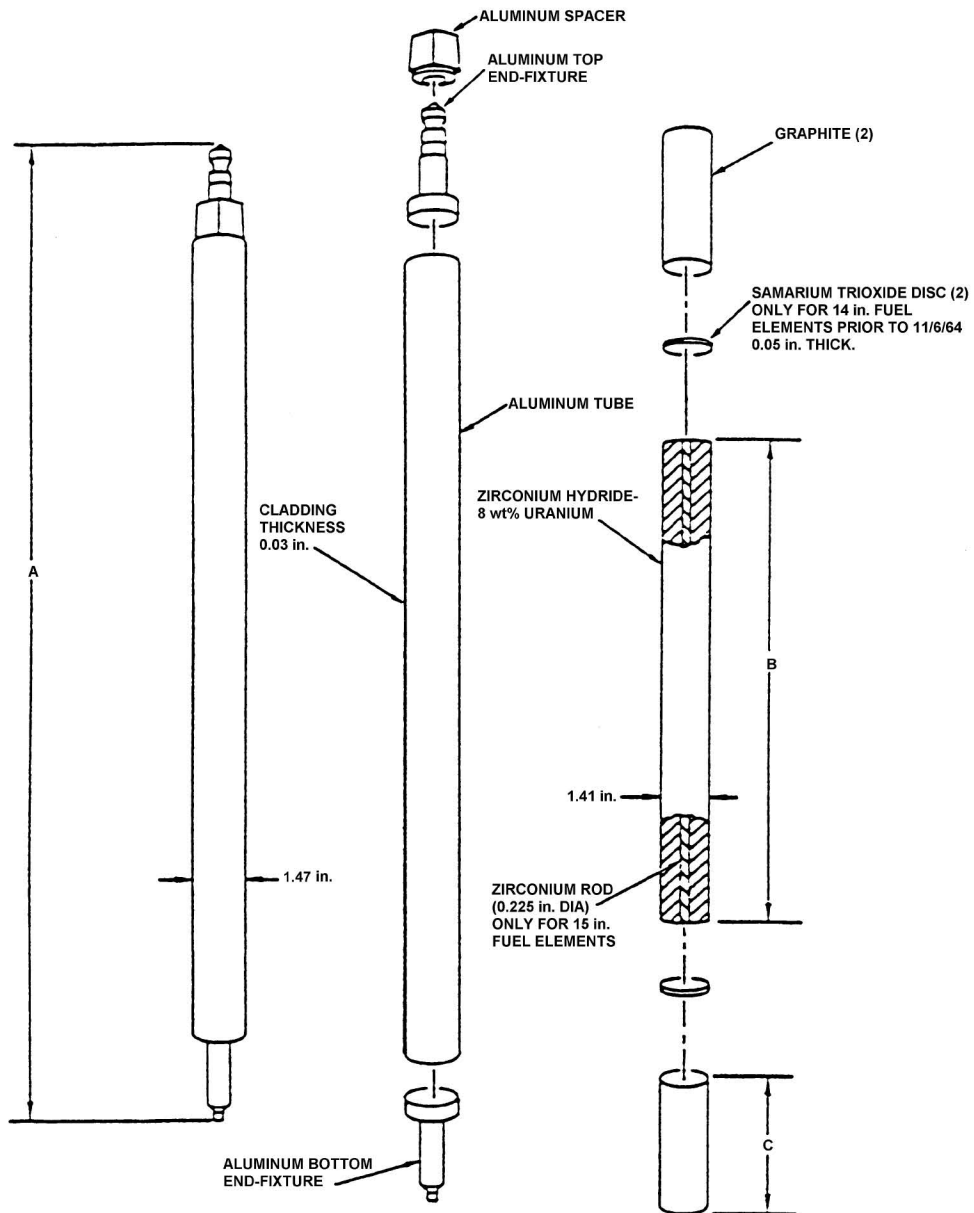
The TRIGA SNF analyzed contains various uranium loadings as a fine metallic dispersion in the zirconium-hydride matrix with 20 percent or 70 percent enrichment (Tomsio 1986, Table 3-3, p. 3-11). The H/Zr ratio is nominally 1.6, although earlier fuels used an H/Zr ratio of 1.0. Most of the earlier TRIGA SNF contained a nominal 8.5 wt percent uranium, but TRIGA SNF with up to 12-wt% uranium has also been used. The spent nuclear fuel burnup on both aluminum and standard stainless-steel-clad elements range typically from 10 wt% to 20 wt% of ^{235}U (DOE 1999c, Table 3-7, p. 20). However, the Fuel Life Improvement Program (FLIP) stainless-steel-clad rods (the only one with 70 percent uranium enriched) have burnups from 30 to 50 percent by weight (Tomsio 1986, pp. 1-1, 3-11, 3-13, and 5-1).

The inventory of TRIGA SNF investigated in *Evaluation of Codisposal Viability for UZrH (TRIGA) DOE-Owned Fuel* (CRWMS M&O 2000b) falls into the following three basic categories: aluminum-clad rods, stainless-steel-clad rods, and fuel-follower control rod rods (fuel rod with control rod inside) (Tomsio 1986, p. 3-1). Each of these fuel types has differences in loading, enrichment, dimensions, and rod components. The TRIGA rods contain fuel rods with a homogeneous mixture of uranium and zirconium-hydride. For example, $\text{U}_{20}\text{ZrH}_{1.6}$ identifies a fuel composition with uranium 20 percent enriched in ^{235}U , and a hydrogen-to-zirconium ratio of 1.6 (Tomsio 1986, p. 3-11). Aluminum-clad TRIGA is referred to as TRIGA-Al, and stainless-steel-clad TRIGA as TRIGA-SS.

It is noted that all fuel element types, except the fuel-follower type, may be instrumented with thermocouples extending from the top fitting into the fuel rod (Tomsio 1986, pp. 3-4, 3-7, and 3-13). Thermocouple lead wires pass through a seal contained in a tube welded to the upper end fixture. This tube is extended by two sections of tubing connected by unions to provide a watertight path to the monitors. Before the fuel is shipped for storage, the tubing is removed from the element. The balance of the instrumented rod is identical to the standard element.

3.2.2.1 Aluminum-Clad TRIGA (TRIGA-Al) Rods

The source of information in this section is (DOE 1999c, pp. 10 and 11). There are two types of TRIGA-Al rods, as shown in Figure 3-5. One has a 355.6-mm (14.0-in) fuel length, and the other has a 381.0-mm (15.0-in) fuel length. Both are 35.8-mm (1.41-in) diameter $\text{U}_{20}\text{ZrH}_{1.0}$ fuel rods loaded with 36 grams of ^{235}U with 8 percent of the total fuel mass being uranium. The rods are clad with 0.76-mm (0.03-in) thick aluminum, with a 37.34-mm (1.47-in) outside diameter. A 6.35-mm (0.25-in) diameter hole is drilled through the center of the 381-mm (15.0-in) rods, and a 5.72-mm (0.225-in) diameter zirconium rod is placed in the hole. The 381-mm (15.0-in) rods have an 89.66-mm (3.53-in) long graphite reflector on each end. These rods are 718.82-mm (28.3-in) long. The 355.6-mm (14.0-in) rods have no hole drilled through, and have a 100.33-mm (3.95-in) graphite reflector on each end. These rods are 720.6-mm (28.37-in).

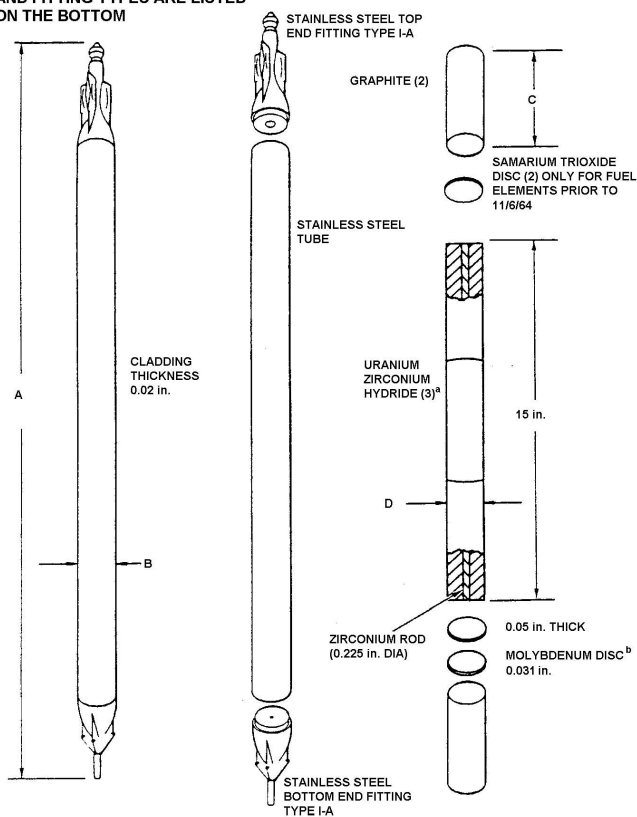


TRIGA Fuel Type	A (in.)	B (in.)	C (in.)
Original - 14 in.	28.37	14.0	3.95
Original - 15 in.	28.3	15.0	3.53

Source: DOE 1999c, Figure 3-1

Figure 3-5. Sketch of Aluminum-Clad TRIGA Rods (TRIGA-AI)

NOTE:
 APPLICABLE DIMENSION "A-D"
 AND FITTING TYPES ARE LISTED
 ON THE BOTTOM



NOTES: ^a ACPR FUEL ELEMENT CONSIST OF ONE 15 in. FUEL ROD
^b NOT INCLUDED IN FUEL ELEMENTS PRIOR TO 4/15/71 AND IN ACPR FUEL ELEMENTS

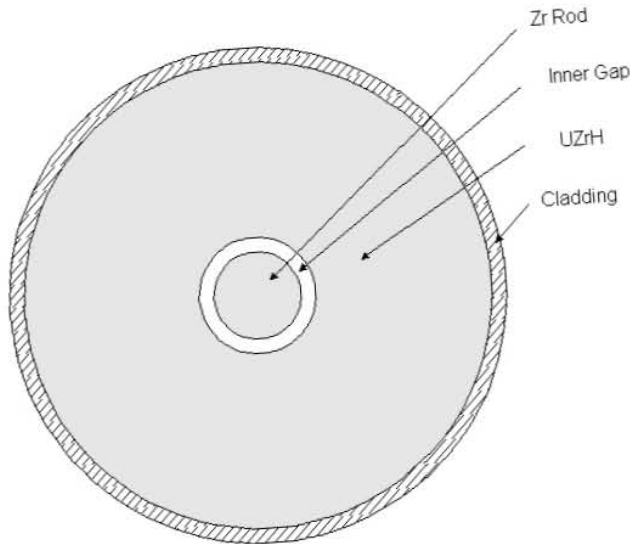
STAINLESS STEEL CLAD FUEL ELEMENTS DIMENSIONS

TRIGA Fuel Type	Fitting Type	A (in.)	B (in.)	C (in.)	D (in.)
Standard-streamline	I-A	29.68	1.478	2.56 ^a	1.435
Standard-plain	II-A	28.9	1.478	3.42	1.435
4 rod cluster	III-A	29.88	1.414	3.42	1.37
ACPR ^b	IV-A	28.89	1.478	3.45	1.40

NOTES: ^a Lower graphite is longer than upper graphite. Lower graphite 3.72 in.
^b Annular Core Pulsed reactor

Source: DOE 1999c, Figure 3-2

Figure 3-6. Sketch of TRIGA-SS Rods



Source: DOE 1999, Figure 3-3

Figure 3-7. Cross-Section Sketch of TRIGA-SS Rod

Standard Streamline Type Rods—The standard streamline type is a 36.45-mm (1.435-in) diameter fuel rod, with a 65.02-mm (2.56-in) long upper graphite reflector and a 94.49-mm (3.72-in) long lower graphite reflector (DOE 1999c, p. 12). The cladding for these rods is 753.87-mm (29.68-in) long with a 37.54-mm (1.478-in) outer diameter. There are five variations for the uranium loading of these rods. Before 1965, the standard (TRIGA-SS Standard) rods were $U_{20}ZrH_{1.0}$ loaded with 39 g ^{235}U ; 8 wt% of the total fuel mass was uranium. After 1965, the TRIGA-SS standard rods were $U_{20}ZrH_{1.7}$ loaded with 39 g ^{235}U ; 8.5-9 wt% of the total fuel mass was uranium. Also, there are three types of TRIGA-SS FLIP loadings: TRIGA-SS, TRIGA-SS Low Enriched Uranium I (FLIP-LEU-I), and TRIGA-SS LEU-II. The TRIGA-SS FLIP rods are $U_{70}ZrH_{1.6}$ fuel rods loaded with 137 g ^{235}U , 8.5 percent of the total fuel mass was uranium. The TRIGA-SS FLIP-LEU-I rods are $U_{20}ZrH_{1.6}$ fuel rods loaded with 101 g ^{235}U , and 20.2 wt% of the total fuel mass is uranium. TRIGA-SS FLIP-LEU-II rods are $U_{20}ZrH_{1.6}$ fuel rods loaded with 165 g ^{235}U , and 30 percent of the total fuel mass is uranium.

Standard Plain Type Rods—Standard plain-type rods have 36.45-mm (1.435-in) diameter fuel region, with an 86.87-mm (3.42-in) long graphite reflector on both ends (DOE 1999c, p. 14). The rod cladding is 734.06-mm (28.9-in) long with a 37.54-mm (1.478-in) outer diameter.

Four-Rod Cluster Type Rods—Four-rod cluster type rods have a 34.80-mm (1.37-in) diameter fuel region, with an 86.87-mm (3.42-in) long graphite reflector on both ends of the fuel region (DOE 1999c, p. 15). The rod cladding has a 758.95-mm (29.88-in) overall length, and a 35.92-mm (1.414-in) outer diameter. The rods may be configured in a cluster of four rods (in a 2×2 array) with unknown center-to-center spacing. The rods may be loaded in the first five ways listed in Table 3-5. Analyses performed at INEEL show that the four-rod cluster-type TRIGA-SS FLIP is the most reactive (DOE 1999c, p. 19) under a limited range of conditions.

ACPR Type—ACPR rods have 35.56-mm (1.40-in) diameter fuel region with an 87.63-mm (3.45-in) long graphite reflector on both ends of the fuel (DOE 1999c, p. 15). The rod cladding is 733.81-mm (28.89-in) long and has a 37.54-mm (1.478-in) outer diameter. There is a 0.56-

mm (0.022-in) gap between the fuel and the cladding. The rods are $U_{20}ZrH_{1.7}$ fuel rods loaded with 54 g ^{235}U , and 12 percent of the total mass is uranium.

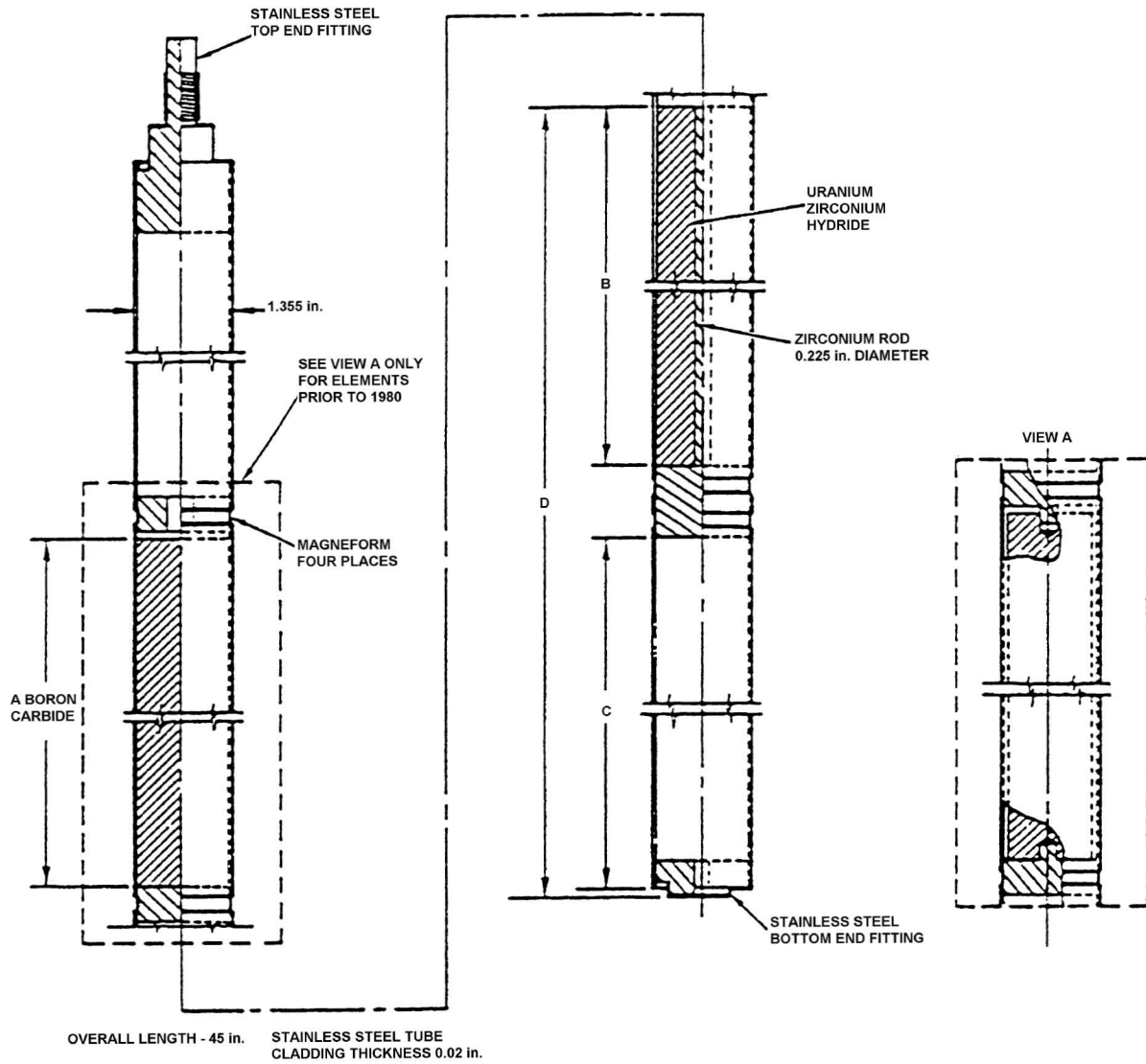
3.2.2.3 Fuel-Follower TRIGA-SS Rods

The fuel-follower rods contain control rods. They serve differing functions within the core, such as safety rods, regulating rods, and shim rods. There are two types of fuel-follower TRIGA-SS rods (DOE 1999c, p. 16): standard (Figure 3-8) and the ACPR fuel-follower control rod element (Figure 3-9). Both types are clad with 0.51-mm (0.02-in) thick stainless steel (Type 304). The 1143.0-mm (45.0-in) long fuel rods are $U_{20}ZrH_{1.6}$ with 381.0-mm (15.0-in) of boron carbide neutron absorber above the fuel. In addition, both types have a 5.72-mm (0.225-in) diameter zirconium rod inserted in the 6.35-mm (0.25-in) diameter hole drilled through the center of the fuel rod. Standard-type follower rods are 381.0-mm (15.0-in) long, have a 33.40-mm (1.315-in) diameter, and have two possible fuel loadings. The TRIGA-SS standard loading is 38 g ^{235}U , and 8.5 percent of the total mass being uranium. The TRIGA-SS FLIP-LEU-I loading for the standard fuel-follower is 97 g ^{235}U , 20 percent of the total fuel mass being uranium. These 1143.0-mm (45.0-in) long fuel rods will be stacked in two stainless steel baskets in the DOE SNF container to provide 74 rods per canister. ACPR-type follower rods are 1689.1-mm (66.5-in) long, 36.53-mm (1.438-in) in diameter, and are loaded with 54 g ^{235}U , 12 percent of the total mass being uranium. For this type of rods, one stainless steel basket will be stacked in the DOE SNF container to provide 37 rods per canister. Table 3-2 shows the dimensions and fuel loading for the TRIGA-SS FLIP fuel (DOE 1999c, p. 19).

Table 3-2. TRIGA-SS FLIP Dimensions and Fuel Loading

Parameter	Value
Outer diameter mm (in)	34.80 (1.37)
Inner diameter mm (in)	6.35 (0.25)
Gap mm (in)	0.05 (0.002)
Cladding mm (in)	0.51 (0.02)
Height mm (in)	381.00 (15)
^{235}U (g)	137
^{238}U (g)	59
Zr (g)	2073.7
H (g)	36.7

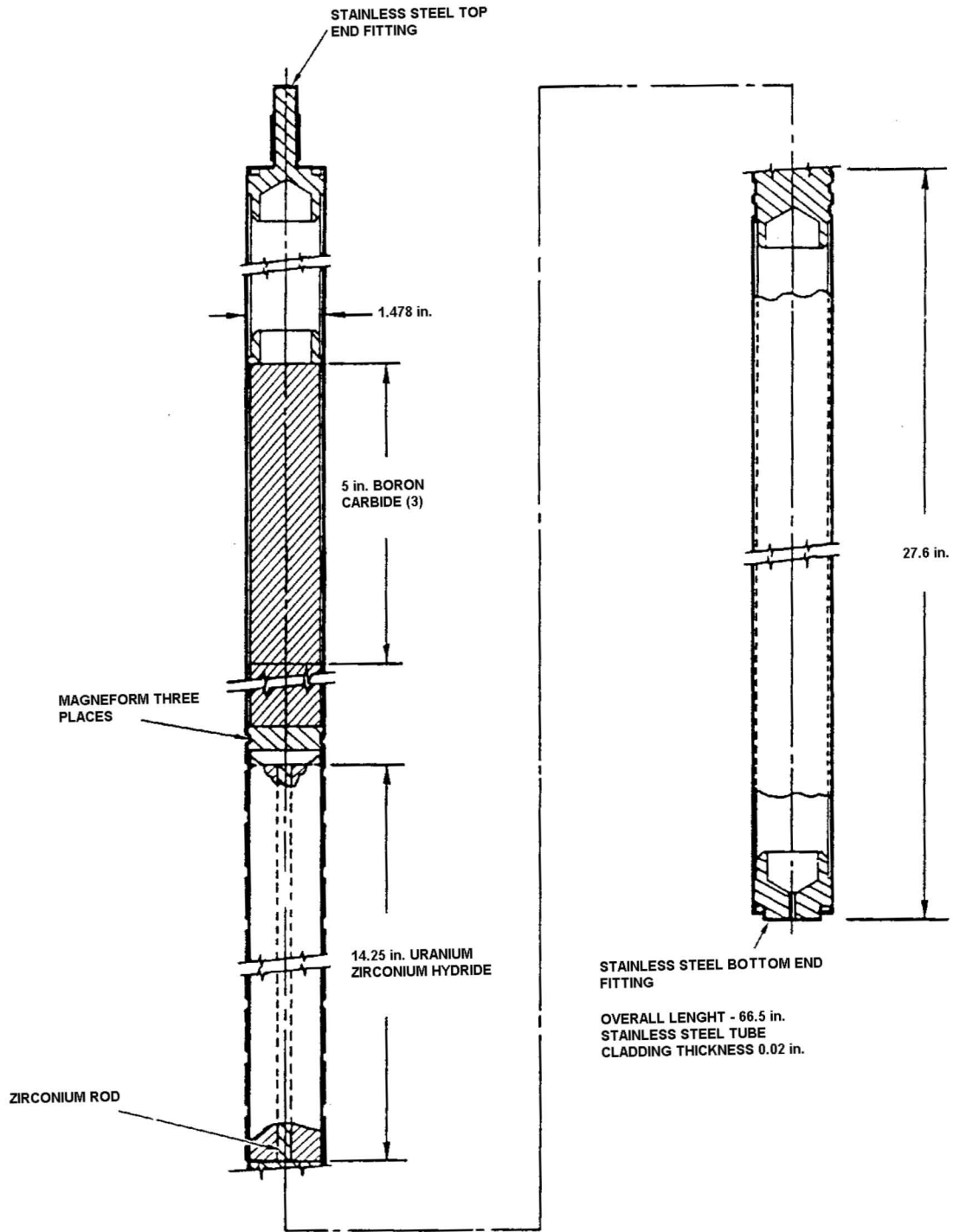
Source: DOE 1999c, Table 3-6



TRIGA FUEL TYPE	A (in.)	B (in.)	C (in.)	D (in.)
Present	15.0	15.0	5.88	22.06
Prior to 1980	14.25	15.0	6.0	22.03

Source: DOE 1999c, Figure 3-5

Figure 3-8. Sketch of Standard Fuel-Follower Control Rod



Source: CRWMS M&O 2000b, Figure 2-10

Figure 3-9. Sketch of ACPR Fuel-Follower Control Rod Element

The BOL characteristics per element for four different TRIGA SNF element types are shown in Table 3-3. This table also provides the typical burnup for each of these types of rods. Table 3-4 lists the nominal densities for the TRIGA UZrH fuels for several uranium weight percentages.

Table 3-3. Beginning-of-Life Characteristics for Four TRIGA Spent Nuclear Fuel Rod Types

	Al-Clad Standard	SS-Clad Standard	FLIP	FLIP-LEU-I
BOL ²³⁵ U (g)	36.0	39.0	137.0	101.0
BOL ²³⁸ U (g)	144.0	156.0	59.0	403.0
BOL uranium (g)	180.0	195.0	196.0	504.0
Enrichment (%)	20.0	20.0	70.0	20.0
Cladding	Al	Stainless Steel	Stainless Steel	Stainless Steel
U wt% in ZrH	8.0	8.5	8.5	20.0
H/Zr Atom Ratio	1.0	1.7	1.6	1.6
Erbium neutron absorber (g)	0.0	0.0	36.0	20.0
Neutron absorber disc	19.7 g Sm ₂ O ₃ (2 Discs)	8.38 g Mo Disc	None	None
Graphite (g)	450.0	450.0	450.0	450.0
Stainless Steel Type 204 (g)	0.0	800.0		
Aluminum 1100 (g)	280.0	0.0	0.0	0.0
Zr (g)	2,070.0	2,088.0	2,060.0	1,988.0
Typical Burnup (% ²³⁵ U)	10 to 20	10 to 20	30 to 50	10 to 20

Source: DOE 1999c, p. 20

Table 3-4. Nominal Compositions and Densities of TRIGA UZrH Fuels

Uranium (wt%)	Uranium (vol %)	Uranium (g/cm³)	UZrH (g/cm³)
8.5	2.7	0.51	6.02
12	3.9	0.74	6.18
20	6.9	1.32	6.60
30	11.3	2.15	7.21
45	19.5	3.73	8.37

Source: DOE 1999c, Table 3-8

3.2.2.4 TRIGA SNF Quantities by Type

Table 3-5 shows the approximate quantities of each basic TRIGA SNF. The exact number of a particular type is not presently known (DOE 1999c, p. 22).

Table 3-5. TRIGA Spent Nuclear Fuel Type Quantities

Fuel Type	Number of Rods
TRIGA-SS FLIP (4 rod cluster type, standard streamline type, and standard plain type)	228
TRIGA-SS FLIP-LEU Standard (4 rod cluster type, standard streamline type, and standard fuel-follower type; FLIP-LEU-I and FLIP-LEU-II loading)	502
TRIGA-SS ACPR (Standard ACPR type and fuel-follower type)	15
TRIGA-SS Standard (4 rod cluster type, standard streamline type, standard plain type, and standard fuel-follower type; pre1965 and post1965 fuel loading)	900
TRIGA-AL (355.6-mm (14.0-in) type, 381.0-mm (15.0-in) type)	528
TRIGA-SS Standard or TRIGA-AL (FRR reactors) ^a	1,061
TRIGA-In (93% enriched)	878
TRIGA-In (20% enriched)	498

NOTE: ^a Current information from foreign reactors does not distinguish between TRIGA-SS standard and TRIGA-Al rods. These must be distributed into the appropriate category when additional information is received.

Table 3-6 lists the lengths of the various TRIGA rods. There are four to six fuel-follower rods for 1 MW reactors and zero to four for reactors operating at less than 1 MW (Tomsio 1986, p. 3-18). The longest fuel rod is 774.70-mm (30.5-in). It is noted that instrumented rods may have a portion of the stainless steel lead-out tube attached to the end fitting. This may add additional length (approximately 76.20-mm) to these rods. The standard fuel-follower control rod is a fuel rod with a control rod inside. This rod is 1143.0-mm (45-in) long, about 1.5 times the length of the fuel rods. The ACPR fuel-follower control rod is 1,689.1-mm (66.5-in) long, more than twice the length of the standard fuel rods.

Table 3-6. TRIGA SNF-Element Lengths

TRIGA SNF Type	Number of Rods	Length of Fuel Element		
		Range (in)	Maximum (in)	Maximum (cm)
TRIGA-AL	528^b			
Fuel		28.3 - 28.37	28.37	72.06
Instrument ^a		28.53	28.53	72.47
TRIGA-SS	1645^b			
Fuel		28.89 - 29.88	29.88	75.90
Instrument ^a		30 (33 ^a)	30 (33 ^a)	76.20 (83.82 ^a)
TRIGA-In	1376			
Fuel		30.5	30.5	77.47
Instrument ^a		30	30	76.20
Fuel-Follower				
Standard		45	5	114.30
ACPR		66.5	66.5	168.91

Source: DOE 1999c, p. 23

NOTES: ^a The instrument tubes have portions of the stainless steel lead-out tubes attached to the top end fitting. This may extend the length of the element by 3 inches.

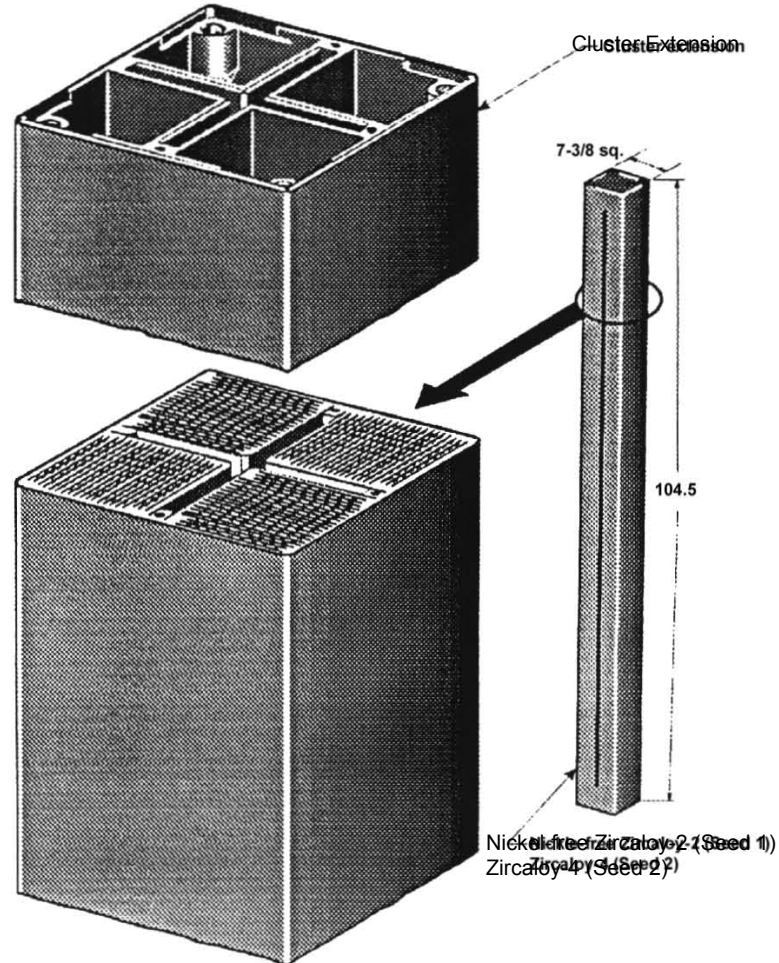
^b Does not include about 1,061 additional rods that have not been identified as either Al or stainless steel.

3.2.3 Shippingport PWR

The Shippingport PWR was a “seed and blanket” reactor, which underwent multiple modifications to provide higher thermal outputs. The blankets will be shipped and handled as bare assemblies. The low enrichments (less than 1 percent) allows use of the same packaging associated with either PWR or BWR commercial fuels (DOE 1999d, p. 1). Therefore, this report does not specifically address the disposal of blanket assemblies in the repository.

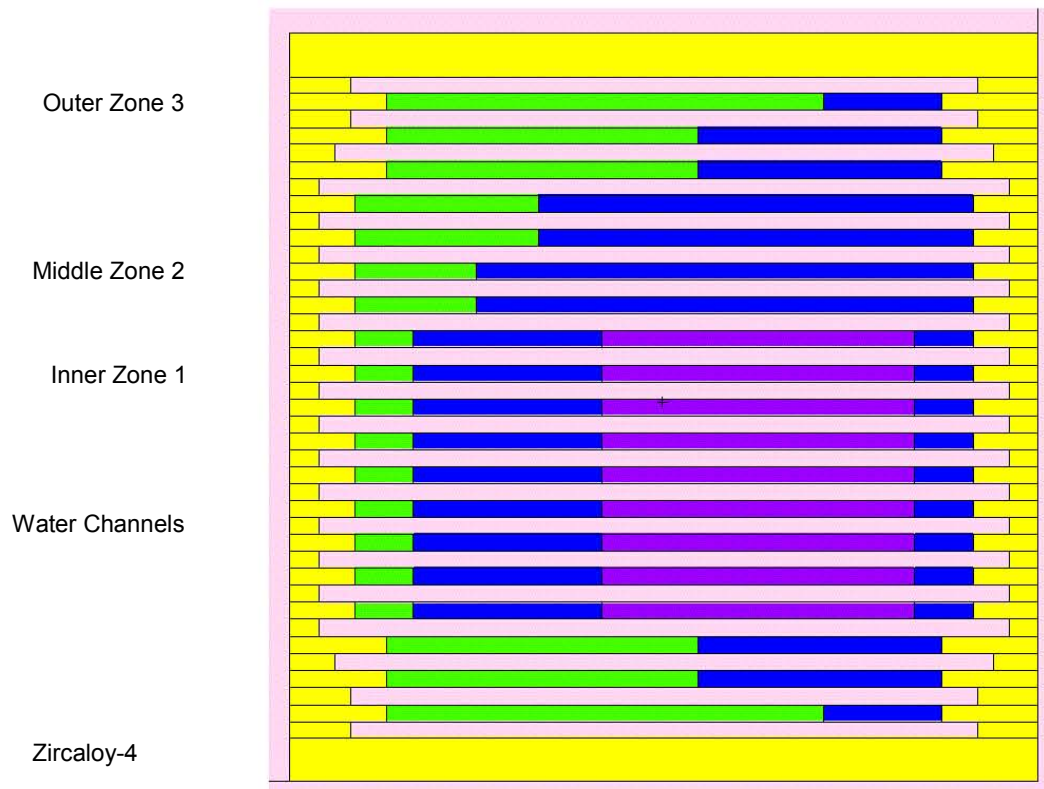
Two seeds, Seed 1 (S1) and Seed 2 (S2), which had identical geometrical dimensions but different ²³⁵U enrichment and chemical composition, were designed for Shippingport PWR Core 2 (C2) operation. The Shippingport PWR C2 S2 fuel assembly is shown in Figure 3-10 (DOE 1999d, p. 11). The assembly is composed of Zircaloy-4 and consists of four subassemblies and a cruciform-shaped channel in the center to accommodate a control rod. Figure 3-11 shows the cross-section of a single subassembly. Each subassembly is composed of 19 fuel plates and 20 channels. Each plate is formed by sandwiching an enriched U-Zr alloy strip between two Zircaloy-4 cover plates and four side strips. Note that there are five types of

fuel plates located in the assembly: end (Y), transition (T), secondary (W), standard (R), and intermediate (L). As shown in Table 3-7, the three assembly regions (i.e., Zones 1, 2, and 3) have different fissile loadings. Figure 3-12 gives a cross-sectional representation of a typical fuel plate (DOE 1999d, p. 10).



Source: DOE 1999d, Figure 3-2

Figure 3-10. Shippingport C2 S2 Spent Nuclear Fuel Assembly



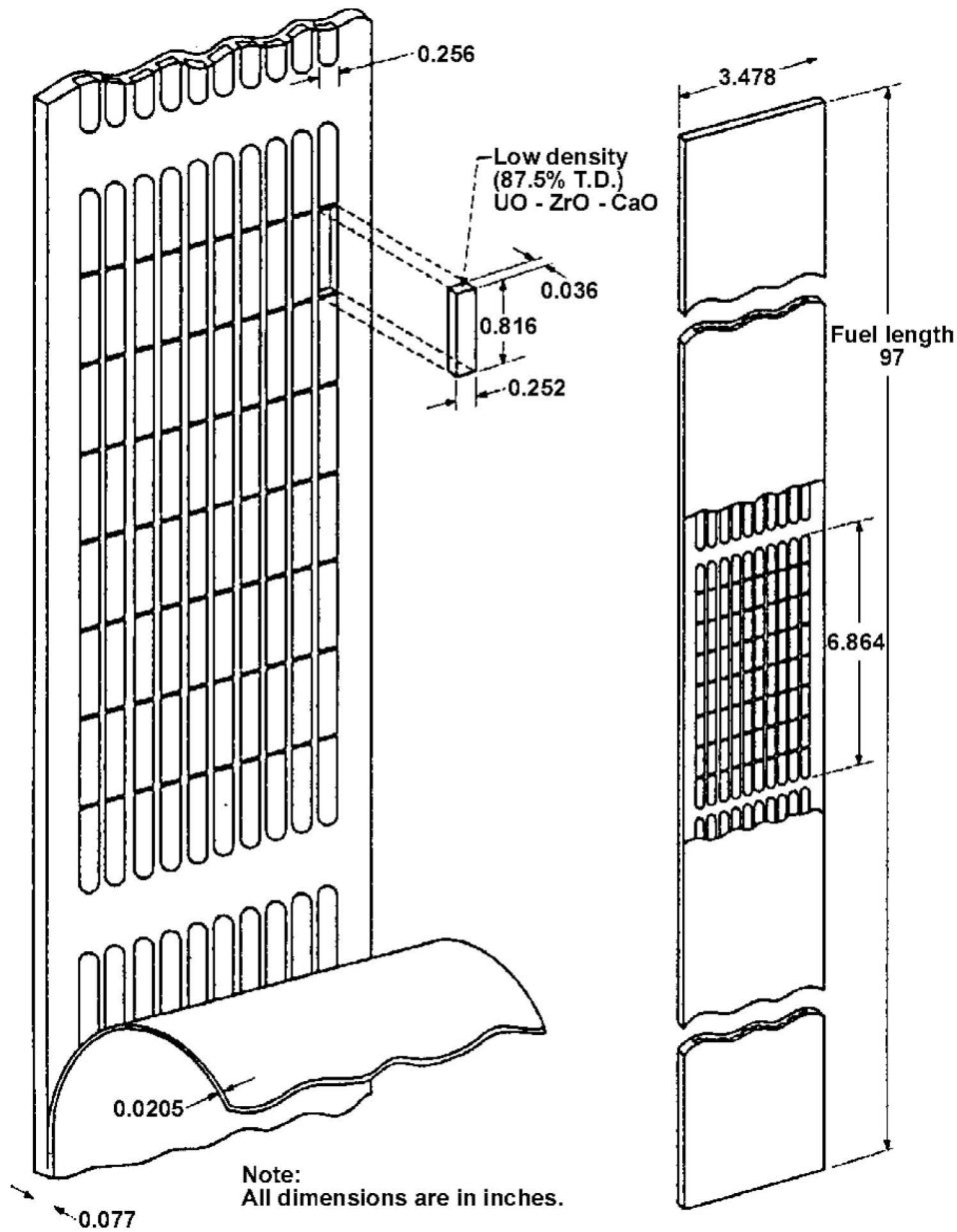
Source: DOE 1999d, Figure 3-3

Figure 3-11. Shippingport C2 S2 Spent Nuclear Fuel Subassembly Cross-Section

Table 3-7. Geometry and Material Specifications for the Shippingport C2 S2 Assembly

Component	Material	Characteristic	Value
Assembly		Total mass (kg)	357
		Length (cm)	265.43
		Transverse dimensions (cm)	18.7325
Fuel plate		Active fuel length (cm)	246.38
Fuel wafer	UO ₂ -ZrO ₂ -CaO 93.2% ²³⁵ U beginning of life (BOL) enrichment	Length (cm)	2.07264
		Width (cm)	0.64008
		Thickness (cm)	0.09144
Fuel Zone 1	UO ₂ -ZrO ₂ -CaO	weight (wt)% UO ₂	54.9
		wt% CaO	5.2
		wt% ZrO ₂	39.9
		Fissile loading (kg)	7.076
Fuel Zone 2	UO ₂ -ZrO ₂ -CaO	wt% UO ₂	40.2
		wt% CaO	5.8
		wt% ZrO ₂	54
		Fissile loading (kg)	8.987
Fuel Zone 3	UO ₂ -ZrO ₂ -CaO	wt% UO ₂	26.5
		wt% CaO	6.4
		wt% ZrO ₂	67.1
		Fissile loading (kg)	3.437
Borated stainless steel	Stainless Steel Type 304	Mass (g)	6,001
	¹⁰ B	Mass (g)	26
	¹¹ B	Mass (g)	114
Spacer rings	Inconel X	Mass (g)	546
Chrome plating	Cr	Mass (g)	325
Cladding	Zircaloy-4	—	—

Source: DOE 1999d, pp. 6, 7, 8, C-16, C-17, and C-18



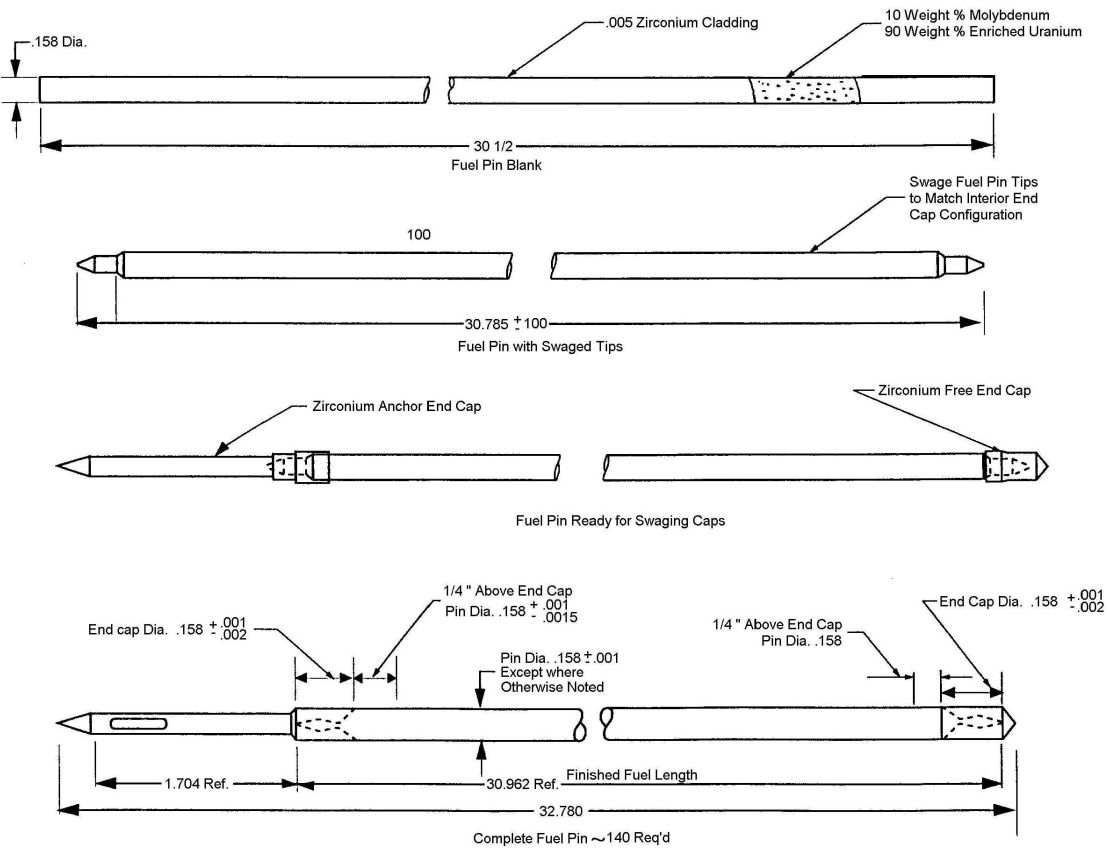
Source: DOE 1999d, Figure 3-1

Figure 3-12. Shippingport C2 S2 Spent Nuclear Fuel Fuel Plate

3.2.4 Enrico Fermi

The Enrico Fermi SNF fuel pin is made of a solid uranium-molybdenum alloy, 3.759 mm (0.148 in) in diameter, and is metallurgically bonded to a zirconium tube (i.e., no gaps). The zirconium cladding has a thickness of 5 mils (5 thousandth of an inch). The fuel material is 84.6 wt% uranium (enriched to a nominal 25.69 wt% ^{235}U), 10.22 wt% molybdenum, and the balance is zirconium cladding and impurities. The fuel pin mass is 159 grams, therefore a fuel section of 140 pins has a total mass of approximately 22.3 kg, of which 4.8 kg is ^{235}U . The fuel pins were

originally fabricated in lengths of 3.66 m (12 feet) or greater and were later cut into 774.7-mm (30.5-in) lengths. The ends of the pins were swaged to a point. Figure 3-13 shows the characteristics and dimensions of the fuel pin design.



Source: DOE 1999b, Figure 3.1-2

Figure 3-13. Enrico Fermi Fuel Pin Details (all dimensions are in inches)

Zirconium end caps were placed on the end of each pin and secured in place by cold swaging. The end caps were removed before storing the fuel in existing cans. The total length of the fuel pin after cold swaging (including the pointed swaged ends but without the free end caps) is 781.94 mm (30.785 in). The cold swaging process provides mechanical seal between the cladding on the pointed ends and the end cap to protect the U-Mo alloy.

3.2.5 Shippingport LWBR

The Shippingport LWBR was a “seed and blanket” reactor that used the movable seed fuel assemblies for the core reactivity control. The method of shipping and handling the blankets is yet to be decided. Therefore, the disposal of blanket assemblies in the repository has not been evaluated.

The source of the information in this section is *Shippingport LWBR (Th/U Oxide) Fuel Characteristics for Disposal Criticality Analysis* (DOE 1999e).

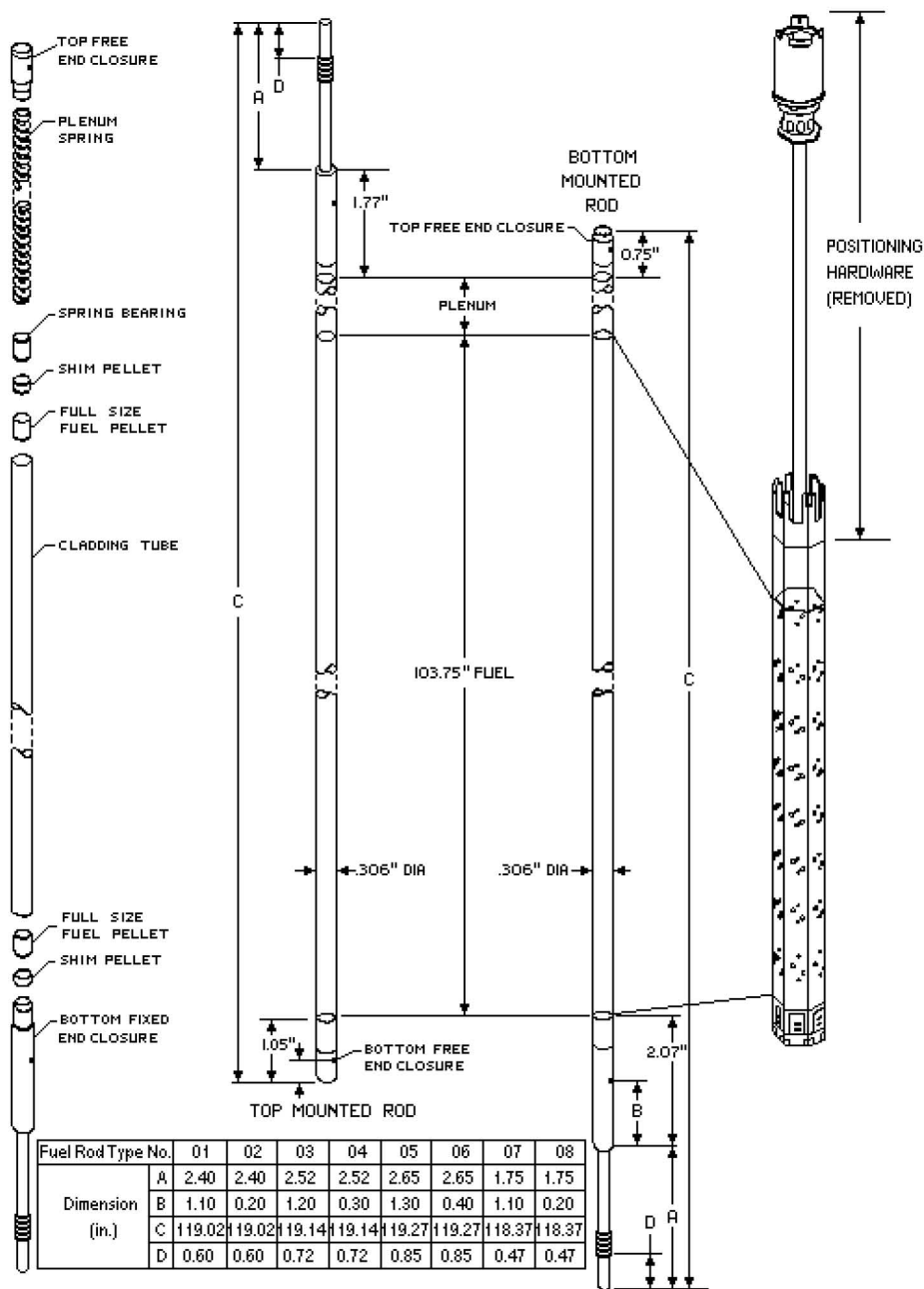
The Shippingport LWBR seed fuel assembly is shown in Figure 3-14. The LWBR core was fueled with fertile ^{232}Th and fissile ^{233}U , the relative concentrations of which varied axially and radially across the core to promote high neutron economy. The uranium that was used in fabricating the fuel was mostly ^{233}U , but some isotopic impurities were also present (Table 3-8). The design called for vertical fuel rods on a triangular pitch (i.e., the distance between the centers of two adjacent rods) with the space between taken up by circulating cooling water. The fuel rods featured cladding tubes loaded with cylindrical fuel pellets of thoria (ThO_2) or a binary mixture of thoria and UO_2 and backfilled with helium at one atmosphere during welding. The binary fuel is a solid solution fabricated from the two oxides in powder form. Processing of the well-mixed powder preparation achieved a nearly homogeneous structure owing to diffusion at elevated temperature during sintering. Axial variation in fissile material concentration was achieved by loading individual fuel rods such that part of the length bore a binary mixture of fissile and fertile material and the rest bore only fertile material. Radial variation was achieved by the arrangement of fuel rods that differed in their axial loading and by using binary pellets of different binary mixtures, depending on the radial location of the rod. Zircaloy-4 with hafnium content less than 40 ppm was used for the cladding tubes and all other structures in the fuel region, except the grids, which were made of AM-350 stainless steel. The fuel and fuel components suffered minimal damage during operation. Extensive destructive and nondestructive examinations after shutdown confirmed that the fuel was in good condition with minimal deformation of the cladding and minimal cracking of fuel pellets.

Table 3-8. Isotopic Composition of the Uranium

Isotope	Weight Percent (wt%)
U-232	<0.001
U-233	98.23
U-234	1.29
U-235	0.09
U-236	0.02
U-238	0.37

Source: DOE 1999e, Table 3-1

The as-built core was conceptually segregated into four regions. Although the relative concentrations of fissile and fertile material varied axially and radially within each region, the regions can be broadly described as follows: (1) the Seed Region constituted islands of fuel initially rich in ^{233}U ; (2) the Standard Blanket Region surrounded the islands of concentrated seed material with a fuel initially less rich in ^{233}U , and consequently richer in ^{232}Th ; (3) the Power Flattening Blanket Region enveloped the Seed and Standard Blanket Regions with fuel of



Source: DOE 1999e, Figure 3-9

Figure 3-14. Schematic Representation of Seed Fuel Assembly and Rods

3.2.5.1 Description of SNF from the Seed Region

Two different binary mixtures were used to fabricate the fuel in the Seed Region, resulting in binary fuel of higher and lower fissile concentrations. The tops and bottoms of the fuel rods

were stacked with ThO₂ pellets. Between the two fertile end stacks was a variable length binary ThO₂-UO₂ stack, which began 254 mm (10 in) from the bottom of the stack. Any given fuel rod contained fuel that was fabricated from only one of the two binary mixtures. Rods in the Seed Region were grouped into movable hexagonal seed assemblies, each of which contained 619 fuel rods. The twelve Seed assemblies together initially contained 198.59 kg of fissile material, with 61.28 kg in rods of the lower fissile concentration (low zone) and 137.31 kg in rods of the higher fissile concentration (high zone).

Fuel Pellets—Seed pellets were right circular cylinders, with chamfers (bevels) on both ends. The seed pellets had dished ends to reduce axial expansion of the stack. Fuel pellets in the Seed Region were smaller in diameter than pellets elsewhere in the core. Binary pellets of two different lengths and two different binary mixtures were used in the Seed Region. The shorter pellets were made of the binary mixture with the lower fissile concentration, while the longer pellets were made of the binary mixture of greater fissile concentration. The length of the thoria pellets was about midway between the two different lengths of the binary pellets. Much shorter thoria shim pellets were used near the top and bottom of the fuel stack to make up the desired stack length. A spring-bearing thoria pellet with only one dished end was used at the top of the fuel stack. During fabrication, the pellets were sintered to a large fraction of their theoretical densities to ensure dimensional stability. Table 3-9 gives dimensions and other characteristics for seed fuel pellets. The void fraction listed in Table 3-9 and elsewhere is defined as the fraction of the volume of a right circular cylindrical pellet of the nominal dimensions that is missing due to end dishes, chamfers, and pellet chips.

Table 3-9. Characteristics of Pellets in the Seed Region

Characteristic (units)	Seed Region Enrichment Zone		
	High	Low	ThO ₂
Diameter ^a (mm [in])	6.4008 (0.2520)	6.4008 (0.2520)	6.49224 (0.2556)
Diameter ^b (mm [in])	6.4008 ± .0127 (0.252 ± 0.0005)	6.4008 ± .0127 (0.252 ± 0.0005)	6.4897 ± .0127 (0.2555 ± .0005)
Length ^a (mm [in])	15.621 (0.615)	11.2776 (0.444)	13.462 (0.530)
Length ^b (mm [in])	15.621 ± .508 (0.615 ± .020)	11.303 ± .508 (0.445 ± .020)	13.462 ± .508 (0.530 ± .020)
Taper or Chamfer Depth ^b (mm [in])	0.381 ± 0.127 (0.015 ± 0.005)	0.381 ± 0.127 (0.015 ± 0.005)	0.381 ± 0.127 (0.015 ± 0.005)
Taper or Chamfer Length ^b (mm [in])	0.381 ± 0.127 (0.015 ± 0.005)	0.381 ± 0.127 (0.015 ± 0.005)	0.381 ± 0.127 (0.015 ± 0.005)
End Dish Spherical Radius ^b (mm [in])	9.144 (0.360)	9.144 (0.360)	7.5692 (0.298)
End Shoulder Width ^b (mm [in])	1.1684 ± 0.20 (0.046 ± 0.008)	1.1684 ± 0.20 (0.046 ± 0.008)	1.397 ± 0.254 (0.055 ± 0.010)
End Face Dish Depth ^b (mm [in])	0.2286 ± 0.0762 (0.009 ± 0.003)	0.2286 ± 0.0762 (0.009 ± 0.003)	0.2286 ± 0.0762 (0.009 ± 0.003)
Void Fraction ^a (of chamfers, dishes, and chip defects)	0.01172	0.01704	0.01253
Percent Theoretical Density ^a	97.554	97.712	98.013
Theoretical Density (g/cm ³)	10.042	10.035	9.999

Source: DOE 1999e, Table 3-5

NOTES: ^a Average as built.

^b Design specification.

Fuel Rods—Fuel rods from the Seed Region differed amongst themselves in several ways. A classification based on differences in the overall length of the rod and whether the rod was fixed to the seed assembly at the top or the bottom yields eight rod types (Figure 3-14, Table 3-10). Rods with odd type numbers were fixed to the bottom of the assembly, while even numbered rods were fixed at the top. The bottom 254 mm (10.0 in) of each stack consists of thoria pellets. The binary stack begins at the 254-mm level. Thoria pellets make up the rest of the stack above the binary stack. Total pellet stack length is 2635.25 mm (103.75 in). Other as-built characteristics of the Seed Region fuel rods are given in Table 3-11. The diameter of the mounting stems is not precisely known but historical documents imply that it does not exceed 5.766 mm (0.227 in). The seamless cladding tubes were welded at both ends to solid end plugs of Zircaloy-4. Cladding dimensions are given in Table 3-12. The cladding tubes in the Seed Region are freestanding; that is, they were designed to withstand operating pressures and temperatures without collapsing onto the pellet stack. However, irradiation of the rods caused a reduction in diameter of 0.03 to 0.06 mm (1.2 to 2.5 mils). Within the tube and above the pellet stack there is a 254 ± 2.54 -mm (10.0 ± 0.1 -in) plenum at the top of the fuel stack to accommodate fission gases. The plenum houses an Inconel X-750 wire compression spring (Table 3-13). The approximate masses of unirradiated fuel rod components for all core regions are given in Table 3-14.

Table 3-10. As-Built Characteristics of Seed Fuel Rods

Fuel Rod Type	Number per Assembly	Overall Length (mm [in])	Length of Fixed End Plug (mm [in])	Length of Mounting Stem (mm [in])	Length of Free-End Plug (mm [in])
01	30	3023.108 (119.02)	52.578 (2.07)	60.96 (2.40)	19.05 (0.75)
02	84	3023.108 (119.02)	44.958 (1.77)	60.96 (2.40)	26.67 (1.05)
03	72	3026.156 (119.14)	52.578 (2.07)	64.008 (2.52)	19.05 (0.75)
04	66	3026.156 (119.14)	44.958 (1.77)	64.008 (2.52)	26.67 (1.05)
05	181	3029.458 (119.27)	52.578 (2.07)	67.31 (2.65)	19.05 (0.75)
06	150	3029.458 (119.27)	44.958 (1.77)	67.31 (2.65)	26.67 (1.05)
07	30	3006.598 (118.37)	52.578 (2.07)	44.45 (1.75)	19.05 (0.75)
08	6	3006.598 (118.37)	44.958 (1.77)	44.45 (1.75)	26.67 (1.05)

Source: DOE 1999e, Table 3-6

Table 3-11. Further As-Built Characteristics of Fuel Rods in the Seed Region

Rod Type	Initial Fissile Mass Loading (g/rod)	Fissile Concentration of the Binary Stack ^a (wt% fissile)	Length of Binary Stack (mm [in])
01, 02, 07, 08	14.33	4.337	1066.8 (42)
03	19.14	4.337	1422.4 (56)
04	23.92	4.337	1778 (70)
05,06	34.57	5.202	2133.6 (84)

Source: DOE 1999e, Table 3-7

NOTE: ^a Weight percent fissile ($^{233}\text{U} + ^{235}\text{U}$)/(ThO₂+UO₂).

Table 3-12. Average As-Built Cladding Dimensions for all Core Regions

Core Region	Outside Diameter (mm [in])	Thickness (mm [in])
Seed	7.78002 (0.3063)	0.563118 (0.02217)
Standard Blanket	14.52118 (0.5717)	0.713232 (0.02808)
Power Flattening Blanket	13.39596 (0.5274)	0.671068 (0.02642)
Reflector	21.14042 (0.8323)	1.06426 (0.0419)

Source: DOE 1999e, Table 3-8

Table 3-13. Plenum Spring Dimensions for All Core Regions

Core Region	Number of Coils	Wire Diameter (mm [in])	Spring Diameter (mm [in])
Seed	190	1.0795 (0.0425)	5.2578 (0.207)
Standard Blanket	125	1.81102 (0.0713)	9.1694 (0.361)
Power Flattening Blanket	135	1.66624 (0.0656)	8.4328 (0.332)
Reflector	33	2.7686 (0.109)	13.3858 (0.527)

Source: DOE 1999e, Table 3-9

Table 3-14. Estimated Masses of Unirradiated Fuel Rod Components for All Core Regions

Core Region	Mass per Rod (kg)			
	Fuel Pellets	Cladding and End Caps	Internal Hardware	Total
Seed	0.83	0.27	0.02	1.12
Standard Blanket	3.38	0.69	0.14	4.21
Power Flattening Blanket	2.85	0.59	0.12	3.56
Reflector	6.94	1.47	0.12	8.53

Source: DOE 1999e, Table 3-10

Seed Assemblies—There were twelve nominally identical seed assemblies, or modules, in the Shippingport LWBR documentation. The categorization of modules into Types I through IV refers to the blanket and reflector assemblies, although seed assemblies can be categorized according to the same system due to their unique associations with particular blanket assemblies. The numbering of assemblies by Arabic numerals within each type gives each assembly a unique identifier. Key dimensions of the horizontal cross-sections of the various types of fuel assembly are given in *Shippingport LWBR (Th/U Oxide) Fuel Characteristics for Disposal Criticality Analysis* (DOE 1999e, p. 22). Figure 3-15 depicts the layout of the different types of fuel rod in the seed assemblies. The fuel rod in the center of a seed assembly is said to occupy the first row. Each successive hexagonal layer of rods wrapping around the central fuel rod forms another consecutively numbered row. The fuel of higher fissile concentration occupied the central eleven rows of the seed assemblies, where the binary stack length was at its maximum. Fuel rods bearing fuel of the lower fissile concentration occupied the remaining four outer rows. In the four outer rows, the binary stack length declined toward the edges of the assemblies. Base plates of Inconel 600 alloy held the fuel rods in position axially. Approximately half of the fuel rods were secured to the top base plate and the others were secured to the bottom base plate. The base plates were 38.1-mm (1.5-in) thick and were perforated to accept the rod mounting stems and to allow the flow of cooling water. Average as-built fissile masses in assemblies from all

core regions are given in Table 3-15. The quantities of thorium and uranium isotopes in the Seed assembly with the maximum fissile loading are given in Table 3-16.

Table 3-15. Average As-Built Fissile Loading of Assemblies from All Core Regions

Core Region	Average As-Built Fissile Loading (kg)		
	Type I	Type II	Type III
Seed	16.53	16.55	16.56
Blanket	16.18	25.00	29.85

Source: DOE 1999e, Table 3-11





Table 3-16. Composition of the Seed Assembly with Maximum Fissile Loading

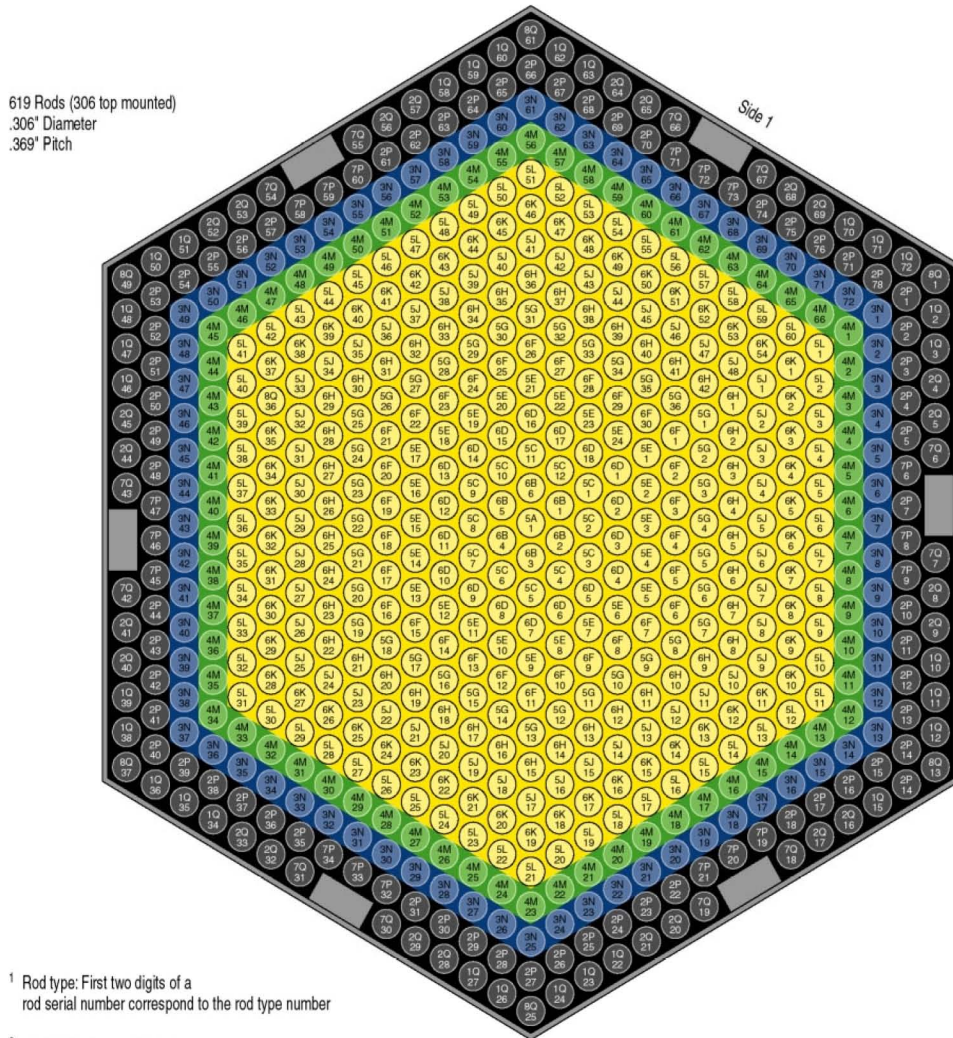
Nuclide	Mass (g)
²³² Th	434090
²³² U	0.10
²³³ U	16568.7
²³⁵ U	215.20
²³⁵ U	11.49
²³⁶ U	2.49
²³⁸ U	45.85
²³³ U+ ²³⁵ U	16580.2

Source: DOE 1999e, Table 3-12

A nominal 9.362-mm (0.3686-in) center-to-center spacing between fuel rods was maintained along the length of each seed assembly by nine AM-350 stainless steel grids. The uppermost grid was entirely above the fuel, and half of the lowermost grid was below the fuel. Leaving out the portions of the grids above and below pellet stacks, the grids displaced 2.130 cm³ (0.130 in³) of cooling water for each fuel rod in the seed assemblies. Grids in the seed region weighed, on average, 1,542 g each grid, whereas the assembly with the most massive grids had an average grid mass of 1,557 g.

The outer support shell of the seed assemblies was a 2.032-mm (0.080-in) thick hexagonal shell of Zircaloy-4. The length of the support shell may be taken to be 3,302 mm (130.00 in), though this length includes that of the bottom cover plate. The distance between the inner surfaces of the top and bottom base plates was 3,009.9 mm (118.500 in). The distance between the bottom of the assembly and the inner surface of the bottom base plate was greater than 111.76 mm (4.4 in) and less than 254 mm (10 in); halfway between the bounds (182.88 mm) is a reasonable approximation. For top- and bottom-mounted fuel rods, the distance to the bottom of the pellet stack from the inner surface of the bottom base plate is 52.578 mm (2.07 in). Therefore, the total distance between the bottom of the fuel assembly and the bottom of the fuel stack is approximately 235 mm. The maximum corner-to-corner width of the seed assemblies was 281.432 mm (11.08 in).

Rod Type ¹	Binary Stack Length	Enrichment (U-fissile wt %) ²	Theoretical Density (g/cm ³) ²	Mass Initial Fissile (g/Rod) ³	Number of Rods/Core	F
	05, 06	84°	5.195	10.042	34.57	3,972
	04	70°	4.327	10.035	23.92	792
	03	56°	4.327	10.035	19.14	864
	01, 02, 07, 08	42°	4.327	10.035	14.33	1,800
					7,428	



Source: DOE 1999e, p. 6

NOTE: ^a Rod type: First two digits of a rod serial number correspond to the rod type number. Illegibility does not impact the technical meaning or content of the record.

Figure 3-15. Layout of Fuel Rods in a Seed Assembly

Hardware removed from the seed assembly tops included the support shaft, the uppermost hexagonal portion of the assembly, the cover plate, and the top base plate bolts. The removal of mounting hardware from the assemblies necessitated the attachment of shipping plates at the tops so that the assemblies could be picked up. The shipping plates on the seed assemblies consist of 50.8-mm (2-in) thick rings of Stainless Steel Type 304 with 155.956-mm (6.140-in) inner diameter and 244.551-mm (9.628-in) outer diameter. There are a number of holes and recessions in the shipping plates. Of the many holes and recessions, the 9 largest are: 6 holes 14.224 mm (0.560 in) in diameter and 3 holes 25.4 mm (1.00 in) in diameter. Records of the total weights of intact assemblies in storage are available (DOE 1999e, Table 3-4). The intact assemblies, including attached shipping plates, are between 3,302 mm (130 in) and 3,327.4 mm (131 in) long, allowing for the 1-in maximum extent that the studs and nuts for attaching the shipping plates were allowed to protrude beyond the Zircaloy-4 support shell.

3.2.6 N-Reactor

Detailed information on N-Reactor fuel and MCO design used in this report is documented in *N-Reactor (U-metal) Fuel Characteristics for Disposal Criticality Analysis* (DOE 2000a). The N-Reactor core was fueled with slightly enriched (0.947 wt%, and 0.947 to 1.25 wt% ²³⁵U in Mark IV and Mark IA fuels, respectively) uranium metal clad with Zircaloy-2. Differences in the enrichment were selected based on the intended mode of reactor operation (i.e., plutonium or power production).

The N-Reactor fuel elements consist of the two basic design variants, both of which use two concentric tubes of uranium metal co-extruded with Zircaloy-2 cladding. Lengths and diameters vary slightly by fuel type; these differences are described in the following text. There is a special case of twelve Mark IA fuel elements that are the same maximum length as the longest Mark IV fuels (i.e., 66.3 cm [26.1 in]). The data contained in Table 3-17 is representative of the fuel “envelope” as it may affect packaging strategies.

3.2.6.1 Mark IV Fuel Details

Mark IV fuel elements (Figure 3-16) used two concentric tubes of uranium metal co-extruded into Zircaloy-2 cladding. The uranium enrichment for both layers was specified to be 0.947 wt% ²³⁵U, yielding an average uranium mass of 22.7 kg (50 lb) per element. These fuels had an outer diameter of 6.147 cm (2.42 in) and lengths varied (to facilitate reactor fuel loading configurations) as follows: 44, 59, 62, and 66 cm (17.4, 23.2, 24.6, and 26.1 in). The Mark IV fuel inner and outer elements have Zircaloy-2 end caps with an axial length of 0.48 cm (0.19 in) on each end. Table 3-17 gives the dimensions and material composition of the fuel elements.

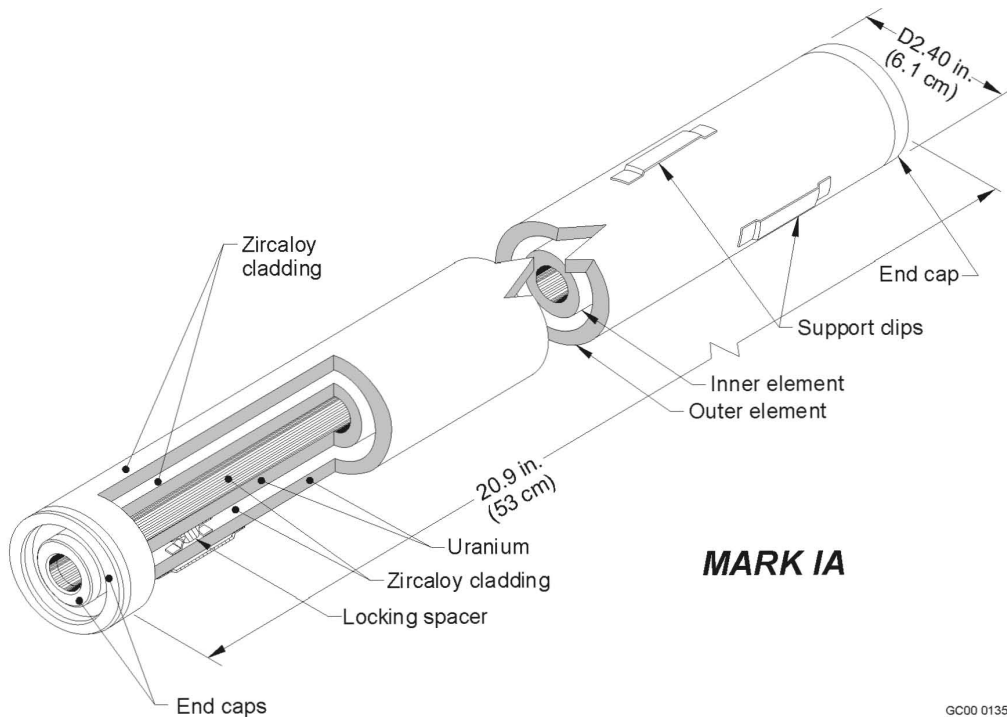
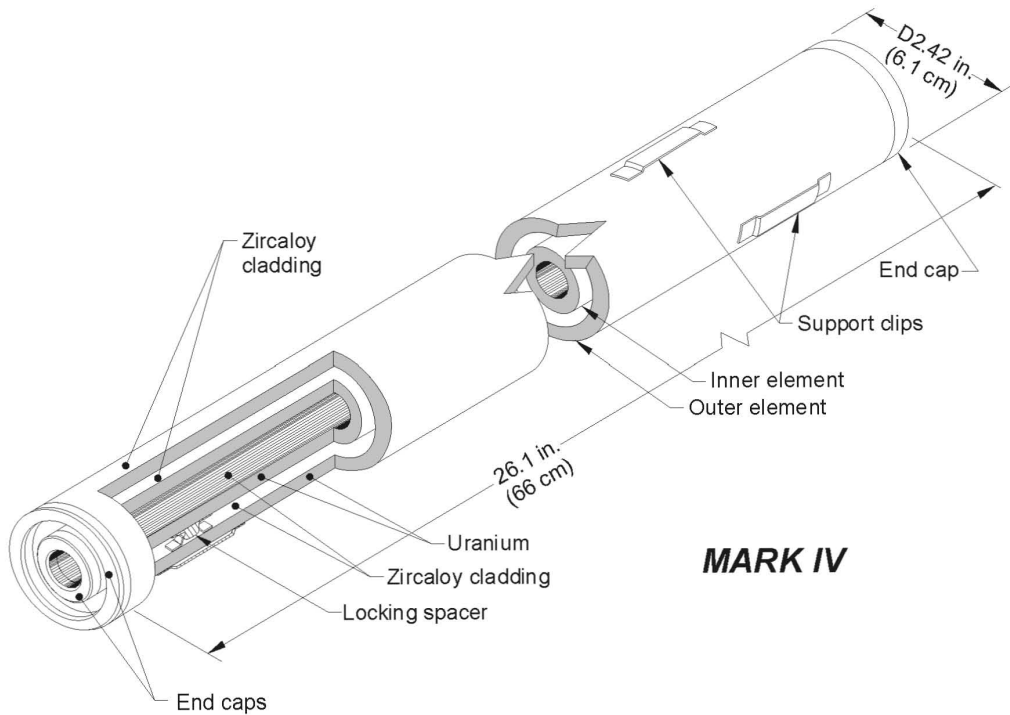
Table 3-17. N-Reactor Fresh Fuel Elements Description

	Mark IV				Mark IA			
Preirradiation enrichment of ²³⁵ U	0.947% enriched				0.947% and 1.25% enriched for the inner and outer of the fuel element, respectively			
Type-length code ^a	E	S	A	C	M	T	F	
Length, cm (in)	66 (26.1)	62 (24.6)	59 (23.2)	44 (17.4)	53 ^b (20.9)	50 (19.6)	38 (14.9)	
Element Diameter, mm (in)								
1. Outer of outer fuel element	61.47 (2.42)				60.96 (2.40)			
2. Inner of outer fuel element	43.18 (1.70)				44.96 (1.77)			
3. Outer of inner fuel element	32.51 (1.28)				31.75 (1.25)			
4. Inner of inner fuel element	12.19 (0.48)				11.18 (0.44)			
Cladding weight, kg (lb.)								
1. Outer element	1.094 (2.41)	1.041 (2.29)	0.991 (2.18)	0.791 (1.74)	0.882 (1.94)	0.832 (1.83)	0.659 (1.45)	
2. Inner element	0.550 (1.21)	0.523 (1.15)	0.500 (1.10)	0.400 (0.88)	0.536 (1.18)	0.509 (1.12)	0.405 (0.89)	
Weight of U in outer fuel element								
1. 0.947% ²³⁵ U,	kg (lb)	16.0 (35.2)	15.0 (33.1)	14.2 (31.2)	10.5 (23.1)	---	---	
2. 1.25% ²³⁵ U,	kg (lb)	---	---	---	---	11.1 (24.4)	10.4 (22.9)	
U isotopics		(0.947 wt%)				(1.25 wt%)		
²³⁵ U		0.9470				1.2500		
²³⁶ U		0.0392				0.0392		
²³⁸ U		99.0138				98.7108		
Weight of U in inner fuel element, kg @ 0.947% ²³⁵ U, (lb)		7.5 (16.5) (10.9)	7.0 (15.5)	6.6 (14.6)	5.0	5.5 (12.1)	5.1 (11.3)	3.9 (8.6)
Maximum weight of a fuel element, kg (lb)		25.15 (55.32)	23.65 (52.04)	22.31 (49.08)	16.65 (36.62)	18.01 (39.62)	16.89 (37.15)	12.84 (28.24)
Weighted average of U in a fuel element, kg (lb)		22.73 (50.0)				16.32 (35.9)		
Ratio of Zircaloy-2 to uranium, kg/MT		140	141.6	143.2	154.1	171.0	172.5	180.7

Source: DOE 2000a, p. 11

NOTES: ^a Letter code differentiates the various lengths of Mark IV or Mark IA fuel elements (i.e., a type “E” element is 26.1 inches long).

^b There are 12 Mark IA elements that have an overall length of 66.3 cm; they will be dealt with as a special case fuel loading in a Mark IV fuel basket.



GC00 0135

Source: DOE 2000a, Figure 3-1

Figure 3-16. Characteristic N-Reactor Fuel Types

The construction of the N-Reactor fuel elements includes the use of annular cylinders of co-extruded uranium with Zircaloy-2 cladding. This method of construction ultimately lead to the use of concentric tubes filled with uranium metal alloy and an inner and outer cladding with

attendant end caps. There is variability in the cladding thickness that is dependent not only on which tube is being examined but which fuel type. Table 3-18 provides a summary of calculated thickness based on specified dimensions of the fuel elements.

Table 3-18. Calculated Cladding Thickness for Mark IA and Mark IV Fuel Elements

	Mark IV cm, (inches)	Mark IA cm, (inches)
Outer layer - outer tube	0.0640 (0.0252)	0.0635 (0.0250)
Inner layer - outer tube	0.0505 (0.0199)	0.0555 (0.0219)
Outer layer - inner tube	0.0765 (0.0301)	0.1015 (0.0400)
Inner layer - inner tube	0.0510 (0.0201)	0.0635 (0.0250)
End cap thickness	0.4830 (0.1900)	0.4830 (0.1900)

Source: DOE 2000a, Table 3-2

3.2.6.2 Mark IA Fuel Details

The Mark IA fuels (Figure 3-16) are differentiated from the Mark IV fuel elements in that the outer concentric tube of uranium metal consists of 1.25 wt% enriched in ^{235}U ; the inner concentric tube still consists of a 0.947 wt% uranium enrichment. These fuels have a slightly smaller diameter of 6.096 cm (2.40 in) than the Mark IV fuels, and their U-metal weight of 16.3 kg (35.9 lbs.) is somewhat less than that found in the average Mark IV elements. Fuel lengths varied by the following values: 38, 50, or 53 cm (14.9, 19.6, and 20.9 in). An exception to these quoted lengths must include twelve Mark IA elements that measure 66.3 cm (26.1 in) long; a separate analysis has analyzed loading these special case fuels in a Mark IV basket configuration because of the added length. The Mark IA fuel element inner and outer elements have Zircaloy-2 end caps with an axial length of 0.483 cm (0.190 in) on each end.

Both Mark IV and Mark IA fuels were co-located in the N-Reactor during operation, with the more highly enriched Mark IA elements functioning as the seed or driver fuel.

3.2.7 Melt and Dilute

The information on MD ingots used in this report was obtained from *Statement of Work for DOE—Office of Civilian Radioactive Waste Management, Technical Assistance on Melt-Dilute Criticality and Shielding Analyses, Revision 2, May 30, 2001* (BSC 2001b). The MD ingots are homogeneous monolithic cylinders composed primarily of a U-Al alloy. These ingots will range in height from 381.0 to 762.0 mm (15 to 30 in) and will likely be contained in a plain carbon steel crucible liner. This liner will be standardized at approximately 508.0 to 762.0 mm (20 to 30 in). The crucible liner will have a maximum outer diameter of 393.7 to 419.1 mm (15.5-16.5 in) and a thickness of up to 12.5 mm (0.5 in). Due to uncertainty in the presence of a crucible liner, the analysis should consider a crucible liner thickness ranging from 0.0 mm (i.e., no liner) to 12.5 mm (0.5 in). The outer diameter and thickness of the crucible liner assumed in a given configuration will provide the outer diameter of the MD ingot. The mass of a MD ingot will be dictated by the geometry assumed for a given configuration assuming an ingot density of approximately 3 g/cm³ and an ingot porosity of 5 to 10 percent. Two general ingot compositions should be considered in the criticality and geochemistry analyses. The first composition is

13.2±5 wt% uranium, enriched at less than 20 wt% ²³⁵U and 0.5 wt% gadolinium metal, with the balance of the ingot being aluminum. The second composition is 13.2±5 wt% uranium, enriched at less than 20 wt% ²³⁵U, 0.5 wt% gadolinium metal, and 2.5 wt% hafnium metal, with the balance of the ingot being aluminum. Consideration is given for the presence of 2 wt% silicon and 3 wt% calcium. These considerations account for the silicate and oxide Al-based SNF forms. The values used for the MD ingots composition are presented in Table 3-19.

Table 3-19. Values Used for the MD Ingots Composition

Element	First Composition (wt%)	Second Composition (wt%)
U (20 wt% U-235)	18.2	18.2
Gd	0.5	0.5
Hf	0.0	2.5
Al (balance)	81.3	78.8

3.2.8 Fort Saint Vrain

The information on FSVR SNF used in this report is from *Fort Saint Vrain HTGR (Th/U Carbide) Fuel Characteristics for Disposal Criticality Analysis* (Taylor 2001).

3.2.8.1 Fuel Element Characteristics

There are four main types of FSVR fuel elements: standard elements, control elements, bottom control elements, and neutron source elements with the neutron sources removed. All four types are made of graphite and have the same external dimensions, but differ in mass, number of coolant holes, reactivity holes, and neutron source holes. No metallic components are present in the fuel elements. Descriptions of the physical characteristics of each element are shown in Table 3-20.

Table 3-20. Physical Characteristics of FSVR Fuel Elements

Characteristic	Control Element	Bottom Control Element	Standard Element
Approximate Mass (with fuel compacts/matrix, kg)	109	111	128
Graphite Body Mass (kg)	85	94	86
Number of Coolant Holes (12.7 mm and 15.9 mm diameter)	57	57	108
Number of Fuel Holes (12.7 mm diameter)	120	120	210
Fuel Hole Pitch (mm)	18.8	18.8	18.8
Number of Control Rod Drive Holes (101.6 mm diameter)	2	2	0
Number of Reserve Shutdown Holes (95.3 mm)	1	1	0

Source: Taylor 2001, Table 2-1

NOTE: The characteristics of the standard fuel elements are also applicable to the neutron source fuel elements.

The FSVR graphite blocks for the initial core were machined from H-327 graphite cylinders. The graphite was produced from needle coke filler material, pitch blend, and additives processed to minimize impurity content.

The FSVR fuel element (Figure 3-17) is hexagonal in cross-section with dimensions of 360.0 mm (14.172 in) across flats by 793.0 mm (31.22 in) high. The active fuel is contained in an array of small-diameter holes, which are parallel with the coolant channels, and occupy alternating positions in a triangular array within the graphite structure. The fuel holes are drilled from the top face of the element to within approximately 7.6 mm (0.3 in) of the bottom face. A cemented graphite plug that is 12.7 mm (0.5 in) long closes the top of each fuel channel after the fuel compacts were installed. The fuel holes in all elements are 12.7 mm (0.5 in) in diameter. The bonded rods (also referred to as “fuel compacts”) of coated fuel particles are stacked within the hole. These rods had a nominal dimension of 12.5 mm (0.49 in) in diameter. At least one standard fuel block used 3,130 compacts (which is the maximum number of compacts in a fuel block) to distribute the Th and U throughout the block. The fuel holes and coolant channels are distributed on a triangular array with a pitch of approximately 18.8 mm (0.74 in).

The control element is similar to the standard fuel elements, but contains enlarged channels for the two control rods and the reserve shutdown absorber material. The control rod channels have a 246.9 mm (9.72 in) centerline spacing and a diameter of 101.6 mm (4.0 in). The reserve shutdown channel has a diameter of 95.3 mm (3.75 in).

All of the standard elements have 12.7-mm (0.5-in) diameter holes in each of their six corners for possible insertion of burnable neutron absorber rods. All of the control and bottom control elements have similar holes on four corners for burnable neutron absorber rods. The burnable neutron absorber rods are 50.8-mm (2.0-in) long and 11.43 mm (0.45 in) in diameter, and are made of boron carbide particles in a carbon matrix. They are added as required and did not always fill the complete hole.

The lateral alignment of the six-layered fuel element column in the core is maintained by a system of three graphite dowels located on the top face of each element. A normal coolant channel passes through the center of each dowel. The dowels are threaded into the graphite structure and affixed with carbonaceous cement. Height of the dowels measured from the block surface is 22.2 mm (0.875 in). The bottom side of all fuel blocks have three dowel sockets for interlocking with the block underneath.

The fuel blocks are made of nuclear grade graphite, type H-327 (needle-coke graphite) or type H-451 (near-isotropic graphite). Dowels and plugs used in the fuel element are of the same type of graphite as the element.

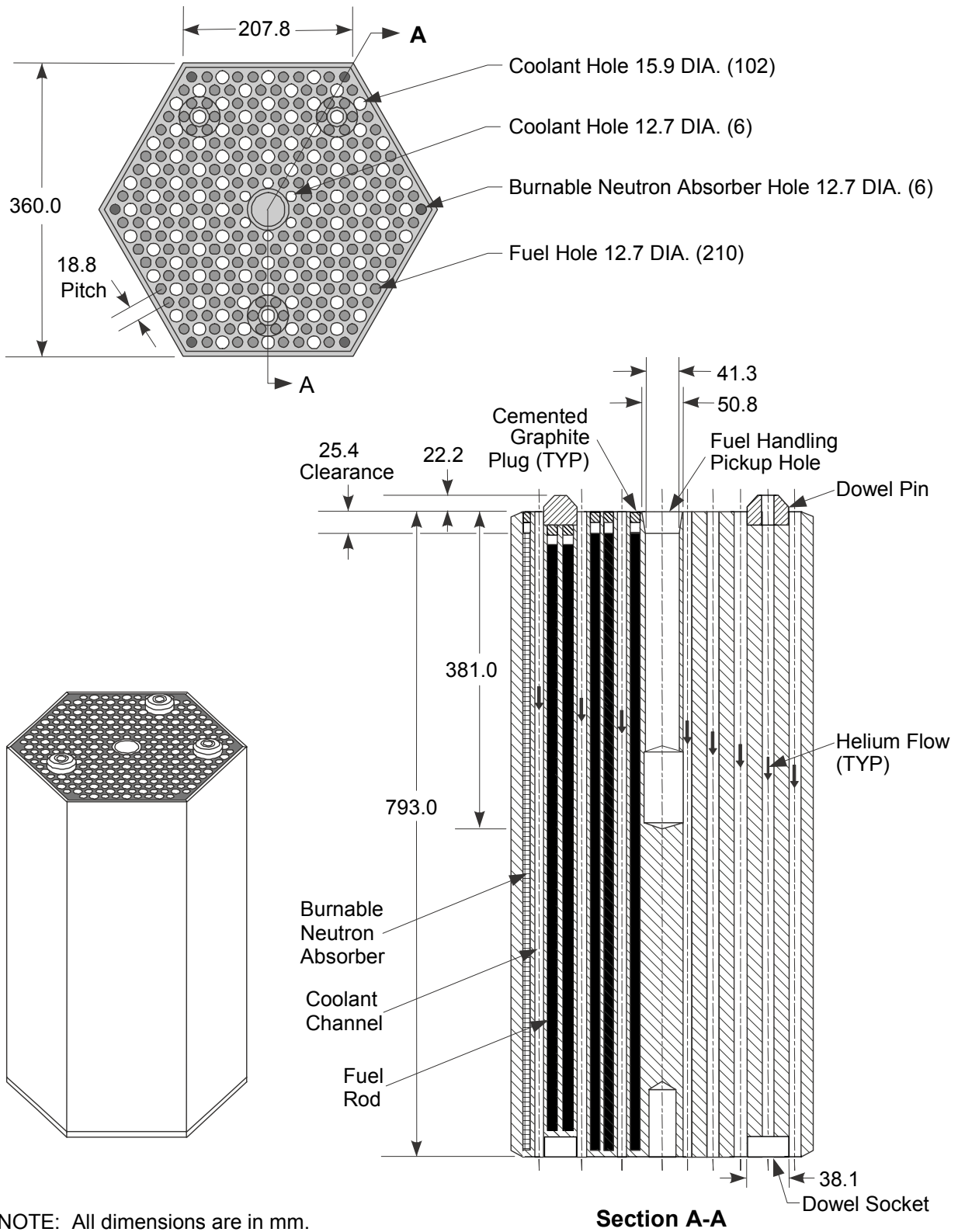


Figure 3-17. Standard FSVR Fuel Element

Based on the apparent (production) densities reported and a reported amorphous carbon density (maximum) of 2.1 g/cm^3 , there is a corresponding calculated porosity of the fuel block of 16.67 percent and 18.10 percent for H-451 and H-327 materials, respectively. The 18.10 percent porosity was used to calculate the maximum water uptake in a block for criticality modeling. Calculating void space within the fuel channels must also account for the interstitial gap between the fuel compacts and fuel channels, as well as the porosity of the compacts. The interstitial gap used to calculate void space between the compacts of 12.5 mm (0.49 in) diameter and the fuel channel of 12.7 mm (0.5 in) diameter represents a maximum gap. The fabrication techniques used materials similar to the graphite blocks, but the allowable macroporosity was specified to less than 45 percent for the compacts. The calculation for the displaced volume of the compacts also assumed a fuel column length of 15 compacts per fuel channel. In combination, these additive voids yield a calculated “porosity” or void volume of 50.76 percent within each fuel channel. While irradiation may have altered the properties of the compacts, the original displaced volume would remain the same within each sealed fuel channel.

3.2.8.2 Fuel Particles Characteristics

The fissile and fertile fuel particles are coated microspheres of uranium and thorium dicarbide. As shown in Figure 3-18, each fuel particle consists of a spherical kernel covered with four main layers of coating material plus a thin intermediate seal coating, which is not represented.

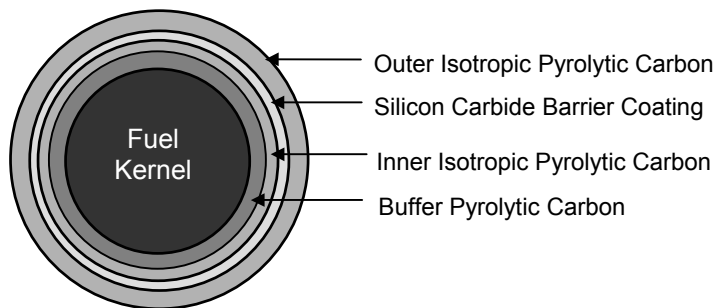


Figure 3-18. Cross-Section View of Fertile and Fissile Fuel Particles Used in FSVR

The maximum uranium load per FSVR fuel element at BOL was 1,485 g with a specified $93.15 \pm 0.15 \text{ wt\%}$ enrichment in ^{235}U , which results in a nominal 1,383.3 g of ^{235}U .

The graphite reactors are generally considered to be “converter” reactors, where a near-equivalent quantity of fissile atoms is produced as it is consumed. In the case of FSVR, this conversion resulted from the production of ^{233}U from ^{232}Th . ^{233}U is known to be more reactive than an equivalent gram quantity of ^{235}U , therefore it is reasonable to account for ^{233}U end of life (EOL) values in addition to any ^{235}U BOL values (since the DOE SNF is not taking burnup credits).

The average content of fertile and fissile species at BOL was 11.3 kg ^{232}Th per fuel block and 0.5 kg ^{235}U per fuel block. Specific data, on a block by block basis, indicates a BOL range of ^{235}U fissile loading values of 131.4 to 1,256.61 g, with a computed average of 574.4 g (Taylor 2001, Section 2.1.2.2 and Appendix B). The maximum uranium (total U with 93.15 wt% ^{235}U enrichment) was 1,485 g per fuel block.

Selection of the appropriate fissile loading is paramount to criticality analysis, both for fissile material accountability and storage/transportation issues for FSVR SNF. The production of ^{233}U is proportional to the ThO_2 loading and burnup, and inversely proportional to the UO_2 loading in a given element (i.e., lower ^{233}U production associated with higher ^{235}U loading).

For purposes of criticality safety evaluations, it is always the goal to describe and analyze the most reactive configuration. To this end, it will be necessary to identify the most reactive isotopic mixture given the blended quantities of ^{233}U and ^{235}U in the FSVR SNF. To establish a base-case fissile load limit per fuel element, there are three apparent combinations and one hypothetical set of values that should be analyzed for reactivity. The first three combinations are derived from the BOL ^{235}U load (maximum) and EOL ^{233}U load (associated maximum) and a similar construct reported in the FSVR fuel database (Taylor 2001, Appendix B). The following four isotopic combinations were evaluated and compared for maximum k_{eff} in the same MCNP representation (the load values are reported per fuel element):

- BOL ^{235}U load of 1,256.61 g, EOL ^{233}U load of 135.79 g.
- BOL ^{235}U load of 1,172.0 g, EOL ^{233}U load of 239.63 g; there should be a “defacto” ^{238}U composition of at least 73.8 g (from adjacent U group loading in database) since ^{235}U was never available in the 100 percent enrichments inferred in the database.
- BOL ^{235}U load of 1,168 g, EOL ^{233}U load of 248.95 g; use a “defacto” ^{238}U composition of at least 73.8 g.
- Total U load of 1,485.0 g with 93.15 wt% enrichment (from FSVR fuel specification); use 1,485.0 g BOL ^{235}U load as maximum case and EOL $^{233}\text{U} + ^{238}\text{U}$ load of 0.0 g.

The kernel dimensions, coating designations, and coating thickness for the fissile and fertile particles are listed in Table 3-21.

The various coatings applied to the outside of the fuel matrix are installed using vapor deposition from some combination of carbon-based gases in a heated fluidized bed. In the case of the application of SiC on a pyrolytically coated fuel particle, methyltrichlorosilane (CH_3SiCl_3) is fed into the fluidized-bed reactor at temperatures greater than or equal to $1,450^\circ\text{C}$ and less than or equal to $1,700^\circ\text{C}$. Coating thicknesses are controlled for a sample mean value of 20-30 μm , and the target density layer is greater than or equal to 3.18 g/cm^3 ; theoretical density of SiC is 3.217 g/cm^3 .

The theoretical density of ThC_2 is 8.96 g/cm^3 , and that of UC_2 is 11.28 g/cm^3 with production (fuel particle kernels) densities being greater than or equal to 8.8 g/cm^3 .

Table 3-21. FSVR Fuel Particle Characteristics (all dimensions are in μm)

Parameter	Fissile		Fertile	
	Small	Large	Small	Large
Th:U	3.6:1, 4.25:1		All Th	
Kernel composition	$(\text{Th:U})\text{C}_2$		ThC_2	
Average fuel kernel diameter	140	225	375	525
	100-275		300-500	
	220		490	
Seal layer	<5		<5	
Buffer carbon layer	50	50	50	50
	45-110		45-65	
	50		50	
Isotropic carbon layer	20	20	20	20
	20-30		20-40	
	20		20	
SiC layer	20	20	20	20
	20-30		20-30	
	20		20	
Isotropic carbon layer	30	40	40	50
	≥ 25		≥ 30	
	30		30	
Average coated fuel diameter	380	485	635	805
	460		730	
	460		730	

Source: Taylor 2001, Table 2-5

The porosity of the fuel matrix material can be calculated using the following expression:

$$\text{Porosity (\%)} = (\text{TD}-\text{PD}) \cdot 100/\text{TD}$$

where

TD = theoretical density

PD = production density of the respective U and Th materials.

For example, using the Th/U ratio equal to 3.6, $\text{TD} = (3.6 \cdot 8.96 + 1.0 \cdot 11.28)/(3.6 + 1.0) = 9.464 \text{ g/cm}^3$ and maximum porosity is 7.016 percent. For the Th/U ratio equal to 4.25, $\text{TD} = 9.402 \text{ g/cm}^3$ and porosity is 6.403 percent.

3.2.8.3 Fuel Rod Characteristics

A fuel rod is a column of coated fuel particles bonded together by a binder matrix. Fuel rods are cylinders 12.45 mm (0.49 in) in diameter and 49.276-mm (1.94-in) long. The chemical characteristics can be varied considerably depending upon blending ratios of the fuel kernels. For initial core loading, and the first reload segment, the FSVR fuel rod design utilized a homogeneous mixture of a graphite filler material and carbonized coal tar pitch as the binder. Beginning with the second reload (segment 8), petroleum-derived pitch was used as the binder, and isotropic shim particles, nominally 800 μm in diameter, were used to accommodate differences in heavy metal loading within the compacts. Hot injection molding process is the reference process for FSVR fuel rod fabrication.

The fuel rods and their individual fissile gram loading of ²³⁵U were controlled by the fuel blend number used during the extrusion process. Similarly, the fissile distributions within the individual fuel blocks were used to adjust the fuel block loading to effect reactor core flux leveling.

The individual fuel compact fissile loading in a fuel block may have incorporated either a single or binary fuel mix number as shown in the following table. The data in Table 3-22 incorporates prescribed fissile loading from the General Atomics FSVR fuel specification (for the first core).

Table 3-22. FSVR Fuel Compact Composition Used

Element		Compact Composition (g)	Comments
Thorium (as ThC ₂)		3.447	Based on 10,789.97 g Th (EOL), and 3,130 compacts per fuel element
Uranium (as ²³⁵ UC ₂)		0.474	Based on 1,485 g maximum total U (BOL) and 100% ²³⁵ U enrichment (combination 4 at page 3-42)
Silicon (as SiC)		0.800	Based on assumption of uniform coating on particles
Carbon	Pyrolytic Coating	4.100	Based on assumption of uniform coating on particles
	Compact Matrix	3.858	Calculated based on mass differences between loaded fuel elements (Table 3-20) and components
	Fuel Matrix	0.399	Calculated from ThC ₂ and UC ₂ masses (per compact)
	SiC Layer	0.341	Calculated as a percentage of SiC from reported pure Si mass

Source: Taylor 2001, Table 2-7

Postirradiation destructive examination was conducted on selected fuel compacts from a single fuel element, 1-0743. The fuel element experienced a burnup of 6.2 percent fissile and 0.3 percent fertile (from ²³³U during the transmutation of ²³²Th). The analysis reported that approximately 0.3 percent of the fissile and 0.2 percent of the fertile microspheres were failed. These failures were due to manufacturing defects such as no coating, cracks, thin coatings, etc. Approximately 3 percent of the compacts were broken; most of them were likely broken by the disassembly process involved by pushing them out from the bottom of the fuel block. These data were used in the criticality safety evaluations for cases where the FSVR was considered to be degraded (Section 10.2.8).

3.3 STRUCTURAL

A two-dimensional (three-dimensional for FSVR SNF) finite element representation of the waste package was developed to determine the effects of loads on the structural components due to a tip over design basis event. Calculations of maximum stress intensity for each waste package handling accident scenario (horizontal drop, vertical drop, and tip over design basis event) showed that the bounding dynamic load is obtained from a tip over case in which the rotating end of the waste package experiences the highest impact load. Therefore, the structural evaluations presented in this technical report are bounding for all handling-accident scenarios. The finite element representation was developed using the dimensions provided for each fuel type.

3.4 THERMAL

3.4.1 DHLW Glass

The thermal conductivity of the DHLW glass is conservatively approximated as that of pure borosilicate glass, while the density and specific heat are approximated as those of Pyrex glass (Assumption 5.2.9). The values of thermal conductivity, specific heat, and density for borosilicate glass are 1.1 W/m/K, 835.0 J/kg/K, and 2,225.0 kg/m³, respectively. The thermal conductivity is the mid-range value for a temperature range of 100°C to 500°C (CRWMS M&O 2000f, p. 28). The density and specific heat are taken to be the same as that of Pyrex glass at 27°C (300 K) (CRWMS M&O 2000f, p. 28).

The Hanford 4.5-m- (15-ft-) long DHLW canister heat output history was derived from the Hanford regular DHLW canister heat output and scaled up by a factor of 2.9155. This factor is based on the ratio of initial heat output from the Hanford long canister (Taylor 1997) to that of Hanford regular canister (CRWMS M&O 1997b, Attachment LI) ($2,540/871.2 = 2.9155$). The heat output rates used in the thermal analyses for the rest of the waste packages, for times up to a thousand years from emplacement are listed in Table 3-23.

Table 3-23. Heat Output History of a Hanford 4.5-m- (15-ft-) Long DHLW Glass Canister

Time Emplaced (years)	Values used for the FFTF, Shippingport PWR, and N-Reactor Waste Packages (W) ^a	Values used for the Shippingport LWBR Waste Package (W) ^b	Values used for the FSVR Waste Package (W) ^c
0	2540.0	1473.4	56.38
0.1	2461.6	1427.9	Value not available
0.2	2389.9	1386.3	Value not available
0.3	2324.0	1348.1	Value not available
0.4	2263.6	1313.1	Value not available
0.5	2208.2	1280.9	Value not available
0.6	2157.2	1251.4	Value not available
0.7	2110.0	1224.0	Value not available
0.8	2066.8	1198.9	Value not available
0.9	2026.9	1175.8	Value not available
1	1989.8	1154.3	55.08
2	1739.7	1009.2	53.78
3	1609.7	933.7	52.48
4	1530.4	887.7	51.28
5	1473.8	854.9	50.08
6	1428.3	828.5	48.88
7	1389.0	805.7	47.68
8	1353.7	785.2	46.58
9	1320.4	766.0	45.48
10	1289.0	747.7	44.38
15	Value not available	666.0	39.48
20	1024.8	594.5	34.98
30	819.0	475.1	27.68
40	657.2	381.2	21.78
50	529.5	307.1	17.27
60	429.2	249.0	13.67
70	349.9	202.9	10.77
80	287.5	166.8	8.56
90	237.9	138.0	6.79
100	199.1	115.5	5.41
200	61.8	35.9	0.72
300	41.7	24.2	0.26
400	33.2	19.3	0.21
500	27.4	15.9	0.19
600	22.4	13.0	0.18
700	18.4	10.7	0.17
800	15.2	8.8	0.16
900	12.5	7.3	0.15
1000	10.2	5.9	0.14

Sources: ^aValues from CRWMS M&O 1997b, Attachment LI, and multiplied by 2.9155

^bCRWMS M&O 2000e, Table 13.

^cCRWMS M&O 2000g, Attachment III.

The heat output rate history of a SRS DHLW glass canister Attachment LII of *Preliminary Design Basis for WP Thermal Analysis* (CRWMS M&O 1997b), is listed in Table 3-24.

Table 3-24. Heat Output History of an SRS 3.0-m- (10-ft-) Long DHLW Glass Canister

Time Emplaced (years)	Heat Output of a SRS DHLW Canister
0	710.1
0.1	699.2
0.2	689.0
0.3	679.6
0.4	670.8
0.5	662.6
0.6	654.9
0.7	647.7
0.8	641.0
0.9	634.8
1	628.9
2	585.9
3	559.9
4	541.5
5	526.7
6	513.7
7	501.7
8	490.4
9	479.4
10	468.8
20	376.0
30	302.5
40	244.2
50	198.0
60	161.2
70	131.9
80	108.5
90	89.82
100	74.84
200	18.33
300	8.15
400	4.55
500	2.79
600	1.87
700	1.37
800	1.11
900	0.96
1000	0.88

Source: CRWMS M&O 1997b, Attachment LII

3.4.2 FFTF

The total heat released from the fuel irradiated to 150 MWd/kgHM (megawatt day per kilogram of heavy metal) burnup is given in Table 3-25. The thermal properties of the FFTF fuel are determined as described in *Thermal Evaluation of the FFTF Codisposal Waste Package* (CRWMS M&O 1999c).

Table 3-25. FFTF Spent Nuclear Fuel Assembly Heat Output

Time	Type 4.1 Fuel (W/assembly)	Type 4.2 Fuel (W/assembly)
Discharge	2.367E+05	3.153E+05
1 year	1.521E+03	1.783E+03
5 years	2.307E+02	2.447E+02
10 years	1.388E+02	1.379E+02
20 years	1.135E+02	1.103E+02
30 years	9.992E+01	9.617E+01
40 years	8.928E+01	8.522E+01
50 years	8.064E+01	7.639E+01
60 years	7.356E+01	6.921E+01
100 years	5.588E+01	5.137E+01

Source: DOE 1998b, Table B-3

3.4.3 TRIGA

The heat output history for five burnup values is shown in Tables 3-26 and 3-27 for TRIGA-Al/Stainless Steel and TRIGA-SS FLIP, respectively (Sterbentz 1997, pp. 14 to 16). Table 3-26 lists data for low-enriched TRIGA-SS fuel with burnup values below the typical average values of 10 – 20 g ²³⁵U burnup. Table 3-26 lists an enrichment of 70.0 percent ²³⁵U with a burnup of 70.0 g ²³⁵U that is well in excess of typical fuel burnup.

The data in Table 3-27 show that for the highest burnup case, the heat output decreases from 2,459 W following removal from the core to 14.970 W after one year of decay, and to 1.777 W after 20 years.

Table 3-26. TRIGA-AI/SS Standard Assembly Heat Output as a Function of Decay Time and Burnup (Low Burnups)

Burnup Measure	Burnup per Single Fuel Element				
BU ^a : ²³⁵ U (g)	0.5	1.0	3.0	5.0	7.0
BU ^a : % ²³⁵ U	1.39	2.78	8.33	13.89	19.44
BU ^a : MWd	0.48	0.95	2.85	4.75	6.65
BU ^a : MWd/MTU	2,639	5,278	15,833	26,389	36,944
²³⁵ U Depletion ^b (g)	0.6	1.18	3.5	5.8	8.07
Decay Time (years)					
	Heat Output, Watts per Single Fuel Element				
0	20.670	40.820	121.400	200.200	277.600
1	0.079	0.157	0.489	0.845	1.225
5	0.018	0.036	0.120	0.217	0.330
10	0.014	0.028	0.091	0.163	0.244
20	0.011	0.022	0.068	0.118	0.172

Source: Sterbentz 1997, pp. 14 to 16

NOTES: ^a BU = Burnup or Fissioned ²³⁵U.
^b ²³⁵U Depletion = Depletion due to fission and transmutation.

Table 3-27. TRIGA-SS FLIP Heat Output as a Function of Decay Time and Burnup (High Burnups)

Burnup Measure	Burnup per Single Fuel Element						
BU ^a : ²³⁵ U (g)	5.0	10.0	20.0	40.0	45.0	50.0	70.0
BU ^a : % ²³⁵ U	3.65	7.3	14.6	29.2	32.85	36.5	51.09
BU ^a : MWd	4.75	9.50	19.00	38.01	42.76	47.51	66.52
BU ^a : MWd/MTU	24,235	48,481	96,962	193,920	218,170	242,410	339,370
²³⁵ U Depletion ^b (g)	6.1	12.1	24.2	47.82	53.63	59.4	81.84
Decay Time (years)							
	Heat Output, Watts per Single Fuel Element						
0	201.9	401.4	792.4	1,532	1,705	1,872	2,459
1	0.894	1.806	3.690	7.758	8.852	9.983	14.970
5	0.239	0.485	0.999	2.141	2.457	2.789	4.318
10	0.168	0.339	0.689	1.437	1.639	1.847	2.776
20	0.114	0.228	0.460	0.946	1.073	1.205	1.777

Source: Sterbentz 1997, pp. 14 to 16

NOTES: ^a BU = Burnup or Fissioned ²³⁵U.
^b ²³⁵U Depletion = Depletion due to fission and transmutation.

3.4.4 Shippingport PWR

The Shippingport PWR waste package contains five Hanford 4.5-m- (15-ft-) long DHLW glass canisters, with a heat output history given in Table 3-23, and one DOE SNF canister containing a single Shippingport PWR Core 2 Seed 2 SNF assembly. The heat output of the SNF assembly and the waste package are listed in Table 3-28.

Table 3-28. Heat Output of the Shippingport PWR Spent Nuclear Fuel and the Waste Package

Time Emplaced (years)	Shippingport Fuel Zone 1 (W)	Shippingport Fuel Zone 2 (W)	Shippingport Fuel Zone 3 (W)	Waste Package Total (W)
0	46.749	59.375	22.707	12828.8
0.1	46.749	59.375	22.707	12436.8
0.2	46.749	59.375	22.707	12078.3
0.3	46.749	59.375	22.707	11748.8
0.4	46.749	59.375	22.707	11446.8
0.5	46.749	59.375	22.707	11169.8
0.6	46.749	59.375	22.707	10914.8
0.7	46.749	59.375	22.707	10678.8
0.8	46.749	59.375	22.707	10462.8
0.9	46.749	59.375	22.707	10263.3
1	46.749	59.375	22.707	10077.8
2	46.749	59.375	22.707	8827.3
3	46.749	59.375	22.707	8177.3
4	46.749	59.375	22.707	7780.8
5	46.749	59.375	22.707	7497.8
6	46.749	59.375	22.707	7270.3
7	46.749	59.375	22.707	7073.8
8	46.749	59.375	22.707	6897.3
9	46.749	59.375	22.707	6730.8
10	46.749	59.375	22.707	6573.8
20	31.252	39.692	15.180	5210.1
30	31.252	39.692	15.180	4181.1
40	31.252	39.692	15.180	3372.1
50	31.252	39.692	15.180	2733.6
60	31.252	39.692	15.180	2232.1
70	31.252	39.692	15.180	1835.6
80	31.252	39.692	15.180	1523.6
90	31.252	39.692	15.180	1275.6
100	31.252	39.692	15.180	1081.6
200	31.252	39.692	15.180	395.1
300	31.252	39.692	15.180	294.6
400	31.252	39.692	15.180	252.1
500	31.252	39.692	15.180	223.1
600	31.252	39.692	15.180	198.1
700	31.252	39.692	15.180	178.1
800	31.252	39.692	15.180	162.1
900	31.252	39.692	15.180	148.6
1000	31.252	39.692	15.180	137.1

Source: CRWMS M&O 2000c, Table 2-5

3.4.5 Enrico Fermi

The waste package contains five SRS DHLW glass canisters, with a heat output history given in Table 3-24, and one DOE SNF canister containing twenty-four Enrico Fermi SNF sections (i.e., 3360 fuel pins) in two stacks with a maximum heat output history given in Appendix B of *Fermi*

(U-Mo) Fuel Characteristics for Disposal Criticality Analysis (DOE 1999b). The heat output of the Enrico Fermi SNF is equal to 1.1 watts per section of 140 fuel pins. Since the axial power peaking factor for the Fermi SNF is not known, a bounding value of 1.25 was used for the axial power peaking factor in the analysis. Table 3-29 lists the heat output of the Enrico Fermi SNF and the waste package.

Table 3-29. Heat Output History of the Enrico Fermi Spent Nuclear Fuel and the Waste Package

Time After Emplacement (years)	Enrico Fermi SNF (W/-04 canister)	Waste Package Total Heat Output (W)
0	1.1	3576.9
0.1	1.1	3522.4
0.2	1.1	3471.4
0.3	1.1	3424.4
0.4	1.1	3380.4
0.5	1.1	3339.4
0.6	1.1	3300.9
0.7	1.1	3264.9
0.8	1.1	3231.4
0.9	1.1	3200.4
1	1.1	3170.9
2	1.1	2955.9
3	1.1	2825.9
4	1.1	2733.9
5	1.1	2659.9
6	1.1	2594.9
7	1.1	2534.9
8	1.1	2478.4
9	1.1	2423.4
10	1.1	2370.4
20	1.1	1906.4
30	1.1	1538.9
40	1.1	1247.4
50	1.1	1016.4
60	1.1	832.4
70	1.1	685.9
80	1.1	568.9
90	1.1	475.5
100	1.1	400.6
200	1.1	118.1
300	1.1	67.2
400	1.1	49.2
500	1.1	40.4
600	1.1	35.8
700	1.1	33.3
800	1.1	32.0
900	1.1	31.2
1000	1.1	30.8

Source: CRWMS M&O 2000d, Table 5

3.4.6 Shippingport LWBR

The Shippingport PWR waste package contains five Hanford 4.5-m- (15-ft-) long DHLW glass canisters, with a heat output history given in Table 3-23, and one DOE SNF canister containing a single Shippingport LWBR SNF seed assembly. The heat output of Shippingport LWBR SNF and the waste package is listed in Table 3-30. The time of emplacement considered is year 2010.

Decay heat for intact assemblies can be estimated from predicted decay heat curves that were developed for the Shippingport LWBR SNF. The decay heat curves represent the decay heat generation rates as a function of cooling time for the hottest intact seed, blanket, and reflector assemblies. The maximum estimated heat generation rates for the various assemblies in 1992 (ten years after shutdown) are (DOE 1999e, p. 34):

Seed Assemblies (for 619 rods): 630 W (2,150 BTU/hr)
 Blanket Assemblies (for 564 rods): 527 W (1,800 BTU/hr)
 Reflector Assemblies (for 228 rods): 175 W (600 BTU/hr).

Estimates of axial thermal peaking factors can be derived from average and peak burnup data for individual fuel rods (see Table 3-31).

Table 3-30. Heat Output of the Shippingport LWBR Spent Nuclear Fuel and the Waste Package

Time After Emplacement (years)	Shippingport LWBR SNF Seed Assembly (W)	Waste Package Total (W)
0	640.0	8007.1
0.1	638.8 ^a	7778.4
0.2	637.7 ^a	7569.3
0.3	636.5 ^a	7377.0
0.4	635.4 ^a	7200.8
0.5	634.2 ^a	7038.9
0.6	633.0 ^a	6889.6
0.7	631.9 ^a	6751.7
0.8	630.7 ^a	6625.3
0.9	629.6 ^a	6508.4
1	628.4 ^a	6399.8
2	616.8 ^a	5662.6
3	605.2 ^a	5273.9
4	593.6 ^a	5032.3
5	582.0	4856.6
6	571.6 ^a	4714.3
7	561.2 ^a	4589.7
8	550.8 ^a	4477.0
9	540.4 ^a	4370.2
10	530.0	4268.5
15	482.0	3812.1
20	442.0	3414.4
30	442.0	2817.4
40	442.0	2348.1

Table 3-30. Heat Output of the Shippingport LWBR Spent Nuclear Fuel and the Waste Package
(Continued)

Time After Emplacement (years)	Shippingport LWBR SNF Seed Assembly (W)	Waste Package Total (W)
50	442.0	1977.7
60	442.0	1686.8
70	442.0	1456.7
80	442.0	1275.8
90	442.0	1132.0
100	442.0	1019.6
200	442.0	621.3
300	442.0	562.9
400	442.0	538.4
500	442.0	521.5
600	442.0	507.1
700	442.0	495.3
800	442.0	486.0
900	442.0	478.4
1000	442.0	471.6

Source: CRWMS M&O 2000d, Table 13

NOTE: ^a Value derived from linear interpolation between given values.

Table 3-31. Axial Peaking Factors Estimated from Peak and Average Burnups

Core Region	Peak Burnup (MWd/MTHM)	Maximum Rod Average Burnup (MWd/MTHM)	Estimated Axial Peaking Factor
Seed	53400	29800	1.79
Standard Blanket	23200	13200	1.76
Power Flattening Blanket	25200	14700	1.71
Reflector	4500	2200	2.05

Source: DOE 1999e, Table 3-22

3.4.7 N-Reactor

The boundary conditions used for the thermal analysis are as follow:

- The spacing between the waste packages is 0.1 m (BSC 2003d, p. 1)
- The repository will be ventilated for 50 years after initial emplacement. *Repository Design Project, Repository/PA IED Emplacement Drift Configuration 1 of 2* (BSC 2003d, p. 1) states that the repository will be ventilated for 50 years after final emplacement, therefore there will be more than 50 years of ventilation after the waste package containing N-Reactor SNF will be emplaced.
- There will be no backfill in the emplacement drift (Stroupe 2000, Attachment I).

The surface temperature history of the 2-MCO/2-DHLW waste package is given in Table 3-32.

Table 3-32. Upper Bound of the 2-MCO/2-DHLW Waste Package Surface Temperature

Time after Emplacement (years)	Waste Package Bottom Temperature (°C)	Waste Package Side Temperature (°C)	Waste Package Top Temperature (°C)
0.0	57.2	62.9	64.7
0.1	83.7	80.6	79.9
0.2	88.2	85.0	84.3
0.3	90.9	87.8	87.1
0.4	93.0	89.8	89.1
0.5	94.6	91.5	90.8
0.6	96.0	92.9	92.2
0.7	97.2	94.1	93.4
0.8	98.3	95.2	94.5
0.9	99.2	96.1	95.5
1	100.1	97.0	96.3
2	105.4	102.4	101.7
3	108.0	105.0	104.4
4	109.5	106.6	106.0
5	110.4	107.6	107.1
6	111.0	108.2	107.6
7	111.2	108.5	108.0
8	111.3	108.7	108.1
9	111.2	108.7	108.1
10	111.1	108.6	108.0
15	109.3	106.9	106.5
20	106.7	104.5	104.1
25	103.9	101.9	101.5
30	226.6	221.9	220.3
35	238.5	234.3	232.8
45	234.2	230.5	229.2
55	224.2	220.8	219.6
65	214.2	211.1	210.0
75	204.7	201.9	200.9
85	196.5	193.9	192.9
95	189.7	187.3	186.4
105	184.8	182.5	181.6
125	176.9	174.8	174.0
225	152.4	150.9	150.4
325	142.1	140.9	140.4
425	136.6	135.5	135.1
525	131.7	130.8	130.5
625	127.7	126.9	126.6
725	124.2	123.5	123.2
825	121.2	120.6	120.3
925	118.6	118.0	117.7
1025	116.5	116.0	115.8
2025	98.7	98.4	98.2
3025	92.2	92.0	91.9
4025	87.3	87.1	87.0
5025	83.7	83.5	83.4
6025	80.5	80.3	80.2
7025	78.1	77.9	77.8
8025	76.0	75.8	75.8
9025	73.5	73.3	73.2
10025	71.3	71.2	71.1

Source: CRWMS M&O 2000h, Attachment VI

Table 3-33 lists the heat output of the MCO and the waste package. For simplicity in thermal analysis, only the Mark IV fuel element is considered (Assumption 5.2.7). It is also assumed that the heat output of each fuel element remains at the value estimated for time of emplacement (Assumption 5.2.10). Both these assumptions are conservative. The heat output per spent nuclear fuel element is taken to be 776 watts (DOE 2000a, p. 16).

Table 3-33. 2-MCO/2-DHLW Waste Package Heat Output History

Time after Emplacement (years)	Per MCO (W)	Per Waste Package (W)
0.00	776.0	6632.0
0.10	776.0	6475.1
0.20	776.0	6331.7
0.30	776.0	6199.9
0.40	776.0	6079.2
0.50	776.0	5968.4
0.60	776.0	5866.4
0.70	776.0	5771.9
0.80	776.0	5685.6
0.90	776.0	5605.7
1.0	776.0	5531.7
2.0	776.0	5031.4
3.0	776.0	4771.3
4.0	776.0	4612.7
5.0	776.0	4499.6
6.0	776.0	4408.6
7.0	776.0	4329.9
8.0	776.0	4259.3
9.0	776.0	4192.9
10	776.0	4129.9
20	776.0	3601.6
30	776.0	3189.9
40	776.0	2866.3
50	776.0	2610.9
60	776.0	2410.3
70	776.0	2251.7
80	776.0	2126.9
90	776.0	2027.8
100	776.0	1950.3
200	776.0	1675.6
300	776.0	1635.4
400	776.0	1618.5
500	776.0	1606.8
600	776.0	1596.9
700	776.0	1588.7
800	776.0	1582.3
900	776.0	1577.1
1000	776.0	1572.4

Source: CRWMS M&O 2001a, Table 2-6

3.4.8 Melt and Dilute

No thermal analysis was performed for this fuel type.

3.4.9 FSVR

The FSVR waste package contains five Hanford 4.5-m- (15-ft-) long DHLW glass canisters, with a heat output history given in Table 3-23, and one DOE SNF canister containing up to five FSVR SNF elements. Table 3-34 lists the maximum heat output history of the FSVR waste package.

Table 3-34. Maximum Heat Output History of the FSVR Waste Package

Year	Heat Output (W / Waste Package)
2010	776
2020	620
2030	496
2040	398
2050	320
2060	258
2070	209
2080	170
2090	138
2100	113
2200	21.7
2300	8.15
2400	4.55
2500	3.08
2600	2.37
2700	1.99
2800	1.77
2900	1.63
3000	1.52
4000	1.13
5000	1.05
6000	1.02
7000	1.00
8000	0.986
9000	0.937
10000	0.960

Source: BSC 2001d, Table 5.3-2

The boundary conditions for the thermal analysis are:

- The spacing between the waste packages will be 0.1 m (BSC 2003d, p. 1).
- The repository will be ventilated for 50 years after initial emplacement. *Repository Design Project, Repository/PA IED Emplacement Drift Configuration 1 of 2* (BSC 2003d, p. 1) states that the repository will be ventilated for 50 years after final emplacement, therefore there will be more than 50 years of ventilation after the waste package containing FSVR SNF will be emplaced.
- There will be no backfill in the emplacement drift (Stroupe 2000, Attachment I).

The surface temperature of the waste package was taken from Table 6-18 in *Drift Scale Thermal Analysis* (CRWMS M&O 2000h) under the heading “Waste Package 1.” “Waste Package 1” was chosen because it most closely matches 5-DHLW/DOE SNF-long waste package with FSVR fuel output in terms of total heat generation and is bounding. This choice is conservative since “Waste Package 1” column is based on a heat source approximately three times than that of 5-DHLW/DOE SNF-long waste package with FSVR fuel, and the volume where the heat is generated is smaller. The temperatures used are listed in Table 3-35. The sudden increase in temperature at 50 years is due to the end of forced ventilation.

Table 3-35. FSVR Waste Package Boundary Conditions

Time Emplaced (years)	Temperature (°C)	Time Emplaced (years)	Temperature (°C)
0	36	50.6	126
0.1	56	50.7	128
0.2	62	50.8	129
0.3	65	50.9	130
0.4	67	51	131
0.5	69	52	141
0.6	71	53	148
0.7	72	54	152
0.8	74	55	155
0.9	75	56	158
1	76	57	161
2	83	58	162
3	86	59	163
4	88	60	163
5	90	70	163
6	91	80	163
7	92	90	159
8	92	100	155
9	92	110	152
10	93	120	150
15	92	130	147
20	91	140	144
25	89	150	141
30	87	250	128

Table 3-35. FSVR Waste Package Boundary Conditions (Continued)

Time Emplaced (years)	Temperature (°C)	Time Emplaced (years)	Temperature (°C)
35	85	350	123
40	83	450	119
45	82	550	116
50	80	650	113
50.01	87	750	110
50.02	95	850	109
50.03	100	950	107
50.04	103	1050	106
50.05	105	2050	93
50.06	107	3050	87
50.07	108	4050	83
50.08	110	5050	80
50.09	110	6050	77
50.1	111	7050	75
50.2	116	8050	73
50.3	119	9050	71
50.4	121	10050	69
50.5	124		

Source: CRWMS M&O 2000h, Table 6-18

3.5 SHIELDING SOURCE TERM

3.5.1 DHLW Glass

The SRS DHLW glass gamma and neutron source spectra per one 3.0-m- (10-ft-) long canister that were used for the dose calculations for TRIGA and Enrico Fermi waste packages were based on *DHLW Canister Source Terms for Waste Package Design* (CRWMS M&O 1997c, Attachment IX, p. 1 and Attachment X, p. 1).

The radiation source terms for the projected DHLW glass forms have been generated in *Source Terms for HLW Glass Canisters* (CRWMS M&O 2000g). The bounding radiation source term for all projected DHLW glass forms pertains to the Design-Basis glass from the DWPF at SRS (CRWMS 2000g, Attachments V and VI). The Design-Basis glass represents an upper bound in terms of the dose rate and the heat generation rate, expected from the DWPF canistered waste forms. Table 3-36 lists the gamma and neutron source terms per 3-m- (10-ft-) long SRS DHLW glass canister at year 2010.1.

Table 3-36. Gamma and Neutron Sources for a 3-m- (10-ft-) Long Canister Loaded with SRS DHLW Glass at Day One after Pouring

Gamma Source			Neutron Source		
Upper Energy Boundary (MeV)	Intensity Value Used for TRIGA, Enrico Fermi Waste Packages (photons/s) ^a	Intensity Value Used for Melt and Dilute Waste Packages (photons/s) ^b	Upper Energy Boundary (MeV)	Intensity Value Used for TRIGA, Enrico Fermi Waste Packages (neutrons/s) ^a	Intensity Value Used for Melt and Dilute Waste Packages (neutrons/s) ^b
0.05	1.3213E+15	1.29E+15	0.10	1.970E+05	1.54E+05
0.10	3.9581E+14	3.89E+14	0.40	1.893E+06	1.60E+06
0.20	3.0959E+14	3.02E+14	0.90	6.337E+06	5.58E+06
0.30	8.7394E+13	8.58E+13	1.40	6.919E+06	5.98E+06
0.40	6.3931E+13	6.27E+13	1.85	6.123E+06	5.21E+06
0.60	8.8265E+13	8.55E+13	3.00	2.614E+07	2.12E+07
0.80	1.3478E+15	1.34E+15	6.43	3.416E+07	2.74E+07
1.00	2.1344E+13	2.08E+13	20.00	3.069E+05	2.99E+05
1.33	2.9649E+13	2.91E+13			
1.66	6.4161E+12	6.18E+12			
2.00	5.1377E+11	4.86E+11			
2.50	2.9370E+12	2.70E+12			
3.00	2.0440E+10	1.91E+10			
4.00	2.2835E+09	2.15E+09			
5.00	5.2534E+05	5.20E+05			
6.50	2.1058E+05	2.09E+05			
8.00	4.1263E+04	4.09E+04			
10.00	8.7544E+03	8.67E+03			
Total	3.6750E+15	3.61E+15	Total	8.208E+07	6.74E+07

Source: ^a CRWMS M&O 1997c, Attachment IX, p. 1 and Attachment X, p. 1

^b CRWMS M&O 2000g, Attachment V, p. 1, and Attachment VI, p. 1

As the Design-Basis glass represents an upper bound in terms of the dose rate and the heat generation rate, expected from the DWPF canistered waste forms, it is assumed that the DHLW glass that fills the 4.5-m-long Hanford glass pour canisters is the SRS Design-Basis DHLW glass (Assumption 5.5.2). Therefore, the gamma and neutron source terms per one 4.5-m- (15-ft-) long Hanford DHLW glass canister (Tables 3-36 and 3-37) were obtained by multiplying the gamma and neutron source terms of the 3-m- (10-ft-) long SRS DHLW glass canister (Table 3-36) with the scale up factor given by Taylor (1997), which is $3.67/2.17=1.6912$.

Table 3-37. Gamma Sources for a Hanford 4.5-m- (15-ft-) Long DHLW Glass Canister at One Day Decay Time

Upper Energy Boundary (MeV)	Average Energy (MeV)	Intensity Value Used for FFTF, Shippingport PWR, and Shippingport LWBR Waste Packages (photons/sec) ^a	Intensity Value Used for N-Reactor Waste Package (photons/sec) ^b	Intensity Value Used for FSVR Waste Package (photons/sec) ^c
0.05	0.0300	2.0480E+15	2.23E+15	2.18E+15
0.10	0.0750	6.1351E+14	6.69E+14	6.58E+14
0.20	0.1500	4.7986E+14	5.24E+14	5.11E+14
0.30	0.2500	1.3546E+13	1.48E+14	1.45E+14
0.40	0.3500	9.9093E+13	1.08E+14	1.06E+14
0.60	0.5000	1.3681E+14	1.49E+14	1.45E+14
0.80	0.7000	2.0891E+15	2.28E+15	2.27E+15
1.00	0.9000	3.3083E+13	3.61E+13	3.52E+13
1.33	1.1650	4.5956E+13	5.01E+13	4.92E+13
1.66	1.4950	9.9450E+12	1.09E+13	1.05E+13
2.00	1.8300	7.9634E+11	8.69E+11	8.22E+11
2.50	2.2500	4.5524E+12	4.97E+12	4.57E+12
3.00	2.7500	3.1682E+10	3.46E+10	3.23E+10
4.00	3.5000	3.5394E+09	3.86E+09	3.64E+09
5.00	4.5000	8.1428E+09	8.88E+05	8.79E+05
6.50	5.7500	3.2640E+05	3.56E+05	3.53E+05
8.00	7.2500	6.3958E+04	6.98E+04	6.92E+04
10.00	9.0000	1.3569E+04	1.48E+04	1.47E+04
	Total	5.6962E+15	6.22E+15	6.11E+15

Source: ^a CRWMS M&O 1998b, Attachment III, p. 1.

^b Calculated by multiplying the gamma and neutron source terms of the 3-m-long SRS DHLW glass canister provided in CRWMS M&O 1997c, Attachment IX, p. 1 and Attachment X, p. 1) with the scale up factor given in Taylor 1997, which is $3.67/2.17=1.69$.

^c Calculated by multiplying the gamma and neutron source terms of the 3-m-long SRS DHLW glass canister provided in CRWMS M&O 2000g, Attachment V, p. 1 and Attachment VI, p. 1 with the scale up factor given in Taylor 1997, which is $3.67/2.17=1.69$.

Table 3-38. Neutron Sources for a Hanford DHLW Glass Canister at One Day Decay Time

Upper Energy Boundary (MeV)	Average Energy (MeV)	Intensity Value Used for FFTF, Shippingport PWR, and Shippingport LWBR Waste Packages (n/sec) ^a	Intensity Value Used for N-Reactor Waste Package (n/sec) ^b	Intensity Value Used for FSVR Waste Package (n/sec) ^c
0.100	0.0585	7.144E+04	3.33E+05	2.60E+05
0.400	0.2500	5.419E+05	3.20E+06	2.71E+06
0.900	0.6500	1.563E+06	1.07E+07	9.44E+06
1.400	1.1500	1.835E+06	1.17E+07	1.01E+07
1.850	1.6250	1.733E+06	1.04E+07	8.81E+06
3.000	2.4250	8.683E+06	4.42E+07	3.59E+07
6.430	4.7150	1.145E+07	5.78E+07	4.63E+07
20.000	13.2150	4.000E+04	5.19E+05	5.06E+05
	Total	2.591E+07	1.39E+08	1.14E+08

Source: ^a CRWMS M&O 1998b, Attachment III, p. 1.

^b Calculated by multiplying the gamma and neutron source terms of the 3-m-long SRS DHLW glass canister provided in CRWMS M&O 1997c, Attachment IX, p. 1 and Attachment X, p. 1 with the scale up factor given in Taylor 1997, which is $3.67/2.17=1.69$.

^c Calculated by multiplying the gamma and neutron source terms of the 3-m-long SRS DHLW glass canister provided in CRWMS M&O 2000g, Attachment V, p. 1 and Attachment VI, p. 1 with the scale up factor given in Taylor 1997, which is $3.67/2.17=1.69$.

3.5.2 FFTF

The maximum irradiation exposure of any standard DFA or test DFA is less than 150 MWd/kgHM. The photon spectrum for outer Type 4.1 and inner Type 4.2 DFAs with a burnup of 150 MWd/kgHM and 5 years decay are given in Table 3-39. The total neutron source for outer Type 4.1 and inner Type 4.2 DFAs with a burnup rate of 150 MWd/kgHM and 5 years decay are 5.532E+06 and 5.304E+06, respectively (DOE 1998b, Tables B-2 and B-3).

Table 3-39. Gamma and Neutron Sources for a FFTF Type 4.1 (Outer) Assembly at 150 MWd/kg Burnup (decay of 5 years)

Upper Energy Boundary (MeV)	Average Energy (MeV)	Type 4.1 (Outer) Assembly Gamma Intensity (photons/sec)	Type 4.2 (Inner) Assembly Gamma Intensity (photons/sec)
0.02	0.0150	3.948E+14	4.324E+14
0.03	0.0250	1.084E+14	1.192E+14
0.05	0.0375	1.088E+14	1.170E+14
0.07	0.0575	8.088E+13	8.850E+13
0.10	0.0850	5.942E+13	6.503E+13
0.15	0.1250	5.091E+13	5.659E+13
0.30	0.2250	4.498E+13	5.026E+13
0.45	0.3750	3.533E+13	3.936E+13
0.70	0.5750	6.744E+14	7.092E+14
1.00	0.8500	9.899E+13	1.168E+14
1.50	1.2500	3.812E+13	4.495E+13
2.00	1.7500	1.210E+12	1.394E+12
2.50	2.2500	6.720E+11	8.051E+11
3.00	2.7500	3.660E+10	4.274E+10
4.00	3.5000	4.726E+09	5.515E+09
6.00	5.0000	2.234E+05	2.147E+05
8.00	7.0000	2.564E+04	2.465E+04
14.00	11.0000	2.941E+03	2.827E+03
	Total	1.697E+15	1.842E+15

Source: DOE 1998b, Tables B-2 and B-3

3.5.3 TRIGA

The total photon spectrum from high-burnup and isotopics associated with TRIGA-SS FLIP element is given in Table 3-40. The source term is bounding because it is increasing with burnup and initial enrichment. The overall neutron source is given in Table 3-41. The sources are provided as a function of decay time. These data represent a TRIGA-SS FLIP Element with 70.0 percent ²³⁵U enrichment and a burnup of 70 grams of ²³⁵U (66.52 MWd).

Table 3-40. Total Gamma Source for the Maximum Burnup TRIGA-SS FLIP Element

Period		1-yr Cooled	5-yr Cooled	10-yr Cooled	20-yr Cooled
Upper Energy Boundaries (MeV)	Average Energy (MeV)	Total (photons/s)	Total (photons/s)	Total (photons/s)	Total (photons/s)
0.02	1.500E-02	3.850E+13	1.073E+13	8.53E+12	6.601E+12
0.03	2.500E-02	8.610E+12	2.354E+12	1.80E+12	1.368E+12
0.05	3.750E-02	9.140E+12	2.082E+12	1.59E+12	1.206E+12
0.07	5.750E-02	7.920E+12	2.079E+12	1.65E+12	1.286E+12
0.10	8.500E-02	5.520E+12	1.293E+12	1.00E+12	7.719E+11
0.15	1.250E-01	6.770E+12	1.039E+12	7.29E+11	5.355E+11
0.30	2.250E-01	4.570E+12	1.099E+12	8.60E+11	6.663E+11
0.45	3.750E-01	2.360E+12	5.486E+11	3.90E+11	2.898E+11
0.70	5.750E-01	1.840E+13	9.076E+12	6.47E+12	4.816E+12
1.00	8.500E-01	1.150E+13	1.666E+12	4.21E+11	9.894E+10
1.50	1.250E+00	1.150E+13	6.397E+12	3.31E+12	9.141E+11
2.00	1.750E+00	5.820E+10	8.556E+09	4.77E+09	2.629E+09
2.50	2.250E+00	2.280E+11	6.706E+09	1.03E+08	4.665E+06
3.00	2.750E+00	1.050E+09	6.073E+07	2.22E+06	3.578E+05
4.00	3.500E+00	1.120E+08	7.155E+06	2.34E+05	2.564E+03
6.00	5.000E+00	2.610E+03	1.714E+03	1.43E+03	9.914E+02
8.00	7.000E+00	3.000E+02	1.973E+02	1.64E+02	1.139E+02
14.0	1.100E+01	3.450E+01	2.264E+01	1.88E+01	1.306E+01
Totals	---	1.251E14	3.8385E+13	2.6754E+13	1.8556E+13

Source: DOE 1999c, p. B-7

Table 3-41. Neutron Source at 20-Year Decay Time for the TRIGA-SS FLIP SNF Element

Nuclide	20-yr Decay Time		
	Activity (Ci)	(α , n) Production (neutrons/s)	Spontaneous Fission Production (neutrons/s)
Bi-211	3.78E-08	5.51E-03	
Po-212	1.72E-05	1.84E+01	
Po-215	3.78E-08	2.57E-01	
Rn-219	3.78E-08	9.24E-03	
U-235	1.19E-04	9.71E-03	1.82E-02
U-238	1.83E-05	9.49E-04	6.43E-01
Pu-238	3.24E-00	1.31E+03	
Pu-239	9.35E-02	4.66E+01	4.70E-00
Pu-240	7.69E-02	2.70E+01	
Am-241	7.80E-01	4.57E+02	
Totals	---	1.86E+03	5.36E-00

Source: DOE 1999c, p. B-8

3.5.4 Shippingport PWR

Although the material and geometry specifications of the Shippingport PWR C2 S2 fuel assembly are used in the dose analysis, the gamma and neutron source terms are from the C2 S1 assembly. These sources are the bounding values for the Shippingport PWR fuel (DOE 1999d, pp. B-2 and B-3). Table 3-42 gives the details of the gamma sources and the total intensity of each component.

Table 3-42. Gamma and Neutron Sources of the Shippingport C2 S1 Fuel Assembly at Year 2005

Upper Energy Boundary (MeV)	Gamma Intensity (photons/s)			Neutron Intensity (neutrons/s)
	Activation Products	Actinides and Daughters	Fission Products	
0.02	2.8410E+10	4.5890E+12	5.3430E+14	
0.03	9.1100E+09	5.9580E+10	1.1110E+14	
0.05	3.4820E+09	1.6890E+10	9.7230E+13	
0.07	2.3590E+09	8.6340E+11	1.0380E+14	
0.10	9.3670E+08	1.1830E+10	6.2650E+13	
0.15	3.9480E+08	6.3100E+09	4.2030E+13	
0.30	5.9420E+08	4.4630E+09	5.4170E+13	
0.45	2.8350E+09	2.3510E+09	2.3530E+13	
0.70	3.5670E+09	6.3060E+07	3.9300E+14	
1.00	4.4320E+09	4.9280E+07	5.5290E+12	
1.50	7.6130E+11	8.5050E+06	3.1620E+12	
2.00	2.9270E+05	4.4900E+06	1.5510E+11	
2.50	4.0350E+06	3.5760E+05	1.0790E+07	
3.00	1.2490E+04	3.9030E+07	2.2920E+00	
4.00	4.1600E-08	1.8430E+05	2.9960E-01	
6.00	8.8690E-09	7.8270E+04	1.5730E-05	
8.00	5.7540E-10	8.9510E+03	1.0210E-06	
14.00	3.6390E-11	1.0240E+03	6.4560E-08	
Total	8.1743E+11	5.5540E+12	1.4370E+15	2.680E+06

Source: DOE 1999d, pp. B-2 and B-3

3.5.5 Enrico Fermi

The maximum exposure of any standard Fermi fuel assembly is less than 3,130 MWd/MTU. For a typical Fermi fuel assembly with a burnup rate of 3,130 MWd/mtU and 9,404-day decay time, the gamma spectrum is given in Table 3-43 and the total neutron source is 1.042E+03 neutrons/s (CRWMS M&O 1999d, p. 15).

Table 3-43. Gamma Sources for a Typical Fermi Spent Nuclear Fuel Assembly at 9,404-Day Cooling Time

Upper Energy Boundary (MeV)	Gamma Intensity, (photons/s)
0.02	4.984E+12
0.03	1.037E+12
0.05	9.112E+11
0.07	9.651E+11
0.10	5.861E+11
0.15	3.796E+11
0.30	5.008E+11
0.45	2.192E+11
0.70	3.824E+12
1.00	3.578E+10
1.50	4.807E+10
2.00	9.240E+08
2.50	2.921E+05
3.00	1.414E+04
4.00	6.003E+01
6.00	1.414E+01
8.00	1.516E+00
14.00	1.665E-01
Total	1.349E+13

Source: CRWMS M&O 1999d, p. 15

3.5.6 Shippingport LWBR

A burnup and decay simulation of the Shippingport LWBR seed assembly provided the radiation source terms as a function of cooling time (DOE 1999e, p. 34). The initial fissile loading of the simulated assembly is 16892.84 g, which is approximately 2 percent greater than the actual initial fissile loading. The simulated burnup for the assembly is 10,269.14 MWd. Table 3-44 presents the gamma radiation source terms of a Shippingport LWBR SNF seed assembly at year 2005. The total neutron intensity at year 2005 is 5.770E+08 neutrons/s (DOE 1999e, p. B-4). Estimates of axial radiation peaking factors can be derived from average and peak burnup data for individual fuel rods (Table 3-31).

Table 3-44. Gamma Source Terms of a Shippingport LWBR Spent Nuclear Fuel Seed Assembly at Year 2005

Mean Photon Energy (MeV)	Gamma Intensity (photons/s)		
	Activation Products	Actinides and Daughters	Fission Products
1.50E-02	1.208E+11	1.546E+13	1.123E+15
2.50E-02	1.034E+11	1.215E+12	2.340E+14
3.75E-02	6.585E+10	9.808E+11	2.006E+14
5.75E-02	1.967E+10	1.159E+12	2.185E+14
8.50E-02	1.187E+10	7.029E+12	1.322E+14
1.25E-01	5.647E+10	5.412E+11	8.913E+13
2.25E-01	1.869E+10	9.856E+12	1.143E+14
3.75E-01	4.747E+10	7.169E+11	4.979E+13
5.75E-01	7.054E+10	6.543E+12	7.568E+14
8.50E-01	6.130E+10	3.041E+12	1.275E+13
1.25E+00	3.202E+12	1.741E+11	7.310E+12
1.75E+00	1.979E+09	5.637E+11	3.450E+11
2.25E+00	1.662E+07	3.567E+05	2.293E+07
2.75E+00	5.144E+04	5.682E+12	1.706E+04
3.50E+00	1.468E-06	2.298E+04	2.219E+03
5.00E+00	5.276E-09	7.014E+03	2.227E-05
7.00E+00	3.423E-10	5.310E+02	1.445E-06
1.10E+01	2.165E-11	4.255E+01	9.138E-08
Total	3.781E+12	5.296E+13	2.939E+15

Source: DOE 1999e, pp. B-2 and B-3

3.5.7 N-Reactor

Table 3-45 presents the maximum gamma source term per MCO, which is provided in *N Reactor (U-Metal) Fuel Characteristics for Disposal Criticality Analysis* (DOE 2000a, p. 39). The maximum neutron source intensity per MCO is 1.17E+07 neutrons/s (DOE 2000a, p. 41).

Table 3-45. Maximum Gamma Source Term per MCO

Upper Energy Boundary (MeV)	Average Group Energy (MeV)	Gamma Intensity per MCO (photons/s)
0.02	1.50E-02	1.75E+15
0.03	2.50E-02	3.87E+14
0.05	3.75E-02	4.21E+14
0.07	5.75E-02	3.46E+14
0.10	8.50E-02	1.95E+14
0.15	1.25E-01	1.48E+14
0.30	2.25E-01	1.66E+14
0.45	3.75E-01	8.64E+13
0.70	6.62E-01	2.81E+15
1.00	8.50E-01	1.04E+14
1.50	1.25E+00	4.33E+13
2.00	1.75E+00	1.29E+12
2.50	2.25E+00	9.42E+10
3.00	2.75E+00	4.67E+09
4.00	3.50E+00	6.04E+08
6.00	5.00E+00	3.71E+05
8.00	7.00E+00	4.23E+04
14.00	1.10E+01	4.84E+03
Total		6.45E+15

Source: DOE 2000a, p. 39

3.5.8 Melt and Dilute

The gamma and neutron source terms are presented in Table 3-46. The radiation source terms, which are provided per kilogram of MD ingot, have been derived for several fuel assemblies of various high-enriched U-Al SNF types (BSC 2001b) and by selecting the values that generate the highest dose rate at the external surface of the DOE SNF canister. The calculations assumed a decay time of one year, which will conservatively bound all expected shipments of MD ingots to the repository.

Table 3-46. Gamma and Neutron Source Terms per Kilogram of Melt and Dilute Ingots

Photon Upper Energy Group Boundaries (MeV)	Gamma Intensity (photons/s)	Neutron Upper Energy Group Boundaries (MeV)	Neutron Intensity (neutrons/s)
0.05	2.1605E+13	0.10	0.0000E+00
0.10	7.0742E+12	0.40	1.7633E+04
0.20	7.3063E+12	0.90	9.0075E+04
0.30	1.6334E+12	1.40	8.2275E+04
0.40	1.2655E+12	1.85	6.0413E+04
0.60	7.0238E+12	3.00	1.0575E+05
0.80	1.8281E+13	6.43	9.6825E+04
1.00	2.7830E+12	20.00	8.6175E+03
1.33	4.1610E+11		
1.66	3.1092E+11		
2.00	2.3501E+10		
2.50	2.1331E+11		
3.00	8.7773E+08		
4.00	8.8118E+07		
5.00	1.4215E+04		
6.50	5.7054E+03		
8.00	1.1193E+03		
10.00	2.3766E+02		
Total	6.7936E+13	Total	4.6159E+05

Source: BSC 2001e, Table 14

3.5.9 FSVR

The gamma and neutron source terms of the FSVR SNF are presented in Table 3-47. The radiation source terms, which are provided per FSVR fuel element, have been calculated for a fuel element with maximum burnup. A bounding peaking factor has been applied to the calculations to conservatively consider the variation of the fuel irradiation flux during the fuel cycles (Taylor 2001, pp. 32 and 35). The dose rate evaluations used the radiation source terms at the time of fuel discharge, which conservatively bound all expected shipments of FSVR SNF to the repository.

Table 3-47. Gamma and Neutron Sources per FSVR Fuel Element

Photon Mean Energy ^a (MeV)	Gamma Intensity ^a (photons/s)	Neutron Energy Group Boundaries ^a (MeV)	Neutron Intensity ^a (neutrons/s)
3.00E-01	3.27E+13	0.00-0.10	0.000E+00
6.50E-01	4.68E+14	0.10-0.40	7.931E+03
1.13E+00	9.15E+12	0.40-0.90	4.067E+04
1.57E+00	4.22E+12	0.90-1.40	3.961E+04
2.00E+00	3.11E+12	1.40-1.85	3.274E+04
2.40E+00	5.58E+10	1.85-3.00	7.086E+04
2.80E+00	6.86E+09	3.00-6.43	5.263E+04
3.25E+00	7.81E+08	6.43-20.00	3.812E+03
3.75E+00	3.44E+05		
4.25E+00	7.70E-07		
4.75E+00	3.86E-07		
5.50E+00	2.86E-07		
Total	5.17E+14	Total	2.483E+05

Source: ^a Taylor 2001, pp. 35 and 36

3.6 MATERIAL COMPOSITIONS

The chemical compositions of the materials used in the analyses are given in Tables 3-48 through 3-56.

Table 3-48. Chemical Composition of ASTM B 575 (Alloy 22) (UNS N06022)

Element	Composition (wt%)	Value Used (wt%)
Carbon (C)	0.015 (max)	0.015
Manganese (Mn)	0.50 (max)	0.50
Silicon (Si)	0.08 (max)	0.08
Chromium (Cr)	20.0 - 22.5	21.25
Molybdenum (Mo)	12.5 - 14.5	13.5
Cobalt (Co)	2.50 (max)	2.50
Tungsten (W)	2.5 - 3.5	3.00
Vanadium (V)	0.35 (max)	0.35
Iron (Fe)	2.0 - 6.0	4.00
Phosphorus (P)	0.02 (max)	0.02
Sulfur (S)	0.02 (max)	0.02
Nickel (Ni)	Balance	54.765
Density = 8.69 g/cm³		

Source: DTN: MO0003RIB00071.000

Table 3-49. Chemical Composition of ASTM A 516 Grade 70 Carbon Steel (UNS K02700)

Element	Composition (wt%)	Value Used (wt%)
Carbon (C)	0.28 (max)	0.28
Manganese (Mn)	0.79-1.30	1.045
Phosphorus (P)	0.035 (max)	0.035
Sulfur (S)	0.035 (max)	0.035
Silicon (Si)	0.13-0.45	0.29
Iron (Fe)	Balance	98.325
Density = 7.85 g/cm³		

Source: DTN: MO9906RIB00053.000

Table 3-50. Chemical Composition of Stainless Steel Type 304

Element	Weight Percent Range	Value Used (wt%)
Carbon	0.08 (max)	0.080
Manganese	2.00 (max)	2.000
Phosphorus	0.045 (max)	0.045
Sulfur	0.03 (max)	0.030
Silicon	1.0 (max)	1.0
Chromium	18.00 – 20.00	19.000
Nickel	8.00 – 10.50	9.250
Nitrogen	0.10 (max)	0.100
Iron	68.495 (balance)	68.495
Density = 7.940 g/cm³		

Source: DTN: MO9906RIB00054.000

Table 3-51. Chemical Composition of Stainless Steel Type 304L (UNS S30403)

Element	Composition ^a (wt%)	Value Used (wt%)
Carbon (C)	0.03 (max)	0.03
Manganese (Mn)	2.00 (max)	2.00
Phosphorus (P)	0.045 (max)	0.045
Sulfur (S)	0.03 (max)	0.03
Silicon (Si)	0.75 (max)	0.75
Chromium (Cr)	18.00 - 20.00	19.00
Nickel (Ni)	8.00 - 12.00	10.00
Nitrogen (N)	0.10	0.10
Iron (Fe)	Balance	68.045
Density^b = 7.94 g/cm³		

Source: DTN: MO9906RIB00054.000

Table 3-52. Chemical Composition of SS Type 316L (UNS S31603)

Element	Composition ^a (wt%)	Value Used (wt%)
Carbon (C)	0.03 (max)	0.03
Manganese (Mn)	2.00 (max)	2.00
Phosphorus (P)	0.045 (max)	0.045
Sulfur (S)	0.03 (max)	0.03
Silicon (Si)	1.00 (max)	1.00
Chromium (Cr)	16.00 - 18.00	17.00
Nickel (Ni)	10.00 - 14.00	12.00
Molybdenum (Mo)	2.00 - 3.00	2.50
Nitrogen (N)	0.00	0.10 ^c
Iron (Fe)	Balance	65.295
Density^b = 7.98 g/cm³		

Source: DTN: MO9906RIB00054.000

Table 3-53. Chemical Composition of Zircaloy-2 (UNS R60802)

Element	Composition (wt %) ^a	Value Used (wt %)
Sn	1.20-1.70	1.45
Fe	0.07-0.20	0.135
Cr	0.05-0.15	0.10
Ni	0.03-0.08	0.055
O	0.09-0.16	0.125
Zr	Balance	98.135
Density^b = 6.55 g/cm³		

Source: DTN: MO9906RIB00048.000

Table 3-54. Chemical Composition of Zircaloy-4 (UNS R60804)

Element	Composition (wt%) ^a	Value Used (wt%)
Iron (Fe)	0.18-0.24	0.20
Chromium (Cr)	0.7-0.13	0.10
Iron and Chromium (Fe+Cr)	0.28-0.37	0.00
Tin (Sn)	1.2-1.7	1.40
Oxygen (O)	0.09-0.16	0.12
Zirconium (Zr)	Balance	98.18
Density^b = 6.56 g/cm³		

Source: DTN: MO9906RIB00048.000

Table 3-55. Composition of the Advanced Neutron Absorber Matrix

Element	Weight Percent	Element	Weight Percent
C	0.012	Mn	0.409
Si	0.065	Cr	17.369
Mo	11.034	Co	2.043
W	2.452	V	0.286
Fe	3.269	P	0.016
S	0.016	Gd	18.264
Ni	44.763		
Density^a = 8.55 g/cm³			

Source: CRWMS M&O 1999c, p. 22

NOTE: ^a The density is calculated using the density of the Alloy-22, the density of Gd, and the weight percentage of Gd in the Alloy-22.

Table 3-56. Chemical Composition of SRS DHLW Glass

Element/Isotope	Composition ^a (wt %)	Element/Isotope	Composition ^a (wt %)
O	4.4770E+01	Ni	7.3490E-01
U-234	3.2794E-04	Pb	6.0961E-02
U-235	4.3514E-03	Si	2.1888E+01
U-236	1.0415E-03	Th	1.8559E-01
U-238	1.8666E+00	Ti	5.9676E-01
Pu-238	5.1819E-03	Zn	6.4636E-02
Pu-239	1.2412E-02	B-10	5.9176E-01
Pu-240	2.2773E-03	B-11	2.6189E+00
Pu-241	9.6857E-04	Li-6	9.5955E-02
Pu-242	1.9168E-04	Li-7	1.3804E+00
Cs-133	4.0948E-02	F	3.1852E-02
Cs-135	5.1615E-03	Cu	1.5264E-01
Ba-137	1.1267E-01	Fe	7.3907E+00
Al	2.3318E+00	K	2.9887E+00
S	1.2945E-01	Mg	8.2475E-01
Ca	6.6188E-01	Mn	1.5577E+00
P	1.4059E-02	Na	8.6284E+00
Cr	8.2567E-02	Cl	1.1591E-01
Ag	5.0282E-02		
Density^b at 25 °C = 2.85 g/cm³			

NOTES: ^a CRWMS 1999d, p. 7.

^b The average glass density is 2.65 g/cm³ (CRWMS M&O 2000a). Stout and Leider (1991, p. 2.2.1.1-4) give an upper limit of the glass density of 2.85 g/cm³. The upper limit is the value used unless otherwise noted.

4 FUNCTIONS AND DESIGN CRITERIA

The design criteria are based on *DOE and Commercial Waste Package System Description Document* (BSC 2003a), hereafter referred to as the SDD. In this section, the key waste package design criteria from the SDD are identified for the following areas: structural, thermal, shielding, criticality within a breached but otherwise intact waste package, degradation and geochemistry, and criticality of a degraded waste package and waste form. These criteria are subject to verification.

The disposal container accommodates either five SRS 3.0-m- (10-ft-) short or Hanford 4.5-m- (15-ft-) long DHLW canisters and one DOE SNF canister containing FFTF, TRIGA, Shippingport PWR, Enrico Fermi, Shippingport LWBR, Melt and Dilute, or FSVR DOE SNF, or two Hanford 4.5-m- (15-ft-) long DHLW canisters and two DOE SNF canisters containing N-Reactor DOE SNF.

The disposal container consists of two cylinders; an inner cylinder that is made of Stainless Steel Type 316 (UNS S31600), and an outer cylinder that is made of Alloy 22 (UNS N06022).

4.1.1 Structural Criteria

4.1.1.1 The sealed waste package shall not breach during normal operations or during credible preclosure event sequences (BSC 2003a, Functional Requirement 3.1.1.1, Performance Requirement 1).

4.1.1.2 The waste package shall be designed and constructed to the codes and standards specified in Section 5.1.1 of *Project Design Criteria Document* (Minwalla 2003), which is the 1997 Addenda of *1995 ASME Boiler and Pressure Vessel Code* (ASME 1995) (BSC 2003a, Functional Requirement 3.1.1.1, Performance Requirement 2).

4.1.1.3 Normal operations and credible event sequence loads combinations are defined in *Project Design Criteria Document* (Minwalla 2003), Section 5.1.1, Table 5.1.1-1 (BSC 2003a, Functional Requirement 3.1.1.1, Performance Requirement 3).

The structural evaluation of the waste package shall include the load conditions identified in Table 4-1.

Table 4-1. Summary of Load Combinations for Normal and Hypothetical Accident Conditions for the Waste Package at the Repository on the Surface and to the Emplaced Condition

Applicable Initial Conditions							
	Ambient Temperature		Decay Heat ¹		Internal Pressure ²		Dead Weight ³
	116 °F	2 °F	Max.	Zero	Max.	Min.	
Vertical Lift ⁴	X		X		X		X
		X		X		X	X
Horizontal Lift ⁴	X		X		X		X
		X		X		X	X
Accident Conditions ⁵ (Event Sequences)							
Seismic – Frequency Category 2 Event ⁶	X		X		X		X
		X		X		X	X
Spherical object fall while vertical from 6.1 ft (2 m) of 5,100 lbs. (2.3 MT)	X		X		X		X
		X		X		X	X
Free drop Horizontal 7.3 ft (2.4 m) ⁷	X		X		X		X
		X		X		X	X
Free drop Vertical 6.1 ft (2.0 m) ⁷	X		X		X		X
		X		X		X	X
Tip Over Slap Down	X		X		X		X
		X		X		X	X
Free drop w/emplacement pallet 6 ft (2 m)	X		X		X		X
		X		X		X	X
Missile Impact from Internal source 1.1 lb (0.5 kg) at 15.7 ft/s (5.7 m/s)	X		X		X		X
		X		X		X	X
Rockfall while Horizontal 13,230 lbs. (6 MT)	X		X		X		X
		X		X		X	X
Thermal fire accident	X		X		X		X

- NOTES: ¹ Maximum Decay Heat may take credit for the time prior to arrival at the site or before closure for the waste form involved.
- ² Maximum internal pressure would be maximum pressure at waste package closure plus any additional pressure from failure of fuel and temperature increase.
- ³ Dead Weight will include the maximum weight for the specific type of waste package and will consider any significant loading deviations of weight distribution and center of gravity.
- ⁴ The waste package is lifted from one end in the vertical position and from both ends in the horizontal position as it is processed.
- ⁵ Event sequences include those events identified below. These will be taken one event at a time since after an event sequence occurs, work will be stopped until a recovery plan is developed.
- ⁶ If the waste package survives the Frequency Category II Event provided in Minwalla 2003, Section 6.1.3, it can be assumed to survive the Frequency Category I Event.
- ⁷ Drop accidents should evaluate the waste package for any drop from the indicated position or condition onto a flat unyielding horizontal surface. The waste package should strike the surface in a position that is expected to inflict maximum damage. Impacts with the maximum and minimum weight of contents should be considered.

4.1.1.4 Normal operations and event sequence loads combinations are defined in Table 5.1.1-2 of *Project Design Criteria Document* (Minwalla 2003) (BSC 2003a, Functional Requirement 3.1.1.2, Performance Requirement 3).

The structural evaluation of the waste package shall include the load conditions identified in Table 4-2.

Table 4-2. Summary of Load Combinations for Normal and Hypothetical Accident Conditions for the Waste Package at the Repository in the Emplaced Postclosure Condition on Pallet

Applicable Initial Conditions							
	Ambient Temperature		Decay Heat ¹		Internal Pressure ²		Dead Weight ³
	116 °F	2 °F	Max.	Zero	Max.	Min.	
Static on pallet	X		X		X		X
		X		X		X	X
Accident Conditions							
Postclosure Seismic Event	X		X		X		X
		X		X		X	X

- NOTES: ¹ Maximum Decay Heat may take credit for the time prior to arrival at the site or before closure for the waste form involved.
² Maximum internal pressure would be maximum pressure at waste package closure plus any additional pressure from failure of fuel and temperature increase.
³ Dead Weight will include the maximum weight for the specific type of waste package and will consider any significant loading deviations of weight distribution and center of gravity.

Calculations of maximum potential energy for each handling accident scenario (horizontal drop, vertical drop, and tip over design-basis events) show that the bounding dynamic load is obtained from a tip over case in which the waste package experiences the highest impact load with maximum rotational velocity of 1.89 rad/s (CRWMS M&O 2000a, p. 14). This equates to a maximum velocity of the rotating top end of the waste package of 9.86 m/s ($v = r \cdot \omega$, where r is the length of the waste package and ω is the rotational velocity in rad/s). The maximum velocities of the waste package for 2.4-m horizontal and 2.0-m vertical drops are approximately 6.86 m/s ($v = \sqrt{2 \cdot g \cdot h}$, where g is the gravitational acceleration and h is drop height) and 6.26 m/s, respectively. Therefore, tip over structural evaluations are bounding for all waste package handling accident scenarios.

The tip over design-basis event may only take place during a waste package transfer operation from vertical to horizontal position (just after waste package closure) or horizontal to vertical position (upon retrieval).

4.1.2 Thermal Criteria

4.1.2.1 The maximum cladding temperature limit is 350°C, as specified in Section 5.1.3.2 in *Project Design Criteria Document* (Minwalla 2003).

4.1.2.2 The maximum waste package power at emplacement is 11.8 kW (BSC 2003a, Functional Requirement 3.1.1.5).

4.1.3 Shielding Criteria

There are no shielding criteria in the SDD to address.

4.1.4 Degradation and Geochemistry Criteria

There are no degradation and geochemistry criteria in the SDD to address.

4.1.5 Intact and Degraded Criticality Criteria

According to Functional Requirement 3.1.1.5 in *DOE and Commercial Waste Package System Description Document* (BSC 2003a), the sealed waste package shall provide criticality control.

5 ASSUMPTIONS

In the course of developing the evaluations of codisposal viability for the DOE SNF, assumptions were made regarding the waste package structural, thermal, shielding, intact criticality, degradation and geochemistry, and degraded component criticality analyses. These assumptions were used in the various calculations and analyses that support this report, and are not used directly in this report. The listing of assumptions that are essential to these calculations analyses is provided below.

5.1 STRUCTURAL

5.1.1 The Viability Assessment Design Waste Package Containment Barriers Have Solid Connections at the Adjacent Surfaces

Assumption: The Viability Assessment design waste package containment barriers have solid connections at the adjacent surfaces.

Rationale: The inner and outer barriers will be either shrunk fit or the inner barrier will be weld cladding onto the outer barrier inner surface (CRWMS M&O 1997a). For each one of these fabrication processes, it is reasonable to assume solid contact between the barriers. Newer designs have a 0 to 4-mm gap between barriers. However, gaps within this range are negligible for the structural analysis, therefore the solid contact assumption between barriers is still applicable.

Confirmation Status: This assumption refers to the Viability Assessment design, which is superseded by the License Application design, and does not require confirmation.

Use in the Analysis: This assumption is used in Section 7.

5.1.2 Target Surface Elastic Characteristics

Assumption: The target surface is unyielding and the target surface material has a large elastic modulus compared to the waste package materials.

Rationale: A bounding set of results was required in terms of stresses, and it was known that the use of an unyielding surface with high stiffness conservatively ensures slightly higher stresses in the waste package.

Confirmation Status: This assumption does not require confirmation.

Use in the Analysis: This assumption is used in Section 7.

5.1.3 MCO Internals Mass Distribution Simplification

Assumption: The exact geometry of the MCO internals was simplified for the purpose of this calculation in such a way that its total mass, 8746.4 kg minus the mass of the external shell, was assumed to be distributed equally as mass elements along the nodes of the inner wall of the MCO.

Rationale: It is a conservative assumption since the mass elements along the inner shell have inertial effects that will increase the deformation of the MCO shell wall and cause tensional stresses at the point of contact of the MCO. These tensional stresses are more critical than compressive stresses that may occur from the modeling of the MCO internals. Also, the rationale for this conservative assumption was to provide the set of bounding results, while simplifying the finite element representation.

Confirmation Status: This assumption does not require confirmation.

Use in the Analysis: This assumption is used in Section 7.

5.1.4 The Total Mass of DOE SNF Canister Loaded with MD Ingots is Distributed Uniformly Within the Volume of the Canister

Assumption: The total maximum mass of the DOE SNF canister loaded with MD ingots, 2270 kg, is distributed uniformly within the volume of the canister.

Rationale: The homogenous ingots (with 419.1 mm maximum outer diameter) fill almost completely the inside volume of the canister (438.2 mm inner diameter).

Confirmation Status: This assumption does not require confirmation.

Use in the Analysis: This assumption is used in Section 7.

5.1.5 Mass of FSVR Fuel Element is Distributed Uniformly Within its Volume

Assumption: The exact geometry of the DOE SNF FSVR fuel element is simplified in such a way that its total maximum mass, 128 kg, is assumed to be distributed within a hexagonal prism with uniform mass density and constructed of H-327 graphite.

Rationale: The FSVR fuel geometry is anticipated to be similar to a hexagonal prism and have a center of gravity at or near that of a hexagonal prism with uniform mass density. This assumption provides a set of bounding results, while simplifying the finite element representation.

Confirmation Status: This assumption does not require confirmation.

Use in the Analysis: This assumption is used in Section 7.

5.1.6 Mass of DHLW Glass Canister is Distributed Uniformly Within its Volume

Assumption: The exact geometry of the DHLW glass canister was simplified for the purpose of the calculation in such a way that its total mass was assumed to be distributed within a cylinder with uniform mass density.

Rationale: To provide a set of bounding results, while simplifying the finite element representation.

Confirmation Status: This assumption does not require confirmation.

Use in the Analysis: This assumption is used in Section 7.

5.2 THERMAL

5.2.1 The Axial Power Peaking Factor (PPF) for the FFTF SNF Assemblies, TRIGA, and Enrico Fermi SNF Pins is 1.25

Assumption: The axial PPF for the FFTF SNF assemblies, TRIGA, and Enrico Fermi SNF pins is 1.25.

Rationale: The value of 1.25 is a conservative value for PWR fuel (CRWMS M&O 1997b, p. 29).

Confirmation Status: This assumption does not require confirmation.

Use in the Analysis: This assumption is used in Section 8.

5.2.2 The Volumetric Heat Generation of DHLW Glass Canisters and Shippingport PWR C2 S2 SNF Assemblies is Uniform

Assumption: The volumetric heat generation of DHLW glass canisters and Shippingport PWR C2 S2 SNF assemblies is constant over the axial and radial cross-section of each heat-generating element.

Rationale: Heat generation for a DHLW glass canister, which is geometrically uniform, does not exhibit any peaking behavior. Heat generating elements are dispersed (from vitrification) throughout the glass matrix. In addition, the Shippingport PWR C2 S2 SNF assembly has small heat generating fuel wafers distributed in axial and radial arrays. This even distribution of heat generating elements would negate any thermal peaking effect.

Confirmation Status: This assumption does not require confirmation.

Use in the Analysis: This assumption is used in Section 8.

5.2.3 The Axial PPF for Shippingport LWBR SNF is 2.0

Assumption: The axial PPF for Shippingport LWBR SNF is 2.0.

Rationale: This assumption allows for the inclusion of a radial uncertainty in the maximum axial peaking factor, reported as 1.79 (DOE 1999e, Assumption 3.11), which is conservative.

Confirmation Status: This assumption does not require confirmation.

Use in the Analysis: This assumption is used in Section 8.

5.2.4 The First Arrival and Emplacement of Shippingport LWBR SNF Will Occur in 2010

Assumption: The first arrival and emplacement of Shippingport LWBR SNF will occur in the year 2010.

Rationale: To assure correspondence with *Waste Quantity, Mix and Throughput Study Report* (CRWMS M&O 1997d, p. 7), and its evaluation of the throughput of waste forms.

Confirmation Status: This assumption does not require confirmation.

Use in the Analysis: This assumption is used in Section 8.

5.2.5 Heat Output of the Shippingport LWBR Seed SNF is Held Constant after 2030

Assumption: The heat output of the Shippingport LWBR seed SNF is based on decay heats starting at 2010 and continuing until 2030, after which time the decay heat is held constant.

Rationale: In reality, the Shippingport LWBR seed SNF will continue to decay after 2030. Thus, the assumption is conservative, resulting in higher waste package temperatures.

Confirmation Status: This assumption does not require confirmation.

Use in the Analysis: This assumption is used in Section 8.

5.2.6 The MCO Contains Intact Mark IV Fuel Elements Only

Assumption: The MCO contains intact Mark IV fuel elements only.

Rationale: The MCO-heat generation is higher (resulting in more conservative temperatures) for Mark IV than for Mark IA elements (DOE 2000a, p. 16). Moreover, since the scrap baskets contain less uranium than the intact ones (DOE 2000a, pp. 11 and 26) they generate less heat (under the reasonable assumption that all fuel elements have experienced approximately the same burnup).

Confirmation Status: This assumption does not require confirmation.

Use in the Analysis: This assumption is used in Section 8.

5.2.7 Basis for the Heat Output History of Hanford DHLW Glass Canisters

Assumption: The 2-MCO/2-DHLW waste package contains two Hanford 4.5-m- (15-ft-) long canisters. The heat output history of these canisters is projected from the heat output history of the SRS 3-m (10-ft-) long canister with a conversion factor stated in *Thermal Evaluation of the Shippingport PWR Codisposal Waste Package* (CRWMS M&O 1999f, p. 23).

Rationale: The decay rate for these specific canisters is unknown; thus, using a decay rate based on the thermal output of the Hanford 4.5-m- (15-ft-) long canister is intended to capture the major heat contributor of these canisters.

Confirmation Status: This assumption does not require confirmation.

Use in the Analysis: This assumption is used in Section 8.

5.2.8 The Thermal Conductivity of the DHLW Glass is Equal to that of Borosilicate Glass, and its Density and Specific Heat to that of Pyrex Glass

Assumption: The thermal conductivity of the DHLW glass is conservatively approximated as that of pure borosilicate glass, and the density and specific heat are approximated as those of Pyrex glass. The values of thermal conductivity, specific heat, and density for borosilicate glass are 1.1 W/m/K, 835.0 J/kg/K, and 2,225.0 kg/m³, respectively. The thermal conductivity is the mid-range value for a temperature range of 100°C to 500°C (CRWMS M&O 2000f, p. 28). The density and specific heat are taken to be the same as that of Pyrex glass at 27°C (300 K) (CRWMS M&O 2000f, p. 28).

Rationale: According to *DOE SRS HLW Glass Chemical Composition* (CRWMS M&O 1999d, p. 7), the weight percent of heavy metal present in the DHLW glass is negligible.

Confirmation Status: This assumption does not require confirmation.

Use in the Analysis: This assumption is used in Section 8.

5.2.9 The Heat Output of the MCO Filled with Mark IV Fuels is Constant over the Entire Period of Emplacement

Assumption: The heat output of the MCO filled with Mark IV fuels is constant over the entire period of emplacement.

Rationale: This assumption is conservative since the heat output will actually decay further during this period. This assumption is also needed because the only thermal output available is based on a radionuclide inventory estimate at time of emplacement (DOE 2000a, p. 16). The full decay curve of Mark IV fuels is not available.

Confirmation Status: This assumption does not require confirmation.

Use in the Analysis: This assumption is used in Section 8.

5.2.10 The Zircaloy-2 Cladding of the Mark IV Fuel Pins is Completely Oxidized

Assumption: The Zircaloy-2 cladding of the Mark IV fuel pins is completely oxidized.

Rationale: The emissivity of the cladding depends on the thickness of the oxide layer. Because the state of the oxide layer is not known, and since the cladding thicknesses are small (between 0.5 and 0.8 mm, according to DOE 2000a, p. 13), it is reasonable (and slightly conservative) to assume that all the cladding is oxidized.

Confirmation Status: This assumption does not require confirmation.

Use in the Analysis: This assumption is used in Section 8.

5.2.11 Basis for 2-MCO/2-DHLW Waste Package Surface Temperature History

Assumption: The surface temperature history of the 2-MCO/2-DHLW waste package is based on the results of the three-dimensional thermal analysis in *Drift Scale Thermal Analysis* (CRWMS M&O 2000h, Attachment VI), in which the temperature history obtained for a 21-PWR waste package was selected.

Rationale: The temperatures obtained for the 21-PWR waste package are bounding the temperatures expected on the waste package surface (CRWMS M&O 2000h, pp. 50 and 51).

Confirmation Status: This assumption does not require confirmation.

Use in the Analysis: This assumption is used in Section 8.

5.2.12 The Fill Gas Within the N-Reactor Waste Package is Same as the Gas Filling the MCO

Assumption: The fill gas within the N-Reactor waste package is same as the gas filling the MCO. Within the waste package, the fill gas located between the inner and outer shells is same as the gas surrounding the two MCOs and the two DHLW canisters.

Rationale: To develop the most conservative evaluation.

Confirmation Status: This assumption does not require confirmation.

Use in the Analysis: This assumption is used in Section 8.

5.2.13 The DHLW Glass Filling the Hanford 4.5-m- (15-ft-) long Canister Has an Age of Zero

Assumption: The DHLW glass filling the Hanford 4.5-m- (15-ft-) long canister has an age of zero.

Rationale: There is no criterion for minimum aging time of the DHLW glass. This assumption may result in conservative temperature results.

Confirmation Status: This assumption does not require confirmation.

Use in the Analysis: This assumption is used in Section 8.

5.2.14 A Two-Dimensional Finite Element Representation of a Cross-Section of the Waste Package is Representative of the Hottest Portion of the Waste Package

Assumption: A two-dimensional finite element representation of a cross-section of the waste package is representative of the hottest portion of the waste package.

Rationale: The axial heat transfer does not significantly affect the solution (i.e., the flow of heat in the radial direction dominates the solution since the waste package internal components have

uniform heat generation and material properties along the waste package axis, and the waste package is a cylinder with a length approximately 2.5 times larger than its diameter).

Confirmation Status: This assumption does not require confirmation.

Use in the Analysis: This assumption is used in Section 8.

5.2.15 The Thermal Conductivity of Helium at Atmospheric Pressure is Representative of the Waste Package Conditions

Assumption: The thermal conductivity of helium at atmospheric pressure is representative of the conditions which helium will experience in the waste package.

Rationale: One atmosphere fill pressure at ambient temperature is representative of the industry standard for storage casks. *Analysis of Degradation Due to Water and Gases in MPC* (CRWMS M&O 1995, p. 10) states the highest pressure to which storage casks may be filled is approximately 1.5 atmospheres. Also, most industry vendors use substantially lower pressure in their designs. Although the internal pressure of the waste package will increase due to the temperature rise, according to Bird et al. (1960, p. 255) the thermal conductivity of most gasses is pressure independent. Thus, using the thermal conductivity at atmospheric pressure is reasonable.

Confirmation Status: This assumption requires confirmation when the exact helium fill pressure for the waste packages will become available.

Use in the Analysis: This assumption is used in Section 8.

5.2.16 Modeling only Conduction and Radiation Heat Transfer Provides Conservative Results

Assumption: Modeling only conduction and radiation heat transfer provides conservative results.

Rationale: Although the fill gas in the waste package will allow a convective heat transfer path to exist, the natural convective heat transfer will have a small or negligible impact on the total heat transfer. Attachment X of *Thermal Evaluation of the Codisposal Canister in the 5-Pack DHLW Waste Package* (CRWMS M&O 1997e) estimates the effect of the convective heat transfer inside the 5-DHLW waste package. The analysis indicates a potential for convection cells to develop in the larger cavities near the top and sides of the waste package internals. Convection will likely not play a role in transferring heat near the bottom of the waste package where heat transfer will be clearly dominated by conduction and thermal radiation. The total impact of convection on heat transfer within the waste package is estimated to be less than 10 percent. Thus, the problem may be modeled with only the dominant heat transfer modes with a slightly conservative impact upon the results.

Confirmation Status: This assumption does not require confirmation.

Use in the Analysis: This assumption is used in Section 8.

5.2.17 The Equations for Unirradiated Graphite are Used to Calculate the Thermal Conductivity of the Graphite Block

Assumption: The equations for unirradiated graphite are used to calculate the thermal conductivity of the graphite block.

Rationale: For the time frame considered (1 to 10⁶ years) the thermal conductivity of the DOE SNF canister internal components has a negligible effect on the DHLW glass temperature.

Confirmation Status: This assumption does not require confirmation.

Use in the Analysis: This assumption is used in Section 8.

5.2.18 The Glass Volume in the Hanford 4.5-m- (15-ft-) long Canister is 1.08 m³

Assumption: The volume of glass contained in the Hanford 4.5-m- (15-ft-) long canister is 1.08 m³.

Rationale: The difference between the glass volume information by Picha (1997, Table RL-3) and the actual value is anticipated to have a negligible effect on any results reported.

Confirmation Status: This assumption requires confirmation when the exact volume of glass contained in the Hanford 4.5-m- (15-ft-) long canister will become available.

Use in the Analysis: This assumption is used in Section 8.

5.2.19 The Fill Gas Used in the DOE SNF Canister is Air

Assumption: The fill gas used in the DOE SNF canister is air. In *Preliminary Design Specification for Department of Energy Standardized Spent Nuclear Fuel Canisters* (DOE 1999a, p. 6) it is indicated that the DOE SNF canister shall be backfilled with an inert cover gas (e.g., helium).

Rationale: For the time frame considered (1 to 10⁶ years) the thermal conductivity of the DOE SNF canister internal components has a negligible effect on the DHLW glass temperature.

Confirmation Status: This assumption does not require confirmation.

Use in the Analysis: This assumption is used in Section 8.

5.3 SHIELDING

5.3.1 For FFTF, TRIGA, and Fermi SNF the Contents of the DOE SNF Canister are Homogenized Inside the Cavity of Canister

Assumption: For FFTF, TRIGA, and Fermi SNF the contents of the DOE SNF canister are homogenized inside the cavity of canister.

Rationale: This representation is conservative, because the homogenization process essentially moves the radiation source closer to the outer surfaces of the waste package, allowing more particles to reach the outer surface and decreases the self-shielding effect of the fuel (Parks et al. 1988, p. 85).

Confirmation Status: This assumption does not require confirmation.

Use in the Analysis: This assumption is used in Section 9.

5.3.2 An Axial PPF of 1.25 is used for the FFTF, TRIGA, Fermi, and Shippingport PWR SNF Source

Assumption: An axial PPF of 1.25 is used for the FFTF, TRIGA, Fermi, and Shippingport PWR SNF source to bound the axial source distribution.

Rationale: This value is based on the axial peaking factor shown by Creer et al. (1987, p. 3-29, Figure 3-18).

Confirmation Status: This assumption does not require confirmation.

Use in the Analysis: This assumption is used in Section 9.

5.3.3 The dose rate due to secondary gamma rays is negligible

Assumption: The dose rate due to secondary gamma rays is negligible and no coupled neutron-photon calculation is performed.

Rationale: The neutron source intensity is nine and eight orders of magnitude smaller than the gamma source intensity for the SNF (FFTF, Shippingport PWR, Fermi fuel) and DHLW glass, respectively. The neutron source intensities are about six and seven orders of magnitude smaller than the gamma source intensity for the Shippingport LWBR SNF and DHLW glass, respectively.

Confirmation Status: This assumption does not require confirmation.

Use in the Analysis: This assumption is used in Section 9.

5.3.4 The inner, the outer brackets, and the divider plates supporting the DHLW glass canisters in the waste package are neglected

Assumption: The inner, the outer brackets, and the divider plates supporting the DHLW glass canisters in the waste package are neglected.

Rationale: The basis for this is that the calculated surface dose rates will be conservative (higher) since the structural components that would attenuate radiation are not modeled.

Confirmation Status: This assumption does not require confirmation.

Use in the Analysis: This assumption is used in Section 9.

5.3.5 The active fuel region of the Shippingport LWBR seed fuel assembly, Shippingport PWR C2 S1 fuel assembly and FSVR fuel element is homogenized inside its transverse dimensions

Assumption: The active fuel region of the Shippingport LWBR seed fuel assembly, Shippingport PWR C2 S1 fuel assembly and FSVR fuel element is homogenized inside its transverse dimensions.

Rationale: Homogenization of the components inside the fuel assembly or element volume statistically gives the same waste package surface dose rate as does the heterogeneous representation (as demonstrated in CRWMS M&O 1998d, pp. 22 and 23).

Confirmation Status: This assumption does not require confirmation.

Use in the Analysis: This assumption is used in Section 9.

5.3.6 The Shippingport LWBR fuel source terms has an axial PPF factor of 2.0

Assumption: A PPF factor of 2.0 is used for the Shippingport LWBR fuel source terms for bounding the axial source distribution.

Rationale: This value is based on the rounded peaking factor for a seed assembly of 1.79 (DOE 1999e, Assumption 3.11), for conservative (higher) dose rate calculations.

Confirmation Status: This assumption does not require confirmation.

Use in the Analysis: This assumption is used in Section 9.

5.3.7 The density of the SRS DHLW glass is 2.56 g/cm³

Assumption: The density of the SRS DHLW glass (which is assumed to fill the Hanford DHLW glass canisters) is 2.56 g/cm³.

Rationale: According to Plodinec and Marra (1994, p. 22), the density of the SRS DHLW glass may vary between 2.56 and 2.75 g/cm³. Stout and Leider (1991, p. 2.2.1.1-4) gives an upper limit for the glass density of 2.85 g/cm³. A lower glass density provides conservative (higher) gamma dose rates.

Confirmation Status: This assumption does not require confirmation.

Use in the Analysis: This assumption is used in Section 9.

5.3.8 The head and neck of the DHLW glass canisters are neglected

Assumption: The head and neck of the DHLW glass canisters are neglected.

Rationale: Radiation transport in the upper part of the canister is not affected because this portion of the canister is empty and the wall thickness is maintained.

Confirmation Status: This assumption does not require confirmation.

Use in the Analysis: This assumption is used in Section 9.

5.3.9 The source distribution of the N-Reactor SNF has axial PPF of 2.0

Assumption: An axial peaking factor of 2.0 bounds the axial source distribution of the N-Reactor SNF.

Rationale: This value provides conservative (higher) dose rates. However, the calculations show that the surface dose rates next to the MCOs are lower than those next to the DHLW glass canisters. Therefore, the maximum dose rate on the waste package external surfaces is not sensitive to the axial peaking factor value of the N-Reactor SNF.

Confirmation Status: This assumption does not require confirmation.

Use in the Analysis: This assumption is used in Section 9.

5.3.10 For elements' composition with weight percent range, the midpoint value is assumed

Assumption: The material compositions used in dose calculations have elements with allowable ranges of weight percentages. For elements with weight percent range, the midpoint value is used, and the weight percent of the most abundant element is adjusted.

Rationale: Small weight variations for the affected elements do not affect the accuracy of dose results, as long as the total weight is maintained.

Confirmation Status: This assumption does not require confirmation.

Use in the Analysis: This assumption is used in Section 9.

5.3.11 The MD ingots do not contain a liner, and the ingot stack occupies the entire cavity volume of the 18-in-outer diameter DOE SNF canister

Assumption: The MD ingots do not contain a liner, and the ingot stack occupies the entire cavity volume of the 18-in-outer diameter DOE SNF standardized canister.

Rationale: These considerations are conservative for dose rate calculations. A liner, if present, attenuates the radiation originating inside the ingot, and a larger ingot volume has higher radiation intensity.

Confirmation Status: This assumption does not require confirmation.

Use in the Analysis: This assumption is used in Section 9.

5.3.12 The MD ingots composition consists of 13.2±5 wt% uranium with aluminum being the balance element

Assumption: The MD ingots composition consists of 13.2±5 wt% uranium with aluminum being the balance element.

Rationale: The rationale for replacing the neutron absorbers and other elements contained in the silicide and oxide Al-SNF forms with aluminum is that this generates higher (conservative) gamma dose rates.

Confirmation Status: This assumption does not require confirmation.

Use in the Analysis: This assumption is used in Section 9.

5.4 INTACT AND DEGRADED COMPONENT CRITICALITY

5.4.1 Preirradiation nuclear fuel compositions were used

Assumption: BOL preirradiation nuclear fuel compositions updated (where applicable) with the most reactive fissile concentration (for fuels that contained fertile species during irradiation) were used for all criticality analyses. No credit was taken for fuel burnup in the criticality analyses of DOE SNF.

Rationale: It is conservative to assume fresh nuclear fuel as it is more neutronically reactive than SNF.

Confirmation Status: This assumption does not require confirmation.

Use in the Analysis: This assumption is used in Section 10.

5.4.2 Ident-69 pin containers are assumed to contain a most reactive configuration of FFTF fuel pins for the intact fuel cases

Assumption: Ident-69 pin containers are assumed to contain a most reactive configuration of FFTF fuel pins for the intact fuel cases.

Rationale: Conservative (i.e., highest k_{eff}) values are obtained for these configurations, and they are bounding for all configurations.

Confirmation Status: This assumption does not require confirmation.

Use in the Analysis: This assumption is used in Section 10.

5.4.3 The DHLW canister is represented as a right circular cylinder completely filled with DHLW glass and the flanged head and neck are neglected

Assumption: The flanged head and neck of the DHLW canister is neglected and the canister is represented as a right circular cylinder with the same top-to-bottom height as the canister. The canister is assumed completely filled with DHLW glass.

Rationale: It is conservative since the additional waste will make the system more reactive by increasing the total amount of fissile elements (by less than 1 percent) in the waste package.

Confirmation Status: This assumption does not require confirmation.

Use in the Analysis: This assumption is used in Section 10.

5.4.4 The radial FFTF pellet spacing in degraded cladding configurations never becomes greater than the original pitch of the DFA

Assumption: For configurations where the FFTF fuel pin cladding has become completely degraded the remaining fuel pellets maintain their axial alignment (as in the fuel pin), and the radial spacing which can be affected by the expansion of corrosion products never becomes greater than the original spacing (pitch) of the DFA.

Rationale: There is no known physical mechanisms to push the fuel pins apart.

Confirmation Status: This assumption does not require confirmation.

Use in the Analysis: This assumption is used in Section 10.

5.4.5 The erbium burnable neutron absorber for fresh TRIGA nuclear fuel was neglected.

Assumption: The neutron absorber (referred to as advanced neutron absorber matrix) for the TRIGA waste package is made of Alloy 22 with 8 wt% of gadolinium.

Rationale: It is conservative to assume fresh nuclear fuel without the burnable absorber as this increases its reactivity.

Confirmation Status: This assumption does not require confirmation.

Use in the Analysis: This assumption is used in Section 10.

5.4.6 The neutron absorber for the TRIGA waste package is made of Alloy 22 with 8 at% of gadolinium

Assumption: The neutron absorber (referred to as advanced neutron absorber matrix) for the TRIGA waste package is made of Alloy 22 with 8 at% of gadolinium.

Rationale: The composition of this material is given in *TRIGA Fuel Phase I and II Criticality Calculation* (CRWMS M&O 1999c). This assumption is conservative, as the components of Alloy 22 do have low, but significant, thermal neutron absorption cross-sections.

Confirmation Status: This assumption does not require confirmation.

Use in the Analysis: This assumption is used in Section 10.

5.4.7 For Fermi SNF, the impurities in the undegraded fuel matrix (B, C, Cr, Fe, Ni, N, O, Zr, Cu, and others) are replaced with molybdenum (Mo)

Assumption: For the purposes of k_{eff} calculations for Fermi SNF, the impurities in the undegraded fuel matrix (B, C, Cr, Fe, Ni, N, O, Zr, Cu, and others) (DOE 1999b, p. 9) are replaced with molybdenum (Mo).

Rationale: The replacement makes the calculations more conservative, as the majority of the elements present in the impurities have higher thermal neutron absorption cross-sections than Mo. This assumption does not impact the geochemistry calculations that consider the solubility of all of these elements individually.

Confirmation Status: This assumption does not require confirmation.

Use in the Analysis: This assumption is used in Section 10.

5.4.8 If aluminum is present in the DOE SNF canister its degradation (oxidizing) produces AlOOH (diaspore)

Assumption: If aluminum is present in the DOE SNF canister its degradation (oxidizing) produces AlOOH (diaspore).

Rationale: The diaspore formation, instead of gibbsite, can have little effect on the criticality calculations because the additional hydrogen in the gibbsite would be much less than that in the water assumed to be present for all the criticality calculations.

Confirmation Status: This assumption does not require confirmation.

Use in the Analysis: This assumption is used in Section 10.

5.4.9 For the degraded configurations with intact fuel pins, the pins are assumed to be stacked at the bottom of the waste package in a regular array

Assumption: For the degraded configurations with intact fuel pins surrounded by degraded waste package internals, the placement and stacking of the pins is chosen to give a more reactive configuration rather than a more realistic stacking due to gravity.

Rationale: It is conservative since it gives a larger k_{eff} for the system.

Confirmation Status: This assumption does not require confirmation.

Use in the Analysis: This assumption is used in Section 10.

5.4.10 Boron in two end plates of the Shippingport PWR SNF subassembly were represented as water

Assumption: Burnable neutron absorber material (boron) in two end plates (referred to as “poison wafers”) of the Shippingport PWR SNF subassembly were represented as water.

Rationale: It is conservative to neglect burnable neutron absorber material since it provides some additional amount of neutron absorption.

Confirmation Status: This assumption does not require confirmation.

Use in the Analysis: This assumption is used in Section 10.

5.4.11 The iron in the iron shot and Stainless Steel degrades to goethite rather than hematite

Assumption: For the degraded component criticality calculations, it is assumed that the iron in the iron shot (for the waste packages where it is used), carbon steel and stainless steel degrades to goethite (FeOOH) rather than hematite (Fe₂O₃).

Rationale: It is conservative to consider goethite rather than hematite since hydrogen (neutron moderator) is a component of goethite. All the other constituents or impurities of iron shot and/or steel are neglected since they are neutron absorbers, and, hence, their absence provides a conservative (higher) value of the k_{eff} of the system. This assumption does not impact the geochemistry calculations.

Confirmation Status: This assumption does not require confirmation.

Use in the Analysis: This assumption is used in Section 10.

5.4.12 The length of the FSVR fuel in the fuel elements is same as the length of the fuel elements

Assumption: The length of the FSVR fuel in the fuel elements is assumed to be the same as the length of the fuel elements rather than the actual length of the fuel holes, which is slightly smaller.

Rationale: This gives a larger void fraction and thus the potential for more water in the fuel. This is a conservative assumption since it is shown (BSC 2001c, Section 7.3, Table 7-2) that it is more reactive to have more water in the fuel (i.e., this gives a higher value of the k_{eff} for the system).

Confirmation Status: This assumption does not require confirmation.

Use in the Analysis: This assumption is used in Section 10.

5.4.13 A most reactive fissile concentration is used for the FSVR fuel that is shown to bound fuel compositions for actual fuel elements

Assumption: A most reactive fissile concentration is used for the FSVR fuel that is shown (BSC 2001f, Table 12) to bound fuel compositions for actual fuel elements.

Rationale: These selected fuel compositions use the larger fissile masses from either the BOL or EOL, neglect any ²³⁸U and use EOL values for ²³²Th. These selected compositions are conservative since they maximize the fissile isotope content while minimizing the effect of

neutron absorbers. Therefore, the fuel composition used for the FSVR fuel is even more conservative since it bounds these actual (conservative) compositions.

Confirmation Status: This assumption does not require confirmation.

Use in the Analysis: This assumption is used in Section 10.

5.5 GENERAL

5.5.1 The limits for each fuel group, which are established by the technical information related to that specific SNF, are bounding

Assumption: The limits for each fuel group, which are established by the technical information related to that specific SNF (DOE 1998b; DOE 1999b; DOE 1999c; DOE 1999d; DOE 1999e; DOE 2000a; BSC 2001b; Taylor 2001), are bounding.

Rationale: The technical information for a representative fuel type was supplied for criticality and related design calculations as a bounding case within each fuel group. The fuel grouping is the activity in which the DOE SNF program has evaluated the parameters and properties of the DOE SNF important to criticality, design events, and performance assessment, and categorized the DOE SNF into fuel groups. Therefore, the burden is placed on the custodian of the SNF to demonstrate, before acceptance of SNF by BSC that SNF characteristics identified as important to criticality control or other analyses herein are not exceeded.

Confirmation Status: This assumption does not require confirmation.

Use in the Analysis: This assumption is used in Sections 7, 8, 9 and 10.

5.5.2 SRS Design-Basis DHLW glass fills the 4.5-m-long glass pour canisters

Assumption: The DHLW glass that fills the 4.5-m-long glass pour canisters is the SRS Design-Basis DHLW glass.

Rationale: The Hanford DHLW glass composition is not known at this time and the characteristics of the two types of glass are expected to be similar. The composition of SRS Design-Basis DHLW glass is taken from *DOE SRS HLW Glass Chemical Composition* (CRWMS M&O 1999d, p. 7). Also, radiation source terms of the SRS Design-Basis DHLW glass bound the source terms of all projected high-level radioactive waste glass forms (CRWMS M&O 2000g, Attachments V and VI), and generates conservative (higher) dose rates at the external surfaces of the waste package.

Confirmation Status: This assumption does not require confirmation.

Use in the Analysis: This assumption is used in Sections 7, 8, 9, and 10.

6 ANALYSIS METHODOLOGY

6.1 STRUCTURAL

ANSYS Versions 5.4 (ANSYS V5.4L2, STN: 10027-5.4L2-00) and 5.6.2 (ANSYS V5.6.2, STN: 10364-5.6.2-00), and Livermore Software Technology Corporation (LSTC) LS-DYNA V950 (LS-DYNA V950, STN: 10300-950-00)—finite-element analysis (FEA) computer codes—were used for the structural analysis of the 5-HLW/DOE SNF-long and short waste packages with SNF loads inside the DOE SNF canister, which is placed in the center of the waste package. ANSYS Version 5.4 and LS-DYNA V950 were used for the structural analysis of the 2-MCO/2-DHLW waste package with N-Reactor fuel loads inside the MCOs. A two-dimensional (three-dimensional for FSVR waste package) finite-element representation of the waste package was developed to determine the effects of loads on the waste package structural components due to a waste package tipover design-basis event (DBE). There is no finite element representation developed specifically for the MD ingots waste package. However, a bounding two-dimensional finite element representation of the 5-DHLW/DOE SNF-short waste package was developed to determine the effects of loads on the structural components due to a tipover design basis event (BSC 2002a).

The analyses considered the configurations with the maximum total mass of the DOE SNF canister, and the maximum total mass for each DHLW glass canister. Calculations of maximum stress intensity for each waste package handling accident scenario (2.4 m horizontal drop, 2.0 m vertical drop, and tipover DBEs) show that the bounding dynamic load results from a tipover case in which the rotating top end of the waste package experiences the highest impact load. Therefore, tipover structural evaluations are bounding for all handling accident scenarios considered in the DBEs document.

Finite element solutions result from structural analyses for the components of the 5-DHLW/DOE SNF and 2-MCO/2-DHLW waste packages. A detailed description of the finite element representations, the method of solution, and the results are provided in *Tip-Over of the 5 DHLW/DOE SNF - Long Waste Package Containing Fort Saint Vrain HTGR Fuel Onto an Unyielding Surface* (BSC 2001g). The results are presented in terms of maximum stress intensities, then compared to the design criteria obtained from Sections F-1340 and F-1341 of the 1997 Addenda of *1995 ASME Boiler and Pressure Vessel Code* (ASME 1995). Conclusions can be drawn regarding the structural performance of the 5-DHLW/DOE SNF and 2-MCO/2-DHLW waste package designs using the stated criteria. The results of the calculation must meet the criteria specified in Table 6-1. The structural performance of the DHLW canister is not evaluated.

The design approach for determining the adequacy of a structural component is based on the stress limits given in the 1997 Addenda of *1995 ASME Boiler and Pressure Vessel Code* (ASME 1995). S_u is defined as the ultimate tensile strength of the materials and is compared to the design stress intensity of the materials. Table 6-1 summarizes design criteria as obtained from appropriate sections of the 1997 Addenda of *1995 ASME Boiler and Pressure Vessel Code* (ASME 1995). All three conditions must be met.

Table 6-1. Containment Structure Allowable Stress-Limit Criteria

Category	Containment Structure Allowable Stresses
	Accident Conditions
Primary membrane stress intensity	0.7S _u
Maximum primary stress intensity	0.9S _u
Average primary shear stress across a section loaded in pure shear	0.42S _u

Source: ASME 1995, Division 1, Section F-1341.2

6.2 THERMAL

The FEA computer code used for the thermal evaluations of 5-DHLW/DOE SNF waste package was ANSYS V5.4. Version 5.4 was used because Version 5.6.2 could not be used for times past 60 years from waste package emplacement in the repository.

A detailed description of the finite element representations, the method of solution, and the results are provided in the thermal evaluations for each SNF type. The finite element representations were created as a two-dimensional representation. The two-dimensional method was chosen because it was assumed that radial heat transfer will dominate the solution and that axial heat transfer will be minor (Section 5.1.2).

The boundary conditions on the outer surface of the waste package were taken from *Drift Scale Thermal Analysis* (CRWMS M&O 2000h, Table 6-18). The actual numbers are from an initial 50-year forced ventilation period with 0.1 m spacing between waste packages and no backfill. The waste package cross-section was modeled (taking advantage of symmetry) and the boundary conditions were applied.

The time period covered by the thermal analysis was from the time of waste package emplacement in the repository to 1,000 years after emplacement. This ensures that the time when the maximum temperatures inside the waste package will be experienced, is covered.

6.3 SHIELDING

The Monte Carlo method for solving the integral radiation transport equation, which is implemented in the MCNP computer program, is used to calculate radiation dose rates for the waste packages. MCNP uses continuous-energy cross-sections processed from the evaluated nuclear data files ENDF/B-V (Briesmeister 1997, Appendix G). These cross-section libraries are part of the qualified MCNP code. The flux averaged over a surface tally is specified in calculations and the neutron and gamma flux-to-dose rate conversion factors, which were extracted from *Neutron and Gamma-Ray Flux-to-Dose-Rate Factors* (ANSI/ANS-6.1.1-1977), are applied to obtain surface dose rates.

6.4 GEOCHEMISTRY

The EQ3/6 geochemistry software package (EQ3/6 V7.2b, STN: UCRL-MA-110662; EQ6 V7.2bLV, STN: 10075-7.2bLV-00), was used for the geochemistry evaluations. The information regarding the code and its use for the degradation and geochemistry analysis is

documented in *EQ6 Calculation for Chemical Degradation of Fort St. Vrain (Th/U Carbide) Waste Packages* (BSC 2001h).

6.4.1 Design Analysis

6.4.1.1 Systematic Investigation of Degradation Scenarios and Configurations

Degradation scenarios comprise a combination of features, events, and processes that result in degraded configurations to be evaluated for criticality. A configuration is defined by a set of parameters characterizing the amount and physical arrangement, at a specific location, of the materials that can significantly affect criticality (e.g., fissile materials, neutron absorbing materials, reflecting materials, and moderators). The variety of possible configurations is best understood by grouping them into classes. A configuration class is a set of similar configurations whose composition and geometry is defined by specific parameters that distinguish one class from another. Within a configuration class, the values of configuration parameters may vary over a given range.

A master scenario list and set of configuration classes relating to internal criticality is given in *Disposal Criticality Analysis Methodology Topical Report* (YMP 2003, pp. 3-12 to 3-14) and also shown in Figures 6-1 and 6-2. This list was developed through a process that involved workshops and peer review. The comprehensive evaluation of disposal criticality for any waste form must include variations of the standard scenarios and configurations to ensure that no credible degradation scenario is neglected. All of the scenarios that can lead to criticality begin with the breaching of the waste package, followed by entry of water, which eventually leads to degradation of the SNF and/or other internal components (OIC) of the waste package.

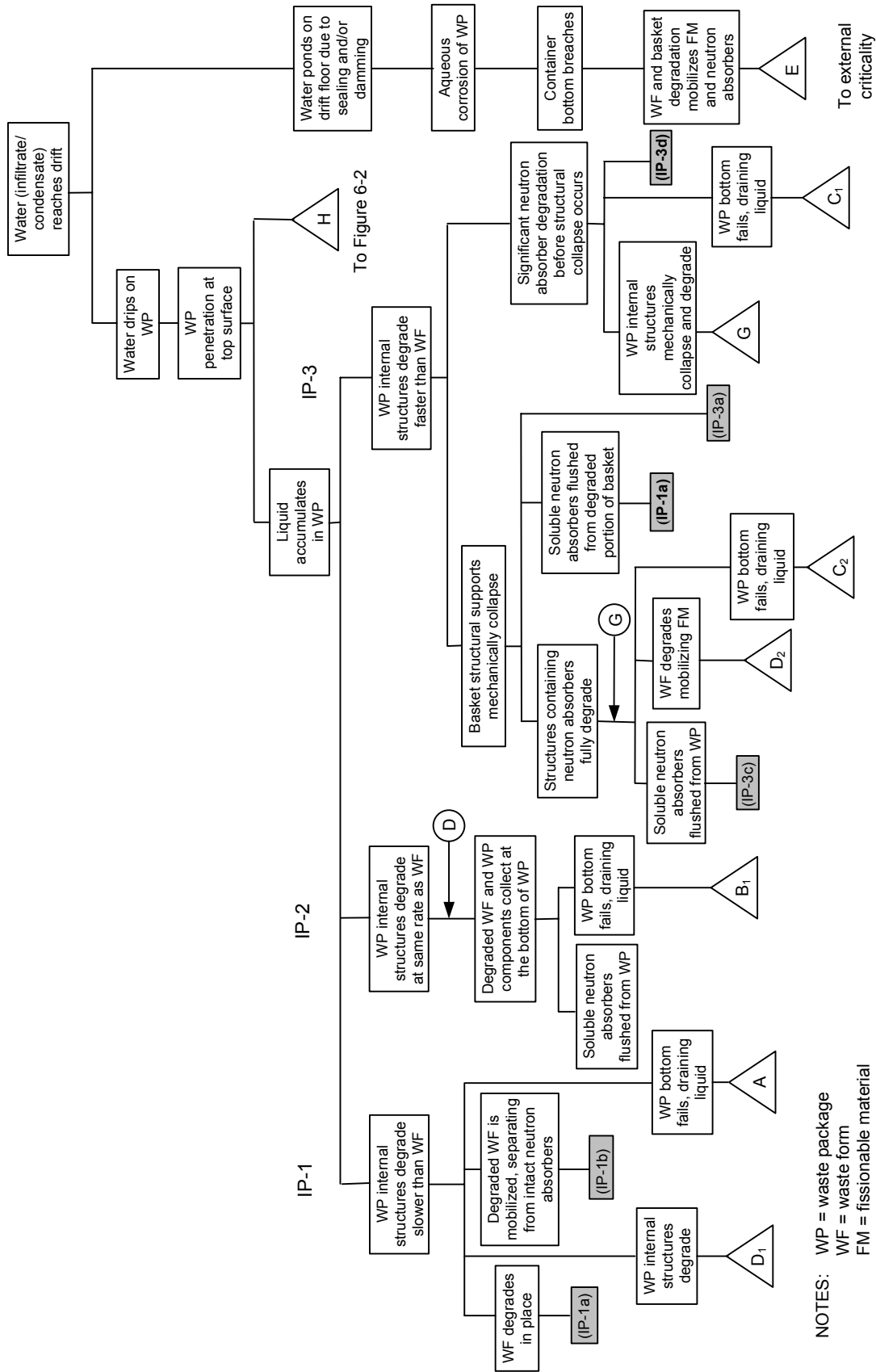
The standard scenarios for internal criticality divide into two groups:

1. When the waste package is breached only on the top, water flowing into the waste package collects and fills the waste package. This water provides moderation to potentially increase the possibility of criticality. Further, after a few hundred years of steady dripping, the water can overflow through the hole on the top of the waste package and flush out any dissolved degradation products.
2. When the waste package breach occurs on the bottom as well as the top, the water can flow through the waste package. This group of scenarios allows the soluble degradation products to be removed more quickly but does not directly provide water for moderation. Criticality is possible, however, if the waste package fills with corrosion products that can retain water and/or plug any holes in the bottom of the waste package while fissile material is retained.

The standard scenarios for the first group shown in Figure 6-1, which have the waste package breached only at the top, are designated IP-1, -2, and -3 (IP stands for internal to the package) according to whether the waste form degrades before the waste package OIC, at approximately the same time (but not necessarily at the same rate) or later than the waste package OIC. The standard scenarios for the second group shown in Figure 6-2, which have the waste package breached at both the top and the bottom, are designated IP-4, -5, or -6 based on the same criteria. The internal criticality configurations resulting from these scenarios fall into six generic

configuration classes described below (YMP 2003, pp. 3-13 to 3-14). These configuration classes are intended to comprehensively represent the configurations that can result from physically realizable scenarios. As presented here, the configuration classes do not distinguish between waste package internal components inside versus outside the DOE SNF canister. It should be noted that the waste package studied in this technical report has no added neutron absorbers, no basket structure inside the DOE SNF canister, and no credit is taken for SNF burnup (or fission product neutron absorbers).

1. Basket is degraded but waste form is relatively intact and sits on the bottom of the waste package (or the DOE SNF canister) surrounded by, and/or beneath, the basket corrosion products. This configuration class is reached from scenario IP-3.
2. Both basket and waste form are degraded. The sludge at the bottom of the waste package is a mixture consisting of fissile material, corrosion products, and iron oxides and may contain clay. It is more complex than for configuration class 1 and is determined by geochemistry calculations as described in *EQ6 Calculation for Chemical Degradation of Fort St. Vrain (Th/U Carbide) Waste Packages* (BSC 2001h). This configuration class is most directly reached from standard scenario IP-2 in which all the waste package components degrade at the same time. However, after many tens of thousands of years the scenarios IP-1 and IP-3, in which the waste form degrades before or after the other components, also lead to this configuration.
3. Fissile material is moved some distance from the neutron absorber, but both remain in the waste package. This configuration class can be reached from IP-1.
4. Fissile material accumulates at the bottom of the waste package (or the DOE SNF canister), together with moderator provided by water trapped in clay. The clay composition is determined by geochemistry calculations (BSC 2001h). This configuration class can be reached by any of the scenarios, although IP-2 and IP-5 lead to this configuration by the most direct path; the only requirement is that there be a large amount of glass in the waste package (as in the waste package) to form the clay.
5. Fissile material is incorporated into the clay, similar to configuration class 4, but with the fissile material not at the bottom of the waste package. Generally, the mixture is spread throughout most of the waste package volume but could vary in composition so that the fissile material is confined to one or more layers within the clay. Generally, the variations of this configuration are less reactive than for configuration class 4. Either standard scenario IP-1 or IP-4 can reach this configuration class.
6. Fissile material is degraded and spread into a more reactive configuration. This configuration class can be reached by scenario IP-1.

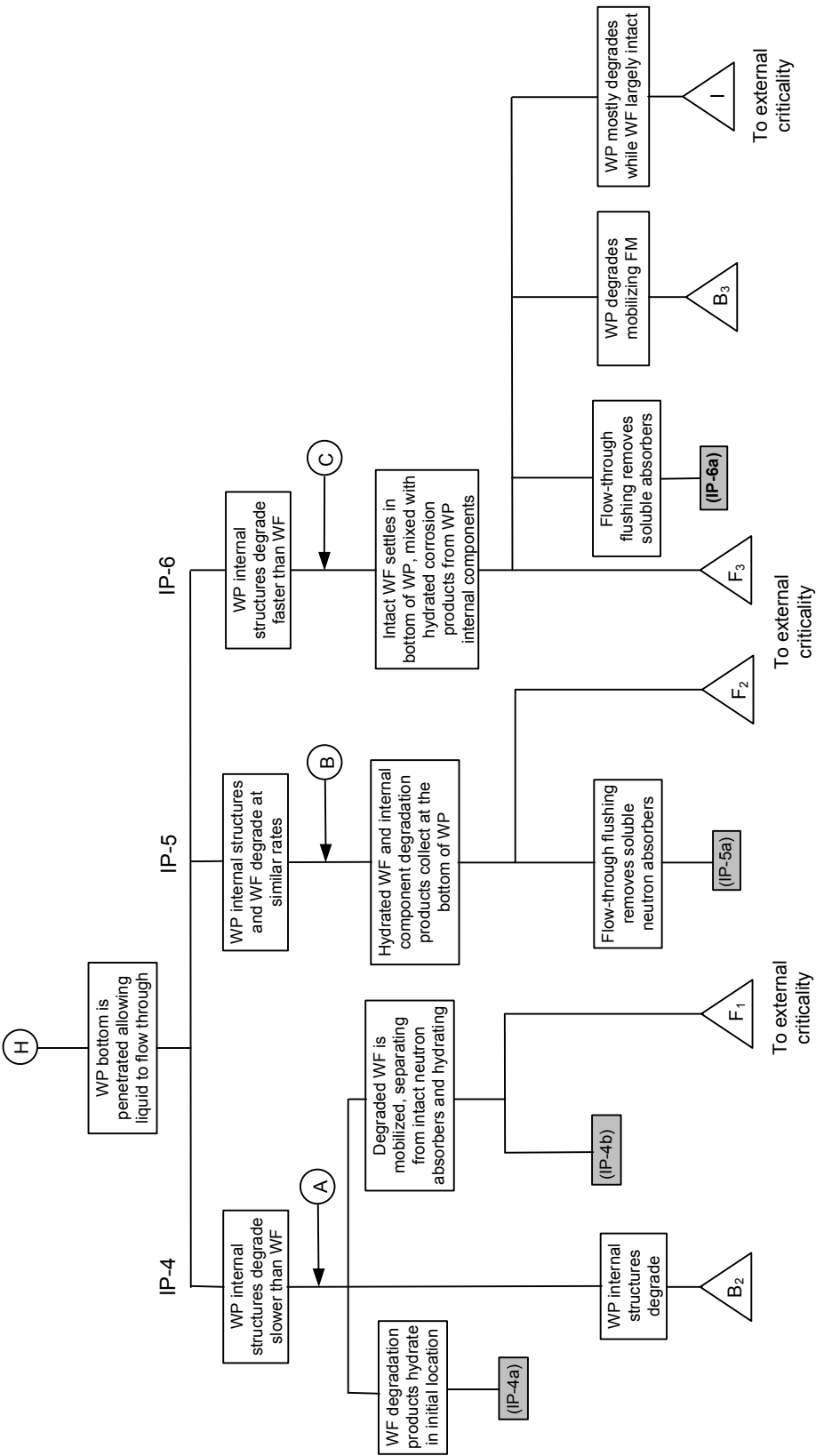


NOTES: WP = waste package
 WF = waste form
 FM = fissionable material

Source: YMP 2003, p. 3-8

Figure 6-1. Internal Criticality Master Scenarios, Part 1

From Figure 6-1



NOTE: Hydrated degradation products may include hydrated metal oxides, metal hydroxides, and clayey materials

Source: YMP 2003, p. 3-9

Figure 6-2. Internal Criticality Master Scenarios, Part 2

Generic Degradation Scenario and Configuration Analysis for DOE Codisposal Waste Package (CRWMS M&O 1999g) serves as the basis for the specific degraded waste package criticality analysis to be performed for any type of DOE SNF that will be codisposed with the high-level radioactive waste in a waste package. Starting from these guidelines, a set of degradation scenarios and resultant configurations has been developed for the waste package containing FSVR SNF. The following description focuses on the correspondence between different classes of configurations and their refinements. This approach allows a systematic treatment of the degraded internal criticality analysis, taking into account all possible configurations with potential for internal criticality. In Sections 6.3 and 6.4, the scenarios and the resulting configuration classes that are applicable to a waste package with a DOE standardized SNF canister containing FSVR SNF are discussed.

6.4.1.2 Generic Degraded Configuration Classes

Configuration classes resulting from degradation scenario IP-1, in which the SNF degraded before the OICs:

IP-1-A: SNF degraded, DOE SNF canister and internal supporting structure not degraded.

IP-1-B: SNF degraded, DOE SNF canister and supporting structure partially degraded.

IP-1-C: All waste package components degraded.

Configuration classes resulting from degradation scenario IP-2, in which waste package components degrade concurrently with the SNF:

IP-2-A: All waste package components degraded.

Configuration classes resulting from degradation scenario IP-3, in which the SNF degrades after the OICs:

IP-3-A: Degraded DOE SNF canister internal structure; intact SNF and DOE SNF canister shell; degraded waste package basket structure and DHLW glass canister(s).

IP-3-B: Degraded waste package basket structure, DHLW glass canister(s), and DOE SNF canister; intact SNF.

IP-3-C: All waste package components degraded.

Configuration classes resulting from flow-through degradation scenario IP-4, in which the SNF degrades before the OICs:

IP-4-A: SNF degraded, DOE SNF canister shell not fully degraded.

IP-4-B: All waste package components degraded.

Configuration classes resulting from flow-through degradation scenario IP-5, in which the waste package components including the SNF, are degrading concurrently:

IP-5-A: All waste package components degraded.

Configuration classes resulting from flow-through degradation scenarios of IP-6, in which the SNF degrades after the OICs:

IP-6-A: All waste package components degraded.

6.4.2 Basic Design Approach for Geochemistry Analysis

The method used for this analysis involves eight steps as described below:

1. Use of the modified and qualified version of the EQ3/6 reaction-path code to trace the progress of reactions as the chemistry evolves, including estimating the concentrations of materials remaining in solution as well as the composition of precipitated minerals. EQ3NR is used to determine a starting fluid composition for EQ6 reaction-path calculations.
2. Evaluate available data on the range of dissolution rates for the materials involved, to be used as material/species input for each time step.
3. Use the “solid-centered flow-through” mode in EQ6. In this mode, an increment of aqueous “feed” solution is added continuously to the waste package system, and a like volume of the existing solution is removed. This mode simulates a continuously stirred tank reactor.
4. Determine the concentrations of fissile material in solution as a function of time (from the output of EQ6 simulated reaction times up to $6.34 \cdot 10^5$ years).
5. Calculate the amount of fissile material released from the waste package as a function of time (fissile material loss reduces the chance of criticality within the waste package).
6. Determine the concentrations of neutron absorbers (most importantly Th) in solution as a function of time (from the output of EQ6 over times up to $6.34 \cdot 10^5$ years).
7. Calculate the amount of neutron absorber retained within the waste package as a function of time.
8. Calculate the composition and amounts of solids (precipitated minerals or corrosion products and unreacted waste package materials).

The calculations begin using selected representative values from known ranges for composition, amounts, surface areas, and reaction rates of the various components of the FSVR SNF waste package. The input to EQ6 includes the composition of J-13 well water, a rate of influx to the waste package that corresponds to suitably chosen percolation rates into a drift, and a drip rate into the waste package (Section 2.1.9.3), which is also the flow rate out of the waste package. In some cases, the degradation of the waste package is divided into stages (e.g., degradation of the

DHLW glass before breach of the DOE SNF canister and exposure of the fuel material to the water).

6.5 CRITICALITY METHODOLOGY

The approach to addressing postclosure criticality as described in *Disposal Criticality Analysis Methodology Topical Report* (YMP 2003) is intended to provide a rigorous method of demonstrating that public health and safety are protected against the consequences of any potential postclosure criticality. That approach is consistent with 10 CFR Part 63. The approach is based on risk-informed, performance-based analyses.

The analysis methodology approach presented in *Disposal Criticality Analysis Methodology Topical Report* (YMP 2003) does not attempt to support a demonstration that postclosure criticality either will not occur or is totally incredible (that is, guaranteed to have a probability below the threshold of concern). Instead, the methodology approach focuses on evaluation of the probability of occurrence of configurations and, for configurations with potential for criticality, the probability of criticality for the configuration.

The risk-informed, performance-based methodology approach described in *Disposal Criticality Analysis Methodology Topical Report* (YMP 2003) defines a critical limit for the multiplication factor (k_{eff}) of the system, which is used to identify systems that have the potential to become critical. The critical limit is the value of k_{eff} at which the configuration class is considered potentially critical as characterized by statistical tolerance limits.

The criticality model used in analyzing the configurations, which encompasses the Monte Carlo code (MCNP) and the appropriately selected neutron cross-section libraries, is validated using evaluated critical benchmark experiments and the methodology detailed in *Disposal Criticality Analysis Methodology Topical Report* (YMP 2003). Critical limit values are obtained by analysis of experimental systems with a range of neutronic parameters that are representative of the configuration parameters expected for the repository. The calculated bias and uncertainty of the criticality model are incorporated in the critical limit.

The last revision of *Disposal Criticality Analysis Methodology Topical Report* (YMP 2003) indicates that postclosure criticality evaluations are performed only for those degraded configuration classes of the waste form/engineered barrier system for which the probability of occurrence of the configuration class exceeds the probability screening criterion. This predetermined probability screening criterion is set well below the 10 CFR 63.114(d) criterion of one chance in 10,000 of occurring over 10,000 years. Thus, the probability of occurrence for a configuration class is used as an upper bound for the probability of criticality for that configuration class if the screening criterion is satisfied. If the probability screening criterion is not satisfied, then a criticality analysis of the specific configuration class is performed. These criticality evaluations are performed for the configuration classes in each waste form over the range of parameters for the particular class. The process continues with an evaluation of the probability of criticality for configurations that have potential for criticality and an estimation of consequences for those potential critical configurations that cannot be screened from further consideration by low probability. Finally, an estimation of the dose in the accessible environment or risk resulting from such consequences is performed and an identification of

candidates for additional criticality control measures is done if the 10 CFR 63.113(b) criteria for risk to the accessible environment cannot be met.

Application to Waste Package—The current report presents in Chapter 10 a summary of the results of the criticality screening analyses that have been performed to date as part of the overall process of defining and evaluating the conceptual design for the waste package containing various DOE-owned SNF groups. The available results reflect the historical evolution of the postclosure criticality methodology (various revisions of the criticality topical report) and also the iterative efforts required to define an acceptable conceptual design for each SNF group. The differences from the above general postclosure criticality methodology are summarized below. A more detailed presentation is included in Section 10.1.

The main difference from the current postclosure criticality methodology is that the criticality analyses to date have been performed for all anticipated configurations of the waste package regardless of their probability of occurrence. This approach is more conservative than the methodology presented in *Disposal Criticality Analysis Methodology Topical Report* (YMP 2003) and enabled a complete characterization of the potential for criticality of the investigated systems. In order to address the specific configurations of the waste package containing DOE SNF, the general scenarios and configuration classes presented in Section 3 of *Disposal Criticality Analysis Methodology Topical Report* (YMP 2003) have been itemized in *Generic Degradation Scenario and Configuration Analysis for DOE Codisposal Waste Package* (CRWMS M&O 1999g). SNF specific geochemistry calculations were performed to evaluate the degradation of the internal constituents (Phase II) using various scenarios and their results were used in defining the possible configurations of the waste package.

The criticality analyses of the intact and degraded configurations (Phase I and II) resulted in a comprehensive assessment of the effectiveness of the added neutron absorber (where applicable) for a large category of possible configurations spanning periods of time going well beyond the regulatory period.

Another difference from the current methodology was the utilization of a so called “interim critical limit” derived for each SNF group based on a limited number of criticality benchmark experiments and established without the use of the rigorous method described in *Disposal Criticality Analysis Methodology Topical Report* (YMP 2003). Recent work, summarized for each waste package in Section 10, presents the results of the critical model validation for the most reactive configurations identified in the screening analyses using the methodology proposed in *Disposal Criticality Analysis Methodology Topical Report* (YMP 2003). The results show that the interim critical limit is in all situations well below the lower bound tolerance limit (see definition in BSC 2003e) and confirm that the criticality screening analysis was conservative with respect to this criterion.

The Monte Carlo particle transport code, MCNP (MCNP V4B2LV, CSCI: 30033 V4B2LV), was used to estimate the effective neutron-multiplication factor (k_{eff}) of the waste package. The information regarding the code and its use for the criticality analyses is documented in *Criticality Model Report* (BSC 2003e). The k_{eff} results represent the average combined collision, absorption, and track-length estimator from the MCNP calculations. The standard deviation (σ) represents the standard deviation of k_{eff} related to the average combined collision, absorption,

and track-length estimate of the Monte Carlo calculation statistics. The calculations were performed using ENDF/B-V continuous energy cross-section libraries that are part of the qualified MCNP code system.

Currently, efforts are in place to evaluate the probabilities associated with the different configurations using the configurations generator model according to the methodology presented in *Disposal Criticality Analysis Methodology Topical Report* (YMP 2003). Since the criticality screening analysis has not identified areas of concern with respect to the criticality potential within the limits of the assumptions used, the probabilistic analysis is expected to assure the completeness of the postclosure criticality analysis according to the current risk-informed methodology.

INTENTIONALLY LEFT BLANK

7 STRUCTURAL ANALYSIS

7.1 FFTF

7.1.1 Description of the Finite-Element Representation

A two-dimensional finite-element representation of the 5-DHLW/DOE SNF-long waste package was developed to determine the effects of loads from the tipover DBE on the structural components. The representation of the waste package includes the outer and inner barriers, the basket, the support tube, the DOE SNF canister and its basket and support tube, and the DHLW glass canisters. This representation corresponds to a two-dimensional (x-y) slice from the middle of the waste package. After a tipover DBE onto an unyielding surface, the waste package lies horizontally as shown in Figure 7-1. A half-symmetry finite-element representation of the waste package was used. The barriers are assumed to have solid connections at the adjacent surfaces (Section 5.1.1.) and are constrained in a direction perpendicular to the symmetry plane. For the first of the finite-element representations, the DOE SNF canister is included as a point mass at the bottom of the waste package support tube (the waste package lies horizontally), and no credit is taken for its structure. Therefore, the resulting closure of gap between the support tube and the DOE SNF canister is realistically calculated. If it is determined that the gap is not closed, there will be no structural load transferred from the support tube to the DOE SNF canister. Since all calculations are two-dimensional, masses per unit length are calculated based on the maximum allowable weight limits. Although the weight limit for the DOE SNF canister is 2,721 kg (DOE 1999a, Table 3-2), the maximum weight limit from the SDD that was current at the time when the analysis was performed, was 3,400 kg (CRWMS M&O 1998e, Table 1-2), was used to calculate the stresses. Therefore, actual deformations will be smaller than the ones reported in this technical report.

For the second part of the calculations, the finite-element representation is modified to take structural credit for the DOE SNF canister and basket components. This representation is used to determine the maximum closure of the clearance gaps inside the FFTF DFA and the Ident-69 fuel pin container. The deformation values can then be compared to the fuel assembly and the Ident-69 pin container dimensions to determine if there is contact between these components and the basket structure.

First, the impact velocity of the inner lid's outer surface is calculated for a waste package tipover DBE. Then, this velocity is conservatively used in the two-dimensional finite-element analysis. Since the two-dimensional representation does not model a lid, the calculations will indicate that the waste package components undergo more deflection and stress than would actually occur. The target surface is conservatively assumed to be essentially unyielding by using a large elastic modulus for the target surface compared to the waste package (see Section 5.1.2). The target surface is constrained at the bottom to prevent horizontal and vertical motion. Contact elements are defined between the top DHLW glass canister and the inner brackets, and between the outer barrier and the target surface. Initial configuration of the finite-element representation includes a negligibly small gap for each contact element defined in the representation. This configuration allows enough time and displacement for the waste package and its internals to ramp up to the specified initial velocity before the impact. With this initial velocity, the simulation is then

continued through the impact until the waste package begins to rebound. At that time, the stress peaks and the maximum displacements have been obtained.

The vitrified DHLW material properties are represented by ambient material properties of general borosilicate glass. This document does not specifically report any results for the DHLW glass canisters.

7.1.2 Results with No Credit for the Structural Components of the DOE SNF Canister

The first finite-element representation does not take structural credit for the DOE SNF canister; the mass is included by using a point mass element at the lowest point inside the support tube. The structural response of the waste package to tipover accident loads is reported using maximum stress values and displacements obtained from the finite-element solution to the problem. The results indicate that the maximum deformation inside the waste package support tube is 32.3 mm (CRWMS M&O 1998a, Section 6.1). Available space between the support tube and the DOE SNF canister is 44.3 mm (CRWMS M&O 1998a, Section 6.1). Hence, there will be no interference between the two components because of tipover DBE. The stresses on the waste package components and the DOE SNF canister are shown in Figure 7-1. Table 7-1 presents the stresses in each component of the waste package, and shows that the inner barrier of the waste package will not breach since the peak stresses are below the $0.9S_u$, which is the ASME code allowance stress limit shown in Table 6-1.

Table 7-1. 5-DHLW/DOE SNF-Long Waste Package FEA Stress Results

Component	Ultimate Tensile Strength (MPa)	$0.7S_u$ (MPa)	$0.9S_u$ (MPa)	Maximum Stress Intensity (MPa)	Maximum Membrane Stress (MPa)	Maximum Membrane Plus Bending Stress (MPa)
Outer barrier	483	338	435	372	25	486
Inner barrier	690	483	621	418	412	418
Basket plates and support tube	483	338	435	474	27	555

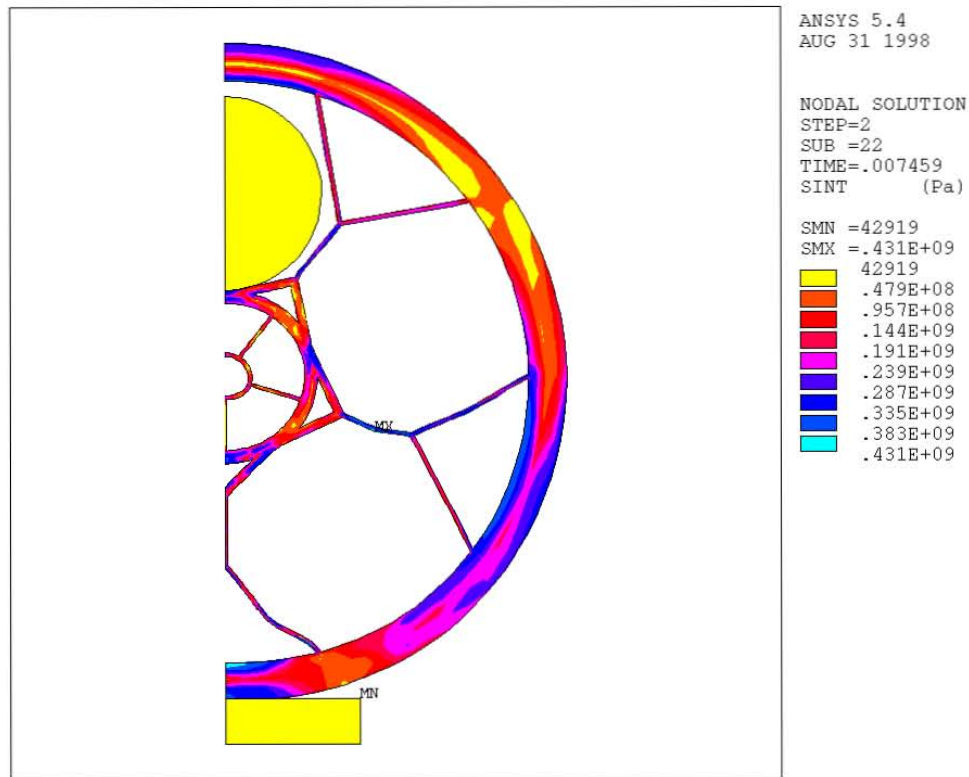
Source: CRWMS M&O 1998a, Section 6.1

7.1.3 Results with Structural Credit for the DOE SNF Canister Components

The maximum deformation causing cavity closure around the fuel assembly is determined for the case of 5-DHLW waste package representation that includes the structural components of the DOE SNF canister. The displacement results of the waste package tipover structural analysis showed that the maximum FFTF DFA cavity closure is 7.3 mm due to the deformation of the DOE SNF canister basket (CRWMS M&O 1998a, Section 6.2). The available gap between the FFTF DFA and the basket is 11.6 mm (CRWMS M&O 1998a, Section 6.2). Therefore, the DFA will not be crushed by the basket structure.

Similarly, the maximum deformation inside the Ident-69 container shell is determined to be 12.8 mm (CRWMS M&O 1998a, Section 6.2). On the other hand, available space between the FFTF DOE SNF canister center tube and the Ident-69 pin container is 11.7 mm (CRWMS M&O 1998a, Section 6.2). This seems to result in an interference (1.1 mm) between these two parts

due to impact. This is an artifact of the computational representation. The case was setup with the DOE SNF canister in contact with the waste package basket (support tube), which simplifies the calculations and reduces computing time. Since the 44.3 mm gap between the DOE SNF canister and the waste package support tube was not utilized, a significant part of the load that deformed the support tube in the waste package basket was transmitted directly to the DOE SNF canister and its basket structure in this representation. This causes excessive deformation of the DOE SNF canister basket and appears to trap the Ident-69 pin container in the center tube. As shown in Section 7.1.2, since the gap between the DOE SNF canister and the waste package support tube does not fully close, there is no load transferred to the DOE SNF canister and its basket. Thus the deformation will be much less and there will be no interference between any of the fuel-assemblies or the Ident-69 container and the basket structure.



Source: CRWMS M&O 1999a, Figure 3-1

Figure 7-1. Stresses in 5-DHLW/DOE SNF-Long Waste Package Loaded with FFTF Fuel

7.1.4 Summary

The results given in Sections 7.1.2 and 7.1.3 show that there is sufficient clearance between the inner diameter of the support tube and the outer diameter of the DOE SNF canister in the case of a tipover DBE. Hence, there will be no interference between the two components, and the DOE SNF canister can be removed from the support tube if necessary to be placed in another waste package.

7.2 TRIGA

7.2.1 Description of the Finite-Element Representation

A two-dimensional finite-element representation of the waste package (containing five DHLW glass canisters and one DOE SNF canister) was developed to determine the effects of loads on the structural components from the tipover DBE. The representation of the waste package includes the outer and inner barriers, the basket assembly (inner and outer brackets and divider plate), the support tube, the DOE SNF canister and its basket and support tube, and the DHLW glass canisters. A half-symmetry finite-element representation of the waste package is used. The barriers are assumed to have solid connections at the adjacent surfaces (Section 5.1.1) and are constrained in a direction perpendicular to the symmetry plane. One of the DHLW glass canisters, which are located around the 18-in-outer diameter DOE SNF canister, is represented using two-dimensional elements. The remaining DHLW glass canisters are included in the representation by placing point mass elements at the points of contact of the pour canister with the basket assembly. These locations are approximately at the mid-point of each component or segment. The finite-element representation is used to determine the maximum closure of the gap between the structural tubes and fuel rods so that they can be compared to the fuel element dimensions to determine whether there is contact between the tubes and the fuel element during the transient analysis.

First, the impact velocity of the outer surface of the inner lid is calculated for a waste package tipover DBE. Then, this velocity is conservatively used in the two-dimensional finite-element analysis. Since the two-dimensional representation does not include a lid, the calculations will indicate that the waste package components undergo more deflection and stress than would actually occur. The target surface is conservatively assumed essentially unyielding by using a large elastic modulus for the target surface compared to the waste package (Section 5.1.1). The target surface is constrained at the bottom to prevent horizontal and vertical motion. Contact elements are defined between: the top DHLW canister and the inner bracket, the lower and upper corner (apex) tube and the DOE SNF canister, the lower and upper basket support bracket and the DOE SNF canister, the DOE SNF canister and the support tube and finally, the outer waste package barrier and the target surface. The initial configuration of the finite-element representation of waste package internals includes the maximum possible gap for each contact element in order to account for the worst case scenario. On the other hand, the initial gap between the entire waste package and the target surface is small in comparison with the others. This allows enough time and displacement for the waste package and its internals to ramp up to the specified initial velocity before the impact. With this initial velocity, the simulation is then continued throughout the impact until the waste package and its internals begin to rebound, at which time the stress peaks and the maximum displacements have been obtained.

The vitrified DHLW glass material properties are represented by ambient material properties of general borosilicate glass. This document does not specifically report any results for the individual DHLW glass canisters.

7.2.2 Results with No Credit for the TRIGA SNF Rod Inside of the DOE SNF Canister

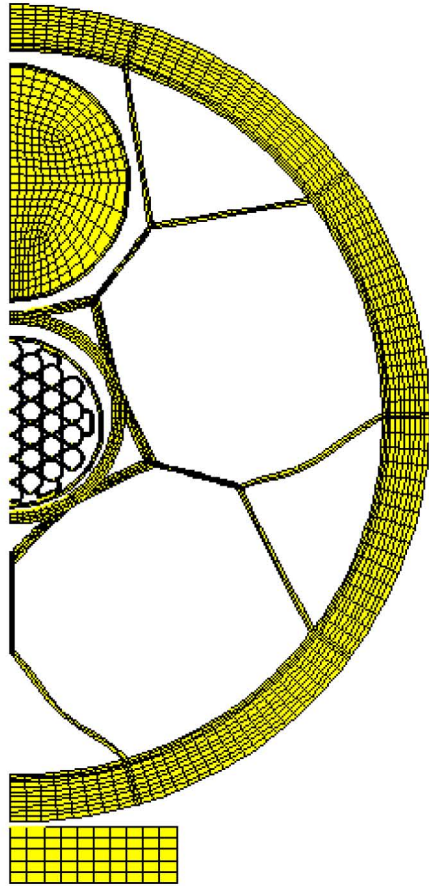
The first finite-element representation does not take any structural credit for the TRIGA SNF rod inside of the DOE SNF canister; the mass is included using a point mass element at the lowest point inside the support grid tube. The structural response of the waste package to tipover accident loads is reported using maximum stress intensity magnitudes and displacements obtained from the finite-element solution to the problem. The results indicate that the maximum deformation inside the waste package support tube is 8.28-mm (0.326-in) (CRWMS M&O 1999h, Section 6). Available space inside of the structure tube after deformation is 40.9-mm (1.61-in) (CRWMS M&O 1999h, Section 6). Hence, there will be no interference between the two components because of tipover DBE. The deformed configuration and stresses on the waste package components and the support grid tubes are shown in Figures 7-2 and 7-3. Table 7-2 presents the stress intensity magnitudes in the waste package components, and shows that the inner barrier of the waste package does not exceed the peak stresses of $0.9S_u$ which is the ASME code allowance stress limit in Table 6-1.

Table 7-2. 5-DHLW/DOE SNF-Short Waste Package FEA Stress Results

Component	Ultimate Tensile Strength (MPa)	$0.7S_u$, (MPa)	$0.9S_u$, (MPa)	Maximum Stress Intensity (MPa)	Maximum Membrane Stress (MPa)	Maximum Membrane Plus Bending Stress (MPa)
Outer barrier	483	338	435	372 ^b	25 ^b	486 ^b
Inner barrier	690	483	621	418 ^b	412 ^b	418 ^b
Basket plates ^a and support tube	483	338	435	474 ^b	27 ^b	555 ^b

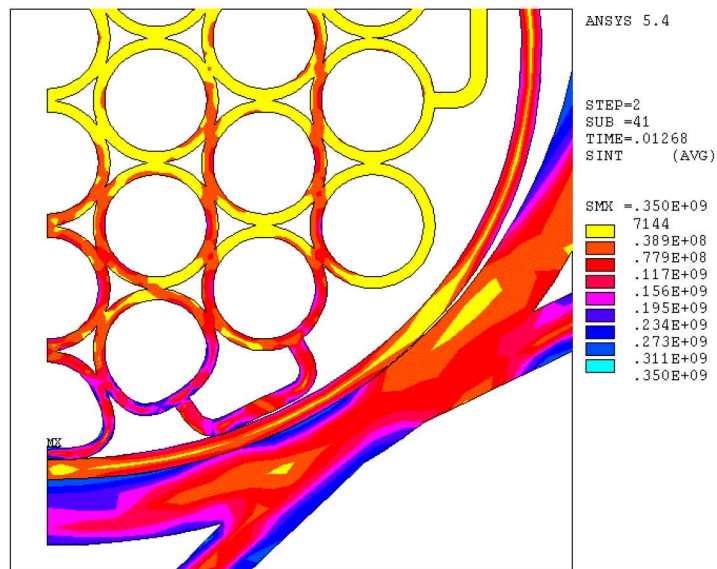
Source: CRWMS M&O 1999h

NOTES: ^a Basket plates include the inner bracket, the outer bracket, and the divider plate.
^b CRWMS M&O 1998a.



Source: CRWMS M&O 1999h

Figure 7-2. Stresses in the 5-DHLW/DOE SNF-Short Waste Package Loaded with TRIGA Fuel



Source: CRWMS M&O 1999h

Figure 7-3. Stresses Inside of the DOE Spent Nuclear Fuel Canister Loaded with TRIGA Fuel

The structural response of the waste package to tipover accident loads is reported using maximum stress values and displacements obtained from the finite-element solution to the problem. The results show that the maximum cavity closure inside the fuel tube is 8.28 mm (0.325-in) (CRWMS M&O 1999h, Section 6). The available space inside of an individual tube was reduced from 49.20-mm (1.937-in) to 40.92-mm (1.611-in), and since the maximum outer diameter of the fuel element is 37.5 mm (1.476-in), the space between the most deformed apex tube and the fuel rod is 3.44 mm (0.135-in) (CRWMS M&O 1999h, Attachment V, line #553). Hence, there is no interference between the two components from a tipover DBE. The maximum stress in the 18-in-outer diameter DOE SNF canister structural components including internals is 350 MPa, which is 27.5 percent less than the ultimate tensile strength of Stainless Steel Type 316L, 483 MPa (CRWMS M&O 1999h, Section 6).

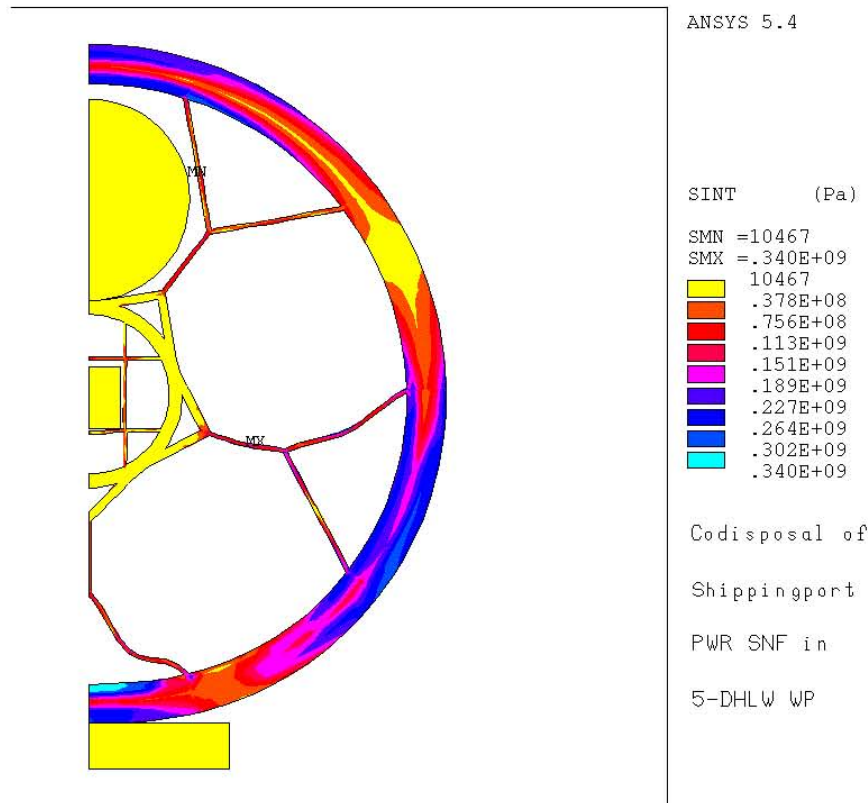
7.2.3 Summary

The results given in Section 7.2.2 show that there is sufficient clearance between the inner diameter of the support tube and the outer diameter of the DOE SNF canister in the case of a tipover DBE. Hence, there will be no interference between the two components, and the DOE SNF canister can be removed from the support tube if necessary to be placed in another waste package.

7.3 SHIPPINGPORT PWR

7.3.1 Description of the Finite-Element Representation

A two-dimensional finite-element representation of the 5-DHLW/DOE SNF-long waste package is developed to determine the effects of loads from the tipover DBE on the structural components (CRWMS M&O 1999i). The representation of the waste package includes the outer and inner barriers, the basket, the support tube, the DOE SNF canister and its basket and support tube, and the DHLW glass canisters. This representation corresponds to a two-dimensional (x-y) slice from the middle of the waste package. After a tipover DBE onto an unyielding surface, the waste package lies horizontally as shown in Figure 7-4. A half-symmetry finite-element representation of the waste package was used. The barriers are assumed to have solid connections at the adjacent surfaces (Assumption 5.1.1) and are constrained in a direction perpendicular to the symmetry plane. It was shown in *5-High Level Waste DOE Spent Fuel Waste Package Structural Calculations* (CRWMS M&O 1998a) that there is no closure of gap between the support tube and the DOE SNF canister, and there is no structural load transferred from the support tube to the DOE SNF canister. Since all calculations are two-dimensional, masses per unit length are calculated based on the maximum allowable weight limits. The maximum weight limits, which are higher than the weight limits in *FFTF (MOX) Fuel Characteristics for Disposal Criticality Analysis* (DOE 1998b, p. 6), from the SDD (CRWMS M&O 1998e, Table 1-2) is used to calculate the stresses on the support tube and waste package basket plates.



Source: CRWMS M&O 1999i

Figure 7-4. Stresses in 5-DHLW/DOE SNF-Long Waste Package Loaded with Shippingport PWR Fuel

The finite-element representation is used to determine the maximum closure of the clearance gaps inside the DOE SNF canister-basket plates so that they can be compared to the Shippingport fuel assembly dimensions to determine whether there is contact between the basket plates and the fuel assembly. A two-dimensional finite-element representation of the 5-DHLW/DOE SNF-long waste package is developed to determine the effects of tipover DBE loads on the structural components of the DOE SNF canister. The design concept is developed to contain one Shippingport fuel assembly in the DOE SNF canister (see CRWMS M&O 1999i, pp. I-3 and II-2). Since the Shippingport PWR assembly mass is far below the DOE SNF canister mass limit, a second design is developed to contain two Shippingport PWR fuel assemblies in the DOE SNF (CRWMS M&O 1999i, pp. I-2 and II-1) to show that the 5-DHLW/DOE SNF-Long waste package for Shippingport PWR can handle loads greater than the ones with a single assembly in a DOE SNF canister. The difference between the two designs is limited to the internal components of the DOE SNF canister only.

First, the impact velocity of the outer surface of the inner lid is calculated for a waste package tipover DBE. Then, this velocity is conservatively used in the two-dimensional finite-element analysis. Since the two-dimensional representation does not model a lid, the calculations will indicate that the waste package components undergo more deflection and stress than would actually occur. The target surface is conservatively assumed to be essentially unyielding by using a large elastic modulus for the target surface compared to the waste package (Section

5.1.2). The target surface is constrained at the bottom to prevent horizontal and vertical motion. Contact elements are defined between the top DHLW glass canister and the inner brackets, and between the outer barrier and the target surface. The initial configuration of the finite-element representation includes a negligibly small gap for each contact element defined in the representation. This configuration allows enough time and displacement for the waste package and its internals to ramp up to the specified initial velocity before the impact. With this initial velocity, the simulation is then continued through the impact until the waste package begins to rebound. At that time, the stress peaks and the maximum displacements have been obtained.

The vitrified DHLW material properties are represented by ambient material properties of general borosilicate glass. This document does not specifically report any results for the individual DHLW glass canisters.

7.3.2 Results of Structural Calculations

The structural response of the waste package to tipover accident loads is reported using maximum stress values and displacements obtained from the finite-element solution to the problem. The results show that the cavity between the Shippingport basket and the basket plates does not close, but on the contrary, becomes larger because of the dynamic load applied on the bottom plate by the Shippingport fuel assembly as shown in Figure 7-5. Hence, there will be no interference between the fuel assembly and the basket plates because of tipover DBE. The maximum stress in the DOE SNF canister-structural components including internals is determined to be 217 MPa (CRWMS M&O 1999i, p. 20). This magnitude of stress is also less than the tensile strength of 316L, 483 MPa.

The results obtained with two Shippingport PWR assemblies are similar to the results with one Shippingport PWR assembly. The results show that the cavity between the Shippingport fuel assembly and the basket plates does not close, but on the contrary, becomes larger because of the dynamic load applied on the bottom plate by the Shippingport fuel assembly (see CRWMS M&O 1999i, Figure II-3). Hence, there will be no interference between the fuel assembly and the basket plates because of tipover DBE. The maximum stress in the DOE SNF canister-structural components including internals is determined to be 228 MPa (CRWMS M&O 1999i, p. 20). This magnitude of stress is less than the tensile strength of Stainless Steel Type 316L, 483 MPa (CRWMS M&O 1999i, p. 20).

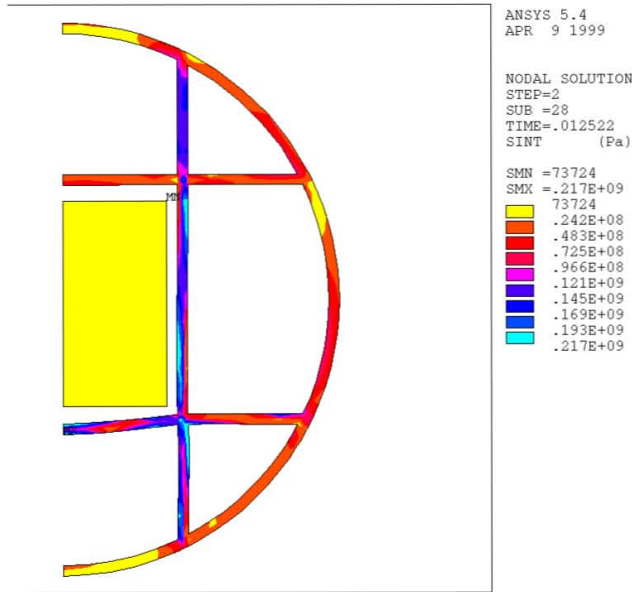


Figure 7-5. Stresses in the DOE Spent Nuclear Fuel Canister Loaded with Shippingport PWR Fuel

The calculations in *Structural Calculations for the Codisposal of Shippingport Spent Nuclear Fuel in a Waste Package* (CRWMS M&O 1999i) also show that the maximum bending stress on the base plate due to the weight of the structural components and the fuel is 55 MPa which is less than the yield strength of Stainless Steel Type 316L (172 MPa, CRWMS M&O 1999i, p. 20).

The calculations given in Sections 5.7 and 5.8 of *Structural Calculations for the Codisposal of Shippingport Spent Nuclear Fuel in a Waste Package* (CRWMS M&O 1999i) utilize the maximum DOE SNF canister mass; therefore, the results of the bending and buckling calculations are bounding for all design concepts.

7.3.3 Summary

The results given in Section 7.3.2 show that there is sufficient clearance between the inner diameter of the support tube and the outer diameter of the DOE SNF canister in the case of a tipover DBE. Hence, there will be no interference between the two components, and the DOE SNF canister can be removed from the support tube if necessary to be placed in another waste package.

7.4 ENRICO FERMI

7.4.1 Description of the Finite-Element Representation

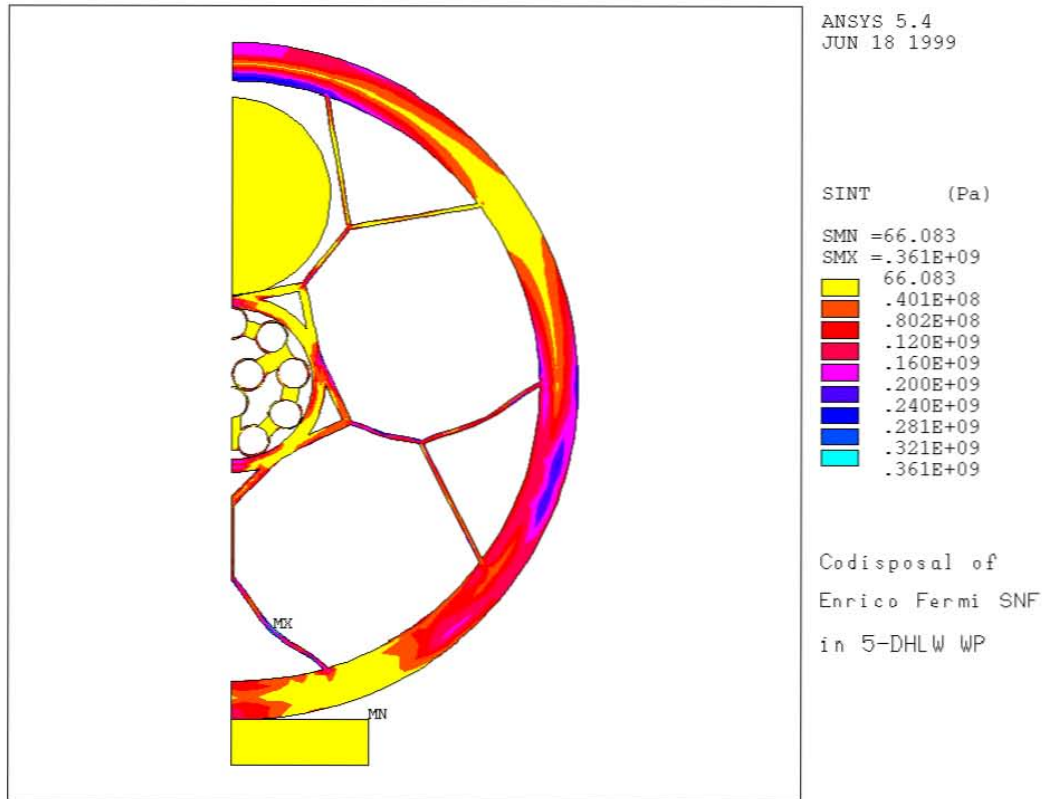
A two-dimensional transient dynamic calculation has been performed for the structural analysis of the Enrico Fermi SNF canister within the 5-DHLW (defense high-level waste) DOE SNF waste package. This analysis, performed with ANSYS V5.4, considers a bounding dynamic load from a tip-over design basis event on the cross-section of the waste package at its rotating end. Since the potential energy of the rotating end is larger than the potential energy of any other

DBEs, the tipover DBE is considered both bounding and appropriately conservative for structural design purposes. The finite-element representation of the fuel assemblies includes the minimum level of detail needed to represent the mass and mechanical/physical properties of the fuel assemblies and to meet the computational requirements of ANSYS V5.4.

The two-dimensional finite-element representation is developed. A one-half-symmetry finite-element representation is developed for the waste package (see Figure 7-6). The finite-element representation includes the outer and inner barriers, basket assembly, support pipe, uppermost DHLW pour canister, DOE SNF canister shell, 4-in pipes and the dividers. The finite-element representation also includes masses of the other four pour canisters, the aluminum canisters and the fuel. The barriers are assumed to have solid connections at the adjacent surfaces (Section 5.1.1) and are constrained in a direction perpendicular to the symmetry plane. The DHLW pour canister that is located above the DOE SNF canister is created using two-dimensional elements. The remaining pour canisters are included in the representation as point mass elements at the points of contact of the pour canisters with the inner barrier and the divider plates. These locations are approximately at the mid-point of each component or segment at which the pour canisters would be in contact. This approach is a realistic way to simulate the effect of each pour canister in contact with the waste-package internals. This approach reduces the computer execution time needed for this analysis. The finite-element representation is used to determine the maximum closure of the clearance space between components inside the 4-in pipes and the aluminum canister to determine whether there is contact between the pipes and the aluminum canister during the DBE.

First, the impact velocity of the outer surface of the inner lid is calculated for a waste package tipover DBE. Then, this velocity is conservatively used in the two-dimensional finite-element analysis. Since the two-dimensional representation does not model the lids, the calculations will indicate that the waste package components undergo more deflection and stress than would actually occur if the lids were included. The target surface is conservatively assumed to be essentially unyielding because the elastic modulus used for the target surface is large compared to the elastic modulus used for the waste package (Section 5.1.2). The target surface is constrained at the bottom to prevent its horizontal and vertical motion. Contact elements are defined between the top pour canister and the inner brackets, and between the outer barrier and the target surface. Initial configuration of the finite-element representation includes a negligibly small gap for each contact element. This approach allows enough time and displacement for the waste package and its internals to ramp up to the specified initial velocity before the impact. With this initial velocity, the simulation is then continued throughout the impact until the waste package begins to rebound; at that time, the stress peaks, and the maximum displacements are obtained.

The vitrified DHLW material properties are represented by ambient temperature properties of general borosilicate glass. This document does not specifically report any results for the individual DHLW glass canisters.



Source: CRWMS M&O 1999j

Figure 7-6. Stresses in the 5-DHLW/DOE SNF-Short Waste Package Loaded with Enrico Fermi Fuel

7.4.2 Results

The structural response of the waste package to tipover accident loads is reported using maximum stress values and displacements obtained from the finite-element solution to the problem. The results show that the maximum cavity closure inside the 4-in pipe is 6.97 mm (CRWMS M&O 1999j). Available space between an individual 4-in pipe and an aluminum -01 canister shell is 9.49 mm (CRWMS M&O 1999j). Hence, there is no interference between the two components from a tipover DBE. The maximum stress in the DOE SNF canister structural components and internals is 265 MPa (CRWMS M&O 1999j), which is less than the 483 MPa tensile strength of Stainless Steel Type 316L (CRWMS M&O 1999j).

In performing the structure analysis, the maximum DOE canister mass of 2,270 kg was used. The mass of the iron shot was not specifically considered in the structural analysis but was implicitly included in the maximum mass.

7.4.3 Summary

The results given in Section 7.4.2 show that there is sufficient clearance between the inner diameter of the support pipe and the outer diameter of the DOE SNF canister in the case of a tipover DBE. Hence, there will be no interference between the two components, and the DOE

SNF canister can be removed from the support pipe if necessary to be placed in another waste package. Additionally, there will be no breach of the DOE SNF canister.

7.5 SHIPPINGPORT LWBR

7.5.1 Description of the Finite-Element Representation

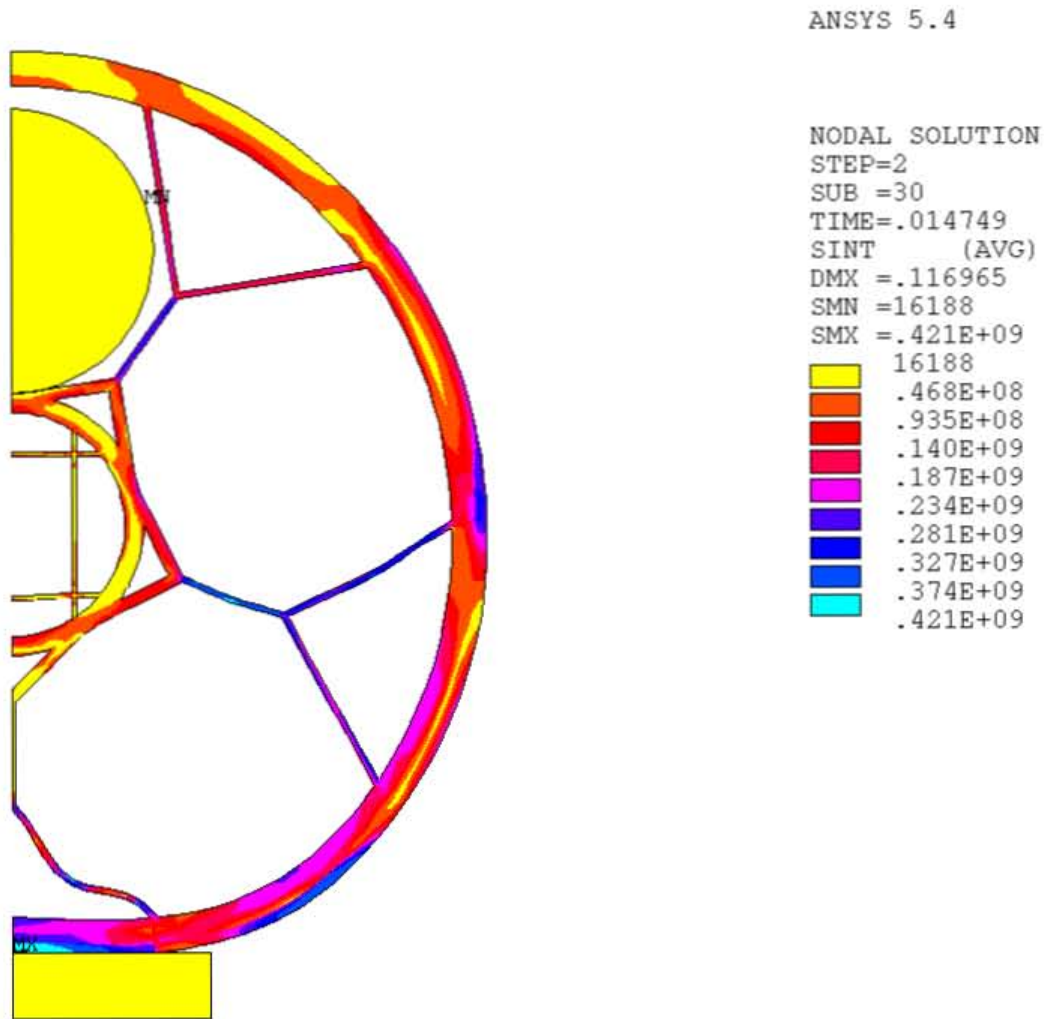
A two-dimensional transient dynamic calculation has been performed for the structural analysis of the Shippingport LWBR SNF canister within the 5-DHLW DOE SNF-long waste package. This analysis, performed with ANSYS V5.4, considers a bounding dynamic load from a tip-over design basis event on the cross-section of the waste package at its rotating end. Since the potential energy of the rotating end is larger than the potential energy of any other DBEs, the tipover DBE is considered both bounding and appropriately conservative for structural design purposes. The Shippingport LWBR seed fuel assembly is represented as a single lumped mass, since the worst-case loading is a point loading in the middle of the canister assembly plates. Aluminum shot is to be placed within the 18-in-outer diameter DOE SNF canister, and is represented in the calculation as individual lumped masses.

The two-dimensional finite-element representation is developed. A one-half-symmetry finite-element representation is developed for the waste package (see Figure 7-7). The finite-element representation includes the outer and inner barriers, basket assembly, support tube, uppermost DHLW pour canister, DOE SNF canister shell and basket. The finite-element representation also includes masses of the other four pour canisters and the fuel assembly. The barriers are assumed to have solid connections at the adjacent surfaces (Assumption 5.1.1) and are constrained in a direction perpendicular to the symmetry plane. The DHLW pour canister that is located above the DOE SNF canister is created using two-dimensional elements. The remaining pour canisters are included in the representation as point mass elements at the points of contact of the pour canisters with the inner barrier and the divider plates. These locations are approximately at the mid-point of each component or segment at which the pour canisters would be in contact. This approach is a realistic way to simulate the effect of each pour canister in contact with the waste-package internals. This approach reduces the computer execution time needed for this analysis. The finite-element representation is used to determine the maximum closure of the clearance space inside the DOE SNF canister basket plates so that they can be compared to the Shippingport LWBR seed fuel assembly dimensions to determine whether there is contact between the basket plates and the fuel assembly.

First, the impact velocity of the outer surface of the inner lid is calculated for a waste package tipover DBE. Then, this velocity is conservatively used in the two-dimensional finite-element analysis. Since the two-dimensional representation does not model the lids, the calculations will indicate that the waste package components undergo more deflection and stress than would actually occur if the lids were included. The target surface is conservatively assumed to be essentially unyielding because the elastic modulus used for the target surface is large compared to the elastic modulus used for the waste package (Assumption 5.1.2). The target surface is constrained at the bottom to prevent its horizontal and vertical motion. Contact elements are defined between the top pour canister and the inner brackets, and between the outer barrier and the target surface. Initial configuration of the finite-element representation includes a negligibly small gap for each contact element. This approach allows enough time and displacement for the

waste package and its internals to ramp up to the specified initial velocity before the impact. With this initial velocity, the simulation is then continued throughout the impact until the waste package begins to rebound; at that time, the stress peaks, and the maximum displacements are obtained.

The DHLW glass material properties are represented by ambient material properties of general borosilicate glass. This document does not specifically report any results for the individual DHLW glass canisters.



Source: CRWMS M&O 1999k

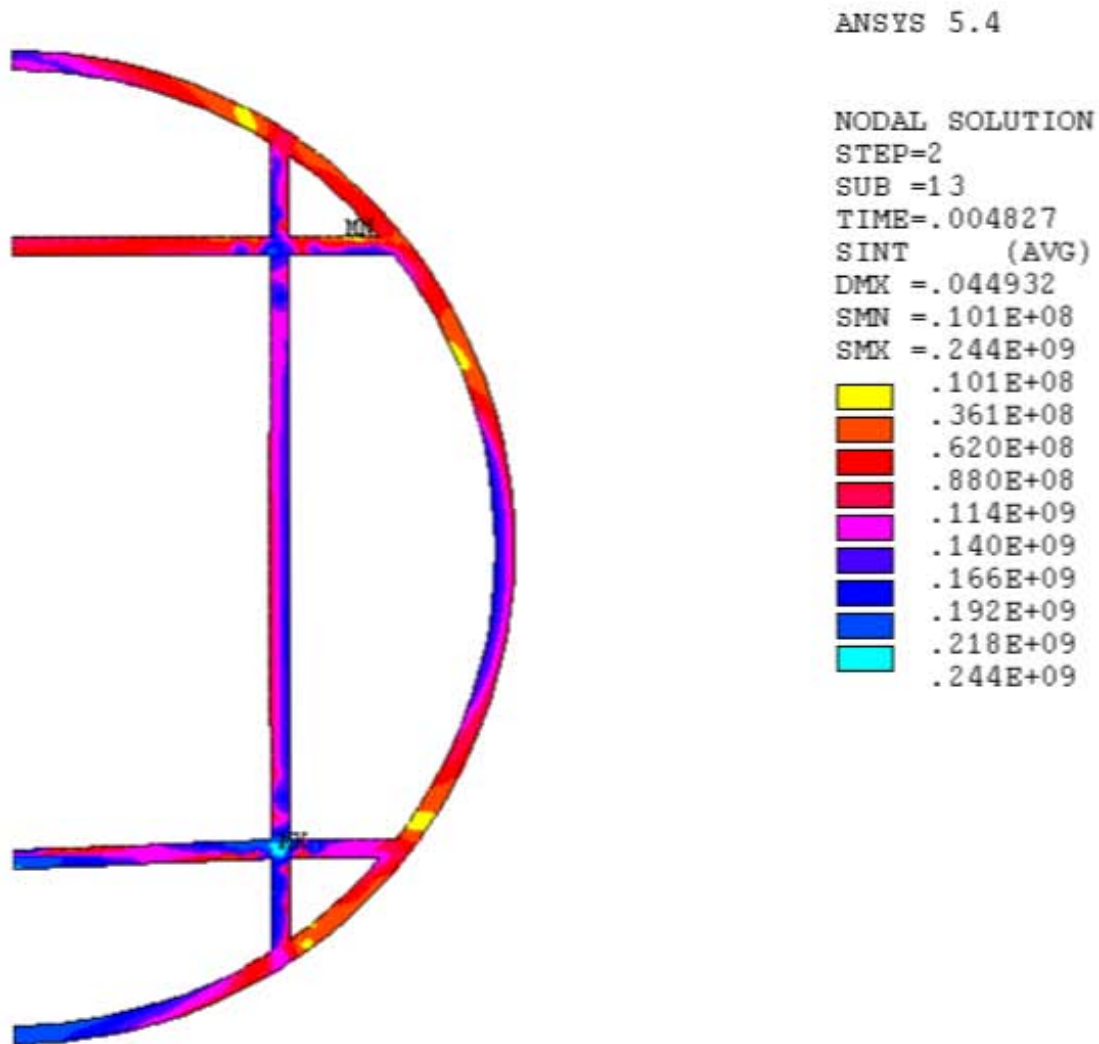
Figure 7-7. Stresses in the 5-DHLW/DOE SNF-Long Waste Package

7.5.2 Results

The structural response of the waste package to tipover accident loads is reported using maximum stress values and displacements obtained from the finite-element solution to the problem. The results show that the cavity between the Shippingport LWBR seed fuel assembly and the basket plates does not close, but on the contrary, becomes larger because of the dynamic load applied on the bottom plate by the fuel assembly as shown in Figure 7-8. Hence, there will

be no interference between the fuel assembly and the basket plates because of a tipover DBE. The maximum stress in the DOE SNF canister structural components and internals is 243.6 MPa (CRWMS M&O 1999k, p. 21), which is less than 0.9 or 0.7 of the ultimate tensile strength of Stainless Steel Type 316L, 483 MPa (CRWMS M&O 1999k, p. 21), therefore the allowable stress-limit criteria presented in Table 6-1 are met.

The calculations in *Structural Calculations for the Codisposal of Shippingport LWBR Spent Nuclear Fuel in a Waste Package* (CRWMS M&O 1999k) also show that the maximum bending stress on the base plate due to the weight of the structural components and the fuel is 16.6 MPa which is less than the 172 MPa yield strength of Stainless Steel Type 316L (CRWMS M&O 1999k, p. 21).



Source: CRWMS M&O 1999k

Figure 7-8. Stresses in the DOE Spent Nuclear Fuel Canister

Finally, the critical stress for buckling to take place on the spacer tube (see Figure 7-7) is 1.43 GPa, whereas the compressive stress is only 2.06 MPa (CRWMS M&O 1999k, p. 21). Therefore, the Shippingport LWBR fuel assembly will not be crushed within the basket structure.

The calculations given in *Structural Calculations for the Codisposal of Shippingport LWBR Spent Nuclear Fuel in a Waste Package* (CRWMS M&O 1999k, Sections 5.7 and 5.8) utilize the maximum DOE SNF canister mass, 2,721 kg, and the maximum DHLW glass canister mass, 4200 kg; therefore, the results of the bending and buckling calculations given in this section are bounding for all design concepts.

7.5.3 Summary

The results given in Section 7.5.2 show that there is sufficient clearance between the inner diameter of the support tube and the outer diameter of the DOE SNF canister in the case of a tipover DBE. Hence, there will be no interference between the two components, and the DOE SNF canister can be removed from the support tube if necessary to be placed in another waste package. Additionally, there will be no breach of the DOE SNF canister.

7.6 N-REACTOR

7.6.1 Description of the Finite Element Representation

A full three-dimensional finite element representation of the waste package was developed in ANSYS V5.4 by using the dimensions provided in Appendix A. The finite element representation was created with the largest possible radial gap of 4 mm between the inner and outer shells (CRWMS M&O 2000i, Section 8.1.8). The initial orientation of the inner shell maintains this 4-mm gap around the circumference of the shell. This gap results in a slightly lower total mass of the waste package than that listed in Appendix A, which shows a nominal 0-mm radial gap between the inner and outer shells, but the difference is small, and the impact was anticipated to be negligible. The internal structure of the waste package was simplified in several ways. First, the A-plate dividers were created as shell elements with an assigned thickness of 10 mm. Next, the internals of the MCO were reduced to mass elements uniformly distributed along the inner walls of the MCO (Assumption 5.1.3). Finally, the structure of the DHLW glass canisters was reduced to cylinders of uniform mass density (Assumption 5.1.5). The total mass and geometric dimensions of the DHLW glass canister define the density. The benefit of using this approach was to reduce the computer execution time while preserving all features of the problem relevant to the structural calculation.

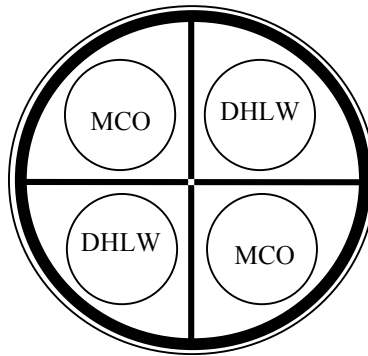


Figure 7-9. Cross-Section View of Tipover (Case 1 Orientation)

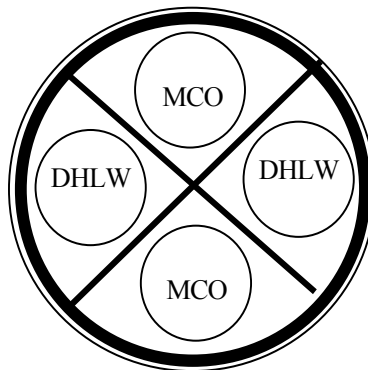


Figure 7-10. Cross-Section View of Tipover (Case 2 Orientation)

The MCOs and DHLW glass canisters were placed in the waste package such that they were diagonally across from each other (Figures 7-9 and 7-10). This configuration will have the center of gravity lie on the axis of the cylinder (except for movement tolerance within the cells of the basket). In this way the waste package will be as close as possible to balanced with respect to rotations about the cylinder axis. The tipover calculation was performed for two different initial configurations. This was done to find the most critical tipover orientation of the two limiting configurations. The first was oriented such that one MCO and one DHLW glass canister were at the bottom and the same on top, with the vertical A-plate divider being perpendicular to the unyielding surface (Figure 7-9). The second was oriented such that one MCO was directly at the bottom of the waste package and the DHLW glass canisters were at the sides (Figure 7-10).

The target surface was conservatively assumed to be unyielding with a large elastic modulus (Assumption 5.1.2).

The initial tipover angle was reduced to 0.1° , and the waste package was given an initial angular velocity corresponding to the rigid-body motion of the waste package. This configuration reduces the computer execution time while preserving all features of the problem relevant to the structural calculation.

The finite element representation was then used in LS-DYNA V950 to perform the transient dynamic analysis for the 2-MCO/2-DHLW waste package tipover DBE.

7.6.2 Results of Structural Calculations

The structural response of the waste package to tipover accident loads was reported using maximum stress values and displacements obtained from the finite element solution to the problem. The results show that the maximum stress intensities occurred in the first case for each part, except for the upper trunnion collar sleeve, and all components had stresses greater than their corresponding yield strengths. The maximum stress intensities were in the upper trunnion collar sleeve with a magnitude of 532 MPa, which exceeded seven tenths of the ultimate tensile strength but was less than the ultimate tensile strength of Alloy 22, 690 MPa (CRWMS M&O 2000j, Section 5.1). However, the upper trunnion collar sleeve was not part of the containment barrier. It acted as an impact limiter for the containment barrier in this case. The maximum stress intensity in the outer shell had a magnitude of 429 MPa, which was less than seven tenths of the ultimate tensile strength of Alloy 22.

The maximum stress intensity in the inner shell was 325 MPa, which was less than the seven tenths of the ultimate tensile strength of Stainless Steel Type 316NG, 515 MPa (CRWMS M&O 2000j, Section 5.1).

For the A-plate dividers, the maximum stress intensity was 437 MPa, which exceeded seven tenths of the ultimate tensile strength of 516 carbon steel, 483 MPa (CRWMS M&O 2000j, Section 5.1). However, the A-plate dividers are not part of the containment barrier and only separate the MCO and defense high-level waste canisters.

The maximum stress intensity in the MCO outer shell occurred in the MCO placed in the bottom and had a magnitude of 226 MPa, which was less than seven tenths of the ultimate tensile strength of Stainless Steel Type 304L, 485 MPa (CRWMS M&O 2000j, Section 5.1).

The results also show that the cavity of the entire waste package (between the MCOs and the DHLW glass canister) is significantly decreased as the A-plate dividers are bent under the load. However, the bending of the A-plate dividers is concentrated at the top of the waste package and does not appear to be a hindrance to the removal of the MCOs or DHLW glass canisters.

7.6.3 Summary

The results given show that the containment of the MCO is sufficient, and clearance between the inner A-plate dividers in diameter of the waste package canister will be adequate in the case of a tipover design basis event. Hence, there will be no breach of the waste package or MCO, and there will not be a great enough interference from the A-plate dividers to prevent removal of the MCOs and defense high-level waste glass canisters from the waste package for emplacement inside another waste package. Therefore, there will be no criticality induced by a tipover event.

The ultimate strengths of the materials of the waste package and MCOs are given in Section 7.4.2. A comparison of these values reveals that all stresses, except for in the A-plate dividers, are less than the stress limit (70 percent of the ultimate tensile strength of the material) given in the 1997 Addenda of *1995 ASME Boiler and Pressure Vessel Code* (ASME 1995). Therefore, it is concluded that the performance of the 2-MCO/2-DHLW waste package internal design is structurally acceptable when exposed to a tipover event and therefore meet the structural criteria (Section 4.1.1) as long as the MCOs loaded mass limit (9298.7 kg and 7906.4 kg for MCOs

loaded with Mark IV and Mark IA, respectively) and the DHLW glass canisters mass limit (4,200 kg) are not exceeded.

7.7 ALUMINUM-BASED FUELS (MELT AND DILUTE)

7.7.1 Description of the Finite Element Representation

A full three-dimensional finite element representation of the waste package was developed in ANSYS V5.4. The finite element representation was created with the largest possible radial gap of 4 mm between the inner and outer shells. The initial orientation of the inner shells maintains this 4-mm gap around the circumference of the shell. The internal structure of the waste package was simplified in several ways. First the support tube, brackets, and divider plates were combined and created as shell elements with an assigned thickness of 31.75, 25.4, and 12.7 mm in the respective regions. Next, the structure of the DHLW glass canisters and DOE SNF canister, were reduced to cylinders of uniform mass density (Sections 5.1.4 and 5.1.6). The total mass and geometric dimensions of the DHLW canister and DOE SNF canister define the density. The benefit of using this approach was to reduce the computer execution time while preserving all features of the problem relevant to the structural calculation.

The target surface was conservatively assumed to be unyielding with a large elastic modulus (Section 5.1.4).

The initial tip-over angle with respect to the horizontal plane was reduced to 0.1°, and the waste package was given an initial angular velocity corresponding to the rigid-body motion of the waste package (BSC 2002a, Section 5.5). This configuration reduces the computer execution time while preserving all features of the problem relevant to the structural calculation.

The finite element representation was then solved using LS-DYNA V950 to perform the transient dynamic analysis for the 5-DHLW/DOE SNF-short waste package tip-over design basis event at room temperature (20°C), 204°C, and 316°C.

LS-DYNA uses true stress and true strain as material property inputs. The ASME Code reports only engineering stress and engineering strain. The material properties needed to be converted to the proper form in order for the solution to execute correctly. Table 7-3 reports the true ultimate tensile strength (σ_u) for Alloy 22 and Stainless Steel Type 316NG. σ_u values are given in *Waste Package Tip-Over of 5-DHLW/DOE Short* (BSC 2002a, p. 14). σ_u should be substituted for S_u in Table 6-1 in order to remain consistent.

Table 7-3. True Stress of Alloy 22 and Stainless Steel Type 316NG

Temperature	σ_u of Alloy 22 (MPa)	σ_u of Stainless Steel Type 316 (MPa)
Room Temperature	973	700
204°C	940	630
316°C	904	619

Source: BSC 2002a, p. 14

7.7.2 Results of Structural Calculations

The results obtained from LS-DYNA V950 were reported in terms of maximum shear stress. Since the maximum stress intensities were desired, the results needed to be converted. The maximum shear stress is defined as one-half the difference between maximum and minimum principal stress (Shigley and Mischke 1989, p. 31). Stress intensity is defined as the difference between maximum and minimum principal stress. Therefore, the results obtained from LS-DYNA V950 were multiplied by two to obtain the corresponding stress intensities.

The maximum stresses were found by carefully examining each time step taken by LS-DYNA V950, which outputs the element with the highest magnitude of stress, at each step, for each defined part. Table 7-4 lists the maximum stress intensities in the outer shell and inner shell at room temperature, 204°C, and 316°C.

Table 7-4. Maximum Stress Intensities

Temperature	Maximum Stress Intensity in the Outer Shell (MPa)	0.9 σ_u of Alloy 22 (MPa)	Maximum Stress Intensity in the Inner Shell (MPa)	0.9 σ_u of SS 316 ^a (MPa)
Room Temperature	519	875	394	630
204°C	419	846	373	567
316°C	397	813	211	557

Source: BSC 2002a, Section 5.1 and Table 1

NOTE: ^a The material properties of Stainless Steel Type 316 (SS 316) are the same as Stainless Steel Type 316NG.

The above table shows that for each temperature condition, the maximum stress intensity was less than the allowable of the corresponding material.

Since the waste package is not internally pressurized, the stress intensity consists primarily of bending stresses. In this case, the membrane stress is close to or approaches zero and meets the first criterion in Table 6-1.

During the tip-over calculation, no components were loaded in pure shear.

7.7.2.1 Summary

Table 6-1 states the applicable criteria, according to paragraph F-1341.2 of the 1997 Addenda of *1995 ASME Boiler and Pressure Vessel Code* (ASME 1995).

The primary membrane stress intensity is at or near zero (therefore lower than 0.7 σ_u) since the waste package is not pressurized. Therefore, the first criterion is met.

Table 7-4 clearly shows the highest stress calculated during tip-over is lower than 0.9 σ_u . Therefore, the second criterion in Table 6-1 is met.

None of the components are loaded in pure shear during tip-over. The third and final criterion is met. Therefore, the waste package meets the safety standards stated in Appendix F of the 1997 Addenda of *1995 ASME Boiler and Pressure Vessel Code* (ASME 1995).

It is concluded that the performance of the 5-DHLW/DOE SNF-short waste package internal design is structurally acceptable when exposed to a tipover event, therefore meets the structural criteria (Section 4.1.1) as long as the DOE SNF canister loaded mass limit (2,270 kg) and the DHLW glass canisters mass limit (2,500 kg) are not exceeded.

7.8 FORT SAINT VRAIN

7.8.1 Description of the Finite Element Representation

A full three-dimensional finite element representation of the waste package and the DOE SNF standardized canister was developed in ANSYS V5.6.2 by using the dimensions provided in Sections 2.1 and 2.3, respectively. The finite element representation was created with the largest possible radial gap of 4 mm between the inner and outer shells (CRWMS M&O 2000i, Section 8.1.8). The initial orientation of the inner shells maintains this 4-mm gap around the circumference of the shell.

The structure of the DHLW glass canister, was reduced to a cylinder of uniform mass density (Sections 5.1.5 and 5.1.6). The total mass and geometric dimensions of the DHLW canister define the density. The benefit of using this approach was to reduce the computer execution time while preserving all features of the problem relevant to the structural calculation.

The target surface was conservatively assumed to be unyielding with a large elastic modulus (Section 5.1.2).

The initial tip-over angle with respect to the horizontal plane was reduced to 0.1°, and the waste package was given an initial angular velocity corresponding to the rigid-body motion of the waste package (BSC 2002a, Section 5.5). This configuration reduces the computer execution time while preserving all features of the problem relevant to the structural calculation.

The finite element representation was solved using LS-DYNA V950 to perform the transient dynamic analysis for the 5-DHLW/DOE SNF-long waste package tip-over design basis event at room temperature (20°C), 204°C, and 316°C.

LS-DYNA uses true stress and true strain as material property inputs. the 1997 Addenda of *1995 ASME Boiler and Pressure Vessel Code* (ASME 1995) reports only engineering stress and engineering strain. The material properties needed to be converted to the proper form in order for the solution to execute correctly. Table 7-5 reports the true ultimate tensile strength (σ_u) for Alloy 22 and Stainless Steel Type 316NG. σ_u values are given in *Waste Package Tip-Over of 5-DHLW/DOE Short* (BSC 2002a, p. 14). σ_u should be substituted for S_u in Table 6-1 in order to remain consistent.

Table 7-5. True Stress of Alloy 22 and Stainless Steel Type 316NG

Temperature	σ_u of Alloy 22 (MPa)	σ_u of Stainless Steel Type 316 (MPa)	σ_u of Stainless Steel Type 316L (MPa)
Room Temperature (20°C)	971	703	575
204°C	926	675	511
316°C	885	673	506

Source: BSC 2002a, p. 14

7.8.2 Results

The results obtained from LS-DYNA V950 were reported in terms of maximum shear stress. Since the maximum stress intensities were desired, the results needed to be converted. The maximum shear stress is defined as one-half the difference between maximum and minimum principal stress (Shigley and Mischke 1989, p. 31). Stress intensity is defined as the difference between maximum and minimum principal stress. Therefore, the results obtained from LS-DYNA V950 were multiplied by two to obtain the corresponding stress intensities.

The maximum stresses were found by carefully examining each time step taken by LS-DYNA V950, which outputs the element with the highest magnitude of stress, at each step, for each defined part. Table 7-5 lists the maximum stress intensities in the outer shell and inner shell at room temperature, 204°C, and 316°C.

Table 7-6. Maximum Stress Intensities Comparison

Temperature	Maximum Stress Intensity in the Waste Package Outer Shell (MPa)	Trunnion Collars (MPa)	0.9 σ_u of Alloy 22 (MPa)	Maximum Stress Intensity in the Waste Package Inner Shell (MPa)	0.9 σ_u of SS 316 ^a (MPa)	Maximum Stress in the DOE SNF Canister (MPa)	0.9 σ_u of SS 316L ^a (MPa)	FSVR Fuel Elements
Room Temperature	575	724	874	370	633	561	518	716
204°C	520	644	833	337	608	515	460	556
316°C	505	632	797	325	606	504	455	572
316°C (with modified elongation)	495	634	820	355	557	578	432	564

Source: BSC 2002a, Section 5.1 and Table 1

NOTE: ^a The material properties of Stainless Steel Type 316 (SS 316) are the same as Stainless Steel Type 316NG.

Table 7-6 shows that for each temperature condition, the maximum stress intensity was less than the allowable for the waste package outer and inner shells, and higher than the allowable for the DOE SNF canister.

Since the waste package is not internally pressurized, the stress intensity consists primarily of bending stresses. In this case, the membrane stress is close to or approaches zero and meets the first criterion in Table 6-1.

During the tip-over calculation, no components were loaded in pure shear.

The ultimate tensile strength of graphite H-327 at 25°C (which is the lowest of the two types of graphite used) is 6.481 MPa in the radial direction (Table 2-4). This value is two orders of magnitude less than the calculated value shown in Table 7-6 (669 MPa), therefore it is expected that the graphite blocks inside the DOE SNF canister will fail during a tip-over event.

7.8.3 Summary

Table 6-1 states the applicable criteria, according to paragraph F-1341.2 of the 1997 Addenda of *1995 ASME Boiler and Pressure Vessel Code* (ASME 1995)

The primary membrane stress intensity is at or near zero (therefore lower than $0.7\sigma_u$) since the waste package is not pressurized. Therefore, the first criterion in Table 6-1 is met.

Table 7-6 clearly shows the highest stress calculated during tip-over is lower than $0.9\sigma_u$ for the waste package outer shell, inner shell, and the DOE SNF canister. Therefore, the second criterion in Table 6-1 is met.

None of the components are loaded in pure shear during tip-over. The third and final criterion in Table 6-1 is met. Therefore, the waste package meets the safety standards stated in Appendix F of the 1997 Addenda of *1995 ASME Boiler and Pressure Vessel Code* (ASME 1995)

The 5-DHLW/DOE SNF-long waste package internal design with a DOE SNF canister loaded with FSVR SNF meets SDD criteria in Section 4.1.1 if the DOE SNF canister loaded mass limit (2,721 kg) and the DHLW glass canisters mass limit (4200 kg) are not exceeded.

INTENTIONALLY LEFT BLANK

8 THERMAL ANALYSIS

8.1 FFTF

8.1.1 Thermal Design Analysis

A detailed description of the finite-element representations, the method of solution, and the results are provided in *Thermal Evaluation of the FFTF Codisposal Waste Package* (CRWMS M&O 1999c). Each DFA and the Ident-69 fuel pin container holds 217 fuel pins in this representation. The FFTF standard DFA representation in this calculation is a two-dimensional section of the hexagonal duct containing 217 pins, as shown in Figures 3-1 and 3-2. The wire spacers around each fuel pin are conservatively neglected in this calculation (wire spacers provide contact and thus increase the transfer of thermal energy by conduction to the outside), so that the pins are represented as floating within the driver duct. In this analysis, the axial cross-section at the center of the fuel pin is represented.

The cross-section of the Ident-69 fuel pin container is shown in Figure 3-4. For this analysis, which represents a loading of 217 pins, the pins are loosely consolidated into the container and are allowed to settle. The pins are considered packed together near the center of the container. In reality, the settled configuration of the pins would vary significantly between each of the six partitioned sections. However, in this analysis, the settled configuration of fuel pins is represented as a constant since this approach simplifies the calculation and is considered conservative.

As shown in Figure 2-1, the waste package outside of the support tube for the DOE SNF canister is divided into five sections by the plates of the waste package basket. The plates of the FFTF DOE SNF canister also divide the space around the central support tube for the Ident-69 container into five sections. Due to this symmetry, thermal conditions within each of the five sections (representing 72° of the entire 360° of the waste package) will be approximately the same. In addition, within each of the 72° sections, the waste package components possess a further radial line of symmetry. Therefore, transient conditions in the waste package can be represented by one-tenth of the total radial geometry (a 36° slice of the full 360°) as shown in Figure 8-1.

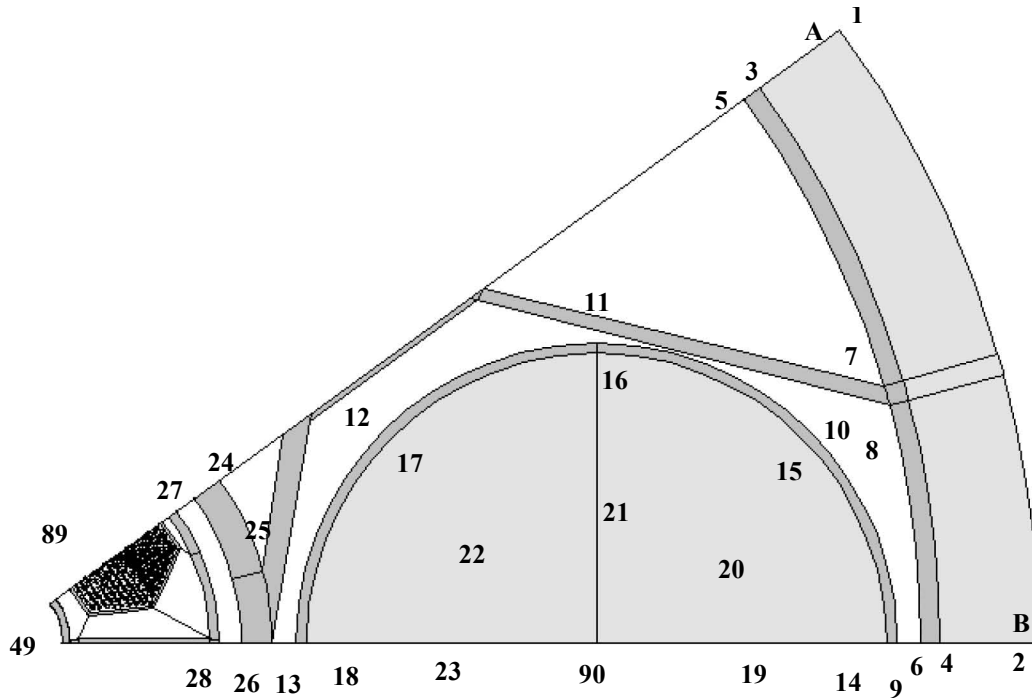


Figure 8-1. Node Locations and Numbers on Part 1 of the Finite-element Representation (Waste Package Basket and Hanford 15-ft DHLW Canister)

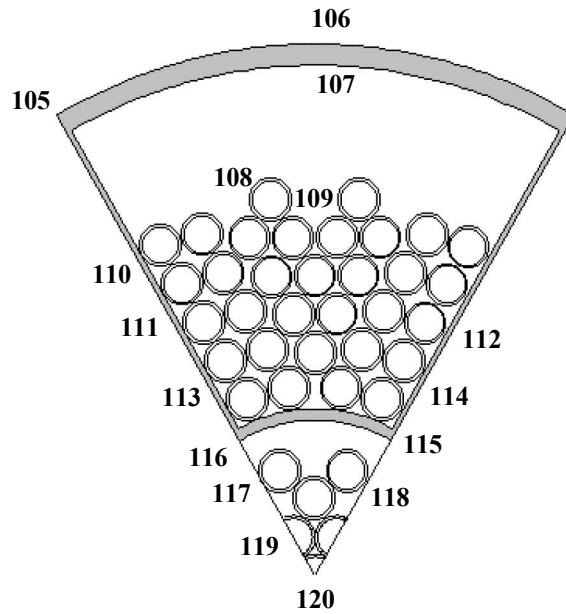


Figure 8-2. Node Locations and Numbers on Part 2 of the Finite-element Representation (Ident-69 Fuel Pin Container)

The waste package outside of the Ident-69 fuel pin container is divided evenly into 72° slices, but the interior of the Ident-69 container is symmetrically divided by 60° slices. For this reason, the interior of the Ident-69 fuel pin container cannot be accurately included in the same 36°-slice finite-element representation as the waste package outside of the Ident-69. The calculation is therefore divided into two parts, corresponding to the two parts of the finite-element representation.

Figures 8-1 and 8-2 give the designated node locations and numbers on each component of the finite-element representations. Note that the outer shell of the Ident-69 fuel pin container is included, in Part 1 of the finite-element representation.

Two cases are considered, one with helium as the fill gas for the FFTF DOE SNF canister and the other with argon as the fill gas. The final fuel irradiations in FFTF were completed in March 1992 (DOE 1998b). Therefore, in all cases, the FFTF fuel is represented after ten years from discharge. The waste package total heat output is 13,533 W, and is based on five DHLW glass canisters, five DFAs, and one Ident-69 pin container (Ident-69 pin container heat output is the same as one DFA).

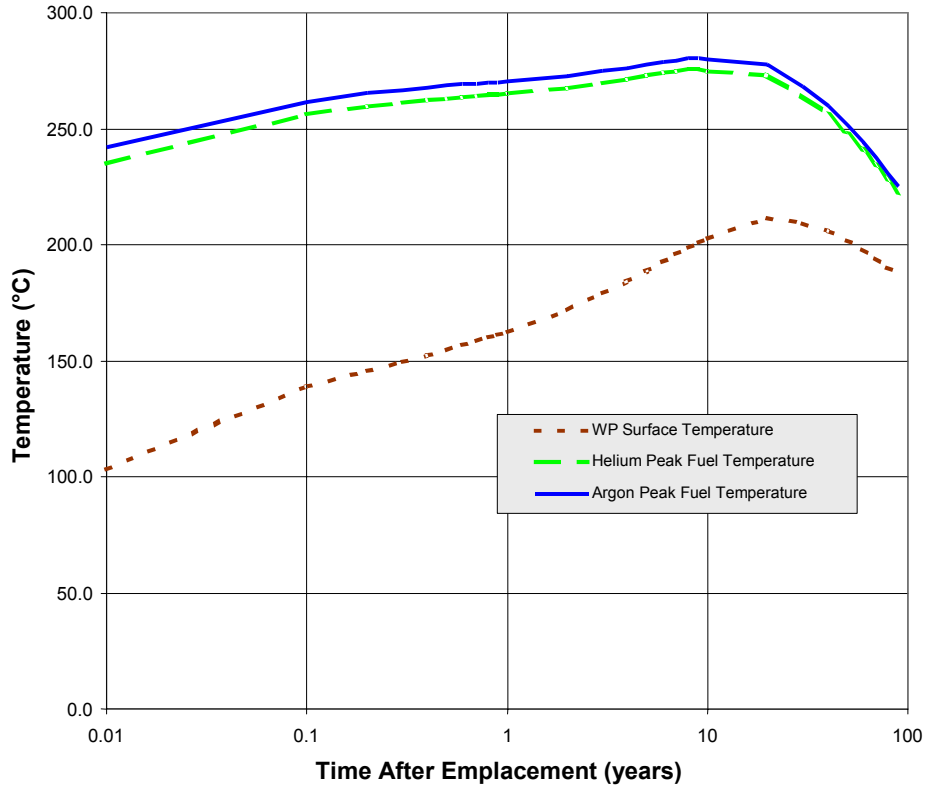
8.1.2 Calculations and Results

Table 8-1 lists the physical location of the most important nodes shown in Figures 8-1 and 8-2. Figure 8-3 shows the surface and peak fuel temperatures calculated in each case. The temperature distribution in the waste package at the time of peak fuel temperature can be found in Attachments XIV through XVII of *Thermal Evaluation of the FFTF Codisposal Waste Package* (CRWMS M&O 1999c). Table 8-2 summarizes the peak temperatures and time of occurrence for each case. The results indicate that argon fill gas in the FFTF DOE SNF canister causes the peak fuel temperature, which occurs after nine years, to be approximately 1.5 percent higher than helium fill gas. The peak DHLW glass and waste package surface temperatures are not affected by the choice of the fill gas in the FFTF DOE SNF canister.

Table 8-1. Physical Locations of Nodes of Interest

Node Number	Physical Location
2	Waste package outer surface
90	DHLW center
89	Standard DFA center fuel pin
49	Ident-69 outer surface, given as output of FEA, Part 1
106	Ident-69 outer surface, given as input to FEA, Part 2
120	Ident-69 center fuel pin

Source: CRWMS M&O 1999c, Table 6-2



Source: CRWMS M&O 1999c, Figure 6-1

Figure 8-3. Temperature History for FFTF Waste Package

Table 8-2. Peak Temperatures and Time of Occurrence for Each Case

Case; FFTF DOE SNF Canister Fill Gas	Peak Fuel Temperature (°C)	Time of Peak Fuel Temperature (yr.)	Peak Surface Temperature (°C)	Time of Peak Surface Temperature (yr.)	Peak DHLW Glass Temperature (°C)	Time of Peak DHLW Glass Temperature (yr.)
1; Helium	276.0	9	211.7	20	247.6	20
2; Argon	280.3	9	211.7	20	247.6	20

Source: CRWMS M&O 1999c, Table 6-5

8.1.3 Summary

The results indicate that the maximum fuel and DHLW glass temperatures occur with argon fill gas in the DOE SNF canister and are 280.3°C and 247.6°C, respectively.

8.2 TRIGA

8.2.1 Design Analysis

A detailed description of the finite-element representations, the method of solution, and the results are provided in *Thermal Evaluation of the TRIGA Codisposal Waste Package* (CRWMS M&O 1999). The temperature histories for 13 node locations within the waste package were calculated for two cases. The first case calculation assumes the entire waste package and the

DOE SNF canister are filled with helium. The second case calculation assumes the DOE SNF canister is filled with argon and the rest of the waste package is filled with helium.

The highest temperature results at two specified node locations (the assembly cladding at the geometric center of the DOE SNF canister and the centerline of the SRS DHLW canister) within the finite-element representation are given in Table 8-3. The finite element representation of the TRIGA waste package and the node locations on each component is shown in Figures 8-4 and 8-5. These node locations are used in Figure 8-7. Note that these temperatures occur at different times within the waste package.

Results for each case are given in Section 4.3. The Case 1 calculation assumes the entire waste package and DOE SNF canister are filled with helium. The Case 2 calculation assumes the DOE SNF canister is filled with argon and the rest of the waste package is filled with helium.

8.2.2 Calculations and Results

Table 8-3 contains the peak temperature for the TRIGA SNF assembly cladding at the center of the DOE SNF canister and the center of the SRS DHLW canister. It assumes one year decay prior to start of emplacement period. Table 8-4 lists the time and location of peak temperature for the center of fuel rod, the center of DHLW glass canister, and the glass canister shell. Figure 8-6 shows the temperature histories until 50 years for TRIGA SNF assembly cladding at the center of the DOE SNF canister and the center of the SRS DHLW canister. After 50 years, the temperature decreases gradually.

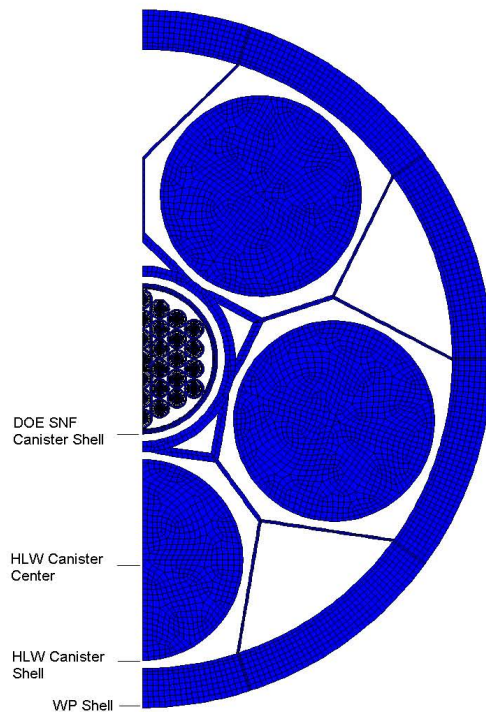


Figure 8-4. The Finite Element Representation of TRIGA Waste Package

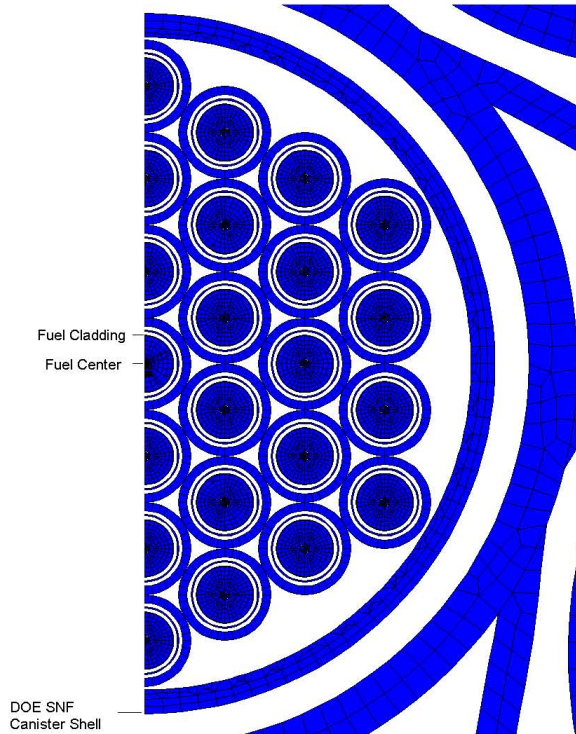
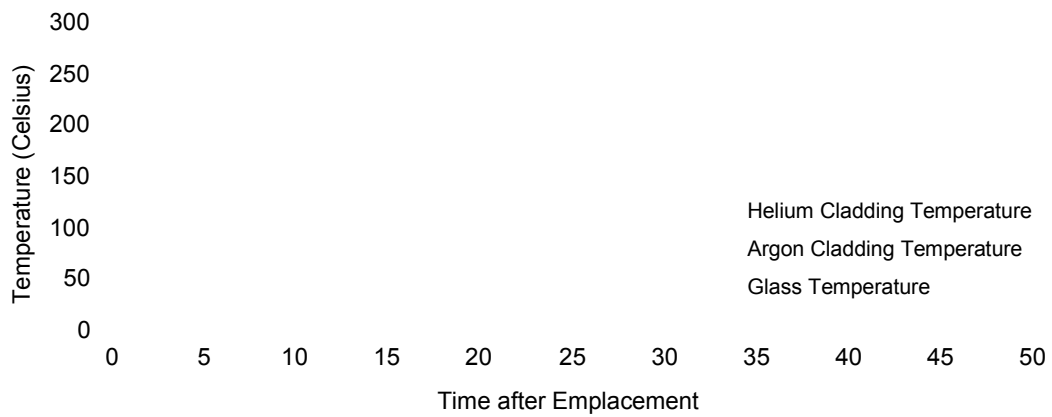


Figure 8-5. Location of DOE Spent Nuclear Fuel Canister Temperature Nodes



Source: CRWMS M&O 1999I

Figure 8-6. Temperature History for TRIGA Waste Package

Table 8-3. Peak Temperature Histories of Fuel Cladding and Glass

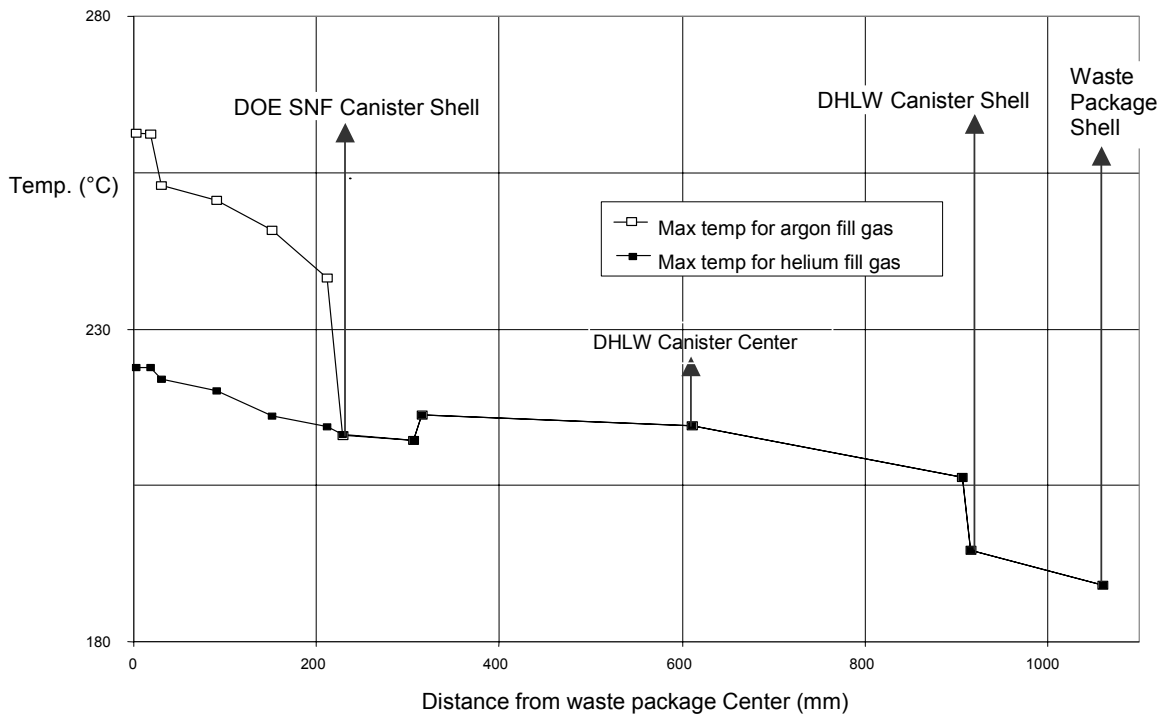
Time after Emplacement (years)	Helium		Argon	
	Fuel Cladding Temperature (°C)	Glass Temperature (°C)	Fuel Cladding Temperature (°C)	Glass Temperature (°C)
0.1	223.1	166.0	261.2	166.0
0.2	223.8	169.4	260.5	169.4
20	216.6	214.5	221.9	214.5
1,000	155.1	145.9	162.0	145.9

Source: CRWMS M&O 1999I

Table 8-4. Time and Location of Peak Temperature

Location	Peak Temperature (°C)	Time of Peak Temperature (years)	Peak Temperature (°C)	Time of Peak Temperature (years)
Center of the fuel rod	223.9	0.2	261.3	0.1
Center of SRS DHLW	214.5	20	214.5	20
SRS DHLW canister shell	206.3	20	206.3	20

Source: CRWMS M&O 1999I



Source: CRWMS M&O 1999I

Figure 8-7. Peak Temperature versus Distance from the Center of the Waste Package

8.2.3 Summary

The results indicate that the maximum fuel cladding temperature is 261.2°C (Argon), which is less than the temperature limit of 350°C indicated in Section 4.1.2.1. Also the maximum DHLW canister shell temperature occurs, after 20 years, with argon fill gas in the DOE SNF canister, and is 206.3°C. The peak temperature in the center of the DHLW glass is 214.5°C.

8.3 SHIPPINGPORT PWR

8.3.1 Thermal Design Analysis

A detailed description of the finite-element representations, the method of solution, and the results are provided in *Thermal Evaluation of the Shippingport PWR Codisposal Waste Package* (CRWMS M&O 1999f). This waste package is loaded with five Hanford 15-foot DHLW glass canisters (Figure 2-2) and one DOE SNF canister (Figures 2-3 and 2-4). The DOE SNF canister holds one Shippingport PWR C2 S2 SNF assembly (Figures 2-5 through 2-7). Three different fill gases are considered for the Shippingport PWR DOE SNF canister: helium, argon, and nitrogen. The waste package is filled with helium.

The finite-element representation used in this calculation is shown in Figures 8-8 and 8-9. Figure 8-8 presents a finite-element representation of the 5-DHLW/DOE SNF-long waste package with the DOE SNF canister containing Shippingport PWR SNF. Figure 8-9 presents a finite-element representation of the Shippingport PWR C2 S2 SNF assembly.

As shown in these figures, symmetry is across the center of the waste package. Therefore, this representation includes half of the 5-DHLW/DOE SNF-long waste package, half of the DOE SNF canister, two-and-a-half Hanford long DHLW glass canisters, and two subassemblies of the Shippingport PWR assembly. In addition, the DHLW glass canisters and the Shippingport PWR assembly are positioned in the center of their compartments to maximize radiation heat transfer to waste package surfaces.

8.3.2 Calculations and Results

Table 8-5 lists the locations of components of interest. Table 8-6 summarizes the peak temperatures and time of occurrence for each DOE SNF canister fill gas. The results indicate that argon fill gas in the Shippingport PWR DOE SNF canister causes the peak Shippingport PWR fuel temperature, which occurs after ten years, to be approximately 1 percent higher than for helium fill gas. The peak DHLW glass and waste package surface temperatures are not affected by the choice of the fill gas in the Shippingport PWR DOE SNF canister. Figure 8-10 plots peak temperatures versus radial location from the center of the waste package with the Shippingport PWR DOE SNF canister filled with argon, nitrogen or helium gas.

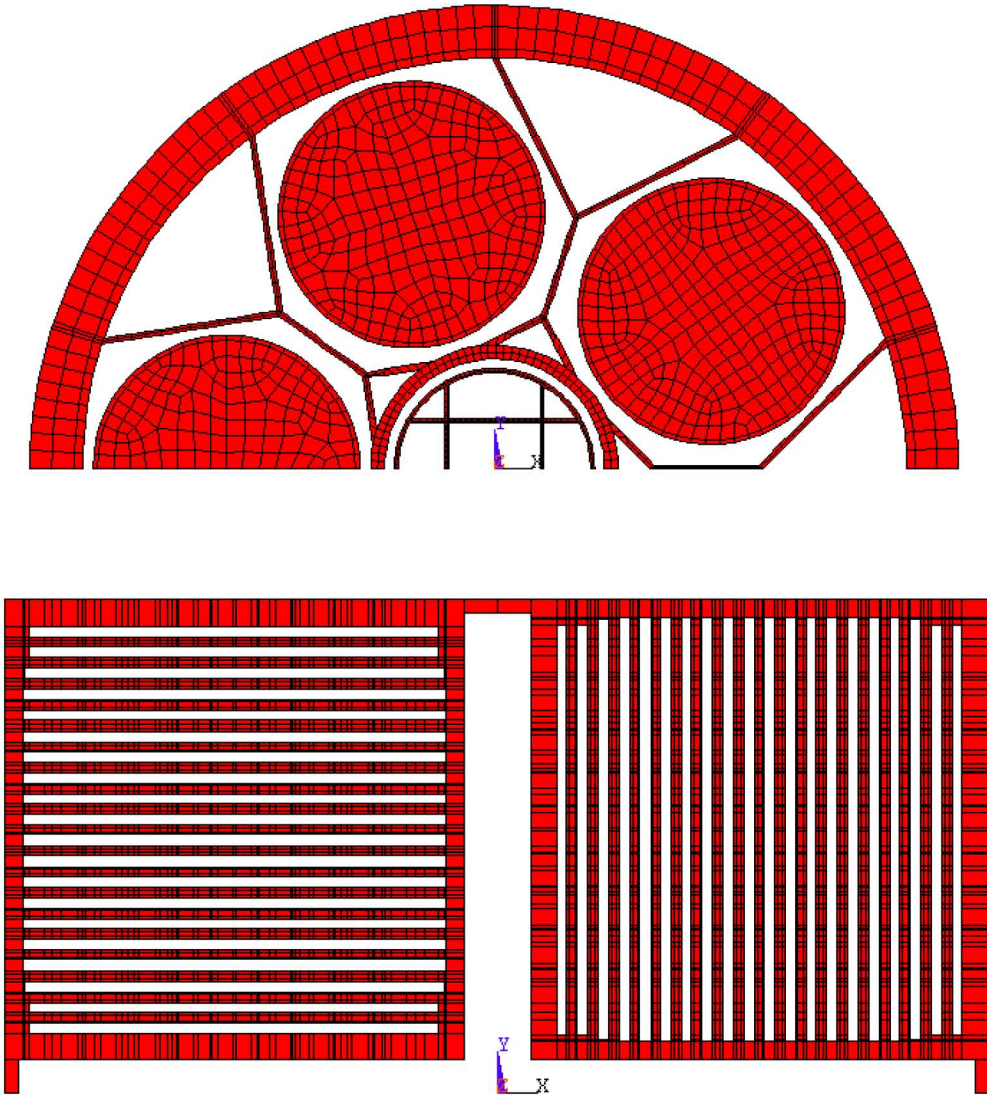


Figure 8-9. Finite-element Representation of the Shippingport PWR C2 S2 Spent Nuclear Fuel Assembly

Table 8-5. Physical Locations of Nodes of Interest

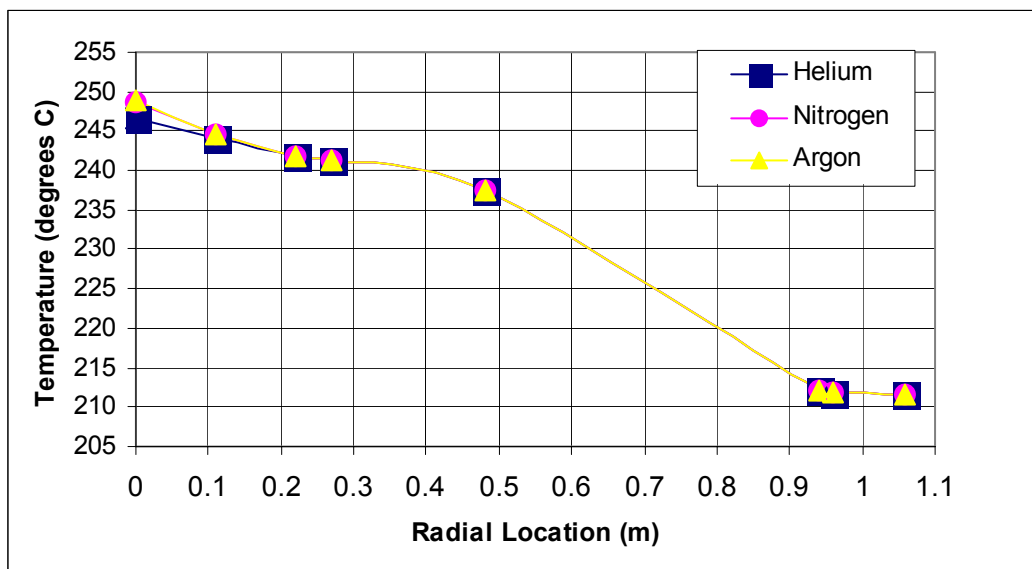
Component and location	Location from Center of Waste Package (m)
Center of Shippingport assembly	0.00
Center of Shippingport canister A-guide	0.11
Center of Shippingport canister wall	0.22
Center of 5-DHLW/DOE Waste Package support tube	0.27
Center of 5-DHLW/DOE Waste Package divider plate	0.48
Inside of Waste Package inner barrier	0.94
Waste package inner and outer barrier interface	0.96
Outside of Waste Package outer barrier	1.06

Source: CRWMS M&O 1999f, Table 6-3

Table 8-6. Peak Temperatures and Time of Occurrence for Each DOE Spent Nuclear Fuel Canister Fill Gas

	DOE SNF Canister Fill Gas		
	Helium	Nitrogen	Argon
Peak Fuel Temperature (°C)	246.7	248.7	248.9
Time of Peak Fuel Temperature (years)	10	10	10
Peak Waste Package Outer Barrier Surface Temperature (°C)	211.7	211.7	211.7
Time of Peak Waste Package Outer Barrier Surface Temperature (years)	20	20	20
Peak DHLW Glass Temperature (°C)	252.3	252.3	252.3
Time of Peak DHLW Glass Temperature (years)	10	10	10
Peak Fuel Cladding Temperature (°C)	246.8	248.9	249.2
Time of Peak Fuel Cladding Temperature (years)	10	10	10

Source: CRWMS M&O 1999f, Table 6-3



Source: CRWMS M&O 1999f, Figures 6-3 to 6-5

Figure 8-10. Axial Temperature Profile of the 5-DHLW/DOE SNF-Long Waste Package

8.3.3 Summary

The results indicate that the maximum fuel and fuel cladding temperatures are 248.9°C and 249.2°C, respectively, with argon fill gas in the DOE SNF canister. The maximum cladding temperature is less than the temperature limit of 350°C indicated in SDD criterion 4.1.2.1. Also the maximum DHLW glass temperature occurs, after 10 years, with argon fill gas in the DOE SNF canister and is 252.3°C.

8.4 ENRICO FERMI

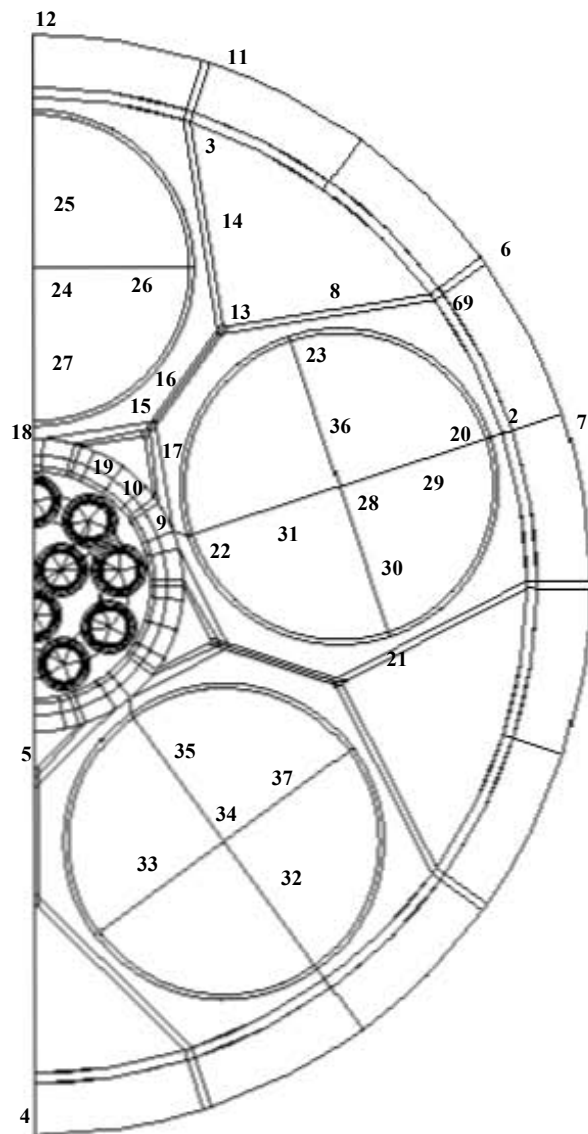
8.4.1 Thermal Design Analysis

A detailed description of the finite-element representation, the method of solution, and the temperature history results at specified node locations (designated by numbers 1-70) within the finite-element representation are given in Section 6 of *Thermal Evaluation of the Enrico Fermi Co-Disposal Waste Package* (CRWMS M&O 1999m). Figures 8-11 and 8-12 give the designated node locations and numbers on each component of the finite-element representation. Details of the internals of the Fermi DOE SNF canister is shown in Appendix A of this report.

Two cases were considered. The first one is the “nominal” case with the actual heat outputs. The second one is a “bounding” case, which was obtained by applying a multiplier on the SRS DHLW canister heat output. This multiplier, equal to 5.8, leads to the temperature that is close to the maximum acceptable temperature of the DHLW (400°C).

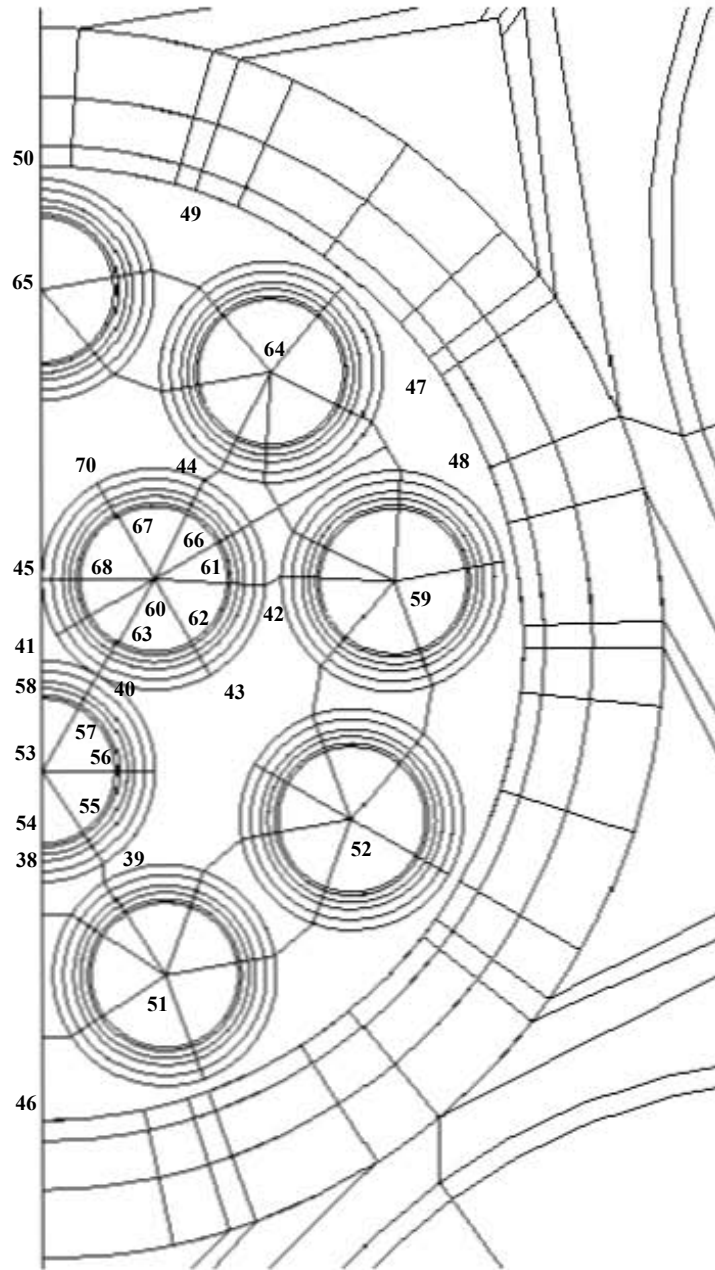
Two sizes of iron shot were considered, Grades S230 and S330. The S330 thermal conductivity was used, which is most conservative since it is the lower of the two. The average of S230 and S330 densities was used in the calculations. A vibrated or settled condition, which may be expected to occur while transporting the waste package, is also assumed to obtain the iron shot density value.

The waste package is assumed to be evacuated, then filled with helium gas. Representing only conduction and radiation heat transfer inside the waste package provides conservative temperature results for the calculation. The fill gas placed inside the waste package will allow a natural convective heat transfer to exist; however, since only a few small enclosed basket cavities exist and the temperature gradient in the enclosure is very small, the heat transferred by helium circulation is insignificant.



Source: CRWMS M&O 1999m

Figure 8-11. Node Locations and Numbers of the Finite-Element Representation of Waste Package with Fermi Spent Nuclear Fuel Canister and the DHLW Canisters



Source: CRWMS M&O 1999m

Figure 8-12. Node Locations and Numbers of the Finite-Element Representation of Fermi Spent Nuclear Fuel Canister

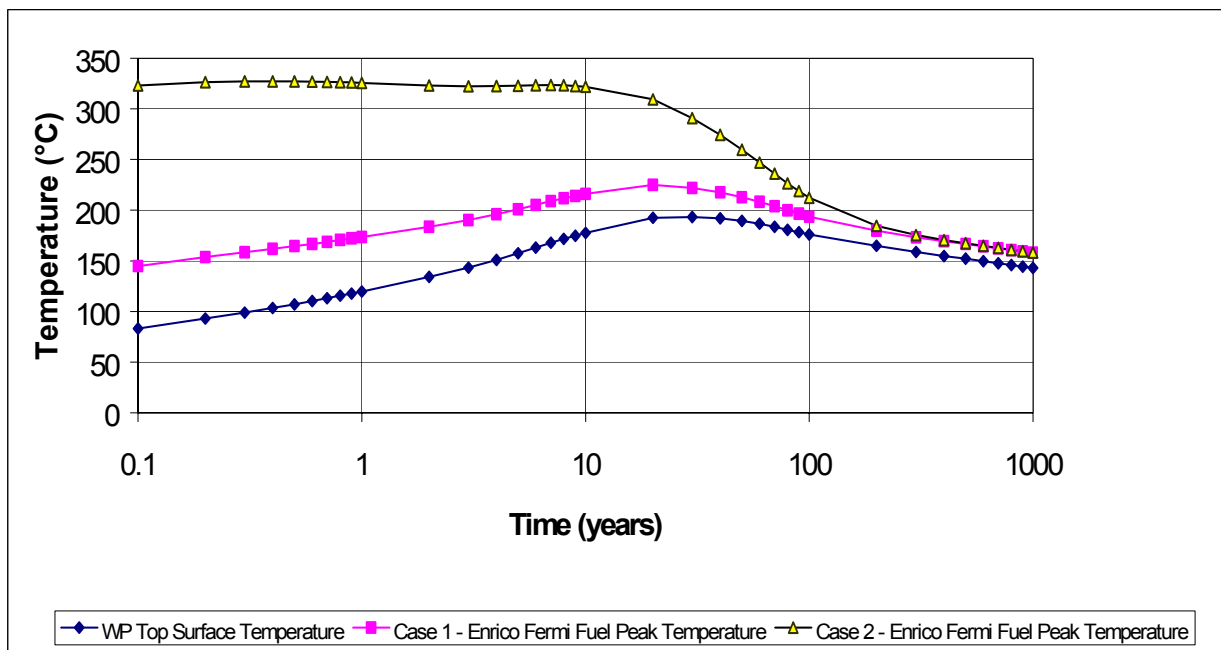
8.4.2 Calculations and Results

The results provided in this section were derived from the ANSYS V5.4 calculations. Table 8-7 lists the physical location of the most important nodes shown in Figures 8-11 and 8-12.

Table 8-7. Physical Locations of Nodes of Interest

Node Number	Physical Location
12	Waste Package outer surface top
35	DHLW glass (maximum temperature)
53	4-in-diameter pipe center with fuel

Figure 8-13 shows the peak surface temperature of the waste package and the peak fuel temperatures calculated for each case (“nominal” case and bounding case). The temperature distribution in the waste package at the time of peak fuel temperature can be found in Tables 6-1 through 6-10 of *Thermal Evaluation of the Enrico Fermi Co-Disposal Waste Package* (CRWMS M&O 1999m). Table 8-8 summarizes the Enrico Fermi peak fuel temperatures and time of occurrence for each case.



Source: CRWMS M&O 1999m

NOTE: Case 1 is nominal, while Case 2 is bounding.

Figure 8-13. Temperature History for Enrico Fermi Waste Package

Table 8-8. Enrico Fermi Peak Fuel Temperatures and Time of Occurrence

Case	Peak Fuel Temperature (°C)	Time of Occurrence (years)
1 - Nominal	225.0	20
2 - Bounding	327.2	0.4

Source: CRWMS M&O 1999m

8.4.3 Summary

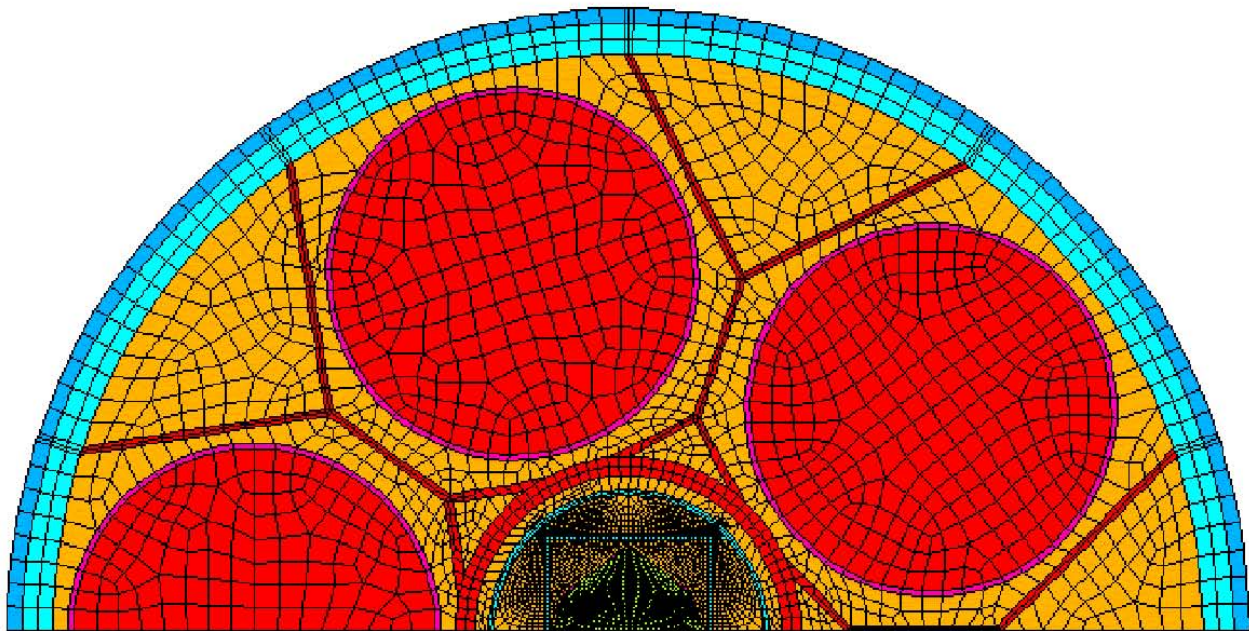
The results indicate that the maximum fuel and DHLW glass temperatures for the bounding case are 327.2°C (Node 53) and 394.5°C (Node 35), respectively. The maximum fuel temperature is below the maximum cladding temperature limit of 350°C (Section 4.1.2).

8.5 SHIPPINGPORT LWBR

8.5.1 Thermal Design Analysis

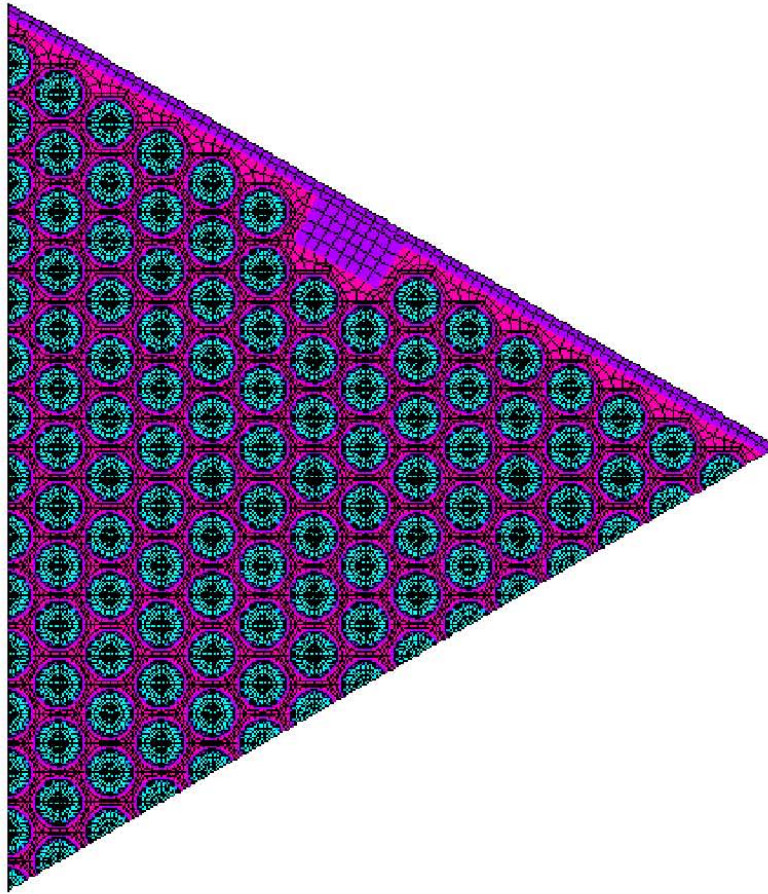
A detailed description of the finite-element representations, the method of solution, and the temperature history results are provided in *Structural Calculations for the Codisposal of Shippingport LWBR Spent Nuclear Fuel in a Waste Package* (CRWMS M&O 1999k). This waste package is loaded with five Hanford 15-foot DHLW glass canisters and one DOE SNF canister. The DOE SNF canister holds one Shippingport LWBR seed assembly. Two different fill gases are considered for the Shippingport LWBR DOE SNF canister: helium and argon. The waste package is filled with helium. These calculations evaluate heat conduction and thermal radiation within the waste package. Heat transfer by means of natural convection is assumed to be insignificant and is not considered (see Section 5.2.17).

Figure 8-14 is a finite-element representation of the 5-DHLW/DOE SNF-long waste package with the DOE SNF canister containing Shippingport LWBR SNF. Figure 8-15 is a finite-element representation of one-sixth section of the Shippingport LWBR SNF seed assembly.



Source: CRWMS M&O 1999k

Figure 8-14. Finite-Element Representation of the 5-DHLW/DOE SNF-Long Waste Package



Source: CRWMS M&O 1999k

Figure 8-15. Finite-Element Representation of the Shippingport LWBR Seed Assembly Fuel (One-Sixth Section)

As shown in these figures, symmetry is across the center of the waste package. Therefore, this representation includes half of the 5-DHLW/DOE SNF-long waste package, half of the DOE SNF canister, two-and-a-half Hanford long DHLW glass canisters, and half of the Shippingport LWBR seed assembly. In addition, the DHLW glass canisters and the Shippingport LWBR seed assembly are positioned in the center of their compartments to maximize radiation heat transfer to waste package surfaces.

8.5.2 Calculations and Results

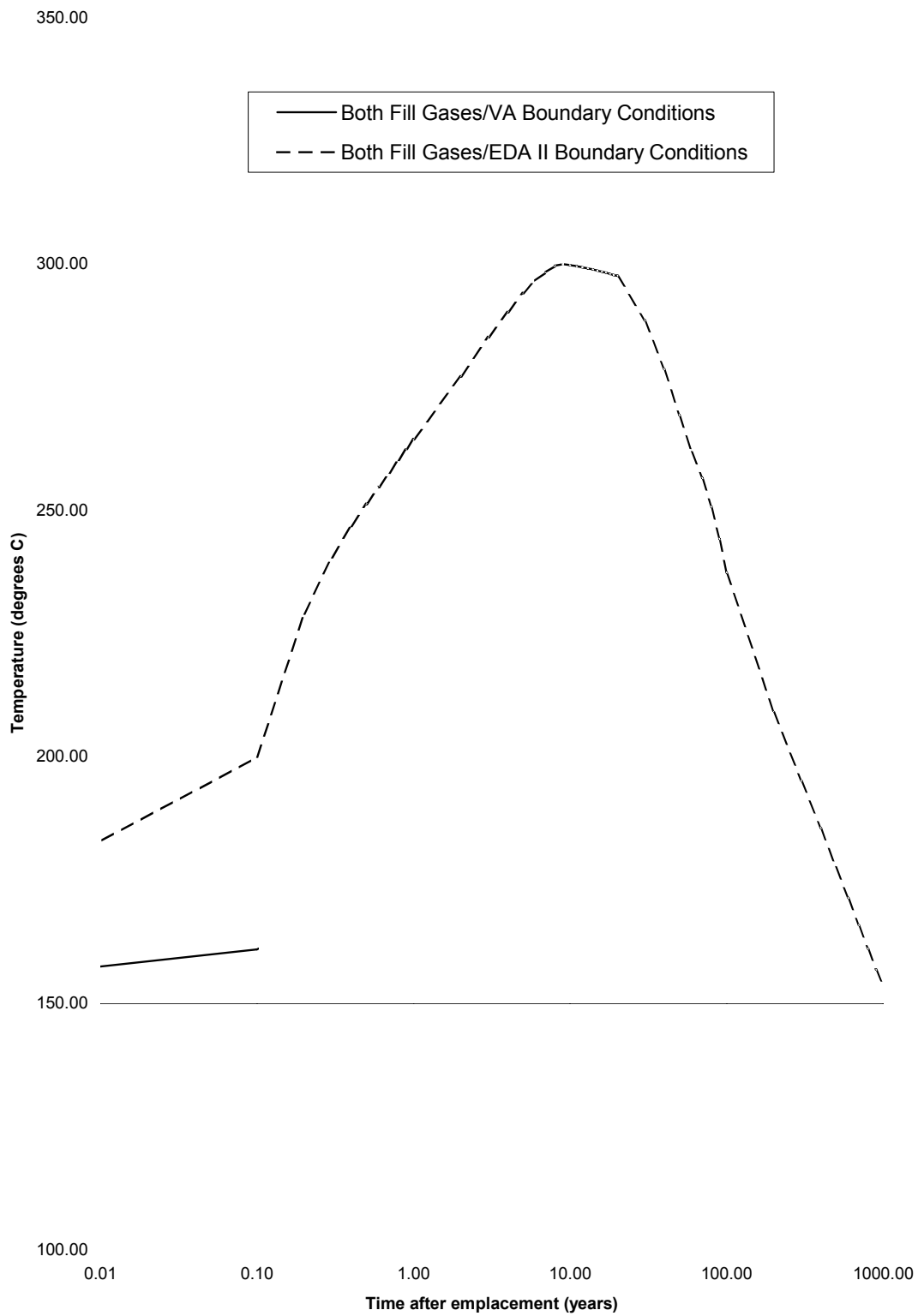
Table 8-9 summarizes the peak temperatures for components of interest and time of occurrence for each DOE SNF canister fill gas (CRWMS M&O 2000f). For the EDA II waste package designs and emplacement parameters, the results indicate that argon fill gas in the DOE SNF canister causes the peak Shippingport LWBR fuel temperature, which occurs after nine years, to be approximately 7 percent higher than for helium fill gas. The peak DHLW glass and waste package surface temperatures are not affected by the choice of the fill gas in the Shippingport LWBR DOE SNF canister (see also Figure 8-16). Figure 8-17 plots waste package peak temperatures versus radial location from the center of the waste package with the Shippingport LWBR DOE SNF canister filled with argon or helium gas for both Viability Assessment and EDA II designs.

Table 8-9. Peak Temperature versus Time for Various Components

Viability Assessment Waste Package Design and Emplacement Parameters					
Component and Location	Location from Center of Waste Package (m)	Helium Fill Gas		Argon Fill Gas	
		Peak Temperature (°C)	Time of Peak Temperature (years)	Peak Temperature (°C)	Time of Peak Temperature (years)
Inside the DOE Shippingport LWBR SNF Canister					
Center of Shippingport LWBR Seed SNF Assembly	0.000	249.46	20.0	285.57	9.0
Center of A-Plate	0.133	231.46	20.0	234.41	234.41
Center of SNF Canister Outer Shell	0.224	223.63	20.0	225.66	20.0
Outside the DOE Shippingport LWBR SNF Canister but Inside the Waste Package					
Center of Support Tube	0.267	220.43	20.0	220.44	20.0
Center of Divider Plate	0.484	214.54	20.0	214.55	20.0
Inside of Waste Package Corrosion Resistant Shell	0.940	193.78	30.0	193.78	30.0
Waste Package Corrosion Resistant and Corrosion Allowance Shells Interface	0.960	193.68	30.0	193.68	30.0
Outside of Waste Package Corrosion Allowance Shell	1.060	193.61	30.0	193.61	30.0
License Application Waste Package Design and Emplacement Parameters					
Inside the DOE Shippingport LWBR SNF Canister					
Center of Shippingport LWBR Seed SNF Assembly	0.000	325.55	9.0 ^a	347.46	9.0
Center of A-Plate	0.133	310.85	9.0 ^a	312.50	9.0
Center of SNF Canister Outer Shell	0.224	304.91	9.0 ^a	305.97	9.0
Outside the DOE Shippingport LWBR SNF Canister but Inside the Waste Package					
Center of Support Tube	0.267	302.55	9.0 ^a	302.54	9.0
Center of Divider Plate	0.484	298.68	9.0 ^a	298.68	9.0
Inside of Waste Package Inner Shell	0.940	287.97	9.0 ^a	287.98	9.0
Waste Package Inner and Outer Shell Interface	0.990	287.33	9.0 ^a	287.84	9.0
Outside of Waste Package Outer Shell	1.015	287.77	9.0 ^a	287.77	9.0

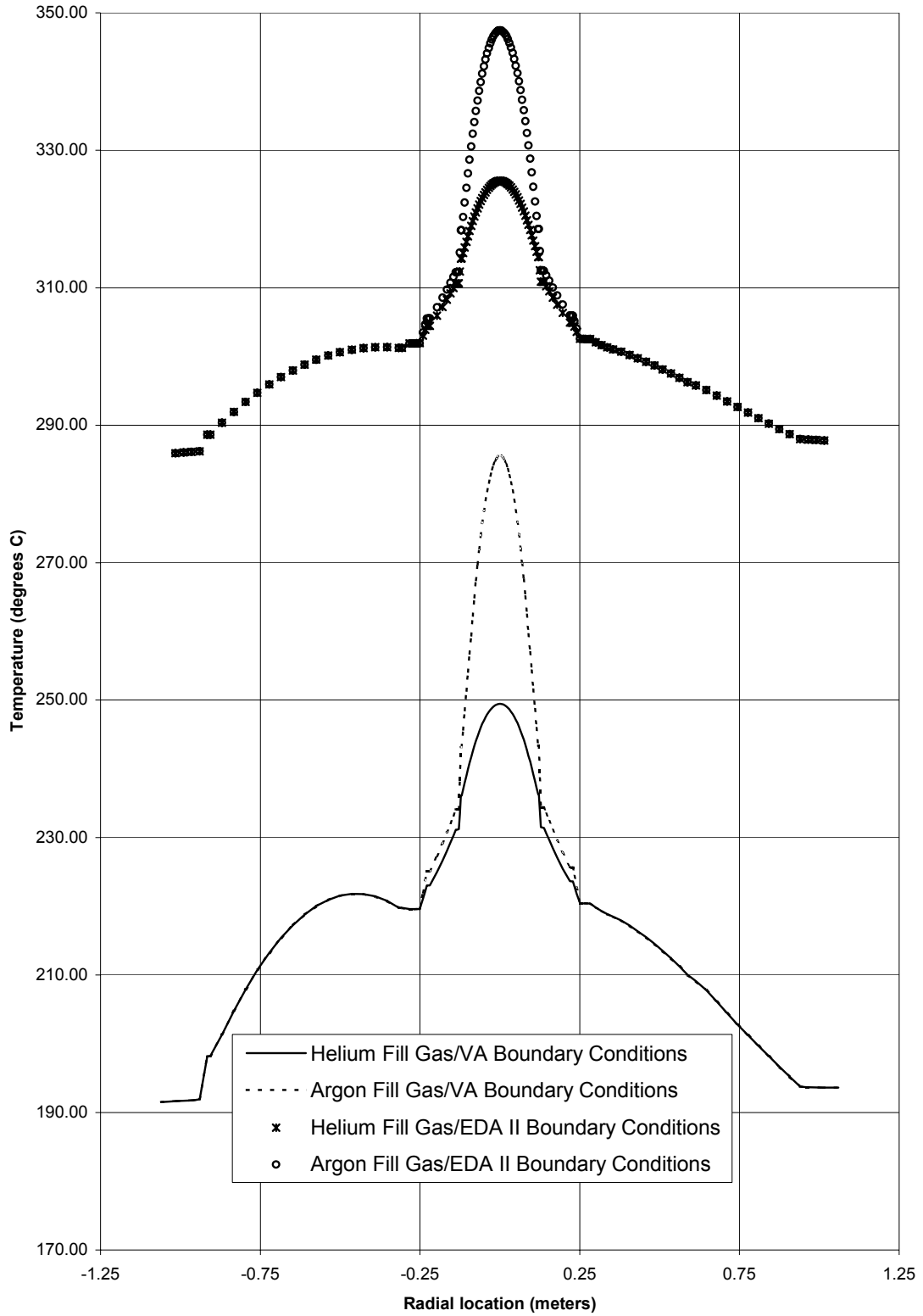
Source: CRWMS M&O 2000f, Table 6-3

NOTE: ^a Time after 50 years ventilation period.



Source: CRWMS M&O 2000f

Figure 8-16. DHLW Peak Temperature Versus Time



Source: CRWMS M&O 2000f

Figure 8-17. Radial Temperature Profile of the Waste Package

8.5.3 Summary

The results indicate that the maximum DHLW glass temperature for the EDA II design is 300.04°C (Argon) (CRWMS M&O 2000f, Table 6-2). The waste package thermal output at emplacement is 8007.1 W for both Viability Assessment and License Application design and emplacement parameters. Both are less than the SDD criterion of 11,800 W (Section 4.1.2.2).

8.6 N-REACTOR

8.6.1 Thermal Design Analysis

A detailed description of the finite element representations, the method of solution, and the results are provided in *Thermal Evaluation of the 2-MCO/2-DHLW Waste Package* (CRWMS M&O 2000k). Two geometrical configurations, corresponding to different relative positions of MCOs and DHLW canisters, were investigated, as displayed in Figure 8-18. The configuration shown on the left will be referred to as configuration 1 and the one on the right as configuration 2. Although the waste package will be loaded as shown in configuration 2, the thermal analysis was also conducted for a waste package loaded as shown in configuration 1. Since configuration 2 is the nominal design, configuration 1 should be viewed as resulting only from misload, and is evaluated here only for conservatism. Different fill gases (helium, nitrogen, and argon) for the MCOs were also investigated.

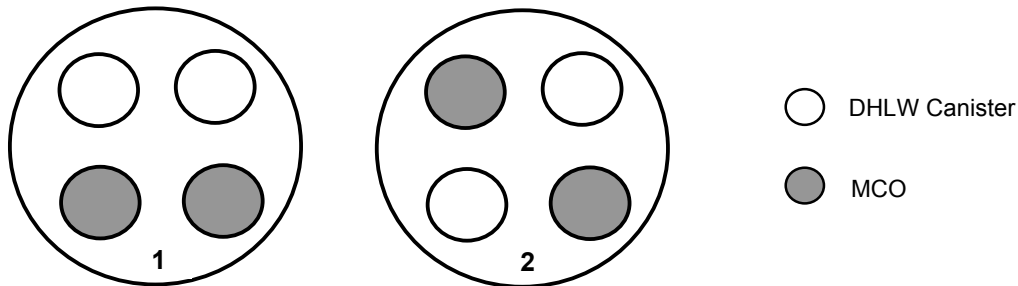


Figure 8-18. 2-MCO/2-DHLW Waste Package Configurations

Figure 8-19 displays a cross-section view of the 2-MCO/2-DHLW waste package. The dimensions of the structures are given in Section 2.

Figure 8-20 displays a view of the MCO containing intact Mark IV fuel elements. A total of 54 fuel elements are included in each basket (DOE 2000a, p. 25). The dimensions of the Mark IV fuel elements come from pages 11 and 13 of *N Reactor (U-Metal) Fuel Characteristics for Disposal Criticality Analysis* (DOE 2000a), while the dimensions of the MCOs come from page 23 of that document.

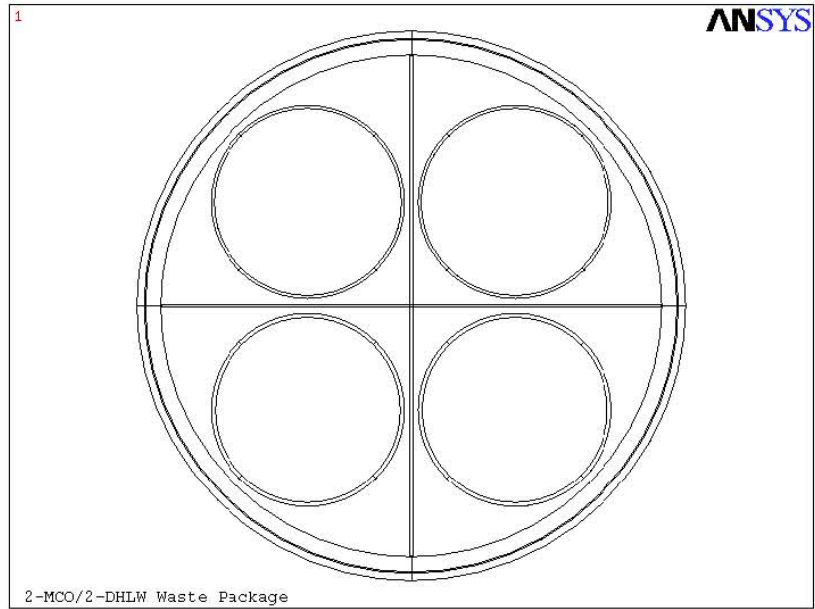


Figure 8-19. Cross-Section View of the 2-MCO/2-DHLW Waste Package for the Thermal Analysis

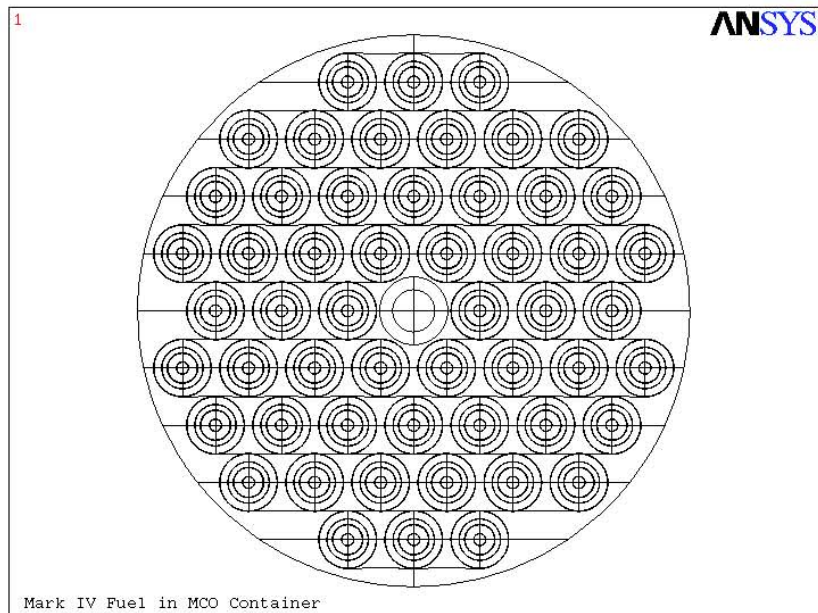


Figure 8-20. Cross-Section of the MCO

The MCO materials information is from *N Reactor (U-Metal) Fuel Characteristics for Disposal Criticality Analysis* (DOE 2000a, p. 23). The information about the materials of the DHLW canisters is from Section 2.1.2. The waste material is assumed to be borosilicate glass (see Section 5.2.9). The materials of the Mark IV fuel elements come from *N Reactor (U-Metal) Fuel Characteristics for Disposal Criticality Analysis* (DOE 2000a, p. 10).

8.6.2 Calculations and Results

Tables 8-10 and 8-11 provide the upper bound estimate of the peak temperatures obtained within the DHLW canisters and within the MCOs for the different fill gases (argon, nitrogen, and helium). The temperature calculations take no credit for the decay of the heat in the spent nuclear fuel, so the results should be interpreted as the upper bound of the temperatures. For this reason, the time of occurrence of the peak temperature will actually be sooner than indicated. However, at no time will the temperature be greater than that given in Tables 8-10 and 8-11 or Figures 8-21 and 8-22.

Table 8-10. Peak Temperatures and Time of Occurrence for Each DOE Spent Nuclear Fuel Canister Fill Gas: Configuration 1

Waste Package Metric	DOE Spent Nuclear Fuel Canister Fill Gas		
	Helium	Nitrogen	Argon
Peak Fuel Temperature (°C)	322.9	349.1	351.9
Time of Peak Fuel Temperature (years)	40	40	40
Peak High-Level Waste Glass Temperature (°C)	276.1	284.9	286.3
Time of Peak High-Level Waste Glass Temperature (years)	40	40	40

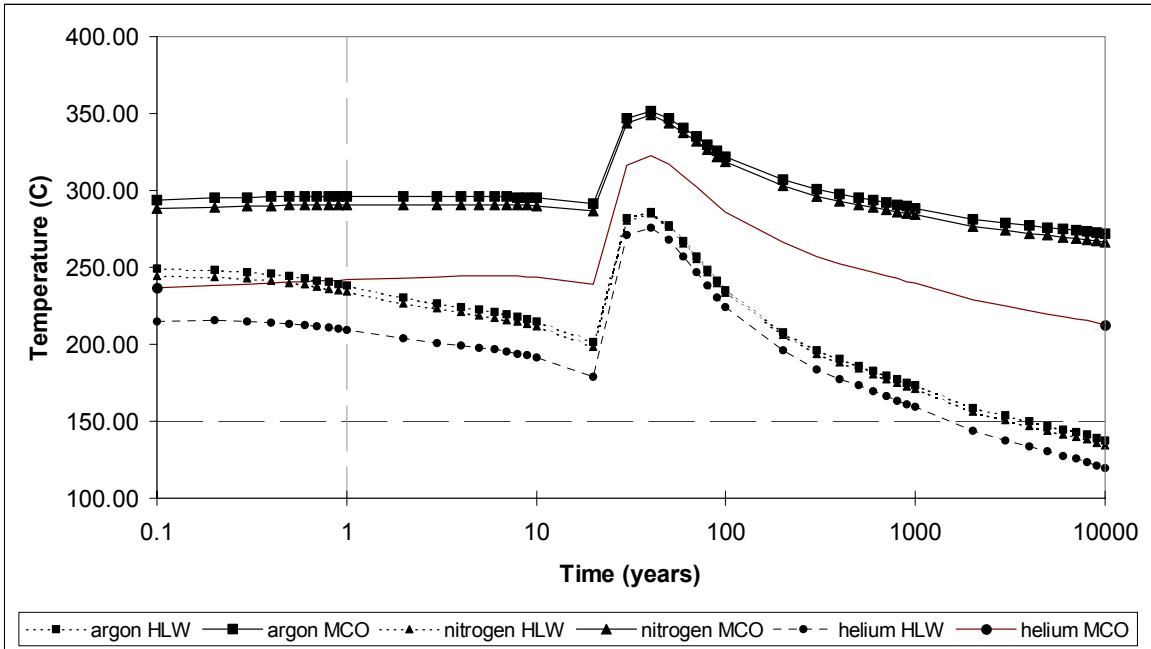
Source: CRWMS M&O 2000k

Table 8-11. Peak Temperatures and Time of Occurrence for Each DOE Spent Nuclear Fuel Canister Fill Gas: Configuration 2

Waste Package Metric	DOE Spent Nuclear Fuel Canister Fill Gas		
	Helium	Nitrogen	Argon
Peak Fuel Temperature (°C)	320.5	346.6	349.3
Time of Peak Fuel Temperature (years)	40	40	40
Peak High-Level Waste Glass Temperature (°C)	279.0	288.0	289.4
Time of Peak High-Level Waste Glass Temperature (years)	40	40	40

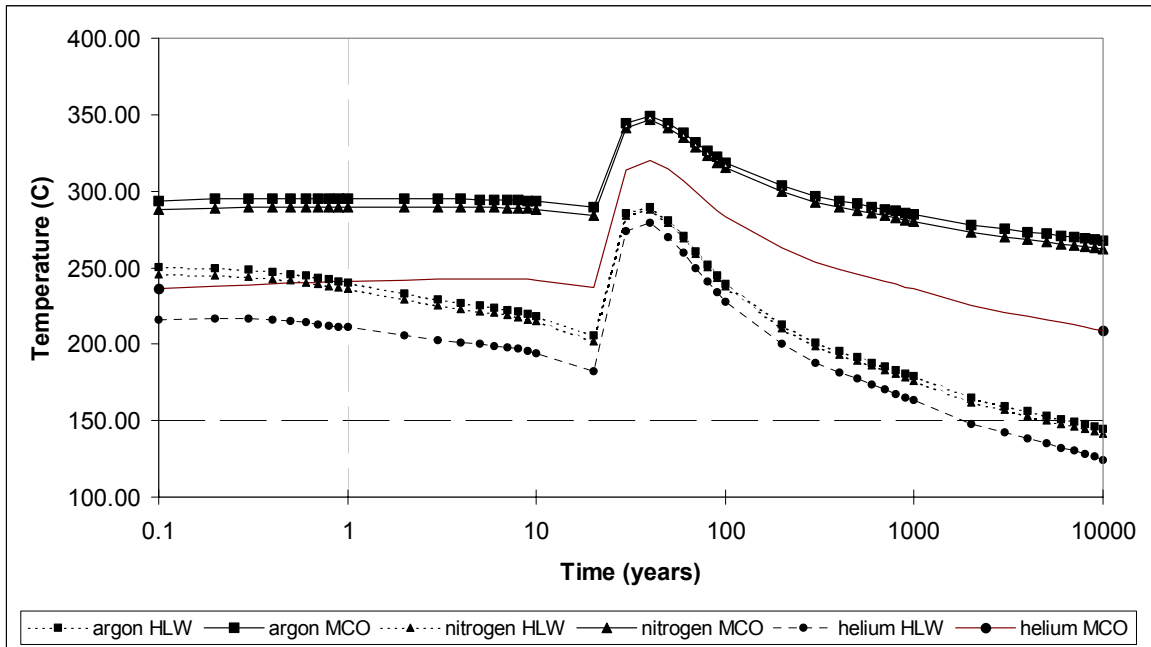
Source: CRWMS M&O 2000k

Figures 8-21 and 8-22 display the peak temperatures obtained within the DHLW canisters and within the MCOs for the different fill gases (argon, nitrogen, and helium).



Source: CRWMS M&O 2000k

Figure 8-21. Peak Temperatures – Configuration 1



Source: CRWMS M&O 2000k

Figure 8-22. Peak Temperatures – Configuration 2

8.6.3 Summary

The results indicate that the maximum DHLW glass temperature for 2-MCO/2-DHLW waste package is 289.4°C (Argon as a filler gas and waste package in configuration 2 – see Table 8-11). The maximum temperature within the MCO is 351.9°C (Argon as a filler gas and waste package in configuration 1 – see Table 8-10). The maximal thermal output of the 2-MCO/2-DHLW waste package is 6,632 W (CRWMS M&O 2000k, Table 5-3), which is less than the SDD criterion of 11,800 W (Section 4.1.2.2).

8.7 MELT AND DILUTE

No thermal analysis has been performed for Melt and Dilute ingots.

8.8 FORT SAINT VRAIN

A detailed description of the finite element representations, the method of solution, and the results are provided in *Thermal Evaluation of the Fort Saint Vrain Codisposal Waste Package* (BSC 2001d). The finite element representations were created as two-dimensional representations. The two-dimensional method was chosen because it was assumed that radial heat transfer will dominate the solution and that axial heat transfer will be minor (see Section 5.2.15).

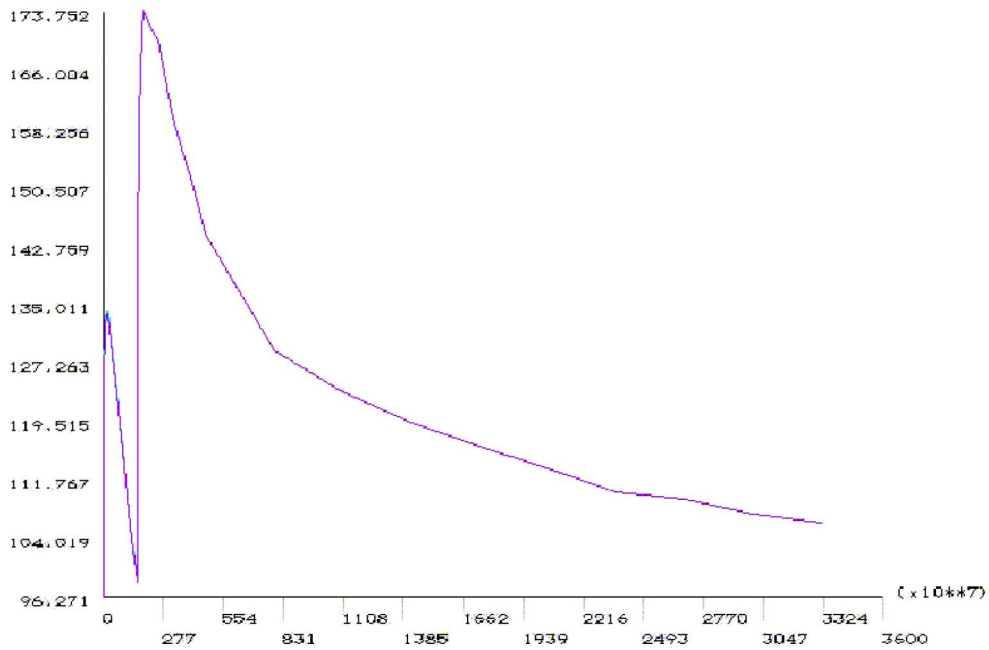
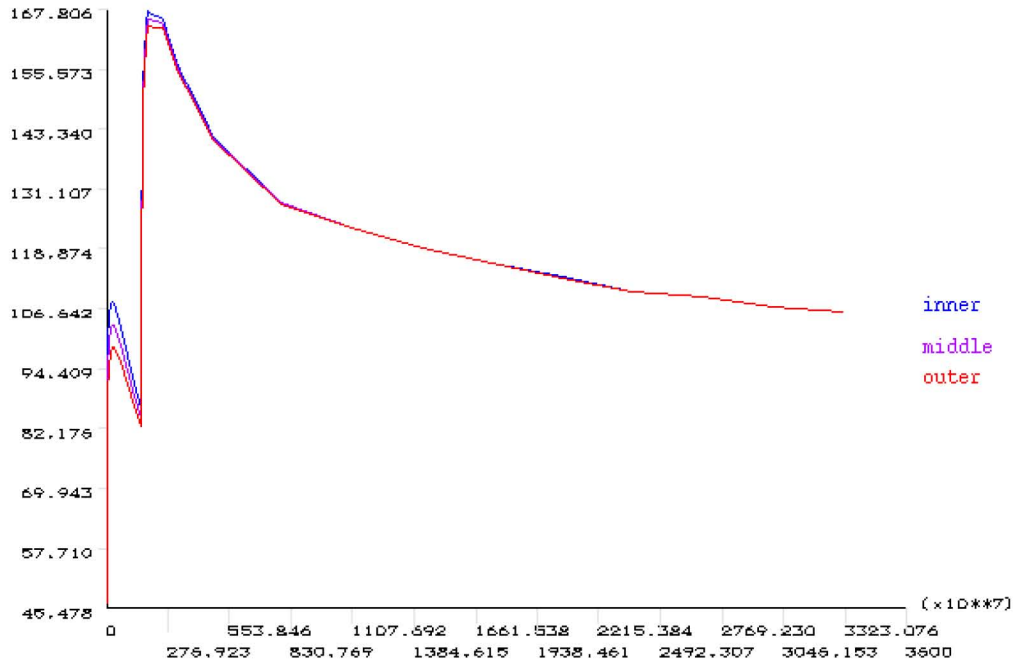
The boundary conditions on the outer surface of the waste package were taken from *Drift Scale Thermal Analysis* (CRWMS M&O 2000h, Table 6-18). The actual values are from an initial 50-year forced ventilation period with 0.1 m spacing between waste packages and no backfill. The waste package is loaded with five Hanford 4.5-m- (15-ft-) long DHLW glass canisters and one DOE SNF canister containing FSVR SNF. The waste package cross-section was modeled (taking advantage of symmetry) and the boundary conditions were applied. However, the detail of the FSVR fuel element in the center of the waste package required too many elements to make a feasible finite element representation. Therefore, the FSVR fuel element was given distributed properties in the large model. The boundary temperatures were saved and applied to a second finite element representation of the FSVR fuel element only, to obtain an accurate, continuous temperature profile from the center of the waste package to the edge of its outer shell.

The time period covered by the thermal analysis was from the time of waste package emplacement in the repository to 1,000 years after emplacement. This ensures that the time when the maximum temperatures inside the waste package will be experienced, is covered.

8.8.1 Calculations and Results

The maximum thermal output of the 5-DHLW/DOE SNF-long waste package loaded with FSVR SNF is 1,037 W. This value was calculated using the thermal outputs of the Hanford DHLW canister and DOE SNF canister containing FSVR SNF at the time of waste package emplacement in the repository ($5 \cdot 52.21 \text{ W} + 776 \text{ W} = 1,037 \text{ W}$; the values were taken from Tables 2-7 and 2-8 in BSC 2001d).

Figure 8-23 shows the plot of temperature versus time for three positions across the DHLW glass canisters. The location nearest the center of the waste package is labeled “inner.” The location farthest from the center of the waste package is labeled “outer.” The location labeled “middle” is between “inner” and “outer” locations.



Source: BSC 2001d, p. 25

Figure 8-24. Plot of Temperature Versus Time for the FSVR Spent Nuclear Fuel Element

Figures 8-23 and 8-24 show a rapid temperature increase immediately after waste package emplacement, followed by a drop that continues until the 50 years (i.e., $1.578 \cdot 10^9$ seconds) forced ventilation period ends. Then another rapid increase and peaking of the temperature is followed by a slow decrease as the fission products in the FSVR SNF continue to decay.

8.8.2 Summary

The temperature between any two points in the FSVR SNF element did not vary by more than 1°C at any time (see Figure 8-24). The maximum temperature in the FSVR SNF element was 173.8°C and was attained at 59 years after waste package emplacement.

The maximum DHLW glass temperature for the 5-DHLW/DOE SNF-long waste package loaded with FSVR SNF was 167.4°C at 59 years after waste package emplacement. The maximum thermal output of the 5-DHLW/DOE SNF-long waste package loaded with FSVR SNF is 1,037 W, which is less than the SDD criterion of 11,800 W (Section 4.1.2.2).

8.9 CONCLUSIONS

The SDD requirements changed between the time when the first and last thermal analyses were performed (FFTF and FSVR, respectively). Therefore, different types of results were sought and obtained for analyses performed for different fuel types.

The thermal analyses for FFTF and Shippingport LWBR waste packages did not provide the fuel or cladding temperatures, therefore no results are available for comparison with SDD criterion 4.1.2.1. The other thermal analyses performed (for TRIGA, Shippingport PWR, Enrico Fermi, N-Reactor, and FSVR waste packages) met the SDD criterion 4.1.2.1.

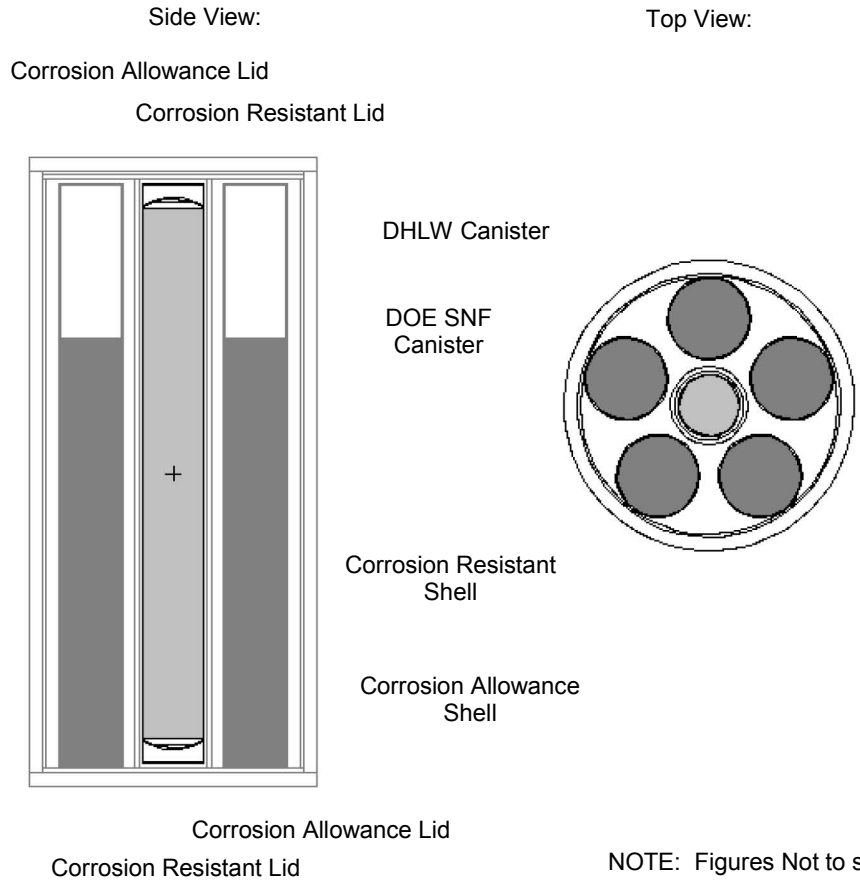
Earlier thermal analyses (FFTF, Shippingport PWR, Shippingport LWBR) used an overly conservative value for the thermal output of the Hanford DHLW canister, which was based on the maximum value allowed. The latest values of the thermal output of the Hanford DHLW canister (Table 3-23) showed that waste packages loaded with any of the fuel types addressed in this report have maximum thermal outputs that are less than the SDD criterion of 11,800 W (Section 4.1.2.2).

9 SHIELDING ANALYSIS

9.1 FFTF

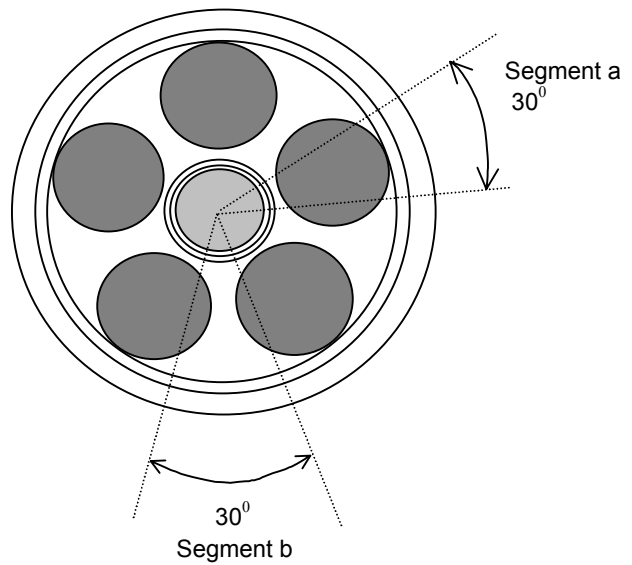
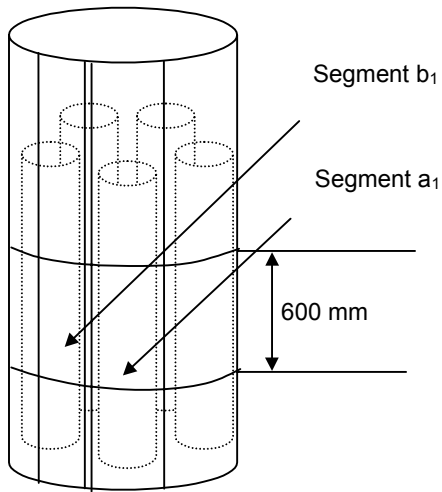
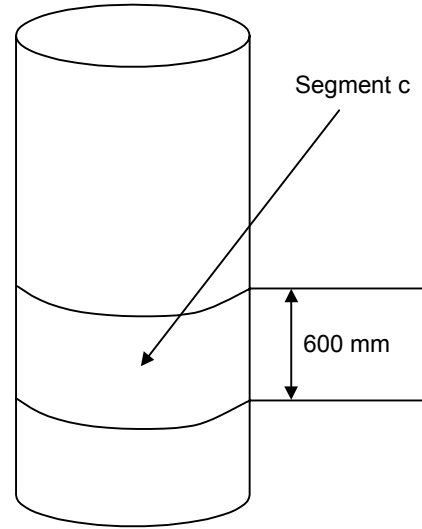
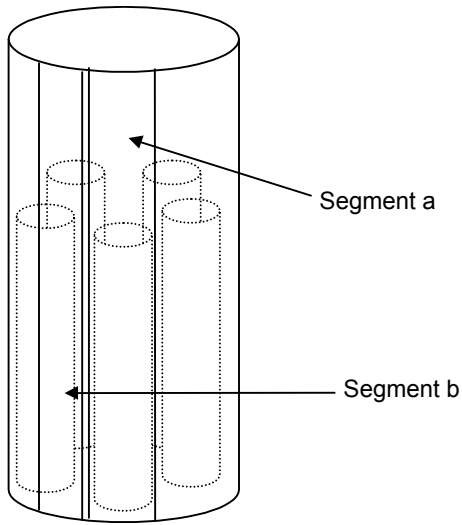
Dose rate calculations are performed for four cases: a waste package containing SRS DHLW glass and FFTF fuel, a waste package containing only SRS DHLW glass, a waste package containing Hanford DHLW glass and FFTF fuel, and a waste package containing only Hanford DHLW glass. All calculations use the glass composition given in Section 3.6. These calculations evaluated dose rates on all barrier boundaries of the waste package. Details of the calculations and the results for all cases considered are given in *Dose Calculations for the Co-Disposal WP of HLW Canisters and the Fast Flux Test Facility (FFTF) Fuel* (CRWMS M&O 1998b). The geometric representation, which ignores the waste package basket, for the MCNP calculations is shown in Figure 9-1. The surface-dose rates of the waste package containing Hanford DHLW glass are approximately 20 percent higher than those of the waste package containing SRS DHLW glass. In addition, only the dose rates on the waste package outer surfaces are of most interest. Therefore, only the results from Hanford cases for the surfaces of interest are summarized.

Figure 9-2 shows the segments and surfaces of interest. Segment c is a 600-mm long radial surface segment axially centered at the middle of glass canisters. Segment a_1 is a 30° wide angular segment of the 600-mm long radial surface (segment c) near glass canisters. Segment b_1 is a 30° wide angular segment of the 600-mm long radial surface (segment c) near the gap between glass canisters. Axial surface segment d is at the center of the waste package (Figure 9-3).



Source: CRWMS M&O 1998b, Figure 5.3-1

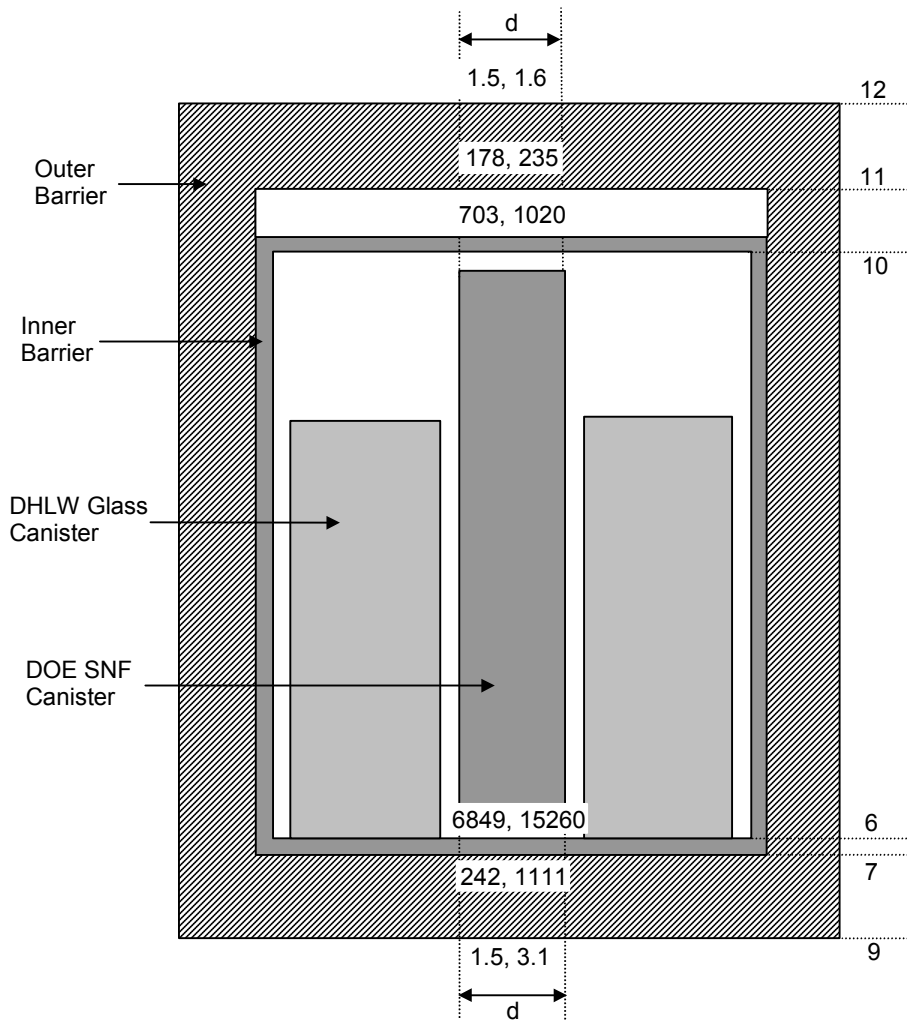
Figure 9-1. Axial and Transversal Cross-Sections of MCNP Geometry Representation for FFTF Waste Package



NOTE: Figures not to scale

Source: CRWMS M&O 1998b, Figures 6-1 and 6-2

Figure 9-2. Radial Segments Used for Dose-Rate Calculations



NOTE: Figure not to scale.

Source: CRWMS M&O 1999a, Figure 5-3

Figure 9-3. MCNP Estimates for Dose Rates in rem/h over Axial Surfaces and Segments

9.1.1 Waste Package Containing Hanford DHLW and FFTF Fuel

Tables 9-1 and 9-2 show the dose rates in rem/h on the surfaces of interest of the waste package containing the Hanford DHLW glass and FFTF DOE SNF canister.

Table 9-1. Total Radial Dose Rates Averaged over a Height of 60 cm

Radial Position	Angular Position					
	Segment a ₁		Segment b ₁		Segment c	
	Dose Rate (rem/h)	Relative Error	Dose Rate (rem/h)	Relative Error	Dose Rate (rem/h)	Relative Error
Inner surface of inner barrier	9328.1	0.0246	9869.5	0.0238	9967.3	0.0086
Outer surface of outer barrier	15.9	0.0603	15.0	0.0716	15.0	0.0184

Source: CRWMS M&O 1999a, Table 5-1

Table 9-2. Dose Rates Averaged over Segment d

Axial Surface	Gamma Dose Rate (rem/h)	Relative Error	Neutron Dose Rate (rem/h)	Relative Error	Total Dose Rate (rem/h)	Relative Error
Outer surface of outer barrier bottom lid	1.52	0.1514	2.84E-02	0.0089	1.55	0.1486
Outer surface of outer barrier top lid	1.47	0.1317	1.28E-02	0.0131	1.48	0.1306

Source: CRWMS M&O 1999a, Table 5-2

9.1.2 Waste Package Containing Only Hanford DHLW Canisters

Tables 9-3 and 9-4 show dose rates on the surfaces of interest of the waste package containing the Hanford DHLW glass canisters only.

Table 9-3. Radial Gamma Dose Rates Averaged over a Height of 60 cm

Radial Position	Angular Position					
	Segment a ₁		Segment b ₁		Segment c	
	Dose Rate (rem/h)	Relative Error	Dose Rate (rem/h)	Relative Error	Dose Rate (rem/h)	Relative Error
Inner surface of inner barrier	9392.8	0.0219	10099	0.0237	9959.5	0.0070
Outer surface of outer barrier	15.83	0.0507	13.73	0.0679	14.45	0.0159

Source: CRWMS M&O 1999a, Table 5-3

Table 9-4. Dose Rates in rem/h Averaged over Segment d

Axial Surface	Gamma Dose Rate (rem/h)	Relative Error
Outer surface of outer barrier bottom lid	3.11	0.1462
Outer surface of outer barrier top lid	1.57	0.2212

Source: CRWMS M&O 1999a, Table 5-4

9.1.3 Summary

The results of dose rate calculations are analyzed for the cases containing Hanford DHLW and FFTF fuel, since that case has the highest dose rate among all cases investigated. The highest dose rate of 15.9 ± 1.9 rem/h (uncertainties reported correspond to two standard deviations) is calculated on the 600-mm long, 30° wide angular segment of radial outer surface of the waste package (Segment a₁, see Figure 9-2). The primary gamma dose rate dominates the neutron dose rate by approximately three orders of magnitude.

The axial dose rates are higher on the bottom surfaces of waste packages because the DHLW canisters rest on the bottom lids. The average dose rates on the outside of outer barrier of the bottom lid, and the outside of the outer barrier of the top lid are 1.52 ± 0.46 rem/h and 1.47 ± 0.39 rem/h, respectively.

The dose on Segment a₁ is primarily due to the gamma rays of the adjacent DHLW glass canister, while the dose on Segment b₁ is a contribution of gamma rays emitted from nearby

DHLW glass canisters. Source strength, geometry, and spectrum lead to a uniform angular dose over the radial surfaces of the waste packages for all analyzed cases.

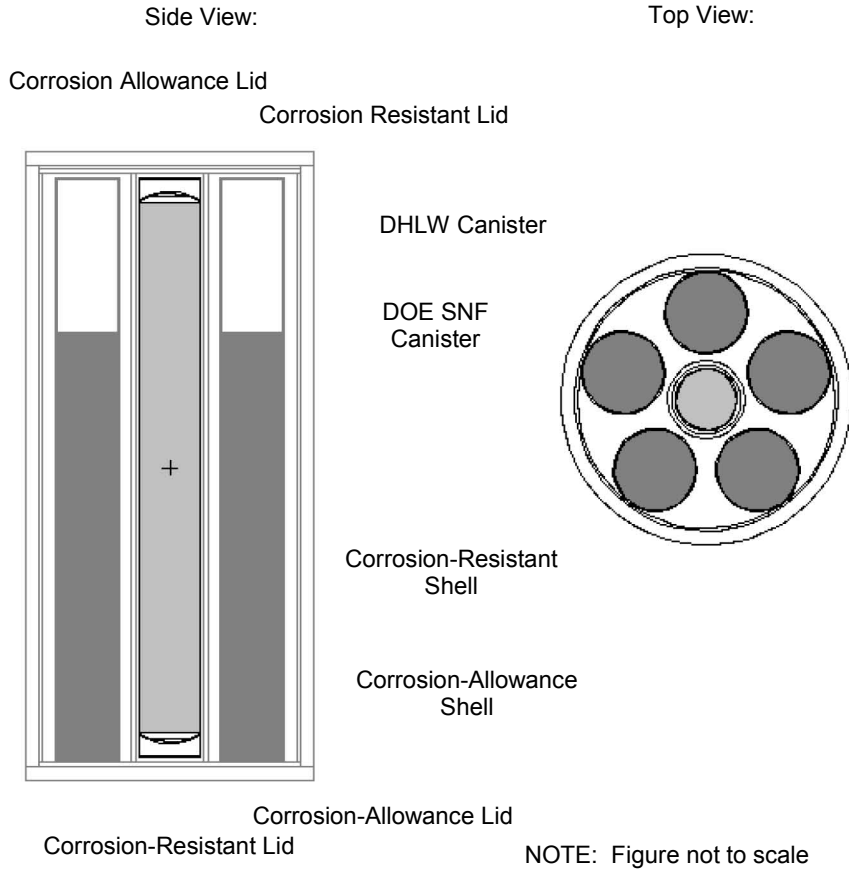
The contribution to the total dose rate by the FFTF DOE SNF canister is approximately 10 percent for the waste package containing SRS DHLW glass and approximately 5 percent for the waste package containing Hanford DHLW glass. Figure 9-3 shows the MCNP estimates for dose rates over axial surfaces and segments in rem/h. The first value of each set is the surface dose rate for the waste package containing Hanford DHLW glass canisters and FFTF DOE SNF canister, while the second value is the surface dose rate for the waste package containing only Hanford DHLW glass canisters. The axial dose rate on Surface 10 (the inner surface of the inner barrier of the top lid) is about one order of magnitude lower than the axial dose rate on Surface 6 (inner surface of inner barrier bottom lid). The difference indicates that the doses on the axial surfaces are mainly due to DHLW glass canisters. The upper surface of DHLW glass canisters is about 1 m below the inner top lid and their bottom surfaces lay on the inner bottom lid, while the FFTF DOE SNF canister is symmetrically positioned at the center of the waste package.

The peak dose on the outside of top and bottom waste package outer lids (Figure 9-3, Segment d) is mainly produced by the gamma rays emitted in the DHLW glass. The gamma rays from the DHLW glass undergo multiple collisions and lose energy in the FFTF fuel and in the walls of the DOE SNF canister. The spectrum of gamma rays that enter the FFTF DOE SNF canister and then reach the Segment d of Surface 6 (see Figure 9-3) is much softer than that of the gamma rays that propagate through the less dense material of the DHLW glass and reach the surrounding axial surface. The dose rate on Segment d is doubled when the FFTF DOE SNF canister is removed, indicating that its presence in the center of the waste package reduces the axial dose rates. This is mainly due to the fact that placing the FFTF DOE SNF canister in the center of the waste package provides shielding for the gamma rays from the DHLW glass, which otherwise would only attenuate through air (or a fill gas) with a much smaller attenuation coefficient. The combined dose rate due to the gamma rays from the DHLW glass that are shielded by the FFTF DOE SNF canister, and the gamma rays from the FFTF DOE SNF canister itself is, therefore, less than the dose rate due to the gamma rays from the DHLW glass in the absence of the FFTF DOE SNF canister.

9.2 TRIGA

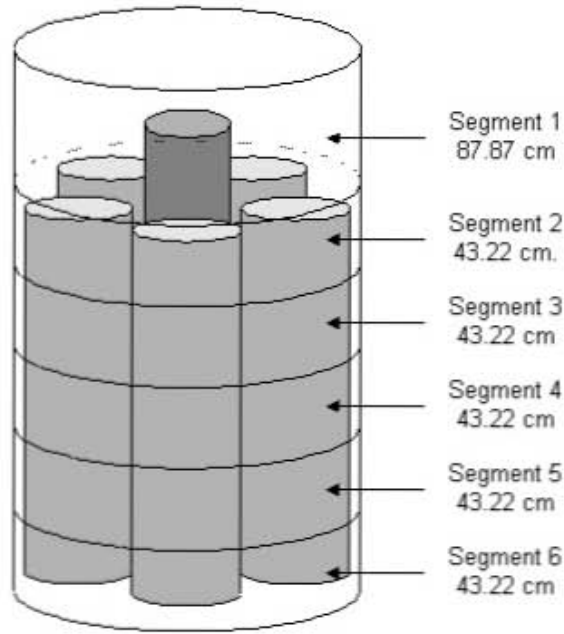
The waste package load consists of five SRS DHLW glass canisters and one 18-in-outer diameter DOE SNF canister containing the TRIGA SNF. There are two different radiation sources in this calculation, the DHLW glass canisters and the contents of the DOE SNF canister. All calculations use the glass composition given in Section 3.6. These calculations evaluated the dose rates on all barrier boundaries of the waste package. Details of the calculations and the results for all cases considered are given in *Dose Calculations for the Codisposal WP of HLW Glass and the TRIGA SNF* (CRWMS M&O 1999n). The geometric representation for the MCNP calculations is shown in Figure 9-4. Figure 9-5 shows the surfaces and segments of the waste package used in the dose-rate calculations. The radial surfaces of the waste package are divided into six axial segments. The first five axial segments are equal segments of the radial surfaces between the top and bottom planes of the DHLW glass. Each of these segments has a height of 432.25 mm. The last axial segment, of 878.74 mm height, is the portion between the top of waste package cavity and the top of DHLW glass.

The source term used in these calculations for the TRIGA SNF corresponds to 1-year decay time. Tables 9-5 and 9-6 show the radial and axial gamma dose rates on the outer surface of the waste package containing the SRS DHLW glass canisters and the DOE SNF canister containing TRIGA SNF.



Source: CRWMS M&O 1999n, Figure 5.2-1

Figure 9-4. Vertical and Horizontal Cross-Sections of MCNP Geometry Representation



not to scale

Source: CRWMS M&O 2000b, Figure 5-2

Figure 9-5. Radial-Surface Segments of the Waste Package Used in Dose Rate Calculations

Table 9-5. Gamma Dose Rates Averaged over Waste Package Outer Radial Surface

Axial Location ^a	Dose Rate (rem/h)	Relative Error
Segment 1	7.3403	0.0168
Segment 2	12.978	0.0206
Segment 3	14.060	0.0201
Segment 4	13.811	0.0202
Segment 5	13.489	0.0218
Segment 6	10.891	0.0238

Source: CRWMS M&O 1999n, Table 6-3

NOTE: ^a Exact locations are indicated in Figure 9-5.

Table 9-6. Gamma Dose Rates Averaged over Waste Package Axial Surfaces

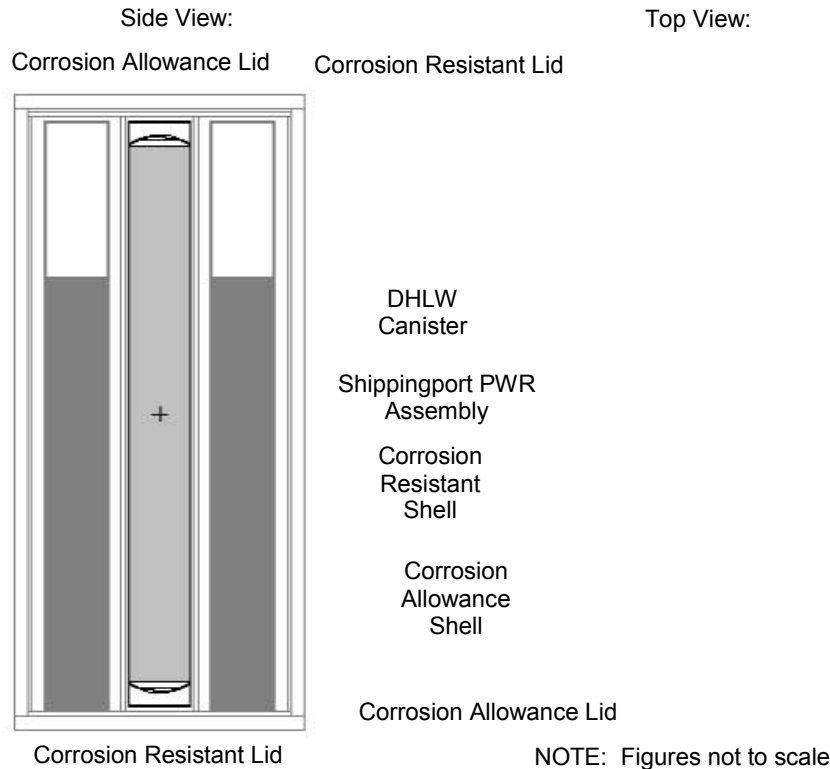
Axial Location	Dose Rate (rem/h)	Relative Error
Top surface of waste package	1.7518	0.0411
Bottom surface of waste package	3.5951	0.0320

Source: CRWMS M&O 1999n, Table 6-6

The highest dose rates for the outer surfaces of the waste package have been obtained for the middle segments of the radial surface (segments 3 and 4). The maximum surface dose rate is 14.06 ± 0.57 rem/h. The contribution of the neutron dose rate to the total dose rate is negligible.

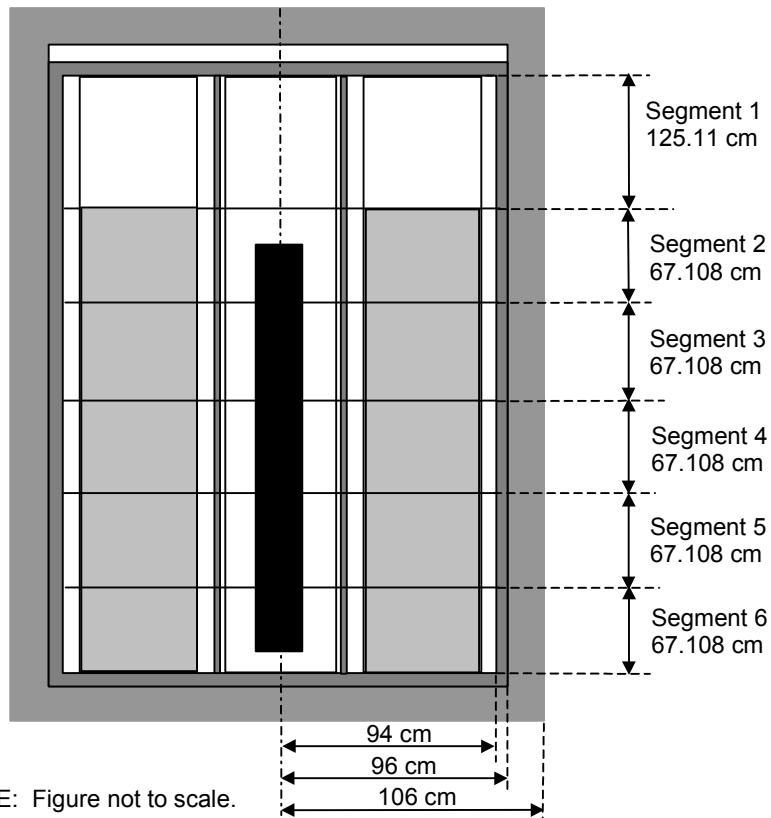
9.3 SHIPPINGPORT PWR

The details of the dose calculations and the results for Shippingport PWR waste package are provided in *Dose Calculation for the Co-Disposal WP of HLW Canisters and the Shippingport PWR Fuel* (CRWMS M&O 1999o). The geometric representation used in MCNP calculations is shown in Figure 9-6. Previous dose-rate calculations for the waste package containing SRS DHLW glass canisters show that the angular dose over the waste package radial surfaces is uniform (CRWMS M&O 1998b, pp. 30 and 33). Therefore, only axial variation of the dose rate on the waste package radial surfaces and the radial variation of the dose rate on the waste package axial surfaces are studied. The surfaces and segments that are used in the dose-rate calculations are shown in Figure 9-7. The radial surfaces, cut by the bottom and top planes of DHLW glass, are equally divided into five segments, each of which is 67.108-cm high. The sixth radial segment, 125.11-cm high, is the portion between the top of waste package cavity and the top of DHLW glass. Previous analyses used Hanford DHLW glass neutron and gamma sources, which resulted in approximately 20 percent higher dose rates, for 5-DHLW/DOE SNF-long waste packages. Because this approach yielded overly conservative results, the SRS DHLW glass neutron and gamma sources were used in the analyses of the Shippingport PWR SNF. Although the sources are from 3-m SRS DHLW glass canisters, they were scaled up to account for longer (4.5-m or 15-foot) DHLW glass canisters.



Source: CRWMS M&O 1999o, Figure 5.2-1

Figure 9-6. Waste Package Cross-Sections of MCNP Geometry Representation



Source: CRWMS M&O 1999o, Figure 6-1

Figure 9-7. Radial Surfaces and Segments of the Waste Package Used in Dose Rate Calculations

Tables 9-7 and 9-8 show the dose rates in rem/h on the surfaces of interest of the waste package containing the SRS DHLW glass and Shippingport PWR DOE SNF canister. The dose rates in rem/h and rad/h are practically the same due to the insignificant contribution of the neutron dose rate to the total dose rate (CRWMS M&O 1999o, pp. 21 to 25).

Table 9-7. Dose Rates on Waste Package Outer Radial Surface

Axial Location	Gamma		Neutron		Total	
	Dose Rate (rem/h)	Relative Error (%)	Dose Rate (rem/h)	Relative Error (%)	Dose Rate (rem/h)	Relative Error (%)
Segment 1	1.0624	0.0431	2.3274E-02	0.0065	1.0856	0.0422
Segment 2	9.4949	0.0191	6.9035E-02	0.0047	9.5640	0.0190
Segment 3	9.9406	0.0180	8.4840E-02	0.0042	10.025	0.0178
Segment 4	10.231	0.0176	8.5894E-02	0.0042	10.317	0.0175
Segment 5	9.7283	0.0174	8.5034E-02	0.0042	9.8133	0.0172
Segment 6	9.2088	0.0184	7.3792E-02	0.0046	9.2826	0.0183

Source: CRWMS M&O 1999o, Table 6-3

Table 9-8. Dose Rates on Waste Package Axial Surfaces

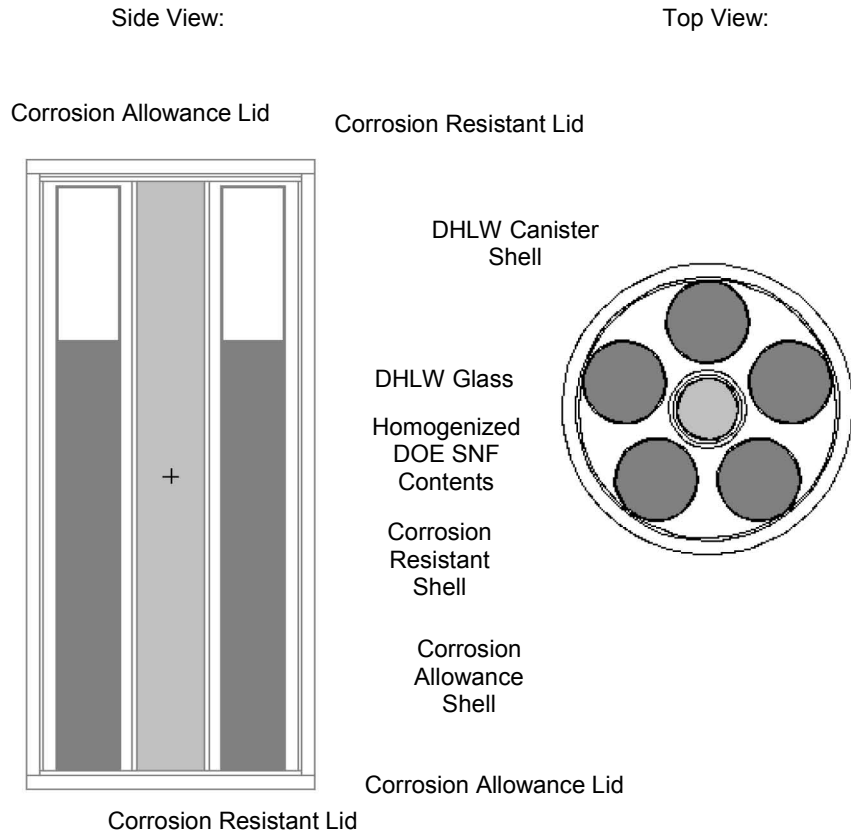
Axial Location	Gamma		Neutron		Total	
	Dose Rate (rem/h)	Relative Error (%)	Dose Rate (rem/h)	Relative Error (%)	Dose Rate (rem/h)	Relative Error (%)
Bottom surface of waste package	2.5216	0.0368	5.2263E-02	0.0063	2.5738	0.0361
Top surface of waste package	0.49322	0.0805	1.3585E-02	0.0118	0.5068	0.0783

Source: CRWMS M&O 1999o, Table 6-6

For the radial surfaces, the maximum surface dose rate occurs at the middle segments of the DHLW glass canisters. The maximum surface dose rates, for the middle segment of the waste package outer radial surface is 10.32 ± 0.36 rem/h. The maximum dose rates on the axial surfaces for the bottom and top surfaces are about one to one-half orders of magnitude lower than the maximum dose rates on the corresponding radial surfaces.

9.4 ENRICO FERMI

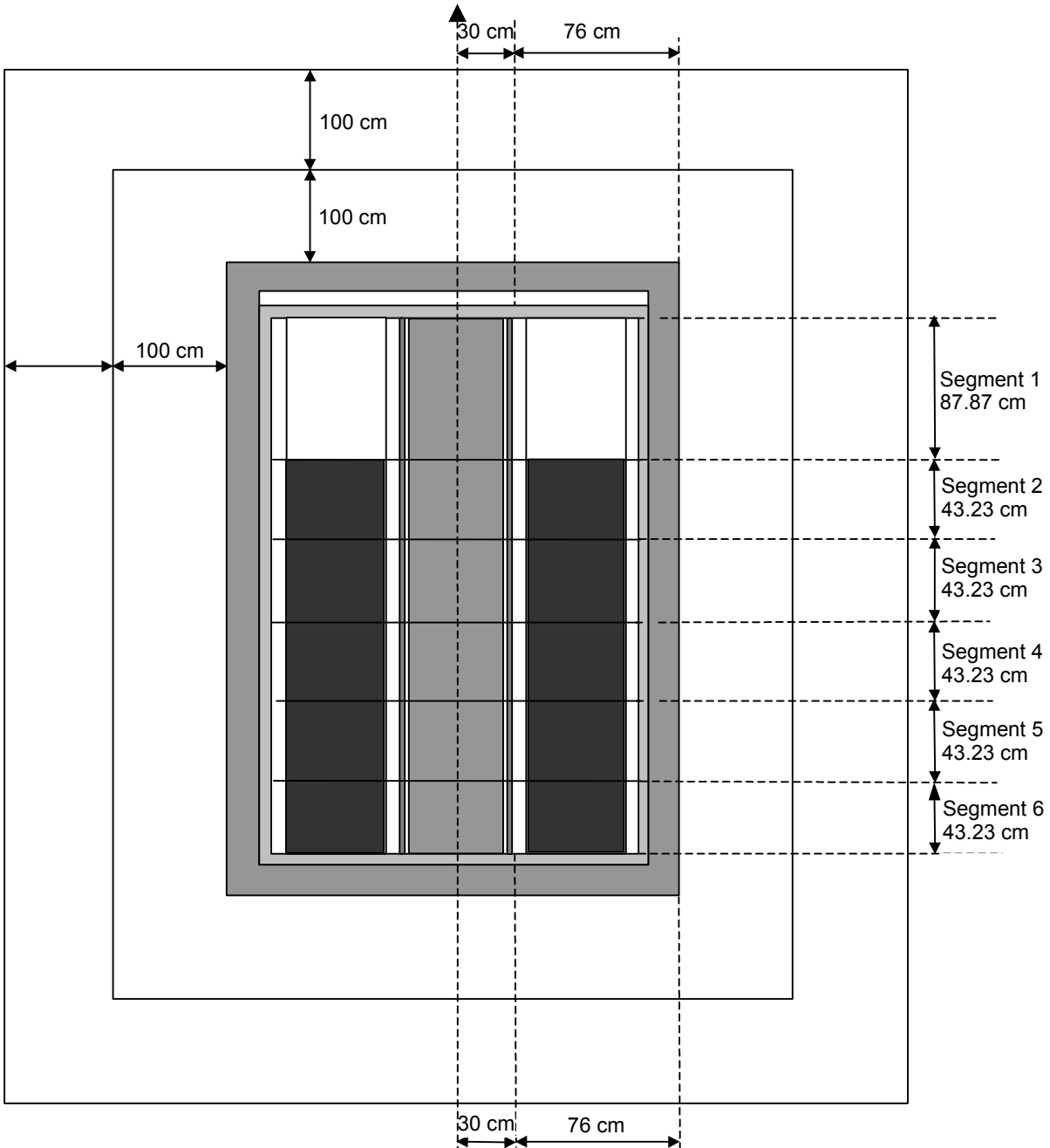
The details of the dose calculations and the results for Enrico Fermi waste package are provided in *Dose Calculations for the Co-Disposal WP of HLW Canisters and Fermi U-Mo Alloy SNF* (CRWMS M&O 1999d). The geometric representation used in MCNP calculations is shown in Figure 9-8. Previous dose-rate calculations for the waste package containing only SRS DHLW glass canisters show that the angular dose rate over waste package radial surfaces is uniform (CRWMS M&O 1998b, p. 33). Therefore, only axial variation of the dose rate on the waste package radial surfaces and the radial variation of the dose rate on the waste package top and bottom axial surfaces are studied. Figure 9-9 shows the surfaces and segments that are used in the dose-rate calculations. The radial surface, between the bottom and top planes of DHLW glass, are equally divided into five segments, each of which is 43.23-cm high. The first radial segment (segment 1), 87.87-cm high, corresponds to the empty portion of the DHLW glass canister, which is between the top of the waste package cavity and the top of the DHLW glass. The waste package top and bottom axial surfaces are divided into two radial segments of 0-30 cm and 30-106 cm.



NOTE: Figures not to scale

Source: CRWMS M&O 1999d

Figure 9-8. Vertical and Horizontal Cross-Sections of MCNP Geometry Representation



Source: CRWMS M&O 2000d, Figure 14

Figure 9-9. Surfaces and Segments Used for Dose-Rate Calculations

Tables 9-9 through 9-11 present the radial and axial dose rates on the outer surface of the waste package containing the five SRS DHLW glass canister and the Fermi DOE SNF canisters. The dose rates in rem/h and rad/h are practically the same due to the insignificant contribution of the neutron dose rate to the total dose rate (CRWMS M&O 1999d, pp. 21 to 24 and Attachment V).

Table 9-9. Radial Dose Rates Averaged over Waste Package Outer-Radial Surface

Axial Location	Gamma Dose Rate (rem/h)	Neutron Dose Rate (rem/h)	Total Dose Rate (rem/h)
Segment 1	1.688	0.029	1.717
Segment 2	10.005	0.067	10.072
Segment 3	10.747	0.083	10.830
Segment 4	10.866	0.085	10.951
Segment 5	10.769	0.083	10.852
Segment 6	9.499	0.067	9.566

Source: CRWMS M&O 1999d

NOTE: The dose rates listed in this table are the upper limits of the 95% confidence intervals of the Monte Carlo dose rate calculations.

Table 9-10. Axial Dose Rates Averaged over a 30-cm Radius Surface

Axial Location	Gamma Dose Rate (rem/h)	Neutron Dose Rate (rem/h)	Total Dose Rate (rem/h)
Bottom surface of waste package	0.986	0.061	1.047
Top surface of waste package	0.477	0.020	0.497

Source: CRWMS M&O 1999d

NOTE: The dose rates listed in this table are the upper limits of the 95% confidence intervals of the Monte Carlo dose rate calculations.

Table 9-11. Axial Dose Rates Averaged over the Circular Segment Outside the 30-cm Radius

Axial Location	Gamma Dose Rate (rem/h)	Neutron Dose Rate (rem/h)	Total Dose Rate (rem/h)
Bottom surface of waste package	3.153	0.052	3.205
Top surface of waste package	1.121	0.020	1.141

Source: CRWMS M&O 1999d

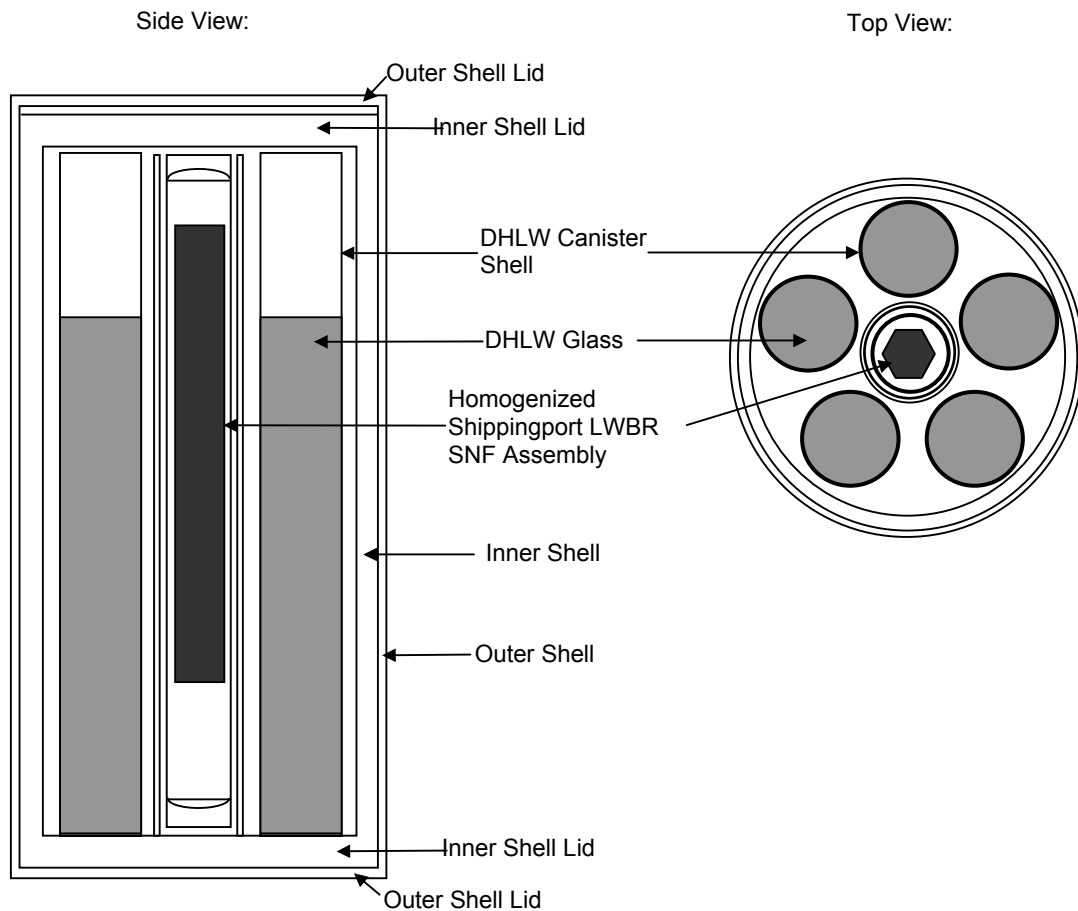
NOTE: The dose rates listed in this table are the upper limits of the 95% confidence intervals of the Monte Carlo dose rate calculations.

The maximum dose rate on the external surfaces of the waste package is 10.95 rem/h. It occurs on the outer radial surface at Segment 4 of the waste package. The dose rates on the bottom and top surfaces of the waste package are about one-third and about one-tenth, respectively, of the maximum dose rate on the outer radial surface.

9.5 SHIPPINGPORT LWBR

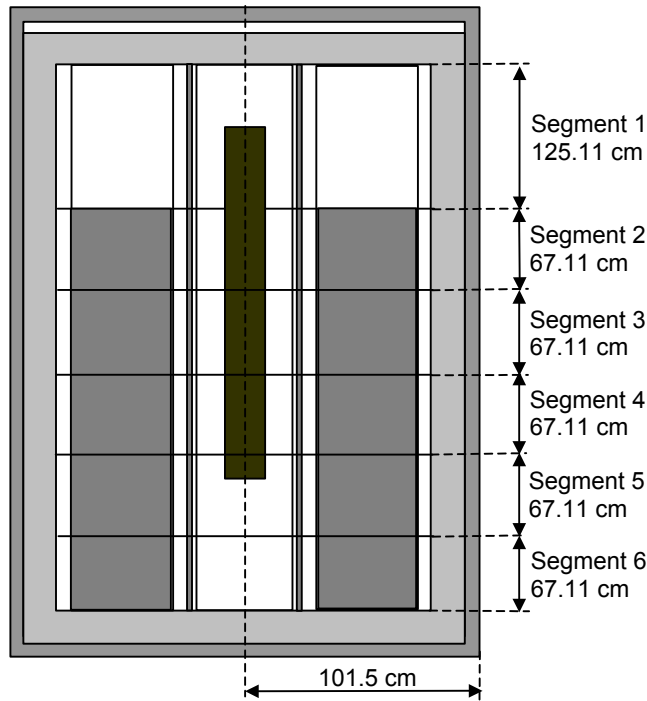
Dose Calculations for the Codisposal WP of HLW Glass and the Shippingport LWBR SNF (CRWMS M&O 1999p) gives the details of the calculations and the results. The geometric representation of the waste package used in MCNP calculations is shown in Figure 9-10. Previous dose-rate calculations for the 5-DHLW/DOE SNF waste package have shown that the

angular dose rate over waste package radial surfaces is uniform (CRWMS M&O 1998b, p. 33). Therefore, only axial variation of the dose rates on the waste package radial surfaces and the radial variation of the dose rates on the waste package top and bottom axial surfaces are studied. Figure 9-11 shows the surfaces and segments that are used in the dose-rate calculations. The radial surface, between the bottom and top planes of DHLW glass, are equally divided into five segments, each of which is 67.11-cm high. The first radial segment (segment 1), 125.11-cm high, corresponds to the empty portion of the DHLW canister, which is between the top of the waste package cavity and the top of the DHLW glass.



Source: CRWMS M&O 1999p, Figure 5.2-1

Figure 9-10. Vertical and Horizontal Cross-Sections of the MCNP Geometry Representation



Source: CRWMS M&O 1999p, Figure 5.2-2

Figure 9-11. Surfaces and Segments Used for Dose-Rate Calculations

Tables 9-12 and 9-13 present the MCNP estimates of the radial and axial dose rates on the outer surface of the waste package containing five 4.5-m-long DHLW glass canisters and the Shippingport LWBR DOE SNF canister. The estimated relative error, which is the ratio of the estimated standard deviation and the estimated tally, is also provided for each segment dose rate in Tables 9-13 and 9-14. The dose rates in rem/h and rad/h are practically the same due to the insignificant contribution of the neutron dose rate to the total dose rate (CRWMS M&O 1999p, pp. 19 to 21, and Attachment VI).

Table 9-12. Dose Rates on the Waste Package Outer Radial Surface

Axial Location (Figure 15)	Gamma		Neutron		Total	
	Dose Rate (rem/h)	Relative Error	Dose Rate (rem/h)	Relative Error	Dose Rate (rem/h)	Relative Error
Segment 1	9.6170E+00	0.0191	2.5418E-01	0.0038	9.8712E+00	0.0186
Segment 2	7.2129E+01	0.0109	2.5634E-01	0.0050	7.2385E+01	0.0109
Segment 3	8.0643E+01	0.0104	2.5985E-01	0.0050	8.0902E+01	0.0104
Segment 4	8.0426E+01	0.0104	2.3333E-01	0.0053	8.0660E+01	0.0104
Segment 5	8.1163E+01	0.0106	1.7181E-01	0.0062	8.1334E+01	0.0106
Segment 6	7.4584E+01	0.0109	1.1881E-01	0.0076	7.4703E+01	0.0109

Source: CRWMS M&O 1999p, Table 6.1-3

Table 9-13. Dose Rates on the Waste Package Axial Surfaces

Axial Location (Figure 15)	Gamma		Neutron		Total	
	Dose Rate (rem/h)	Relative Error	Dose Rate (rem/h)	Relative Error	Dose Rate (rem/h)	Relative Error
Bottom surface of waste package	3.0317E+00	0.0379	6.3251E-02	0.0113	3.0950E+00	0.0371
Top surface of waste package	6.0081E-01	0.0802	9.0493E-02	0.0088	6.9130E-01	0.0697

Source: CRWMS M&O 1999p, Table 6.1-6

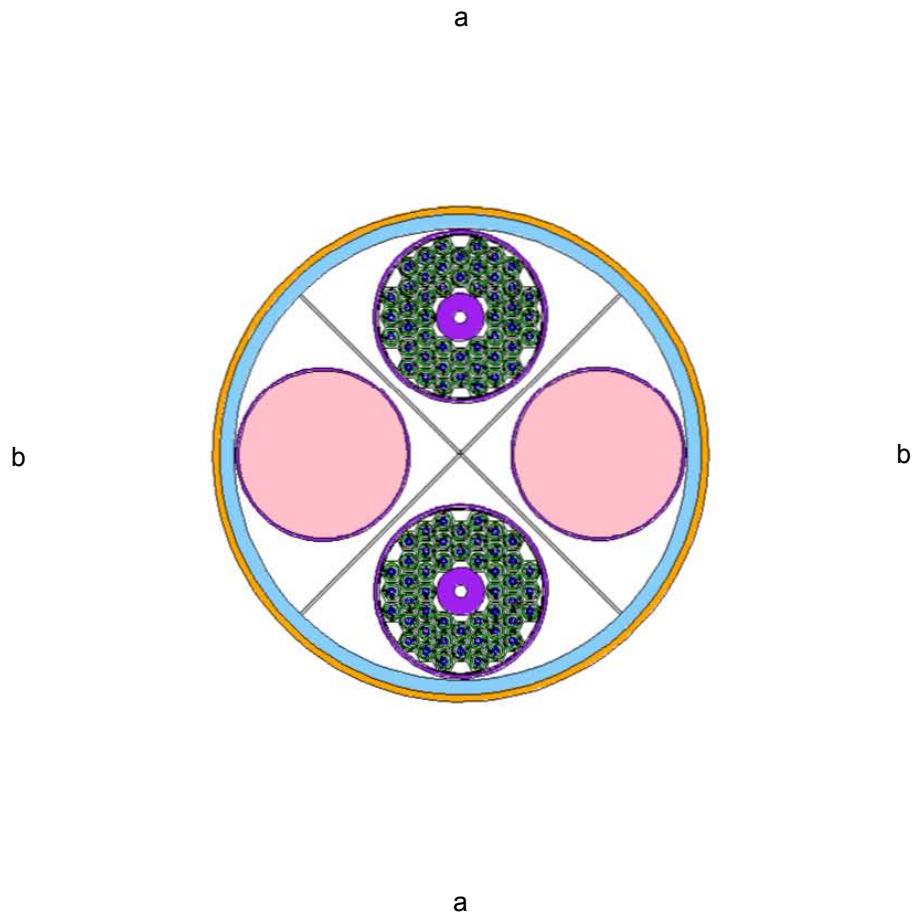
The maximum dose rate at the external surfaces of a waste package that contains only the five 4.5-m-long DHLW glass canisters is 83.05 rem/h (dose rate + 2 σ) (CRWMS M&O 1999p, p. 20).

The maximum dose rate on the external surfaces of the waste package is 83.05 rem/h. It occurs on segment 5 of the outer radial surface of the waste package. The dose rates on the bottom and top surfaces of the waste package are one and two orders of magnitude, respectively, smaller than the maximum dose rate on the outer radial surface.

9.6 N-REACTOR

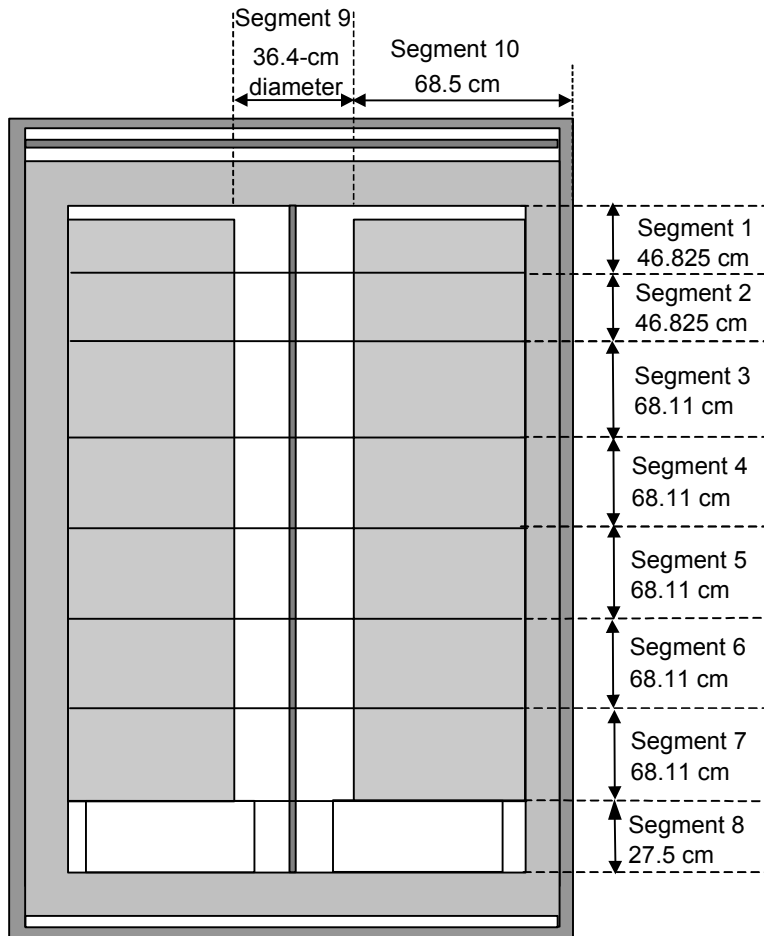
The details of the calculations and the results are provided in *Dose Rate Calculation for the 2-MCO/2-DHLW Waste Package* (CRWMS M&O 2000l). The calculation provides dose rates at the external surfaces of a waste package that contains two 4.5-m (15-ft) -long Hanford DHLW glass canisters and two Hanford MCOs. Each MCO is loaded with intact N-Reactor SNF Mark IA. Because an MCO loaded with Mark IA fuels is less self-shielded than an MCO loaded with Mark IV fuels (i.e., density of the MCO loaded with Mark IA fuel is lower than that of MCO loaded with Mark IV fuel) (DOE 2000a, p. 33), the calculation provides conservative (higher) dose rate evaluations.

A horizontal cross-section of the waste package geometric representation in MCNP calculations is shown in Figure 9-12. This figure also shows the angular segments of the radial surfaces, each 90° wide, used in surface dose-rate calculations. Figure 9-13 shows the radial and axial segments used in dose rate tallies. Segments 1 and 2, each 46.825-cm long, are segments of the radial surfaces between the top plane of glass and the top plane of waste package cavity. Segments 3 through 7, each 68.11-cm long, are radial surface segments between the bottom plane of the MCO and the top plane of DHLW glass. Segment 8 is between the bottom of the waste package cavity and the bottom of MCOs. Each waste package axial surface is divided into two segments by a circle of 36.4-cm diameter.



Source: CRWMS M&O 2001a, Figure 5-1

Figure 9-12. Waste Package Cross-Section of MCNP Geometry Representation and the Angular Segments Used in Dose Rate Calculations



Source: CRWMS M&O 2001a, Figure 5-2

NOTES: Drawing not to scale. The figure shows a vertical cross-section through the MCOs. The contents of the MCOs (fuel elements and storage baskets) are not shown in this figure.

Figure 9-13. Radial and Axial Surfaces and Segments of the Waste Package Used in Dose Rate Calculations

Tables 9-14 and 9-15 present the total radial and axial dose rates (and the corresponding standard deviations) averaged over waste package radial and axial surface segments, respectively. The dose rates in rem/h and rad/h are practically the same due to the insignificant contribution (less than four percent) of the neutron dose rate to the total dose rate (CRWMS M&O 2000l, Attachment III).

In case of canister misplacement, with the DHLW glass canister occupying successive positions inside the waste package (configuration 1 of Figure 8-18), the bounding surface dose rates are less than twice of those of segment b shown in Table 9-14.

Table 9-14. Dose Rates on Waste Package Outer Radial Surface

Axial Location ^a	Segment a ^b		Segment b ^c	
	Dose Rate (rem/h)	Standard Deviation (rem/h)	Dose Rate (rem/h)	Standard Deviation (rem/h)
Segment 1	0.5920	0.0679	1.9578	0.1290
Segment 2	11.0123	0.3582	17.5959	0.4953
Segment 3	28.3893	0.4761	67.3416	0.8206
Segment 4	30.7318	0.5122	72.2033	0.8509
Segment 5	30.3483	0.4997	75.0814	0.8924
Segment 6	28.8816	0.4698	72.0221	0.8488
Segment 7	27.2182	0.4699	70.9662	0.8506
Segment 8	12.0523	0.5201	58.4442	1.2260

Source: CRWMS M&O 2000I, Table 15

NOTES: ^a See Figure 5-2 for segment locations.

^b Segment a is adjacent to an MCO (see Figure 5-1 for segment location).

^c Segment b is adjacent to a high-level waste glass canister (see Figure 5-1 for segment location).

Table 9-15. Dose Rates on Segments of Waste Package Axial Surfaces

Axial Location	Segment	Dose Rate (rem/h)	Standard Deviation (rem/h)
Bottom surface of the waste package	Segment 9	1.1907	0.1657
	Segment 10	1.7729	0.0544
Top surface of the waste package	Segment 9	0.2513	0.0680
	Segment 10	0.2709	0.0208

Source: CRWMS M&O 2000I, Table 18

NOTE: See Figure 5-2 for segment locations.

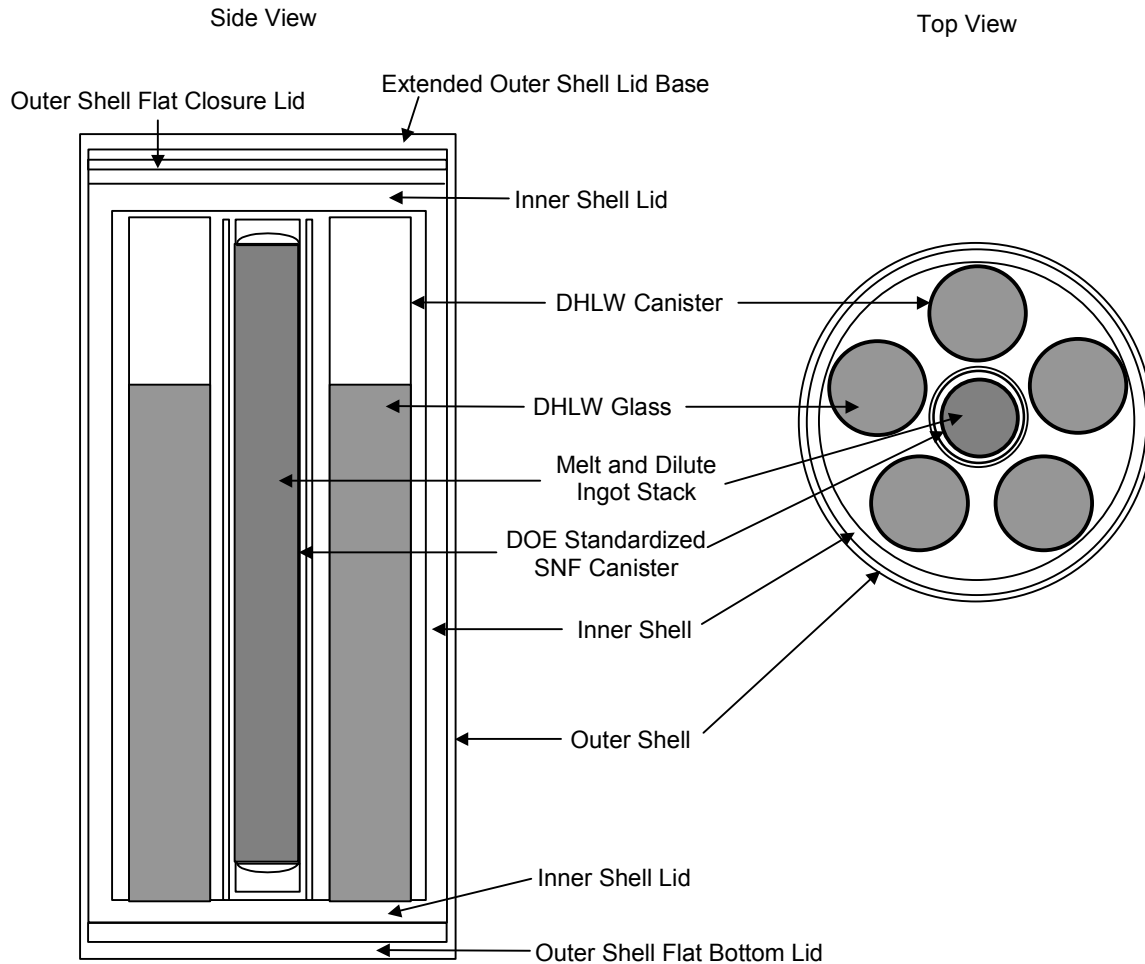
The gamma source spectra of an MCO and a DHLW glass canister are similar, and the gamma-source intensity of an MCO is higher than that of a DHLW glass canister (see Tables 3-47 and 3-45). However, because of radiation self-shielding inside an MCO due to higher-density materials, the dose rate at the external surface of the waste package adjacent to the glass canisters is higher than the dose rate at the external surface of the waste package adjacent to MCOs.

The maximum dose rate at the external surfaces of the waste package is 75.08 ± 1.78 rem/h. The location of the maximum surface dose rate is a segment of the waste package radial surface adjacent to a DHLW glass canister. The maximum surface dose rate on a segment of the waste package radial surface adjacent to an MCO canister is 30.73 ± 1.02 rem/h. The dose rates on the bottom and top waste package surfaces are about 40 times and 250 times, respectively, lower than the maximum surface dose rate. The neutron dose rates represent less than four percent of the gamma dose rates. Therefore, the gamma dose rates dominate the total dose rates.

9.7 ALUMINUM-BASED FUELS (MELT AND DILUTE)

Dose Rate Calculation for the Codisposal Waste Package of HLW Glass and the Melt-Dilute Al SNF (BSC 2001e) gives the details of the calculations and the results. The geometric representation of the waste package used in MCNP calculations is shown in Figure 9-14. The

waste package contains two different radiation sources, which are volumetric sources uniformly distributed inside the cavity of the DOE SNF canister and the glass volume, respectively. A conservative approach is used, in which lower material densities for the SRS DHLW glass and the MD ingots are employed (see Sections 5.3.8 and 5.3.12).

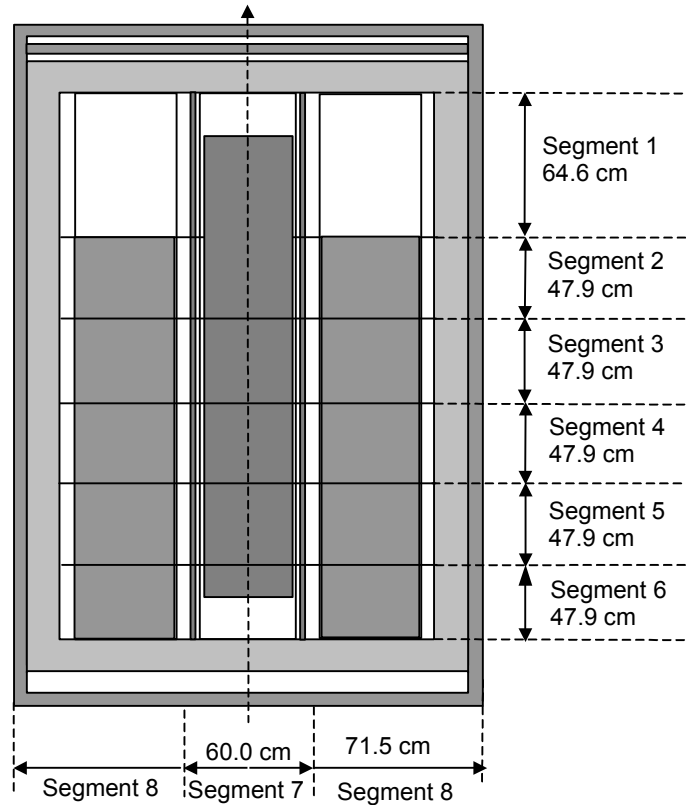


Source: BSC 2001e, Figure 1

Figure 9-14. Vertical and Horizontal Cross-Sections of MCNP Geometry Representation

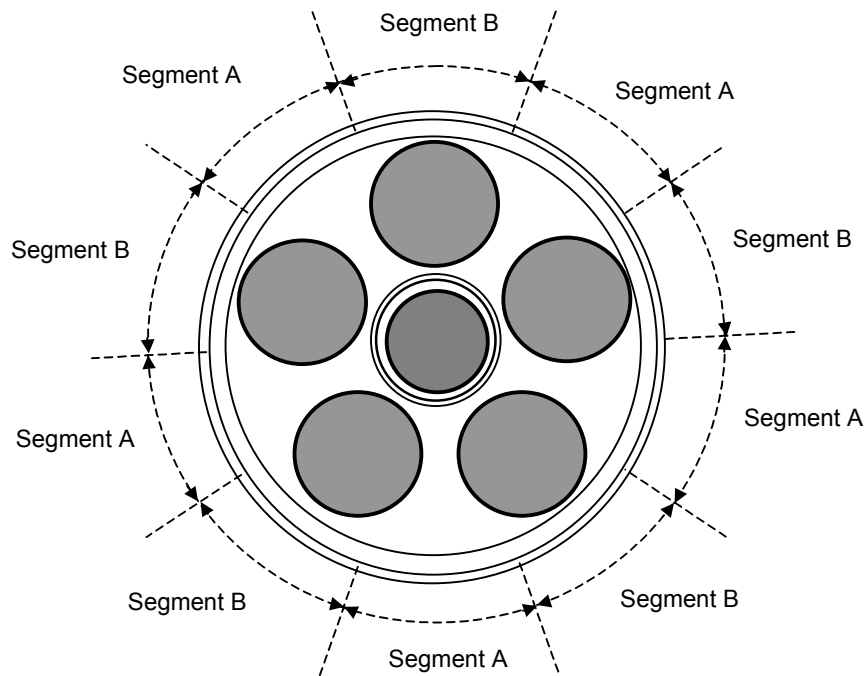
In the calculation, the external surfaces of the waste package are divided in segments and the dose rate is averaged over each segment to evaluate the spatial distribution of the dose rate. Figures 9-15 and 9-16 show the segments of the radial and axial segments used in the dose-rate calculations. The radial surface, between the bottom and top planes of DHLW glass, is equally divided into five segments, each of which is 47.886-cm high. The first radial segment (Segment 1), 64.57-cm high, corresponds to the empty portion of the DHLW canister, which is between the top of the waste package cavity and the top of the DHLW glass. The waste package top and bottom axial surfaces are divided into two radial segments of 0-30 cm (Segment 7) and 30-101.5 cm (Segment 8). For this waste package, the DOE canister is positioned in the center of the waste package and gamma source intensity of the MD ingots is twenty times the gamma source intensity of each individual SRS DHLW glass canister. Because the DHLW glass canisters are positioned near the disposal container, they attenuate the radiation emitted by the

MD SNF and mostly determine the dose rates on the angular segments adjacent to them (Segments B). However, due to their higher source intensity, the MD ingots contribute to the dose rates averaged over Segments A. Therefore, an angular dependence of the waste package radial dose is expected and the radial surface is divided into ten equal angular segments, as shown in Figure 9-16.



Source: BSC 2001e, Figure 2

Figure 9-15. Surfaces and Segments (Axial and Radial) Used for Dose Rate Calculations



Source: BSC 2001e, Figure 3

Figure 9-16. Angular Segments of the Waste Package Outer Radial Surface Used in Dose Rate Calculations

Tables 9-16 and 9-17 are lists of the radial and axial dose rates on the outer surface of the waste package containing the five SRS DHLW glass canisters and the MD DOE SNF canister. The neutron source has an insignificant contribution to the total dose and the gamma dose dominates the total dose.

Table 9-16. Dose Rates Averaged over Axial and Radial Segments of the Waste Package Outer-Radial and Axial Surfaces

Location	Gamma Dose Rate (rem/h)	Neutron Dose Rate (rem/h)	Total Dose Rate (rem/h)
Radial surface: Segment 1	85.47	0.14	85.61
Radial surface: Segment 2	133.53	0.14	133.67
Radial surface: Segment 3	144.49	0.15	144.64
Radial surface: Segment 4	143.34	0.15	143.49
Radial surface: Segment 5	136.42	0.14	136.57
Radial surface: Segment 6	105.20	0.11	105.31
Bottom surface: Segment 7	47.50	0.22	47.71
Bottom surface: Segment 8	13.76	0.08	13.84
Top surface: Segment 7	27.30	0.15	27.45
Top surface: Segment 8	4.82	0.08	4.89

Source: BSC 2001e, Tables 17 and 20

NOTE: The dose rates listed in this table are the upper limits of the 95% confidence intervals of the Monte Carlo dose rate calculations.

The radial surface dose rates have an angular dependence, as shown in Table 9-17. The dose rate averaged over Segment A is approximately twice as much as the dose rate averaged over Segment B.

Table 9-17. Dose Rates Averaged Over Angular Segments of the Waste Package Outer-Radial Surface

Axial Location	Angular Segment A			Angular Segment B		
	Gamma Dose Rate (rem/h)	Neutron Dose Rate (rem/h)	Total Dose Rate (rem/h)	Gamma Dose Rate (rem/h)	Neutron Dose Rate (rem/h)	Total Dose Rate (rem/h)
Segment 1	104.33	0.16	104.49	74.42	0.14	74.56
Segment 2	182.66	0.19	182.85	98.68	0.11	98.79
Segment 3	199.69	0.20	199.89	103.21	0.11	103.32
Segment 4	199.13	0.20	199.33	101.38	0.10	101.48
Segment 5	185.52	0.20	185.72	100.46	0.11	100.57
Segment 6	132.09	0.14	132.23	92.80	0.08	92.88

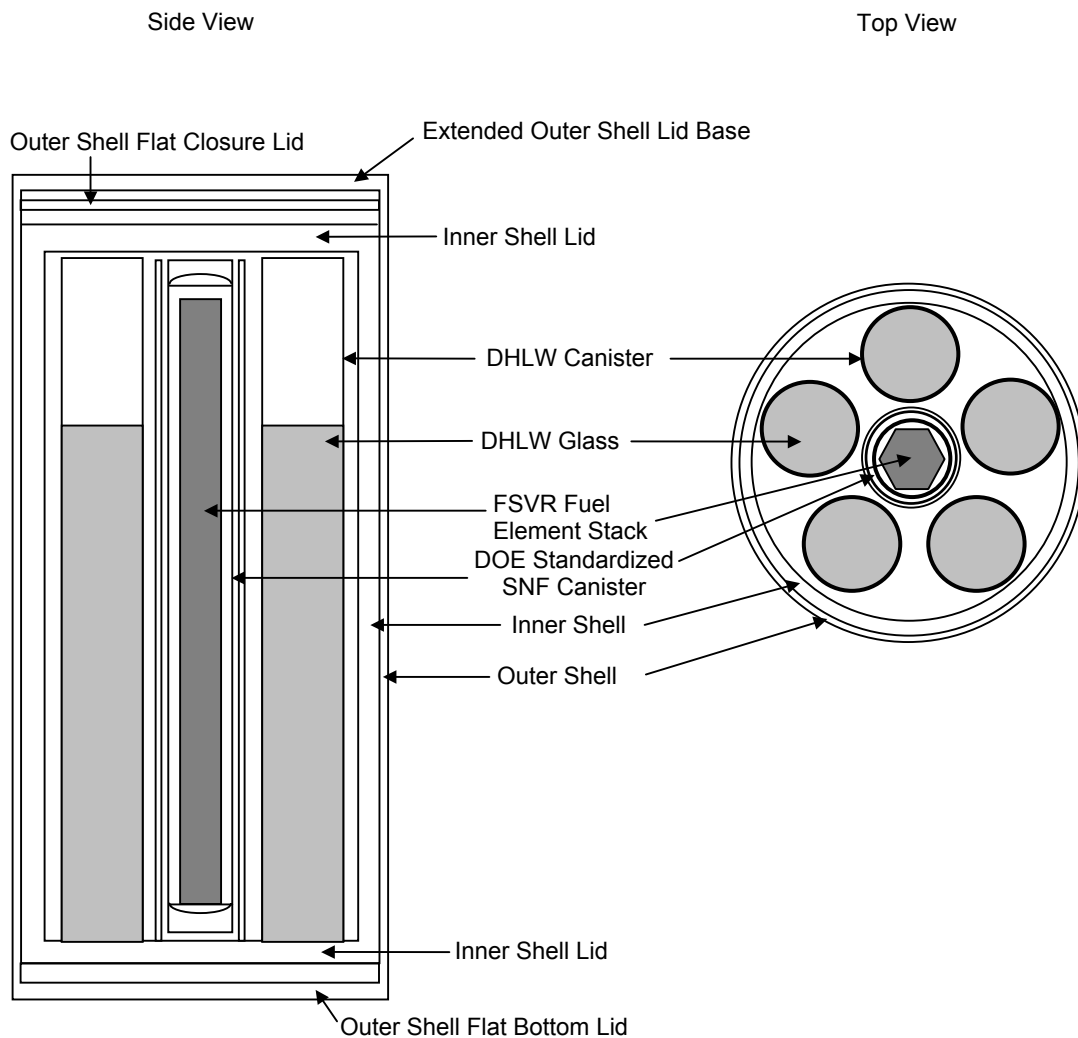
Source: BSC 2001e, Table 21

NOTE: The dose rates listed in this table are the upper limits of the 95% confidence intervals of the Monte Carlo dose rate calculations.

The maximum dose rate at the external surfaces of the waste package occurs on the radial surface and is 199.89 rem/h. The radial dose rate shows an angular distribution, with dose rates on Segments A being approximately twice as much as those on Segments B. The dose rates on the bottom and top surfaces of the waste package are about one-third and about one-fifth, respectively, of the maximum dose rate on the outer radial surface. The dose rates in rem/h and rad/h are practically the same due to the insignificant contribution of the neutron dose rate to the total dose rate.

9.8 FORT SAINT VRAIN

Dose Rate Calculation for the Codisposal Waste Package of HLW Glass and the FSVR Fuel (BSC 2001i) gives the details of the calculations and the results. The geometric representation of the waste package used in the MCNP calculations is shown in Figure 9-17. The waste package contains two different radiation sources (see Section 3.5.8), which are volumetric sources uniformly distributed inside the FSVR element stack and the glass volume, respectively.

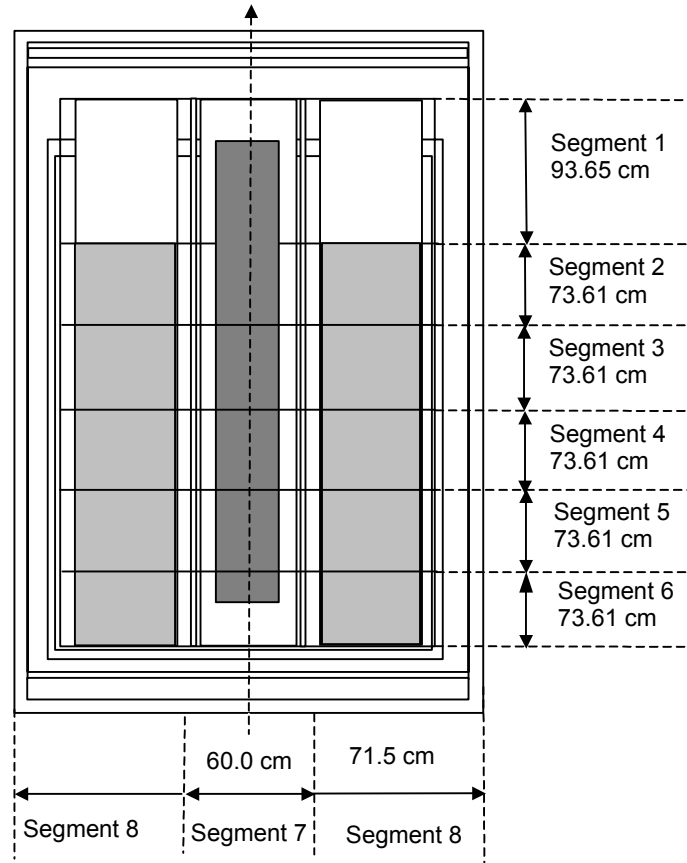


Source: BSC 2001i, Figure 1

Figure 9-17. Vertical and Horizontal Cross-Sections of MCNP Geometry Representation

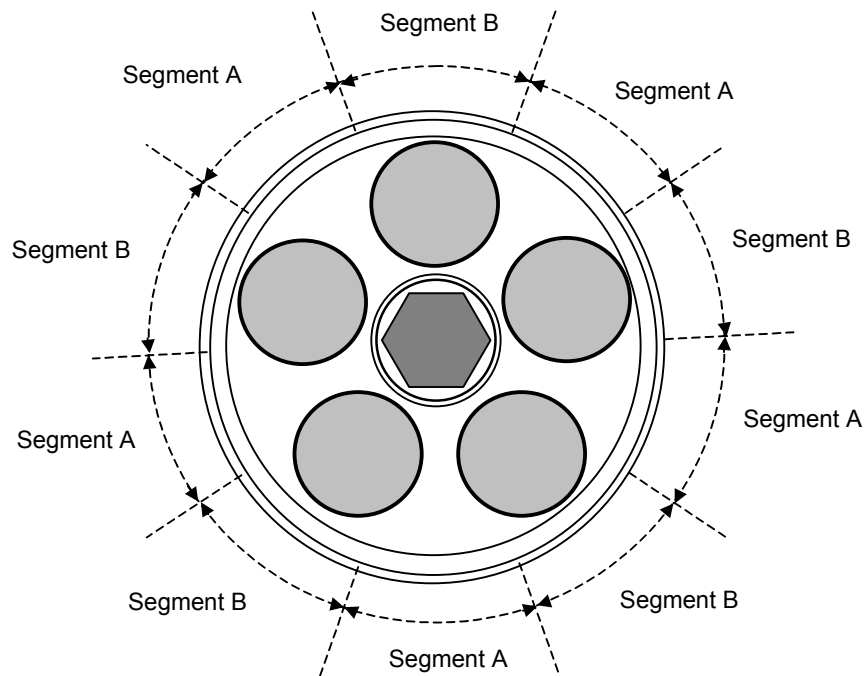
In the calculation, the external surfaces of the waste package are divided into segments and the dose rate is averaged over each segment to evaluate the spatial distribution of the dose rate. Figures 9-18 and 9-19 show the radial and axial segments used in the dose-rate calculations. The radial surface, between the bottom and top planes of DHLW glass, is equally divided into five segments, each of which is 73.61-cm high. The first radial segment (segment 1), 93.65-cm high, corresponds to the empty portion of the DHLW canister, which is between the top of the waste package cavity and the top of the DHLW glass. The waste package top and bottom axial surfaces are divided into two radial segments of 0-30 cm (segment 7) and 30-101.5 cm (segment 8). For this waste package, the DOE canister is positioned in the center of the waste package and the gamma source intensity of the FSVR SNF is approximately half of that of each individual DHLW glass canister. Therefore, it is expected that the gamma radiation generated inside the DHLW glass canisters are the primary contributors to the doses on the axial segments of the waste package external surface between the bottom and top planes of the glass canisters

(segments 2 through 6). To evaluate any angular dependence of the waste package radial dose, the radial surface is divided into ten equal angular segments, as shown in Figure 9-19. The angular segments adjacent to the DHLW glass canister are denoted by “Segment B” and the other segments are denoted as “Segment A” since only statistical variations of the dose rate averaged over each of these two angular segments are expected.



Source: BSC 2001i, Figure 2

Figure 9-18. Surfaces and Segments (Axial and Radial) Used for Dose Rate Calculations



Source: BSC 2001i, Figure 3

Figure 9-19. Angular Segments of the Waste Package Outer Radial Surface Used in Dose Rate Calculations

Tables 9-18 and 9-19 provide the radial and axial dose rates on the outer surface of the waste package containing the five 4.5-m-long DHLW glass canisters and the DOE SNF canister loaded with FSVR SNF. The dose rates listed in both tables are the upper limits of the 95 percent confidence intervals of the Monte Carlo dose rate calculations.

Table 9-18. Dose Rates Averaged over Axial and Radial Segments of the Waste Package Outer-Radial and Axial Surfaces

Location	Gamma Dose Rate (rem/h)	Neutron Dose Rate (rem/h)	Total Dose Rate (rem/h)
Radial surface: Segment 1	20.639	0.029	20.668
Radial surface: Segment 2	88.732	0.081	88.812
Radial surface: Segment 3	94.363	0.095	94.458
Radial surface: Segment 4	95.214	0.096	95.309
Radial surface: Segment 5	94.346	0.095	94.440
Radial surface: Segment 6	84.535	0.083	84.616
Bottom surface: Segment 7	2.841	0.046	2.886
Bottom surface: Segment 8	3.632	0.038	3.670
Top surface: Segment 7	1.071	0.012	1.083
Top surface: Segment 8	0.681	0.012	0.693

Source: BSC 2001i, Tables 19 and 22

Table 9-19. Dose Rates Averaged Over Angular Segments of the Waste Package Outer-Radial Surface

Axial Location	Angular Segment A			Angular Segment B		
	Gamma Dose Rate (rem/h)	Neutron Dose Rate (rem/h)	Total Dose Rate (rem/h)	Gamma Dose Rate (rem/h)	Neutron Dose Rate (rem/h)	Total Dose Rate (rem/h)
Segment 1	23.11	0.03	23.14	20.32	0.03	20.35
Segment 2	88.31	0.08	88.39	96.23	0.08	96.32
Segment 3	93.18	0.10	93.28	100.82	0.10	100.91
Segment 4	94.59	0.10	94.69	101.36	0.10	101.46
Segment 5	93.84	0.10	93.93	101.87	0.10	101.97
Segment 6	80.28	0.09	80.36	93.67	0.09	93.75

Source: BSC 2001i, Table 23

A maximum dose rate of 101.97 rem/h occurs at the external radial surface. Axially over the length of the DHLW glass canisters, the dose rate at the outer waste package radial surface is approximately uniform. The radial dose rate shows a weak angular dependence. Thus, over the length of the glass canisters (segments 2 through 6), the dose rates on segments B are approximately 10 percent higher than those on segments A. For the axial segment corresponding to the empty portion of the glass canister (segment 10), the dose rate on segments A is approximately 15 percent higher than that on segments B. The dose rates on the bottom and top surfaces of the waste package are about 4 percent, and about 1 percent of the maximum dose rate on the outer radial surface, respectively. The dose rates in rem/h and rad/h are basically the same due to the insignificant contribution of the neutron dose rate to the total dose rate (less than 0.2 percent).

10 CRITICALITY ANALYSIS

The criticality analyses performed to date for investigating the nuclear criticality potential of the configurations resulting from the degradation of the waste package containing various DOE-owned SNF have addressed multiple purposes, dictated by the necessities of the particular stage of design development and/or criticality methodology development. A list of the main purposes is as follows:

- The initial purpose in performing the criticality analyses was to evaluate the conceptual design of the waste package containing specific DOE-owned SNF and to identify the items that are important for criticality control.
- The criticality analyses have allowed a screening of the configurations with potential for criticality and calculation of the adequate amount of neutron absorber that need to be placed inside the DOE SNF canister to control the criticality potential.
- Performing criticality analyses on a variety of configurations have provided sufficient information to define the specific range of parameters (ROP) that is required in assessing the validity of the criticality model. The comparison between the ROP and the range of applicability (ROA) of the criticality benchmark experiments is the basic step in defining the applicability of the critical limits calculated using the current validation methodology.

As discussed in Section 6.5, the general methodology approach for assessing the postclosure criticality potential is detailed in *Disposal Criticality Analysis Methodology Topical Report* (YMP 2003). The base tool for performing the criticality analysis is the criticality model (BSC 2003e) that comprises the Monte Carlo computer code MCNP coupled with appropriately selected neutron cross-section libraries. The criticality model is used to estimate the effective neutron-multiplication factor (k_{eff}) of the various configurations of the waste package.

In order to address the multiple purposes presented above, the criticality analyses were performed following a more comprehensive approach than that discussed in *Disposal Criticality Analysis Methodology Topical Report* (YMP 2003). Typically, the analysis was performed for all configurations classes that were anticipated in the degradation analysis of the waste package, regardless of their probability of occurrence. The analysis was deterministic in nature and did not use a probability screening criterion for selecting the configurations to be further investigated with the criticality model. The process made use of an interim critical limit conservatively defined based on a limited number of criticality benchmark experiments. The selection of the interim critical limit was later verified using the validation methodology described in *Disposal Criticality Analysis Methodology Topical Report* (YMP 2003), including the comparison between the ROP of the configurations with the ROA of the criticality benchmark experiments.

This section is structured to present the results obtained to date for each DOE SNF group focusing on the purposes mentioned above. The scope is limited to eight DOE-owned SNF groups that have been analyzed. The general assumptions used in modeling the intact and degraded configurations of the waste package are listed and discussed in Section 5.4. For each DOE SNF group a detailed summary of the criticality analyses performed is given, starting with

the description of the investigated configuration classes and their refinements, the results of the degradation analyses used to support the criticality calculations and the results of the criticality screening calculations performed with the criticality model. The results cover the full range of configurations possible for repository postclosure, which extend well beyond the regulatory period of 10,000 years. Finally, the significant results obtained during the process of validation of the criticality model for each DOE SNF group are presented.

10.1 FFTF SNF WASTE PACKAGE

The description and main characteristics of the waste package containing FFTF SNF are presented in Section 3.2.1. In this section a summary of the results of criticality analyses performed to date is presented together with the current status of the validation of the criticality model for the configurations that are specific to the codisposal of this fuel group.

The first step in applying the criticality model to the intact and degraded configurations of this waste package is identification and characterization of the specific configurations anticipated for postclosure of the repository. The results of the degradation analysis coupled with the geochemistry calculations (CRWMS M&O 1999a, Section 6) provided an insight into the possible arrangements and compositions of the degraded materials placed within the waste package.

The initial analyses on FFTF SNF codisposal conceptual design have been performed almost simultaneously with the development of the postclosure degradation and criticality methodology. This situation has generated a more specific path followed during the analyses in comparison with all the other DOE-owned SNF groups presented in this document. The differences are related to the lack of an established methodology for the initial degradation analysis that resulted in a large number of postulated degraded configurations that were investigated.

Another particularity is the fact that after the results of the criticality analyses have been summarized in the technical report (CRWMS M&O 1999a) it was discovered that additional information that was not available initially could affect some of the conclusions of the criticality analysis. This information was related to the possible loading of the Ident-69 containers with more reactive experimental fuel pins (INEEL 2002). The criticality analyses have been repeated using the new information but only for the configurations that have been identified as limiting (most reactive) from the initial criticality analyses. The new analyses also incorporated the subsequent changes due to evolution of the initial conceptual design of the waste package (from Viability Assessment to Site Recommendation design) and made use of the updated results of new degradation analyses (BSC 2001j). The results of this new set of criticality analyses have been included in a separate calculation (BSC 2002b). The major finding was that a higher amount of neutron absorber (gadolinium phosphate) must be initially loaded in the DOE canister in order to minimize the potential for criticality during postclosure phase of the repository for the waste packages that contain an Ident-69 container.

Beside the results of the above mentioned criticality calculation for the most reactive cases, this section will also summarize the results of the initial criticality evaluations that are not affected by the additional information. There is still a need to verify the conservatism of the remaining

initial calculations using the increased amount of neutron absorber, but it is expected that the results will be bounded by the cases summarized in this report.

The results of the three-dimensional Monte Carlo criticality calculations for the intact configurations of the waste package containing six DFAs show that the requirement of $k_{\text{eff}}+2\sigma$ less than or equal to the interim critical limit of 0.93 (CRWMS M&O 1999a, Section 7.3.4) is satisfied for the FFTF waste package without any added neutron absorber.

The results from the recent criticality analysis (BSC 2002b) on the most reactive degraded configurations containing an Ident-69 container in the central position show that the criteria of $k_{\text{eff}}+2\sigma$ less than or equal to the interim critical limit of 0.93 is satisfied with the following restrictions: a) at least 9.29 kg of Gd must be distributed on (e.g., flame deposit) or in the material used to fabricate the DOE SNF canister basket; b) an additional amount of 30.8 kg of Gd (49.3 kg of GdPO_4) must be uniformly distributed in the initial void spaces of the DOE SNF canister outside the Ident-69 container; b) one of the basket positions must be blocked so only four DFAs can be disposed of with this design. The calculations have also considered the decay effects of Pu isotopes and their influence on the reactivity of the system. All analyses were based on the fuel pins types that have the highest plutonium enrichment (enriched in Pu-239) and the highest plutonium loading.

It is expected that all other intact and degraded configurations of the waste package containing an Ident-69 container and loaded using the above restrictions will be bounded by the results obtained for the most reactive configuration.

The following sections summarize the relevant stages and results of the degradation and criticality analysis, starting with the degradation scenarios and ending with the validation of the criticality model. Only the ROP that characterizes the most reactive cases is used in the process of validation of the criticality model. The process includes selection of appropriate critical benchmark experiments and derivation of specific lower bound tolerance limit for each major group of configuration classes.

10.1.1 Degradation Scenarios and Configurations

The degradation analysis summarized in *Evaluation of Codisposal Viability for MOX (FFTF) DOE-Owned Fuel* (CRWMS M&O 1999a, Section 6.2.1) discusses only the correspondence between the general degradation scenarios from Section 3 of *Disposal Criticality Analysis Methodology Topical Report* (YMP 2003) and the possible arrangements in the waste package containing FFTF SNF. This resulted in an exhaustive set of degraded configurations that have been analyzed in three different preliminary criticality calculations (CRWMS M&O 1999q; CRWMS M&O 1999r; CRWMS M&O 1999s).

The configurations investigated can be categorized using the description of the generic configuration classes given in Section 3.3.1 of *Disposal Criticality Analysis Methodology Topical Report* (YMP 2003). As indicated in Section 6.5 for the purpose of fully identifying the potential for criticality, all representative configurations classes have been analyzed in the preliminary analyses. The configurations are briefly described in the following with headings

that follow the description given in Section 6.2.1 of *Evaluation of Codisposal Viability for MOX (FFTF) DOE-Owned Fuel* (CRWMS M&O 1999a).

Degraded FFTF SNF Assemblies with Intact DOE SNF Canister—For these cases of degraded fuel assemblies within the DOE SNF canister (intact basket), the scenarios and configuration classes are applied to the DOE SNF canister and its contents. Since the SNF degrades before the basket in these configurations, this is an example of standard scenario IP-1. The resultant configurations correspond to refinements of configuration class 6. The varying levels of degradation of DFAs are given by the following sequence:

1. Degradation of fuel pin clips and spacers
2. Partial and complete degradation of fuel cladding
3. Degradation of assembly duct along with fuel pin clips and spacers
4. Complete degradation of the assembly resulting in pellets stacked randomly in each basket location.

The results of the initial criticality analysis for these configurations were summarized in *Evaluation of Codisposal Viability for MOX (FFTF) DOE-Owned Fuel* (CRWMS M&O 1999a, Sections 7.4.1 and 7.4.2). The current report describes only the criticality results for six intact DFAs disposed in the DOE SNF canister. The results for the configurations containing an Ident-69 container are not conservative in their entirety. The cases with the most reactive configurations have been recently redone (BSC 2002b) using the newly identified most reactive Ident-69 container and using the final amount recommended for the neutron absorber distributed in the DOE SNF canister.

Degraded Basket in DOE SNF Canister and Intact SNF Assemblies—The basket is more than three times as thick as the FFTF assembly duct, thus it is virtually impossible for it to completely degrade before the FFTF assembly duct and therefore the configurations are very unlikely. This configuration is a variation of configuration class 1 and can be reached from standard scenario IP-3. The refinements of this configuration are characterized by the varying levels of degradation of the DFAs and are given in the following sequence (CRWMS M&O 1999a, Sections 7.4.3 to 7.4.6):

1. All DFAs and Ident-69 pin container (if present) are intact.
2. All DFAs are degraded resulting in intact fuel pins stacked inside the DOE SNF canister round an intact Ident-69 pin container.
3. Intact Ident-69 surrounded by a homogeneous mixture resulting from complete degradation of all DFAs and the basket.
4. Degraded Ident-69 mixed with homogeneous mixture resulting from complete degradation of all DFAs and the basket.
5. A homogeneous mixture resulting from complete degradation of six DFAs (the nominal five, plus one replacing the Ident-69).

Although these configurations are all very unlikely, they were considered in the initial analysis for reasons of completeness and conservatism. A more likely set of configurations with some basket degradation would contain some partly degraded basket plates between the remaining assemblies or rods that fall to the bottom of the DOE SNF canister. Such a configuration could arise because of the collapse of the basket structure.

A variation of the configuration with an intact Ident-69 container (having the rest of the components inside and outside DOE SNF canister degraded) has been identified in the initial set of analyses (CRWMS M&O 1999a, Section 7.4.7) as being the limiting case driving the design/loading solution. This configuration was used to investigate the system after identification of additional information regarding the Ident-69 container content. The most reactive container was subsequently used in evaluating the new/design/loading solution (BSC 2002b) and the results are summarized in this report.

Degraded DOE SNF Canister Contents and Degraded DHLW and Other Waste Package Components—In this case, the concepts of scenario and configuration are applied to the entire waste package. These configurations have an intact DOE SNF canister shell surrounded by clay formed by degraded DHLW and waste package basket. All DOE SNF canister internals, such as the basket, DFAs, and the Ident-69, if present, are degraded to form a homogeneous mixture. These configurations are a refinement of configuration class 2 and can be reached from any of the standard scenarios IP-1 to IP-3 (CRWMS M&O 1999a, Section 7.4.8).

Completely Degraded DOE SNF Canister Above Clay from DHLW and Waste Package Internals—In this case, the concepts of scenario and configuration are also applied to the entire waste package. These configurations represent the DOE SNF canister as completely degraded and forming a layer above the clay that results from complete degradation of waste package basket and DHLW glass canisters. Various combinations of the fuel and clay layers were investigated (CRWMS M&O 1999a, Section 7.5.1). This configuration is also a variation of configuration class 2.

Clay from DHLW and Waste Package Internals Above Completely Degraded DOE SNF Canister—This case also applies the concepts of scenario and configuration to the entire waste package. These configurations have the clay from the degradation of the waste package basket and DHLW glass canisters above the completely degraded DOE SNF canister (CRWMS M&O 1999a, Section 7.5.2). This configuration is a refinement of configuration class 2 and can be reached from scenarios IP-1 or IP-2.

10.1.2 Criticality Calculations and Results

10.1.2.1 Results for Intact Mode

This section presents the results of the intact-mode criticality analysis only for the configurations containing six DFAs inside the DOE SNF canister. As mentioned above in the beginning of Section 10, the calculations for the most reactive configurations containing an Ident-69 container in the center position need to be reevaluated due to the identification of a more reactive arrangement of experimental fuel pins within the container.

Although the components (fuel pins, cladding, supporting clips, and canisters) are considered structurally intact, water intrusion into the components is assumed in order to determine the highest k_{eff} resulting from optimum moderation. The contents of the waste package outside the DOE SNF canister are considered intact in all cases considered in this section.

For the intact mode, the contents of the DOE SNF canister are in an “as-welded/loaded position and condition,” as depicted in Figure 10-1 with a typical arrangement of six DFAs. No Gd neutron absorber was considered in analyzing these configurations.

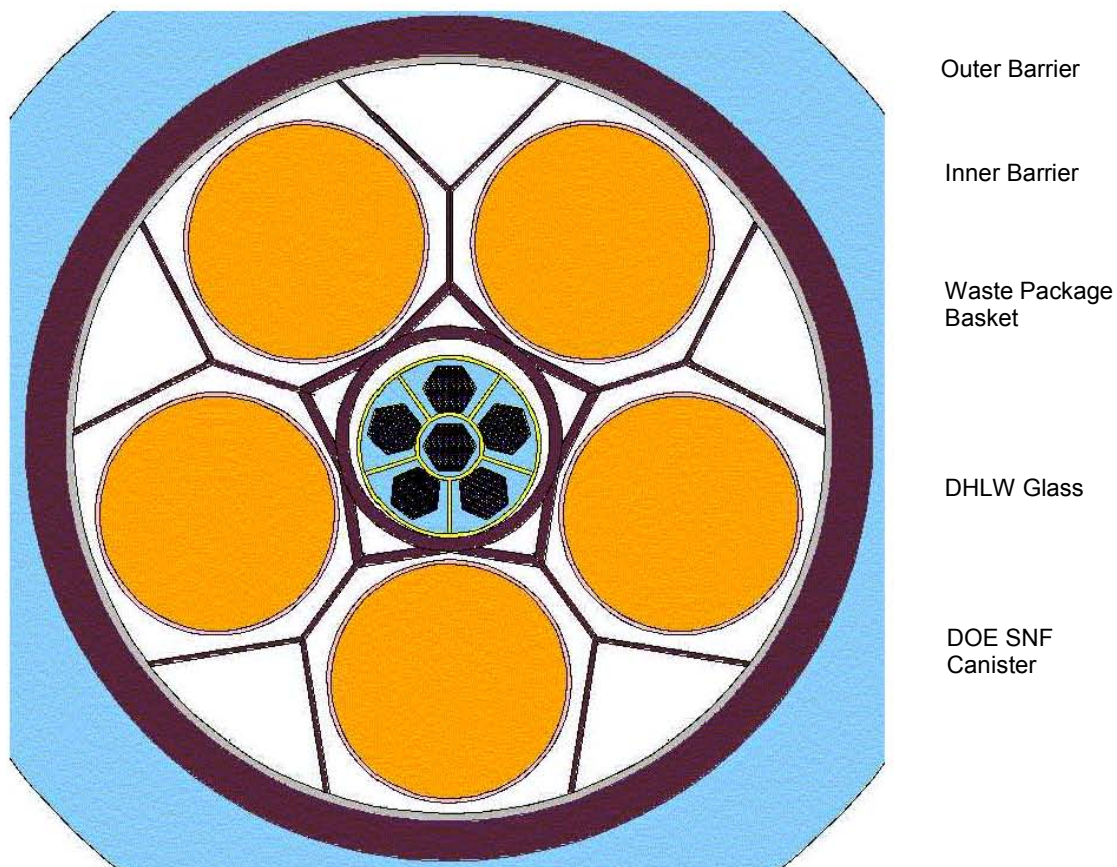


Figure 10-1. Cross-Section View of the 5-HLW/DOE SNF-Long Waste Package (Viability Assessment Design) with Six DFAs

Several comparison calculations were performed to determine the type of fuel elements that results in the highest k_{eff} . Types 3.2 and 4.1 DFAs were compared because they contain the lowest and the highest fissile loading of the four DFA types, respectively. The results show that the Type 4.1 DFAs are more reactive and result in approximately 4 percent higher k_{eff} than the Type 3.2 DFAs (CRWMS M&O 1999q, p. 19). Therefore, Type 4.1 DFAs were used for the remainder of the criticality analyses.

Water intrusion into the fuel pins was also investigated. Based on the calculation results, it was concluded that water intrusion into the fuel pins causes a 2 percent increase in k_{eff} (CRWMS M&O 1999q, Table 6-13). Therefore, all fuel pins were further modeled with water occupying all void spaces inside the fuel pins.

Cases were investigated where the DOE SNF canister is either centered in the waste package or offset from the center to account for settling due to gravity. This change in canister position has no effect on the k_{eff} of the system (results are within 1σ). Also varying levels of flooding and different spacings (between assemblies in outer basket positions or another assembly occupying the inner basket position) were investigated. In all cases, even though the environment outside the waste package, whether tuff, water, or a mixture, has no significant impact on the configuration k_{eff} , the waste package is water reflected. The amount of outgoing neutrons penetrating the waste package barriers is less than 1 percent of the total number of neutrons in the system; and typically less than 0.2 percent based on the evaluation of the neutron activity reported in the outputs. When the factor of four attenuation through the waste package barriers is factored in, even mirror reflection of these neutrons would have no statistically significant effect. Hence, having a different reflector (e.g., tuff, rock, clay, etc.) on the outside of the waste package would have negligible or no effect on the results of the intact configurations.

The maximum $k_{\text{eff}} + 2\sigma$ for intact configurations with six DFAs is 0.9081 (CRWMS M&O 1999r, Table 6-21). This k_{eff} is obtained when fuel pins, fuel assemblies, and the DOE SNF canister are flooded and the plutonium isotopes are decayed for 48,200 years, which corresponds to two half-lives of Pu-239 isotope. The analysis of the results indicates that for the intact criticality configurations the k_{eff} increases by as much as 5 percent after approximately 48,200 years of plutonium decay. No Gd was required for this configuration.

The results for all intact configurations containing an Ident-69 container from Sections 7.3.2, 7.3.3, and 7.3.4 of *Evaluation of Codisposal Viability for MOX (FFTF) DOE-Owned Fuel* (CRWMS M&O 1999a) have not been summarized here because they do not include the latest information on the Ident-69 container content.

10.1.2.2 Results for Configurations with Intact DFAs and Degraded Basket in DOE SNF Canister

The cases where the basket is fully degraded with all other fuel components intact were analyzed. These configurations (belonging to configuration class 1) are not considered credible, as the basket structure is approximately three times thicker than the assembly ducts and the Ident-69 container. Therefore the DFA ducts will degrade before the basket structure. These cases are presented to provide insight into specific contributions to the overall reactivity of the system. In these configurations, the DFAs (including the center DFA) are at the bottom of the DOE SNF canister and the degradation products, with varying water volume fractions, are settled around the fuel components. All analyzed cases that contain an intact Ident-69 container that were summarized in *Evaluation of Codisposal Viability for MOX (FFTF) DOE-Owned Fuel* (CRWMS M&O 1999a, Section 7.4.3) are not reported here due to the incomplete information on the loading of the Ident-69 at the time the analysis was performed. Only the results for the cases with six DFAs loaded in the DOE SNF canister are presented. The results (CRWMS M&O 1999r, Table 6-7) show that the $k_{\text{eff}} + 2\sigma$ for the system with six DFAs and only 7.62 kg of Gd present in the DOE SNF canister is below the critical limit of 0.93 ($k_{\text{eff}} + 2\sigma = 0.9205$).

Another set of configurations, that assumed the gradual degradation of the DFAs before the basket structure, have been investigated and summarized in *Evaluation of Codisposal Viability*

for MOX (FFTF) DOE-Owned Fuel (CRWMS M&O 1999a, Sections 7.4.1, 7.4.2, 7.4.4, and 7.4.5). The results for these degraded configurations containing an Ident-69 container are not presented in this report because they have not used the most recent information on the Ident-69 container content, being less conservative. It is expected that the final amount of neutron absorber recommended (see Section 10.3.1.6) will keep the $k_{\text{eff}} + 2\sigma$ below the interim critical limit of 0.93.

10.1.2.3 Results for Degraded Configurations Postulated Beyond the Regulatory Period

The degradation and criticality analyses performed have also investigated configurations that require very long times to be attained. These configurations are anticipated to happen well beyond the regulatory period of 10,000 years but they have been analyzed for completeness. For the purpose of this document, these results (CRWMS M&O 1999a, Sections 7.4.6, 7.4.7, 7.4.8, 7.5.1, and 7.5.2) have been summarized and grouped together in this section. The results of Section 7.4.7 of *Evaluation of Codisposal Viability for MOX (FFTF) DOE-Owned Fuel* (CRWMS M&O 1999a) containing the limiting case driving the design/loading solution have been reevaluated using new information on Ident-69 container loading (BSC 2002b).

DOE SNF Canister Containing Degraded Fuel (Ident-69 Container Nondegraded) with Waste Package Contents Degraded—The most reactive degraded configuration (limiting case) for the waste package design containing FFTF SNF described in Section 7.4.7 of *Evaluation of Codisposal Viability for MOX (FFTF) DOE-Owned Fuel* (CRWMS M&O 1999a) has been revisited in order to evaluate the impact of the loading information that was not available during the original analysis. The configuration (Figure 10-2) comprises an intact Ident-69 container surrounded by degraded material resulted from the degradation of four DFAs containing Type 4.1 fuel pins and the supporting basket structure inside the DOE SNF canister. The fissile material is contained inside the DOE SNF canister by its stainless steel shell that is not completely degraded. The remaining space of the waste package is filled by water mixed with a clayey material surrounding the DOE SNF canister. The clayey material (clay) results from the degradation of the DHLW glass canisters and supporting structures, and its composition was calculated by revised criticality calculations using Site Recommendation design for the waste package and updated degradation rates (BSC 2002b). The configuration can be categorized as belonging to configuration class 6.

The new information given in the revision of *FFTF (MOX) Fuel Characteristics for Disposal Criticality Analysis* (INEEL 2002) provides the exact fissile content in each Ident-69 container. This information was sufficient to support a new criticality analysis of the possible arrangements of the fuel pins inside the Ident-69 container using a consistent approach in identifying the most reactive inner arrangement. As a first stage of the new criticality calculation a comprehensive parametric analysis of the Ident-69 internal arrangements has been performed. In a second stage, the waste package degraded configuration that produced the highest k_{eff} in previous analyses was investigated using the most reactive arrangements of the fuel pins inside the Ident-69 container.

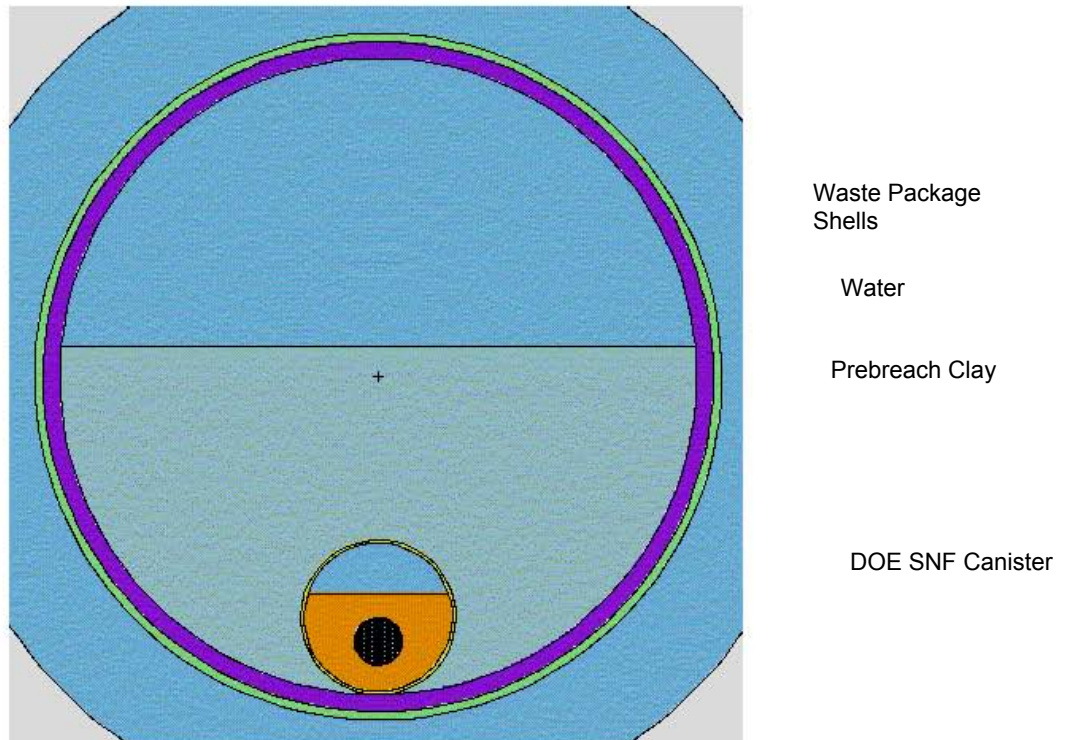


Figure 10-2. Cross-Section View of the Degraded Configuration of the Waste Package with an Intact Ident-69 Container

The results presented in *Criticality Calculation for the Most Reactive Degraded Configurations of the FFTF SNF Codisposal WP Containing an Intact Ident-69 Container* (BSC 2002b, Sections 6.1, 6.2.1, and 6.2.2) show that the previous calculations on the most degraded configuration for the FFTF SNF waste package have not identified the full spectrum of possible values for the k_{eff} . Utilization of the new information regarding the actual content of the Ident-69 containers demonstrates that the higher diameter experimental MOX fuel pins placed inside the Ident-69 container results in the highest values of the k_{eff} for the given configuration. The most important findings of the new criticality analysis can be summarized as follows (BSC 2002b, p. 40):

- The reactivity of the Ident-69 container increases with the pitch for a given number of fuel pins (the system is always undermoderated) and with the enrichment of the fuel. The Ident-69 containers loaded with experimental MOX fuel pins are the most reactive. The arrays of saturated fuel pins (water filling all void spaces inside a fuel pin) are more reactive than the arrays with dry fuel pins.
- The envelope of the maximum k_{eff} values for the investigated configuration shows a broad maximum for various combinations of number of pins/lattice pitch. Differences in results between hexagonal lattice arrays and square lattice arrays are small for the spectrum of combinations investigated, requiring a final analysis considering each type of lattice.
- Among the 3 decay times analyzed (0, 24,100 and 48,200 years), the decay of Pu isotopes produces the highest k_{eff} values at a decay time of 24,100 years.

- The maximum values of $k_{\text{eff}}+2\sigma$ for the most reactive configuration using the previous recommended amount of neutron absorber (2.75 wt% Gd in the initial basket structure) are well above the interim critical limit of 0.93). Adding at least 30.8 kg of Gd (49.3 kg GdPO_4) uniformly distributed in the initial void spaces outside the Ident-69 container and the 4 DFAs results in lowering the $k_{\text{eff}}+2\sigma$ of the most reactive degraded configuration identified to 0.9098. Using a filler to homogeneously distribute the absorber can further reduce the reactivity of the system.

DOE SNF Canister with Completely Degraded Inner Basket and SNF—Configurations with a fully degraded Ident-69 container that holds various numbers of fuel pins (maximum 217 fuel pins) and five degraded DFAs were analyzed. The degraded Ident-69 pin container with 217 fuel pins is equivalent to a degraded DFA; therefore, this configuration (belonging to configuration class 1) also bounds the configurations with the DOE SNF canister containing six completely degraded DFAs. Since the Ident-69 container is completely degraded and was assumed to contain the maximum loading of fissile material, the new information regarding details of possible arrangements inside the container are not relevant for these cases, so the original calculations summarized in Section 7.4.6 of *Evaluation of Codisposal Viability for MOX (FFTF) DOE-Owned Fuel* (CRWMS M&O 1999a) are conservative. This rationale is applicable to all following configurations that include a DOE SNF canister with the content fully degraded.

The criticality results are for configuration that assumed a 0.9144 m (3 ft) fuel slurry and a basket that contains only 7.62 kg Gd. The space not occupied by fuel slurry or goethite in the DOE SNF canister is filled with water at 1 g/cm³ density. The goethite volume in the fuel sludge was varied from 60 percent to a low of 45.71 percent corresponding to a volume that radially fills the DOE SNF canister for a 0.9144 m (3 ft) length. Vacant space in the waste package is treated as a void. The waste package is fully reflected by water. The results show that the highest $k_{\text{eff}} + 2\sigma$ is 0.920 with 217 fuel pins in the Ident-69 pin container, 45.71 percent goethite volume fraction, and 7.62 kg Gd in the DOE SNF canister basket (CRWMS M&O 1999r, Section 6.1.10.2).

DOE SNF Canister with Degraded FFTF Fuel Surrounded by Degraded Waste Package Contents—The results for the configurations of the waste package with degraded DHLW canisters and degraded SNF are summarized in Section 7.4.8 of *Evaluation of Codisposal Viability for MOX (FFTF) DOE-Owned Fuel* (CRWMS M&O 1999a). This set of configurations is a refinement of the general configuration class 2. The DOE SNF canister shell is represented as being intact, and confines the degraded FFTF SNF. The DOE SNF canister contents are completely homogenized and distributed inside the DOE SNF canister. This is different from the previous configurations in that the fuel length is not preserved during homogenization. Instead, the degraded FFTF fuel (equivalent fissile amount of six DFAs, which is the maximum amount in an FFTF DOE SNF canister) is distributed into the homogenized mixture axially and radially.

The effect of the position of the DOE SNF canister was investigated by placing the DOE SNF canister either in the middle or on the bottom of the waste package. The amount of water in the clay, the amount of water in the fuel, the minimum amount of absorber required, and flooding in the DOE SNF canister are among the parameters that were varied.

In investigating the intact DOE SNF canister shell with the degraded FFTF fuel settled at the bottom of the flooded canister, the percentage of water in the clay (along with the volume of clay) is increased. The position of the DOE SNF canister in the waste package was also varied. The results show that the $k_{\text{eff}} + 2\sigma$ is less than 0.3 for all cases (CRWMS M&O 1999s, Section 6.1), and the position of the DOE SNF canister in the waste package has no effect on criticality. The amount of Gd considered present in the DOE SNF canister was 7.73 kg.

The next configuration investigated is an intact DOE SNF canister shell having degraded FFTF fuel located in the center of the waste package, with the FFTF fuel mixed with different amounts of water. The k_{eff} of a degraded waste package as a function of the amount of water in the hematite is investigated. In all of these cases, the clay is not diluted. Results of the variations show that the $k_{\text{eff}} + 2\sigma$ is less than 0.6 for all cases (CRWMS M&O 1999s, Section 6.1). In this configuration, the optimal moderation of the waste package is achieved when the fuel contains 50-65 percent by volume water. The amount of Gd considered present in the DOE SNF canister was also 7.73 kg.

If some of the main absorbers (Gd and Fe_2O_3) are lost, the k_{eff} of the waste package will increase. In the configurations investigated, some of the principal absorbers have been intentionally removed. With all of the hematite remaining in the waste package, the minimal mass of Gd needed in the DOE SNF canister to meet the interim critical limit in such a configuration is 0.387 kg (CRWMS M&O 1999s, Section 6.1). This configuration results in a $k_{\text{eff}} + 2\sigma$ of 0.9217. In the absence of hematite, 7.7 kg Gd is required to be distributed in the DOE SNF canister. This configuration results in a $k_{\text{eff}} + 2\sigma$ of 0.6288 at time zero, which corresponds to the time of disposal (CRWMS M&O 1999s, Tables 6.1-3 and 6.4-1). Geochemistry results indicate that maximum Gd loss is less than 10.4 percent in 100,000 years. Therefore, this configuration is not a concern for criticality.

Completely Degraded DOE SNF Canister Above Settled Clay in Waste Package—The configurations investigated assumed that the DHLW degrades and settles before the DOE SNF canister. The degraded DHLW forms a clay material that is collected at the bottom of the waste package, and the degraded FFTF SNF deposits in a layer at the top of the clay material. The analysis investigated the k_{eff} of the waste package for different degrees of hydration of both the FFTF SNF and the DHLW clay layers (CRWMS M&O 1999s, Section 6.2). Since all configurations consider completely degraded fuel, the worst-case is achieved with the maximum amount of fissile elements in the DOE SNF canister. This is obtained by assuming that all basket locations are initially filled with a DFA (a total of six DFAs). These configurations correspond to the configuration class 2.

In analyzing the configurations, parametric studies have been performed to determine the optimum moderation and configuration. These parametrics included varying the amount of water in the clay and fuel layers, varying the density of water in the clay and fuel layers, varying the amount of absorbers, and varying the amount of clay mixed with the fuel layer. The bounding results are not dependent on the retention of the clay in the waste package, since the iron oxides-fuel mixture with no clay is included. The plutonium decay effects due to long times considered in performing the criticality calculations were also determined.

The results show that the $k_{\text{eff}} + 2\sigma$ of the configurations investigated are all below 0.5 with 7.62 kg Gd. When Gd is present, the k_{eff} of the system decreases as plutonium isotopes decay. In these configurations, even if all the Gd is driven out of the waste package, the $k_{\text{eff}} + 2\sigma$ of the system is still below the interim critical limit of 0.93 with a maximum of 0.9025 after 24,100 years of plutonium radioactive decay.

Completely Degraded DOE SNF Canister at the Bottom of Settled Clay in the Waste Package—This set of configurations assumed that the DOE SNF canister sinks to the bottom of the degraded DHLW clay during the degradation process. As the DOE SNF canister degrades, some of the DHLW clay and the FFTF SNF will mix. The water fractions in the bottom layer and in the clay material are represented as being the same (CRWMS M&O 1999s, Section 6.3). These configurations are representing refinements of the configuration class 2. The results indicate that the highest k_{eff} is achieved if the fuel and clay layers do not mix. Even without any credit for Gd or iron oxide, the maximum $k_{\text{eff}} + 2\sigma$ of the system is 0.9145 after 24,100 years of plutonium decay.

The results from considering the effect of Pu decay indicate that for homogenous layers of fuel and clay, if Gd is present in the waste package, the k_{eff} is maximized at time zero and decreases in time. When Gd is present, the thermal neutrons are absorbed by Gd rather than by ^{240}Pu . Therefore, ^{240}Pu decay has no significant effect on k_{eff} . However, as ^{239}Pu decays to ^{235}U , the k_{eff} decreases. If the Gd is not present, the decay of ^{240}Pu reduces the overall neutron absorption (^{240}Pu is a much stronger absorber than ^{236}U). As a consequence, the k_{eff} peaks at approximately 24,100 years. At that time, approximately 92 percent of the ^{240}Pu has decayed to ^{236}U and only 50 percent of the ^{239}Pu has decayed to ^{235}U . As more ^{239}Pu decays to ^{235}U , k_{eff} decreases.

10.1.3 ROP for Configurations of Waste Package Containing FFTF SNF

ANSI/ANS-8.1-1998 and *Disposal Criticality Analysis Methodology Topical Report* (YMP 2003) provide basic requirements for validation of a calculational method used in the criticality analysis of a system. The bias of a code system (in this case the criticality model containing the Monte Carlo computer code MCNP, and selected cross-section libraries) is determined by correlating the results of critical and near-critical experiments with calculated results for those experiments. The common practice, and that considered by the current validation methodology (BSC 2003e), is for comparison of the calculated k_{eff} to a critical or near critical system.

Prior to the initiation of the validation activity, the operating conditions and parameters for which the validation is to apply must be identified. The fissile isotope, enrichment of fissile isotope, fuel density, chemical form of fuel, types of neutron moderators and reflectors, range of moderator to fissile isotope ratio, neutron absorbers and physical configurations are among the parameters to specify. These parameters will define the area of applicability for the selection of the critical experiments for the validation effort.

The preliminary degradation analyses of the contents of the waste package containing FFTF SNF (CRWMS M&O 1999a) and the subsequent criticality analysis performed for the resulting internal configurations have followed the guidance suggested by the Internal Criticality Master Scenarios presented in *Disposal Criticality Analysis Methodology Topical Report* (YMP 2003,

Section 3.3). The resultant configuration classes internal to the waste package have been screened systematically for their criticality potential in comprehensive criticality analyses. The main results and their applicability have been summarized in the above sections.

For the purpose of the criticality model validation and identification of the ROP that characterize representative internal configurations of the degraded waste package, only the degraded configurations investigated in the latest criticality analysis (BSC 2002b) (most reactive configurations) have been used. The limiting case configurations comprise an intact Ident-69 container containing experimental MOX SNF surrounded by degraded material resulting from the degradation of the 4 DFAs containing Type 4.1 fuel pins. The fissile material is contained inside the DOE SNF canister by its stainless steel shell. This configuration can be categorized as belonging to the general configuration class 6. The remaining space of the waste package is filled by water mixed with a clayey material surrounding the DOE SNF canister. The clayey material results from the degradation of the DHLW glass canisters and supporting structures. The other degraded configurations investigated in the criticality analyses (homogeneous mixtures) have not yet been included in the validation process.

The most reactive configurations described above are very complex with respect to the characteristics of interest in criticality analysis, being a combination of heterogeneous and homogeneous regions. Selected cases (the most reactive or the limiting cases as presented in BSC 2002b and in Section 10.1.2 above) have been rerun with tallies calculating the neutron flux and the fission rate in the regions containing the fissile material. The results of the cases that were rerun with tallies are summarized in Attachment VII of *Criticality Model Report* (BSC 2003e) together with a summary of the key physical and neutronic parameters characterizing the most reactive configurations (ROP).

10.1.4 Selection of the Criticality Benchmark Experiments Used in the Validation of the Criticality Model

The benchmark experiments selected in the validation of the criticality model used for the analysis of the waste package containing FFTF SNF come from *International Handbook of Evaluated Criticality Safety Benchmark Experiments* (NEA 2001) unless otherwise noted. The selection process was initially based on previous knowledge regarding the possible configurations of degraded waste packages, and the subsets have been constructed to accommodate large variations in the ROP of the configurations and also to provide adequate statistics for lower bound tolerance limit calculations. The selected benchmark experiments for the selected subset (applicable to the most limiting set of configurations) are presented in *Benchmark and Critical Limit Calculation for DOE SNF* (BSC 2002c) together with the MCNP cases constructed and the results of the calculations. For the present application (codisposal of FFTF SNF), the selected benchmark experiments are included in one subset (BSC 2002c), that include moderated heterogeneous experiments. The cases, corresponding k_{eff} results and their uncertainties for all benchmark experiments are also summarized in Attachment II of *Analysis of Critical Benchmark Experiments and Critical Limit Calculation for DOE SNF* (BSC 2003f). Table 10-1 presents the list of the benchmark experiments and the number of cases for each subset selected for the partial validation of the criticality model applicable to the limiting cases for FFTF SNF codisposal.

Table 10-1. Critical Benchmarks Selected for Validation of the Criticality Model for the Limiting Cases of FFTF Spent Nuclear Fuel Waste Package

Subset	Benchmark Experiment Identification ^a	Number of Cases Included
Heterogeneous moderated ^b	MIX-COMP-THERM-001	4
	MIX-COMP-THERM-003	6
	MIX-COMP-THERM-004	11
	MIX-COMP-THERM-010	11

Source: Subset defined and evaluated in BSC 2002c

NOTES: ^a The convention for naming the benchmark experiments is from NEA 2001.

^b Identification of each subset from BSC 2002c has been modified to better reflect the subset's main characteristics. The benchmark experiments in each subset have not been affected.

The experiments listed in Table 10-1 are considered appropriate to represent intact (non degraded) configurations and degraded configurations of the waste package containing FFTF SNF that belong to the configuration class 6. Their ROA is detailed in Attachment VII of *Criticality Model Report* (BSC 2003e).

10.1.5 Comparison between ROA of Benchmark Experiments and ROP

The validation of the criticality model needs to show that the range of the fundamental parameters of the benchmark critical experiments (ROA) and the range of the fundamental parameters of the system (ROP) evaluated are nearly identical. This is not usually practical, and for those parameters that do not show a trend in bias, it is acceptable to use critical benchmark experiments that cover most, but not all, of the ROP of the system under evaluation. In these situations, expert judgment may be used to determine if there is a reasonable assurance that the two are sufficiently close. In cases where a trend in bias is identified, the ROA can be extended, but a penalty on the critical limit determined for the subset of benchmark experiments needs to be evaluated and applied.

The comparison between ROA and ROP was performed (BSC 2003e, Attachment VII) only on the subset of benchmark experiments selected to cover the most reactive (limiting cases) configurations of the waste package containing FFTF SNF.

Heterogeneous Moderated Configurations—The comparison of ROA vs. ROP for the heterogeneous moderated configurations is detailed in Attachment VII of *Criticality Model Report* (BSC 2003e). The collective area of applicability of the selected critical benchmarks is based on the ROA of the benchmark experiments included in Table VII-7 of *Criticality Model Report* (BSC 2003e).

The findings from the comparison ROP vs. ROA can be summarized as follows:

- The ROA for this subset of experiments covers the ROP for a number of the parameters that characterize the most limiting degraded configurations of FFTF SNF waste package. The complexity of the investigated system is better described by the spectral parameters which show the existence of two distinct regions due to the different moderation and

neutron absorber content. The existing results for the experiments do not have similar characteristics. The only experiment that has Gd absorber distributed in solution (MIX-COMP-THERM-010) does not have yet the spectral characteristics evaluated.

This situation can be alleviated by addressing one or more of the following possible solutions:

- Spectral characteristics of the benchmark experiment with Gd distributed in solution (MIX-COMP-THERM-010) need to be evaluated.
- Addition of new criticality experiments (very difficult due to the complexity of the arrangement)
- Penalty applied to the critical limit (if trend in bias is identified).
- Change in design (new ROP).

10.1.6 Calculation of the Lower Bound Tolerance Limit

The results of the trending parameter analysis for the critical benchmark subset representative for moderated intact (heterogeneous) configurations of the waste package containing FFTF DOE SNF are presented in Attachment VII of *Criticality Model Report* (BSC 2003e). The results show that the pool of k_{eff} values calculated with the criticality model for this subset of benchmark experiments (moderated heterogeneous subset) does not show any trending. The lower bound tolerance limit value for this subset calculated with the distribution-free tolerance limit (DFTL) method (BSC 2003f, Section 6.2.5) is 0.9786.

The above results and the comparison ROA vs. ROP indicate that the criticality model is partially validated for use in assessing the criticality potential of the intact (nondegraded) configurations and of the configurations belonging to configuration class 6 for the degraded waste package containing FFTF SNF.

10.1.7 Summary of Criticality Model Results and Validation for the Waste Package Containing FFTF SNF

The criticality analyses considered the most important aspects of intact and degraded configurations of the waste package containing FFTF SNF, including optimum moderation condition, rearrangements of the fuel pins and fissile material, and neutron absorber distribution.

The summarized results of three-dimensional Monte Carlo criticality calculations were limited to the intact and degraded configurations for DOE SNF canister loaded with six DFAs and degraded configurations with the updated loading on Ident-69 container. All other configurations containing an intact Ident-69 container analyzed in previous calculations do not include latest data on Ident-69 container loading and were not included in the present report.

The results summarized for the intact and degraded component criticality analyses involving the limiting set of configurations show that the interim critical limit requirement of $k_{\text{eff}}+2\sigma$ be less than or equal to 0.93 is satisfied for the proposed design. The amount of neutron absorber (gadolinium phosphate) required to satisfy the above criterion is 9.29 kg of Gd that must be

distributed on (e.g., flame deposit) or in the material used to fabricate the DOE SNF canister basket for the packages loaded with six DFAs. For the packages containing an Ident-69 container, one basket position must be blocked (limiting the load to maximum 4 DFAs) and an additional amount of 30.8 kg Gd (49.3 kg of GdPO₄ must be uniformly distributed in the initial void spaces of the DOE SNF canister outside the Ident-69 container.

The cases analyzed with highly degraded SNF and internal structures require only a fraction of the indicated insoluble neutron absorber in order to be below the interim critical limit. The overall limiting case was obtained for an extremely conservative configuration comprising an Intact Ident-69 container surrounded by degraded material from 4 DFAs inside the DOE canister. This configuration required an additional amount of insoluble neutron absorber beside the Gd that was included in the basket structure. The plutonium decay typically increases the reactivity of the system with a maximum for k_{eff} placed for configurations containing intact pins between 24,100 and 48,200 years.

All calculations are based on a maximum mass of fissile elements (²³⁵U and ²³⁹Pu) in a fuel assembly of 8.6 kg, with total fissile to ²³⁸U ratio of 0.34 or less. All analyses are based on the fuel pin type that has the highest plutonium enrichment (enriched in ²³⁹Pu) and the highest plutonium loading per pin.

Intact and degraded component criticality calculations included variations on moderators and moderator densities, which encompass flooding the waste package. Occurrence of design basis events, including those with the potential for flooding the disposal container prior to disposal container sealing, is considered and analyzed using very conservative assumptions for many different intact configurations.

Table 10-2 presents a summary of the criticality and geochemistry results with a focus on the correspondence with the degradation classes and resultant configuration classes presented in *Disposal Criticality Analysis Methodology Topical Report* (YMP 2003). The results of the geochemistry analyses (BSC 2001j) show that the calculated maximum loss of Gd is small (10.4 percent) assuring its presence for all anticipated internal configurations, and consequently minimizing the potential for criticality.

The criticality model (MCNP code and appropriated selected neutron cross-section libraries) used in analyzing the configurations of the waste package containing FFTF SNF was validated using the methodology described in *Disposal Criticality Analysis Methodology Topical Report* (YMP 2003) and *Criticality Model Report* (BSC 2003e). Current results indicate that the lower bound tolerance for the heterogeneous moderated configurations limit is well above the interim critical limit used in evaluating the design (Table 10-2).

Table 10-2. Summary of Geochemistry and Criticality Analyses for Internal Configurations (phase I and II) of the Waste Package Containing FFTF Spent Nuclear Fuel

Master Scenario	Description	Configuration Classes and Summary Description	Summary of Geochemistry Calculations	Summary of Criticality and Criticality Model Validation Results				
				($k_{eff}+2\sigma$) _{max}	Interim Critical Limit	Lower Bound Tolerance Limit	Comments	
Initial water intrusion	Initial stage; water fills all available spaces inside the waste package and DOE SNF canister	Intact flooded configurations: SNF and internal structures not degraded	N/A	0.9081 (only for configurations with 6 DFAs)	0.93	0.9786 (heterogeneous moderated configurations)	Maximum $k_{eff}+2\sigma$ was calculated only for the intact configurations containing 6 DFAs (no Gd considered). It is expected that configurations containing an Ident-69 and the design amount of Gd to be below the interim critical limit	
IP-1	The top of the waste package is breached and liquid accumulates inside	Configuration class #6: SNF partially degraded in place (various stages)	For all cases investigated (IP-1, IP-2 and IP-3 scenarios) the loss ranges were: U: 0 to 100% Pu: 6 to 100% Gd: 0 to 10.4%	0.9098 (configuration include one Ident-69 container and 4 DFAs)	0.93	0.9786 (heterogeneous moderated configurations)	Limiting overall case. At least 9.29 kg Gd in the basket structure + an additional 30.8 kg Gd distributed within the empty spaces. One basket position for DFAs blocked (maximum 4 DFAs plus Ident-69 container)	
		Configuration class #3: SNF partially or totally degraded inside the waste package with intact internal structures		N/A		N/A	Configurations with fissile material moved from the neutron absorber are not credible for this design	
IP-2	SNF degrades concurrently with the waste package internals	Configuration class #2: Both SNF and internal structures of the waste package degraded (various stages)		0.9025	0.93	Not available	No Gd considered. Configurations include 6 degraded DFAs and bound configurations with degraded Ident-69 container and 4 DFAs	
IP-3	SNF degrades after the waste package internals	Configuration class #1: SNF intact (as assembly or pins) and degraded internal structures (various stages)		0.9205 (only for configurations with 6 DFAs)	0.93	0.9786 (heterogeneous moderated configurations)	At least 7.62 kg of the initial Gd amount must be present in the mixture surrounding the DFAs. It is expected that configurations containing an Ident-69 and the design amount of Gd to be below the interim critical limit	
IP-4	SNF degrades before the waste package internals	The configurations resulting from these scenarios (configurations classes #4, #5) have not been investigated in the geochemistry and criticality analyses due to the fact that they are less moderated (no pooling of water) and are bounded by the variations of the configurations investigated above.						
IP-5	SNF degrades concurrently with the waste package internals	The bottom of waste package is penetrated allowing liquid to flow through						
IP-6	SNF degrades after the waste package internals							

10.2 TRIGA SNF

The description and main characteristics of the waste package containing TRIGA SNF are presented in Section 3.2.2. In this section a summary of the results of the criticality analyses performed is presented together with the current status of the validation of the criticality model for the configurations that are specific to this fuel group.

The first step in applying the criticality model to the specific intact and degraded configurations of this waste package is identification and characterization of the specific configurations anticipated for postclosure. The results of the degradation analysis coupled with the geochemistry calculations (CRWMS M&O 2000b, Section 6) provided an insight into the possible arrangements and compositions of the degraded materials placed within the waste package. All configuration classes analyzed and the most probable degradation scenario that was identified are summarized in the next section (Section 10.2.1). The results of the criticality calculations for the most representative intact and degraded configurations are presented in Section 10.2.2. The limiting cases identified during the analysis are also providing the basis for deriving the final design solution (amount of neutron absorber to be distributed within the initial waste package). The range of parameters that characterize the limiting or the most reactive cases is subsequently used in the process of validation of the criticality model. The process includes selection of appropriate critical benchmark experiments and derivation of the specific lower tolerance bound limit for each major group of configurations.

The results of three-dimensional Monte Carlo calculations from the criticality analyses showed the requirement of $k_{\text{eff}} + 2\sigma$ less than or equal to the interim critical limit of 0.93 (CRWMS M&O 2000b, Section 2.4.3) is satisfied for any credible configurations of the waste package containing TRIGA SNF. In the intact configuration, the presence of Gd in the DOE SNF canister basket is not necessary to meet this requirement.

The results for the degraded analysis indicate that the highest k_{eff} is achieved if the fuel rods are intact in the degraded DOE SNF canister (basket fully degraded). This configuration results in $k_{\text{eff}} + 2\sigma$ of less than or equal to 0.93 with at least 8.9 kg Gd included in the DOE SNF Canister. The state of the other internal components of the waste package has a negligible impact on k_{eff} .

The final baseline design incorporates a basket for the DOE SNF canister that holds 37 fuel rods. A 1-mm advanced neutron absorber matrix tube (Alloy 22 with 8 at% Gd) is placed inside the tubes such that at least 8.9 kg of Gd is distributed in the baskets in the DOE SNF Canister.

All calculations were based on 111 TRIGA fuel rods per waste package. The total mass of ^{235}U in a fuel rod should not exceed the one of TRIGA FLIP with 70 percent enrichment and 137 g ^{235}U per rod. This results in a waste package mass limit of 15.2 kg of ^{235}U .

10.2.1 Degradation Scenarios and Configurations

Based on the corrosion rates and the material thicknesses presented in Table 10-3, the most probable degradation path for the waste package, the DOE SNF canister and the TRIGA SNF follows the following sequence (CRWMS M&O 2000b, Section 6.2.1.1):

1. Waste package internal cavity is flooded first. Then, waste package basket, (inner brackets and supporting tube) degrade because of the A516 material.
2. Thin stainless steel shell of the DHLW glass canister and subsequently the glass begin to degrade.
3. The DOE SNF canister is penetrated and flooded inside.
4. SNF stainless steel cladding and stainless steel support grid tubes contact with water directly.
5. The thin stainless steel cladding (0.51 mm) degrade faster than the support grid tubes (5.5 mm). After this, there are two degradation paths:
 - 5a. SNF rods are exposed to water but stay intact.
 - 5b. SNF rods are exposed to water and degrade in place inside the support grid tubes. Neutron absorber tubes stay intact also.
6. Support tubes begin to degrade including the tubes with neutron absorber.
 - 6a. Following (5a) and (6), intact SNF rods fall, settle on the bottom of the DOE SNF canister and mix with neutron absorber.
 - 6b. Following (5b) and (6), degraded SNF mix with degraded steel and neutron absorber and accumulate on the bottom of the DOE SNF canister.
7. Given time, eventually everything degrades and the degradation products become a uniform mixture settling on the bottom of the waste package (scenario IP-2). There may be some separation of the fissile material from the neutron absorber.

Table 10-3. Materials and Thicknesses for TRIGA Spent Nuclear Fuel Waste Package

Components	Material	Thickness (mm)
Waste package basket	A516 Carbon Steel	12.7
Waste package inner bracket	A516 Carbon Steel	25.4
Waste package support tube	A516 Carbon Steel	31.75
DHLW glass shell	Stainless Steel Type 304L	9.5
DHLW glass	Glass	N/A
DOE canister	Stainless Steel Type 316L	9.5
SNF support basket (Tubes)/ bottom plates	Stainless Steel Type 316L	5.5
Neutron absorber tubes	GdPO ₄ /C-22	1.0
SNF stainless steel cladding	Stainless Steel Type 304L	0.51
SNF top/bottom end fittings	Stainless Steel Type 304L	Solid Cone (Bottom radius=18.8 mm)
SNF	UZrH rod	15 mm

Source: CRWMS M&O 2000b

The configurations investigated can be categorized using the description of the generic configuration classes given in Section 3 of *Disposal Criticality Analysis Methodology Topical Report* (YMP 2003). As indicated in Section 6.5, for the purpose of fully identifying the potential for criticality, all representative configurations classes have been analyzed and not only the configurations resulting from the most probable degradation path presented above. The next subtitles follow the original description given in Section 6.2.1.2 of *Evaluation of Codisposal Viability for UZrH (TRIGA) DOE-Owned Fuel* (CRWMS M&O 2000b).

TRIGA SNF Degrades Before the Internal Components of the Waste Package—For these scenarios the SNF degrades faster than the surrounding components (i.e., the DOE SNF canister, DHLW glass, and the supporting baskets inside and outside the DOE SNF canister). The waste package and the DOE SNF canister are considered breached at the top and flooded with water. Since the waste package is horizontally emplaced, “the top” corresponds to the side of the waste package and the DOE SNF canister. This configuration is an example of standard scenario IP-1 (CRWMS M&O 1999g, p. 27). Note that since the TRIGA SNF rods including the end fittings are very thick as compared to the other materials external to the TRIGA SNF, the degradation scenario of IP-1 (i.e., SNF degrades faster than the other materials) is not probable. The resultant configuration class refinements and their relevant variations with respect to criticality are presented as follows

TRIGA SNF Degraded, DOE SNF Canister and Internal Supporting Structure Not Degraded—In this configuration class refinement, the DOE SNF canister interior is flooded but not degraded. The configurations result from the application of the IP-1 scenario to the DOE SNF canister. Inside the DOE SNF canister, the supporting internals are in place but the TRIGA SNF has degraded. The neutron absorber remains with its carrier. The degradation materials are distributed at the bottom of each support grid tubes, or else dissolved and distributed uniformly with the water. The configurations obtained have the potential for a more reactive geometry with respect to criticality, especially for the highly enriched TRIGA SNF. Since the TRIGA SNF degrades in place, this configuration group is a refinement of the configuration class 6 (CRWMS M&O 1999g, Section 6.1.2).

TRIGA SNF Degraded, DOE SNF Canister Supporting Structure Partially Degraded—In this configuration refinement group obtained also by applying the standard scenario IP-1 to the DOE SNF canister, some of the inner supporting structures (inside the flooded DOE SNF canister) have partially degraded (e.g., localized corrosion). As a result, some degraded TRIGA SNF could fall to the bottom of the DOE SNF canister and be separated from the neutron absorber. This configuration group is a refinement of the configuration class 3 (CRWMS M&O 1999g, p. 21). Its increased potential for criticality is generally a result of separation of the fissile form from the neutron absorber.

All Waste Package Components Degraded—This configuration group results from the subsequent degradation of the waste package internals and DHLW canisters after the above intermediate configurations have been reached. It also represents the final configuration obtained by applying scenario IP-2 or IP-3 to the whole waste package. These configurations are refinements of the configuration class 2 from Section 6.1.2 of *Generic Degradation Scenario and Configuration Analysis for DOE Codisposal Waste Package* (CRWMS M&O 1999g).

TRIGA SNF Degrades After the Other Internal Components—The components external to the flooded DOE SNF canister will be the first ones exposed to aqueous attack, and will start to degrade first. The carbon steel of the waste package structural web supporting the DHLW canisters will degrade fastest, and leave a significant amount of iron oxide in the bottom of the waste package. Much of the DHLW glass will degrade before the DOE SNF canister is breached, and the silica released will form a clay layer at the bottom of the waste package.

Degraded DOE SNF Canister Internal Structure; Intact TRIGA SNF and DOE SNF Canister Shell; Degraded Waste Package Basket Structure and DHLW Glass Canister(s)—In this configuration (IP-3-A), which results after the application of scenario IP-3 to the flooded DOE SNF canister, the supporting structure inside the DOE SNF canister degrades and the fuel cladding before the TRIGA SNF. The intact TRIGA SNF falls to the bottom of DOE SNF canister. This configuration group is a refinement of configuration class 1 (CRWMS M&O 1999g, Section 6.1.2). The configurations are relatively insensitive to whether the materials outside the DOE SNF canister are degraded or not. Modified geometry and separation from the neutron absorber make this group of configurations susceptible to criticality.

Degraded Waste Package Basket Structure, DHLW Glass Canister(s), and DOE SNF Canister; Intact TRIGA SNF—In this configuration (IP-3-B, CRWMS M&O 1999g, p. 32), which results from the application of scenario IP-3 to the whole waste package, all the waste package internal structure materials and the DHLW glass are degraded first, followed by the degradation of the DOE SNF canister and the supporting structure inside. If the TRIGA SNF stays in solid form due to its high resistance to bulk corrosion, it can fall to the bottom of waste package. If the TRIGA SNF matrix stays intact, the configuration may be characterized by the intact TRIGA SNF matrix stacked at the bottom of the waste package, surrounded by clay and layers of steel degradation materials. This configuration group is a refinement of the configuration class 1 (CRWMS M&O 1999g, Section 6.1.2).

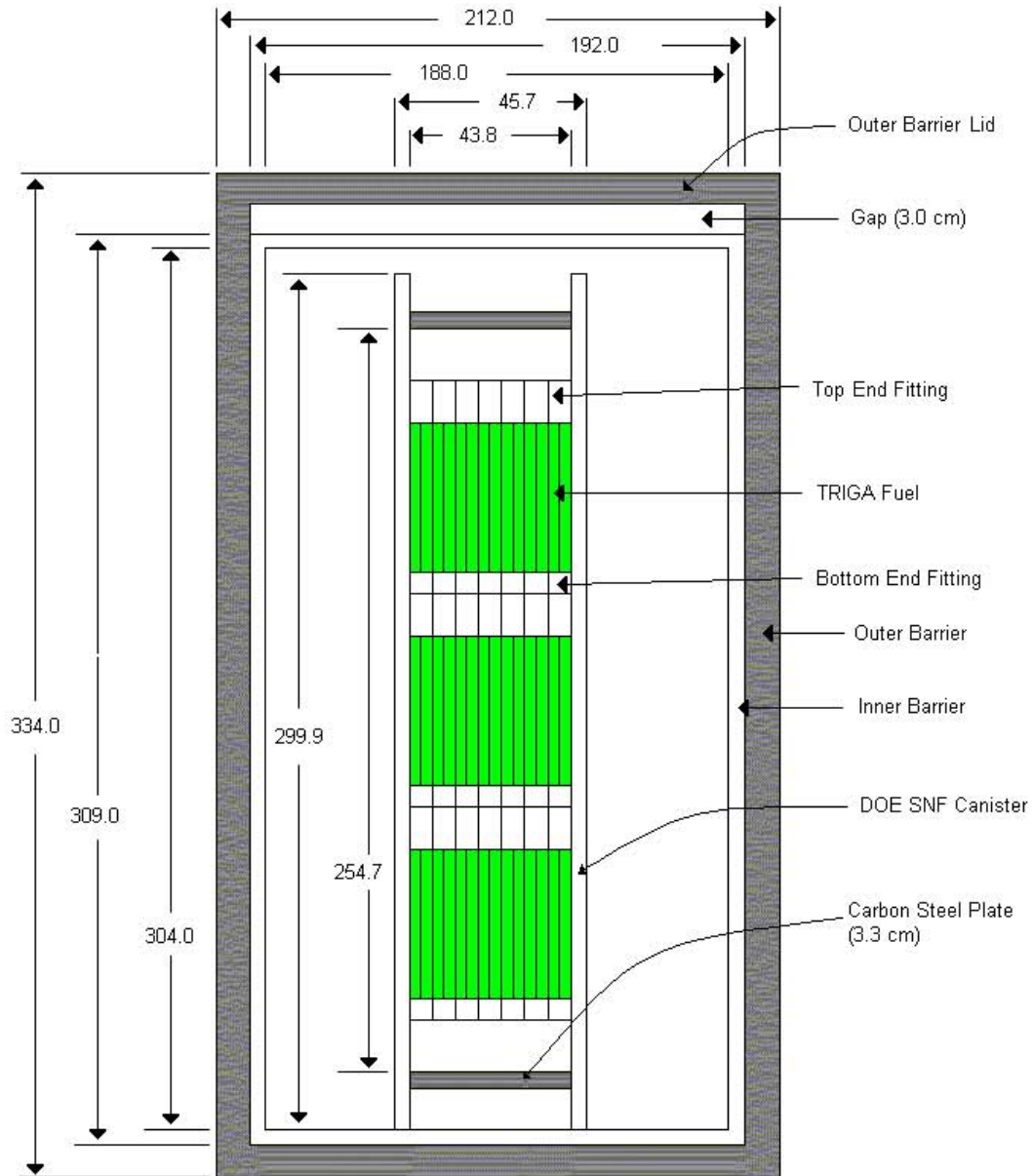
10.2.2 Criticality Calculations and Results

10.2.2.1 Results for Intact Mode

This section summarizes the results of the criticality analyses for intact configurations (CRWMS M&O 2000b, Section 7.3.1). Although the components (fuel rod, cladding, and DOE SNF canister) are considered structurally intact, water intrusion into the components is allowed to determine the highest k_{eff} resulting from the optimum moderation. The TRIGA SNF is described in detail in Section 3.2.2 of this document.

The most reactive fuel based on the fuel type and optimum moderation is determined to be the FLIP type rod, which has a BOL U-235 enrichment of 70 wt%. Analyses of intact fuel rods in the configuration shown in Figure 10-3 indicated that four rod cluster type rods, FLIP, standard streamline type rods, and FLIP-LEU-I are well below interim critical limit of 0.93 (CRWMS M&O 2000b). The maximum $k_{\text{eff}} + 2\sigma$ is 0.7890 for the TRIGA-SS FLIP type rods (CRWMS M&O 2000b, Table 6-1).

The density of water in the DOE SNF canister was also varied. The results indicate that the DOE SNF canister is under moderated even when it is completely flooded, and the maximum k_{eff}



Dimension are in cm.

Not to scale

Source: CRWMS M&O 2000b, p. 72

Figure 10-3. TRIGA Waste Package and DOE Spent Nuclear Fuel Canister Dimensions

10.2.2.2 Results for Degraded Cases

The criticality evaluations conducted for the degraded cases are discussed in the following paragraphs. In the calculations described below, the configurations with the lowest uranium loss (2.1 percent) and the highest Gd loss (53 percent) were analyzed. The fuel type used in the calculations is FLIP in a standard streamline stainless-steel-clad rod unless otherwise specified.

The DOE SNF canister is flooded unless otherwise specified.

Degraded TRIGA SNF, Intact DOE SNF Canister and Basket—In the configurations investigated, the TRIGA SNF was considered to degrade first. All other internal components of the waste package remain intact. The configurations obtained under this situation have the potential for a more reactive geometry with respect to criticality. The configurations belong to configuration class 6 resulting from the standard scenario group IP-1 (the SNF degrades faster than the other internal components). Since the TRIGA SNF rods including the end fittings are very thick as compared to the other materials external to the TRIGA SNF the occurrence of IP-1 scenario is not likely.

Cladding Degrades—In this case the structural tubes and the DOE SNF canister are intact. The waste package basket, the SRS DHLW glass pour canisters and the SRS DHLW glass are also intact. The stainless steel cladding is degraded, but the fuel is intact. A maximum $k_{\text{eff}} + 2\sigma$ of 0.8069 is obtained when no advanced neutron absorber matrix is introduced (CRWMS M&O 2000b, Table 6-2). A representation of this configuration is shown in Figure 10-4.

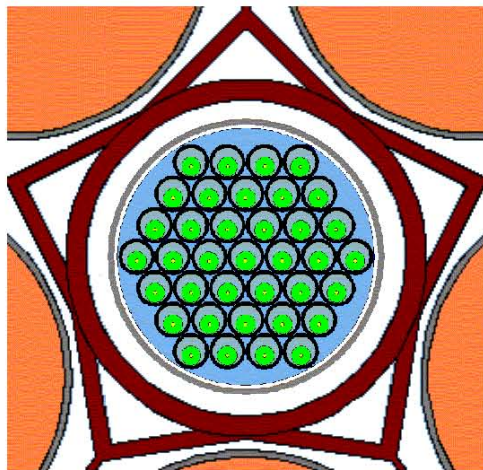


Figure 10-4. Cross-Section of the DOE Spent Nuclear Fuel Canister (Basket Intact, Cladding Degraded)

Fuel Degrades—This configuration is similar to the previous one except that the fuel has degraded. The maximum $k_{\text{eff}} + 2\sigma$ is 0.8158 (CRWMS M&O 2000b, Table 6-5). These are the bounding configurations for degraded SNF with intact basket components. A representation of this configuration is shown in Figure 10-5.

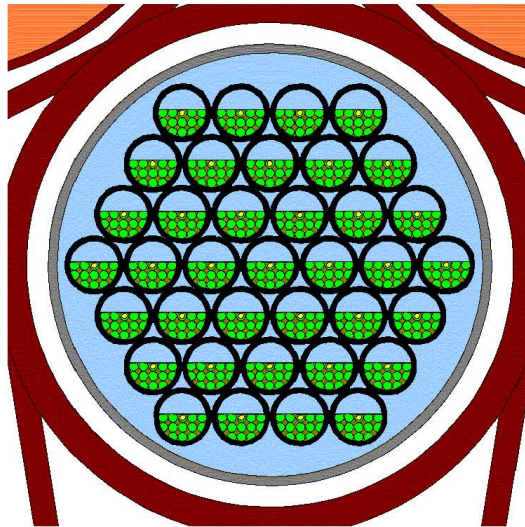


Figure 10-5. Cross-Section of the DOE Spent Nuclear Fuel Canister (Fuel Partially Fractured)

Degraded TRIGA SNF and Basket—In this configuration group, the DOE SNF canister basket has degraded. Therefore, the degraded fuel elements could fall to the bottom of the DOE SNF canister. Different stages of degradation of the fuel element were considered. The configuration obtained under this condition corresponds to class 1. Some of the inner structure has partially degraded. Therefore, some degraded TRIGA SNF could fall to the bottom of the DOE SNF canister and be separated from the neutron absorber. As stated before since the TRIGA SNF rods including the end fittings are very thick as compared to the other materials external to the TRIGA SNF, in general, the probability of occurrence for this degradation group is very small.

Degraded Fuel Cladding—In this configuration, the bare fuel pins have settled on the bottom of the DOE SNF canister and the Zr rods are intact. The degradation products of both the cladding and the basket with a variable fraction of water surround the fuel pins. In this configuration, not only is it not probable for the SNF to degrade faster than the components outside the DOE canister there also is no path for the neutron absorber to escape out of the waste package since all the components outside the DOE canister stay intact.. A representation of this configuration is shown in Figure 10-6. $k_{\text{eff}} + 2\sigma$ is maximized (0.839) when the mixture of advanced neutron absorber matrix, goethite and water is homogenized over the entire volume of the DOE SNF canister (CRWMS M&O 2000b, Table 6-6).

The number of absorber matrix tubes needed to keep the system subcritical after the degradation process was also investigated. $k_{\text{eff}} + 2\sigma$ of the waste package is 0.9050 if the DOE SNF canister basket contains 18 1-mm tubes of advanced neutron absorber matrix (which corresponds to 3.6 kg of Gd homogenized over the entire DOE SNF canister volume) (CRWMS M&O 2000b, Table 6-6). The density of water added to the goethite/advanced neutron absorber matrix mixture was also varied from 1 g/cm³ to 0.3 g/cm³. k_{eff} is maximum for a water density of 1 g/cm³. This case presumes the loss of 5.3 kg (60 percent) of the neutron absorber matrix, which, as mentioned above, is very improbable.

A configuration where the advanced neutron absorber matrix (8.9 kg) settles on the bottom of the DOE SNF Canister is investigated. This configuration can be regarded as belonging to

configuration class 3. In this case, the waste package is subcritical with $k_{\text{eff}} + 2\sigma$ of 0.8339, if at least 1.5 kg (17 percent of initial amount) Gd remains between the rods (CRWMS M&O 2000b, Table 6-6). A representation of this configuration is shown in Figures 10-6 and 10-7.

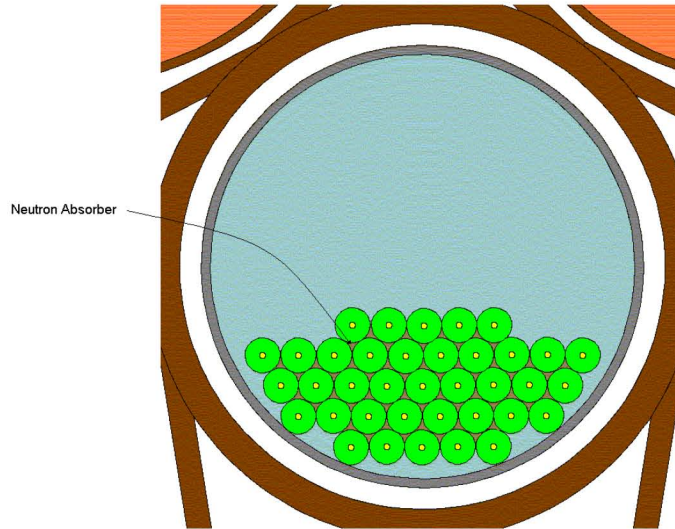


Figure 10-6. Cross-Section of the DOE Spent Nuclear Fuel Canister (Stainless Steel Tubes Degraded)

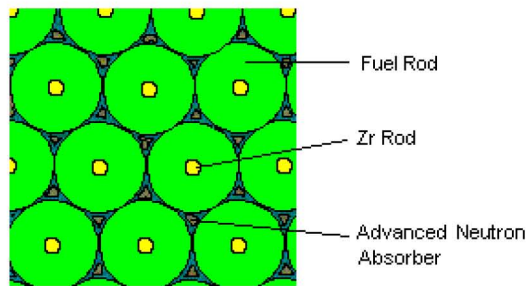


Figure 10-7. Cross-Section of the DOE Spent Nuclear Fuel Canister with Advanced Neutron Absorber Matrix between the Rods

Degraded Cladding and Partially Fractured Fuel—Partially fractured fuel is represented as spheres. The radius of the spheres varies. A mixture of water and degraded stainless steel (goethite) surrounds each sphere. In these configurations, the graphite reflector and the Zr rods form layers above the goethite. There is no advanced neutron absorber matrix in the DOE SNF canister. A maximum $k_{\text{eff}} + 2\sigma$ of 0.6670 was achieved when the radius of the sphere is 0.1 cm (CRWMS M&O 2000b, Table 6-7). A representation of this configuration is shown in Figure 10-8.

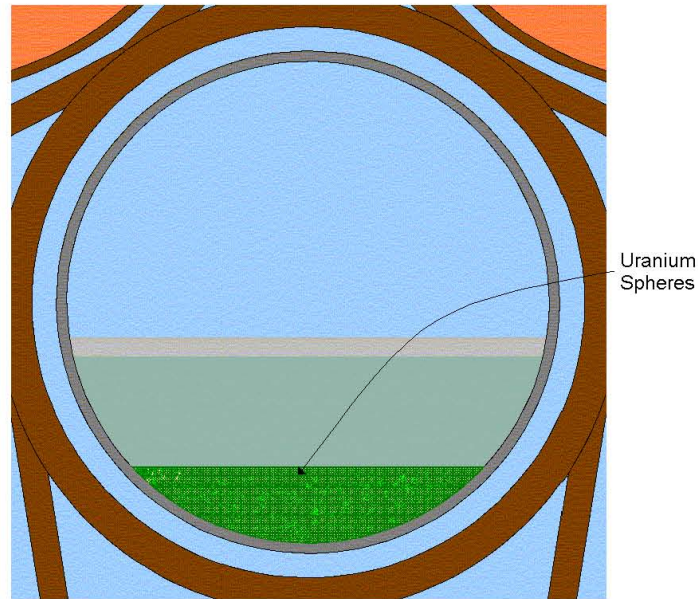


Figure 10-8. Cross-Section of the DOE Spent Nuclear Fuel Canister (Fuel Degraded)

Fully Degraded Fuel, Zr Rods, Graphite Reflector, and Cladding—In this configuration, the fuel and the degradation products from the cladding and the basket form a slurry. The amount of water in the slurry varies. In this configuration, everything is degraded forming a uniform mixture inside the DOE canister. This configuration is also not very likely. Only 0.1 kg (1 percent) Gd is required to remain in the mixture to keep the canister configuration subcritical with the $k_{\text{eff}} + 2\sigma$ of 0.8288 (CRWMS M&O 2000b, Table 6-8).

10.2.2.3 Results for Degraded Configurations Postulated beyond the Regulatory Period

The degradation and criticality analyses performed have also investigated configurations that require very long times to be attained. These configurations are anticipated to happen well beyond the regulatory period of 10,000 years but they have been analyzed to fully investigate the potential for criticality of the waste package containing TRIGA SNF. For the purpose of this document, these results have been summarized and grouped together in this section.

TRIGA SNF Degrades After Other Internal Components—In these cases, the components external to the DOE SNF canister are the first ones exposed to aqueous attack, and start to degrade first (CRWMS M&O 1999g, p. 31). The waste package basket (made of carbon steel) degrades fastest and much of the SRS DHLW glass is degraded before water penetrates the DOE SNF canister. Then the DOE SNF canister contents start to degrade. This configuration requires the degradation of all steel materials inside the waste package and DOE canister except the fuel rods. This is very unlikely to occur since the corrosion rate of the fuel rod material is about the same as the steel. Additionally, the combined probability for all of the sequence of events to occur, from the degradation of all the materials to uniform mixing within the waste package, is very small.

Intact DOE SNF Canister Shell with Intact Pins, Degraded Internals in Waste Package—In this group of configurations, the DOE SNF canister shell is partially intact with some degradation on the outer surface (CRWMS M&O 2000b, Table 6-11). In this configuration,

4.1 kg (46 percent) Gd is required to be distributed in the clay layer to reduce the $k_{\text{eff}} + 2\sigma$ to 0.9095. This configuration occurs when the clay resulting from the degradation of the DHLW glass and the DHLW glass pour canisters have no water. The DOE SNF canister is on the bottom of the waste package.

TRIGA SNF Intact, Other Internal Components Degraded—In this group of configurations, all internal components of the waste package including the DOE SNF canister are degraded, but the fuel is intact. This configuration corresponds to configuration class 1, which results from the degradation of waste package basket and DHLW glass canisters, followed by the degradation of the DOE SNF canister and the supporting structure inside. The configuration may be characterized by intact TRIGA SNF settled on the bottom of the waste package, surrounded by clay. This configuration is highly unlikely because the fuel could not stay intact while all other components degrade. Based on geochemistry calculation results, with average reaction rates it takes more than 300,000 years for the glass to degrade while it takes only 75,000 years for the TRIGA SNF to degrade. 4.1 kg Gd homogenized in a layer of clay that covers only the fuel is needed for $k_{\text{eff}} + 2\sigma$ below the interim critical limit ($k_{\text{eff}} + 2\sigma$ is 0.9146).

Intermediate Degraded Configuration—These degradation configurations assume partial degradation of the DHLW glass and the SNF, and full degradation of the DOE canister and are described in *Evaluation of Codisposal Viability for UZrH (TRIGA) DOE-Owned Fuel* (CRWMS M&O 2000b, Section 7.3.2.3). Based on the discussion presented in Section 10.2.2.1, from the material property point of view, the sequence of events associated with these configurations are not probable. The results show that $k_{\text{eff}} + 2\sigma$ is 0.6892 (CRWMS M&O 1999c, Table 6-14) provided that the Gd remains around the fuel.

All Waste Package Components Degraded—The configurations with degraded waste package internal components and the DOE SNF canister were investigated in *Evaluation of Codisposal Viability for UZrH (TRIGA) DOE-Owned Fuel* (CRWMS M&O 2000b, Section 7.3.2.1.3). The results show that the maximum k_{eff} occurs when both the fuel and the clay layers are without free water; the remaining volume of the waste package is filled with water. No Gd is added to the fuel layer and $k_{\text{eff}} + 2\sigma$ is then equal to 0.6359 (CRWMS M&O 1999c, Table 6-13).

10.2.3 ROP for Configurations of Waste Package Containing TRIGA DOE SNF

ANSI/ANS-8.1-1998 and *Disposal Criticality Analysis Methodology Topical Report* (YMP 2003) provides basic requirements for validation of a calculational method used in the criticality analysis of a system. The bias of a code system (in this case the criticality model containing the Monte Carlo computer code MCNP, selected cross-section libraries and computer hardware) is determined by correlating the results of critical and near-critical experiments with calculated results for those experiments. The common practice, and that considered by the current validation methodology (BSC 2003e), is for comparison of the calculated k_{eff} to a critical or near critical system.

Prior to the initiation of the validation activity, the operating conditions and parameters for which the validation is to apply must be identified. The fissile isotope, enrichment of fissile isotope, fuel density, chemical form of fuel, types of neutron moderators and reflectors, range of moderator to fissile isotope ratio, neutron absorbers and physical configurations are among the

parameters to specify. These parameters will define the area of applicability for the selection of the critical experiments for the validation effort.

The preliminary degradation analysis of the content of the waste package containing TRIGA SNF (CRWMS M&O 2000b, Section 6) and the subsequent criticality analysis performed for the resulting internal configurations have followed the guidance suggested by the Internal Criticality Master Scenarios presented in *Disposal Criticality Analysis Methodology Topical Report* (YMP 2003) and also by *Generic Degradation Scenario and Configuration Analysis for DOE Codisposal Waste Package* (CRWMS M&O 1999g). The resultant configuration classes internal to the waste package have been screened systematically for their criticality potential in comprehensive criticality analyses (CRWMS M&O 1999c).

For the purpose of the criticality model validation for the configurations specific to the waste package containing TRIGA SNF and identification of the range of parameters that characterize the internal configurations of the degraded waste package, the most reactive degraded configurations previously investigated (see Section 10.2.2.) have been categorized into two large groups:

1. Configurations containing intact fuel (heterogeneous configurations)
2. Configurations containing degraded fuel (relatively homogeneous configurations).

The first category contains the configurations described in *Evaluation of Codisposal Viability for UZrH (TRIGA) DOE-Owned Fuel* (CRWMS M&O 2000b, Sections 7.3.1, 7.3.2.1.2, 7.3.2.2, and 7.3.2.3). These configurations represent intact fuel (nondegraded fuel matrix but other components degraded) configurations and refinements of the general configuration class 1 and 6. The second category includes the configurations for degraded fuel described in *Evaluation of Codisposal Viability for UZrH (TRIGA) DOE-Owned Fuel* (CRWMS M&O 2000b, Section 7.3.2.1.2). These configurations represent refinements of the general configuration class 2. This proposed categorization allows a simple and systematic way of identifying the key parameters that characterize the degraded configurations.

The process employed in *TRIGA Fuel Phase I and II Criticality Calculation* (CRWMS M&O 1999c) for investigating the potential for criticality of the possible degraded configurations of the waste package used a screening approach, the goal being to identify the most reactive configurations in a given class of degraded configurations. Due to this approach, the number of configurations analyzed varies among the classes of configurations depending on the complexity of the possible arrangements and the initial screening results. Selected cases (typically the most reactive or the limiting cases as presented in CRWMS M&O 2000b, Section 7) have been rerun with tallies calculating the neutron flux and the fission rate in the regions containing the fissile material. The results of the cases that were rerun with tallies are summarized in Tables IX-2 and IX-3 of *Criticality Model Report* (BSC 2003e) together with a summary of the key physical and neutronic parameters characterizing the most reactive configurations (ROP).

10.2.4 Selection of the Criticality Benchmark Experiments

The benchmark experiments selected in the validation of the criticality model used for the analysis of the waste package containing TRIGA SNF come from *International Handbook of*

Evaluated Criticality Safety Benchmark Experiments (NEA 2001) unless otherwise noted. The selection process was initially based on previous knowledge regarding the possible configurations of degraded waste package, and the subsets have been constructed to accommodate large variations in the range of parameters of the configurations and also to provide adequate statistics for lower bound tolerance limit calculations. The selected benchmark experiments for each subset are presented in *Benchmark and Critical Limit Calculation for DOE SNF* (BSC 2002c, Tables 6-5 and 6-7) together with the MCNP cases constructed and the results of the calculations. For the application to the codisposal of TRIGA SNF, the selected benchmark experiments have been grouped in two subsets (BSC 2002c), that include moderated heterogeneous and homogeneous experiments. The cases, corresponding k_{eff} results and their uncertainties are also summarized in *Analysis of Critical Benchmark Experiments and Critical Limit Calculation for DOE SNF* (BSC 2003f, Attachment II). Table 10-4 presents the list of the benchmark experiments and the number of cases for each subset selected for validation of the criticality model for TRIGA SNF.

Table 10-4. Critical Benchmarks Selected for Validation of the Criticality Model for TRIGA Spent Nuclear Fuel

Subset	Benchmark Experiment Identification ^a	Number of Cases Included
Heterogeneous moderated ^b	HEU-COMP-THERM-002	25
	HEU-COMP-THERM-003	15
	HEU-COMP-THERM-004	4
	HEU-COMP-THERM-005	1
	HEU-COMP-THERM-006	3
	HEU-COMP-THERM-007	3
	HEU-COMP-THERM-008	2
	HEU-COMP-THERM-010	21
	HEU-COMP-THERM-011	3
	HEU-COMP-THERM-012	2
	HEU-COMP-THERM-013	2
	HEU-COMP-THERM-014	2
	HEU-MET-THERM-006	23
	IEU-COMP-THERM-003	2
	Homogeneous moderated ^b	HEU-SOL-THERM-001
HEU-SOL-THERM-005		17
HEU-SOL-THERM-006		29
HEU-SOL-THERM-008		5
HEU-SOL-THERM-009		4
HEU-SOL-THERM-010		4
HEU-SOL-THERM-011		2
HEU-SOL-THERM-012		1
HEU-SOL-THERM-013		4
HEU-SOL-THERM-014		3
HEU-SOL-THERM-015		5
HEU-SOL-THERM-016		3
HEU-SOL-THERM-017		8
HEU-SOL-THERM-018		12
HEU-SOL-THERM-019		3
HEU-SOL-THERM-021		32
HEU-SOL-THERM-025		18
HEU-SOL-THERM-027		9
HEU-SOL-THERM-028		18
HEU-SOL-THERM-029		7
HEU-SOL-THERM-030		7
HEU-SOL-THERM-031		4
HEU-SOL-THERM-032		1
HEU-SOL-THERM-033		26
HEU-SOL-THERM-035		9
HEU-SOL-THERM-036		4
HEU-SOL-THERM-037		9
HEU-SOL-THERM-043		3
HEU-SOL-THERM-044	16	

Source: Subsets defined in BSC 2002c

NOTE: ^a The convention for naming the benchmark experiments is from NEA 2001.

^b Identification of each subset from BSC 2002c has been changed to better reflect the subset's main characteristics. The benchmark experiments in each subset have not been affected.

The experiments listed in Table 10-4 are considered appropriate to represent intact (non degraded) configurations and degraded configurations of the waste package containing TRIGA SNF that belong to the configuration classes 1 and 2.

10.2.5 Comparison between ROA of Benchmark Experiments and ROP

The validation of the criticality model needs to show that the range of the fundamental parameters of the benchmark critical experiments (ROA) and the range of the fundamental parameters of the system (ROP) evaluated are nearly identical. This is not usually practical, and for those parameters that do not show a trend in the bias, it is acceptable to use critical benchmark experiments that cover most, but not all, of the ROP of the system under evaluation. In these situations, expert judgment may be used to determine if there is a reasonable assurance that the two are sufficiently close. In cases where a trend in the bias is identified, the ROA can be extended, but a penalty on the critical limit determined for the subset of benchmark experiments needs to be evaluated and applied.

The comparison between ROA and ROP was structured (BSC 2003e, Attachment IX) on the two subsets of benchmarks experiments selected to cover the majority of the analyzed configurations of the waste package containing TRIGA SNF.

Heterogeneous Moderated Configurations—The comparison of ROA vs. ROP for the heterogeneous moderated configurations is detailed in *Criticality Model Report* (BSC 2003e, Appendix IX). The collective area of applicability of the selected critical benchmarks is based on the information regarding ROA of the benchmark experiments included in Tables IX-6 through IX-9 of *Criticality Model Report* (BSC 2003e).

The findings from the comparison of ROP vs. ROA can be summarized as follows:

- The ROA for this subset of experiments covers the ROP for the majority of parameters that characterize the heterogeneous configurations (with or without Gd). The effect of Gd on the spectra is marginal. The criticality model is adequate for performing the screening of the configurations.
- For the configurations containing Gd dispersed in the DOE SNF internal space, the comparison shows that the ROA of benchmarks is not within the range of parameters (with respect to Gd concentration and spatial distribution) but the ROA of spectral parameters for benchmarks covers ROP (benchmarks cover spectra).

This situation can be alleviated by addressing on or more of the following possible solutions:

- More experiments need to be added covering the Gd presence.
- Penalty can be applied to the critical limit (if trend in bias is identified).

Homogeneous Moderated Configurations—The comparison of ROA vs. ROP for the homogeneous moderated configurations is detailed in Attachment IX of *Criticality Model Report* (BSC 2003e). The collective area of applicability of the selected critical benchmarks is based on the ROA of the benchmark experiments included in Tables IX-10 to IX-15 of *Criticality Model Report* (BSC 2003e).

The findings from the comparison can be summarized as follows:

- The ROA does cover most of the range of parameters characterizing moderation of the systems (e.g., H atomic density, H/X) except for lower values of H atomic density (atoms/b-cm). The spectral parameters show good match of ROP with ROA.

10.2.6 Calculation of the Lower Bound Tolerance Limit

The following results are excerpted from *Analysis of Critical Benchmark Experiments and Critical Limit Calculation for DOE SNF* (BSC 2003f), which present in detail the methodology and calculations performed for evaluating the lower bound tolerance limit for each set of configurations of the waste package containing TRIGA DOE SNF.

The results of the trending parameter analysis for the critical benchmark subset representative for moderated intact (heterogeneous) configurations of the waste package containing TRIGA DOE SNF show a trend with AENCF and are presented in Attachment IX of *Criticality Model Report* (BSC 2003e).

The lower bound tolerance limit function for intact-moderated configurations of TRIGA DOE SNF is calculated as:

$$\begin{aligned} \text{Lower bound tolerance limit} &= 0.9668 && \text{for } 0 < \text{AENCF} < 0.0404 \\ \text{Lower bound tolerance limit} &= -0.3315 * (\text{AENCF}) + 0.9788 && \text{for } 0.0404 < \text{AENCF} < 0.0922 \end{aligned}$$

The normality test results and the critical limit calculations are detailed in *Analysis of Critical Benchmark Experiments and Critical Limit Calculation for DOE SNF* (BSC 2003f, Attachment III).

The results of the trending parameter analysis for the critical benchmark subset representative for moderated degraded configurations of the waste package containing TRIGA DOE SNF are presented in Table IX-19 of *Criticality Model Report* (BSC 2003e). The results show that the pool of k_{eff} values calculated with the criticality model for this subset of benchmark experiments (moderated heterogeneous subset) does not show any trending.

The normality test results and the lower bound tolerance limit calculation are detailed in Attachment III of *Analysis of Critical Benchmark Experiments and Critical Limit Calculation for DOE SNF* (BSC 2003f). The lower bound tolerance limit value calculated with DFTL method for this subset (normality test failed) is 0.9796.

Table 10-5 presents a summary of the results of the analyses performed on the subsets of critical benchmark experiments applicable to the waste package containing TRIGA DOE SNF and the calculated lower bound tolerance limit values.

Table 10-5. Lower Bound Tolerance Limits for Benchmark Subsets Representative for the Configurations of the Waste Package Containing TRIGA Spent Nuclear Fuel

Subset	Trend Parameter	Test for Normality	Applied Computational Method	Lower Bound Tolerance Limit or Lower Bound Tolerance Limit Function
Intact (heterogeneous) Moderated	AENCF	N/A	LUTB	0.9668 for $0 < \text{AENCF} < 0.0404$ $0.3315 * (\text{AENCF}) + 0.9788$ for $0.0404 < \text{AENCF} < 0.0922$
Degraded (homogeneous) Moderated	None	Failed	DFTL	0.9796

Source: BSC 2003f, p. 34

The results above and the comparison ROA vs. ROP indicate that the criticality model is partially validated for use in assessing the criticality potential of the intact (nondegraded) configurations and of the configurations belonging to the general configurations classes 1 and 2 for the degraded waste package containing TRIGA DOE SNF.

10.2.7 Summary of the Criticality Model Results and Validation for the Waste Package

All possible intact configurations, including different fuel enrichments and rod geometries, optimum moderation conditions, and neutron absorber distribution were investigated. The results of three-dimensional Monte Carlo calculations from the criticality analyses showed the requirement of $k_{\text{eff}} + 2\sigma$ less than or equal to 0.93 is satisfied for any credible configurations of TRIGA fuel. In the intact configuration, the presence of Gd in the DOE SNF canister basket is not necessary to meet this requirement.

A number of parametric analyses were run to address or bound the degraded configuration classes. These parametric analyses addressed identification of optimum moderation, optimum spacing, optimum fissile concentration, and neutron absorber concentration/distribution requirements.

The results for the degraded analysis indicate that the highest k_{eff} is achieved if the fuel rods are intact in the degraded DOE SNF canister (basket fully degraded). This configuration results in $k_{\text{eff}} + 2\sigma$ of less than or equal to 0.93 with at least 8.9 kg Gd included in the DOE SNF canister. The state of the other internal components of the waste package has a negligible impact on k_{eff} .

In summary, 111 rods of the most reactive TRIGA SNF with 8.9 kg Gd in the DOE SNF canister basket can be disposed of in the 5-DHLW/DOE spent nuclear fuel waste package without any criticality concern. The analyzed intact and degraded waste package configurations cover all anticipated scenarios. Bounding cases have been used for analyzing the configuration classes that include a great number of variations. All calculations are based on a maximum mass of 15.2 kg of ^{235}U in a waste package. Table 10-6 presents a summary of the criticality and geochemistry results with a focus on the correspondence with the degradation classes and resultant configuration classes presented in *Disposal Criticality Analysis Methodology Topical Report* (YMP 2003). The results of the geochemistry analyses show for all cases investigated (IP-1, IP-2 and IP-3 scenarios) the loss ranges were U: 0 to 99.9 percent and Gd: 0 to 53 percent

and that the degradation in sequence resulted in essentially no loss of Gd, and a few percent loss of U from the SNF (CRWMS M&O 2000b, Section 8.4).

The criticality model (MCNP code and appropriated selected neutron cross-section libraries) used in analyzing the configurations of the waste package containing TRIGA SNF was validated using the methodology described in *Disposal Criticality Analysis Methodology Topical Report* (YMP 2003). Current results indicate that the lower bound tolerance limit is well above the interim critical limit used in evaluating the design.

Table 10-6. Summary of Geochemistry and Criticality Analyses for Internal Configurations (Phase I and II) of the Waste Package Containing TRIGA Spent Nuclear Fuel

Master Scenario	Description	Configuration Classes and Summary Description	Summary of Geochemistry Calculations	Summary of Criticality and Criticality Model Validation Results			
				$(k_{eff}+2\sigma)_{max}$	Interim Critical Limit	Lower Bound Tolerance Limit	Comments
Initial water intrusion	Initial stage; water fills all available spaces inside the waste package and DOE SNF canister	Intact flooded configurations: SNF and internal structures not degraded	N/A	0.7890	0.93	0.9668 for $0 < AENCF < 0.0404$ -0.3315 * AENCF + 0.9788 for $0.0404 < AENCF < 0.0922$ (heterogeneous moderated configurations)	No Gd needed for intact case.
IP-1	The top of the waste package is breached and liquid accumulates inside	Configuration class #6: SNF partially degraded in place (various stages)		0.8158	0.93	0.9668 for $0 < AENCF < 0.0404$ -0.3315 * AENCF + 0.9788 for $0.0404 < AENCF < 0.0922$ (heterogeneous moderated configurations)	No Gd needed
		Configuration class #3: SNF partially or totally degraded inside the waste package with intact internal structures					
IP-2	SNF degrades before the internals of the waste package	Configuration class #2: Both SNF and internal structures of the waste package degraded (various stages)	For all cases investigated (IP-1, IP-2 and IP-3 scenarios) the loss ranges were: U: 0 to 99.9% Gd: 0 to 53 %.	0.6359	0.93	0.9796 (homogeneous moderated configurations)	No Gd needed
		Configuration class #1: SNF intact (as assembly or pins) and degraded internal structures (various stages)					
IP-3	SNF degrades after the internals of the waste package			0.9146	0.93	0.9668 for $0 < AENCF < 0.0404$ -0.3315 * AENCF + 0.9788 for $0.0404 < AENCF < 0.0922$ (heterogeneous moderated configurations)	4.1kg of Gd needed homogenized in layer of clay that covers fuel.
IP-4	The bottom of waste package is penetrated allowing liquid to flow through	The configurations resulting from these scenarios (configurations classes #4, #5) have not been investigated in the geochemistry and criticality analyses due to the fact that they are less moderated (no pooling of water) and All cases are bounded by IP-1, IP-2 and IP-3 as the latter have better moderation (water is pooling inside waste package), and more favorable conditions for neutron absorber loss.					
IP-5	SNF degrades concurrently with the internals of the waste package						
IP-6	SNF degrades after the internals of the waste package						

10.3 SHIPPINGPORT PWR SNF

The description and main characteristics of the waste package containing Shippingport PWR SNF are presented in Section 3.2.3. In this section a summary of the results of the criticality analyses performed is presented together with the current status of the validation of the criticality model for the configurations that are specific to the codisposal of this fuel group.

The first step in applying the criticality model to the specific intact and degraded configurations of this waste package is identification and characterization of the specific configurations anticipated for postclosure. The results of the degradation analysis coupled with the geochemistry calculations (CRWMS M&O 2000c, Section 6) provided an insight into the possible arrangements and compositions of the degraded materials placed within the waste package. All configuration classes analyzed and the most probable degradation scenario that was identified are summarized in the next section (Section 10.3.1). The results of the criticality calculations for the most representative intact and degraded configurations are presented in Section 10.3.2. The limiting cases identified during the analysis are also providing the basis for deriving the final design solution (amount of neutron absorber to be distributed within the initial waste package). The range of parameters that characterize the limiting or the most reactive cases is subsequently used in the process of validation of the criticality model. The process includes selection of appropriate critical benchmark experiments and derivation of the specific lower tolerance bound limit for each major group of configurations.

The results of three-dimensional Monte Carlo calculations from the intact and degraded component criticality analyses show that the requirement of $k_{\text{eff}} + 2\sigma$ less than or equal to 0.93 is satisfied for one Shippingport PWR fuel assembly in the DOE SNF canister. This configuration, which corresponds to the baseline design, does not need any neutron absorber in the basket or elsewhere in the waste package to meet this requirement (CRWMS M&O 2000c, Section 7.5).

The total mass of fissile element (^{235}U) in a waste package should not exceed 19.5 kg of ^{235}U per DOE SNF canister, with total ^{235}U to ^{238}U ratio of 13.7 (93.5 percent enriched in ^{235}U), or less. In addition, the linear density of the fissile (^{235}U) should not exceed 79 g/cm, which is calculated by dividing the total fissile mass (19.5 kg ^{235}U) by the active fuel length (246.38 cm) (CRWMS M&O 2000c, Section 8.6).

10.3.1 Degradation Scenarios and Configurations

Based on the corrosion rates and the material thicknesses that are given in Table 10-7, the most probable degradation path for the waste package, the DOE SNF canister, and the Shippingport PWR SNF follows the following sequence (CRWMS M&O 2000c, Section 6.2.1.1):

1. The waste package is penetrated and flooded internally. The waste package basket (inner brackets and support tube) is likely to degrade first because of the A516 carbon steel material.
2. DHLW glass stainless steel shell and glass begin to degrade. After this, there are two degradation paths.

- 2a. DOE SNF canister stays intact. Intact DOE SNF canister and intact SNF assembly fall on top of degraded products near the bottom of the waste package.
- 2b. DOE SNF canister starts to degrade.
3. DOE SNF canister is penetrated and flooded inside.
4. DOE SNF canister basket and SNF assembly gets in contact with water.
5. SNF plates get in contact with water.
6. DOE SNF canister basket degrades. After this, there are two paths:
 - 6a. SNF assembly and plates stay intact and fall on top of degraded DOE SNF canister basket and settle on the bottom of the DOE SNF canister.
 - 6b. DOE SNF canister degrades. Intact SNF assembly and plates fall and scatter on top of all degradation products near the bottom of the waste package. There could be some separation between the stainless steel and fuel assembly.

Given a very long period of time, it is postulated that everything will degrade including cladding and fuel. This corresponds to degradation scenario group IP-2. This is not likely because of very long lifetime of Zircaloy-4, which will most likely outlast the waste package. To bound the potential degraded cases, degradation of the SNF can be considered. The degraded SNF and other degradation products could mix and pile up near the bottom of waste package. However, there is no mechanism to cause complete and uniform mixing of all the degradation products inside the waste package.

Table 10-7. Materials and Thicknesses

Components	Material	Thickness (mm)
Waste Package basket	A516 Carbon Steel	12.7
Waste Package inner bracket	A516 Carbon Steel	25.4
Waste Package support tube	A516 Carbon Steel	31.75
DHLW glass shell	Stainless Steel Type 304L	9.5
DHLW glass	Glass	N/A
DOE SNF canister	Stainless Steel Type 316L	9.5
DOE SNF canister basket	Stainless Steel Type 316L	9.5
SNF cover plate	Zircaloy-4	0.52
Neutron absorber (in wafer form)	Borated Stainless Steel	0.91
SNF (wafer form)	UO ₂ -ZrO ₂ -CaO ₂	0.91
SNF wafer coating	Pyrolytic carbon	a few microns

Source: CRWMS M&O 1999t; DOE 1999d

The configurations investigated can be categorized using the description of the generic configuration classes given in Section 3.3.1 of *Disposal Criticality Analysis Methodology Topical Report* (YMP 2003). As indicated in Section 6.5 for the purpose of fully identifying the potential for criticality, all representative configurations classes have been analyzed and not only

the configurations resulting from the most probable degradation path presented above. The next subtitles follow the original description given in Sections 6.2.1.2 through 6.2.1.7 of *Evaluation of Codisposal Viability for HEU Oxide (Shippingport PWR) DOE-Owned Fuel (CRWMS M&O 2000c)*.

Degraded DOE SNF Canister Basket and Intact SNF—For these cases of intact fuel assembly within degraded basket, the scenarios and configuration classes are applied to the DOE SNF canister and its contents. This configuration is a variation of configuration class 1 and can be reached from standard scenario IP-3.

Intact DOE SNF Canister and Degraded Waste Package Internals—In this case, the concepts of scenario and configuration are applied to the entire waste package. The fuel assembly and the DOE SNF canister internals are intact. This configuration is a variation of configuration class 1 and can be reached from standard scenario IP-3.

Degraded DOE SNF Canister and Waste Package Internals—In this case, the concepts of scenario and configuration are applied to the entire waste package. The DOE SNF canister, waste package internals, and DHLW glass canisters are degraded. The fuel assembly is intact. This configuration is achievable because of very low degradation rate of Zircaloy-4, which envelops and protects the fuel. This configuration is a variation of configuration class 1 and can be reached from standard scenario IP-3.

Intact DOE SNF Canister and Waste Package Internals and Degraded SNF—For these cases of degraded fuel assembly within intact basket, the scenarios and configuration classes are applied to the DOE SNF canister and its contents. This configuration is a variation of configuration class 6 and can be reached from standard scenario IP-1.

Intact Waste Package Internals and Degraded DOE SNF Canister and SNF—For these cases of degraded fuel assembly within degraded basket, the scenarios and configuration classes are applied to the DOE SNF canister and its contents. This configuration is a variation of configuration class 3 and can be reached from standard scenario IP-1.

Completely Degraded DOE SNF Canister and Waste Package Internals—In this case, the concepts of scenario and configuration are applied to the entire waste package. Degradation products from the DOE SNF canister and contents form a layer on the bottom of the waste package. The degradation products (clay) from waste package internals and DHLW glass canisters form a layer above. This configuration is a variation of configuration class 2 and can be reached from standard scenarios IP-1, IP-2, and IP-3.

The most probable degradation configuration is the one with the degradation of all components inside the waste package and the DOE SNF canister. The SNF assembly remains intact and positioned on the bottom of the waste package (CRWMS M&O 2000c, Section 7.4.1.3). The degradation scenario of IP-1 (i.e., SNF degrades faster than the other materials) is not probable, since the SNF is sealed inside the Zircaloy-4 plates, which practically do not degrade as compared to stainless steel.

10.3.2 Criticality Calculations and Results

10.3.2.1 Results for Intact Mode

This section summarizes, the criticality analyses for intact mode (phase I) (CRWMS M&O 2000c, Section 7.3). Although the components (fuel plates, assembly, and DOE SNF canister) are considered structurally intact, water intrusion into the available internal volume is assumed in order to determine the highest k_{eff} resulting from optimum moderation. It must be noted that no credit for burnable poison material (boron) is taken in any of the calculations that are analyzed in this section.

The intact canister with the intact fuel cluster is represented in the intact waste package as shown in Figure 10-9. The k_{eff} of the intact fuel cluster is calculated based on the fuel cluster centered in the DOE SNF canister and the DOE SNF canister centered inside the waste package. The DOE SNF canister is assumed to be fully flooded internally, and reflected externally (outside of the waste package) with water. The highest $k_{\text{eff}} + 2\sigma$ of 0.8437 is obtained with water with 1.0 g/cm^3 density in both the DOE SNF canister and the waste package (CRWMS M&O 2000m, Section 6.1.1). The density of water in the center cruciform area only is also varied to determine the effect of water density around the fuel assembly. The results indicated that decreasing the density of water in the cruciform area results in decrease in k_{eff} . Therefore, in all configurations in the following sections the DOE SNF canister and the waste package are modeled as being flooded.

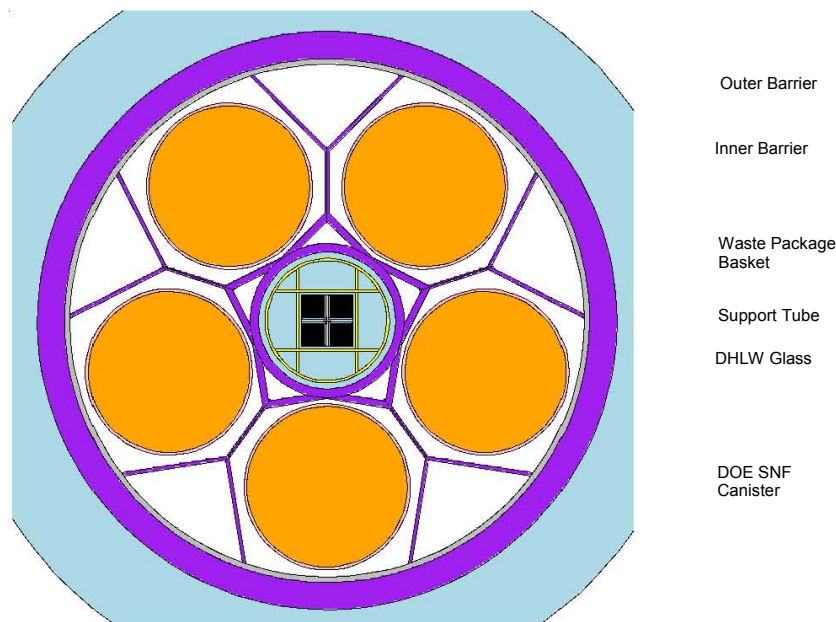


Figure 10-9. Cross-Section View of the 5-DHLW/DOE Spent Nuclear Fuel-Long Waste Package

In all cases the waste package is water reflected. Water intrusion into plate void space (with 1.0 g/cm^3 density) increases k_{eff} by approximately 3 percent with a maximum $k_{\text{eff}} + 2\sigma$ of 0.8678 (CRWMS M&O 2000m, Section 6.1.2). Water intrusion into fuel wafer porosity volume (with 1.0 g/cm^3 density) increases k_{eff} by approximately 2 percent with a maximum $k_{\text{eff}} + 2\sigma$ of 0.8574 (CRWMS M&O 2000m, Section 6.1.2). Water intrusion into both of these regions

simultaneously increases k_{eff} by approximately 5 percent with a maximum $k_{\text{eff}} + 2\sigma$ of 0.8819 (CRWMS M&O 2000m, Section 6.1.2).

10.3.2.2 Results for Degraded Guide Plates

The guide plates, which comprise the DOE SNF canister basket are represented as being completely degraded and converted into goethite. This configuration is characterized by a degraded DOE SNF canister basket and intact SNF configuration as described in Section 10.2.3.1 and corresponds to the configuration class 1. Figure 10-10 shows the cross-section view of the waste package in this configuration. The highest $k_{\text{eff}} + 2\sigma$ of 0.9042 is obtained when the DOE SNF canister is filled with only water at 1 g/cm³ density (goethite volume fraction of 0) (CRWMS M&O 2000m, Table 6-6.)

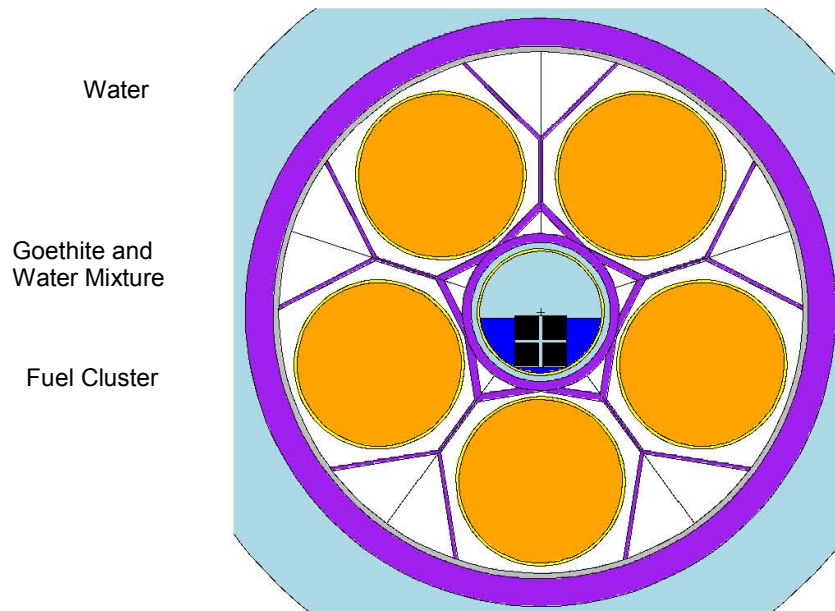


Figure 10-10. Cross-Section View of the Configuration with Degraded Guide Plates and Intact Spent Nuclear Fuel

10.3.2.3 Results for Degraded Fuel Cluster

The Shippingport PWR SNF cluster is degraded for all cases in this section. Partially and fully degraded fuel cases are calculated. The partial degradation is represented as a fraction of fuel ($\text{UO}_2\text{-ZrO}_2\text{-CaO}$) redistributed outside the fuel plates and homogeneously mixed with water, goethite, and/or clay. The fuel cluster is assumed to be physically intact in the partial degradation calculations. The fully degraded fuel is represented as a homogeneous mixture of UO_2 , water, goethite, and clay. The degraded fuel is assumed to be chemically unchanged. The waste package is assumed to be fully reflected by water for all cases.

The degradation configurations presented in this section are for analyzing the effect of the generic degradation scenario group IP-1 (i.e., SNF degrades faster than the other surrounding components). As discussed in Section 10.3.1, the degradations associated with IP-1 are not probable since for Shippingport PWR the SNF is sealed inside the highly corrosion resistant material of Zircaloy-4, which is considered inert.

Partially Degraded Fuel Cluster in the Intact DOE SNF Canister—The fuel cluster is partially degraded and $\text{UO}_2\text{-ZrO}_2\text{-CaO}$ is redistributed into the coolant channels and the cruciform areas as well as into the central-basket area of the canister. The central-basket area is the central square area excluding the fuel cluster. The redistributed fuel (ranging from 10 to 99 percent of the total fuel mass) is mixed with water in the coolant channel, the cruciform, and/or central-basket areas. The remaining portion of the fuel mass stays inside the fuel plates. This configuration is characterized by intact DOE SNF canister and waste package internals and degraded SNF as described in Section 10.2.3.1 and corresponds to the configuration class 6.

The k_{eff} for the configuration with 10 percent of the fuel redistributed (due to aqueous transport) into the coolant channel, cruciform, and central-basket areas is first calculated. It is observed that the 10 percent fuel redistribution to the coolant channel, cruciform, and the central-basket areas results in the largest $k_{\text{eff}} + 2\sigma$ (0.8736) compared to the fuel redistribution to the coolant channel only (0.8460), or to the coolant channel and the cruciform areas (0.8625). Therefore, when the fuel redistribution fraction is varied from 10 to 99 percent, the redistributed fuel is placed in the coolant channel, cruciform, and central-basket areas. The results indicate that k_{eff} increases as the amount of redistributed fuel increases (CRWMS M&O 2000m, Table 6-12). The highest $k_{\text{eff}} + 2\sigma$ of 0.9300 is obtained with 80 percent fuel redistribution. This would require essentially all the cladding to fail and expose the fuel wafers, which is extremely unlikely as discussed in Section 6.4.1.1.

Partially Degraded Fuel Cluster in Degraded DOE SNF Canister—The partially redistributed fuel is mixed with goethite and water with varying volume fraction simulating degradation of the guide plates and the canister. This configuration is characterized by intact waste package internals and degraded DOE SNF canister and SNF as described in Section 10.3.1 and corresponds to the configuration class 3. Figure 10-11 gives a representation of this partial degradation case. The fuel cluster is physically intact in this representation. The coolant channel and cruciform areas of the fuel cluster are filled with water instead of goethite and water mixture.

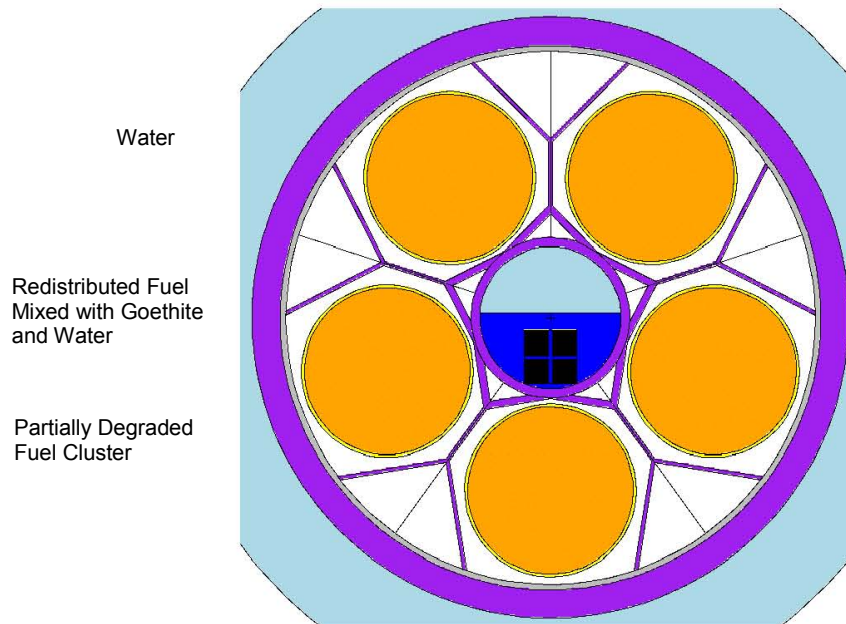


Figure 10-11. Partially Degraded Fuel Cluster in the Waste Package

The results indicate that varying the fraction of fuel that is redistributed through aqueous transport effects the k_{eff} by as much as 28 percent with a maximum $k_{\text{eff}} + 2\sigma$ of 0.9188 with 40 percent fuel redistribution (CRWMS M&O 2000m, Table 6-13). This configuration does not contain any water mixed with the fuel/goethite mixture. Varying the amount of water mixed with the fuel/goethite mixture effects the k_{eff} by as much as 1 percent with a maximum $k_{\text{eff}} + 2\sigma$ of 0.9254 with 40 percent fuel redistribution and 40 percent water in the fuel/goethite/water mixture. The effect of having redistributed fuel, goethite, and water mixture in the coolant channel and cruciform control rod channel areas instead of water is also investigated. Replacing water with fuel/goethite/water mixture reduces k_{eff} by as much as 21 percent. As described in Section 10.3.1 this level of fuel redistribution is extremely unlikely.

10.3.2.4 Results for Degraded Configurations Postulated Beyond the Regulatory Period

The degradation and criticality analyses performed have also investigated configurations that require very long times to be attained. These configurations are anticipated to happen well beyond the regulatory period of 10,000 years but they have been analyzed to fully investigate the potential for criticality of the waste package containing Shippingport PWR. For the purpose of this document, these results (CRWMS M&O 2000c, Sections 7.4.1.2, 7.4.1.3, 7.4.2.3, and 7.4.2.4) have been summarized and grouped together in this section.

Clay Accumulation Inside DOE SNF Canister—Effect of clay intrusion into the canister is calculated based on total degradation of the DHLW glass pour canisters and retained integrity of the canister. The canister is positioned at the bottom of the inner barrier of the waste package. This configuration is characterized by intact DOE SNF canister and degraded waste package internals as described in Section 10.3.1 and corresponds to the configuration class 1. The results show that the k_{eff} is highest when there is no clay in the DOE SNF canister with maximum $k_{\text{eff}} + 2\sigma$ of 0.8429 (CRWMS M&O 2000m, Table 6-8.)

Intact Fuel Cluster with Degraded DOE SNF Canister and Waste Package—In these configurations, the materials surrounding the fuel cluster degrade faster than the fuel, which is likely given the extremely low degradation rate of Zircaloy-4. The DOE SNF canister shell, five DHLW glass pour canisters, waste package basket, and the DOE SNF canister basket are fully degraded. The canister is positioned on the bottom of the waste package before being degraded. This configuration is characterized by degraded DOE SNF canister and waste package internals as described in Section 10.3.1 and corresponds to the configuration class 1. The results show that the maximum $k_{\text{eff}} + 2\sigma$ is 0.922 with goethite, clay, and water fractions of 0.0, 1.0, and 0.0, respectively (CRWMS M&O 2000m, Table 6-9).

Partially Degraded Fuel Cluster with Degraded Canister and Degraded Waste Package—In this scenario, the fuel materials and everything surrounding the fuel degrades at the same rate. The partially degraded fuel (UO_2) is mixed with degradation products from guide plates, DOE SNF canister, waste package basket, DHLW glass pour canisters, and DHLW glass. This configuration is characterized by completely degraded DOE SNF Canister and waste package internals as described in Section 10.3.1 and corresponds to the configuration class 2. The results show that a maximum $k_{\text{eff}} + 2\sigma$ of 0.9194 is obtained when the fuel redistribution fraction is 0.3.

Fully Degraded Fuel in Degraded Canister and Degraded Waste Package—The fully degraded fuel (UO₂) is mixed with goethite, clay, and water. The degraded fuel contains 20.923 kg uranium with effective enrichment of 93.2 wt percent. The fuel, goethite, clay, and water mixture layer is placed on the bottom of the waste package. This configuration is characterized by completely degraded DOE SNF canister and waste package internals as described in Section 10.3.1 and corresponds to the configuration class 2. The results indicate that as the amount of clay in the mixture is increased the k_{eff} decreases. The highest $k_{\text{eff}} + 2\sigma$ of 0.8463 is obtained with no clay or water in the fuel/goethite mixture (CRWMS M&O 2000m, Table 6-16).

10.3.3 Range of Parameters for Configurations of Waste Package Containing Shippingport PWR DOE SNF

ANSI/ANS-8.1-1998 and *Disposal Criticality Analysis Methodology Topical Report* (YMP 2003) provide basic requirements for validation of a calculational method used in the criticality analysis of a system. The bias of a code system (in this case the criticality model containing the computer code MCNP and selected cross-section libraries) is determined by correlating the results of critical and near-critical experiments with calculated results for those experiments. The common practice, and that considered by the current validation methodology (BSC 2003e), is for comparison of the calculated k_{eff} to a critical or near critical system.

Prior to the initiation of the validation activity, the operating conditions and parameters for which the validation is to apply must be identified. The fissile isotope, enrichment of fissile isotope, fuel density, chemical form of fuel, types of neutron moderators and reflectors, range of moderator to fissile isotope ratio, neutron absorbers, and physical configurations are among the parameters to specify. These parameters will define the area of applicability for the selection of the critical experiments for the validation effort.

The preliminary degradation analysis of the contents of the waste package containing Shippingport PWR SNF (CRWMS M&O 2000c, Section 6) and the subsequent criticality analysis performed for the resulting internal configurations have followed the guidance suggested by the Internal Criticality Master Scenarios presented in *Disposal Criticality Analysis Methodology Topical Report* (YMP 2003, Section 3.3) and also by *Generic Degradation Scenario and Configuration Analysis for DOE Codisposal Waste Package* (CRWMS M&O 1999g). The resultant configuration classes internal to the waste package have been screened systematically for their criticality potential in comprehensive criticality analyses (CRWMS M&O 2000m). The main results have been summarized in the above sections.

For the purpose of criticality model validation for the configurations specific to the waste package containing Shippingport PWR SNF and identification of the range of parameters that characterize representative internal configurations of the degraded waste package, the most reactive configurations identified during the screening of the criticality potential have been selected. These comprise various arrangements of the intact and partially degraded fuel mixed with water and/or hydrated products. The configurations, described in Sections 7.4.1.1, 7.4.2.1, 7.4.2.2, and 7.4.1.3 of *Evaluation of Codisposal Viability for HEU Oxide (Shippingport PWR) DOE-Owned Fuel* (CRWMS M&O 2000c) have the fuel contained inside DOE SNF canister or settled at the bottom of the waste package. These configurations represent refinements of the general configuration classes 1, 3 and 6 that are described in Section 6.3.3.1. The voids inside the

fuel assembly are filled with water, degraded fuel or degradation products and clayey material. All other configurations, do not show any criticality potential (e.g., $k_{\text{eff}}+2\sigma$ is much lower than the interim critical limit) and thus have not been considered in the validation process.

The process employed in *Intact and Degraded Criticality Calculations for the Codisposal of Shippingport PWR Fuel in a Waste Package* (CRWMS M&O 2000m) for investigating the potential for criticality of the possible degraded configurations of the waste package used a screening approach, the goal being to identify the most reactive configurations in a given class of degraded configurations. Due to this approach, the number of configurations analyzed varies among the classes of configurations depending on the complexity of the possible arrangements and the initial screening results. Selected cases (typically the most reactive or the limiting cases as presented in CRWMS M&O 2000c, Section 7) have been rerun with tallies calculating the neutron flux and the fission rate in the regions containing the fissile material. The results of the cases that were rerun with tallies are summarized in Table XI-3 of *Criticality Model Report* (BSC 2003e) together with a summary of the key physical and neutronic parameters characterizing the most reactive configurations (ROP).

10.3.4 Selection of the Criticality Benchmark Experiments

The benchmark experiments selected in the validation of the criticality model used for the analysis of the waste package containing Shippingport PWR come from *International Handbook of Evaluated Criticality Safety Benchmark Experiments* (NEA 2001) unless otherwise noted. The selection process was initially based on previous knowledge regarding the possible configurations of degraded waste package, and the subsets have been constructed to accommodate large variations in the range of parameters of the configurations and also to provide adequate statistics for lower bound tolerance limit calculations. The selected benchmark experiments for each subset are presented in *Benchmark and Critical Limit Calculation for DOE SNF* (BSC 2002c) together with the MCNP cases constructed and the results of the calculations. For the present application (codisposal of Shippingport PWR SNF), the selected benchmark experiments include only moderated heterogeneously. The cases, corresponding k_{eff} results and their uncertainties are summarized in *Analysis of Critical Benchmark Experiments and Critical Limit Calculation for DOE SNF* (BSC 2003f, Attachment II). Table 10-8 presents the list of the benchmark experiments and the number of cases for each subset selected for validation of the criticality model for Shippingport PWR SNF.

The experiments listed in Table 10-8 are considered appropriate to represent intact (non degraded) configurations and partially degraded configurations of the waste package containing Shippingport PWR SNF that belong to the configuration classes 1, 3, and 6. Their range of applicability is detailed in Attachment XI of *Criticality Model Report* (BSC 2003e).

Table 10-8. Critical Benchmarks Selected for Validation of the Criticality Model for Shippingport PWR Spent Nuclear Fuel

Subset	Benchmark Experiment Identification ^a	Number of Cases Included
Heterogeneous moderated ^b	HEU-MET-THERM-006	23
	HEU-COMP-THERM-003	15
	HEU-COMP-THERM-005	1
	HEU-COMP-THERM-006	3
	HEU-COMP-THERM-007	3
	HEU-COMP-THERM-008	2
	HEU-COMP-THERM-010	21
	HEU-COMP-THERM-011	3
	HEU-COMP-THERM-012	2
	HEU-COMP-THERM-013	2
	HEU-COMP-THERM-014	2

Source: Subset defined in BSC 2002c

NOTE: ^a The convention for naming the benchmark experiments is from NEA 2001.
^b Identification of the subset from BSC 2002c has been changed to better reflect the subset's main characteristics. The benchmark experiments in the subset have not been affected.

10.3.5 Comparison Between ROA of Benchmark Experiments and ROP

The validation of the criticality model needs to show that the range of the fundamental parameters of the benchmark critical experiments (ROA) and the range of the fundamental parameters of the system (ROP) evaluated are nearly identical. This is not usually practical, and for those parameters that do not show a trend in the bias, it is acceptable to use critical benchmark experiments that cover most, but not all, of the ROP of the system under evaluation. In these situations, expert judgment may be used to determine if there is a reasonable assurance that the two are sufficiently close. In cases where a trend in the bias is identified, the ROA can be extended, but a penalty on the critical limit determined for the subset of benchmark experiments needs to be evaluated and applied.

The comparison between ROA and ROP was focused on the benchmark experiments selected to cover the most reactive cases of the analyzed configurations of the waste package containing Shippingport PWR SNF.

The comparison of ROA vs. ROP for the heterogeneous moderated configurations is detailed in Attachment XI of *Criticality Model Report* (BSC 2003e). The collective area of applicability of the selected critical benchmarks is based on the information regarding ROA of the benchmark experiments included in Tables XI-6 and XI-7 of *Criticality Model Report* (BSC 2003e).

The findings from the comparison in ROP vs. ROA can be summarized as follows:

- The ROA for this subset of experiments covers the ROP for the majority of parameters that characterize the heterogeneous configurations. The coverage in the spectral

parameters indicates the validity of the range of applicability of the selected group of critical benchmarks over the ROP of the most reactive configurations.

10.3.6 Calculation of the Lower Bound Tolerance Limit

The following results are excerpted from *Analysis of Critical Benchmark Experiments and Critical Limit Calculation for DOE SNF* (BSC 2003f), which present in detail the methodology and calculations performed for evaluating the lower bound tolerance limit for each set of configurations of the waste package containing Shippingport PWR SNF.

The results of the trending parameter analysis for the critical benchmark subset representative for moderated intact (heterogeneous) configurations of the waste package containing Shippingport PWR DOE SNF are presented in Attachment XI of *Criticality Model Report* (BSC 2003e). The results show that the pool of k_{eff} values calculated with the criticality model for this subset of benchmark experiments (moderated heterogeneous subset) does show trending.

The value calculated with the lower bound tolerance limit function for the benchmarks applicable to intact-moderated configurations of Shippingport PWR DOE SNF is:

$$\begin{aligned} \text{lower bound tolerance limit} &= 0.969 && \text{for } 0 < \text{AENCF} < 0.0278 \\ \text{lower bound tolerance limit} &= -0.2336 * (\text{AENCF}) + 0.9755 && \text{for } 0.0278 < \text{AENCF} < 0.0922 \end{aligned}$$

The above results and the comparison of ROA vs. ROP indicate that the criticality model is partially validated for use in assessing the criticality potential of the intact (nondegraded) configurations and of the configurations belonging to the general configurations classes 1, 3, and 6 for the degraded waste package containing Shippingport PWR DOE SNF.

10.3.7 Summary of Criticality Model Results and Validation for the Waste Package Containing Shippingport PWR SNF

All aspects of intact and degraded configurations, including optimum moderation conditions, water intrusion into the fuel plates, and positioning of the fuel assembly were investigated. The results of three-dimensional Monte Carlo calculations from the intact and degraded component criticality analyses show that the requirement of $k_{\text{eff}} + 2\sigma$ less than or equal to 0.93 is satisfied for one Shippingport PWR fuel assembly in the DOE SNF canister. This configuration does not need any neutron absorber in the basket or elsewhere in the waste package to meet this requirement.

The results from the criticality analysis for the degraded DOE SNF canister (fissile material distributed in the waste package) indicate that the highest k_{eff} is achieved if the fuel and clay layers do not mix. Therefore, the amount of clay in the waste package has no effect on the bounding case, which is a layer of optimally moderated degraded fuel not mixed with any clay. Although varying the amount of water mixed with the fuel changes the k_{eff} , the peak $k_{\text{eff}} + 2\sigma$ of the system is less than 0.85, which is well below the interim critical limit.

The total mass of fissile element (^{235}U) is 19.5 kg of ^{235}U per DOE SNF canister, with total ^{235}U to ^{238}U ratio of 13.7 (93.5 percent enriched in ^{235}U). In addition, the linear density of the fuel

(²³⁵U) is 79 g/cm, which is calculated by dividing the total fuel mass (19.5 kg ²³⁵U) by the active fuel length (246.38 cm).

Table 10-9 presents a summary of the criticality and geochemistry results with a focus on the correspondence with the degradation classes and resultant configuration classes presented in *Disposal Criticality Analysis Methodology Topical Report* (YMP 2003).

The criticality model (MCNP code and appropriated selected neutron cross-section libraries) used in analyzing the configurations of the waste package containing Shippingport SPWR SNF was validated using the methodology described in *Disposal Criticality Analysis Methodology Topical Report* (YMP 2003) and *Criticality Model Report* (BSC 2003e). Current results indicate that the lower bound tolerance limit is well above the interim critical limit used in evaluating the design.

Table 10-9. Summary of Geochemistry and Criticality Analyses for Internal Configurations (Phase I and II) of the Waste Package Containing Shippingport PWR Spent Nuclear Fuel

Master Scenario	Description	Configuration Classes and Summary Description	Summary of Geochemistry Calculations	Summary of Criticality and Criticality Model Validation Results			
				$(k_{eff} + 2\sigma)_{max}$	Interim Critical Limit	Lower Bound Tolerance Limit	Comments
Initial water intrusion	Initial stage: water fills all available spaces inside the waste package and DOE SNF canister	Intact flooded configurations: SNF and internal structures not degraded	N/A	0.8437	0.93	0.969 for $0 < AENCF < 0.0278$; $0.2336 * (AENCF) + 0.9755$ for $0.0278 < AENCF < 0.0922$ (heterogeneous moderated configurations)	The highest $k_{eff} + 2\sigma$ is obtained with 80% fuel redistribution. This would require essentially all the cladding to fail and expose the fuel wafers, which is extremely unlikely per (CRWMS M&O 2000c)
		Configuration class #6: SNF partially degraded in place (various stages)		0.9300	0.93	0.969 for $0 < AENCF < 0.0278$; $0.2336 * (AENCF) + 0.9755$ for $0.0278 < AENCF < 0.0922$ (heterogeneous moderated configurations)	
IP-1	SNF degrades before the waste package internals	Configuration class #3: SNF partially or totally degraded inside the waste package with intact internal structures	For all cases investigated (IP-1, IP-2 and IP-3 scenarios) the U loss range was 0.06 to 100%	0.9254	0.93	0.969 for $0 < AENCF < 0.0278$; $0.2336 * (AENCF) + 0.9755$ for $0.0278 < AENCF < 0.0922$ (heterogeneous moderated configurations)	Due to high corrosion resistance of Zy-4 cladding, SNF will degrade after internal structures of the DOE SNF canister per (CRWMS M&O 2000c). The configuration assumed that 40% of the fissile migrated outside the fuel.
	The top of the waste package is breached and liquid accumulates inside	Configuration class #2: Both SNF and internal structures of the waste package degraded (various stages)		0.9194	0.93	Not evaluated.	
IP-2	SNF degrades concurrently with the waste package internals	Configuration class #1: SNF intact (as assembly or pins) and degraded internal structures (various stages)		0.9220	0.93	0.969 for $0 < AENCF < 0.0278$; $0.2336 * (AENCF) + 0.9755$ for $0.0278 < AENCF < 0.0922$ (heterogeneous moderated configurations)	
	SNF degrades after the waste package internals						
IP-3	SNF degrades before the waste package internals						
	SNF degrades concurrently with the waste package internals						
IP-4	SNF degrades after the waste package internals						
	The bottom of waste package is penetrated allowing liquid to flow through						
IP-5	SNF degrades concurrently with the waste package internals						
	SNF degrades after the waste package internals						
IP-6							

10.4 ENRICO FERMI

The description and main characteristics of the waste package containing Enrico Fermi SNF are presented in Section 3.2.4. In this section a summary of the results of the performed criticality analyses is presented together with the current status of the validation of the criticality model for the configurations that are specific to the codisposal of this fuel group.

The first step in applying the criticality model to the specific intact and degraded configurations of this waste package is identification and characterization of the specific configurations anticipated for postclosure of the repository. The results of the degradation analysis coupled with the geochemistry calculations (CRWMS M&O 2000d, Section 6) provided an insight into the possible arrangements and compositions of the degraded materials placed within the waste package. All configuration classes analyzed and the most probable degradation scenario that was identified are summarized in the next section (Section 10.4.1). The results of the criticality calculations for the most representative intact and degraded configurations are presented in Section 10.4.2. The limiting cases identified during the analysis are also providing the basis for deriving the final design solution (amount of neutron absorber to be distributed within the initial waste package). The range of parameters that characterize the limiting or the most reactive cases is subsequently used in the process of validation of the criticality model. The process includes selection of appropriate critical benchmark experiments and derivation of the specific lower tolerance bound limit for each major group of configurations.

The results of three-dimensional Monte Carlo criticality calculations for all anticipated intact and degraded configurations show that the requirement of $k_{\text{eff}}+2\sigma$ less than or equal to the interim critical limit of 0.93 is satisfied for the Enrico Fermi waste package with at least 3.0% by volume of gadolinium phosphate (14.5 kg GdPO₄) uniformly distributed in the initial iron shot-GdPO₄ filler.

All calculations are based on a maximum of 4.817 kg of ²³⁵U per -01 canister (one pipe). The analyses are based on the fuel pin type that has the highest uranium enrichment (25.69% in ²³⁵U). The degraded configurations of the Enrico Fermi SNF bound the other types of U-Zr and U-Mo (HEU) DOE-owned SNF, as long as the limits on mass of uranium and its enrichment, and the linear density, are not exceeded. Hence, the total mass of fissile element (²³⁵U) should not exceed the mass used in deriving the conclusions of this report, which is 115.6 kg of ²³⁵U per DOE SNF canister. The linear density of the ²³⁵U should not exceed 62 g/cm in each of the 24 pipes. This value is calculated by dividing the total fuel mass by the number of 4-in-diameter pipes and by the active length of the Enrico Fermi fuel pin.

10.4.1 Degradation Scenarios and Configurations

Based on the corrosion rates and the material thickness given in Table 10-10 below, the most probable degradation path for the waste package, the DOE SNF canister and the Enrico Fermi spent nuclear fuel follows the sequence (CRWMS M&O 2000d, Section 6.2.1.1):

1. Waste package is penetrated and flooded internally. The waste package basket (outer and inner brackets and support pipe) degrades first, because of the high corrosion rate for A 516 carbon steel.

2. DHLW glass canister's stainless steel shell and glass begin to degrade. After this, there are two degradation paths:
 - 2a. DOE SNF canister stays intact. Intact DOE SNF canister and intact SNF assembly fall on top of degraded products near the bottom of the waste package.
 - 2b. DOE SNF canister starts to degrade.
3. DOE SNF canister is penetrated and flooded.
4. Components internal to the DOE canister are in contact with water. These components include the SNF basket structure (4-in pipes, lifting rod, dividers, base plates), -01 and -04 aluminum canisters, and iron shot.
5. The aluminum canisters start to degrade at a rate faster than all other components.
6. Iron shot starts to degrade.
7. Degraded aluminum product mixes with other degraded steel materials locally.
8. SNF is exposed to water. After this, there are two paths:
 - 8a. All SNF stays intact. Iron shot degrades in place and mixes with other degraded products. As a result, SNF and neutron absorber stay in place. The initial void space present inside DOE SNF canister is insufficient to allow complete degradation of the internal constituents. Thus, partial degradation would prevent water flow and further degradation until canister walls are degraded to allow mixing inside the waste package.
 - 8b. All SNF degrades. The degraded SNF mixes with other degraded products and settles at the bottom of the DOE canister.
9. After sequence 8 above, there are two paths:
 - 9a. DOE SNF canister degrades, SNF stays intact. Intact SNF falls and scatters on top of other degraded products near the bottom of the waste package. There could be some separation between the fissile material and neutron absorber.
 - 9b. DOE SNF canister and SNF degrade. Degraded SNF mixes with other degraded products and settle near the bottom of the waste package. There could be some separation between the fissile material and neutron absorber.
10. Given a very long period of time, it is postulated that everything will degrade. This corresponds to the degradation scenario group IP-2 (YMP 2003). To bound the potential degraded cases, degradation of the SNF and other degradation products are assumed to mix to some degree and pile up near the bottom of waste package. Even though there is no mechanism to cause uniform mixing of all the degradation products inside the waste package, it is considered to bound the configurations.

Table 10-10. Materials and Thicknesses

Components	Material	Thickness (mm)
Waste package outer bracket	A 516 carbon steel	12.7
Waste package inner bracket	A 516 carbon steel	25.4
Waste package support pipe	A 516 carbon steel	31.75
DHLW glass shell	304L stainless steel	9.5
DHLW glass	Glass	N/A
DOE SNF canister	316L stainless steel	9.5
DOE SNF canister basket:		
Lifting rod	316L stainless steel	25.4
4-in pipe	316L stainless steel	4.8
Dividers A and B	316L stainless steel	9.5
Base plate	316L stainless steel	9.5
-01 shipping canister	Aluminum	3.175
-04 inner canister	Aluminum	1.651

Source: CRWMS M&O 2000d, Table 24

The most probable degradation configuration of the waste package containing Enrico Fermi SNF is the one with the degradation of all components inside the waste package and the DOE SNF canister. The SNF pins may stay intact but likely will degrade. The degradation scenario of IP-1 (i.e., SNF degrades faster than all of the other materials) is not probable for this waste package because the SNF corrosion rate is much lower than Stainless Steel Types 304L or 316L. As indicated in Section 6.5 for the purpose of fully identifying the potential for criticality, all representative configurations classes have been analyzed and not only the configurations resulting from the most probable degradation path presented above. The subtitles follow the original description given in Section 6.2.1 of *Evaluation of Codisposal Viability for U-Zr/U-Mo Alloy (Enrico Fermi) DOE-Owned Fuel* (CRWMS M&O 2000d).

Total Degradation of the SNF inside Nondegraded DOE Canister—A typical configuration for this class (Class 6 in YMP 2003, Section 3.3.1) is a configuration characterized by a homogeneous mixture of goethite (FeOOH)/diaspore (AlOOH)/degraded fuel inside the intact 4-in-diameter pipes. The 4-in pipes are in their initial locations with the iron shot remaining in place. This configuration is very unlikely due to the high corrosion resistance of the zirconium cladding.

Intact Fuel Pins in Partially Degraded DOE Canister—These configurations comprise the intact fuel pins distributed inside the DOE canister at various stages of degradation of the internal supporting structure. They represent refinements of the configuration Class 1 that is derived from the standard scenario group IP-3, and are described in *Disposal Criticality Analysis Methodology Topical Report* (YMP 2003, Section 3.3.1). Also, the cases with the partially degraded support structure inside the DOE canister are refinements of the configuration Class 1 resulting from standard scenario group IP-3. For Fermi SNF, the 4-in-diameter steel pipes, which are welded to a base plate to maintain the spacing, represent the fuel supporting structure inside the DOE SNF canister.

Different stages of degradation of the supporting structure have been considered. First, rearrangements of the 4-in pipes inside the DOE canister are investigated (see criticality results in Section 10.4.2). Finally, a bounding configuration of an array with the intact fuel pins inside a DOE SNF canister filled with wet goethite (FeOOH) and diaspore (AlOOH) is analyzed at various pitches, to identify the most reactive configuration. The rest of the waste package (outside the DOE SNF canister) is considered filled with a wet clayey material obtained from the degradation of the DHLW glass and the supporting structure.

Degraded Waste Package Internal Components with Nondegraded Fuel Pins—These configurations result from the subsequent degradation stage of the configuration discussed above and represent a refinement of the standard configuration Class 1 (YMP 2003, Section 3.3.1). A bounding arrangement is also selected for this analysis. A hypothetical arrangement of the intact fuel pins in a regular array is placed at the bottom of the waste package filled with clayey material and water. The fuel pins are settled or piled up to form a stack of fuel pins.

Degraded DOE Canister Internals and Fuel Pins—This category includes the waste package configurations that are refinements of the configuration Class 2 (YMP 2003, Section 3.3.1). They are obtained via any of the standard scenario groups from IP-1 to IP-3. The DOE SNF canister outer shell still keeps the degraded mixture with the fissile material from being dispersed in the volume of the DHLW clayey material in the waste package. The refinements include different locations of the DOE SNF canister within the homogeneous wet clayey material.

Degraded DOE Canister and Waste Package Internals—In this case, the whole content of the waste package is considered degraded and settled at the bottom of the waste package. The standard configuration class from *Disposal Criticality Analysis Methodology Topical Report* (YMP 2003, Section 3.3.1) is Class 2, but the refinements include a large number of possible configurations. The approach adopted for analyzing these configurations includes first a screening of the various bounding arrangements of the degraded materials. In the subsequent steps, the actual composition of the degraded mixture is taken into account. This approach covers, in a systematic way, the spectrum of possible configurations from this class. The possible final stage of the waste package internal degradation is a configuration comprising a homogeneous mixture of clay and water. The composition of the clay is given by geochemistry calculations.

10.4.2 Criticality Calculations and Results

10.4.2.1 Results for Intact Mode Configurations

This section summarizes the results of the intact-mode criticality analysis (CRWMS M&O 1999b). Although the components (fuel pins, cladding, supporting pipes, and canisters) are considered structurally intact, water intrusion into the available internal volumes is assumed in order to determine the highest k_{eff} resulting from optimum moderation. The contents of the waste package outside the DOE SNF canister are considered intact in all cases presented in this section.

For the intact mode, the contents of the DOE SNF canister are in an “as-welded/loaded position and condition,” as depicted in Figure 10-12 with a typical fuel pin arrangement. The void space outside and inside the pipes, but outside the -01 canisters, is filled with iron (Fe) shot containing

gadolinium phosphate ($GdPO_4$). For this particular set of configurations the $GdPO_4$ is considered only 1 percent by volume (1 vol%) of the Fe- $GdPO_4$ mixture (approximately 4.84 kg of $GdPO_4$ in 753.1 kg of Fe).

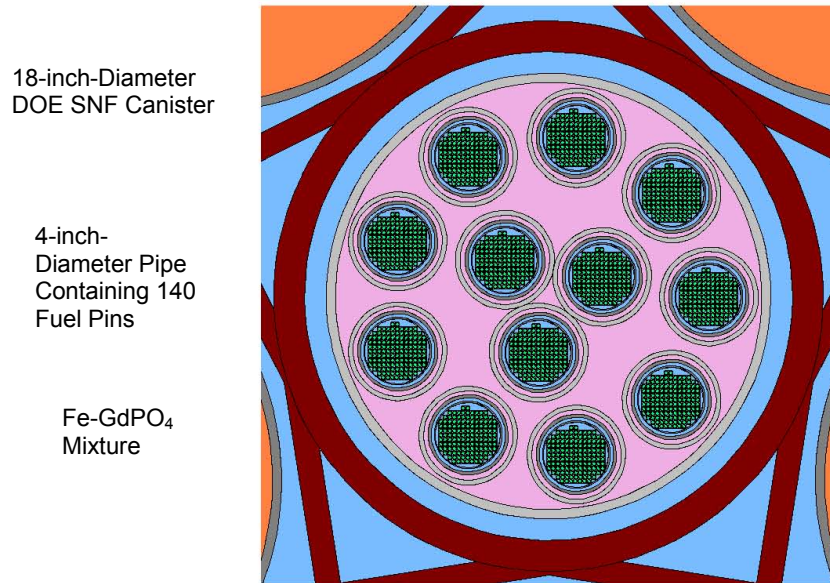


Figure 10-12. Cross-Section View of the Waste Package Showing the Contents of the DOE Spent Nuclear Fuel Canister for the Intact-Mode Analysis

The iron shot is used for moderator (water) exclusion, and the gadolinium phosphate is used as an insoluble neutron absorber. However, since the waste package is to be emplaced horizontally in the repository, the -01 and -04 aluminum canisters inside each pipe are considered to be settled inside the pipe and the -01 canister, respectively.

Water density was also varied for the base case to evaluate its impact on the k_{eff} value. The density variation simulates wetting of the shot to find optimum moderation. The rest of the waste package was considered flooded in all cases. Water fills all void space inside the waste package. Cases with no filler and no $GdPO_4$ were also studied to determine how the k_{eff} of the intact mode is affected by these conditions. It should be noted that while some cases do not seem to be realistic (physically possible), they were considered to obtain more conservative (higher) estimates for k_{eff} .

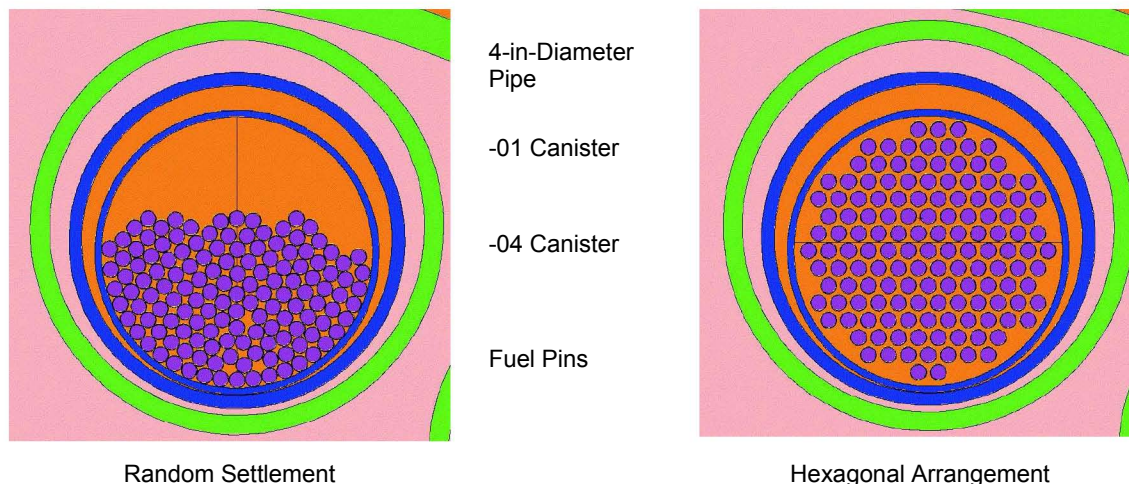


Figure 10-13. Different Arrangement of Fuel Pins Inside 4-in-diameter Pipes

To examine the impact of fuel pin arrangement on the k_{eff} value, different arrangements (hexagonal, square, random; see Figure 10-13) of the fuel pins inside the -04 aluminum canisters were considered. Fuel pin pitch variations and differential flooding of components was investigated for the more reactive configurations.

The results (CRWMS M&O 1999b, Section 7.3.1) show that the variations of the key-waste package parameters from the base intact mode configuration ($k_{\text{eff}}+2\sigma = 0.7295$) cause a relatively small change in the k_{eff} . The highest $k_{\text{eff}}+2\sigma$ of 0.8353 is obtained in a hypothetical configuration with no filler and no neutron absorber. Thus, the $k_{\text{eff}}+2\sigma$ for the system is well within the interim critical limit of 0.93. The decrease of the water density decreased the k_{eff} of the system; and this shows that the nominal system is not over-moderated. The final design has three times more neutron absorber (14.5 kg GdPO_4) than the amount considered in this set of calculations and this is expected to increase the conservatism of the present results.

Occurrence of design basis events, including those with the potential for flooding disposal container prior to disposal container sealing, is considered and bounded by the analysis for many different intact configurations.

It should also be noted that the results from intact cases are bound by those for the degraded cases described in Section 10.4.2.2 (intact pipes with homogenized degraded products inside each pipe). The detailed analysis presented in this section was performed to gain more information regarding the neutronic characteristics of the system.

10.4.2.2 Results for Configurations with Partially Degraded DOE SNF Canister

The partially degraded configurations refers to the cases where the 24 pipes contained in the 18-in diameter DOE SNF canister no longer remain in their original (welded) arrangement and settle into a possibly more reactive configuration. This mode has been analyzed in detail in *Enrico Fermi Fast Reactor Spent Nuclear Fuel Criticality Calculations: Intact Mode* (CRWMS M&O 1999b). The waste-package contents outside the DOE SNF canister are considered intact in all cases considered in this section. The degradation configurations and their refinements

belong to the standard configuration Class 1 that is obtained via standard group scenario IP-3 (YMP 2003, Section 3.3.1).

Moreover, since the waste package is to be emplaced horizontally, the -01 and -04 aluminum canisters are considered to be settled inside the steel pipes and the -01 aluminum canisters, respectively. Alternative pipe arrangements are evaluated to identify their impact on k_{eff} value. Figure 10-14 and Figure 10-15 show the pipe arrangements considered. In the calculations for this degradation mode, the Fe shot and the -01 and -04 aluminum canisters are assumed to be intact (noncorroded). For this particular set of configurations the GdPO_4 is considered only 1 percent by volume (1 vol%) of the Fe- GdPO_4 mixture (approximately 4.84 kg of GdPO_4 in 753.1 kg of Fe).

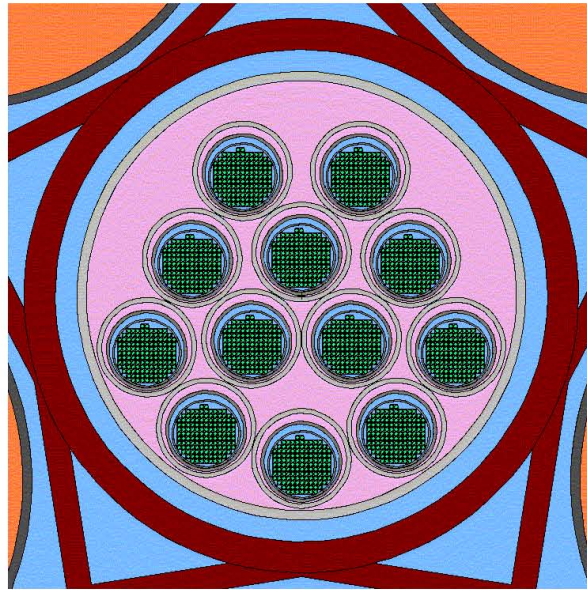


Figure 10-14. Waste Package Showing a Partially Degraded, More Compact Arrangement of Pipes Inside the DOE Spent Nuclear Fuel Canister

The results (CRWMS M&O 1999b, Section 6.2) show that 4-in-diameter pipe rearrangement has a major effect on k_{eff} . By comparing the case in Figure 10-14 with the base intact case from Figure 10-12, $k_{\text{eff}}+2\sigma$ is seen to increase from 0.7295 to 0.8034. A hexagonal closed-packed arrangement (Figure 10-15) is further increasing the $k_{\text{eff}}+2\sigma$ to 0.8336. This is due to the redistribution of the filler and neutron absorber to the periphery of the DOE SNF canister as the pipes are brought closer together. The $k_{\text{eff}}+2\sigma$ for these conditions and configurations do not exceed the interim critical limit of 0.93, even without GdPO_4 and iron shot. With the Fe- GdPO_4 mixture there is a very significant margin to the interim critical limit.

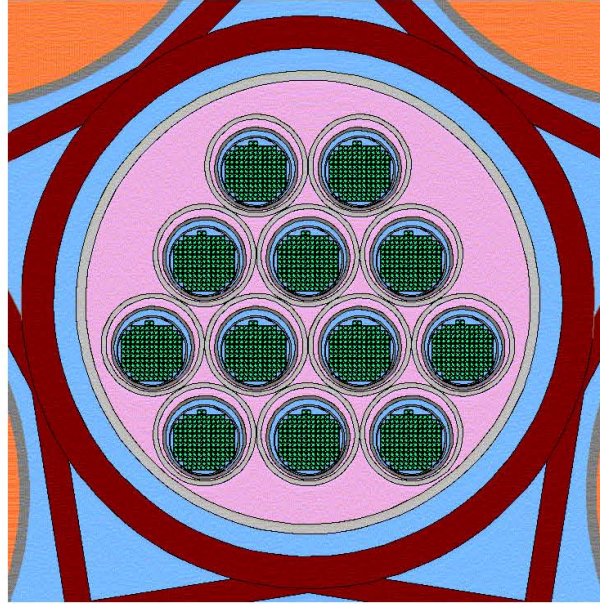


Figure 10-15. Hexagonal Close-Packed Arrangement of the Pipes

A separate set of calculations investigated the effect of fuel pin spacing inside 4-in-diameter pipes and the effect of partial flooding of various volumes. This analysis was performed in the partially degraded mode with more compact pipe configuration, as shown in Figure 10-14, and no oxidation of Fe or Al.

To study the impact of partial flooding on the k_{eff} value, it was assumed that water fills the void space in -01 and -04 aluminum canisters but no water exist in the remaining void space in the DOE SNF canister. This is not credible but is investigated because it minimizes the effectiveness of Gd as a neutron absorber.

The fuel pin spacing was increased from 0.06 cm to 0.48 cm (edge-to-edge distance) to study the impact on the k_{eff} value when there is more space (moderator) between adjacent fuel pins (e.g., less than 140 fuel pins within each -04 aluminum canister).

The combined effects of partial flooding and reduction in the number of pins resulted in a maximum $k_{\text{eff}}+2\sigma$ for the partially degraded mode cases studied of 0.9051 that does not exceed the interim critical limit of 0.93. As already mentioned, the results for all cases with intact pins are bound by those for the cases with homogenized fuel pins inside 4-inch pipes that are described in the next section. The final design has three times more neutron absorber (14.5 kg GdPO_4) than the amount considered in this set of calculations and this is expected to increase the conservatism of the present results.

Results for Totally Degraded Fuel Pins inside Nondegraded DOE Canister—The application of the standard scenario group IP-1 (CRWMS M&O 1999g) to Enrico Fermi SNF in the flooded DOE SNF canister can result in a set of distinct degraded configurations. If the fuel degradation takes place in the initial location (within the supporting structure), the resultant configurations belong to Class 6 (YMP 2003). Since the design of the DOE SNF canister includes a simple supporting structure for the fuel pins (4-in-diameter pipes), the degradation of the fuel pins takes

place in the 4-in-diameter pipes within the DOE SNF canister. This class of configurations can also be regarded as a bounding case for all intact configurations and was expanded in order to cover all possible DOE SNFs fuels that belong to this group.

Due to the highly corrosion-resistant properties of the cladding (Zr), the degradation of the SNF before the supporting structure is very unlikely. This configuration is analyzed in order to include the situation in which the fuel cladding has been mechanically removed or damaged before or during emplacement. At the end of the spectrum of degraded configurations in this class are the cases with the fuel completely degraded within the pipes, forming a mixture with the degradation products and water. The configuration for a more compact arrangement of settled pipes is shown in Figure 10-16.

A direct comparison with an intact configuration analyzed in Section 10.2.4.2.1 can be made for the cases with 1 vol% of GdPO₄ in the iron shot-GdPO₄ mixture (4.84 kg GdPO₄). The $k_{\text{eff}+2\sigma}$ values for these degraded configurations range from 0.8440 to 0.9506 (depending on the volume fraction of water mixed with the degraded products). The $k_{\text{eff}+2\sigma}$ value for the similar arrangement with intact fuel is 0.7295. Note that the degraded cases are more reactive and bound the values obtained with intact fuel.

Different amount of GdPO₄ was added to the iron shot-neutron absorber mixture to reduce k_{eff} . With 9.6 kg of GdPO₄ the $k_{\text{eff}+2\sigma}$ for the system is below 0.93 for all investigated H/X ratios with the exception of the configuration that has the full lengths of 4-in-diameter pipes filled with a homogeneous mixture ($k_{\text{eff}+2\sigma}=0.9308$). This result shows the importance of having some neutron absorber and iron shot distributed in each pipe. A separate set of cases investigated the effect of considering the presence of the filler material in each 4-in-diameter pipe (filling the space between -01 canister and the 4-in-diameter pipe in the Enrico-Fermi design). The goethite in excess of the available volume in each pipe was conservatively neglected (approximately 20 percent). The results show a significant decrease in k_{eff} and also a high effectiveness of the Gd. With 6 kg of Gd (9.6 kg of GdPO₄) uniformly distributed in the initial iron shot-GdPO₄ mixture the highest $k_{\text{eff}+2\sigma}$ drops to 0.8090. Settling the pipes as shown in Figure 10-16 increases $k_{\text{eff}+2\sigma}$ to 0.8843. Removing the water from the rest of the waste package produces an increase in $k_{\text{eff}+2\sigma}$ of approximately 4.5 percent that does not exceed the interim critical limit of 0.93. Reflection of neutrons from the materials outside waste package (water, silica) has no impact on k_{eff} for this class of configurations.

As shown in *Enrico Fermi Fast Reactor Spent Nuclear Fuel Criticality Calculations: Degraded Mode* (CRWMS M&O 2000n, Section 6.1.2), increasing the fuel mixture column length results in a decrease in k_{eff} . A higher $k_{\text{eff}+2\sigma}$ was obtained for a shorter column (64.83 cm) that contains no goethite and no absorber mixed with degraded fuel. The increase in $k_{\text{eff}+2\sigma}$ from the base case (length of fuel section of 77.47 cm, 9.6 kg of GdPO₄) to the shorter column is from 0.8090 to 0.8591.

As will be shown in the next sections, the limiting cases for the fully degraded configurations require at least 14.5 kg of GdPO₄. Repeating some of the above cases with this amount of neutron absorber, $k_{\text{eff}+2\sigma}$ decreased (to 0.7883 from 0.8090 for the base case), further increasing the margin to the interim critical limit of 0.93.

4-in Diameter Pipes with Degraded Fuel Mixture

Water

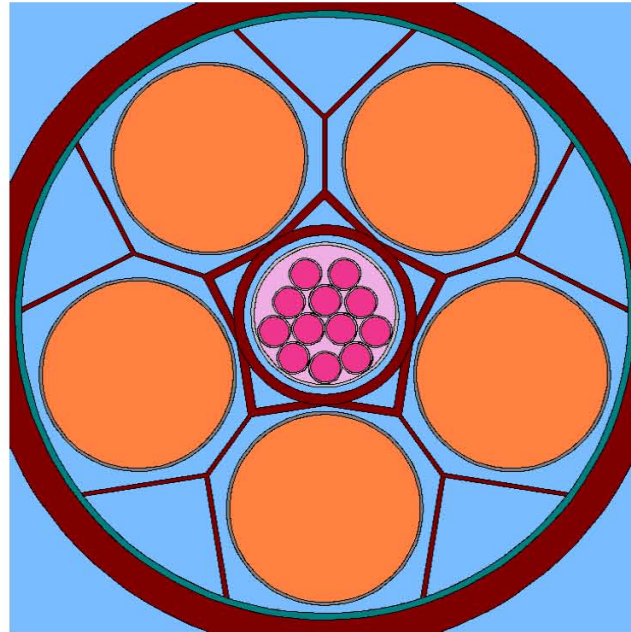


Figure 10-16. Cross-Section View of the Degraded Waste Package Configuration with Degraded Fuel Mixture in 4-in-Diameter Pipes

10.4.2.3 Results for Degraded Configurations Postulated Beyond the Regulatory Period

The degradation and criticality analyses performed have also investigated configurations that require very long times to be attained. These configurations are anticipated to happen well beyond the regulatory period of 10,000 years but they have been analyzed to fully investigate the potential for criticality of the waste package containing Enrico Fermi SNF. For the purpose of this document, these results (CRWMS M&O 2000d, Sections 7.4.2, 7.4.4, and 7.5) have been summarized and grouped together in this section.

Results for Totally Degraded Internal Structures of DOE SNF Canister with Intact Fuel Pins—These configurations comprise the intact fuel pins distributed inside the DOE SNF canister at various stages of degradation of the internal supporting structure. They represent refinements of the configuration Class 1 that results from the standard scenario IP-3 (YMP 2003). Configurations with fuel pins completely separated from the neutron absorber are not possible with the present design because the space between the pipes is filled with a uniform mixture of iron shot and neutron absorber.

For analyzing this class of configurations, a bounding approach is followed, as described in *Enrico Fermi Fast Reactor Spent Nuclear Fuel Criticality Calculations: Degraded Mode* (CRWMS M&O 2000n). It is assumed that the intact fuel pins are arranged in a hypothetical square lattice with constant pitch (defined as the distance between the centers of two adjacent pins). These are incredible cases that bound all possible internal configurations of the intact pins distributed inside DOE SNF canister. The initial void space present inside DOE SNF canister is insufficient to allow complete degradation of the internal constituents. Thus, partial degradation would prevent water flow and further degradation until canister walls are degraded to allow mixing inside the waste package.

Various shapes of the array of pins inside DOE SNF canister are considered. The DOE SNF canister shell is assumed to be breached but structurally intact, and the degradation products resulting from degradation of the canister internals (mainly FeOOH [goethite] and AlOOH [diaspore]) are distributed among fuel pins. The influence of the pitch variation for a hypothetical array of intact pins placed in a mass of hydrated degradation products on k_{eff} of the system is investigated.

An incremental amount of Gd was added to the FeOOH-AlOOH mixture to determine the amount of neutron absorber necessary to keep the k_{eff} of the system below the acceptance criterion. A quantity of 5 kg of Gd (8 kg GdPO₄) per canister is needed to produce a maximum $k_{\text{eff}+2\sigma}$ of 0.9245. It should be noted that while increased pitch promotes a greater k_{eff} , there is no identified mechanism that promotes the increased pitch(es).

Results for Degraded Waste Package and DOE Canister Internal Structures with Intact DOE SNF Canister Shell—The configurations analyzed are refinements of the configuration Class 2 (CRWMS M&O 1999g) and can be obtained via any of the standard scenarios. The configurations include an intact (but breached) DOE SNF canister outer shell that keeps the mixture with degraded fissile material from being dispersed in the DHLW clayey material. All other internal structures inside waste package are considered fully degraded.

Various compositions and densities of the degraded mixture inside DOE SNF canister have been evaluated. The results (CRWMS M&O 2000n, Section 6.1.3) show that a mixture containing UO₂, diaspore, and goethite having a length equal with the initial footprint length of the fuel and completely filling the DOE SNF canister area is the most reactive. The DOE SNF canister shell was evaluated in three locations. One location is at the bottom of the waste package, such that the DOE SNF canister is fully reflected by the clayey material from degraded components. Another location is half submerged into the clayey material. The third location is sitting on top of the clayey material. The most reactive configuration is the one with the DOE SNF canister shell placed at the bottom of the waste package.

The influence of adding an incremental amount of Gd to the content of DOE SNF canister was subsequently investigated. The results (CRWMS M&O 2000n, Section 6.1.3) show that at least approximately 9 kg of Gd (14.5 kg gadolinium phosphate) must be uniformly distributed within the SNF canister to keep k_{eff} of the system (maximum $k_{\text{eff}+2\sigma} = 0.9053$) below the interim critical limit of 0.93 for all investigated configurations. This is the configuration class that contains the overall limiting case for criticality calculations. The results obtained for the configurations with intact pins still contained in the DOE canister are bounded by the results obtained in this section.

Results for Degraded Waste Package Internal Structures with Intact Fuel Pins—This group of configurations, characterized by intact fuel pins immersed in the clayey material resulting from the degradation of the DHLW glass and other internal components of the waste package and the DOE SNF canister, represents a different refinement of the configuration Class 1. It can be reached by applying the standard scenario group IP-3 to both the DOE SNF canister and waste package. The configurations are considered likely due to the high corrosion resistance of the fuel cladding material, zirconium.

In order to perform the criticality calculations for this case, a bounding approach similar to the one presented above has been adopted. The intact fuel pins are dispersed in the clayey material in a regular square lattice with a constant pitch. Two distinct groups of configurations are analyzed. The first one assumes that the clay in the waste package is homogeneously mixed with the degradation products from DOE canister internals and shell. The main constituents of the DOE SNF degradation products considered are goethite and diaspore. Inclusion of the diaspore is conservative since it essentially acts to disperse the more absorbing goethite.

The second group of configurations assumes that the degradation products from DOE SNF canister and the clay are not mixed, with the heaviest components (goethite) settled at the bottom of the waste package. The results of the criticality analysis are presented in Section 6.2.2 of *Enrico Fermi Fast Reactor Spent Nuclear Fuel Criticality Calculations: Degraded Mode* (CRWMS M&O 2000n) and summarized in *Evaluation of Codisposal Viability for U-Zr/U-Mo Alloy (Enrico Fermi) DOE-Owned Fuel* (CRWMS M&O 2000d, Section 7.5.1).

The fuel pins can be settled at the bottom of the waste package or can be stacked forming a stack with a triangular cross-section. The pitch between fuel pins was varied, but the height of the fuel pin arrangement was not higher than the initial DOE SNF canister diameter. Fuel pins are immersed in a uniform mixture of the degradation products of the DOE SNF canister (FeOOH, AlOOH, and GdPO₄). The volume percent of water in this layer is varied from 28.6 percent to 50 percent. The clay layer above has a 37.5 vol% of water. For the configuration optimum moderated configuration (pitch=0.901cm), a minimum quantity of 3.5 kg Gd (5.6 kg GdPO₄) must be uniformly distributed in the mixture to bring $k_{\text{eff}}+2\sigma$ to 0.9205, which is below the critical limit of 0.93.

Similar calculations performed for the configuration containing a stack of fuel pins produce the largest k_{eff} for a pitch of 0.901 cm. In order to reduce the effective neutron multiplication factor of the system ($k_{\text{eff}}+2\sigma$) to a value of 0.8958, 9 kg of Gd (14.5 kg of GdPO₄) must be uniformly dispersed in the goethite layer. A reflective boundary at the outer waste package surface added to this configuration produces $k_{\text{eff}}+2\sigma$ of 0.9216, pointing to a more significant influence of the reflector outside the waste package outer barrier for this class of configurations because the fuel pins are so close to the reflective boundary.

Results for Degraded DOE SNF Canister Mixture Settled at the Bottom of the Waste Package—After the complete degradation of all the waste package internal constituents, including the DOE SNF canister, the resultant configurations can include the degradation products as layers or complex mixtures settled within the waste package. These configurations belong to Class 2 (YMP 2003). It comprises a large number of refinements and variations, and it can be reached by any of the standard top-breach scenarios (IP-1, IP-2, or IP-3). A bounding approach was also adopted for this analysis, investigating various possible combinations of the fissile material with different degradation constituents. The fissile material mixture is settled at the bottom of the waste package. A layer of goethite that results from the degradation of the DOE SNF canister is placed on top of the fissile mixture. The rest of the waste package is filled with a layer of clay and water. The configuration can directly result from subsequent degradation of the configurations presented above. The length of the mixture containing fissile materials is equal to the initial footprint of the fuel pins. The analysis focused on varying the fractions of the degraded constituents in the mixture. The effect of water addition in all layers is

also evaluated in order to identify the optimum-moderated system. The densities of the layers are calculated in order to assure a correct physical representation with the higher densities layers placed at the bottom.

A minimum quantity of 0.935 kg of Gd (1.5 kg GdPO₄) uniformly dispersed in the fuel mixture is sufficient to bring the most reactive configuration below the interim critical limit of 0.93 (CRWMS M&O 2000d, Section 7.5.2). A quantity of 3.5 kg Gd (5.6 kg GdPO₄) distributed uniformly in the degraded fuel mixture decreases the most reactive case to 0.6368. For these fully degraded configurations, the neutron absorber proves to be extremely effective.

Results for Totally Degraded DOE SNF Canister and Waste Package Internal Structure—

The mixture of clayey material obtained after total degradation of the waste package internal constituents and uniformly distributed fissile material was analyzed with varying fractions of water. As expected, the results are well below the interim critical limit of 0.93. For water volume fractions between 0 and 0.3, $k_{\text{eff}}+2\sigma$ varies between 0.4 and 0.363. The clay composition includes the remaining Gd from an initial loading of 3 kg (4.84 kg GdPO₄) (CRWMS M&O 1999u).

10.4.3 Range of Parameters for Configurations of Waste Package Containing Enrico Fermi DOE SNF

ANSI/ANS-8.1-1998 and *Disposal Criticality Analysis Methodology Topical Report* (YMP 2003) provide basic requirements for validation of a calculational method used in the criticality analysis of a system. The bias of a code system (in this case the criticality model containing the software code MCNP and selected cross-section libraries) is determined by correlating the results of critical and near-critical experiments with calculated results for those experiments. The common practice, and that considered by the current validation methodology (BSC 2003e), is for comparison of the calculated k_{eff} to a critical or near critical system.

Prior to the initiation of the validation activity, the operating conditions and parameters for which the validation is to apply must be identified. The fissile isotope, enrichment of fissile isotope, fuel density, chemical form of fuel, types of neutron moderators and reflectors, range of moderator to fissile isotope ratio, neutron absorbers and physical configurations are among the parameters to specify. These parameters will define the area of applicability for the selection of the critical experiments for the validation effort.

The preliminary degradation analysis of the content of the waste package containing Enrico Fermi SNF (CRWMS M&O 2000d, Section 6) and the subsequent criticality analysis performed for the resulting internal configurations have followed the guidance suggested by the Internal Criticality Master Scenarios presented in *Disposal Criticality Analysis Methodology Topical Report* (YMP 2003) and also by *Generic Degradation Scenario and Configuration Analysis for DOE Codisposal Waste Package* (CRWMS M&O 1999g). The resultant configuration classes internal to the waste package have been screened systematically for their criticality potential in comprehensive criticality analyses (CRWMS M&O 1999b; CRWMS M&O 2000n). The main results have also been summarized in the above sections (10.2.4.2.1 to 10.2.4.2.3).

For the purpose of the criticality model validation for the configurations specific to the waste package containing Enrico Fermi SNF and identification of the range of parameters that characterize the most reactive internal configurations of the degraded waste package, the degraded configurations previously investigated have been categorized into two large groups:

1. Configurations containing intact fuel pins (heterogeneous configurations)
2. Configurations containing degraded fuel pins (relatively homogeneous configurations).

The first category contains the configurations described in *Evaluation of Codisposal Viability for U-Zr/U-Mo Alloy (Enrico Fermi) DOE-Owned Fuel* (CRWMS M&O 2000d, Sections 7.3.1 [intact mode], 7.4.1 [partially degraded DOE SNF canister], 7.4.2 [totally degraded internal structures of DOE SNF canister with intact pins], and 7.5.1 [degraded waste package internal structures with intact fuel pins]). These configurations represent intact fuel (nondegraded) configurations and refinements of the general configuration class 1 as described in *Disposal Criticality Analysis Methodology Topical Report* (YMP 2003, Section 3.3.1). The second category includes the configurations described in *Evaluation of Codisposal Viability for U-Zr/U-Mo Alloy (Enrico Fermi) DOE-Owned Fuel* (CRWMS M&O 2000d, Sections 7.4.3 [totally degraded fuel pins inside nondegraded DOE SNF canister], 7.4.4 [degraded internal structures with intact DOE SNF canister shell], 7.5.2 [degraded DOE SNF canister mixture settled at the bottom of the waste package], and 7.5.3 [totally degraded DOE SNF canister and internal structures]). These configurations represent refinements of the general configuration classes 2 and 6 that are described in *Disposal Criticality Analysis Methodology Topical Report* (YMP 2003, Section 3.3.1). This proposed categorization allows a simple and systematic way of identifying the key parameters that characterize the degraded configurations.

The process employed in *Enrico Fermi Fast Reactor Spent Nuclear Fuel Criticality Calculations: Intact Mode* (CRWMS M&O 1999b) and *Enrico Fermi Fast Reactor Spent Nuclear Fuel Criticality Calculations: Degraded Mode* (CRWMS M&O 2000n) for investigating the potential for criticality of the possible degraded configurations of the waste package used a screening approach, the goal being to identify the most reactive configurations in a given class of degraded configurations and testing afterwards the effectiveness of the amount of neutron absorber introduced as a design solution for controlling the criticality potential for the limiting cases. Due to this approach, the number of configurations analyzed varies among the classes of configurations depending on the complexity of the possible arrangements and the initial screening results. Selected cases (typically the most reactive or the limiting cases as presented in CRWMS M&O 2000d, Section 7) have been rerun with tallies calculating the neutron flux and the fission rate in the regions containing the fissile material. The results of the cases that were rerun with tallies are summarized in Tables V-2 to V-4 of *Criticality Model Report* (BSC 2003e) together with a summary of the key physical and neutronic parameters characterizing the most reactive configurations (ROP).

10.4.4 Selection of the Criticality Benchmark Experiments Used in the Validation of the Criticality Model

The benchmark experiments selected for the validation of the criticality model used for the analysis of the waste package containing Enrico Fermi SNF come from *International Handbook of Evaluated Criticality Safety Benchmark Experiments* (NEA 2001). The selection process was initially based on previous knowledge regarding the possible configurations of degraded waste package, and the subsets have been constructed to accommodate large variations in the range of parameters of the configurations and also to provide adequate statistics for lower bound tolerance limit calculations. The selected benchmark experiments for each subset are presented in *Benchmark and Critical Limit Calculation for DOE SNF* (BSC 2002c) together with the MCNP cases constructed and the results of the calculations. For the present application (codisposal of Enrico Fermi SNF), the selected benchmark experiments have been grouped in 4 subsets (BSC 2002c), that include heterogeneous and homogeneous experiments, each of them divided in subsets of moderated (thermal spectrum) and nonmoderated experiments (fast spectrum). The k_{eff} results and their uncertainties are summarized in *Analysis of Critical Benchmark Experiments and Critical Limit Calculation for DOE SNF* (BSC 2003f, Appendix II). Table 10-11 presents the list of the benchmark experiments and the number of cases for each subset selected for validation of the criticality model for Enrico Fermi SNF.

The review of the degraded configurations (BSC 2003e, Attachment V) showed that there are no configurations in the degraded mode (fuel degraded within waste package) without some form of moderator present (in the form of hydrated degradation products). This is the basis for removing the subset of benchmarks for degraded nonmoderated configurations from further comparison with the range of parameters.

The experiments listed in Table 10-11 are considered appropriate to represent intact (nondegraded) and degraded configurations of the waste package containing Enrico Fermi SNF that belong to the configuration classes 1, 2 and 6.

10.4.5 Comparison Between ROA of Benchmark Experiments and ROP

The validation of the criticality model needs to show that the range of the fundamental parameters of the benchmark critical experiments (Range of Applicability-ROA) and the range of the fundamental parameters of the system (Range of Parameters-ROP) evaluated are nearly identical. This is not usually practical, and for those parameters that do not show a trend in bias, it is acceptable to use critical benchmark experiments that cover most, but not all, of the ROP of the system under evaluation. In these situations, expert judgment may be used to determine if there is a reasonable assurance that the two are sufficiently close. In cases where a trend in bias is identified, the ROA can be extended, but a penalty on the critical limit determined for the subset of benchmark experiments needs to be evaluated and applied.

Table 10-11. Critical Benchmarks Selected for Validation of the Criticality Model for Enrico Fermi Spent Nuclear Fuel

Subset	Benchmark Experiment Identification	Number of Cases Included
Heterogeneous moderated ^b	IEU-COMP-THERM-002	6
	IEU-COMP-THERM-003	2
	HEU-COMP-THERM-003	15
	HEU-COMP-THERM-004	4
	HEU-COMP-THERM-005	1
	HEU-COMP-THERM-006	3
	HEU-COMP-THERM-007	3
	IEU-COMP-THERM-001	29
Heterogeneous nonmoderated ^b	IEU-MET-FAST-001	4
	IEU-MET-FAST-002	1
	IEU-MET-FAST-003	1
	IEU-MET-FAST-004	1
	IEU-MET-FAST-005	1
	IEU-MET-FAST-006	1
	IEU-MET-FAST-007	1
	IEU-MET-FAST-008	1
	IEU-MET-FAST-009	1
	IEU-MET-FAST-010	1
Homogeneous moderated ^b	IEU-SOL-THERM-001	4
	IEU-COMP-THERM-001	29
	LEU-SOL-THERM-003	9
	LEU-SOL-THERM-004	7
	LEU-SOL-THERM-006	5
	LEU-SOL-THERM-007	5
	LEU-SOL-THERM-008	4
	LEU-SOL-THERM-009	3
	LEU-SOL-THERM-010	4
	LEU-SOL-THERM-016	7
	LEU-SOL-THERM-017	6
	LEU-SOL-THERM-018	6
	LEU-SOL-THERM-019	6
LEU-SOL-THERM-020	4	
LEU-SOL-THERM-021	4	

Source: Subsets defined in BSC 2002c

NOTE: ^a The convention for naming the benchmark experiments is from NEA 2001.

^b Identification of each subset from BSC 2002c has been modified to better reflect the subset's main characteristics. The benchmark experiments in each subset have not been affected.

The comparison between ROA and ROP was structured (BSC 2003e, Attachment V) on the three subsets of benchmarks experiments selected to cover the majority of the analyzed configurations of the waste package containing Enrico Fermi SNF.

Heterogeneous Moderated Configurations—The comparison of ROA vs. ROP for the heterogeneous moderated configurations is detailed in Attachment V of *Criticality Model Report* (BSC 2003e). The collective area of applicability of the selected critical benchmarks is based on the ROA of the benchmark experiments included in Tables V-7 and V-8 of *Criticality Model Report* (BSC 2003e). The findings from the comparison in ROP vs. ROA can be summarized as follows:

- The ROA for this subset of experiments covers the ROP for the majority of parameters that characterize the heterogeneous configurations without Gd, except those with harder spectra. The criticality model is adequate for performing the screening of the degraded configurations without added neutron absorber.
- For the configurations containing Gd dispersed in the DOE SNF internal space, the comparison shows that the ROA of benchmarks is not within the range of parameters (with respect to Gd concentration and spatial distribution) and the ROA of spectral parameters for benchmarks is outside the ROP (benchmarks cover spectra with peaks in the thermal region).

This situation can be alleviated by addressing on or more of the following possible solutions:

- More experiments need to be added covering the parameters and characteristics of the limiting configurations (metallic U pins, less moderated lattice, distributed Gd as in current design).
- Penalty applied to the critical limit (if trend in bias is identified).
- Change in design (new ROP).

Heterogeneous Nonmoderated Configurations—The comparison of ROA vs. ROP for the heterogeneous nonmoderated configurations is detailed in Attachment V of *Criticality Model Report* (BSC 2003e). The collective area of applicability of the selected critical benchmarks is based on the ROA of the benchmark experiments included in Tables V-9 and V-10 of *Criticality Model Report* (BSC 2003e).

The findings from the comparison can be summarized as follows:

- The comparison shows that the selected experiments cover the range of parameters identified for the nonmoderated configurations of the waste package containing Enrico Fermi SNF.

Homogeneous Moderated Configurations—The comparison of ROA vs. ROP for the homogeneous moderated configurations is detailed in Attachment V of *Criticality Model Report* (BSC 2003e). The collective area of applicability of the selected critical benchmarks is based on the ROA of the benchmark experiments included in Tables V-11, V-12, and V-13 of *Criticality Model Report* (BSC 2003e). The findings from the comparison can be summarized as follows:

- The ROA does not cover the range of parameters characterizing moderation of the systems (e.g., H atomic density, H/X). ROP includes values for less moderated configurations in which fissile material is mixed with hydrated degradation products.
- For the configurations containing Gd dispersed in the DOE SNF internal space, the comparison shows that there are no benchmarks with Gd absorber.

This situation can be alleviated by addressing on or more of the following possible solutions:

- More experiments need to be added close to the characteristics of the limiting configurations (less moderated lattice, distributed Gd).
- Penalty applied to the critical limit based on a sensitivity analysis.

10.4.5.1 Calculation of the Lower Bound Tolerance Limit

The following results are excerpted from *Analysis of Critical Benchmark Experiments and Critical Limit Calculation for DOE SNF* (BSC 2003f), which presents in detail the methodology and calculations performed for evaluating the lower bound tolerance limit for each set of configurations of the waste package containing Enrico Fermi SNF.

The results of the trending parameter analysis for the critical benchmark subset representative for moderated intact (heterogeneous) configurations of the waste package containing Enrico Fermi DOE SNF are presented in Attachment V of *Criticality Model Report* (BSC 2003e). The analysis did not find any trending in k_{eff} and the DFTL method was identified as appropriate for calculating the lower bound tolerance limit (BSC 2003e, Attachment V). The lower bound tolerance limit value calculated with DFTL method for this subset was 0.9751.

The results of the trending parameter analysis for the critical benchmark subset representative for nonmoderated intact (heterogeneous) configurations of the waste package containing Enrico Fermi DOE SNF are presented in Attachment V of *Criticality Model Report* (BSC 2003e). The analysis did not find any trending in k_{eff} and the NDTL method was identified as appropriate for calculating the lower bound tolerance limit (BSC 2003e, Attachment V). The lower bound tolerance limit value calculated with NDTL method for this subset was 0.9872.

The results of the trending parameter analysis for the critical benchmark subset representative for moderated degraded (homogeneous) configurations of the waste package containing Enrico Fermi DOE SNF are presented in Attachment V of *Criticality Model Report* (BSC 2003e). The analysis did not find any trending in k_{eff} and the DFTL method was identified as appropriate for calculating the lower bound tolerance limit (BSC 2003e, Attachment V). The lower bound tolerance limit value calculated with DFTL method for this subset was 0.9659.

Table 10-12 presents a summary of the results of the analyses performed on the subsets of critical benchmark experiments applicable to the waste package containing Enrico Fermi DOE SNF and the calculated lower bound tolerance limit values.

Table 10-12. Lower-Bound Tolerance Limits for Benchmark Subsets Representative for the Configurations of the Waste Package Containing Enrico Fermi Spent Nuclear Fuel

Subset	Trend Parameter	Test for Normality	Applied Computational Method	Lower Bound Tolerance Limit or Lower Bound Tolerance Limit Function
Intact (heterogeneous) Moderated	None	Failed	DFTL	CL = 0.9751
Intact (heterogeneous) Nonmoderated	None	Passed	NDTL	CL = 0.9872
Degraded (homogeneous) Moderated	None	Failed	DFTL	CL = 0.9659

Source: BSC 2003e, p. V-32

The above results and the comparison ROA vs. ROP indicate that the criticality model is partially validated for use in assessing the criticality potential of the intact (nondegraded) configurations and of the configurations belonging to the general configurations classes 1, 2 and 6 (YMP 2003, Section 3.3.1) of the degraded waste package containing Enrico Fermi SNF.

10.4.6 Summary of Criticality Model Results and Validation for the Waste Package Containing Enrico Fermi DOE SNF

The results of three-dimensional Monte Carlo criticality calculations for all anticipated intact and degraded configurations show that the requirement of $k_{\text{eff}}+2\sigma$ less than or equal to the interim critical limit of 0.93 is satisfied for the Enrico Fermi waste package with at least 3.0 percent by volume of gadolinium phosphate (14.5 kg GdPO₄) uniformly distributed in the initial iron shot-GdPO₄ filler.

Most cases analyzed require only a fraction of the indicated insoluble neutron absorber in order to be below the interim critical limit. A number of parametric analyses were run to address or bound the configuration classes discussed in Section 10.4.1. These parametric analyses identified conditions of optimum moderation, optimum spacing between fuel pins, optimum fissile concentration, and minimum neutron absorber requirements. The limiting case for the configurations with the fuel inside DOE SNF canister was obtained for a homogeneous mixture of fuel and hydrated products inside DOE SNF canister, which require 14.5 kg of GdPO₄ uniformly distributed in the canister volume. The overall limiting case was obtained for an extremely conservative configuration comprising a pile of fuel pins stacked at the bottom of the waste package. This configuration required the same amount of insoluble neutron absorber (14.5 kg of GdPO₄) to be distributed in the degraded mixture surrounding the pins.

As expected, the results from analyzing the configurations with the fuel degraded in the 4-in-diameter pipes bound the intact and partially degraded cases with intact fuel in pipes. Also, the results for the configurations with fully degraded DOE SNF internal constituents bound the partially degraded cases. On the other hand, it can be noticed that considering the presence of the aluminum cans (or the aluminum degradation products), which are specific to Enrico Fermi SNF, resulted in higher k_{eff} values for the limiting cases (conservative assumption) than the cases that neglected the cans degradation products.

Much lower amounts of the gadolinium neutron absorber are necessary to keep $k_{\text{eff}}+2\sigma$ below 0.93 for the configurations with fully degraded DOE SNF canister and waste package internals. This finding assures that the margin for criticality is increasing at longer disposal times, as long as the neutron absorber remains dispersed within the waste package. Due to the basket design and the iron shot-GdPO₄ filler, the waste package containing a DOE SNF canister of spent Enrico Fermi fuel will not form critical configurations for any credible degradation scenarios.

All calculations are based on a maximum of 4.817 kg of U-235 per -01 canister (one pipe). The analyses are based on the fuel pin type that has the highest uranium enrichment (25.69 percent in U-235). The degraded configurations of the Enrico Fermi SNF bound the other types of U-Zr and U-Mo (HEU) DOE-owned SNF, as long as the limits on mass of uranium and its enrichment, and the linear density, are not exceeded. Hence, the total mass of fissile element (²³⁵U U-235) should not exceed the mass used in deriving the conclusions of this report, which is 115.6 kg of U-235 per DOE SNF canister.

Table 10-13 presents a summary of the criticality and geochemistry results with a focus on the correspondence with the degradation classes and resultant configuration classes presented in *Disposal Criticality Analysis Methodology Topical Report* (YMP 2003). The results of the geochemistry analyses show that the calculated maximum loss of Gd is very small (2.30 percent) assuring its presence for all anticipated internal configurations, and consequently minimizing the potential for criticality.

The criticality model (software code MCNP and appropriated selected neutron cross-section libraries) used in analyzing the configurations of the waste package containing Enrico Fermi SNF was validated using the methodology described in *Disposal Criticality Analysis Methodology Topical Report* (YMP 2003) and *Criticality Model Report* (BSC 2003e). Current results (Section 10.2.4.6) indicate that the lower bound tolerance limit is well above the interim critical limit used in evaluating the design.

Table 10-13. Summary of Geochemistry and Criticality Analyses for Internal Configurations (Phase I and II) of the Waste Package Containing Enrico Fermi SNF

Master Scenario	Description	Configuration Classes and Summary Description	Summary of Geochemistry Calculations	Summary of Criticality and Criticality Model Validation Results			
				$(k_{eff}+2\sigma)_{max}$	Interim Critical Limit	Lower Bound Tolerance Limit	Comments
Initial water intrusion	Initial stage; water fills all available spaces inside the waste package and DOE SNF canister	Intact flooded configurations: SNF and internal structures not degraded	N/A	0.8353	0.9751 (heterogeneous moderated configurations)	Maximum $k_{eff}+2\sigma$ was obtained assuming no Gd and no filler added. The addition of the final recommended amount of Gd (14.5 kg GdPO ₄) is expected to result in much lower results..	
IP-1	The top of the waste package is breached and liquid accumulates inside	Configuration class #6: SNF partially degraded in place (various stages)	For all cases investigated (IP-1, IP-2 and IP-3 scenarios) the loss ranges were: U: 0 to 100% Gd: 0 to 2.30%	0.8843	0.93 (heterogeneous moderated configurations)	2 vol% of GdPO ₄ distributed with the initial filler mixture. The final Gd amount recommended (3 vol % = 14.5 kg GdPO ₄) is expected to result in much lower results.	
		Configuration class #3: SNF partially or totally degraded inside the waste package with intact internal structures		N/A	0.93 (homogeneous moderated configurations)	Due to high corrosion resistance of the Zr cladding, SNF will degrade after internal structures of the DOE SNF canister.	
IP-2	SNF degrades concurrently with the internals of the waste package	Configuration class #2: Both SNF and internal structures of the waste package degraded (various stages)		0.9053	0.9659 (homogeneous moderated configurations)	3 vol% (14.5 kg GdPO ₄ distributed with the initial filler mixture.	
		Configuration class #1: SNF intact (pins) and degraded internal structures (various stages)		0.9216	0.93 (heterogeneous moderated configurations)	3 vol% (14.5 kg GdPO ₄ distributed with the initial filler mixture.	
IP-4	SNF degrades before the internals of the waste package	SNF degrades before the internals of the waste package	The configurations resulting from these scenarios (configurations classes #4, #5) have not been investigated in the geochemistry and criticality analyses due to the fact that they are less moderated (no pooling of water) and are bounded by the variations of the configurations investigated above.				
IP-5	The bottom of waste package is penetrated allowing liquid to flow through	SNF degrades concurrently with the internals of the waste package					
		SNF degrades after the internals of the waste package					
IP-6							

10.5 SHIPPINGPORT LWBR SNF

The description and main characteristics of the waste package containing Shippingport LWBR SNF are presented in Section 3.2.5. In this section a summary of the results of the criticality analyses performed is presented together with the current status of the validation of the criticality model for the configurations that are specific for the codisposal of this fuel group.

The first step in applying the criticality model to the specific intact and degraded configurations of this waste package is identification and characterization of the specific configurations anticipated for postclosure. The results of the degradation analysis coupled with the geochemistry calculations (CRWMS M&O 2000e, Section 6) provided an insight into the possible arrangements and compositions of the degraded materials placed within the waste package. All configuration classes analyzed and the most probable degradation scenario that was identified are summarized in the next section (Section 10.5.1). The results of the criticality calculations for the most representative intact and degraded configurations are presented in Section 10.5.2. The limiting cases identified during the analysis are also providing the basis for deriving the final design solution (amount of neutron absorber to be distributed within the initial waste package). The range of parameters that characterize the limiting or the most reactive cases is subsequently used in the process of validation of the criticality model. The process includes selection of appropriate critical benchmark experiments and derivation of the specific lower tolerance bound limit for each major group of configurations.

The results of the three-dimensional Monte Carlo criticality calculations for all anticipated intact and degraded configurations show that the requirement of $k_{\text{eff}}+2\sigma$ less than or equal to the interim critical limit of 0.92 (CRWMS M&O 2000e, Section 2.4.3) is satisfied for the Shippingport LWBR waste package with at least 1.0 percent by mass of gadolinium in the aluminum shot-GdPO₄ filler (10.12 kg GdPO₄). The gadolinium must be uniformly distributed in the initial aluminum shot-GdPO₄ filler, and there must be some reasonable degree of mixing of the gadolinium containing filler (or degraded filler) with the fuel mixture layer for many degraded cases. The results show that a uniform distribution of filler material in all available void spaces inside the DOE SNF canister (including void spaces in the fuel assembly) is highly desirable and further increases the margin for criticality.

All calculations are based on a maximum of 16.6 kg ²³³U per DOE SNF canister. The analyses are based on the fuel type that has the highest ²³³U concentration. The degraded configurations of the Shippingport LWBR SNF bound the other types of U-Th DOE-owned SNF, as long as the limits on mass of uranium and its enrichment, and the linear density, are not exceeded (CRWMS M&O 2000e, Section 8.6).

10.5.1 Degradation Scenarios and Configurations

Based on the material thickness given in Table 10-14 and the corresponding corrosion rates, the most probable degradation path for the waste package, the DOE SNF canister, and the Shippingport LWBR SNF follows the following sequence (CRWMS M&O 2000e, Section 6.2.1):

1. Waste package is penetrated and flooded internally. The waste package basket, (outer and inner brackets and support tube) degrades first because of the high corrosion rate for A516 carbon steel.
2. DHLW glass canister's stainless steel shell and glass begin to degrade. After this, there are two degradation paths:
 - 2a. DOE SNF canister stays intact. Intact DOE SNF canister and intact SNF assembly fall on top of degraded products near the bottom of the waste package. The neutron absorber stays together with the fuel rods.
 - 2b. DOE SNF canister starts to degrade.
3. DOE SNF canister is penetrated and flooded.
4. Components internal to the DOE canister are in contact with water. These components include the SNF basket structure, the fuel assembly, and filler material (aluminum shot).
5. The aluminum shot will degrade first. There is a possibility of a partial separation between the neutron absorber and the fuel rods.
6. SNF cladding gets in contact with water.
7. DOE SNF canister basket degrades. After this, there are two paths:
 - 7a. SNF assembly and rods stay intact and fall on top of degraded DOE SNF canister basket and settle on the bottom of the DOE SNF canister.
 - 7b. DOE SNF canister degrades. Intact SNF assembly and rods fall on top of all degradation products near the bottom of the waste package. Given time, the SNF assembly shell might be degraded enough that the rods scatter on top of all degradation products.

Given a very long period of time, it is postulated that everything will degrade including cladding and fuel. This is not likely because of very long lifetime of Zircaloy-4, which will most likely outlast the waste package. To bound the potential degraded cases, degradation of the SNF can be considered. The degraded SNF and other degradation products could mix and pile up near the bottom of waste package. However, there is no mechanism to cause complete and uniform mixing of all the degradation products inside the waste package.

Table 10-14. Materials and Thicknesses

Components	Material	Thickness (mm)
Waste package basket	A516 Carbon Steel	12.7
Waste package inner bracket	A516 Carbon Steel	25.4
Waste package support tube	A516 Carbon Steel	31.75
HLW glass shell	304L Stainless Steel	10.5
HLW glass	Glass	N/A
DOE SNF canister	316L Stainless Steel	9.525
DOE SNF canister basket	316L Stainless Steel	9.5
Neutron absorber (Al shot with 1 wt% Gd)	Al/GdPO ₄	3.0 (nominal diameter)
Seed assembly hexagonal shell	Zircaloy-4	2.032
SNF cladding	Zircaloy-4	0.563118
SNF pellets in seed assembly	ThO ₂ and UO ₂ mixture	6.4008 (nominal diameter)
	ThO ₂ only	6.49224 (nominal diameter)

Source: CRWMS M&O 2000e, p. 59

The configurations investigated can be categorized using the description of the generic configuration classes given in Section 3.3.1 of *Disposal Criticality Analysis Methodology Topical Report* (YMP 2003). As indicated in Section 6.5 for the purpose of fully identifying the potential for criticality, all representative configurations classes have been analyzed and not only the configurations resulting from the most probable degradation path presented above. The subtitles follow the original description given in Section 6.2.1.1 of *Evaluation of Codisposal Viability for Th/U Oxide (Shippingport LWBR) DOE-Owned Fuel* (CRWMS M&O 2000e).

Degraded DOE SNF Canister Basket and Intact SNF—For these cases of intact fuel assembly within degraded basket, the scenarios and configuration classes are applied to the DOE SNF canister and its contents. This configuration is a variation of configuration class 1 and can be reached from standard scenario IP-3 (YMP 2003, Section 3.3.1).

Intact DOE SNF Canister and Degraded Waste Package Internals—In this case, the concepts of scenario and configuration are applied to the entire waste package. The fuel assembly and the DOE SNF canister shell are intact. This configuration is a variation of configuration class 1 and can be reached from standard scenario IP-3 (YMP 2003, Section 3.3.1).

Degraded DOE SNF Canister and Waste Package Internals, Intact SNF—In this case, the concepts of scenario and configuration are applied to the entire waste package. The DOE SNF canister, waste package internals, and DHLW glass canisters are degraded. The fuel assembly is intact. This configuration is achievable because of very low degradation rate of Zircaloy-4, which envelops and protects the fuel. This configuration is a variation of configuration class 1 and can be reached from standard scenario IP-3.

Degraded SNF with Intact DOE Canister or Waste Package—In this case, the SNF could be partially or fully degraded. As a variation, the internal components of DOE SNF canister could be also degraded. This configuration is a variation of configuration class 6 and can be reached from standard scenario IP-1.

Partially or Completely Degraded DOE SNF Canister and Waste Package Internals—In this case, the concepts of scenario and configuration are applied to the entire waste package. Degradation products from the DOE SNF canister and contents form a layer on the bottom of the waste package. The degradation products (clay) from waste package internals and DHLW glass canisters form a layer above. This configuration is a variation of configuration class 2 and can be reached from standard scenario IP-1, IP-2, or IP-3.

10.5.2 Criticality Calculations and Results

10.5.2.1 Results for Intact Mode

This section summarizes the results of the intact-mode (phase I) criticality analysis (CRWMS M&O 2000e, Section 7.3). Although the components of the waste package (fuel assembly, cladding, supporting structures, and canisters) are considered structurally intact, water intrusion into the available internal volumes is assumed in order to determine the highest k_{eff} resulting from optimum moderation. The contents of the waste package outside the DOE SNF canister are intact in all cases considered in this section except as noted.

For the intact mode configurations, the contents of the DOE SNF canister are in an “as-welded/loaded position and condition,” as depicted in Figure 10-17 (showing only the fuel assembly placed inside the DOE SNF canister). The void space outside the fuel assembly and inside the SNF canister is filled with aluminum (Al) shot containing gadolinium phosphate (GdPO_4). Different weight percentages of Gd in the Al-GdPO_4 mixture have been investigated, with a baseline of 1 wt% Gd in the mixture (10.12 kg GdPO_4).

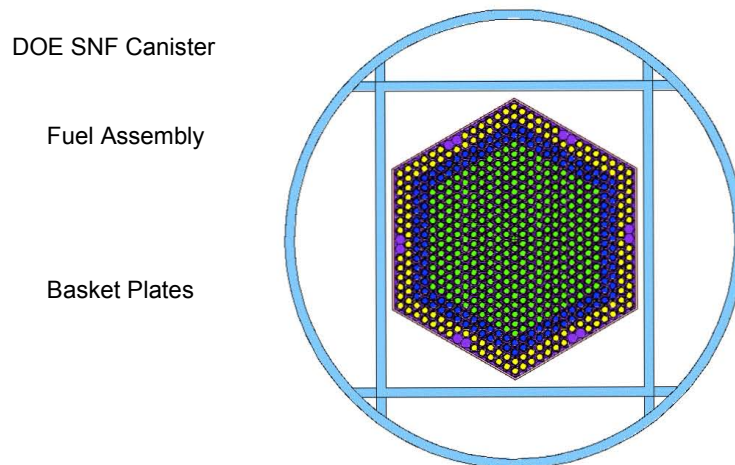


Figure 10-17. Cross-Section View of the Waste Package Showing the Contents of the DOE Spent Nuclear Fuel Canister for the Intact-Mode Analysis

The aluminum shot is used as a means of uniformly distributing the gadolinium phosphate throughout the SNF canister, and the gadolinium phosphate is used as an insoluble neutron absorber. However, since the waste package is to be emplaced horizontally in the repository, the various components inside the waste package are considered to be settled for most cases of interest.

All configurations investigated for intact-mode analysis and the representative results obtained are summarized in *Evaluation of Codisposal Viability for Th/U Oxide (Shippingport LWBR) DOE-Owned Fuel* (CRWMS M&O 2000e, Section 7.3.1). The base intact configuration investigated is similar to the one shown in Figure 10-17, but the DOE SNF canister contains water saturated aluminum fill material and no gadolinium phosphate. Vacant spaces in the waste package outside the SNF canister are treated as voids while the waste package is reflected by full density water. Void spaces in the fuel pins and fuel pellets are saturated with water. The $k_{\text{eff}}+2\sigma$ for the base intact configuration is 0.9140 (with no Gd) and is below the interim critical limit of 0.92 defined in *Evaluation of Codisposal Viability for Th/U Oxide (Shippingport LWBR) DOE-Owned Fuel* (CRWMS M&O 2000e, Section 2.4.3).

Cases with water replacing the filler were also studied to determine how k_{eff} of the intact mode is affected by these conditions. Water density variations were investigated for these cases to evaluate their impact on the value of k_{eff} . The water density was varied inside the DOE SNF canister and also inside the waste package but outside the DOE SNF canister. Effects of partially filling the voids in the fuel pellets with water for the base intact configuration were also investigated. It should be noted that while some cases do not seem to be realistic (i.e., physically possible), they were considered in order to obtain more conservative (higher) estimates for k_{eff} . The results show in all mentioned cases a decrease in $k_{\text{eff}}+2\sigma$ from the base intact configuration, spanning a range of values between 0.4374 to 0.9001 (CRWMS M&O 2000e, Table 35).

The $k_{\text{eff}}+2\sigma$ of 0.9140 for the base intact configuration is reduced to 0.8659 by the addition of 0.1 wt% Gd to the filler. The final baseline design is based on 1.0 wt% Gd in the filler, which provides a large margin for all these cases. The results also show that reducing the water density in the DOE SNF canister produces a significant decrease of k_{eff} . This demonstrates that the system is not over-moderated.

Another important finding for this class of configurations is that the conditions outside the DOE SNF canister have a negligible impact on the k_{eff} of the system. Replacing the water reflector that surrounds the waste package and degrading the contents of the waste package outside the DOE SNF canister have a minor effect on the results.

Occurrence of design basis events, including those with the potential for flooding the disposal container prior to its sealing, is considered and bounded by the analysis results presented above for many different intact configurations.

10.5.2.2 Results for Intact Fuel Assembly in Partially Degraded DOE SNF Canister

The partially degraded mode refers to the cases where the basket plates of the DOE SNF canister have started to degrade to goethite. Cases where the aluminum filler has degraded to diasporite are also considered. The assembly is considered intact and water fills the voids between fuel pins (coolant channels) in the assembly. This mode has been summarized in *Evaluation of Codisposal Viability for Th/U Oxide (Shippingport LWBR) DOE-Owned Fuel* (CRWMS M&O 2000e, Section 7.4.1) and a typical representation is shown in Figure 10-18. The waste package contents outside the DOE SNF canister are considered intact in all cases unless otherwise noted. The degradation configurations and their refinements belong to the standard configuration Class 1 that is obtained via standard group scenario IP-3 (YMP 2003).

Cases have been investigated with different layers of goethite, diaspore or aluminum fill and varying volume fractions of water in these materials (CRWMS M&O 2000e, Table 36). As mentioned in *Evaluation of Codisposal Viability for Th/U Oxide (Shippingport LWBR) DOE-Owned Fuel* (CRWMS M&O 2000e), there is no mechanism to cause significant segregation/stratification of the layers containing degradation products. These cases are overly conservative and unlikely, and have been analyzed only for completeness. Additional cases analyzed had the diaspore, goethite and water mixed together. These cases bound all possible compositions with higher hydrated products of Al (e.g., gibbsite).

The results show that the maximum $k_{\text{eff}}+2\sigma$ is 0.8950 for the baseline design with 1.0 wt% Gd in the Al filler. Complete separation of the layers of the degradation products inside the DOE SNF canister is impossible for the present design, where the fill material is distributed on both sides of the basket. The k_{eff} remains below the interim critical limit of 0.92 if more than 3 percent of the initial amount of Gd is distributed in the mixture that surrounds the fuel assembly. The remaining diaspore and Gd is positioned above the assembly. As mentioned above, the initial Al-GdPO₄ mixture is uniformly distributed around the fuel assembly, therefore a separation in a layer is extremely unlikely. The cases analyzed are very conservative and bound all possible configurations with an intact fuel assembly in the DOE SNF canister.

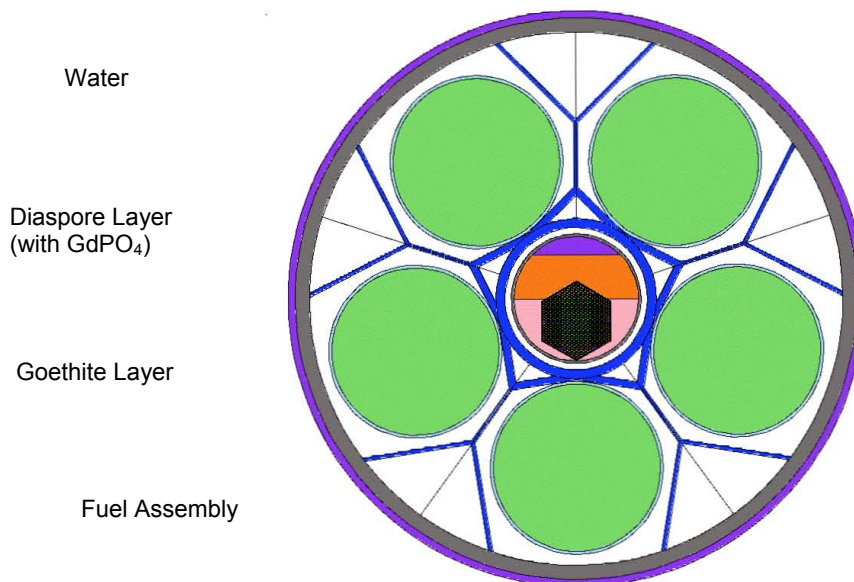


Figure 10-18. Intact Assembly Surrounded by Degraded Contents of the DOE Spent Nuclear Fuel Canister in an Intact Waste Package

Results for Partially Degraded Fuel Assembly in Intact DOE SNF Canister—In these configurations the DOE SNF canister and its internal components are considered intact while the assembly is partially degraded. The degradation of the assembly is partial since only the pitch of the fuel pins or the axial spacing between fuel pellets in the fuel pins are affected. These cases are described in *Evaluation of Codisposal Viability for Th/U Oxide (Shippingport LWBR) DOE-Owned Fuel* (CRWMS M&O 2000e, Section 7.4.2) and are belonging to configuration class 6 (YMP 2003). The typical configuration is depicted by the first representation in Figure 10-19. Aluminum-fill material surrounds the assembly inside the DOE SNF canister for all cases.

As the pitch decreases the configurations become less reactive (CRWMS M&O 2000e, Table 37), which is consistent with the assembly being undermoderated. Increases in pitch were not considered since as long as the pins remain inside the assembly shroud it is highly improbable, if not impossible, for the pitch to increase due to degradation.

Enlarging the axial separation between fuel pellets initially increases the reactivity of the systems, but reaches a maximum value for $k_{\text{eff}}+2\sigma$ of 0.9040 that corresponds to a separation of 1.0 cm between pellets. Changing the boundary conditions outside DOE SNF canister (e.g., prebreach clay) has a minor influence on k_{eff} of the system (CRWMS M&O 2000o, Sections 6.2.1 and 6.2.2). The results show a large margin even for an optimally moderated condition, which is extremely unlikely.

Results for Partially to Totally Degraded Internal Structures of DOE SNF Canister with Intact Fuel Pins—These configurations comprise the intact fuel pins distributed inside the DOE SNF canister at various stages of degradation of the internal supporting structure. Two variations are shown in Figure 10-19. By applying the IP-1 scenario to DOE SNF canister the fuel pins will end up stacked in a configuration with settled pins in the DOE SNF canister (collapsed assembly). The configuration is a variation of the configuration mentioned above. Configurations with fuel pins completely separated from the neutron absorber are not possible with the present configuration because a uniform mixture of aluminum shot and neutron absorber initially surrounds the assembly and there is no identified mechanism to cause significant segregation/stratification of the layers.

For the partially degraded DOE SNF canister, the basket plates are assumed to be intact and cases with the aluminum fill material intact and degraded have been considered. The pins are assumed to remain in a triangular lattice array for all cases. The intact pitch was assumed for most cases, but variations in pitch were also investigated. Since the assembly contains four different types of fuel pins with different fissile loadings, once the pins become loose there is a very large number of configurations possible due to the many different ways of positioning the four pin types. To minimize the number of possible configurations and to still obtain conservative results all pins were replaced by each of the four different types of pins.

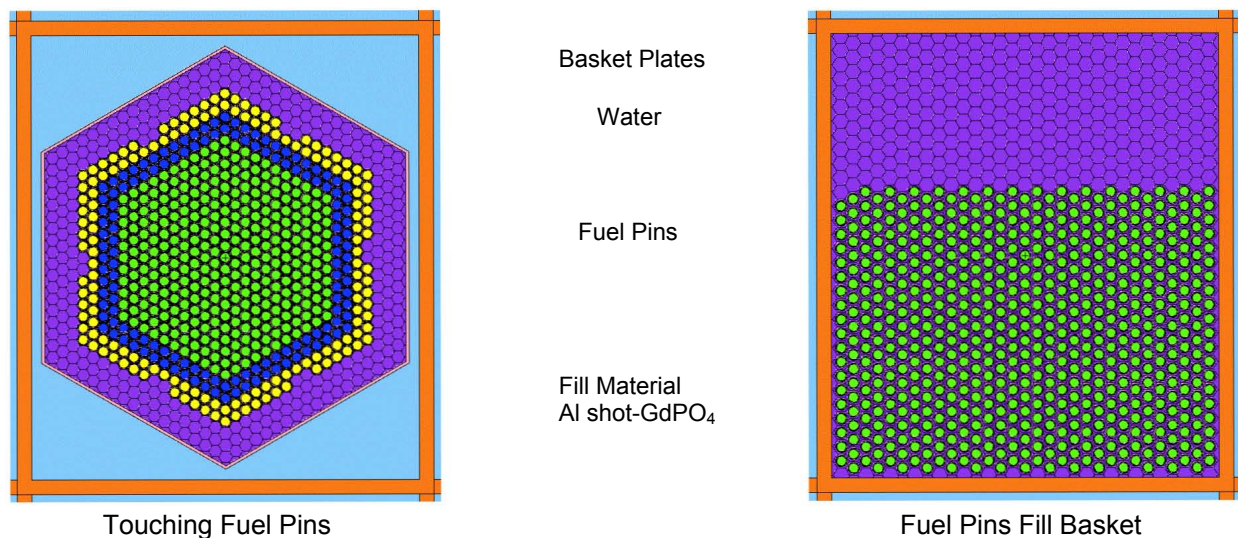


Figure 10-19. Different Arrangements of Fuel Pins Inside DOE Spent Nuclear Fuel Canister

The results (CRWMS M&O 2000e, Table 39) show that the values of $k_{\text{eff}} + 2\sigma$ span a range between 0.6232 to 0.9135 (below the interim critical limit of 0.92) and are significantly reduced if the spaces between fuel pins are filled with the gadolinium-containing material. Any reduction in the pitch of the fuel pins also decreases the configuration's k_{eff} value. Changing the boundary outside DOE SNF canister with dried prebreach clay slightly increases the k_{eff} of the system.

By assuming a further degradation of the basket plates, the loose pins will spread in the DOE SNF canister in a mass of degraded products. For the totally degraded supporting structure and contents of the DOE SNF canister, the canister shell is assumed to be breached but structurally intact. The degradation products resulting from degradation of the canister internals (mainly FeOOH [goethite] and AlOOH [diaspore]) are distributed among the fuel pins. All fuel pins from the assembly are modeled as being from the zone with the highest fissile concentration, therefore the most reactive. The placement of pins in the canister is irregular. The effect of pitch variations for the array of intact pins on k_{eff} of the system was investigated. The minimum necessary amount of neutron absorber to bring k_{eff} below the interim critical limit of 0.92 was determined. The layout of this type of configuration is presented in Figure 10-20.

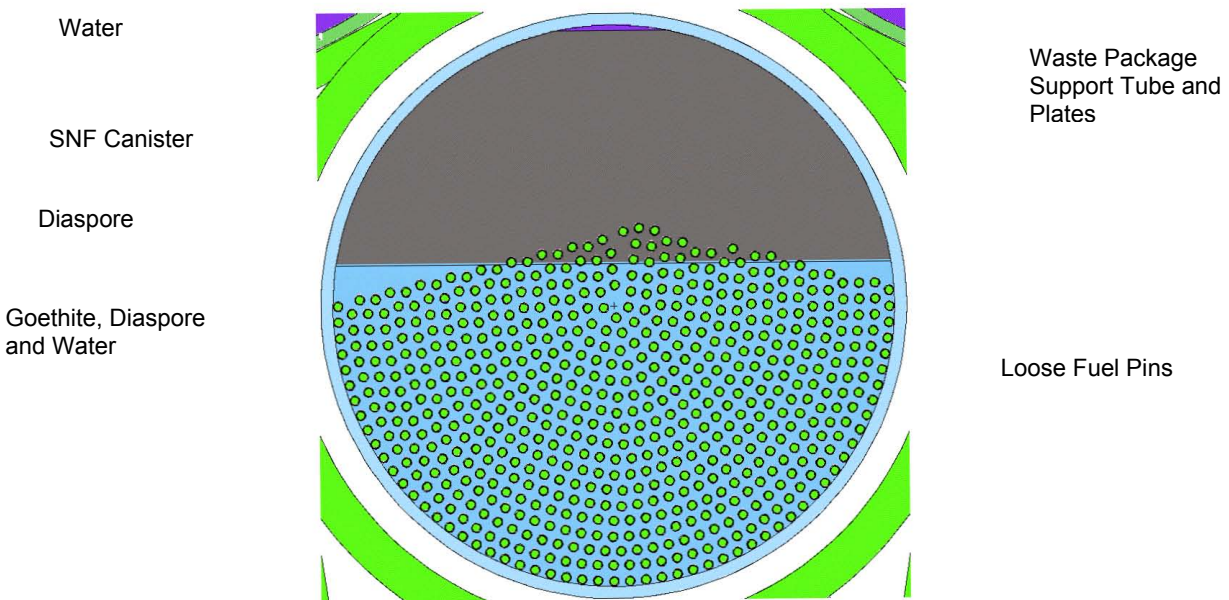


Figure 10-20. Cross-Section View of the Degraded Configuration with Intact Fuel Pins Dispersed within the DOE Canister Shell

These results (CRWMS M&O 2000e, Table 39) show that the greatest effect on k_{eff} of the system results from changes in the fuel pin pitch. The pitch producing the largest value of k_{eff} occurs at about 1.25 cm. For this case, at least 0.18 kg of Gd (approximately 3 percent of the total initial Gd mass of the baseline design in the DOE SNF canister) mixed with the goethite and water is sufficient to reduce k_{eff} well below the interim critical limit of 0.92 ($k_{\text{eff}} + 2\sigma = 0.8978$). Given the relatively uniform initial configuration of the GdPO_4 in the DOE SNF canister the degraded configuration should also be relatively uniform, providing a large margin. If the pitch is no greater than the initial value in the intact assembly and material is mixed between the fuel pins, then values of k_{eff} are well below the interim critical limit. The credibility

of scenarios with separated pins (large pitch) must be demonstrated to insure that they do not defy gravity. Also, there is no identified mechanism to cause significant segregation/separation of the neutron absorber above the fuel. Since the expected values for the mixing fractions of diaspore (containing Gd) with goethite are much higher than the investigated values, there is a large margin to prevent criticality.

10.5.2.3 Results for Degraded Configurations Postulated Beyond the Regulatory Period

The degradation and criticality analyses performed have also investigated configurations that require very long times to be attained. These configurations are anticipated to happen well beyond the regulatory period of 10,000 years but they have been analyzed to fully investigate the potential for criticality of the waste package containing Shippingport LWBR. For the purpose of this document, these results (CRWMS M&O 2000e, Sections 7.4.4 and 7.5) have been summarized and grouped together in this section.

Degraded Waste Package and DOE SNF Canister Internal Structures with Intact DOE SNF Canister Shell—The configurations analyzed in this group are refinements of the configuration Class 2 discussed in *Generic Degradation Scenario and Configuration Analysis for DOE Codisposal Waste Package* (CRWMS M&O 1999g) and can be obtained via any of the standard top-breach scenarios (IP-1, IP-2, or IP-3) after a very long time due to the very low degradation of the DHLW glass logs. The configurations include an intact (but breached) DOE SNF canister outer shell that contains the mixture of degraded fissile material and other degradation products from the DOE SNF canister. All other internal structures inside waste package but external to the DOE SNF canister are degraded. The general configuration (CRWMS M&O 2000e, p. 28) is a very unlikely configuration given the corrosion resistance of the fuel pin cladding, but was analyzed for completeness.

Various compositions and densities of the degraded mixture inside the DOE SNF canister have been evaluated (CRWMS M&O 2000o, Table 6-17). The results show (CRWMS M&O 2000e, Table 40) that if at least 4 percent of the Gd initially present in the DOE SNF canister of the baseline design is distributed in the layer containing the degraded fuel, the k_{eff} for the system will be below the interim critical limit of 0.92 ($k_{\text{eff}} + 2\sigma = 0.8894$). Given the relatively uniform distribution of Gd in the initial configuration, the degraded configuration should have also a relatively uniform distribution of Gd, providing a large margin. The cases discussed above represent overly conservative configurations that will bound any configurations with intact fuel.

Degraded Waste Package Internal Structures with an Intact Fuel Assembly—This group of configurations presented in *Evaluation of Codisposal Viability for Th/U Oxide (Shippingport LWBR) DOE-Owned Fuel* (CRWMS M&O 2000e, Section 7.5.1), are characterized by an intact fuel assembly immersed in the degradation materials resulting from the degradation of the DHLW glass and other internal components of the waste package and the DOE SNF canister. This group represents a refinement of the configuration Class 1 (YMP 2003). It should be noted that spacer grids are made of stainless steel; therefore the preservation of the fuel assembly in the initial configuration is highly improbable.

The configurations have the voids inside the assembly filled with a mixture of prebreach (or postbreach) clay and water. The prebreach clay is formed after few tens of thousands of years

from the complete degradation of components outside the DOE SNF canister: DHLW glass canisters, waste package internal web-like structure, and tube. The postbreach clay is formed through the mixing of the prebreach clay with the completely degraded components of the DOE SNF canister except the fuel assembly.

The results show (CRWMS M&O 2000e, Table 41) that the presence of absorbing impurities inside the assembly has a major role in reducing the reactivity of the system. Increasing the water content in the postbreach clay results in an increase of the $k_{\text{eff}} + 2\sigma$. If at least 10.0 percent of the mixture filling the voids inside the assembly is prebreach clay the k_{eff} of the system is below the interim critical limit, even by neglecting the presence of Gd in the system. The waste package outer boundary conditions have a negligible effect on the reactivity of the system for these configurations. The presence of a very small amount of Gd distributed inside the fuel assembly is also very effective in reducing k_{eff} of the system. These results recommend having some of the neutron absorber distributed from the beginning inside the void spaces of the fuel assembly. This will assure a considerable higher margin for criticality.

The final set of results was obtained using the postbreach clay in the waste package that is also filling the voids inside the assembly. For these cases water fills any voids in the waste package not filled by the postbreach clay. The results show that the presence of postbreach clay results in much lower $k_{\text{eff}} + 2\sigma$ values than in the previous cases (CRWMS M&O 2000e, Table 42).

Degraded Waste Package Internal Structures with Intact Fuel Pins—This group of configurations, characterized by intact fuel pins immersed in the clayey material resulting from the degradation of the DHLW glass and other internal components of the waste package and the DOE SNF canister, represents a further refinement of the configuration Class 1 (YMP 2003). It can be reached by applying the standard scenario group IP-3 to both the DOE SNF canister and waste package and results as a subsequent stage of degradation of the configuration presented above. The configurations are considered likely due to the high corrosion resistance of the zirconium fuel cladding but they require a very long time to reach this stage of degradation (well beyond the regulatory period of 10,000 years). The intact fuel pins are assumed dispersed in the degradation products in a lattice with constant pitch.

The results (CRWMS M&O 2000e, p. 78) show that if only 5.5 percent of the total initial amount of Gd in the waste package is mixed in the layer with the fuel, the maximum $k_{\text{eff}} + 2\sigma$ is 0.8824. The boundary conditions outside the waste package have a more significant effect on the k_{eff} than most other configurations. For example, replacing the water reflector with dry tuff increases k_{eff} with approximately 3 percent (from 0.8824 to 0.9115).

Results for the fuel pins surrounded by postbreach clay show that $k_{\text{eff}} + 2\sigma$ are much smaller than in previous cases. Water fills any vacant spaces in the waste package. The range of the results for $k_{\text{eff}} + 2\sigma$ is between 0.5623 and 0.7475.

There are no criticality concerns for these cases, since these results are well below the limit of 0.92. Any increase or reduction in the pitch or spreading out of the fuel pins would only further reduce these values of k_{eff} .

Degraded DOE SNF Canister Mixture Settled at the Bottom of the Waste Package—After the complete degradation of all waste package internal constituents, including the DOE SNF canister, the resultant configurations can include the degradation products as layers or complex mixtures settled within the waste package. These configurations belong to Class 2 (CRWMS M&O 1999g). This class comprises a large number of refinements and variations, and it can be reached by any of the standard top-breach scenarios (IP-1, IP-2, or IP-3). The time required to reach these configurations is well beyond the regulatory period of 10,000 years. A bounding approach was also adopted for this analysis, investigating various possible combinations of the fissile material with different degradation constituents.

The results (CRWMS M&O 2000e, Section 7.5.3) show that if at least 5 vol% of the mixture containing degraded fuel is diaspore (containing $GdPO_4$), the $k_{eff} + 2\sigma$ is below 0.92 even considering the most conservative reflective boundary conditions. This corresponds to 0.316 kg of Gd being distributed uniformly in the layer containing degraded fuel (5 percent of the initial total amount).

The inclusion of the prebreach clay in the fuel mixture further reduces the k_{eff} of the system, but only for volumes significantly greater than the volume of diaspore. If at least 5 vol% of the fuel mixture is prebreach clay, the presence of 1.75 vol% of diaspore + $GdPO_4$ in the layer, which represents only 1.85 percent of the total Gd in the waste package, will bring the $k_{eff} + 2\sigma$ to 0.8785, well below the interim critical limit. Since these kinds of final mixtures are the most probable due to the evolution of the system, there are no criticality concerns for the fully degraded configurations. Changing the waste package boundary conditions from water reflector to dry tuff produces an increase in $k_{eff} + 2\sigma$ from 0.8785 to 0.9123.

Results for the cases with postbreach clay show that if at least 10 percent by volume of the fuel mixture (fuel, water and clay) is clay then there are no criticality concerns ($k_{eff} + 2\sigma = 0.8941$). If only water is mixed with the fuel then the large amount necessary to raise k_{eff} above the limit of 0.92 would result in the density of the mixture being such that it would not be capable of supporting the clay above it.

Results for Axial Redistribution of Degraded DOE SNF in the Canister and in the Waste Package—Results are presented in *Intact and Degraded Criticality Calculations for the Codisposal of Shippingport LWBR Spent Nuclear Fuel in a Waste Package* (CRWMS M&O 2000o) for cases where the fully degraded fuel in the bottom of either the SNF canister or the waste package is axially redistributed (i.e., its length becomes shorter or longer than its intact footprint length). These results show that as the length becomes greater the k_{eff} of the system becomes smaller. Likewise, any decrease in the length of the fuel region leads to an increase in the system k_{eff} . As an example for the cases presented, a 10.0 percent increase in length leads to at least a 1.5 percent decrease in k_{eff} , while the largest increase in k_{eff} is 5.2 percent for a 10 percent decrease in length. These results suggest the necessity of imposing a limit on the linear loading for the fissile material in the DOE SNF canister. A homogeneous model of the fuel was developed to demonstrate that similar fuels (U/Th oxide), containing the same amount (or less) of fissile material, are bound by the results for Shippingport LWBR SNF. The results (CRWMS M&O 2000o, Table 6-22) show that for the various homogeneous configurations considered (with different degrees of simplification), the k_{eff} of the system is lower or within the uncertainty band of the maximum heterogeneous case. The linear density of the ^{233}U should not

exceed 92.5 g/cm in the canister. This value is calculated for the axial zone with maximum fissile loading by summing the initial linear fissile density per rod for all the rods in the seed assembly.

Results for Uranium Decay Effects—The half-life of ^{233}U is several orders of magnitude smaller than that of ^{235}U , 159,200 years and 704,000,000 years, respectively (Parrington et al. 1996, p. 49). The shorter of these times is certainly of the order of what is of immediate concern for the life of the repository. Therefore, results for selected cases are given in *Intact and Degraded Criticality Calculations for the Codisposal of Shippingport LWBR Spent Nuclear Fuel in a Waste Package* (CRWMS M&O 2000o) for the system k_{eff} after a passage of 50,000, 100,000 and 150,000 years. For the cases examined the minimum decrease in k_{eff} after a passage of 50000 years is about 5.3 percent whereas, the minimum decrease after 150,000 years is 17.5 percent. These results show that uranium decay has a very important effect in reducing the k_{eff} of the system. The highly degraded configurations (that require long times) have a drastically reduced potential for criticality.

10.5.3 Range of Parameters for Configurations of Waste Package Containing Shippingport LWBR DOE SNF

ANSI/ANS-8.1-1998 and *Disposal Criticality Analysis Methodology Topical Report* (YMP 2003) provide basic requirements for validation of a calculational method used in the criticality analysis of a system. The bias of a code system (in this case the criticality model containing software code MCNP and selected cross-section libraries) is determined by correlating the results of critical and near-critical experiments with calculated results for those experiments. The common practice, and that considered by the current validation methodology (BSC 2003e), is for comparison of the calculated k_{eff} to a critical or near critical system.

Prior to the initiation of the validation activity, the operating conditions and parameters for which the validation is to apply must be identified. The fissile isotope, enrichment of fissile isotope, fuel density, chemical form of fuel, types of neutron moderators and reflectors, range of moderator to fissile isotope ratio, neutron absorbers and physical configurations are among the parameters to specify. These parameters will define the area of applicability for the selection of the critical experiments for the validation effort.

The preliminary degradation analysis of the contents of the waste package containing Shippingport LWBR SNF (CRWMS M&O 2000e, Section 6) and the subsequent criticality analysis performed for the resulting internal configurations have followed the guidance suggested by the Internal Criticality Master Scenarios presented in *Disposal Criticality Analysis Methodology Topical Report* (YMP 2003, Section 3.3) and also by *Generic Degradation Scenario and Configuration Analysis for DOE Codisposal Waste Package* (CRWMS M&O 1999g, Section 6.2.2). The resultant configuration classes internal to the waste package have been screened systematically for their criticality potential in comprehensive criticality analyses (CRWMS M&O 2000o). The main results have been summarized in the sections above.

For the purpose of the criticality model validation for the configurations specific to the waste package containing Shippingport LWBR SNF and identification of the range of parameters that characterize the internal configurations of the degraded waste package, the degraded

configurations previously investigated (see Section 10.5.2.1 to 10.5.2.3) have been categorized in two large groups:

1. Configurations containing intact fuel rods (heterogeneous configurations)
2. Configurations containing degraded fuel rods (relatively homogeneous configurations).

The first category contains the configurations described in *Evaluation of Codisposal Viability for Th/U Oxide (Shippingport LWBR) DOE-Owned Fuel* (CRWMS M&O 2000e, Sections 7.3.1 [intact mode], 7.4.1 [intact fuel assembly in partially degraded DOE SNF canister], 7.4.2 [partially degraded fuel assembly in intact DOE SNF canister], 7.4.3 [partially to totally degraded internal structures of DOE SNF canister with intact fuel pins], 7.5.1 [degraded waste package internal structures with intact fuel assembly], and 7.5.2 [degraded waste package internal structures with intact fuel pins]). These configurations represent intact (nondegraded waste form) configurations and refinements of the general configuration class 1 and 6 as described in *Disposal Criticality Analysis Methodology Topical Report* (YMP 2003, Section 3). The second category includes the configurations described in *Evaluation of Codisposal Viability for Th/U Oxide (Shippingport LWBR) DOE-Owned Fuel* (CRWMS M&O 2000e, Sections 7.4.4 [degraded waste package and DOE SNF canister internal structures with intact DOE SNF canister shell] and 7.5.3 [degraded DOE SNF canister mixture settled at the bottom of the waste package]). These configurations represent refinements of the general configuration classes 2 and 6 that are described in *Disposal Criticality Analysis Methodology Topical Report* (YMP 2003, Section 3). This proposed categorization allows a simple and systematic way of identifying the key parameters that characterize the degraded configurations.

The process employed in *Intact and Degraded Criticality Calculations for the Codisposal of Shippingport LWBR Spent Nuclear Fuel in a Waste Package* (CRWMS M&O 2000o) for investigating the potential for criticality of the possible degraded configurations of the waste package used a screening approach, the goal being to identify the most reactive configurations in a given class of degraded configurations. Due to this approach, the number of configurations analyzed varies among the classes of configurations depending on the complexity of the possible arrangements and the initial screening results. Selected cases (typically the most reactive or the limiting cases as presented in CRWMS M&O 2000e, Sections 7.3.1, 7.4.1, 7.4.2, 7.4.3, 7.4.4, 7.5.1, 7.5.2, and 7.5.3) have been rerun with tallies calculating the neutron flux and the fission rate in the regions containing the fissile material. The results of the cases that were rerun with tallies are summarized in Attachment IV of *Criticality Model Report* (BSC 2003e) together with a summary of the key physical and neutronic parameters characterizing the most reactive configurations (ROP).

10.5.4 Selection of the Criticality Benchmark Experiments Used in the Validation of the Criticality Model

The benchmark experiments selected in the validation of the criticality model used for the analysis of the waste package containing Shippingport LWBR come from *International Handbook of Evaluated Criticality Safety Benchmark Experiments* (NEA 2001) unless otherwise noted. The selection process was initially based on previous knowledge regarding the possible

configurations of degraded waste packages, and the subsets have been constructed to accommodate large variations in the range of parameters of the configurations and also to provide adequate statistics for lower bound tolerance limit calculations. The selected benchmark experiments for each subset are presented in *Benchmark and Critical Limit Calculation for DOE SNF* (BSC 2002c) together with the MCNP cases constructed and the results of the calculations. For the present application (codisposal of Shippingport LWBR SNF), the selected benchmark experiments have been grouped in two subsets (BSC 2002c), that include moderated heterogeneous and homogeneous experiments. The cases, corresponding k_{eff} results and their uncertainties for all benchmark experiments are also summarized in Attachment II of *Analysis of Critical Benchmark Experiments and Critical Limit Calculation for DOE SNF* (BSC 2003f). Table 10-15 presents the list of the benchmark experiments and the number of cases for each subset selected for validation of the criticality model for Shippingport LWBR SNF.

Table 10-15. Critical Benchmarks Selected for Validation of the Criticality Model for Shippingport LWBR Spent Nuclear Fuel

Subset	Benchmark Experiment Identification ^b	Number of Cases Included
Heterogeneous moderated ^c	Experiment with SB cores ^a	8
	HEU-COMP-MIXED-001	26
	U233-SOL-THERM-006	12
	HEU-COMP-THERM-003	15
	HEU-COMP-THERM-005	1
	HEU-COMP-THERM-006	3
	HEU-COMP-THERM-007	3
	HEU-COMP-THERM-011	3
	HEU-COMP-THERM-012	2
	HEU-COMP-THERM-013	2
Homogeneous moderated ^c	U233-SOL-THERM-001	5
	U233-SOL-THERM-002	17
	U233-SOL-THERM-003	10
	U233-SOL-THERM-004	8
	U233-SOL-THERM-005	2
	U233-SOL-THERM-006	12
	U233-SOL-THERM-008	1
	HEU-COMP-MIXED-001	26

Sources: Subsets defined and evaluated in BSC 2002c except SB core experiments that are evaluated in BSC 2003f.

NOTE: ^a These experiments were evaluated in BSC 2003f, Section 6.1

^b The convention for naming the benchmark experiments is from NEA 2001.

^c Identification of each subset from BSC 2002c has been modified to better reflect the subset's main characteristics. The benchmark experiments in each subset have not been affected.

The experiments listed in Table 10-15 are considered appropriate to represent intact (non degraded) configurations and degraded configurations of the waste package containing Shippingport LWBR SNF that belong to configuration classes 1, 2, and 6 as described in

Disposal Criticality Analysis Methodology Topical Report (YMP 2003, Section 3.3.1). Their range of applicability is detailed in Attachment IV of *Criticality Model Report* (BSC 2003e).

10.5.5 Comparison Between ROA of Benchmark Experiments and ROP

The validation of the criticality model needs to show that the range of the fundamental parameters of the benchmark critical experiments (ROA) and the range of the fundamental parameters of the system (ROP) evaluated are nearly identical. This is not usually practical, and for those parameters that do not show a trend in bias, it is acceptable to use critical benchmark experiments that cover most, but not all, of the ROP of the system under evaluation. In these situations, expert judgment may be used to determine if there is a reasonable assurance that the two are sufficiently close. In cases where a trend in bias is identified, the ROA can be extended, but a penalty on the critical limit determined for the subset of benchmark experiments needs to be evaluated and applied.

The comparison between ROA and ROP was structured (BSC 2003e, Attachment IV) on the two subsets of benchmark experiments selected to cover the majority of the analyzed configurations of the waste package containing Shippingport LWBR SNF.

Heterogeneous Moderated Configurations—The comparison of ROA vs. ROP for the heterogeneous moderated configurations is detailed in Attachment IV of *Criticality Model Report* (BSC 2003e). The collective area of applicability of the selected critical benchmarks is based on the ROA of the benchmark experiments included in Tables IV-6 and IV-7 of *Criticality Model Report* (BSC 2003e).

The findings from the comparison ROP vs. ROA can be summarized as follows:

- The ROA for this subset of experiments does not cover all ROP. Differences are noted in the isotopic composition of the fissionable material and in the lack of appropriate benchmark experiments with Gd absorber. The ROA is partially adequate for the scoping calculations done to investigate configurations with no neutron absorber. The comparison of spectral parameters shows only a partial coverage but the shape of the spectra is very similar indicating a good selection of the experiments. The information on some experiments (including ^{233}U experiments) that is not presently available (i.e., spectral parameters) can bring more insights regarding the applicability of the selected experiments.

This situation can be alleviated by addressing on or more of the following possible solutions:

- Further investigation of experiments with ^{233}U to evaluate all spectral parameters
- More experiments can be added to cover the parameters and characteristics of the limiting configurations (^{233}U -thoria matrix, distributed Gd)
- Penalty can be applied to the critical limit (if trend in bias is identified).

Homogeneous Moderated Configurations—The comparison of ROA vs. ROP for the homogeneous moderated configurations is detailed in Appendix IV of *Criticality Model Report*

(BSC 2003e). The collective area of applicability of the selected critical benchmarks is based on the ROA of the benchmark experiments included in Tables IV-7 and IV-8 of *Criticality Model Report* (BSC 2003e).

The findings from the comparison can be summarized as follows:

- The comparison shows that the range of applicability of the selected experiments is partially covering the major part of the range of parameters identified for the possible homogeneous moderated configurations of Shippingport LWBR SNF. Differences are noted with respect to spectral parameters but not all experiments have this information available at this time. Also the presence of Gd is not covered by the existing experiments.

This situation can be alleviated by addressing on or more of the following possible solutions:

- Further investigation to evaluate spectral parameters of all experiments
- More experiments can be added to cover the parameters and characteristics of the limiting configurations (U233-thoria mixture, distributed Gd)
- Penalty applied to the critical limit (if trend in bias is identified).

10.5.6 Calculation of the Lower Bound Tolerance Limit

The following results are excerpted from *Analysis of Critical Benchmark Experiments and Critical Limit Calculation for DOE SNF* (BSC 2003f), which present in detail the methodology and calculations performed for evaluating the lower bound tolerance limit for each set of configurations of the waste package containing Shippingport LWBR SNF.

The results of the trending parameter analysis for the critical benchmark subset representative for moderated intact (heterogeneous) configurations of the waste package containing Shippingport LWBR DOE SNF are presented in Attachment IV of *Criticality Model Report* (BSC 2003e). The results show that the pool of k_{eff} values calculated with the criticality model for this subset of benchmark experiments (moderated heterogeneous subset) does not show any trending. The lower bound tolerance limit value for this subset calculated with the distribution-free tolerance limit (DFTL) method (BSC 2003f, Section 6.2.7) is 0.9751.

The results of the trending parameter analysis for the critical benchmark subset representative for moderated degraded configurations of the waste package containing Shippingport LWBR DOE SNF are presented in Table IV-12 of *Criticality Model Report* (BSC 2003e). The results show that the pool of k_{eff} values calculated with the criticality model for this subset of benchmark experiments (moderated heterogeneous subset, see Table 10-15 above) does not show any trending. The lower bound tolerance limit value calculated with DFTL method for this subset (BSC 2003f, Section 6.2.7) is 0.9748.

Table 10-16 presents a summary of the results of the analyses performed on the subsets of critical benchmark experiments applicable to the waste package containing Shippingport LWBR DOE SNF and the calculated lower bound tolerance limit values.

Table 10-16. Lower Bound Tolerance Limits for Benchmark Subsets Representative for the Configurations of the Waste Package Containing Shippingport LWBR Spent Nuclear Fuel

Subset	Trend Parameter	Test for Normality	Applied Computational Method	Lower Bound Tolerance Limit or Lower Bound Tolerance Limit Function
Intact (heterogeneous) Moderated	None	Failed	DFTL	Lower bound tolerance limit = 0.9751
Degraded (homogeneous) Moderated	None	Failed	DFTL	Lower bound tolerance limit = 0.9748

Source: BSC 2003f, p. 57

The above results and the comparison ROA vs. ROP indicate that the criticality model is partially validated for use in assessing the criticality potential of the intact (nondegraded) configurations and of the configurations belonging to the general configurations classes 1, 2 and 6 for the degraded waste package containing Shippingport LWBR SNF.

10.5.7 Summary of Criticality Model Results and Validation for the Waste Package Containing Shippingport LWBR SNF

The criticality analyses considered all aspects of intact and degraded configuration of the waste package containing Shippingport LWBR SNF, including optimum moderation condition, rearrangements of the fuel pins and fissile material, and neutron absorber distribution. The results of three-dimensional Monte Carlo calculations from both the intact and the degraded component criticality analyses show that the interim critical limit requirement of $k_{eff}+2\sigma$ be less than or equal to 0.92 is satisfied for the proposed design. The amount of neutron absorber (gadolinium phosphate) required to satisfy the above criterion is 10.12 kg of GdPO₄ in or on the initial aluminum shot-GdPO₄ filler, which must be placed in void spaces of the DOE SNF canister loaded with the Shippingport LWBR seed fuel assembly. This amount is equivalent to 1 wt% of Gd in the aluminum shot-GdPO₄ filler. The results show that a uniform distribution of filler material in all available void spaces inside the DOE SNF canister (including void spaces in the fuel assembly) is highly desirable and further increases the margin for criticality.

A number of parametric analyses were run to address or bound the configuration classes discussed. These parametric analyses identified conditions of optimum moderation, optimum spacing between fuel pins, optimum fissile concentration, and minimum neutron absorber requirements. The results from the degraded criticality analyses show that the most reactive configurations are the configurations with fully degraded components inside DOE SNF canister and the configurations with intact fuel pins dispersed in the waste package. These configurations result in $k_{eff}+2\sigma$ less than or equal to 0.92 with at least 10.12 kg GdPO₄ distributed in the initial aluminum-GdPO₄ filler. 10 kg or more of GdPO₄ should be loaded to provide extra margin (defense in depth).

Most cases analyzed require only a fraction of the indicated insoluble neutron absorber in order to be below the interim critical limit. The representative intact configurations that were investigated are very near the interim critical limit without neutron absorber and at best would require only a tenth of the amount of neutron absorber that is listed above. The limiting case for the configurations with the fuel inside DOE SNF canister was obtained for a homogeneous

mixture of fuel and hydrated products inside DOE SNF canister, which require 10.12 kg of GdPO₄ in the canister. At least 4 percent of the Gd must be mixed uniformly with the layer containing the degraded fuel. The overall limiting case was obtained for an extremely conservative configuration comprising a pile of fuel pins stacked at the bottom of the waste package that can be obtained after a very long time after repository closing. This configuration required the same amount of insoluble neutron absorber (10.12 kg of GdPO₄) present in the waste package with at least 5.5 percent of it distributed uniformly in the layer that covers the fuel.

Due to the basket design and the aluminum shot-GdPO₄ filler, the waste package containing a DOE SNF canister of spent Shippingport LWBR fuel will not form critical configurations for any credible degradation scenarios. The uranium decay has a beneficial effect on further reducing the k_{eff} of the system containing Shippingport LWBR SNF. The effect is very significant after 50,000 years (at least 5 percent reduction in k_{eff}) and should completely diminish the potential for criticality for postulated waste package breach times of the same order of magnitude.

All calculations are based on a maximum of 16.6 kg ²³³U per DOE SNF canister. The analyses are based on the fuel type that has the highest ²³³U concentration.

Intact and degraded component criticality calculations include variations on moderators and moderator densities, which encompass flooding the waste package. Occurrence of design basis events, including those with the potential for flooding the disposal container prior to disposal container sealing, is considered and analyzed using very conservative assumptions for many different intact configurations.

Table 10-17 presents a summary of the criticality and geochemistry results with a focus on the correspondence with the degradation classes and resultant configuration classes presented in *Disposal Criticality Analysis Methodology Topical Report* (YMP 2003). The results of the geochemistry analyses show that the calculated maximum loss of Gd is very small (3.63 percent) assuring its presence for all anticipated internal configurations, and consequently minimizing the potential for criticality.

The criticality model (software code MCNP and appropriated selected neutron cross-section libraries) used in analyzing the configurations of the waste package containing Shippingport LWBR SNF was validated using the methodology described in *Disposal Criticality Analysis Methodology Topical Report* (YMP 2003) and *Criticality Model Report* (BSC 2003e). Current results indicate that the lower bound tolerance limit is well above the interim critical limit used in evaluating the design (Table 10-17).

Table 10-17. Summary of Geochemistry and Criticality Analyses for Internal Configurations (Phase I and II) of the Waste Package Containing Shippingport LWBR SNF

Master Scenario	Description	Configuration Classes and Summary Description	Summary of Geochemistry Calculations	Summary of Criticality and Criticality Model Validation Results			
				$(k_{eff}+2\sigma)_{max}$	Interim Critical Limit	Lower Bound Tolerance Limit	Comments
Initial water intrusion	Initial stage: water fills all available spaces inside the waste package and DOE SNF canister	Intact flooded configurations: SNF and internal structures not degraded	N/A	0.8659	0.92	0.9751 (heterogeneous moderated configurations)	Maximum $k_{eff}+2\sigma$ was obtained considering only 0.1 wt% added in the package. With 1 wt% Gd dispersed with the Al filler the results are expected to be much lower
IP-1	The top of the waste package is breached and liquid accumulates inside	Configuration class #6: SNF partially degraded in place (various stages)	For all cases investigated (IP-1, IP-2 and IP-3 scenarios) the loss ranges were: U: 0 to 100% Th: 0 to 1.38% Gd: 0 to 3.63%	0.9135	0.92	0.9751 (heterogeneous moderated configurations)	At least 3% of the initial Gd amount must be present in the mixture.
		Configuration class #3: SNF partially or totally degraded inside the waste package with intact internal structures					
IP-2	SNF degrades concurrently with the internals of the waste package	Configuration class #2: Both SNF and internal structures of the waste package degraded (various stages)		0.9123	0.92	0.9748 (homogeneous moderated configurations)	Due to high corrosion resistance of Zr-4 cladding, SNF will degrade after internal structures of the DOE SNF canister.
IP-3	SNF degrades after the internals of the waste package	Configuration class #1: SNF intact (as assembly or pins) and degraded internal structures (various stages)		0.9115	0.92	0.9751 (heterogeneous moderated configurations)	At least 1.85% of initial Gd amount must be mixed with the degraded SNF.
IP-4	SNF degrades before the internals of the waste package	The configurations resulting from these scenarios (configurations classes #4, #5) have not been investigated in the geochemistry and criticality analyses due to the fact that they are less moderated (no pooling of water) and are bounded by the variations of the configurations investigated above.					
IP-5	The bottom of waste package is penetrated allowing liquid to flow through						
IP-6	SNF degrades after the internals of the waste package						

10.6 N-REACTOR

The description and main characteristics of the waste package containing N-Reactor SNF are presented in Section 3.2.6. In this section a summary of the results of the criticality analyses performed is presented together with the current status of the validation of the criticality model for the configurations that are specific to the codisposal of this fuel group.

The first step in applying the criticality model to the specific intact and degraded configurations of this waste package is identification and characterization of the specific configurations anticipated for postclosure. The results of the degradation analysis coupled with the geochemistry calculations (CRWMS M&O 2001a, Section 6) provided an insight into the possible arrangements and compositions of the degraded materials placed within the waste package. All configuration classes analyzed and the most probable degradation scenario that was identified are summarized in the next section (Section 10.6.1). The results of the criticality calculations for the most representative intact and degraded configurations are presented in Section 10.6.2. The range of parameters that characterize the most reactive cases is subsequently used in the process of validation of the criticality model. The process includes selection of appropriate critical benchmark experiments and derivation of specific lower tolerance bound limit for each major group of configuration classes.

The results of three-dimensional Monte Carlo criticality calculations for all anticipated intact- and degraded-mode configurations show that the requirement of $k_{\text{eff}} + 2\sigma$ values less than or equal to the interim critical limit of 0.93 is satisfied for the N-Reactor codisposal package. No neutron absorber material is required as long as the enrichment and the U-metal mass for codisposal are within the specified limit (1.25 percent enrichment; 120.2 kg ^{235}U per waste package [CRWMS M&O 2001a, Section 8.7]).

10.6.1 Degradation Scenarios and Configurations

Based on the corrosion rates and the material thickness given in Table 10-18, the most probable degradation path for the waste package, the MCO, and the N-Reactor spent nuclear fuel follows the following sequence (CRWMS M&O 2001a, Section 6.2.1.1):

1. Waste package is penetrated and flooded internally. Water has not yet penetrated the MCO.
2. The waste package separation plates and MCO support cylinder degrade first because of the high corrosion rate of A516 carbon steel. Degraded steel product (iron oxide) accumulates at the bottom of the waste package.
3. High-level waste glass canister shell and glass degrade. Degraded glass clay product accumulates at the bottom of the waste package. After this, there are two possible degradation paths:
 - 3a. MCO stays intact. Intact MCO with intact spent nuclear fuel fall and are surrounded by the clay material near the bottom of the waste package.
 - 3b. MCO starts to degrade.

4. Following 3b above, MCO shell is penetrated but remains intact and MCO interior is flooded.
5. Components internal to the MCO are in contact with water. These components include the spent nuclear fuel basket structure, the center post, and the spent nuclear fuel elements.
6. Spent nuclear fuel starts to degrade due to its high corrosion rate. For conservatism, credit is not taken for the protection of the Zr-2 cladding material. After this, there are two possible paths.
 - 6a. Baskets and center posts stay intact. In this case, spent nuclear fuel degrades in place and is trapped inside the baskets.
 - 6b. Baskets and center posts degrade. In this case, degraded spent nuclear fuel and iron oxide mix together in a pile and are trapped inside and at the bottom of the MCOs.
7. MCO shell starts to degrade. The degraded iron oxide mixes with the degraded glass clay at the bottom of the waste package. The degraded spent nuclear fuel elements fall out and scatter on top of the clay/iron oxide mixture.

Given a very long period of time, it is postulated that everything will degrade including cladding and fuel. All the internal components of the waste package will then be represented as sludge. This corresponds to degradation scenario group IP-2. The degraded spent nuclear fuel and other degradation products could mix and pile up near the bottom of waste package. However, there is no mechanism to cause complete and uniform mixing of all the degradation products inside the waste package.

Table 10-18. Materials and Thicknesses

Components	Material	Thickness (mm)
Waste package separation plate	A516 Carbon Steel	10
Waste package support cylinder	A516 Carbon Steel	5
High-level waste glass shell	304L Stainless Steel	10.5
High-level waste glass	Glass	N/A
MCO shell	304L Stainless Steel	12.7
MCO center post	304L Stainless Steel	61.9 (for larger hollow cylinder)
Spent nuclear fuel basket shell	304L Stainless Steel	1.22
Spent nuclear fuel basket bottom plate	304L Stainless Steel	3.048
Spent nuclear fuel cladding	Zircaloy-2	Varies depending on fuel type but generally very thin

Source: CRWMS M&O 2001a, Table 6-1

The most likely scenario begins with the localized degradation of the canisters inside the waste package followed by the degradation of the spent nuclear fuel once the MCO is breached and followed by the degradation of the entire MCO. The degradation scenario of IP-3 (i.e., SNF degrades slower than the other materials) is not probable since the corrosion rate of the N-

Reactor spent nuclear fuel is the highest among all of the materials. However, for completeness, configurations associated with scenario group IP-3 have also been analyzed.

The final degraded configurations that are used for criticality calculations are characterized by location of the fissile material and possible displacement from any material that can act as neutron absorber. The assignment of such locations has been consistent with a conservative interpretation of possible physical processes.

The configurations investigated can be categorized using the description of the generic configuration classes given in Section 3.3.1 of *Disposal Criticality Analysis Methodology Topical Report* (YMP 2003). As indicated in Section 6.5 for the purpose of fully identifying the potential for criticality, all representative configurations classes have been analyzed and not only the configurations resulting from the most probable degradation path presented above. The subtitles follow the original description given in Section 6.2.1.1 of *Evaluation of Codisposal Viability for U-Metal (N Reactor) DOE-Owned Fuel* (CRWMS M&O 2001a).

Degraded Spent Nuclear Fuel with Nearly Intact MCO and Waste Package Shells—In this case, the spent nuclear fuel could be partially or fully degraded. As a variation, the other internal components of MCO could also be degraded. This configuration is a variation of configuration class 6 and can be reached from standard scenario IP-1 (YMP 2003, Section 3.3.1).

Spent Nuclear Fuel Degrades After Degradation of the MCO Basket—In this case, the spent nuclear fuel is intact and the degradation scenarios and configuration classes are applied to the MCO and its contents including the baskets and the center post. As a variation, there could be partial degradation of the MCO internals and partial-to-full degradation of the spent nuclear fuel. This configuration is a variation of configuration class 1 and can be reached from standard scenario IP-3 (YMP 2003, Section 3.3.1).

Nearly Intact MCO and Degraded Waste Package Internals—In this case, the concepts of scenario and configuration are applied to the entire waste package. The fuel element and the MCO shell retain their initial configuration. This configuration is a variation of configuration class 1 and can be reached from standard scenario IP-3 (YMP 2003, Section 3.3.1).

Degraded MCO and Waste Package Internals, Intact Spent Nuclear Fuel—In this case, the degradation scenario and configuration are applied to the entire waste package. The MCO and waste package internals including the high-level waste glass canisters are degraded. The fuel elements are intact. This configuration is a variation of configuration class 1 and can be reached from standard scenario IP-3.

Completely Degraded MCO and Waste Package Internals—In this case, the degradation scenario and configuration are applied to the entire waste package including the spent nuclear fuel. Degradation products from the MCO and the waste package and their contents mix uniformly inside the waste package. This configuration is a variation of configuration class 2 and can be reached from standard scenario IP-1, IP-2, or IP-3.

10.6.2 Criticality Calculations and Results

10.6.2.1 Results for Intact Mode

This section summarizes the results of the intact-mode (phase I) criticality analysis (CRWMS M&O 2001a, Section 7.3). Although the components of the waste package (fuel element, cladding, supporting basket structures, and MCO) are considered structurally intact, water intrusion into the available internal volumes is assumed in order to determine the effect of optimal moderation. The contents of the waste package outside the MCO are intact in all cases considered in this section except as noted. For the intact mode configurations, the contents of the MCO are in an “as loaded position and condition,” as depicted in Figure 10-21 for the Mark IV fuel element and Figure 10-22 for the Mark IA fuel element.

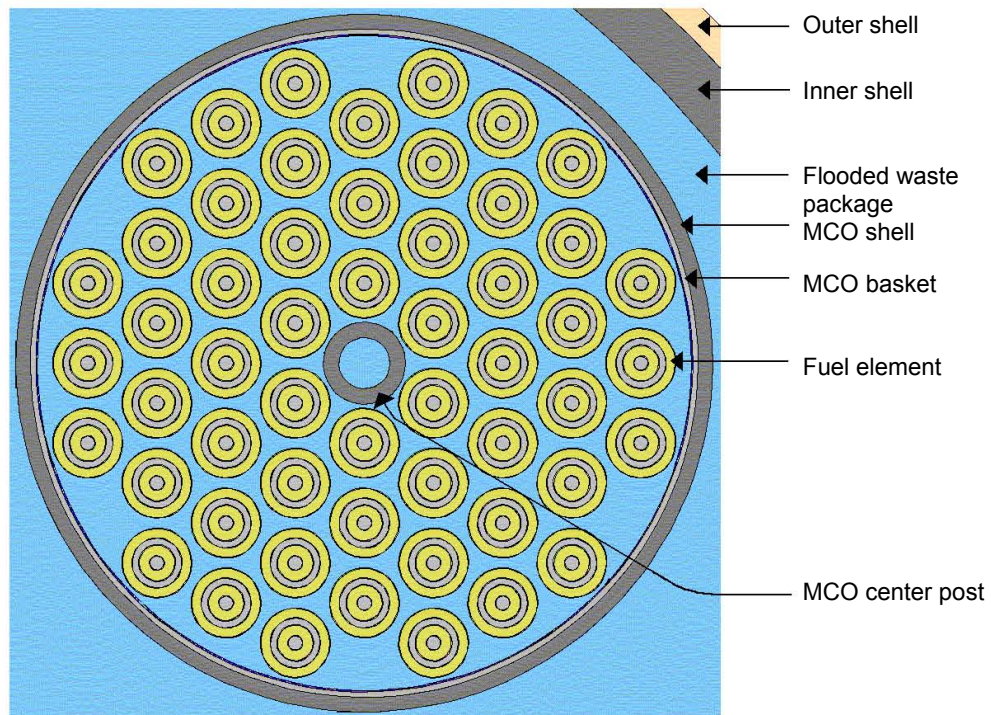


Figure 10-21. Cross-Section of the MCO Loaded with 54 Mark IV Fuel Elements in the Intact Basket

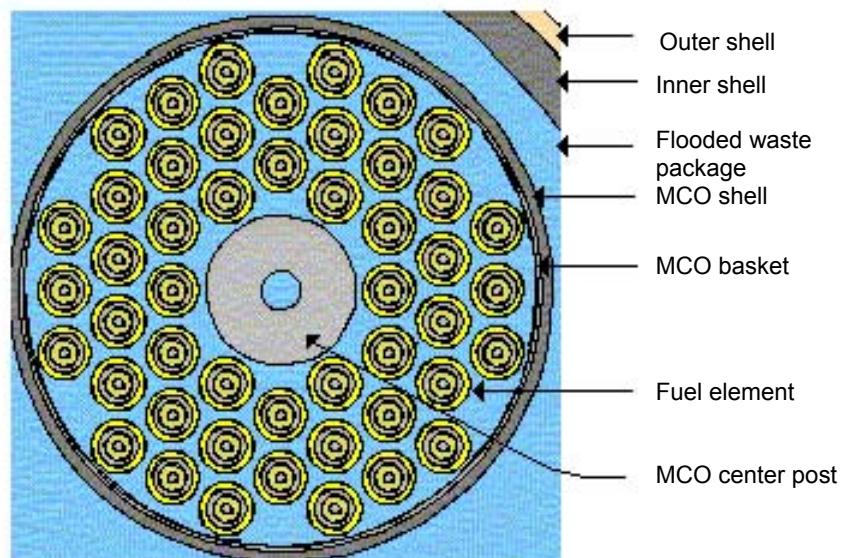


Figure 10-22. Cross-Section of the MCO Loaded with 48 Mark IA Fuel Elements in the Intact Basket

In the intact analyses, the k_{eff} values of a 2-MCO/2-DHLW waste package containing Mark IV and Mark IA fuel elements with intact baskets only or with intact baskets and two scrap baskets were analyzed. Variations included placing MCOs in different quadrants of the waste package, different numbers and arrangements of the intact and scrap baskets, different numbers of fuel elements in the intact basket, different water densities in the MCO (varied from 0 to 1 g/cm³), and different masses of fuel in the intact baskets. Various masses (from 980 kg to 330 kg for Mark IV fuel elements and from 575 kg to 330 kg for Mark IA fuel elements), shapes (intact inner elements, intact outer elements, or fuel elements represented as spheres) and distributions of the fuel in the scrap basket (the pitch of the fuel elements varies from 0.5285 to 1.5520 cm for Mark IV fuel type and from 0.5037 to 1.3672 cm for Mark IA fuel type) were also investigated. Unclad-scrap fuel was represented as spheres because it is shown to be the configuration with the highest k_{eff} . The radius varies from half of the thickness of the outer fuel element to 0.26425 cm and 0.25185 for Mark IV and Mark IA fuel type, respectively.

For all the calculations (unless otherwise specified in CRWMS M&O 2001a), the waste package has reflected boundaries acting as a mirror (i.e., no neutron leakage). This is a very conservative approach. Variations of the intact configurations were run to identify the configuration that results in the highest calculated k_{eff} value within the range of possible conditions as described above. These configurations are investigated in both as loaded position and in a position where the contents of the MCO have settled due to gravity.

The results of the key cases span a range of $k_{\text{eff}} + 2\sigma$ between 0.8248 and 0.8601 for MCO loaded with Mark IV fuel elements and between 0.8161 and 0.8937 MCOs loaded with Mark IA fuel element (CRWMS M&O 2001a, Tables 7-1 and 7-2, respectively). These cases represent the various combinations of possible loading conditions and the highest k_{eff} values under those conditions. As can be seen from these tables, all the k_{eff} values are below the interim critical limit of 0.93 (CRWMS M&O 2001a, Section 2.4.3).

Additionally, a configuration of a waste package containing one MCO loaded with Mark IA fuel and one MCO loaded with Mark IV fuel was investigated. $k_{\text{eff}} + 2\sigma$ of this waste package is

0.8704 (CRWMS M&O 2000b, Section 6.1.3). The result is higher than the k_{eff} of a waste package loaded with 2 MCOs containing Mark IV fuel elements and yet lower than the k_{eff} of a waste package filled with 2 MCOs loaded with Mark IA fuel. Thus, for the degraded analysis Mark IA fuel was the only fuel investigated (unless otherwise specified).

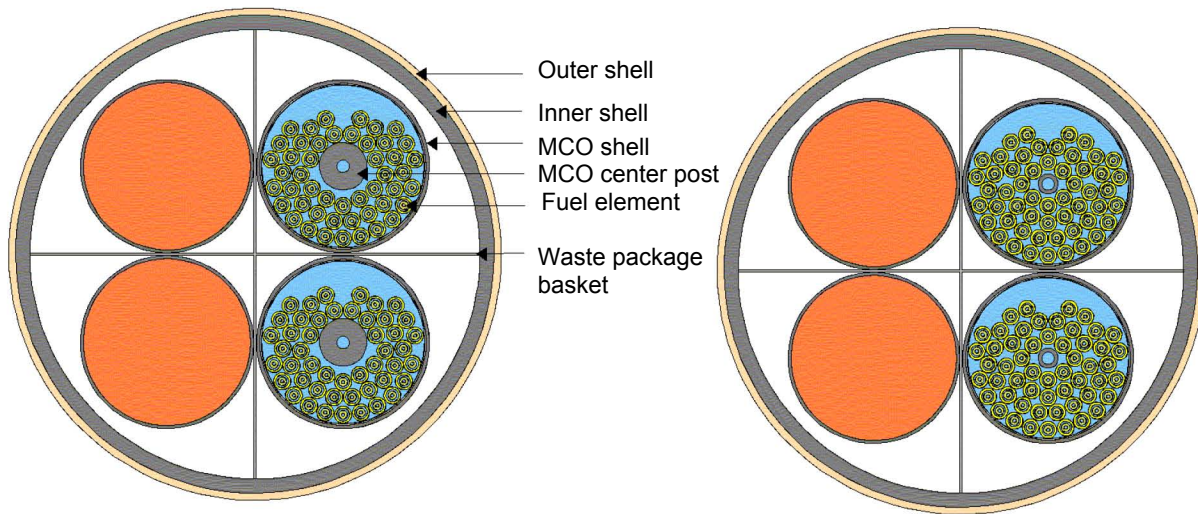
10.6.2.2 Results for Configurations with Fuel Elements Degraded Before the MCO Baskets

This degradation scenario belongs to the generic degradation group IP-1 (YMP 2003) and the resultant configurations are categorized as belonging to configuration class 6. As explained in Section 10.6.1, the relative degradation rates of the waste package internal components make it the most likely degradation scenario. In all cases analyzed, the degraded fuel fragments are represented by spheres. This is the most reactive geometry, and it is, therefore considered bounding. Formation of spheres, however, is physically impossible. Due to the very high degradation rate of the U-metal, the degraded fuel would very quickly form sludge, which is a less reactive configuration (CRWMS M&O 2001b, Tables 65 and 66). In the analyses, the fuel mass present in a basket, the sphere (representing the fuel elements partially degraded) radius, and the lattice pitch are varied. When the fuel is fully degraded, the amount of water in the sludge varies. In the following descriptions, $k_{\text{eff}} + 2\sigma$ are given for the most reactive configurations (optimal pitch, moderation, sphere radius, mass of fuel in the baskets, etc).

All configurations in this degradation group result in the k_{eff} values of less than 0.93. As a first stage, the fuel falls at the bottom of the MCOs as shown in Figure 10-23. k_{eff} of the system is 7.0 percent (from 0.8484 to 0.7935) and 6.5 percent (from 0.8490 to 0.7975) lower in a collapsed configuration than it is an intact configuration if the MCO are loaded with Mark IA fuel elements (Figure 10-23a) and Mark IV (Figure 10-23b), respectively. Then degradation of the inner and outer fuel elements can occur either sequentially or simultaneously. If the degradation of the Mark IA spent nuclear fuel is assumed to occur sequentially, first to the outer elements and then to the inner elements, the results show that $k_{\text{eff}} + 2\sigma = 0.9273$ when the outer fuel elements are represented as spheres and $k_{\text{eff}} + 2\sigma = 0.8950$ when the outer fuel elements are represented as sludge. Then the degradation of the spent nuclear fuel is assumed to occur to both pieces of the fuel elements at the same time. When both inner and outer fuel elements are considered degraded and represented as spheres, $k_{\text{eff}} + 2\sigma$ is at most equal to 0.9293. For fuel elements fully degraded, $k_{\text{eff}} + 2\sigma$ is 0.9088 (CRWMS M&O 2001, Section 7.4.1). In these cases, the lattice pitch of the spheres varies from 0.824 to 1.136 cm. The radius of the spheres varies from half of the thickness of the outer element to 0.37185 cm. The mass of the degraded fuel in each basket varies from 865 kg (mass of 48 intact fuel elements) to 575 kg (weight limit in the basket). Since the k_{eff} value of the system decreases as the mass of degraded fuel in the baskets decreases, lower loads of the basket were not investigated. k_{eff} values ranging from 0.4792 to 0.9088 (depending on the amount of water in the sludge) are obtained when all spent nuclear fuel is fully degraded. The amount of water in the sludge was varied from 0 volume percent to 67.77 volume percent, which corresponds to a homogeneous distribution of the sludge throughout the MCO. The highest k_{eff} is obtained for this latest configuration.

As presented above, the most reactive configurations are the ones with the fuel elements partially degraded in the intact basket and represented as spheres. The pitch of the spheres in the intact basket was conservatively chosen such that the spheres are distributed throughout the intact

basket. The pitch of the spheres in the scrap basket varies such that the spheres are either packed (in a rectangular array) or distributed throughout the scrap basket. This last configuration is the most reactive ($k_{\text{eff}} + 2\sigma = 0.9293$). However, because of the high degradation rate of U-metal, small fragments of U-metal could only exist for a short time. Moreover, since the U-metal would react as it is exposed, the presence of spheres distributed throughout a MCO is not a credible configuration.



a. Waste Package Loaded with Mark IA Fuel Elements b. Waste Package Loaded with Mark IV Fuel Elements

Figure 10-23. Fuel Elements Collapsed at the Bottom of the MCO

Results for Configurations with MCO Basket Degraded Before the Fuel Element—This degradation scenario belongs to the generic degradation scenario IP-3, but its occurrence is very unlikely because of the high degradation rate of the U-metal fuel. From the postulated resultant configurations, several representative cases were analyzed. The degradation of the center post of the basket is assumed to occur first, followed by the degradation of the basket shell and the basket plate. The fuel remains intact. Although the configurations associated with these cases are unlikely to occur, they are analyzed for completeness. In all the cases investigated only the configuration with the center post falling to the bottom of the MCO basket (Figure 10-24) results in the k_{eff} values of more than the interim critical limit of 0.93. In this particular hypothetical configuration, the fuel in the scrap basket is represented as spheres and distributed throughout the basket. However, as discussed earlier, it is not possible for the fuel to form spheres after degradation. There are also no physical mechanisms for the fuel in the scrap basket to be uniformly distributed over the entire volume available in the basket and for the center post to snap and settle down through the fuel elements. The center post is twice thicker than the basket bottom plate and more than sixty times thicker than the basket shell and would be the last component to degrade. No mechanism for shearing off the center post has been identified. The fuel in the scrap basket would be more likely to settle at the bottom of the basket or at the bottom of the MCO if the basket has degraded, which results in the k_{eff} values of less than 0.93 ($k_{\text{eff}} + 2\sigma = 0.8326$ with the basket intact and 0.8275 if the basket degrades [CRWMS M&O 2001b, Table 64]).

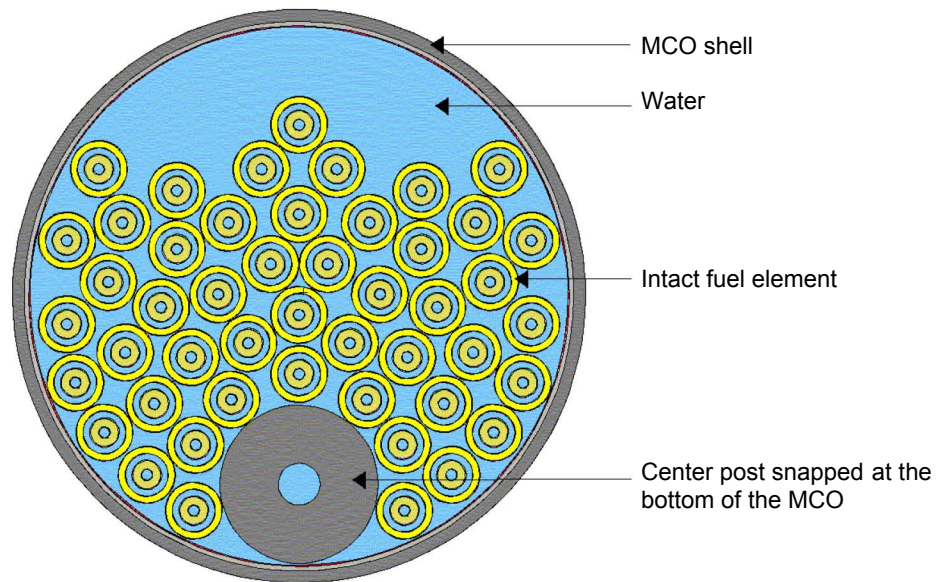


Figure 10-24. Center Post Snapped at the Bottom of the MCO

Cases with the basket fully degraded (basket shell, center post) as shown in Figure 10-25 were also investigated. The amount of water added to the products resulting from this degradation is varied from 50 volume percent (so that the fuel elements are covered by the mixture) to 62 volume percent (uniformly distributed over the entire volume). The highest $k_{\text{eff}} + 2\sigma$ for this configuration is 0.8315, with the degradation product distributed over the entire volume of the MCO (CRWMS M&O 2001b, Section 6.2.1.2.3.1).

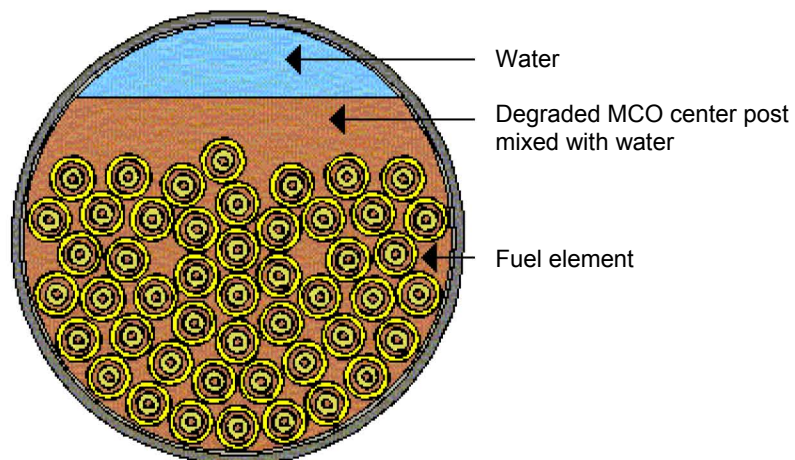


Figure 10-25. Intact Fuel Elements in a Degraded Basket

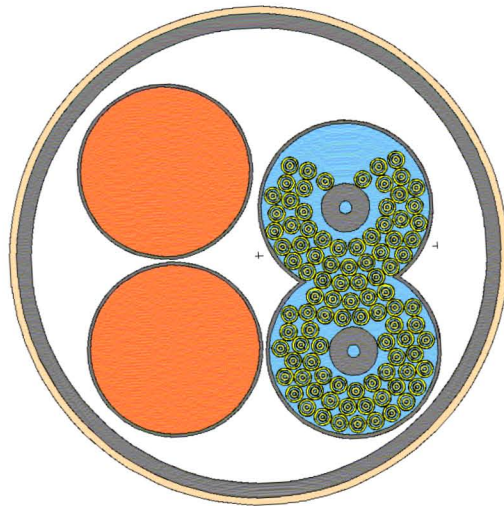
Configurations with partial or full degradation of the center post and basket in combination with the partial or full degradation of the outer fuel elements (inner fuel element intact) were also analyzed. They result in $k_{\text{eff}} + 2\sigma$ values less than the interim critical limit of 0.93 (CRWMS

M&O 2001b, Tables 67 through 69). In the case of full degradation of the center post and basket shells with degraded outer fuel elements, water was added to the degradation products from the steel (the water content mixed with the degraded iron varies from 0 volume percent to 65 volume percent, which corresponds to a mixture uniformly distributed over the entire volume available). This case results in a 3 percent increase in k_{eff} ($k_{\text{eff}} + 2\sigma = 0.9156$) but is still less than the interim critical limit of 0.93. In the case of complete degradation of the MCO internals including the center post, basket and fuel elements, the k_{eff} values are less than 0.7 (CRWMS M&O 2001b, Table 69). The water contents in the sludge resulting from the degradation of the iron and the fuel varies from 0 to 47 volume percent for this configuration (from dry sludge to a sludge uniformly distributed over the entire volume available).

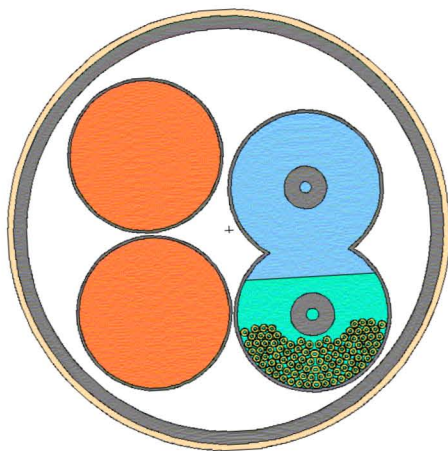
Results for Two MCOs Fused Together—In this configuration, the MCOs shell is partially degraded. Due to gravity, the contents of the MCOs are combined in the cavity formed by the degraded shells as shown in Figure 10-26. Since the U-metal degrades much faster than the steel, once the MCO shell degrades, the fuel element either stays intact (cladded, Figure 10-26a) or is fully degraded (sludge, Figure 10-26b and Figure 10-26c). Water contents in the mixture resulting from the degradation of the baskets and/or fuel were varied from 0 to a content such that the mixture is uniformly distributed over the entire volume available. Results show (CRWMS M&O 2001b, Section 6.2.1.3) that the k_{eff} values exceed the interim critical limit of 0.93 only when the goethite resulting from the degradation of the basket is fully neglected (less absorption), and the fully degraded outer fuel elements are distributed over the entire cavity ($k_{\text{eff}} + 2\sigma = 0.9259$ if the goethite is not neglected). These configurations are very unlikely since there is no physical mechanism to separate the iron oxide from the degraded fuel inside the cavity; therefore it is not possible that the iron oxide can be flushed out of the MCO without flushing out some degraded fuel. Also, there is no physical mechanism to distribute the degraded outer fuel elements over the entire cavity. All other cases investigated have lower k_{eff} values (i.e., less than the interim critical limit of 0.93).

10.6.2.3 Results for Degraded Configurations Postulated Beyond the Regulatory Period

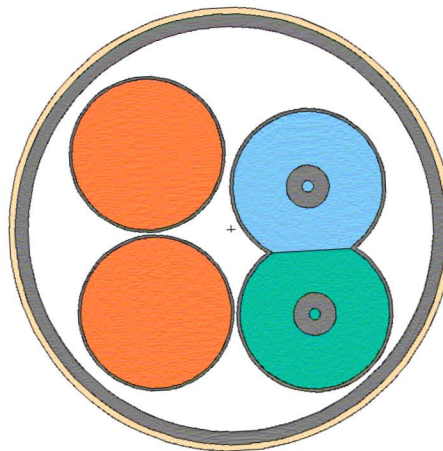
The degradation and criticality analyses performed have also investigated configurations that require very long times to be attained. These configurations are anticipated to happen well beyond the regulatory period of 10,000 years but they have been analyzed to fully investigate the potential for postclosure criticality of the waste package containing Shippingport LWBR. For the purpose of this document, these results (CRWMS M&O 2001a, Section 7.5) have been summarized and grouped together in this section.



a. Intact Basket



b. Partially Degraded Fuel Elements



c. Fully Degraded Fuel Elements

Figure 10-26. MCO Combined

Configurations with MCO Intact and All Internal Components of the Waste Package Degraded—This configuration can result from the generic degradation scenario IP-3 (YMP 2003) and belong to configuration class 1. In this case, MCOs stay intact and all other waste package internal components degrade. The MCOs are surrounded by prebreach clay mainly resulting from the degradation of high-level waste glass. The water content of the prebreach clay was varied from 0 to 67 volume percent, which corresponds to clay distributed throughout the entire waste package and around the MCOs. This variation also is equivalent to losing 67 percent of the prebreach clay around the MCOs. Various configurations of the internals of the MCO are analyzed. The results show that the k_{eff} values are lower for a waste package filled with MCOs and prebreach clay than they are for a waste package filled with the same MCOs and intact high-level waste canisters.

Variations of this class of degraded configurations include a configuration with the waste package containing one MCO intact and the other MCO degraded with the fuel element intact. The calculated results show no effect on k_{eff} . The value of $k_{\text{eff}} + 2\sigma$ is 0.8490, while $k_{\text{eff}} + 2\sigma$ of the waste package with the 2 intact MCOs is also 0.8490 (CRWMS M&O 2001b, Section 6.2.2). The other variation investigated is a case where everything has degraded except the fuel elements. The fuel elements settle at the bottom of the waste package and are surrounded by a clay resulting from the degradation of the other waste package internals. Different clay compositions (depending on the time elapsed since emplacement of the waste packages in the drift) are investigated. The spacing between the fuel elements is varied (pitch varies from 6.1 cm to 13.1cm) as well as the amount of water in the clay (from 0 volume percent to 75.84 volume percent, which corresponds to a mixture uniformly distributed over the entire volume available). The results (CRWMS M&O 2001b, Table 72) show that the calculated k_{eff} values are also less than 0.93 (the highest $k_{\text{eff}} + 2\sigma$ is 0.8781).

Results for Configurations with All Internal Components of the Waste Package Degraded—This configuration belongs to configuration class 2 obtained via any of the generic degradation scenario IP-IP-1, IP-2 or IP-3. The cases analyzed include degradation of the MCO contents and degradation of the other internal components of the waste package. Three clay compositions were analyzed depending on the time after emplacement investigated. The amount of water in the clays was varied from 0 volume percent to 39.41 volume percent, which corresponds to a mixture uniformly distributed over the entire volume available. The final degraded product is a uniform mixture. Water was added to the dry clay to find the most reactive composition. The results show that the k_{eff} values are less than the interim critical limit of 0.93 for all cases analyzed (the highest $k_{\text{eff}} + 2\sigma$ is 0.6184 [CRWMS M&O 2001b, Table 74]).

Range of Parameters for Configurations of Waste Package Containing N-Reactor DOE SNF—ANSI/ANS-8.1-1998 and *Disposal Criticality Analysis Methodology Topical Report* (YMP 2003) provide basic requirements for validation of a calculational method used in the criticality analysis of a system. The bias of a code system (in this case the criticality model containing software code MCNP and selected cross-section libraries) is determined by correlating the results of critical and near-critical experiments with calculated results for those experiments. The common practice, and that considered by the current validation methodology (BSC 2003e), is for comparison of the calculated k_{eff} to a critical or near critical system.

Prior to the initiation of the validation activity, the operating conditions and parameters for which the validation is to apply must be identified. The fissile isotope, enrichment of fissile isotope, fuel density, chemical form of fuel, types of neutron moderators and reflectors, range of moderator to fissile isotope ratio, neutron absorbers and physical configurations are among the parameters to specify. These parameters will define the area of applicability for the selection of the critical experiments for the validation effort.

The preliminary degradation analysis of the content of the waste package containing N-Reactor SNF (CRWMS M&O 2001a, Section 6) and the subsequent criticality analysis performed for the resulting internal configurations have followed the guidance suggested by the Internal Criticality Master Scenarios presented in *Disposal Criticality Analysis Methodology Topical Report* (YMP 2003) and also by *Generic Degradation Scenario and Configuration Analysis for DOE Codisposal Waste Package* (CRWMS M&O 1999g). The resultant configuration classes internal

to the waste package have been screened systematically for their criticality potential in comprehensive criticality analyses (CRWMS M&O 2001a). The main results have been summarized in the sections above.

For the purpose of the criticality model validation for the configurations specific to the waste package containing N-Reactor SNF and identification of the range of parameters that characterize the internal configurations of the degraded waste package, the degraded configurations previously investigated (see Sections 10.6.2.1 to 10.6.2.3 above) have been categorized into two large groups:

1. Configurations containing intact fuel elements (heterogeneous configurations)
2. Configurations containing degraded fuel elements (relatively homogeneous configurations).

The first category contains the configurations described in *Evaluation of Codisposal Viability for U-Metal (N Reactor) DOE-Owned Fuel* (CRWMS M&O 2001a, Sections 7.3.1, 7.4.1, 7.4.2, and 7.5.1). These configurations represent intact fuel (nondegraded) configurations and refinements of the general configuration class 1 as described in Section 10.2.6.1. The second category includes the configurations described in *Evaluation of Codisposal Viability for U-Metal (N Reactor) DOE-Owned Fuel* (CRWMS M&O 2001a, Sections 7.4.1, 7.4.3, and 7.5.2). These configurations represent refinements of the general configuration classes 1, 2 and 6. This proposed categorization allows a simple and systematic way of identifying the key parameters that characterize the degraded configurations.

The process employed in *Intact and Degraded Component Criticality Calculations of N Reactor Spent Nuclear Fuel* (CRWMS M&O 2001b) for investigating the potential for criticality of the possible degraded configurations of the waste package used a screening approach, the goal being to identify the most reactive configurations in a given class of degraded configurations. Due to this approach, the number of configurations analyzed varies among the classes of configurations depending on the complexity of the possible arrangements and the initial screening results. The results of the cases that were rerun with tallies are summarized in *Criticality Model Report* (BSC 2003e). Selected cases (typically the most reactive or the limiting cases as presented in CRWMS M&O 2001a, Sections 7.3.1, 7.4.1, 7.4.2, 7.4.3, 7.5.1, and 7.5.2) have been rerun with tallies calculating the neutron flux and the fission rate in the regions containing the fissile material. The results of the cases that were rerun with tallies are summarized in Attachment VI of *Criticality Model Report* (BSC 2003e) together with a summary of the key physical and neutronic parameters characterizing the most reactive configurations (ROP).

10.6.3 Selection of the Criticality Benchmark Experiments Used in the Validation of the Criticality Model

The critical experiments selected for inclusion in the validation must be representative of the types of materials, conditions, and parameters to be modeled using the calculational method (criticality model). A sufficient number of experiments with varying experimental parameters should be selected for inclusion in the validation to ensure as wide an area of applicability as feasible and statistically significant results. The benchmark experiments selected in the

validation of the criticality model used for the analysis of the waste package containing N-Reactor SNF come from *International Handbook of Evaluated Criticality Safety Benchmark Experiments* (NEA 2001) unless otherwise noted. The selection process was initially based on previous knowledge regarding the possible configurations of degraded waste packages, and the subsets have been constructed to accommodate large variations in the range of parameters of the configurations and also to provide adequate statistics for lower bound tolerance limit calculations.

For the present application (codisposal of N-Reactor SNF), the selected benchmark experiments have been grouped in two subsets (BSC 2002c), that include moderated heterogeneous and homogeneous experiments. The selected benchmark experiments for each subset are presented in *Benchmark and Critical Limit Calculation for DOE SNF* (BSC 2002c) together with the MCNP cases constructed and the results of the calculations. The cases, corresponding k_{eff} results and their uncertainties are also summarized in Attachment II of *Analysis of Critical Benchmark Experiments and Critical Limit Calculation for DOE SNF* (BSC 2003f). Table 10-19 presents the list of the benchmark experiments and the number of cases for each subset selected for validation of criticality model for N-Reactor SNF.

Table 10-19. Critical Benchmarks Selected for Validation of the Criticality Model for N-Reactor Spent Nuclear Fuel

Subset	Benchmark Experiment Identification ^c	Number of Cases Included
Heterogeneous moderated ^d	Experiment with N-Reactor Mark IA Fuel Elements ^a	3
	LEU-COMP-THERM-001	8
	LEU-COMP-THERM-016 ^b	4
	LEU-COMP-THERM-010 ^b	3
	LEU-COMP-THERM-042	7
Homogeneous moderated ^d	Experiment with LEU UO ₃ -H ₂ O solutions ^a	12
	LEU-SOL-THERM-001	1
	LEU-SOL-THERM-002	3
	LEU-SOL-THERM-005	3
	LEU-COMP-THERM-049	18

Source: Subsets defined and evaluated in BSC 2002c

NOTES: ^a These experiments were initially evaluated in CRWMS M&O 1999v.

^b Only the cases evaluated in CRWMS M&O 1999w have been used.

^c The convention for naming the benchmark experiments is from NEA 2001.

^d Identification of each subset from BSC 2002c has been modified to better reflect the subset's main characteristics. The benchmark experiments in each subset have not been affected.

The experiments listed in Table 10-19 are considered appropriate to represent intact (non degraded) configurations and degraded configurations of the waste package containing N-Reactor SNF that belong to the configuration classes 1, 2, and 6. Their range of applicability is detailed in Attachment VI of *Criticality Model Report* (BSC 2003e).

10.6.3.1 Comparison between ROA of Benchmark Experiments and ROP

The validation of the criticality model needs to show that the range of the fundamental parameters of the benchmark critical experiments (ROA) and the range of the fundamental parameters of the system (ROP) evaluated are nearly identical. This is not usually practical, and for those parameters that do not show a trend in bias, it is acceptable to use critical benchmark experiments that cover most, but not all, of the ROP of the system under evaluation. In these situations, expert judgment may be used to determine if there is a reasonable assurance that the two are sufficiently close. In cases where a trend in bias is identified, the ROA can be extended, but a penalty on the critical limit determined for the subset of benchmark experiments needs to be evaluated and applied.

The comparison between ROA and ROP was structured (BSC 2003e, Attachment VI) on the two subsets of benchmark experiments selected to cover the majority of the analyzed configurations of the waste package containing N-Reactor SNF.

Heterogeneous Moderated Configurations—The comparison of ROA vs. ROP for the heterogeneous moderated configurations is detailed in Table VI-9 of *Criticality Model Report* (BSC 2003e). The collective area of applicability of the selected critical benchmarks is based on the ROA of the benchmark experiments included in Table VI-7 of *Criticality Model Report* (BSC 2003e).

The findings from the comparison ROP vs. ROA can be summarized as follows:

- The ROA for this subset of experiments covers the ROP for almost all parameters. The comparison of spectral parameters shows only a partial coverage but the shape of the spectra is very similar. The information on some experiments that is not presently available can bring more insights regarding the applicability of the selected experiments. The criticality model seems to be adequate for performing the criticality potential screening of the heterogeneous degraded configurations of N-Reactor SNF.

Homogeneous Moderated Configurations—The comparison of ROA vs. ROP for the homogeneous moderated configurations is detailed in Table VI-10 of *Criticality Model Report* (BSC 2003e). The collective area of applicability of the selected critical benchmarks is based on the ROA of the benchmark experiments included in Table VI-8 of *Criticality Model Report* (BSC 2003e).

The findings from the comparison ROP vs. ROA can be summarized as follows:

- The comparison shows that the range of applicability of the selected experiments is covering the greatest part of the range of parameters identified for the possible homogeneous moderated configurations of N-Reactor SNF. Differences are noted with respect to spectral parameters but not all experiments have this information available at this time.

10.6.3.2 Calculation of the Lower Bound Tolerance Limit

The following results are excerpted from *Criticality Model Report* (BSC 2003e), which present in detail the methodology and calculations performed for evaluating the lower bound tolerance limit for each set of configurations of the waste package containing N-Reactor SNF.

The results of the trending parameter analysis for the critical benchmark subset representative for moderated intact (heterogeneous) configurations of the waste package containing N-Reactor DOE SNF are presented in Attachment VI of *Criticality Model Report* (BSC 2003e). The analysis identified a linear trending of k_{eff} with AENCF that was used in applying the methodology for calculating the lower bound tolerance limit function (BSC 2003e). The expression calculated for the lower bound tolerance limit function for the benchmarks applicable to intact-moderated configurations of N-Reactor DOE SNF is:

$$\begin{aligned} \text{Lower bound tolerance limit} &= 0.0765 * \text{AENCF} + 0.9434 && \text{for } 0 < \text{AENCF} < 0.175 \\ \text{Lower bound tolerance limit} &= 0.9568 && \text{for AENCF} > 0.175 \end{aligned}$$

The results of the trending parameter analysis for the critical benchmark subset representative for moderated homogeneous configurations of the waste package containing N-Reactor DOE SNF are presented in Table VI-13 of *Criticality Model Report* (BSC 2003e). The analysis did not identify any trending in k_{eff} and the DFTL method was identified as appropriate for calculating the lower bound tolerance limit (BSC 2003f). The lower bound tolerance limit value calculated with DFTL method for this subset was 0.9748.

Table 10-20 presents a summary of the results of the analyses performed on the subsets of critical benchmark experiments applicable to the waste package containing N-Reactor DOE SNF and the calculated lower bound tolerance limit values.

Table 10-20. Lower Bound Tolerance Limits for Benchmark Subsets Representative for the Configurations of the Waste Package Containing N-Reactor Spent Nuclear Fuel

Subset	Trend Parameter	Test for Normality	Applied Computational Method	Lower Bound Tolerance Limit Values or Functions
Intact (heterogeneous) Moderated	AENCF	N/A	LUTB	0.0765 * AENCF + 0.9434 for 0 < AENCF < 0.175 0.9568 for AENCF > 0.175
Degraded (homogeneous) Moderated	None	Failed	DFTL	0.9748

Source: BSC 2003f, p. 59

The above results and the comparison ROA vs. ROP indicate that the criticality model is partially validated for use in assessing the criticality potential of the intact (nondegraded) configurations and of the configurations belonging to the general configurations classes 1, 2, and 6 for the degraded waste package containing N-Reactor DOE SNF.

10.6.3.3 Summary of Criticality Model Results and Validation for N-Reactor SNF

The results of three-dimensional Monte Carlo criticality calculations for all anticipated intact- and degraded-mode configurations show that the requirement of $k_{\text{eff}} + 2\sigma$ values less than or equal to the interim critical limit of 0.93 is satisfied for the N-Reactor codisposal package. No neutron absorber material is required as long as the enrichment and the U-metal mass for codisposal are within the specified limit.

A number of parametric analyses were run to address or bound the configuration classes. These parametric analyses identified conditions of optimum moderation, optimum spacing between the fuel elements, and optimum shape of the degraded fuel (cylinder, sphere, sludge). The results from the degraded criticality analyses show that the most reactive configurations are the configurations with fuel element fragments represented as spheres in the scrap and intact basket ($k_{\text{eff}} + 2\sigma = 0.9293$). However, these configurations are very short lived due to the fact that the degradation rate of the U-metal is five orders of magnitude higher than the steel.

All calculations are based on a maximum of 60.1 kg U-235 per MCO (60.1 kg for MCO loaded with 270 Mark IV fuel elements and 55.0 kg for MCO loaded with 288 Mark IA fuel elements).

Intact and degraded component criticality calculations included variations on moderators and moderator densities, which encompass flooding the waste package. Occurrence of design basis events, including those with the potential for flooding the disposal container prior to disposal container sealing, is considered and analyzed using very conservative assumptions for many different intact configurations.

Table 10-21 presents a summary of the criticality and geochemistry results with a focus on the correspondence with the degradation classes and resultant configuration classes presented in *Disposal Criticality Analysis Methodology Topical Report* (YMP 2003).

The criticality model (software code MCNP and appropriate selected neutron cross-section libraries) used in analyzing the configurations of the waste package containing N-Reactor SNF was validated using the methodology described in *Disposal Criticality Analysis Methodology Topical Report* (YMP 2003) and *Criticality Model Report* (BSC 2003e). Current results indicate that the lower bound tolerance limit is well above the interim critical limit used in evaluating the design Table 10-21.

Table 10-21. Summary of Geochemistry and Criticality Analyses for Internal Configurations (phase I and II) of the Waste Package Containing N-Reactor Spent Nuclear Fuel

Master Scenario	Description	Configuration Classes and Summary Description	Summary of Geochemistry Calculations	Summary of Criticality and Criticality Model Validation Results			
				$(k_{eff}+2\sigma)_{max}$	Interim Critical Limit	Lower Bound Tolerance Limit	Comments
Initial water intrusion	Initial stage; water fills all available spaces inside the waste package and DOE SNF canister	Intact flooded configurations; SNF and internal structures not degraded)	N/A	0.8937	0.93	Maximum $k_{eff}+2\sigma$ was obtained for a configuration with 2 MCOs, loaded with 4 intact baskets containing Mark IA fuel and two scrap baskets filled with outer fuel elements from Mark IA fuel.	
IP-1	The top of the waste package is breached and liquid accumulates inside	Configuration class #6: SNF partially degraded in place (various stages)	For all cases investigated (IP-1, IP-2 and IP-3 scenarios) the loss range for U: 0 to 1.10%	0.9293	0.93	Configuration contains all SNF degraded in small fragments assumed in the shape of sphere and dispersed in a regular array. This perfect geometry is not credible.	
		Configuration class #3: SNF partially or totally degraded inside the waste package with intact internal structures				The internal components of the waste package will degrade before MCO (containing intact or degraded SNF); configuration #6 presented above is the most likely	
IP-2	SNF degrades concurrently with the internals of the waste package	Configuration class #2: Both SNF and internal structures of the waste package degraded (various stages)		0.6184	0.93		
IP-3	SNF degrades after the internals of the waste package	Configuration class #1: SNF intact or partially degraded (as fuel elements or fragments) and degraded internal structures (various stages)		0.9259	0.93	The hypothetical limiting configuration (2 fused MCOs) assumed the presence of iron degradation products within the MCO	
IP-4	SNF degrades before the internals of the waste package	The configurations resulting from these scenarios (configurations classes #4, #5) have not been investigated in the geochemistry and criticality analyses due to the fact that they are less moderated (no pooling of water) and are bounded by the variations of the configurations investigated above.					
IP-5	The bottom of waste package is penetrated allowing liquid to flow through						
	SNF degrades concurrently with the internals of the waste package						
IP-6	SNF degrades after the internals of the waste package						

10.7 MELT AND DILUTE SNF

The description and main characteristics of the waste package containing MD ingots are presented in Section 3.2.7. In this section a summary of the results of the criticality analyses performed is presented together with the current status of the validation of the criticality model for the configurations that are specific to the codisposal of this fuel group.

The first step in applying the criticality model to the specific intact and degraded configurations of this waste package is identification and characterization of the specific configurations anticipated for postclosure. The results of the degradation analysis coupled with the geochemistry calculations (BSC 2001a, Section 5) provided an insight into the possible arrangements and compositions of the degraded materials placed within the waste package. All configuration classes analyzed and the most probable degradation scenario that was identified are summarized in the next section (Section 10.7.1). The results of the criticality calculations for the most representative intact and degraded configurations are presented in Section 10.7.2. The limiting cases identified during the analysis are also providing the basis for deriving the final design solution (amount of neutron absorber to be distributed within the initial waste package). The range of parameters that characterize the limiting or the most reactive cases is subsequently used in the process of validation of the criticality model. The process includes selection of appropriate critical benchmark experiments and derivation of the specific lower tolerance bound limit for each major group of configurations.

The results of three-dimensional Monte Carlo criticality calculations for all anticipated intact-and degraded-mode configurations developed through the degradation analysis show that the requirement of $k_{\text{eff}}+2\sigma$ values less than or equal to the interim critical limit of 0.93 is satisfied for the MD codisposal package if at least 7.5 percent of the original Gd loading (394.2 g from the initial 5.8 kg/waste package) in the ingots without Hf remains mixed with the fissile material. The baseline design assumes Gd content in the ingot of 0.5 wt% (5.8 kg Gd). The geochemistry analysis showed that the loss of more than 20 percent of the initial Gd content is based on extreme and unrealistic conditions. However, the probability of retaining less than 7.5 percent of the initial Gd content and therefore for an increased potential for criticality remains to be assessed. In the alternate MD ingot composition (containing 0.5 wt% Hf), Hf remains in the DOE SNF canister or waste package under all conditions, therefore preventing a critical condition even if all Gd is removed from the system.

All calculations are based on a maximum of 38.3 kg ^{235}U per DOE SNF canister. The degraded configurations of the MD ingots bound the other types of Al-based DOE-owned spent nuclear fuel, as long as the limits on mass of uranium and its enrichment, and the linear density are not exceeded (BSC 2001a, Section 8.6).

10.7.1 Degradation Scenarios and Configurations

Based on the known corrosion rates and the material thicknesses given in Table 10-22, the most probable degradation path for the waste package, the DOE SNF canister, and the MD ingots follows the sequence below (BSC 2001a, Section 5.3.2):

1. Waste package is penetrated and flooded internally. Water has not yet penetrated the DOE SNF canister.
2. The waste package separation plates and DOE SNF canister support cylinder degrade first because of the high corrosion rate of A516 carbon steel. Degraded steel product (iron oxide) accumulates at the bottom of the waste package.
3. DHLW glass canister shell degrades and exposes the DHLW glass. The DHLW glass degrades at a much lower rate than the stainless steel components and only a small percentage degrades while the stainless steel degrades as demonstrated in the geochemistry calculations (BSC 2001k). There are two possible degradation paths:
 - 3a. DOE SNF canister stays intact. Intact DOE SNF canister with intact MD ingots fall and are surrounded by the iron-rich degradation products near the bottom of the waste package (BSC 2001a, Section 7.4.2.1).
 - 3b. DOE SNF canister starts to degrade.
4. Following 3b above, DOE SNF canister shell is penetrated but remains intact and DOE SNF canister interior is flooded (BSC 2001a, Section 7.4.2.1).
5. MD ingots in the DOE SNF canister are in contact with water. MD ingots start to degrade due to their high corrosion rate. The MD ingots degrade into hydrated Al and U oxides and Gd phosphate (BSC 2001a, Section 7.4.2.3).
6. DOE SNF canister shell completely degrades. The degraded iron oxide mixes with the small percentage of degraded glass clay at the bottom of the waste package. The degraded MD ingot material falls out and scatters on top of or mixes with the clay/iron oxide mixture (BSC 2001a, Section 7.4.3).
7. Degraded glass clay product accumulates at the bottom of the waste package over or is mixed with the iron-rich degradation products from the other OICs and the MD ingots (BSC 2001a, Section 7.4.3).

A variation of the above sequence would retain the DOE SNF canister and subsequent degradation products trapped in the center of the DHLW glass logs, but the end result is essentially the same.

Given a very long period of time, it is postulated that everything will degrade. All the internal components of the waste package will then be represented as sludge. This corresponds to degradation scenario group IP-2. The degraded MD ingots and other degradation products could

mix and pile up near the bottom of waste package. However, there is no mechanism to cause complete and uniform mixing of all the degradation products inside the waste package.

Table 10-22. Materials and Thicknesses

Components	Material	Thickness (mm)
Waste package divider plate	A516 Carbon Steel	12.7
Waste package support tube	A516 Carbon Steel	31.75
DHLW glass canister shell	304L Stainless Steel	9.525
DHLW glass	Glass	N/A
DOE SNF canister shell	316L Stainless Steel	9.525
MD ingots	U-Al alloy	381 - 419

Source: BSC 2001a, Section 5.3.2

The configurations investigated can be categorized using the description of the generic configuration classes given in Section 3.3.1 of *Disposal Criticality Analysis Methodology Topical Report* (YMP 2003). For the purpose of fully identifying the potential for criticality, all representative configurations classes have been analyzed and not only the configurations resulting from the most probable degradation path presented above. The subtitles follow the original description given in Section 5.2 of *Evaluation of Codisposal Viability for Melt and Dilute DOE-Owned Fuel* (BSC 2001a).

The MD SNF has the following two characteristics in terms of geometrical arrangement inside the waste package and the distribution of the neutron absorber:

- There is no internal structure inside the DOE SNF canister. The ingots fill most of the space inside the DOE SNF canister and thus does not need a support structure, but a carbon steel crucible liner may encase the MD ingot. This implies that configurations following from degradation of DOE SNF canister basket structure are not valid for disposal of MD SNF.
- Neutron absorber and SNF are merged metallurgically in the ingot. Physical separation of neutron absorber is not possible, as is degradation of the neutron absorber while fuel stays intact. This means that separation mechanisms such as differential settling of solid particles of different densities (CRWMS M&O 1998f, Section 6.4.2) are not applicable for the MD SNF.

In light of these characteristics the application of the standard scenarios follows based on the sequence discussed in Section 5.1.1 of *Evaluation of Codisposal Viability for Melt and Dilute DOE-Owned Fuel* (BSC 2001a).

Melt and Dilute Ingots Degrading Before Other Internal Components—The configurations resulting from IP-1 scenario involve the MD ingots degrading before other internal components and depends on the degradation rates of the various materials that make up the internals of the waste package as compared to the degradation rate of the ingots. The degradation rates show that the ingot high rate is $4.8 \cdot 10^{-12} \text{ mol} \cdot \text{cm}^{-2} \cdot \text{s}^{-1}$ while the low rate of the stainless steel components is $2.5 \cdot 10^{-14} \text{ mol} \cdot \text{cm}^{-2} \cdot \text{s}^{-1}$. The carbon steel has a degradation rate of $1.8 \cdot 10^{-11} \text{ mol} \cdot \text{cm}^{-2} \cdot \text{s}^{-1}$.

Therefore, the degradation of the carbon steel basket and the ingot, with the stainless steel and DHLW glass components intact, is possible. Since there is no basket structure in the DOE SNF canister associated with the MD ingots, configuration variations within the DOE SNF canister are limited. Possible variations are configurations with partial or total degradations of the components outside the DOE SNF canister. The DOE SNF canister falls to the bottom of the waste package. Near the end of this sequence, layers of degradation products in the waste package might result surrounding a partially degraded DOE SNF canister shell.

Melt and Dilute Ingots Degrading Simultaneously with Other Internal Components—In the configurations resulting from IP-2 scenario the SNF may degrade simultaneously with the other components in the waste package if the environmental conditions favor glass degradation rates that are comparable to ingot and steel degradation rates. In this scenario the gradual degradation of the various constituents could result in a configuration where higher density material collects at the bottom of the waste package while lower density material stays on top. The potential for criticality could be significant if the neutron absorber (Gd as $GdPO_4$ – the most likely mineral to form; see Section 6 of BSC 2001a) enters solution and is flushed out of the waste package while the fissile material is in a geometry favorable to criticality. Because the Gd is integral to the MD ingots, this would require complete degradation of the ingots. Gd loss also depends on the fraction of $GdPO_4$ formed as a result of the geochemistry analysis.

Melt and Dilute Ingots Degrading After Other Internal Components—The configurations resulting from IP-3 scenario for SNF degrading after other internal components would require that the ingots have a low degradation rate and the 316L stainless steel of the DOE SNF canister have substantially lower rates than the 304L stainless steel of the DHLW canisters, along with high degradation rates for the DHLW glass. In this configuration the ingots collect at the bottom of the waste package while surrounded by degradation products (e.g., clayey material). As long as the ingots are intact there is no possibility for criticality since the neutron absorber is maintained. Loss of the neutron absorber ($GdPO_4$) if it enters solution and is flushed out of the waste package while the fissile material is in a geometry that is favorable to criticality should be considered. Possible variations are configurations with DOE SNF canister degraded and intact SNF accumulated at the waste package bottom with partial or total degradation of waste package components.

It should be noted that for the scenarios presented “flushing out of the neutron absorber” requires that water overflows through the hole in the top of the waste package.

The standard scenarios for the flow through cases, IP-4, IP-5 and IP-6 require a top and bottom breach of the waste package in order to occur. However, for these scenarios to lead to potential critical configurations there must be some plugging of the hole(s) in the bottom, so that water can accumulate to provide neutron moderation. In addition, geochemistry calculations assume that a material does not get flushed out unless it is in solution. In that case the resulting configurations are the same as the configurations for the top breach only cases (IP-1, IP-2, and IP-3).

10.7.1.1 Criticality Calculations and Results

10.7.1.1.1 Results for Intact Mode

This section summarizes the results of the intact-mode (phase I) criticality analysis (BSC 2001a, Section 7.3). These configurations represent a waste package, which has been breached allowing inflow of water, but the internal components of the waste package are as-loaded (i.e., intact; see also Figure 10-27). For all the calculations (unless otherwise specified), the waste package has reflected boundaries acting as a mirror (i.e., no neutron leakage). This is a very conservative approach. Variations of the intact configurations were examined to identify the configuration that results in the highest calculated k_{eff} value within the range of possible conditions. Intact cases were investigated first with a gadolinium loading of 0.5 wt% and the MD SNF form completely filling the DOE SNF canister. For these cases, approximately 212 kg of U and 5.8 kg of Gd are used. Cases were run with the MD ingot composition filling the interior of the DOE SNF canister and the 10 percent void in the MD ingots dry, half-filled and filled with water. Ingot/gap height combinations from 10 to 60 cm high were also run to investigate the effects of ingot height. In order to demonstrate the effect of 2 wt% Si in the MD ingot composition, an additional case was run.

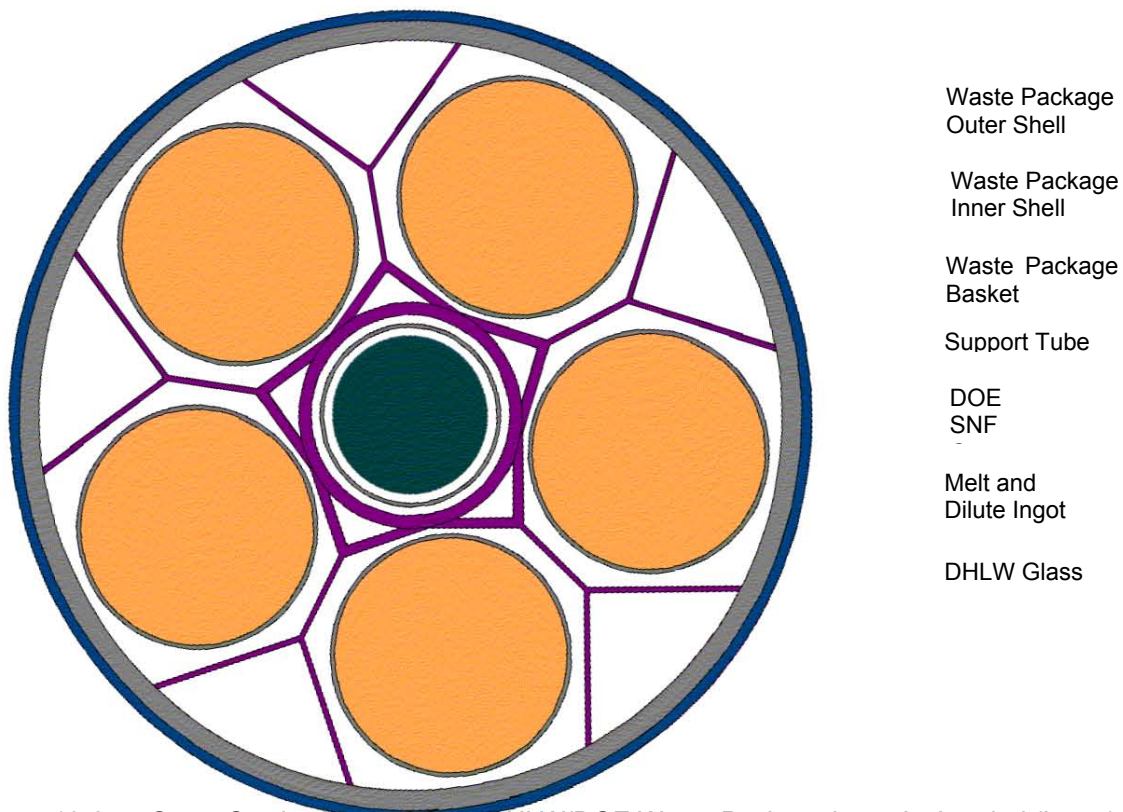


Figure 10-27. Cross-Section View of the 5-DHLW/DOE Waste Package in an As-Loaded (Intact) Configuration

The results show that the configuration with the wet ingot (10 percent voids in the MD ingots filled with water) has higher $k_{\text{eff}}+2\sigma$ than the case with dry ingots. The addition of 2 wt% Si in the MD ingot has negligible effect to criticality (0.3561 versus 0.3571 for case without Si). The

highest $k_{\text{eff}}+2\sigma$ occurs for the case with the wet ingot filling the entire DOE SNF canister. For this case $k_{\text{eff}}+2\sigma = 0.3571$. Variation of ingot height results in lower $k_{\text{eff}}+2\sigma$. A highly moderated case without Gd in the waste package results in a $k_{\text{eff}}+2\sigma$ value of 0.8949 (BSC 20011, Section 6.1). This confirms that, in the intact form, no Gd is required in MD ingots.

Results for Bounding Study of Infinitely Long Mixture of Uranium and Water—A general configuration considered in the evaluation was that of a simple infinitely long cylinder of uranium, gadolinium and water, in order to identify optimum dimensions and moderation. The fuel + water + neutron absorber mixture was considered to be fully reflected with water. This configuration is shown in Figure 10-28. None of the dimensions of the DOE SNF canister or the 5-DHLW/DOE SNF-short waste package are directly relevant to these calculations except that as those dimensions limit the maximum achievable linear uranium density. This linear uranium density was preserved for all the calculations. The cylinder radius was varied from 10 to 35 cm in order to observe the behavior of k_{eff} as the cylinder went from an undermoderated to an overmoderated condition. Water fills the void fraction of the cylinder (difference between full density of UO_2 and the distributed density of UO_2) and varies from 0.75 for the 10 cm radius cylinder up to 0.98 for the 35 cm radius cylinder. The gadolinium linear density was chosen to be consistent with 90 percent of the original gadolinium leaving the system.

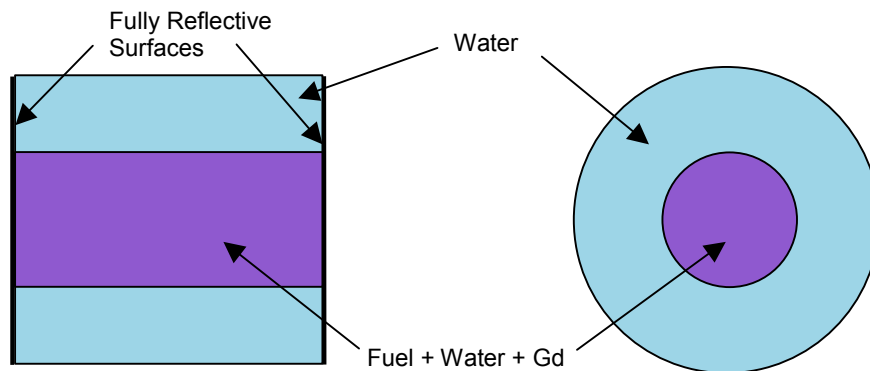


Figure 10-28. Cross-Section View of an Infinitely Long Mixture of Uranium and Water, Reflected with Water

The results show that the maximum $k_{\text{eff}}+2\sigma$ occurs for case with a fissile material radius of 20 cm. The results indicate that as long as 10 percent of the original gadolinium remains intermixed with the uranium and the uranium linear density is less than or equal to the original linear density then $k_{\text{eff}}+2\sigma$ will always be less than 0.79 (BSC 20011, Section 6.2).

10.7.1.1.2 Results for SNF Degrading Before Other Internal Components

In this section, cases where the waste form degrades before any other internal components of the waste package are investigated. This corresponds to configuration class 6 discussed in Sections 5.1.2 and 5.2 of *Evaluation of Codisposal Viability for Melt and Dilute DOE-Owned Fuel* (BSC 2001a). This configuration assumes a rapid degradation of the ingots in the canister while the rest of the waste package internals remain intact. The configuration shown in Figure 10-29 was used.

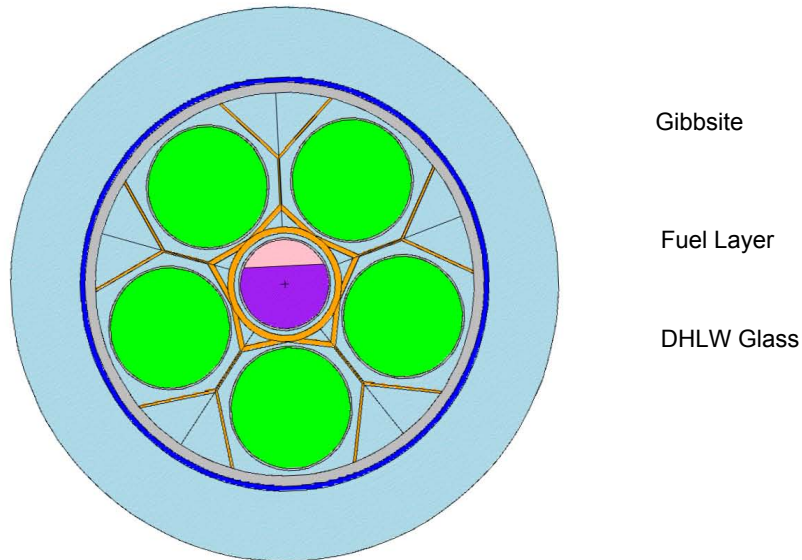


Figure 10-29. Cross-Section View of Degraded Fuel in an Intact Waste Package

The results show that under all circumstances $k_{\text{eff}}+2\sigma$ remained under 0.80 (maximum $k_{\text{eff}}+2\sigma = 0.7994$) with a factor of 8 margin on Gd mass as indicated by the geochemistry results, and the maximum value corresponds to a case with an accumulation 30 cm deep with all the gibbsite present. The cases with void space filled with water have slightly lower $k_{\text{eff}}+2\sigma$ values than corresponding nonphysical cases with empty void space (BSC 2001a, Section 7.4.1).

10.7.1.2 Results for Degraded Configurations Postulated Beyond the Regulatory Period

The degradation and criticality analyses performed have also investigated configurations that require very long times to be attained. These configurations are anticipated to happen well beyond the regulatory period of 10,000 years but they have been analyzed to fully investigate the potential for criticality of the waste package containing Shippingport LWBR. For the purpose of this document, these results (BSC 2001a, Sections 7.4.2 and 7.4.3) have been summarized and grouped together in this section.

Intact Ingots with Internal Components Outside DOE SNF Canister Degraded—This section describes configurations resulting from the scenario IP-3 (BSC 2001a, Sections 5.1.2 and 5.2). The results of the calculations for wet ingots with full Gd content of 0.5 wt% (5.8 kg/waste package) and a U content of 212 kg, corresponding to the MD fuel form completely filling the canister show that $k_{\text{eff}}+2\sigma$ is higher for the case when there is no water present in the prebreach clay and the highest $k_{\text{eff}}+2\sigma$ is 0.4264 (BSC 2001a, Table 7-5).

The results of the calculations for wet ingots with partial Gd content of 0.05 wt% (0.58 kg/waste package) and the MD fuel form completely filling the canister show again that $k_{\text{eff}}+2\sigma$ is highest for the case when there is no water in the prebreach clay and the highest $k_{\text{eff}}+2\sigma$ is 0.6075 (BSC 2001a, Table 7-6).

The results of the calculations for wet ingots with partial Gd content of 0.025 wt% (0.29 kg/waste package) and Gd content of 0.0025 wt% (0.029 kg/waste package) show that $k_{\text{eff}}+2\sigma$ is

highest for the case when there is no water in the prebreach clay. Even without any Gd in the waste package $k_{\text{eff}}+2\sigma$ is well below 0.93. The highest $k_{\text{eff}}+2\sigma$ is 0.7634 for the no Gd case (BSC 2001a, Table 7-7).

Degraded Melt and Dilute Ingots—This configuration has degraded ingots within the intact DOE SNF canister, but with degraded waste package internals. This configuration would be similar to the one shown in Figure 7-4 of *Evaluation of Codisposal Viability for Melt and Dilute DOE-Owned Fuel* (BSC 2001a), but with degraded MD ingots. These cases have approximately 191.3 kg of U.

The results show that retention of at least 7.5 percent of the original Gd inventory assures $k_{\text{eff}}+2\sigma$ below 0.93. The highest $k_{\text{eff}}+2\sigma$ with that amount of Gd is 0.8940.

The thinning of the canister wall down from 0.9525 cm to 0.3175 cm increases $k_{\text{eff}}+2\sigma$ by less than 1 percent ($k_{\text{eff}}+2\sigma$ of 0.8915 versus 0.8850). The effect of a 13.72° tilt to $k_{\text{eff}}+2\sigma$ is an increase of approximately 1.5 percent (BSC 2001a, Table 7-8).

Replacing the reflective boundary condition with a 30-cm water or tuff reflector decreases $k_{\text{eff}}+2\sigma$. This shows that use of the reflective boundary condition is slightly conservative (BSC 2001a, Table 7-8).

All Components Internal to Waste Package Degraded—These configurations represent the final stage of degradation for all the scenarios (BSC 2001a, Section 7.4.3).

Stratified Layers of UO₂ and Postbreach Clay Without Neutron Absorber—The results for cases with a fuel layer (UO₂ and water) on bottom and clay layer on top show that there is no criticality concern for this particular configuration when the water content in the fuel layer is 50 percent. The case with 75 percent water content in the fuel layer shows $k_{\text{eff}}+2\sigma$ of 0.9270, which is just below the critical limit. However, this configuration is not realistic due to lack of physical mechanism that could promote homogenization of 25 percent UO₂ with 75 percent water in stratified layers (BSC 2001a, Section 5.3.3).

Layers of Fuel Mixed with Clay—The results for cases for a layer of UO₂ mixed with the alternate postbreach clay composition corresponding to the extreme case where Gd is lost sitting on the bottom of the waste package show that approximately 2.5 percent of the original Gd loading (131.4 g) must remain with this mixture to prevent criticality or approximately 25 percent of the Hf (approximately 5 kg) in the alternate MD ingot composition must remain (BSC 2001a, Table 7-11). The geochemistry calculation (BSC 2001k) demonstrates that Hf remains in the DOE SNF canister or waste package under all conditions. If confidence in the thermal-dynamic data for GdPO₄ formation is not high enough to make the loss of Gd incredible, then the MD ingot composition with Hf will still prevent a critical condition.

The effect of tilting the waste package is investigated for the maximum tilt angle possible. The $k_{\text{eff}}+2\sigma$ increased to 0.7285 (BSC 2001a, Table 7-11), which is significantly less than the critical limit.

Replacing the reflective boundary condition with a 30-cm thick water or tuff reflector decreases $k_{\text{eff}}+2\sigma$. This shows that use of the reflective boundary condition for this case is very conservative.

10.7.2 Range of Parameters for Configurations of Waste Package Containing Melt and Dilute DOE SNF

ANSI/ANS-8.1-1998 and *Disposal Criticality Analysis Methodology Topical Report* (YMP 2003) provide basic requirements for validation of a calculational method used in the criticality analysis of a system. The bias of a code system (in this case the criticality model containing software code MCNP and selected cross-section libraries) is determined by correlating the results of critical and near-critical experiments with calculated results for those experiments. The common practice, and that considered by the current validation methodology (BSC 2003e), is for comparison of the calculated k_{eff} to a critical or near critical system. Prior to the initiation of the validation activity, the operating conditions and parameters for which the validation is to apply must be identified. The fissile isotope, enrichment of fissile isotope, fuel density, chemical form of fuel, types of neutron moderators and reflectors, range of moderator to fissile isotope ratio, neutron absorbers, and physical configurations are among the parameters to specify. These parameters will define the area of applicability for the selection of the critical experiments for the validation effort.

For the purpose of criticality model validation for the configurations specific to the waste package containing MD DOE SNF and identification of the range of parameters that characterize representative internal configurations of the degraded waste package, the most reactive configurations identified during the screening analyses have been selected. These comprise various arrangements of the degraded fuel mixed with water and/or hydrated products. The first set of configurations has the degraded ingots still contained inside the DOE SNF canister. The second set of configurations represents the final stage of degradation for all possible scenarios. They include the fissile material mixed with water and clayey material in layers placed at the bottom of the waste package (BSC 2001a, Sections 7.4.2 and 7.4.3). All other configurations, including the ones containing intact ingots, do have much lower $k_{\text{eff}}+2\sigma$ (BSC 2001a, Table 7-13) and have not been considered in the validation process.

The configurations considered contain the fissile material homogeneously mixed with hydrated products or water in various fractions and distributed within the DOE SNF canister or in the waste package. The remaining space of the waste package is filled by water mixed with a clayey material. The clayey material has different compositions depending if the DOE SNF canister was degraded or not. The clay composition was calculated in *EQ6 Calculations for Chemical Degradation of Melt and Dilute Waste Packages* (BSC 2001k) using the geochemistry model. These configurations represent refinements of the general configuration class 2 that is described in Section 7 of *Criticality Model Report* (BSC 2003e).

The process employed in *Intact and Degraded Mode Criticality Calculations for the Codisposal of Melt and Dilute Ingots in a Waste Package* (BSC 2001l) for investigating the potential for criticality of the possible degraded configurations of the waste package used a screening approach, the goal being to identify the most reactive configurations in a given class of degraded configurations and testing afterwards the effectiveness of the amount of neutron absorber

introduced as a design solution for controlling the criticality potential for the limiting cases. Due to this approach, the number of configurations analyzed varies among the classes of configurations depending on the complexity of the possible arrangements and the initial screening results.

Selected cases (typically the most reactive cases as presented in BSC 2001a, Section 7) have been rerun with tallies calculating the neutron flux and the fission rate in the regions containing the fissile material. The results of the cases that were rerun with tallies are summarized in *Criticality Model Report* (BSC 2003e) together with a summary of the key physical and neutronic parameters characterizing the most reactive configurations (ROP).

10.7.3 Selection of the Criticality Benchmark Experiments Used in the Validation of the Criticality Model

The benchmark experiments selected in the validation of the criticality model used for the analysis of the waste package containing MD SNF come from *International Handbook of Evaluated Criticality Safety Benchmark Experiments* (NEA 2001) unless otherwise noted. By comparing the characteristics of the selected experiments in each subset with the characteristics of the system that describe the most reactive cases for the degraded configurations of MD SNF waste package, the most appropriate subset of benchmark experiments is the one designated for degraded (homogeneous) moderated (thermal spectrum) configurations (BSC 2002c, Table 6-11). The k_{eff} results and their uncertainties are also summarized in Attachment II of *Analysis of Critical Benchmark Experiments and Critical Limit Calculation for DOE SNF* (BSC 2003f). The benchmarks are listed in Table 10-23.

The experiments listed in Table 10-23 are considered appropriate to represent degraded configurations of the waste package containing Melt and Dilute SNF that belong to the configuration class IP-2a as described in *Disposal Criticality Analysis Methodology Topical Report* (YMP 2003, Section 3). Their range of applicability is detailed in Attachment VIII of *Criticality Model Report* (BSC 2003e).

Table 10-23. Critical Benchmarks Selected for Validation of the Criticality Model for Melt and Dilute Spent Nuclear Fuel

Subset	Benchmark Experiment Identification ^a	Number of Cases Included
Homogeneous moderated ^b	IEU-SOL-THERM-001	4
	IEU-COMP-THERM-001	29
	LEU-SOL-THERM-003	9
	LEU-SOL-THERM-004	7
	LEU-SOL-THERM-006	5
	LEU-SOL-THERM-007	5
	LEU-SOL-THERM-008	4
	LEU-SOL-THERM-009	3
	LEU-SOL-THERM-010	4
	LEU-SOL-THERM-016	7
	LEU-SOL-THERM-017	6
	LEU-SOL-THERM-018	6
	LEU-SOL-THERM-019	6
	LEU-SOL-THERM-020	4
	LEU-SOL-THERM-021	4

Source: Subsets defined in BSC 2002c

NOTES: ^a The convention for naming the benchmark experiments is from NEA 2001.

^b Identification of each subset from BSC 2002c has been modified to better reflect the subset's main characteristics. The benchmark experiments in each subset have not been affected.

10.7.4 Comparison Between ROA of Benchmark Experiments and ROP

The validation of the criticality model needs to show that the range of the fundamental parameters of the benchmark critical experiments (ROA) and the range of the fundamental parameters of the system (ROP) evaluated are nearly identical. This is not usually practical, and for those parameters that do not show a trend in the bias, it is acceptable to use critical benchmark experiments that cover most, but not all, of the ROP of the system under evaluation. In these situations, expert judgement may be used to determine if there is a reasonable assurance that the two are sufficiently close. In cases where a trend in the bias is identified, the ROA can be extended, but a penalty on the lower bound tolerance limit determined for the subset of The comparison between ROA and ROP was structured (BSC 2003e, Attachment VIII) on the subset of benchmark experiments selected to cover the most reactive of the analyzed configurations of the waste package containing MD ingots.

The ROP for the most reactive (homogeneous moderated) configurations was compared to the collective ROA of the selected benchmark experiments described in Tables VIII-4, VIII-5 and VIII-6 of *Criticality Model Report* (BSC 2003e) and the findings are presented in Table VIII-8 of *Criticality Model Report* (BSC 2003e).

The findings from the comparison ROP vs. ROA can be summarized as follows:

- The ROA for this subset of experiments covers the ROP for almost all parameters that characterize the most reactive degraded configurations of MD SNF waste package. The parameter not covered by the ROA is the presence of neutron absorber (Gd). The fact that Gd concentration is very small for the configurations investigated (limiting configurations) makes its impact on the spectral parameters less obvious than for other SNF.

The lack of benchmark experiments with Gd can be substituted with a thorough analysis of the spectral parameters of the system in a sensitivity analysis. Other solutions to completely validate this model for configurations containing Gd are:

- Addition of few new experiments with Gd or analysis of the existing ones (for different fuels/enrichments) in order to extend their ROA.
- Penalty applied to the critical limit (if trend in bias is identified).

10.7.5 Calculation of the Lower Bound Tolerance Limit

The following results are excerpted from *Analysis of Critical Benchmark Experiments and Critical Limit Calculation for DOE SNF* (BSC 2003f), which present in detail the methodology and calculations performed for evaluating the lower bound tolerance limit for each set of configurations of the waste package containing Melt and Dilute SNF.

The results of the trending parameter analysis for the critical benchmark subset representative for moderated degraded configurations of the waste package containing Melt and Dilute DOE SNF are presented in Table VIII-9 of *Criticality Model Report* (BSC 2003e). The results show that the pool of k_{eff} values calculated with the criticality model for this subset of benchmark experiments (moderated heterogeneous subset, see Table 10-23 above) does not show any trending. The lower bound tolerance limit value calculated with the distribution free tolerance limit (DFTL) method is 0.9659.

The above results and the comparison ROA vs. ROP indicate that the criticality model is partially validated for use in assessing the criticality potential of the configurations belonging to the general configuration class 2 of the degraded waste package containing MD ingots.

10.7.6 Summary of the Criticality Model Results and Validation for the Waste Package Containing Melt and Dilute SNF

The criticality analyses considered all aspects of intact and degraded configurations of the waste package containing Melt and Dilute ingots, including optimum moderation condition, optimum reflection, geometry and composition. The results of three-dimensional Monte Carlo criticality calculations for the intact configuration show that the requirement of $k_{\text{eff}}+2\sigma$ values less than or equal to the interim critical limit of 0.93 is satisfied for by a significant margin. The criticality calculations results for all anticipated degraded-mode configurations developed through the degradation analysis show that the requirement of $k_{\text{eff}}+2\sigma$ values less than or equal to the interim

critical limit of 0.93 is satisfied by a significant margin for most of the MD codisposal package degraded configurations. The requirement is satisfied for all MD codisposal package degraded configurations if at least 7.5 percent of the original Gd loading (394.2 g) in the ingots without Hf remains mixed with the fissile material. The geochemistry analysis showed that the loss of more than 20 percent of the initial Gd content is based on extreme conditions or unrealistic unknown errors in the thermal-dynamic data. However, quantifying the probability of retaining less than 7.5 percent of the initial Gd content and therefore for an increased potential for criticality remains to be assessed, but is qualitatively judged to be extremely low as summarized in Section 8.4 of *Evaluation of Codisposal Viability for Melt and Dilute DOE-Owned Fuel* (BSC 2001a). In the alternate MD ingot composition (containing 0.5 wt% Hf), Hf remains in the DOE SNF canister or waste package under all conditions, therefore preventing a critical condition even if all Gd is removed from the system.

All calculations are based on a maximum of 38.3 kg ^{235}U per DOE SNF canister. Hence, the total mass of fissile element (^{235}U) should not exceed the mass used in deriving the conclusions of this report, which is 38.3 kg of ^{235}U per DOE SNF canister. The maximum ^{235}U enrichment is 20 wt%. The linear density of the ^{235}U should not exceed 151 g/cm in the DOE SNF canister. This value is calculated by considering the maximum diameter and the maximum U content (18.2 wt%) for the MD ingots.

Table 10-24 presents a summary of the criticality and geochemistry results with a focus on the correspondence with the degradation classes and resultant configuration classes presented in *Disposal Criticality Analysis Methodology Topical Report* (YMP 2003).

The criticality model (software code MCNP and appropriated selected neutron cross-section libraries) used in analyzing the configurations of the waste package containing MD ingots was validated using the methodology described in *Disposal Criticality Analysis Methodology Topical Report* (YMP 2003) and *Criticality Model Report* (BSC 2003e). Current results indicate that the lower bound tolerance limit is well above the interim critical limit used in evaluating the design.

Table 10-24. Summary of Geochemistry and Criticality Analyses for Internal Configurations (phase I and II) of the Waste Package Containing Melt and Dilute LWBR Spent Nuclear Fuel

Master Scenario	Description	Configuration Classes and Summary Description	Summary of Geochemistry Calculations	Summary of Criticality and Criticality Model Validation Results		Comments
				$(k_{eff}+2\sigma)_{max}$	Interim Critical Limit	
Initial water intrusion	Initial stage; water fills all available spaces inside the waste package and DOE SNF canister	Intact flooded configurations: SNF and internal structures not degraded	N/A	0.3571	0.93	Maximum $k_{eff}+2\sigma$ was obtained for 0.5 wt% Gd in the ingot.
IP-1	MD ingots degrade before the internals of the waste package	Configuration class #6: SNF partially degraded in place (various stages)	For all cases investigated (IP-1, IP-2 and IP-3 scenarios) the loss ranges were: U: 0 to 100% Gd: 0 to 23% (with no suppression of $GdPO_4 \cdot 10H_2O$ formation)	0.7994	0.93	At least 10% of the initial Gd amount must be present in the mixture for this result.
	The top of the waste package is breached and liquid accumulates inside	Configuration class #3: SNF partially or totally degraded inside the waste package with intact internal structures		N/A	0.93	Configurations are covered by refinements of configuration class #2 below
IP-2	SNF degrades concurrently with the internals of the waste package	Configuration class #2: Both SNF and internal structures of the waste package degraded (various stages)		0.8825	0.93	At least 2.5% of initial Gd amount must be mixed with degraded ingots.
IP-3	SNF degrades after the internals of the waste package	Configuration class #1: SNF intact (ingot) and degraded internal structures (various stages)		0.4236	0.93	Maximum $k_{eff}+2\sigma$ was obtained for 0.5 wt% Gd in the ingot.
IP-4	SNF degrades before the internals of the waste package	The configurations resulting from these scenarios (configurations classes #4, #5) have not been investigated in the geochemistry and criticality analyses due to the fact that they are less moderated (no pooling of water) and are bounded by the variations of the configurations investigated above.				
IP-5	The bottom of waste package is penetrated allowing liquid to flow through	SNF degrades concurrently with the internals of the waste package				
IP-6	SNF degrades after the internals of the waste package	SNF degrades after the internals of the waste package				

10.8 FSVR SNF

The description and main characteristics of the waste package containing FSVR SNF are presented in Section 3.2.8. In this section a summary of the results of the criticality analyses performed is presented together with the current status of the validation of the criticality model for the configurations that are specific to this fuel group.

The first step in applying the criticality model to the specific intact and degraded configurations of this waste package is identification and characterization of the specific configurations anticipated for postclosure. The results of the degradation analysis coupled with the geochemistry calculations (BSC 2001c, Section 6) provided an insight into the possible arrangements and compositions of the degraded materials placed within the waste package. All configuration classes analyzed and the most probable degradation scenario that was identified are summarized in the next section (Section 10.8.1). The results of the criticality calculations for the most representative intact and degraded configurations are presented in Section 10.8.2. The limiting cases identified during the analysis are also providing the basis for deriving the final design solution (amount of neutron absorber to be distributed within the initial waste package). The range of parameters that characterize the limiting or the most reactive cases is subsequently used in the process of validation of the criticality model. The process includes selection of appropriate critical benchmark experiments and derivation of the specific lower tolerance bound limit for each major group of configurations.

The results of the three-dimensional Monte Carlo criticality calculations for all anticipated intact- and degraded-mode configurations developed through the degradation analysis, and which are physically possible, show that the requirement of $k_{\text{eff}}+2\sigma$ values less than or equal to the interim critical limit of 0.93 is satisfied for the FSVR SNF waste package. No neutron absorber material is required as long as the U-235 mass for codisposal is within the specified limit. All calculations were based on a maximum of 7.425 kg ^{235}U per DOE SNF canister. This amount is calculated using the maximum number of FSVR fuel elements that can be loaded into the DOE SNF canister, which is five. The degraded configurations of the FSVR SNF bound the other types of Th/U carbide DOE-owned SNF, as long as the limits on mass of uranium and its linear density are not exceeded.

The highest k_{eff} values resulted from the configurations assuming that approximately 10 percent of the fuel contained in the compacts inside the FSVR fuel elements is degraded and leaves the compacts, while the DOE SNF canister is still intact. However, these configurations are not possible because the carbonaceous matrix of the fuel compacts is similar to graphite, therefore chemically inert. Additionally, there is no known degradation mechanism that can remove 10 percent or more of the fuel particles from the compacts. The highest $k_{\text{eff}}+2\sigma$ values also resulted from the configurations that assume either the breaking of the graphite block into a large number of pieces or complete degradation. Neither configuration is attainable through any known degradation mechanism. All possible degraded configurations (intact and degraded) are bounded by the intact configuration with water inside the DOE SNF canister but no water outside the DOE SNF canister (waste package is still reflected with 30 cm of water). In this case the $k_{\text{eff}}+2\sigma$ is just below 0.93.

10.8.1 Degradation Scenarios and Configurations

Based on the corrosion rates and the material thicknesses given in Table 10-25, the most probable degradation path for the waste package, the DOE SNF canister, and the FSVR SNF follows the sequence below (BSC 2001c, Section 6.4.2):

1. Waste package is penetrated and flooded internally. Water has not yet penetrated the DOE SNF canister.
2. The waste package separation plates and DOE SNF canister support cylinder degrade first because of the high corrosion rate of A516 carbon steel. Degraded steel product (iron oxide) accumulates at the bottom of the waste package.
3. DHLW glass canister shell degrades and exposes the DHLW glass. The DHLW glass degrades at a much lower rate than the stainless steel components and only a small percentage degrades while the stainless steel degrades as demonstrated in the geochemistry calculations (BSC 2001c). There are two possible degradation paths:
 - 3a. DOE SNF canister stays intact. Intact DOE SNF canister with intact FSVR SNF fall and are surrounded by the iron-rich degradation products near the bottom of the waste package.
 - 3b. DOE SNF canister starts to degrade.
4. Following 3b above, DOE SNF canister shell is penetrated but remains intact and DOE SNF canister interior is flooded.
5. DOE SNF canister shell completely degrades. The degraded iron oxide mixes with the degraded glass and iron oxide clay at the bottom of the waste package. The intact FSVR fuel elements fall on top of the clay.
6. Given a very long period of time, it is postulated that everything will degrade including the FSVR fuel compacts and graphite block. However, it is very unlikely to attain complete degradation of the graphite block and fuel particles within the time period covered by the geochemistry and criticality analyses (up to $6.34 \cdot 10^5$ years from emplacement) due to very low degradation rates of SiC and graphite. It is expected that rockfall and seismic events could break the graphite blocks and fuel compacts into pieces, but the number of pieces is rather small. The degraded SNF, other degradation products, and water mix and accumulate at the bottom of the waste package.

Table 10-25. Materials and Thicknesses

Components	Material	Thickness (mm)
Waste package divider plate	A516 Carbon Steel	12.7
Waste package support tube	A516 Carbon Steel	31.75
DHLW glass canister shell	Stainless Steel Type 304L	10.5
DHLW glass	Glass	N/A
DOE SNF canister shell	Stainless Steel Type 316L	9.525
Fuel particles layer	SiC	0.020

Source: BSC 2001c, Section 2.1 and Appendix A

The configurations investigated can be categorized using the description of the generic configuration classes given in Section 3 of *Disposal Criticality Analysis Methodology Topical Report* (YMP 2003). As indicated in Section 6.5 for the purpose of fully identifying the potential for criticality, all representative configurations classes have been analyzed and not only the configurations resulting from the most probable degradation path presented above. The subtitles follow the original description given in Section 6.4.3 of *Evaluation of Codisposal Viability for Th/U Carbide (Fort Saint Vrain HTGR) DOE-Owned Fuel* (BSC 2001c).

Intact DOE SNF Canister and Degraded Waste Package Internals—In this case, the SNF is intact or partially degraded. This configuration is a variation of configuration class 1 and can be reached from standard scenario IP-3. The results of criticality calculations for this configuration are given in Section 10.8.2.3 (Intact DOE SNF Canister)

Degraded DOE SNF Canister and Waste Package Internals, Intact SNF—In this case, the DOE SNF canister, waste package internals, and DHLW canisters are degraded. The fuel element is intact. The degradation scenarios and configuration classes are applied to the entire waste package. As a variation, there could be partial degradation of the SNF. This configuration is a variation of the configuration class 1 and can be reached from standard scenario IP-3. The results of the criticality calculations for this configuration are given in Section 10.8.2.3 (Degraded DOE SNF Canister with nonreacted prebreach clay).

Degraded SNF with Intact DOE SNF Canister or Waste Package—In this case, the SNF could be partially or fully degraded. This configuration is a variation of configuration class 6 and can be reached from standard scenario IP-1. The results of the criticality calculations for this configuration are given in Section 10.8.2.2.

Partially or Completely Degraded DOE SNF Canister and Waste Package Internals—In this case, the degradation scenario and configuration are applied to the entire waste package including the SNF. Degradation products from the DOE SNF canister, SNF and the OIC mix uniformly inside the waste package. This configuration is a variation of configuration class 2 and can be reached from standard scenario IP-1, IP-2, or IP-3. The results of the criticality calculations for this configuration are given in Section 10.8.2.3.

10.8.2 Criticality Calculations and Results

10.8.2.1 Results for Intact Mode

This section summarizes the results of the intact-mode (phase I) criticality analysis (BSC 2001c, Section 7.3). These configurations represent a waste package, which has been breached allowing the inflow of water, but the internal components of the waste package are intact (see Figure 10-30). For most of the MCNP representations the waste package was reflected by water, but in order to investigate the effect of different reflective conditions on criticality, the mirror reflection boundary condition was also considered. Use of a mirror reflective boundary condition is conservative since no neutrons leak (escape) from the system. The DOE SNF canister is represented as loaded with five FSVR fuel elements axially aligned. Variations of the intact configurations were examined to identify the configuration that results in the highest calculated k_{eff} value within the range of possible conditions.

The base case is shown in Figure 10-30. The water reflected waste package is in a horizontal storage position where the effect of gravity on the DHLW and DOE SNF canisters is evident. All the voids and porosities in the fuel and graphite block were represented as completely filled with water, the fuel length is considered to be the same as the element length, and the DOE SNF canister is completely flooded. The fourth fuel composition (BSC 2001c, Section 2.1.4.2) was used with an additional 2.59 g of Pu per fuel element (which is equal to the maximum amount of Pu at EOL and was added for conservatism). The amount of Th in the fuel is reduced (arbitrarily) by 5 percent to show the sensitivity of the results to Th content. Other modeling details such as whether the fuel has the same length as the element (neglecting the plugs at the end of the fuel holes) or the slightly smaller length of the actual fuel holes and reflector boundary conditions were also investigated.

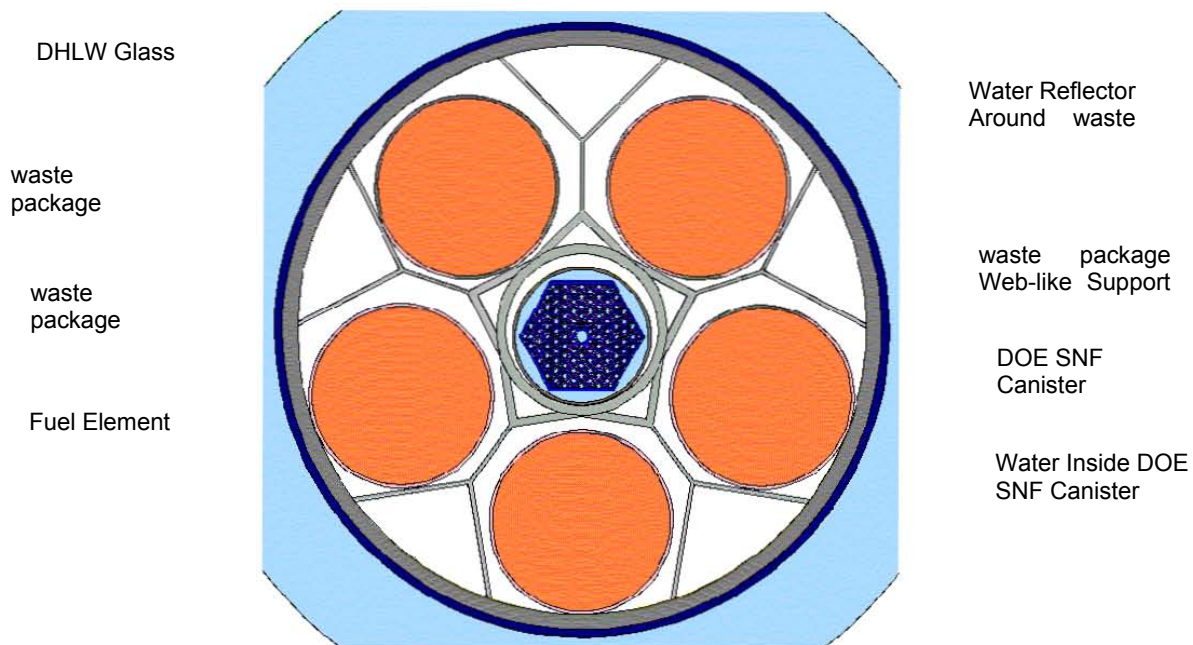


Figure 10-30. Cross-Section View of the 5-DHLW/DOE Waste Package Intact Configuration

The results indicate that the intact configuration of the FSVR waste package has a $k_{\text{eff}}+2\sigma$ below 0.93 ($k_{\text{eff}}+2\sigma = 0.9176$) and the fourth fuel composition from Section 2.1.4.2 of *Evaluation of Codisposal Viability for Th/U Carbide (Fort Saint Vrain HTGR) DOE-Owned Fuel* (BSC 2001c) is the most reactive among the four compositions evaluated, therefore conservatively selected for further use in the analysis. The variations applied to the intact configuration show a statistically insignificant change in results from the base case, except the last case where a 5-percent reduction of the Th amount results in an increase of about 0.5 percent in $k_{\text{eff}}+2\sigma$ (BSC 2001c, Section 7.3).

A separate set of cases was run where the amount of water saturation is varied in the fuel compacts and in the graphite block (BSC 2001c, Table 7.2). The examination of the results shows that the FSVR waste package system is under-moderated, and the absence of water in the fuel and graphite block voids significantly reduces the k_{eff} .

Cases with variations in the positioning of the waste package internal components and other cases demonstrate that changing the positions of internal waste package components has no statistical significance for the $k_{\text{eff}}+2\sigma$ results. Also, there is no statistical difference between water and a perfect (mirror) reflector at the outer boundary of the waste package (BSC 2001c, Table 7.3).

The results in this section show that the most reactive composition of the four considered (BSC 2001c, Section 2.1.4.2) is that using 1,485 g ^{235}U per fuel element. On the basis of conservatism, this is the composition used further in the criticality analyses.

10.8.2.2 Results for Fuel Assembly Degrading Before the Internal Components of the waste package

In this section, cases where the waste form degrades before any other internal components of the waste package were investigated. This corresponds to configuration class 6 resulting from scenario IP-1. This class of configurations assumes a rapid degradation of the FSVR fuel elements inside the DOE SNF canister while the rest of the waste package internals remain intact.

Partial Degradation of Fuel Compacts before the Graphite Block—In this scenario the graphite blocks are intact, but some portion of the fuel compacts has degraded. This degradation is due to either some amount of the fissile material in the fuel having dissolved into solution and reentering the fuel elements, or some portion of the fuel compact has fallen out of the graphite block and settles at the bottom of the canister. In the first case, where the fissile material has dissolved, only the uranium is considered to dissolve and is redistributed in the coolant channels and voids of the fuel elements. This is conservative since otherwise the uranium would redistribute in all the water throughout the entire DOE SNF canister and not just inside the fuel elements. Variations are considered where the water level in the DOE SNF canister is such that only a portion of the fuel elements is submerged and the dissolved fissile material only fills the portion of the fuel elements below the water level. This configuration is shown in Figure 10-31 where the water level is at half of the fuel elements' height and dissolved fissile material fills the coolant channels and voids below the water level.

In the cases where fuel is uniformly removed from the fuel elements, at least 10 percent of the uranium must be redistributed into the channels in order to exceed the interim critical limit (BSC 2001c, Table 7-4). This amount of dissolved uranium is significantly greater than approximately 0.3 percent - the upper bound of the failure rate for all fuel particles (BSC 2001c, Section 2.1.4.3). It should be noted that failure of fuel particles that expose the kernel to water is the only known mechanism resulting in fissile material being dissolved in the surrounding water.

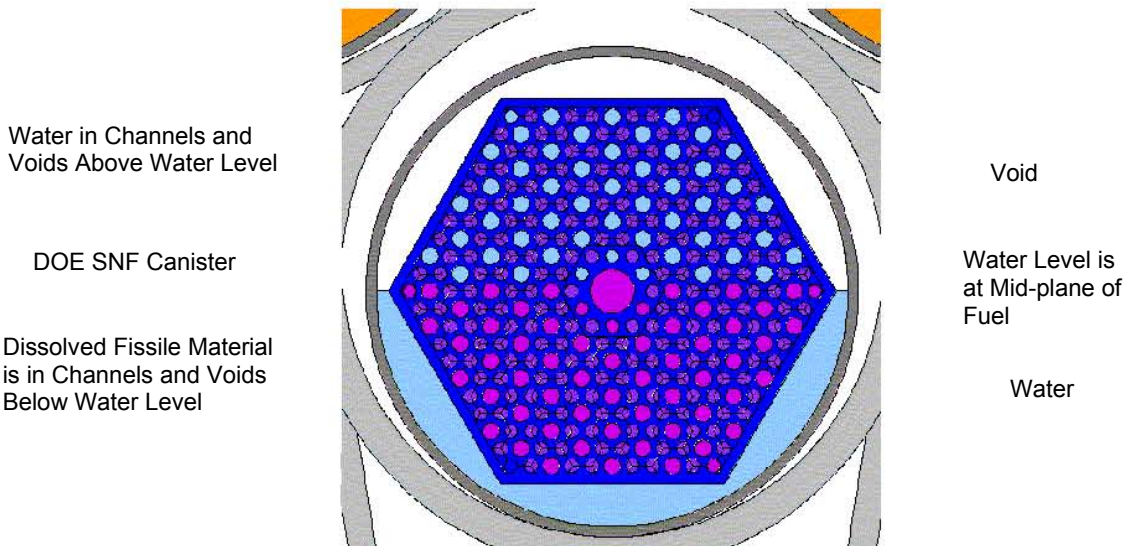


Figure 10-31. Configuration with Fissile Material in Solution in the Lower Half of the Coolant Channels and Voids of the Fuel Element

Cases were analyzed where a portion of the fuel degrades, is removed from an end element in the fuel element stack, and is re-deposited at the bottom of the canister along its entire length (BSC 2001c, Table 7-5). The results indicate that $k_{\text{eff}}+2\sigma$ is greater than 0.93 in cases where more than 10 percent of fuel is removed from fuel elements in the configuration investigated. There are two known mechanisms through which the fuel could be removed from the fuel elements: the failure of fuel particles that expose the kernel to water, and the fuel particles separating from the compacts. As mentioned before, the first mechanism, which results in fissile material being dissolved in the surrounding water, is limited to approximately 0.3 percent failed fuel particles - significantly less than the 10 percent minimum needed to obtain $k_{\text{eff}}+2\sigma$ greater than 0.93. The second mechanism could result in fuel particles accumulating at the bottom of the DOE SNF canister only if the graphite blocks break into a large number of pieces, which is not possible through known degradation processes.

A group of cases also investigated the effect of tilting the DOE SNF canister. The fuel was removed from some portion of a fuel element and re-deposited either in the volume between the end of the fuel element stack and the canister or in the volume between the second and third element of the stack. The re-deposited fuel was composed of degraded fuel compacts homogenized with water. The volume left in the fuel holes by removing fuel was filled either by water or by axially homogenizing the remaining fuel with water over the entire length of the fuel hole. The volume fraction of water in the displaced fuel was also varied. Any unfilled spaces in the canister were filled by water. The results, presented in *Intact and Degraded Mode Criticality Calculations for the Codisposal of Fort Saint Vrain HTGR Spent Nuclear Fuel in a Waste Package* (BSC 2001f, Table 18), show that $k_{\text{eff}}+2\sigma$ was below 0.93 for all physically possible cases.

Results for Degraded Graphite Block with Intact Fuel Compacts—Cases were treated for various degrees of degradation ranging from the graphite block broken into a few pieces to a completely rubblized block. For the cases where the block has broken into pieces the separation

between pieces was varied. An example of a fuel element that has broken into 6 pieces is shown in Figure 10-32.

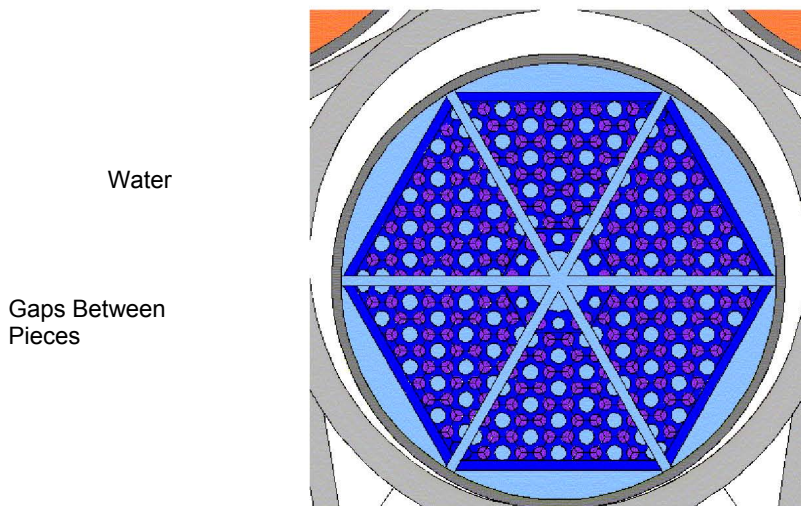


Figure 10-32. Configuration with the Fuel Elements Broken into Six Pieces

The results for this configuration are presented in *Intact and Degraded Mode Criticality Calculations for the Codisposal of Fort Saint Vrain HTGR Spent Nuclear Fuel in a Waste Package* (BSC 2001f, Table 19). The $k_{\text{eff}}+2\sigma$ was below 0.93 for all variations covered (two, four, six or more pieces, moved outward in the radial direction up to 1 cm).

For the cases where the block was treated as rubble, the fuel compacts are represented axially aligned and radially separated so as to form fictitious “fuel rods,” which are surrounded by the graphite from the fuel elements mixed with water. In these cases the radial separation (pitch) between “fuel rods” is varied from touching to just greater than that for the intact fuel elements. Figure 10-33 shows a configuration of these “fuel rods” in the DOE SNF canister. In this configuration the “fuel rods” have settled into the canister with a pitch of 2.0 cm and uniformly fill the DOE SNF canister to an approximately leveled arrangement across the canister. This configuration is considered to be more probable than that shown in Figure 10-34, where the “fuel rods” form a pile heaped at the center of the DOE SNF canister. The configuration in Figure 10-34 is shown to be the more reactive of the two in *Intact and Degraded Mode Criticality Calculations for the Codisposal of Fort Saint Vrain HTGR Spent Nuclear Fuel in a Waste Package* (BSC 2001f, Section 6.2.1.2). The effect of varying the volume fraction of water in the rubble was also investigated, as well as the axial separation between the fuel compacts in the “fuel rods.” For this scenario any unoccupied space in the canister was filled with water. The results for these cases are presented in *Intact and Degraded Mode Criticality Calculations for the Codisposal of Fort Saint Vrain HTGR Spent Nuclear Fuel in a Waste Package* (BSC 2001f, Table 20). Examination of the results shows that k_{eff} increases for increasing pitch and volume fraction of water in the carbon rubble, but decreases slightly for increasing axial separation between fuel compacts. Also, the most reactive cases for a given pitch, volume fraction of water in the rubble, and axial separation occurs for configurations that are more tightly compacted and less spread out in the canister (see Figure 10-34). However, the compacted configurations are less probable since any disturbance of the waste package would

tend to spread out the rods and also decrease the pitch. For all cases analyzed, the calculated $k_{eff}+2\sigma$ was below 0.93.

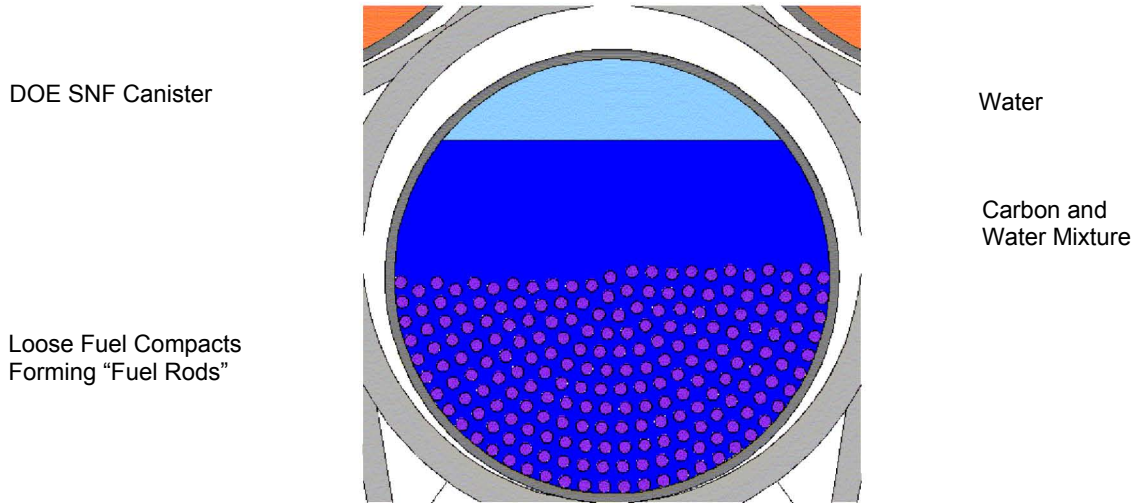


Figure 10-33. Configuration with Graphite Block Broken into Rubble and Fuel Compacts Axially Aligned Forming "Fuel Rods" (level arrangement)

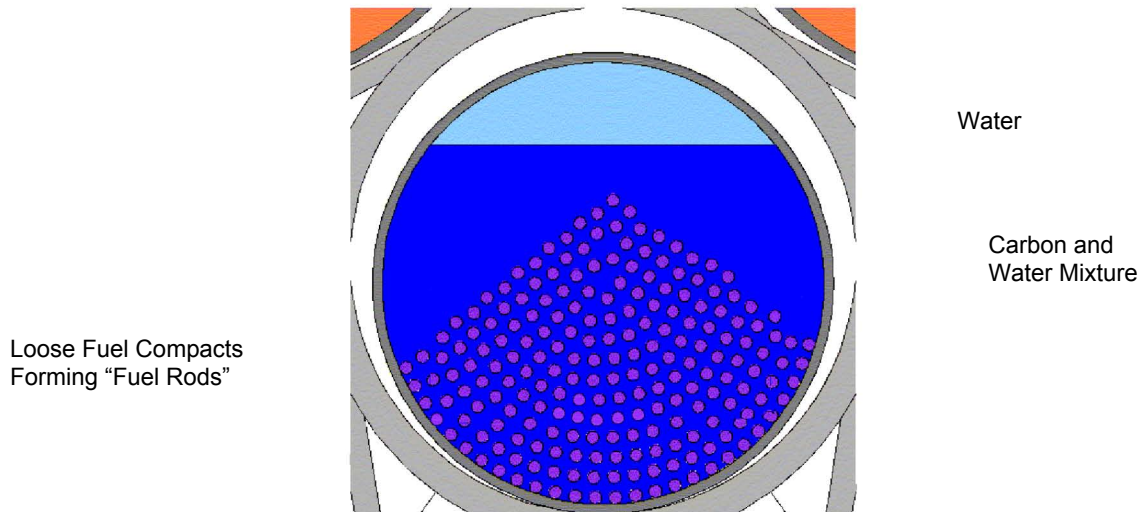


Figure 10-34. Configuration with Graphite Block Broken into Rubble and Fuel Compacts Axially Aligned Forming "Fuel Rods" (mound arrangement)

10.8.2.3 Results for Degraded Configurations Postulated beyond the Regulatory Period

The degradation and criticality analyses performed have also investigated configurations that require very long times to be attained. These configurations are anticipated to happen well beyond the regulatory period of 10,000 years but they have been analyzed to fully investigate the potential for criticality of the waste package containing Shippingport LWBR. For the purpose of this document, these results (BSC 2001c, Sections 7.4.1.3, 7.4.2, and 7.4.3) have been summarized and grouped together in this section.

Results for Configurations with Degraded Graphite Block and Degraded Fuel Compacts—

For this scenario both the graphite block and the fuel compacts have degraded to rubble. The configuration can be regarded as being a refinement of the configuration class 6. The degraded materials would in general mix together, but cases were investigated where these are treated as layers of separate materials to investigate the effect of their segregation on $k_{\text{eff}}+2\sigma$. Values of $k_{\text{eff}}+2\sigma$ above 0.93 were obtained for cases with fuel content between 30 and 60 volume % (vol%) in the bottom layer, and at least 60 vol% carbon in the layer above (for both layers, the difference up to 100 percent is water).

It should be noted that all fuel elements are loaded into the DOE SNF canister and the canister is then loaded into the waste package. The fuel elements are then assumed to be emplaced into the repository in an intact condition (i.e., without any significant cracks and chips in the graphite blocks).

Intact DOE SNF Canister and Degraded Components Inside the Waste Package—The DOE SNF canister configurations investigated include intact and degraded cases and are derived from the most reactive cases identified in the previous sections. The configuration belongs to configuration class 1 resulting from IP-3 degradation scenario. For these cases the intact canister containing the intact or degraded fuel was surrounded by prebreach clay. The location of the DOE SNF canister in the clay was varied from just under the surface of prebreach clay to the bottom of waste package.

The results of the MCNP cases are given in *Intact and Degraded Mode Criticality Calculations for the Codisposal of Fort Saint Vrain HTGR Spent Nuclear Fuel in a Waste Package* (BSC 2001f, Table 23). For all cases with intact fuel elements, the $k_{\text{eff}}+2\sigma$ values were below 0.93. The set of cases that have partially or completely degraded fuel components (based on the most reactive configurations with degraded graphite block from of BSC 2001c, Section 7.4.1) had several $k_{\text{eff}}+2\sigma$ values above 0.93. However, as mentioned also in Section 7.4.1.3 of *Evaluation of Codisposal Viability for Th/U Carbide (Fort Saint Vrain HTGR) DOE-Owned Fuel* (BSC 2001c), at and after emplacement of FSVR SNF in the repository, there is no degradation mechanism to break the graphite blocks in a large number of pieces, therefore the configurations with $k_{\text{eff}}+2\sigma$ values above 0.93 are not physically attainable.

Intact Fuel Elements with Degraded DOE SNF Canister and Waste Package Internals—In these configurations (refinements of class 1 of configurations) the fuel elements are intact and surrounded by prebreach clay and goethite either mixed together or in separate layers. When mixed together, the composition of the mixture was varied to determine how reactive the configuration is. Also, the water volume fraction of the materials in the various layers was varied. For most cases the coolant channels and voids of the fuel elements were filled with water, but for some of the more reactive cases a mixture of clay and water was used to fill the coolant channels and voids of the fuel elements.

A possibly more realistic configuration has the goethite surrounding the intact fuel elements, which in turn are surrounded by clay. This configuration could occur if the canister degrades to goethite after it is trapped in the clay formed from the degraded contents of the waste package. Variations of this case were investigated by changing the volume fraction of water in the goethite surrounding the fuel elements, varying the volume fraction of goethite in the coolant channels

and voids, and by assuming the goethite forms a hexagonal shaped layer around the fuel elements. The results for these cases are given in *Intact and Degraded Mode Criticality Calculations for the Codisposal of Fort Saint Vrain HTGR Spent Nuclear Fuel in a Waste Package* (BSC 2001f, Table 24). The values of $k_{\text{eff}}+2\sigma$ were below 0.93 for all cases.

Intact Fuel Compacts with Degraded Graphite Block, DOE SNF Canister, and Internals of the Waste Package—These cases are similar to those presented in the previous section (refinements of configuration class 1), but the graphite block has been degraded to rubble and the fuel compacts are assumed to remain axially aligned and form “fuel rods” in the waste package. The “fuel rods” can now be surrounded by goethite and clay in addition to the carbon from the degraded graphite block. Variations of these materials and the water volume fraction for the layers surrounding the fuel were investigated. The pitch of the “fuel rods” was also varied. Here the loose “rods” are heaped at the bottom of the waste package and are surrounded by a mixture of goethite, carbon, water, and clay. These cases and the results of the MCNP cases are presented in *Intact and Degraded Mode Criticality Calculations for the Codisposal of Fort Saint Vrain HTGR Spent Nuclear Fuel in a Waste Package* (BSC 2001f, Table 25). The maximum value of $k_{\text{eff}}+2\sigma$ was 0.841 for this set of cases.

Configurations similar to the above ones but where the rods surrounded by goethite and carbon have been trapped in the clay layer were also investigated. Such a configuration has the pins forming an array with a circular cross-section (henceforth referred to as a “circular” array). Here, a mixture of goethite, carbon, and water surrounds the pins that are positioned in the prebreach clay layer. Different compositions, volume fractions of water and pitches were investigated. Also, cases were considered where the “fuel pins” are assumed to be in the same position as in the intact fuel elements and are surrounded by goethite, and the volume fraction of water in the surrounding carbon is varied. All of these cases and the results of the MCNP runs are presented in *Intact and Degraded Mode Criticality Calculations for the Codisposal of Fort Saint Vrain HTGR Spent Nuclear Fuel in a Waste Package* (BSC 2001f, Table 27). Several of the $k_{\text{eff}}+2\sigma$ values are between 0.93 and 0.96. However, the breach of the graphite block in a large number of pieces is nonphysical, therefore the configurations described in this set of cases are not attainable.

Degraded Fuel Compacts, Graphite Block, DOE SNF Canister and Internals of the Waste Package—These configurations (belonging to configuration class 2) have the degraded fuel mixed with goethite and clay in addition to carbon and water in the waste package. Different cases with single and mixed materials in the layers at the bottom of the waste package were investigated. The volume fraction of water was also varied for these different compositions. The materials in each layer were always represented as homogeneously mixed. These cases and the results of MCNP cases are presented in *Intact and Degraded Mode Criticality Calculations for the Codisposal of Fort Saint Vrain HTGR Spent Nuclear Fuel in a Waste Package* (BSC 2001f, Table 28). All the values of $k_{\text{eff}}+2\sigma$ were below 0.76.

Uniform Mixture of Degraded Products in the Waste Package—These configurations represent the final stage of degradation for the scenarios, where the waste form degrades together with the internals of the waste package and correspond to the class 2 of configurations. The composition of the clay resulting from the degradation of all components inside the waste package is given in *EQ6 Calculation for Chemical Degradation of Fort St. Vrain (Th/U Carbide)*

Waste Packages (BSC 2001h, Table 6-14). This clay is referred to as postbreach clay. The amount of water in the clay was varied to determine the most reactive compositions. These cases and the results of the MCNP cases are presented in *Intact and Degraded Mode Criticality Calculations for the Codisposal of Fort Saint Vrain HTGR Spent Nuclear Fuel in a Waste Package* (BSC 2001f, Tables 28 and 29). All the values of $k_{\text{eff}}+2\sigma$ were below 0.93, except one case where $k_{\text{eff}}+2\sigma$ was 0.938. However, this case, like all the others in this set is based on the breaking of the graphite block into a large number of pieces. This configuration cannot be attained by any known degradation mechanism (BSC 2001c, Section 7.4.3).

10.8.3 Range of Parameters for Configurations of Waste Package Containing FSVR DOE SNF

ANSI/ANS-8.1-1998 and *Disposal Criticality Analysis Methodology Topical Report* (YMP 2003) provides basic requirements for validation of a calculational method used in the criticality analysis of a system. The bias of a code system (in this case the criticality model containing software code MCNP and selected cross-section libraries) is determined by correlating the results of critical and near-critical experiments with calculated results for those experiments. The common practice, and that considered by the current validation methodology (BSC 2003e), is for comparison of the calculated k_{eff} to a critical or near critical system.

Prior to the initiation of the validation activity, the operating conditions and parameters for which the validation is to apply must be identified. The fissile isotope, enrichment of fissile isotope, fuel density, chemical form of fuel, types of neutron moderators and reflectors, range of moderator to fissile isotope ratio, neutron absorbers and physical configurations are among the parameters to specify. These parameters will define the area of applicability for the selection of the critical experiments for the validation effort.

The preliminary degradation analysis of the content of the waste package containing FSVR SNF (BSC 2001c, Section 6) and the subsequent criticality analysis performed for the resulting internal configurations have followed the guidance suggested by the Internal Criticality Master Scenarios presented in *Disposal Criticality Analysis Methodology Topical Report* (YMP 2003, Section 3.3) and also by *Generic Degradation Scenario and Configuration Analysis for DOE Codisposal Waste Package* (CRWMS M&O 1999g, Section 6.2.2). The resultant configuration classes internal to the waste package have been screened systematically for their criticality potential in comprehensive criticality analyses (BSC 2001f, Section 7.5). The main results have been summarized in the sections above.

For the purpose of the current criticality model validation for the configurations specific to the waste package containing FSVR SNF and identification of the range of parameters that characterize the internal configurations of the degraded waste package, the degraded configurations previously investigated (see Section 10.8.2.1 to 10.8.2.3) have been categorized into two large groups:

1. Configurations containing intact fuel elements (heterogeneous configurations)
2. Configurations containing degraded fuel elements (relatively homogeneous configurations).

The first category contains the configurations described in Sections 7.3, 7.4.1.1, 7.4.1.2, 7.4.2.1, and 7.4.2.2 of *Evaluation of Codisposal Viability for Th/U Carbide (Fort Saint Vrain HTGR) DOE-Owned Fuel* (BSC 2001c). These configurations represent mostly intact fuel (nondegraded or partially degraded) configurations and refinements of the general configuration class 1 and 6. The second category includes the configurations described in Sections 7.4.1.3, 7.4.2.2.3 and 7.4.3 of *Evaluation of Codisposal Viability for Th/U Carbide (Fort Saint Vrain HTGR) DOE-Owned Fuel* (BSC 2001c). These configurations represent refinements of the general configuration classes 2 and 6. This proposed categorization allows a simple and systematic way of identifying the key parameters that characterize the degraded configurations.

The process employed in *Evaluation of Codisposal Viability for Th/U Carbide (Fort Saint Vrain HTGR) DOE-Owned Fuel* (BSC 2001c) for investigating the potential for criticality of the possible degraded configurations of the waste package used a screening approach, the goal being to identify the most reactive configurations in a given class of degraded configurations. Due to this approach, the number of configurations analyzed varies among the classes of configurations depending on the complexity of the possible arrangements and the initial screening results. Selected cases (typically the most reactive cases as presented in BSC 2001c, Sections 7.3 and 7.4) have been rerun with tallies calculating the neutron flux and the fission rate in the regions containing the fissile material. The original MCNP cases have been obtained from *Intact and Degraded Mode Criticality Calculations for the Codisposal of Fort Saint Vrain HTGR Spent Nuclear Fuel in a Waste Package* (BSC 2001f). The results of the cases that were rerun with tallies are summarized in *Criticality Model Report* (BSC 2003e).

10.8.4 Selection of the Criticality Benchmark Experiments Used in the Validation of the Criticality Model

The benchmark experiments selected in the validation of the criticality model used for the analysis of the waste package containing FSVR SNF come from *International Handbook of Evaluated Criticality Safety Benchmark Experiments* (NEA 2001) unless otherwise noted. The selection process was initially based on a prior knowledge regarding the possible configurations of degraded waste package, and the subsets have been constructed to accommodate large variations in the range of parameters of the configurations and also to provide adequate statistics for lower bound tolerance limit calculations. The selected benchmark experiments for each subset are presented in *Benchmark and Critical Limit Calculation for DOE SNF* (BSC 2002c) together with the MCNP cases constructed and the results of the calculations. For the present application (codisposal of Shippingport LWBR SNF), the selected benchmark experiments have been grouped in two subsets (BSC 2002c), that include moderated heterogeneous and homogeneous experiments. Additional benchmark cases added for the present analysis and the k_{eff} results and their uncertainties are summarized in Attachment II of *Analysis of Critical Benchmark Experiments and Critical Limit Calculation for DOE SNF* (BSC 2003f). Table 10-26 presents the list of the benchmark experiments and the number of cases for each subset selected for validation of the criticality model for FSVR SNF.

Table 10-26. Critical Benchmarks Selected for Validation of the Criticality Model for FSVR Spent Nuclear Fuel

Subset	Benchmark Experiment Identification ^a	Number of Cases Included
Heterogeneous moderated ^b	Experiment with SB Cores ^c	8
	HEU-COMP-THERM-002	25
	HEU-COMP-MIXED-001	4
	HEU-MET-INTER-006	2
	U233-SOL-THERM-006	6
Homogeneous moderated ^b	U-233-SOL-THERM-001	5
	U-233-SOL-THERM-002	17
	U-233-SOL-THERM-003	10
	U-233-SOL-THERM-004	8
	U-233-SOL-THERM-005	2
	U-233-SOL-THERM-008	1
	U-233-SOL-THERM-006	6
	HEU-COMP-THERM-002	25
	HEU-COMP-MIXED-001	4
	HEU-MET-INTER-006	2

Source: Subsets defined and evaluated in BSC 2002c

NOTES: ^a The convention for naming the benchmark experiments is from NEA 2001.

^b Identification of each subset from BSC 2002c has been modified to better reflect the subset's main characteristics. The benchmark experiments in each subset have not been affected.

^c These experiments are described in Section 5.1.1 in BSC 2003f

The experiments listed in Table 10-26 are considered appropriate to represent intact (non degraded) configurations and degraded configurations of the waste package containing FSVR SNF that belong to the configuration classes 1, 2, 3 and 6 as described in *Disposal Criticality Analysis Methodology Topical Report* (YMP 2003, Section 3). Their range of applicability is detailed in Attachment X of *Criticality Model Report* (BSC 2003e)

10.8.5 Comparisons between ROA of Benchmark Experiments and ROP

The validation of the criticality model needs to show that the range of the fundamental parameters of the benchmark critical experiments (ROA) and the range of the fundamental parameters of the system (ROP) evaluated are nearly identical. This is not usually practical, and for those parameters that do not show a trend in bias, it is acceptable to use critical benchmark experiments that cover most, but not all, of the ROP of the system under evaluation. In these situations, expert judgment may be used to determine if there is a reasonable assurance that the two are sufficiently close. In cases where a trend in bias is identified, the ROA can be extended, but a penalty on the critical limit determined for the subset of benchmark experiments need to be evaluated and applied.

The comparison between ROA and ROP was structured (BSC 2003e, Attachment X) on the two subsets of benchmarks experiments selected to cover the majority of the analyzed configurations of the waste package containing FSVR SNF.

Heterogeneous Moderated Configurations—The comparison of ROA vs. ROP for the heterogeneous moderated configurations is detailed in Appendix X of *Criticality Model Report* (BSC 2003e). The collective area of applicability of the selected critical benchmarks is based on the information regarding ROA of the benchmark experiments included in Table X-7 of *Criticality Model Report* (BSC 2003e).

The findings from the comparison of ROP and ROA can be summarized as follows:

The ROA for this subset of experiments covers only a limited subset of the ROP. The atomic density of ^{235}U and the ratio moderator/fissile are not covered but this is difficult to assess for systems with two moderators. The partial coverage for spectral parameters indicates a good selection of the experiments that have spectral parameters available.

Homogeneous Moderated Configurations—The comparison of ROA vs. ROP for the homogeneous moderated configurations is detailed in Appendix X of *Criticality Model Report* (BSC 2003e). The collective area of applicability of the selected critical benchmarks is based on the ROA of the benchmark experiments included in Tables X-7 and X-9 of *Criticality Model Report* (BSC 2003e).

The findings from the comparison can be summarized as follows:

The comparison shows that the range of applicability of the selected experiments is covering the major part of the range of parameters identified for the possible homogeneous moderated configurations of FSVR SNF. Differences are noted with respect to atomic number density of ^{235}U but spectral characteristics are very similar.

10.8.5.1 Calculation of the Lower Bound Tolerance Limit

The following results are excerpted from *Analysis of Critical Benchmark Experiments and Critical Limit Calculation for DOE SNF* (BSC 2003f) which present in detail the methodology and calculations performed for evaluating the lower bound tolerance limit for each set of configurations of the waste package containing FSVR SNF. The calculated k_{eff} values for the critical benchmarks are taken from Attachment II of *Analysis of Critical Benchmark Experiments and Critical Limit Calculation for DOE SNF* (BSC 2003f).

The results of the trending parameter analysis for the critical benchmark subset representative for moderated intact (heterogeneous) configurations of the waste package containing FSVR DOE SNF are presented in Table X-13 of *Criticality Model Report* (BSC 2003e) and show a valid trend with AENCF.

The value calculated for the lower bound tolerance limit function for the benchmarks applicable to intact-moderated configurations of FSVR DOE SNF is:

$$\begin{aligned} \text{Lower bound tolerance limit} &= 0.9575 && \text{for } 0 < \text{AENCF} < 0.386 \\ \text{Lower bound tolerance limit} &= -0.0226 * \text{AENCF} + 0.9674 && \text{for } 0.386 < \text{AENCF} < 0.8015 \end{aligned}$$

The normality test results and the lower bound tolerance limit calculations are detailed in *Analysis of Critical Benchmark Experiments and Critical Limit Calculation for DOE SNF* (BSC 2003f, Attachment III).

The results of the trending parameter analysis for the critical benchmark subset representative for moderated degraded (homogeneous) configurations of the waste package containing FSVR DOE SNF are presented in Table X-14 of *Criticality Model Report* (BSC 2003e) and show a valid trend with AENCF.

The value calculated for the lower bound tolerance limit function for the benchmarks applicable to degraded (homogeneous)-moderated configurations of FSVR DOE SNF is:

$$\begin{aligned} \text{Lower bound tolerance limit} &= 0.9608 && \text{for } 0 < \text{AENCF} < 0.4625 \\ \text{Lower bound tolerance limit} &= -0.0183 * \text{AENCF} + 0.9687 && \text{for } 0.4625 < \text{AENCF} < 0.8015 \end{aligned}$$

The normality test results and the lower bound tolerance limit calculations are detailed in *Analysis of Critical Benchmark Experiments and Critical Limit Calculation for DOE SNF* (BSC 2003f, Attachment III).

Table 10-27 presents a summary of the results of the analyses performed on the subsets of critical benchmark experiments applicable to the waste package containing FSVR DOE SNF and the calculated lower bound tolerance limit values or functions.

Table 10-27. Lower Bound Tolerance Limits for Benchmark Subsets Representative for the Configurations of the Waste Package Containing FSVR Spent Nuclear Fuel

Subset	Trend Parameter	Test for Normality	Applied Computational Method	Lower Bound Tolerance Limit
Intact (heterogeneous) Moderated	AENCF	N/A	LUTB	0.9575 for $0 < \text{AENCF} < 0.386$ -0.0226 * AENCF + 0.9674 for $0.386 < \text{AENCF} < 0.8015$
Degraded (homogeneous) Moderated	AENCF	N/A	LUTB	0.9608 for $0 < \text{AENCF} < 0.4625$ -0.0183 * AENCF + 0.9687 for $0.4625 < \text{AENCF} < 0.8015$

Source: BSC 2003f, p. 52

The above results and the comparison ROA vs. ROP indicate that the criticality model is partially validated for use in assessing the criticality potential of the intact (nondegraded) configurations and of the configurations belonging to the general configurations classes 1, 2, and 6 for the degraded waste package containing FSVR SNF.

10.8.6 Summary of Criticality Model Results and Validation for FSVR SNF

The criticality analyses considered all aspects of intact and degraded configurations of the waste package containing FSVR SNF, including optimum moderation conditions, optimum reflection, geometry, and composition. The results of the three-dimensional Monte Carlo criticality calculations for all anticipated intact and degraded configurations developed through the

degradation analysis, and physically attainable, show that the requirement of $k_{\text{eff}}+2\sigma$ values be less than or equal to the interim critical limit of 0.93 is satisfied. No neutron absorber material is required as long as the ^{235}U mass for codisposal is within the specified limit.

A number of parametric analyses were run to address or bound the configuration classes discussed in Section 10.2.8.1.1. These parametric analyses identified conditions of optimum moderation, optimum spacing between fuel compacts, and optimum neutron reflection. The highest $k_{\text{eff}}+2\sigma$ values resulted from the configurations assuming that approximately 10 percent of the fuel contained in the compacts inside the FSVR fuel elements is degraded and leaves the compacts, while the DOE SNF canister is still intact. However, these configurations are not possible due to the fact that the carbonaceous matrix of the fuel compacts is similar to graphite, therefore chemically inert. Additionally, there is no known degradation mechanism that can remove 10 percent or more of the fuel particles from the compacts. The highest $k_{\text{eff}}+2\sigma$ values also resulted from the configurations assuming either the breakage of the graphite block into a large number of pieces or complete degradation, which are not attainable through any known degradation mechanism. All above conclusions are dependent on the validity of this basic assumption.

Intact and degraded component criticality calculations include variations on moderators and moderator densities, which encompass flooding the waste package. Occurrence of design basis events, including those with the potential for flooding the disposal container prior to disposal container sealing, is considered and analyzed using very conservative assumptions for many different intact configurations.

All calculations were based on a maximum of 7.425 kg ^{235}U per DOE SNF canister. This amount is calculated using the maximum number of FSVR fuel elements that can be loaded into the DOE SNF canister, which is five. The maximum ^{235}U enrichment considered is 100 wt%. The linear density of the ^{235}U is 20.0 g/cm in the DOE SNF canister. This value is calculated by dividing the total mass of fuel (7.425 kg ^{235}U) by the active fuel length of the five FSVR fuel elements stack (369.57 cm).

Table 10-28 presents a summary of the criticality and geochemistry results with a focus on the correspondence with the degradation classes and resultant configuration classes presented in *Disposal Criticality Analysis Methodology Topical Report* (YMP 2003). The results of the geochemistry analyses show that the calculated maximum loss of Gd is very small (3.63 percent) assuring its presence for all anticipated internal configurations, and consequently minimizing the potential for criticality.

The criticality model (software code MCNP and appropriated selected neutron cross-section libraries) used in analyzing the configurations of the waste package containing FSVR SNF was validated using the methodology described in *Disposal Criticality Analysis Methodology Topical Report* (YMP 2003). Current results indicate that the lower bound tolerance limit is well above the interim critical limit used in evaluating the design.

Table 10-28. Summary of Geochemistry and Criticality Analyses for Internal Configurations (Phase I and II) of the Waste Package Containing Shippingport LWBR Spent Nuclear Fuel

Master Scenario	Description	Configuration Classes and Summary Description	Summary of Geochemistry Calculations	Summary of Criticality and Criticality Model Validation Results		Comments
				$(k_{eff}+2\sigma)_{max}$	Interim Critical Limit	
Initial water intrusion	Initial stage; water fills all available spaces inside the waste package and DOE SNF canister	Intact flooded configurations: SNF and internal structures not degraded	N/A	0.9196	0.93	No Gd needed for intact case.
IP-1	SNF degrades before the internals of the waste package	Configuration class #6: SNF partially degraded in place (various stages)	For most conditions and variations of parameters the geochemistry results indicated that the loss ranges were: U: 0% to 100% Th: 0 to 29.8 %	See comment	0.93	All cases where $k_{eff}+2\sigma > 0.93$ were based on 10% or more of the fuel degraded. Postirradiation data indicate that approximately 0.3% of the fuel particles degraded. There is no mechanism that can increase this number significantly after employment (SIC has a very low degradation rate). Therefore, for all possible cases $(k_{eff}+2\sigma)_{max} < 0.93$.
IP-2	The top of the waste package is breached and liquid accumulates inside	Configuration class #3: SNF partially or totally degraded inside the waste package with intact internal structures		N/A	0.93	Configurations are covered by refinements of configuration class #6 above and #2 below
IP-3	SNF degrades concurrently with the internals of the waste package	Configuration class #2: Both SNF and internal structures of the waste package degraded (various stages)		See comment	0.93	All cases where $k_{eff}+2\sigma > 0.93$ were based on partial or complete degradation of the graphite block. The current analysis assumed that there is no mechanism that can cause this degradation. Therefore, for all possible cases $(k_{eff}+2\sigma)_{max} < 0.93$.
IP-4	SNF degrades after the internals of the waste package	Configuration class #1: SNF intact (as assembly or pins) and degraded internal structures (various stages)		See comment	0.93	
IP-5	SNF degrades before the waste package internals	The configurations resulting from these scenarios (configurations classes #4, #5) have not been investigated in the geochemistry and criticality analyses due to the fact that they are less moderated (no pooling of water) and All cases are bounded by IP-1, IP-2 and IP-3 as the latter have better moderation (water is pooling inside waste package), and more favorable conditions for neutron absorber loss (mainly Th).				
IP-6	The bottom of waste package is penetrated allowing liquid to flow through	SNF degrades concurrently with the waste package internals				
IP-6	SNF degrades after the waste package internals					

11 CONCLUSIONS

11.1 STRUCTURAL

The results presented in Section 7 show that the 5-DHLW/DOE SNF waste package internal designs (short and long; Viability Assessment and License Application) with a DOE SNF canister loaded with DOE SNF meets the SDD criteria in Section 4.1.1 if the DOE SNF canister loaded mass limit and the DHLW glass canisters mass limit are not exceeded. Also, the results show that there is sufficient clearance between the inner diameter of the support pipe and the outer diameter of the DOE SNF canister in the case of a tipover DBE (which is shown to be bounding for all handling accident scenarios in Section 4.1.1). Hence, there will be no interference between the two components, and the DOE SNF canister can be removed from the support pipe if necessary to place it inside another waste package. Additionally, there will be no breach of the DOE SNF canister.

In addition, it is concluded that the performance of the 2-MCO/2-DHLW waste package internal design is structurally acceptable when exposed to a tipover design basis event and therefore meets the structural criteria (Section 4.1.1) as long as the MCOs loaded mass limit and the DHLW glass canisters mass limit are not exceeded. There will be no breach of the waste package or multiccanister overpack, and there will not be a great enough interference from the A-plate dividers to prevent removal of the multiccanister overpacks and DHLW glass canisters from the waste package for emplacement inside another waste package.

11.2 THERMAL

The SDD requirements changed during the time period when the thermal analyses were performed. Therefore, different types of results were sought and obtained for analyses performed for different fuel types.

The thermal analyses for FFTF and Shippingport LWBR waste packages did not provide the fuel or cladding temperatures, therefore no results are available for comparison with SDD criterion 4.1.2.1. The other thermal analyses performed (for TRIGA, Shippingport PWR, Enrico Fermi, N-Reactor, and FSVR waste packages) met the SDD criterion 4.1.2.1.

Earlier thermal analyses (FFTF, Shippingport PWR, Shippingport LWBR) used a very conservative value for the thermal output of the Hanford DHLW canister, which was based on the maximum value allowed. Values of the thermal output of the Hanford 4.5-m- (15-ft-) long DHLW canister that were obtained later showed that waste packages loaded with any of the fuel types addressed in this report have maximum thermal outputs that are less than the SDD criterion of 11,800 W (Section 4.1.2.2).

11.3 SHIELDING

The shielding analyses provided the results for maximum gamma and neutron doses on the surfaces of waste packages loaded with DOE SNF and DHLW glass canisters. At the time when the analyses were performed, the SDD criteria were met. There are no current shielding criteria in the SDD to address.

11.4 CRITICALITY

The criticality analyses performed for the intact and degraded configurations of the waste package containing representative fuel types of each DOE SNF group made use of the criticality model comprising software code MCNP and appropriately selected neutron cross-section libraries. The configurations investigated have been identified and characterized using the general degradation scenarios described in *Disposal Criticality Analysis Methodology Topical Report* (YMP 2003) and the results of the specific degradation analysis applied to a representative SNF from each designated DOE SNF group. The main purpose of the criticality analyses was to demonstrate the validity of the design solutions selected for codisposing the DOE SNF and, where applicable, to evaluate the amount of added neutron absorber that minimizes the potential for criticality during postclosure of the repository.

The results of the criticality calculations for all anticipated intact and degraded configurations developed through degradation analysis show that the requirement of $k_{\text{eff}}+2\sigma$ less than or equal to the waste specific interim critical limit is satisfied. For certain configurations, specific conditions must be met with respect to the minimum amount and distribution of the neutron absorbers within the waste package. The existing results of the geochemistry calculations show that these conditions are fulfilled within the assumptions used in the geochemistry analyses.

Various general and specific assumptions have been used in the criticality calculations in order to increase the conservatism of the analysis and to take into account the uncertainties related to the modeling process. All criticality results and associated conclusions are dependent on the validity of the assumptions; which represent the best available knowledge at the time the analyses were performed.

12 REFERENCES

12.1 DOCUMENTS CITED

ASM (American Society of Metals) 1961. *Properties and Selection of Metals*. Volume 1 of *Metals Handbook*. Lyman, T., ed. 8th Edition. Pages 1010-1011. Metals Park, Ohio: American Society for Metals. TIC: 239917.

ASME (American Society of Mechanical Engineers) 1995. *1995 ASME Boiler and Pressure Vessel Code*. New York, New York: American Society of Mechanical Engineers. TIC: 245287.

Bird, R.B.; Stewart, W.E.; and Lightfoot, E.N. 1960. *Transport Phenomena*. New York, New York: John Wiley & Sons. TIC: 208957.

Briesmeister, J.F., ed. 1997. *MCNP-A General Monte Carlo N-Particle Transport Code*. LA-12625-M, Version 4B. Los Alamos, New Mexico: Los Alamos National Laboratory. ACC: MOL.19980624.0328.

BSC (Bechtel SAIC Company) 2001a. *Evaluation of Codisposal Viability for Melt and Dilute DOE-Owned Fuel*. TDR-EDC-NU-000006 REV 00. Las Vegas, Nevada: Bechtel SAIC Company. ACC: MOL.20010809.0070.

BSC 2001b. *Statement of Work for DOE—Office of Civilian Radioactive Waste Management, Technical Assistance on Melt-Dilute Criticality and Shielding Analyses, Revision 2, May 30, 2001*. Las Vegas, Nevada: Bechtel SAIC Company. ACC: MOL.20010619.0626.

BSC 2001c. *Evaluation of Codisposal Viability for Th/U Carbide (Fort Saint Vrain HTGR) DOE-Owned Fuel*. TDR-EDC-NU-000007 REV 00. Las Vegas, Nevada: Bechtel SAIC Company. ACC: MOL.20011017.0092.

BSC 2001d. *Thermal Evaluation of the Fort Saint Vrain Codisposal Waste Package*. CAL-WIS-TH-000012 REV 00. Las Vegas, Nevada: Bechtel SAIC Company. ACC: MOL.20010718.0263.

BSC 2001e. *Dose Rate Calculation for the Codisposal Waste Package of HLW Glass and the Melt-Dilute Al SNF*. CAL-DDC-NU-000004 REV 00. Las Vegas, Nevada: Bechtel SAIC Company. ACC: MOL.20010730.0063.

BSC 2001f. *Intact and Degraded Mode Criticality Calculations for the Codisposal of Fort Saint Vrain HTGR Spent Nuclear Fuel in a Waste Package*. CAL-EDC-NU-000007 REV 00. Las Vegas, Nevada: Bechtel SAIC Company. ACC: MOL.20011015.0020.

BSC 2001g. *Tip-Over of the 5 DHLW/DOE SNF - Long Waste Package Containing Fort Saint Vrain HTGR Fuel Onto an Unyielding Surface*. CAL-DDC-ME-000006 REV 00. Las Vegas, Nevada: Bechtel SAIC Company. ACC: MOL.20011008.0001.

BSC 2001h. *EQ6 Calculation for Chemical Degradation of Fort St. Vrain (Th/U Carbide) Waste Packages*. CAL-EDC-MD-000011 REV 00. Las Vegas, Nevada: Bechtel SAIC Company. ACC: MOL.20010831.0300.

BSC 2001i. *Dose Rate Calculation for the Codisposal Waste Package of HLW Glass and the FSVR Fuel*. CAL-DDC-NU-000003 REV 00. Las Vegas, Nevada: Bechtel SAIC Company. ACC: MOL.20010924.0044.

BSC 2001j. *EQ6 Calculations for Chemical Degradation of Fast Flux Test Facilities (FFTF) Waste Packages: Effects of Updated Design and Rates*. CAL-EDC-MD-000014 REV 00. Las Vegas, Nevada: Bechtel SAIC Company. ACC: MOL.20020102.0191.

BSC 2001k. *EQ6 Calculations for Chemical Degradation of Melt and Dilute Waste Packages*. CAL-EDC-MD-000012 REV 00. Las Vegas, Nevada: Bechtel SAIC Company. ACC: MOL.20010719.0064.

BSC 2001l. *Intact and Degraded Mode Criticality Calculations for the Codisposal of Melt and Dilute Ingots in a Waste Package*. CAL-EDC-NU-000006 REV 00. Las Vegas, Nevada: Bechtel SAIC Company. ACC: MOL.20010730.0062.

BSC 2002a. *Waste Package Tip-Over of 5-DHLW/DOE Short*. CAL-DDC-ME-000004 REV A. Las Vegas, Nevada: Bechtel SAIC Company. ACC: MOL.20020614.0038.

BSC 2002b. *Criticality Calculation for the Most Reactive Degraded Configurations of the FFTF SNF Codisposal WP Containing an Intact Ident-69 Container*. CAL-DSD-NU-000002 REV A. Las Vegas, Nevada: Bechtel SAIC Company. ACC: MOL.20021028.0128.

BSC 2002c. *Benchmark and Critical Limit Calculation for DOE SNF*. CAL-EDC-NU-000008 REV 00. Las Vegas, Nevada: Bechtel SAIC Company. ACC: MOL.20020416.0053.

BSC 2003a. *DOE and Commercial Waste Package System Description Document*. 000-3YD-DS00-00100-000-002. Las Vegas, Nevada: Bechtel SAIC Company. ACC: ENG.20030930.0011.

BSC 2003b. *Technical Work Plan for: Department of Energy Spent Nuclear Fuel Criticality and TSPA Work Packages*. TWP-MGR-MD-000031 REV 00. Las Vegas, Nevada: Bechtel SAIC Company. ACC: DOC.20030328.0006.

BSC 2003c. *Repository Design Project, RDP/PA IED Typical Waste Package Components Assembly (2)*. 800-IED-WIS0-00202-000-00A. Las Vegas, Nevada: Bechtel SAIC Company. ACC: ENG.20030702.0002.

BSC 2003d. *Repository Design Project, Repository/PA IED Emplacement Drift Configuration 1 of 2*. 800-IED-EBS0-00201-000-00A. Las Vegas, Nevada: Bechtel SAIC Company. ACC: ENG.20030630.0002.

BSC 2003e. *Criticality Model Report*. MDL-EBS-NU-000003 REV 02. Las Vegas, Nevada: Bechtel SAIC Company. ACC: DOC.20031013.0002.

BSC 2003f. *Analysis of Critical Benchmark Experiments and Critical Limit Calculation for DOE SNF*. CAL-DSD-NU-000003 REV 00A. Las Vegas, Nevada: Bechtel SAIC Company. ACC: DOC.20030724.0002.

Creer, J.M.; Michener, T.E.; McKinnon, M.A.; Tanner, J.E.; Gilbert, E.R.; Goodman, R.L.; Dziadosz, D.A.; Moore, E.V.; McKay, H.S.; Batalo, D.P.; Schoonen, D.H.; Jensen, M.F.; and Mullen, C.K. 1987. *The TN-24P PWR Spent-Fuel Storage Cask: Testing and Analyses*. EPRI NP-5128. Palo Alto, California: Electric Power Research Institute. TIC: 228305.

CRWMS M&O (Civilian Radioactive Waste Management System Management and Operating Contractor) 1995. *Analysis of Degradation Due to Water and Gases in MPC*. BB0000000-01717-0200-00005 REV 01. Las Vegas, Nevada: CRWMS M&O. ACC: MOL.19960419.0202.

CRWMS M&O 1996. *Waste Package Filler Material Testing Report*. BBA000000-01717-2500-00008 REV 02. Las Vegas, Nevada: CRWMS M&O. ACC: MOL.19970121.0004.

CRWMS M&O 1997a. *Waste Package Materials Selection Analysis*. BBA000000-01717-0200-00020 REV 01. Las Vegas, Nevada: CRWMS M&O. ACC: MOL.19980324.0242.

CRWMS M&O 1997b. *Preliminary Design Basis for WP Thermal Analysis*. BBAA00000-01717-0200-00019 REV 00. Las Vegas, Nevada: CRWMS M&O. ACC: MOL.19980203.0529.

CRWMS M&O 1997c. *DHLW Canister Source Terms for Waste Package Design*. BBA000000-01717-0200-00025 REV 00. Las Vegas, Nevada: CRWMS M&O. ACC: MOL.19970711.0019.

CRWMS M&O 1997d. *Waste Quantity, Mix and Throughput Study Report*. B00000000-01717-5705-00059 REV 01. Las Vegas, Nevada: CRWMS M&O. ACC: MOL.19971210.0628.

CRWMS M&O 1997e. *Thermal Evaluation of the Codisposal Canister in the 5-Pack DHLW Waste Package*. BBAA00000-01717-0200-00021 REV 01. Las Vegas, Nevada: CRWMS M&O. ACC: MOL.19971210.0413.

CRWMS M&O 1998a. *5-High Level Waste DOE Spent Fuel Waste Package Structural Calculations*. BBA000000-01717-0210-00021 REV 00. Las Vegas, Nevada: CRWMS M&O. ACC: MOL.19981006.0187.

CRWMS M&O 1998b. *Dose Calculations for the Co-Disposal WP of HLW Canisters and the Fast Flux Test Facility (FFTF) Fuel*. BBA000000-01717-0210-00019 REV 00. Las Vegas, Nevada: CRWMS M&O. ACC: MOL.19990129.0075.

CRWMS M&O 1998c. *Multiple WP Emplacement Thermal Response - Suite 1*. BBA000000-01717-0210-00001 REV 00. Las Vegas, Nevada: CRWMS M&O. ACC: MOL.19980807.0311.

CRWMS M&O 1998d. *Calculation of the Effect of Source Geometry on the 21-PWR WP Dose Rates*. BBAC00000-01717-0210-00004 REV 00. Las Vegas, Nevada: CRWMS M&O. ACC: MOL.19990222.0059.

CRWMS M&O 1998e. *DOE Spent Nuclear Fuel Disposal Container System Description Document*. BBA000000-01717-1705-00003 REV 00. Two volumes. Las Vegas, Nevada: CRWMS M&O. ACC: MOL.19981214.0036.

CRWMS M&O 1998f. *Evaluation of Codisposal Viability for Aluminum-Clad DOE-Owned Spent Fuel: Phase II Degraded Codisposal Waste Package Internal Criticality*. BBA000000-01717-5705-00017 REV 01. Las Vegas, Nevada: CRWMS M&O. ACC: MOL.19981014.0038.

CRWMS M&O 1999a. *Evaluation of Codisposal Viability for MOX (FFTF) DOE-Owned Fuel*. BBA000000-01717-5705-00023 REV 00. Las Vegas, Nevada: CRWMS M&O. ACC: MOL.19991014.0235.

CRWMS M&O 1999b. *Enrico Fermi Fast Reactor Spent Nuclear Fuel Criticality Calculations: Intact Mode*. BBA000000-01717-0210-00037 REV 00. Las Vegas, Nevada: CRWMS M&O. ACC: MOL.19990125.0079.

CRWMS M&O 1999c. *Thermal Evaluation of the FFTF Codisposal Waste Package*. BBAA00000-01717-0210-00012 REV 01. Las Vegas, Nevada: CRWMS M&O. ACC: MOL.19990610.0180.

CRWMS M&O 1999d. *Dose Calculations for the Co-Disposal WP of HLW Canisters and Fermi U-Mo Alloy SNF*. BBAC00000-01717-0210-00009 REV 00. Las Vegas, Nevada: CRWMS M&O. ACC: MOL.19990421.0152.

CRWMS M&O 1999c. *TRIGA Fuel Phase I and II Criticality Calculation*. CAL-MGR-NU-000001 REV 00. Las Vegas, Nevada: CRWMS M&O. ACC: MOL.19991209.0195.

CRWMS M&O 1999d. *DOE SRS HLW Glass Chemical Composition*. BBA000000-01717-0210-00038 REV 00. Las Vegas, Nevada: CRWMS M&O. ACC: MOL.19990215.0397.

CRWMS M&O 1999e. *Thermal Evaluation of the FFTF Codisposal Waste Package*. BBAA00000-01717-0210-00012 REV 00. Las Vegas, Nevada: CRWMS M&O. ACC: MOL.19990505.0446.

CRWMS M&O 1999f. *Thermal Evaluation of the Shippingport PWR Codisposal Waste Package*. BBA000000-01717-0210-00053 REV 00. Las Vegas, Nevada: CRWMS M&O. ACC: MOL.19990609.0069.

CRWMS M&O 1999g. *Generic Degradation Scenario and Configuration Analysis for DOE Codisposal Waste Package*. BBA000000-01717-0200-00071 REV 00. Las Vegas, Nevada: CRWMS M&O. ACC: MOL.19991118.0180.

CRWMS M&O 1999h. *Structural Calculations for the Codisposal of TRIGA Spent Nuclear Fuel in a Waste Package*. BBA000000-01717-0210-00052 REV 00. Las Vegas, Nevada: CRWMS M&O. ACC: MOL.19990812.0350.

CRWMS M&O 1999i. *Structural Calculations for the Codisposal of Shippingport Spent Nuclear Fuel in a Waste Package*. BBA000000-01717-0210-00050 REV 00. Las Vegas, Nevada: CRWMS M&O. ACC: MOL.19990505.0463.

CRWMS M&O 1999j. *Structural Calculations for the Codisposal of Enrico Fermi Spent Nuclear Fuel in a Waste Package*. BBA000000-01717-0210-00030 REV 00. Las Vegas, Nevada: CRWMS M&O. ACC: MOL.19990505.0462.

CRWMS M&O 1999k. *Structural Calculations for the Codisposal of Shippingport LWBR Spent Nuclear Fuel in a Waste Package*. BBA000000-01717-0210-00057 REV 00. Las Vegas, Nevada: CRWMS M&O. ACC: MOL.20000224.0398.

CRWMS M&O 1999l. *Thermal Evaluation of the TRIGA Codisposal Waste Package*. BBAA00000-01717-0210-00022 REV 00. Las Vegas, Nevada: CRWMS M&O. ACC: MOL.19990712.0195.

CRWMS M&O 1999m. *Thermal Evaluation of the Enrico Fermi Co-Disposal Waste Package*. BBAA00000-01717-0210-00014 REV 00. Las Vegas, Nevada: CRWMS M&O. ACC: MOL.19990325.0216.

CRWMS M&O 1999n. *Dose Calculations for the Codisposal WP of HLW Glass and the TRIGA SNF*. BBAC00000-01717-0210-00015 REV 00. Las Vegas, Nevada: CRWMS M&O. ACC: MOL.19990830.0375.

CRWMS M&O 1999o. *Dose Calculation for the Co-Disposal WP of HLW Canisters and the Shippingport PWR Fuel*. BBAC00000-01717-0210-00012 REV 00. Las Vegas, Nevada: CRWMS M&O. ACC: MOL.19990517.0010.

CRWMS M&O 1999p. *Dose Calculations for the Codisposal WP of HLW Glass and the Shippingport LWBR SNF*. BBAC00000-01717-0210-00016 REV 00. Las Vegas, Nevada: CRWMS M&O. ACC: MOL.19991117.0141.

CRWMS M&O 1999q. *Fast Flux Test Facility (FFTF) Reactor Fuel Criticality Calculations*. BBA000000-01717-0210-00016 REV 00. Las Vegas, Nevada: CRWMS M&O. ACC: MOL.19990426.0142.

CRWMS M&O 1999r. *Fast Flux Test Facility (FFTF) Reactor Fuel Degraded Criticality Calculations: Intact SNF Canister*. BBA000000-01717-0210-00051 REV 00. Las Vegas, Nevada: CRWMS M&O. ACC: MOL.19990607.0075.

CRWMS M&O 1999s. *Fast Flux Test Facility (FFTF) Reactor Fuel Degraded Criticality Calculation: Degraded SNF Canister*. BBA000000-01717-0210-00033 REV 01. Las Vegas, Nevada: CRWMS M&O. ACC: MOL.19990607.0239.

CRWMS M&O 1999t. *EQ6 Calculation for Chemical Degradation of Shippingport PWR (HEU Oxide) Spent Nuclear Fuel Waste Packages*. CAL-EDC-MD-000002 REV 00. Las Vegas, Nevada: CRWMS M&O. ACC: MOL.19991220.0322.

CRWMS M&O 1999u. *EQ6 Calculations for Chemical Degradation of Enrico Fermi Spent Nuclear Fuel Waste Packages*. BBA000000-01717-0210-00029 REV 00. Las Vegas, Nevada: CRWMS M&O. ACC: MOL.19990702.0030.

CRWMS M&O 1999v. *LCE for Research Reactor Benchmark Calculations*. B00000000-01717-0210-00034 REV 00. Las Vegas, Nevada: CRWMS M&O. ACC: MOL.19990329.0394.

CRWMS M&O 1999w. *Summary Report of Laboratory Critical Experiment Analyses Performed for the Disposal Criticality Analysis Methodology*. B00000000-01717-5705-00076 REV 02. Las Vegas, Nevada: CRWMS M&O. ACC: MOL.19990920.0167.

CRWMS M&O 2000a. *Design Analysis for the Defense High-Level Waste Disposal Container*. ANL-DDC-ME-000001 REV 00. Las Vegas, Nevada: CRWMS M&O. ACC: MOL.20000627.0254.

CRWMS M&O 2000b. *Evaluation of Codisposal Viability for UZrH (TRIGA) DOE-Owned Fuel*. TDR-EDC-NU-000001 REV 00. Las Vegas, Nevada: CRWMS M&O. ACC: MOL.20000207.0689.

CRWMS M&O 2000c. *Evaluation of Codisposal Viability for HEU Oxide (Shippingport PWR) DOE-Owned Fuel*. TDR-EDC-NU-000003 REV 00. Las Vegas, Nevada: CRWMS M&O. ACC: MOL.20000227.0240.

CRWMS M&O 2000d. *Evaluation of Codisposal Viability for U-Zr/U-Mo Alloy (Enrico Fermi) DOE-Owned Fuel*. TDR-EDC-NU-000002 REV 00. Las Vegas, Nevada: CRWMS M&O. ACC: MOL.20000815.0317.

CRWMS M&O 2000e. *Evaluation of Codisposal Viability for Th/U Oxide (Shippingport LWBR) DOE-Owned Fuel*. TDR-EDC-NU-000005 REV 00. Las Vegas, Nevada: CRWMS M&O. ACC: MOL.20001023.0055.

CRWMS M&O 2000f. *Thermal Evaluation of the Shippingport LWBR SNF Codisposal Waste Package*. CAL-EDC-ME-000001 REV 00. Las Vegas, Nevada: CRWMS M&O. ACC: MOL.20000307.0808.

CRWMS M&O 2000g. *Source Terms for HLW Glass Canisters*. CAL-MGR-NU-000002 REV 01. Las Vegas, Nevada: CRWMS M&O. ACC: MOL.20000823.0004.

CRWMS M&O 2000h. *Drift Scale Thermal Analysis*. CAL-WIS-TH-000002 REV 00. Las Vegas, Nevada: CRWMS M&O. ACC: MOL.20000420.0401.

CRWMS M&O 2000i. *Waste Package Operations Fabrication Process Report*. TDR-EBS-ND-000003 REV 01. Las Vegas, Nevada: CRWMS M&O. ACC: MOL.20000927.0002.

CRWMS M&O 2000j. *Tip-Over of the 2-MCO/2-DHLW Waste Package on Unyielding Surface*. CAL-EDC-ME-000002 REV 00. Las Vegas, Nevada: CRWMS M&O. ACC: MOL.20000710.0522.

CRWMS M&O 2000k. *Thermal Evaluation of the 2-MCO/2-DHLW Waste Package*. CAL-WIS-TH-000006 REV 00. Las Vegas, Nevada: CRWMS M&O. ACC: MOL.20000913.0450.

CRWMS M&O 2000l. *Dose Rate Calculation for the 2-MCO/2-DHLW Waste Package*. CAL-DDC-NU-000002 REV 00. CRWMS M&O, Nevada: Las Vegas. ACC: MOL.20001016.0006.

CRWMS M&O 2000m. *Intact and Degraded Criticality Calculations for the Codisposal of Shippingport PWR Fuel in a Waste Package*. CAL-EDC-NU-000002 REV 00. Las Vegas, Nevada: CRWMS M&O. ACC: MOL.20000209.0233.

CRWMS M&O 2000n. *Enrico Fermi Fast Reactor Spent Nuclear Fuel Criticality Calculations: Degraded Mode*. CAL-EDC-NU-000001 REV 00. Las Vegas, Nevada: CRWMS M&O. ACC: MOL.20000802.0002.

CRWMS M&O 2000o. *Intact and Degraded Criticality Calculations for the Codisposal of Shippingport LWBR Spent Nuclear Fuel in a Waste Package*. CAL-EDC-NU-000004 REV 00. Las Vegas, Nevada: CRWMS M&O. ACC: MOL.20000922.0093.

CRWMS M&O 2001a. *Evaluation of Codisposal Viability for U-Metal (N Reactor) DOE-Owned Fuel*. TDR-EDC-NU-000004 REV 00. Las Vegas, Nevada: CRWMS M&O. ACC: MOL.20010314.0004.

CRWMS M&O 2001b. *Intact and Degraded Component Criticality Calculations of N Reactor Spent Nuclear Fuel*. CAL-EDC-NU-000003 REV 00. Las Vegas, Nevada: CRWMS M&O. ACC: MOL.20010223.0060.

DOE (U.S. Department of Energy) 1998a. *Preliminary Design Concept for the Repository and Waste Package*. Volume 2 of *Viability Assessment of a Repository at Yucca Mountain*. DOE/RW-0508. Washington, D.C.: U.S. Department of Energy, Office of Civilian Radioactive Waste Management. ACC: MOL.19981007.0029.

DOE 1998b. *FFTF (MOX) Fuel Characteristics for Disposal Criticality Analysis*. DOE/SNF/REP-032, Rev. 0. Washington, D.C.: U.S. Department of Energy. TIC: 241492.

DOE 1999a. *Design Specification*. Volume 1 of *Preliminary Design Specification for Department of Energy Standardized Spent Nuclear Fuel Canisters*. DOE/SNF/REP-011, Rev. 3. Washington, D.C.: U.S. Department of Energy, Office of Spent Fuel Management and Special Projects. TIC: 246602.

DOE 1999b. *Fermi (U-Mo) Fuel Characteristics for Disposal Criticality Analysis*. DOE/SNF/REP-035, Rev. 0. Washington, D.C.: U.S. Department of Energy. TIC: 242461.

DOE 1999c. *TRIGA (UZrH) Fuel Characteristics for Disposal Criticality Analysis*. DOE/SNF/REP-048, Rev. 0. Washington, D.C.: U.S. Department of Energy. TIC: 244162.

DOE 1999d. *Shippingport PWR (HEU Oxide) Fuel Characteristics for Disposal Criticality Analysis*. DOE/SNF/REP-040, Rev. 0. Washington, D.C.: U.S. Department of Energy. TIC: 243528.

DOE 1999e. *Shippingport LWBR (Th/U Oxide) Fuel Characteristics for Disposal Criticality Analysis*. DOE/SNF/REP-051, Rev. 0. Washington, D.C.: U.S. Department of Energy, Office of Environmental Management. TIC: 245631.

DOE 2000a. *N Reactor (U-Metal) Fuel Characteristics for Disposal Criticality Analysis*. DOE/SNF/REP-056, Rev. 0. Washington, D.C.: U.S. Department of Energy, Office of Environmental Management. TIC: 247956.

DOE 2000b. *DOE Spent Nuclear Fuel Grouping in Support of Criticality, DBE, TSPA-LA*. DOE/SNF/REP-0046, Rev. 0. Idaho Falls, Idaho: U.S. Department of Energy, Idaho Operations Office. ACC: DOC.20030905.0021.

DOE 2002. *DOE Spent Nuclear Fuel Information in Support of TSPA-SR*. DOE/SNF/REP-047, Rev. 2. Idaho Falls, Idaho: U.S. Department of Energy, Idaho Operations Office. TIC: 252089.

DOE 2003. *Quality Assurance Requirements and Description*. DOE/RW-0333P, Rev. 13. Washington, D.C.: U.S. Department of Energy, Office of Civilian Radioactive Waste Management. ACC: DOC.20030422.0003.

INEEL (Idaho National Engineering and Environmental Laboratory) 2002. *FFTF (MOX) Fuel Characteristics for Disposal Criticality Analysis*. DOE/SNF/REP-032, Rev. 1. Idaho Falls, Idaho: U.S. Department of Energy, Idaho National Operations Office. TIC: 252933.

Minwalla, H.J. 2003. *Project Design Criteria Document*. 000-3DR-MGR0-00100-000-001. Las Vegas, Nevada: Bechtel SAIC Company. ACC: ENG.20030402.0001.

NEA (Nuclear Energy Agency) 2001. *International Handbook of Evaluated Criticality Safety Benchmark Experiments*. 2001 Edition. NEA/NSC/DOC(95)03. Paris, France: Nuclear Energy Agency, Organization for Economic Co-operation and Development. TIC: 251945.

Parks, C.V.; Broadhead, B.L.; Hermann, O.W.; Tang, J.S.; Cramer, S.N.; Gauthey, J.C.; Kirk, B.L.; and Roussin, R.W. 1988. *Assessment of Shielding Analysis Methods, Codes, and Data for Spent Fuel Transport/Storage Applications*. ORNL/CSD/TM-246. Oak Ridge, Tennessee: Oak Ridge National Laboratory. ACC: NN1.19880928.0023.

Parrington, J.R.; Knox, H.D.; Breneman, S.L.; Baum, E.M.; and Feiner, F. 1996. *Nuclides and Isotopes, Chart of the Nuclides*. 15th Edition. San Jose, California: General Electric Company and KAPL, Inc. TIC: 233705.

Picha, K.G., Jr. 1997. "Response to Repository Environmental Impact Statement Data Call for High-Level Waste." Memorandum from K.G. Picha, Jr. (DOE) to W. Dixon (YMSCO), September 5, 1997, with attachments. ACC: MOL.19970917.0273.

Plodinec, M.J. and Marra, S.L. 1994. *Projected Radionuclide Inventories and Radiogenic Properties of the DWPF Product (U)*. WSRC-IM-91-116-3, Rev. 0. Aiken, South Carolina: Westinghouse Savannah River Company. TIC: 242337.

Shigley, J. E. and Mischke, C.R. 1989. *Mechanical Engineering Design*. Fifth Edition. New York, New York: McGraw-Hill. TIC: 246990.

Sterbentz, J.W. 1997. *Radionuclide Mass Inventory, Activity, Decay Heat, and Dose Rate Parametric Data for TRIGA Spent Nuclear Fuels*. INEL-96/0482. Idaho Falls, Idaho: Idaho National Engineering and Environmental Laboratory. TIC: 243659.

Stout, R.B. and Leider, H.R., eds. 1991. *Preliminary Waste Form Characteristics Report*. Version 1.0. Livermore, California: Lawrence Livermore National Laboratory. ACC: MOL.19940726.0118.

Stroupe, E.P. 2000. "Approach to Implementing the Site Recommendation Design Baseline." Interoffice correspondence from E.P. Stroupe (CRWMS M&O) to D.R. Wilkins, January 26, 2000, LV.RSO.EPS.1/00-004, with attachment. ACC: MOL.20000214.0480.

Taylor, L.L. 2001. *Fort Saint Vrain HTGR (Th/U Carbide) Fuel Characteristics for Disposal Criticality Analysis*. DOE/SNF/REP-060, Rev. 0. [Washington, D.C.]: U.S. Department of Energy, Office of Environmental Management. TIC: 249783.

Taylor, W.J. 1997. "Incorporating Hanford 15 Foot (4.5 Meter) Canister into Civilian Radioactive Waste Management System (CRWMS) Baseline." Memorandum from W.J. Taylor (DOE) to J. Williams (Office of Waste Acceptance Storage and Transportation), April 2, 1997. ACC: HQP.19970609.0014.

Tomsio, N. 1986. *Characterization of TRIGA Fuel*. ORNL/SUB/86-22047/3. Oak Ridge, Tennessee: Oak Ridge National Laboratory. TIC: 229864.

YMP (Yucca Mountain Site Characterization Project) 2003. *Disposal Criticality Analysis Methodology Topical Report*. YMP/TR-004Q, Rev. 02. Las Vegas, Nevada: Yucca Mountain Site Characterization Office. ACC: DOC.20031110.0005.

12.2 CODES, STANDARDS, REGULATIONS, AND PROCEDURES

10 CFR 63. Energy: Disposal of High-Level Radioactive Wastes in a Geologic Repository at Yucca Mountain, Nevada. Readily available.

ANSI/ANS-6.1.1-1977. *Neutron and Gamma-Ray Flux-to-Dose-Rate Factors*. La Grange Park, Illinois: American Nuclear Society. TIC: 239401.

ANSI/ANS-8.1-1998. *Nuclear Criticality Safety in Operations with Fissionable Material Outside Reactors*. La Grange Park, Illinois: American Nuclear Society. TIC: 242363.

ASTM A 240/A 240M-03b. 2003. *Standard Specification for Chromium and Chromium-Nickel Stainless Steel Plate, Sheet, and Strip for Pressure Vessels and for General Applications*. West Conshohocken, Pennsylvania: American Society for Testing and Materials. TIC: 254845.

12.3 DATA, LISTED BY DATA TRACKING NUMBER

MO0003RIB00071.000. Physical and Chemical Characteristics of Alloy 22. Submittal date: 03/13/2000.

MO9906RIB00048.000. Waste Package Material Properties: Waste Form Materials. Submittal date: 06/09/1999.

MO9906RIB00053.000. Waste Package Materials Properties: Corrosion Allowance and Basket Materials. Submittal date: 06/17/1999.

MO9906RIB00054.000. Waste Package Material Properties: Structural Materials. Submittal date: 06/17/1999.

12.4 SOFTWARE CODES

Software Code: ANSYS. V5.4L2. HP-UX-10.20. 10027-5.4L2-00.

Software Code: ANSYS. V5.6.2. HP-UX 10.20. 10364-5.6.2-00.

Software Code: EQ3/6. V7.2b. LLNL: UCRL-MA-110662.

Software Code: EQ6, Version 7.2bLV. V7.2bLV. 10075-7.2bLV-00.

Software Code: LS-DYNA. V950. HP 9000. 10300-950-00.

Software Code: MCNP. V4B2LV. HP, HPUX 9.07 and 10.20; PC, Windows 95; Sun, Solaris 2.6. 30033 V4B2LV.